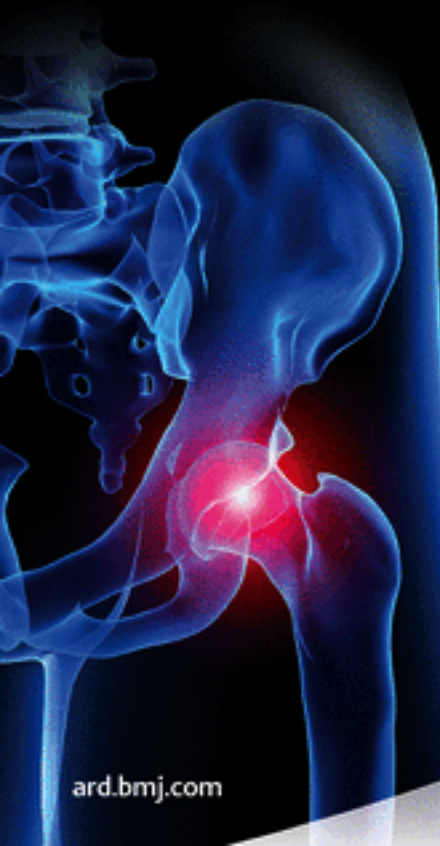


December 2019 Volume 78 Issue 12

Impact
Factor
14.299

Annals of the Rheumatic Diseases

The EULAR Journal



ard.bmj.com

eular **BMJ**
EUROPEAN LEAGUE OF ASSOCIATIONS
OF RHEUMATOLOGISTS

Editor

Josef S Smolen (Austria)

Associate Editors

Francis Berenbaum (France)

Dimitrios Boumpas (Greece)

Gerd Burmester (Germany)

Mary Crow (USA)

Iain McInnes (UK)

Thomas Pap (Germany)

David Pisetsky (USA)

Désirée van der Heijde

(The Netherlands)

Kazuhiko Yamamoto (Japan)

**Methodological and Statistical
Advisor**

Stian Lydersen (Norway)

Social Media Advisors

Alessia Alunno (Italy)

Mary Canavan (Ireland)

Meghna Jani (UK)

Elena Nikiphorou (UK)

Caroline Ospelt (Switzerland)

Christophe Richez (France)

Paul Studenic (Austria)

**Guidelines for Authors and
Reviewers**

Full instructions are available online at <http://ard.bmj.com/pages/authors>. Articles must be submitted electronically at <http://mc.manuscriptcentral.com/ard>. Authors retain copyright but are required to grant ARD an exclusive licence to publish. (<http://ard.bmj.com/pages/authors/>).

Annals of the Rheumatic Diseases publishes original work on all aspects of rheumatology and disorders of connective tissue. Laboratory and clinical studies are equally welcome

Editorial Board

Daniel Aletaha (Austria)
 Johan Askling (Sweden)
 Sang-Cheol Bae (Korea)
 Xenofon Baraliakos (Germany)
 Anne Barton (UK)
 Maarten Boers (The Netherlands)
 Maxine Breban (France)
 Matthew Brown (Australia)
 Maya Buch (UK)
 Loreto Carmona (Spain)
 Carlo Chizzolini (Switzerland)
 Bernard Combe (France)
 Philip Conaghan (UK)
 Maurizio Cutolo (Italy)
 Nicola Dalbeth (Australia)
 Christian Dejaco (Austria)
 Oliver Distler (Switzerland)
 Thomas Dörner (Germany)
 Dirk Elewaut (Belgium)
 Axel Finckh (Switzerland)
 Rebecca Fischer-Betz (Germany)
 Roy Fleischmann (USA)
 Mary Goldring (USA)
 Laure Gossec (France)
 Walter Grassi (Italy)
 Ahmet Gül (Turkey)
 Frederic Houssiau (Belgium)
 Tom Huizinga (The Netherlands)
 Arthur Kavanaugh (USA)
 Margreet Kloppenburg (The Netherlands)
 Robert Landewé (The Netherlands)
 Zhan-Gou Li (China)

Rik Lories (Belgium)
 Ingrid Lundberg (Sweden)
 Gary MacFarlane (UK)
 Xavier Mariette (France)
 Alberto Martini (Italy)
 Marco Mattucci Cerinic (Italy)
 Dennis McGonagle (UK)
 Fred Miller (USA)
 Peter Nash (Australia)
 Michael Nurmohamed (The Netherlands)
 Caroline Ospelt (Switzerland)
 Monika Østensen (Norway)
 Costantino Pitzalis (UK)
 Jane Salmon (USA)
 Georg Schett (Germany)
 José da Silva (Portugal)
 Hendrik Schulze-Koops (Germany)
 Nan Shen (China)
 Greg Silverman (USA)
 Alexander So (Switzerland)
 Hiroshi Takayanagi (Japan)
 Tsutomu Takeuchi (Japan)
 Yoshiya Tanaka (Japan)
 Dimitrios Vassilopoulos (Greece)
 Douglas Veale (Ireland)
 Jiri Vencovsky (Czech Republic)
 Ronald van Vollenhoven (Sweden)
 Erwin Wagner (Spain)
 Michael Ward (USA)
 Kevin Winthrop (USA)
 Huji Xu (China)

**Chairman of Advisory
Committee**Johannes Bijlsma
(The Netherlands)**Advisory Committee**

Ferry Breedveld (The Netherlands)
 Marco Mattucci Cerinic (Italy)
 Michael Doherty (UK)
 Maxime Dougados (France)
 Paul Emery (UK)
 Daniel Furst (USA)
 Steffen Gay (Switzerland)
 Marc Hochberg (USA)
 Joachim Kalden (Germany)
 Edward Keystone (Canada)
 Lars Klareskog (Sweden)
 Tore Kvien (Norway)

Zhan-guo Li (China)
 Peter Lipsky (USA)
 Sir Ravinder Maini (UK)
 Emilio Martín-Mola (Spain)
 Haralampos Moutsopoulos (Greece)
 Karel Pavelka (Czech Republic)
 Yehuda Shoenfeld (Israel)
 Leo van de Putte (The Netherlands)
 Frank Wollheim (Sweden)
 Anthony Woolf (UK)

Contact Details**Editorial Office**

Annals of the Rheumatic Diseases
 BMJ Journals, BMA House, Tavistock Square
 London WC1H 9JR, UK
 E: ard@bmj.com

Production Editor

Teresa Jobson
 E: production.ard@bmj.com

EULAR

EULAR Executive Secretariat
 Seestrasse 240, 8802 Kilchberg, Switzerland
 E: eular@eular.org
www.eular.org

Customer support

For general queries and support with existing and new subscriptions:
 W: support.bmj.com
 T: +44 (0)20 7111 1105
 E: support@bmj.com

Self-archiving and permissions

W: bmj.com/company/products-services/rights-and-licensing/
 E: bmj.permissions@bmj.com

Advertising

W: bmj.com/company/for-advertisers-and-sponsor/

Display Advertising ROW

Sophie Fitzsimmons
 T: +44 (0)20 3655 5612
 E: sfitzsimmons@bmj.com

Online Advertising ROW

Marc Clifford
 T: +44 (0) 20 3655 5610
 E: mclifford@bmj.com

Display & Online Advertising Americas

American Medical Communications (AMC)
 T: +1 973 214 4374
 E: rgordon@americanmedicalcomm.com

Reprints

Author Reprints
 BMJ Reprints Team
 E: admin.reprints@bmj.com

Commercial Reprints ROW
 Nadia Gurney-Randall
 M: +44 07866 262344
 E: ngurneyrandall@bmj.com

Commercial Reprints Americas
 Ray Thibodeau
 T: +1 267 895 1758
 M: +1 215 933 8484
 E: ray.thibodeau@contentednet.com

For all other journal contacts
ard.bmj.com/contact-us

Subscription Information

ARD is published monthly; subscribers receive all supplements
 ISSN 0003-4967 (print); 1468-2060 (online)

Institutional Rates 2019

Print
 £1036

Online

Site licences are priced on FTE basis and allow access by the whole institution. Details available online at <http://journals.bmj.com/content/subscribers> or contact the Subscription Manager in the UK (see above right)

Personal print or online only and institutional print subscriptions may be purchased online at <http://journals.bmj.com/content/subscribers> (payment by Visa/Mastercard only)

Residents of some EC countries must pay VAT; for details, call us or visit <http://journals.bmj.com/content/subscribers>

For more information on subscription rates or to subscribe online please visit [ard/bmj.com/pages/contact-us/](http://ard.bmj.com/pages/contact-us/)

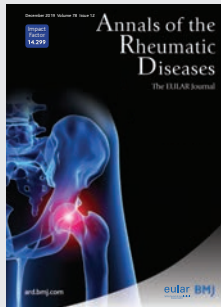
Personal Rates 2019

Print (includes online access at no additional cost)
 £428

Online only
 £182

EULAR congress delegates

Delegates receive a Continuous Professional Development package that includes a 12 month complimentary subscription to *ARD* in print and/or online

**Editor**

Josef S Smolen

Associate Editors

Francis Berenbaum
 Dimitrios Boumpas
 Gerd Burmester
 Mary Crow
 Iain McInnes
 Thomas Pap
 David Pisetsky
 Désirée van der Heijde
 Kazuhiko Yamamoto

Editorial office

Annals of the Rheumatic Diseases
 BMJ Publishing Group Ltd
 BMA House
 Tavistock Square
 London WC1H 9JR, UK
 T: +44 (0)20 3655 5889
 E: ard@bmj.com
 Twitter: @ARD_BMJ
 ISSN: 0003-4967 (print)
 ISSN: 1468-2060 (online)

Disclaimer: ARD is owned and published by BMJ Publishing Group Ltd (a wholly owned subsidiary of the British Medical Association) and the European League Against Rheumatism. The owners grant editorial freedom to the Editor of ARD. ARD follows guidelines on editorial independence produced by the World Association of Medical Editors and the code on good publication practice of the Committee on Publication Ethics.

ARD is intended for medical professionals and is provided without warranty, express or implied. Statements in the journal are the responsibility of their authors and advertisers and not authors' institutions the BMJ Publishing Group, the European League Against Rheumatism or the BMA unless otherwise specified or determined by law. Acceptance of advertising does not imply endorsement.

To the fullest extent permitted by law, the BMJ Publishing Group shall not be liable for any loss, injury or damage resulting from the use of ARD or any information in it whether based on contract, tort, or otherwise. Readers are advised to verify any information they choose to rely on.

Copyright: © 2019 BMJ Publishing Group and European League Against Rheumatism. All rights reserved; no part of this publication may be reproduced stored in a retrieval system, or transmitted in any form or by any means, electronic, mechanical, photocopying recording, or otherwise without prior permission

ARD is published by BMJ Publishing Group Ltd typeset by Exeter Premedia Services Private Ltd, Chennai, India and printed in the UK on acid-free paper.

Annals of the Rheumatic Diseases (ISSN No: 0003-4967) is published monthly by BMJ Publishing Group and distributed in the USA by Air Business Ltd. Periodicals postage paid at Jamaica NY 11431 POSTMASTER: send address changes to *Annals of the Rheumatic Diseases*, Air Business Ltd, c/o WN Shipping USA, 156-15, 146th Avenue, 2nd Floor, Jamaica, NY 11434, USA.

Rheumatoid arthritis

1609 Effect of disease duration and prior disease-modifying antirheumatic drug use on treatment outcomes in patients with rheumatoid arthritis
D Aletaha, J Maa, S Chen, S-H Park, D Nicholls, S Florentinus, D Furtner, J S Smolen

1616 On the presence of HLA-SE alleles and ACPA-IgG variable domain glycosylation in the phase preceding the development of rheumatoid arthritis
T Kissel, K A van Schie, L Hafkenscheid, A Lundquist, H Kokkonen, M Wuhrer, T WJ Huizinga, H U Scherer, R Toes, S Rantapää-Dahlqvist

1621 Anticitrullinated protein antibodies facilitate migration of synovial tissue-derived fibroblasts
M Sun, B Rethi, A Krishnamurthy, V Joshua, A Circiumaru, A H Hensvold, E Ossipova, C Grönwall, Y Liu, M Engstrom, S B Catrina, J Steen, V Malmstrom, L Klareskog, C Svensson, C Ospelt, H Wähämaa, A I Catrina

1632 CD109 regulates the inflammatory response and is required for the pathogenesis of rheumatoid arthritis
G Song, T Feng, R Zhao, Q Lu, Y Diao, Q Guo, Z Wang, Y Zhang, L Ge, J Pan, L Wang, J Han

Early arthritis

1642 Synovial tissue signatures enhance clinical classification and prognostic/treatment response algorithms in early inflammatory arthritis and predict requirement for subsequent biological therapy: results from the pathobiology of early arthritis cohort (PEAC)
G Lliso-Ribera, F Humby, M Lewis, A Nerviani, D Mauro, F Rivellese, S Kelly, R Hands, F Bene, N Ramamoorthi, J A Hackney, A Cauli, E H Choy, A Filer, P C Taylor, I McInnes, M J Townsend, C Pitzalis

Spondyloarthritis

1653 HLA-B27 alters BMP/TGF β signalling in *Drosophila*, revealing putative pathogenic mechanism for spondyloarthritis
B Grandon, A Rincheval-Arnold, N Jah, J-M Corsi, L M Araujo, S Glatigny, E Prevost, D Roche, G Chiochia, I Guéna, S Gaumer, M Breban

Systemic lupus erythematosus

1663 Safety and immune response of a live-attenuated herpes zoster vaccine in patients with systemic lupus erythematosus: a randomised placebo-controlled trial
C C Mok, K H Chan, L Y Ho, Y F Fung, W F Fung, P C Y Woo

1669 Ultrasensitive serum interferon- α quantification during SLE remission identifies patients at risk for relapse

A Mathian, S Mouries-Martin, K Dorgham, H Devilliers, H Yssel, L Garrido Castillo, F Cohen-Aubart, J Haroche, M Hié, M Pineton de Chambrun, M Miyara, M Pha, F Rozenberg, G Gorochov, Z Amoura

1677 A WHO Reference Reagent for lupus (anti-dsDNA) antibodies: international collaborative study to evaluate a candidate preparation
B J Fox, J Hockley, P Rigsby, C Dolman, P L Meroni, J Rönnelid

Systemic sclerosis

1681 Revised European Scleroderma Trials and Research Group Activity Index is the best predictor of short-term severity accrual
S Fasano, A Riccardi, V Messiniti, P Caramaschi, E Rosato, B Maurer, V Smith, E Siegert, E De Langhe, V Riccieri, P Airó, C Mihai, J Avouac, E Zanatta, U A Walker, F Iannone, P García De la Peña Lefebvre, J H W Distler, A Vacca, O Distler, O Kowal-Bielecka, Y Allanore, G Valentini

1686 Vascularised human skin equivalents as a novel in vitro model of skin fibrosis and platform for testing of antifibrotic drugs
A-E Matei, C-W Chen, L Kiesewetter, A-H Györfi, Y-N Li, T Trinh-Minh, X Xu, C Tran Manh, T van Kuppevelt, J Hansmann, A Jüngel, G Schett, F Groeber-Becker, J H W Distler

MORE CONTENTS ►



EDITOR'S CHOICE

This article has been chosen by the Editor to be of special interest or importance and is freely available online.



OPEN ACCESS

This article has been made freely available online under the BMJ Journals open access scheme.

See <http://authors.bmj.com/open-access/>



Member since 2008

JMD0004

This journal is a member of and subscribes to the principles of the Committee on Publication Ethics

<http://publicationethics.org/>



When you have finished with this please recycle it

Osteoarthritis

1693 Knee osteoarthritis risk in non-industrial societies undergoing an energy balance transition: evidence from the indigenous Tarahumara of Mexico

I J Wallace, D T Felson, S Worthington, J Duryea, M Clancy, P Aliabadi, G N Eick, J J Snodgrass, A L Baggish, D E Lieberman

1699 Discovery of an autoantibody signature for the early diagnosis of knee osteoarthritis: data from the Osteoarthritis Initiative



M Camacho-Encina, V Balboa-Barreiro, I Rego-Perez, F Picchi, J VanDuin, J Qiu, M Fuentes, N Oreiro, J LaBaer, C Ruiz-Romero, F J Blanco

Osteoporosis

1706 Diagnosis of osteoporosis in statin-treated patients is dose-dependent



M Leutner, C Matzhold, L Bellach, C Deischinger, J Harreiter, S Thurner, P Klimek, A Kautzky-Willer

Paediatric rheumatology

1712 Immunome perturbation is present in patients with juvenile idiopathic arthritis who are in remission and will relapse upon anti-TNF α withdrawal



J Y Leong, P Chen, J G Yeo, F Ally, C Chua, S Nur Hazirah, S L Poh, L Pan, L Lai, E S C Lee, L D/O T Bathi, T Arkachaisri, D Lovell, S Albani, Pediatric Rheumatology Collaborative Study Group

1722 Emergent high fatality lung disease in systemic juvenile arthritis

V E Saper, G Chen, G H Deutsch, R P Guilleman, J Birgmeier, K Jagadeesh, S Canna, G Schuler, R Deterding, J Xu, A N Leung, L Bouzoubaa, K Abulaban, K Baszis, E M Behrens, J Birmingham, A Casey, M Cidon, R Q Cron, A De, F De Benedetti, I Ferguson, M P Fishman, S I Goodman, T B Graham, A A Grom, K Haines, M Hazen, L A Henderson, A Ho, M Ibarra, C J Inman, R Jerath, K Khawaja, D J Kingsbury, M Klein-Gitelman, K Lai, S Lapidus, C Lin, J Lin, D R Liptzin, D Milojevic, J Mombourquette, K Onel, S Ozen, M Perez, K Phillippi, S Prahalad, S Radhakrishna, A Reinhardt, M Riskalla, N Rosenwasser, J Roth, R Schneider, D Schonenberg-Meinema, S Shenoj, J A Smith, H E Sönmez, M L Stoll, C Towe, S O Vargas, R K Vehe, L R Young, J Yang, T Desai, R Balise, Y Lu, L Tian, G Bejerano, M M Davis, P Khatri, E D Mellins, the Childhood Arthritis and Rheumatology Research Alliance Registry Investigators

Letters

1733 Evidence to support or guide glucocorticoid tapering in rheumatoid arthritis is lacking

B I Wallace, D M Wallace, A K Waljee, D J Clauw

1734 Association of human papillomavirus infection with risk for rheumatoid arthritis: a population-based cohort study

Y-T Liu, H-K Tsou, J-Y Chiou, Y-H Wang, M-C Chou, J C-C Wei

1736 Real-world effectiveness of apremilast in multirefractory mucosal involvement of Behçet's disease

G Lopalco, V Venerito, P Leccese, G Emmi, L Cantarini, N Lascaro, G Di Scala, C Fabiani, D Rigante, F Iannone

1738 'Slope sign': a feature of large vessel vasculitis?

B Dasgupta, K Smith, A A S Khan, F Coath, R J Wakefield

Electronic pages

e131 Metering the METEOR in methotrexate failure: is propensity score a falling star?

S Ahmed

e132 Response to: 'Metering the METEOR in methotrexate failure: is propensity score a falling star?' by Ahmed *et al*

S A Bergstra, C F Allaart, R B M Landewé

e133 Tocilizumab in patients with adult-onset Still's disease refractory to glucocorticoid treatment

Y H Lee

e134 Response to: 'Tocilizumab in patients with adult-onset Still's disease refractory to glucocorticoid treatment' by Lee

Y Kaneko, H Kameda, K Ikeda, T Ishii, K Murakami, H Takamatsu, Y Tanaka, T Abe, T Takeuchi

e135 Inflammation in SLE-PAH: good news or not?

J Qian, M Li, J Zhao, Q Wang, Z Tian, X Zeng

e136 Response to: 'Inflammation in SLE-PAH: good news or not?' by Junyan Qian *et al*

F Sun, Y Lei, X Zhang, S Ye

e137 Chronic hydroxychloroquine/chloroquine exposure for connective tissue diseases and risk of Alzheimer's disease

Y H Lee

- e138** Response to: 'Chronic hydroxychloroquine/chloroquine exposure for connective tissue diseases and risk of Alzheimer's disease' by Lee
L Fardet, I Petersen, I Nazareth
- e139** 'MAINRITSAN2-the future', with some doubts!
A Chattopadhyay, N Acharya, D Mishra, V Sharma, GSRSNK Naidu, A Sharma
- e140** Response to: "'MAINRITSAN2-the future", with some doubts!' by Chattopadhyay *et al*
P Charles, L Guillevin
- e141** Knee osteoarthritis and bisphosphonates: Could BCP crystals be the missing link?
C-L M Murphy, G McCarthy
- e142** Response to: 'Knee osteoarthritis and bisphosphonates: Could BCP crystals be the missing link?' by Murphy *et al*
W Lems
- e143** Correction: *Mitochondrial DNA haplogroups influence the risk of incident knee osteoarthritis in OAI and CHECK cohorts. A meta-analysis and functional study*
- e144** Correction: *Multi-dimensional analysis identified rheumatoid arthritis-driving pathway in human T cell. A meta-analysis and functional study*

CLINICAL SCIENCE

Effect of disease duration and prior disease-modifying antirheumatic drug use on treatment outcomes in patients with rheumatoid arthritis

Daniel Aletaha,¹ Jen-fue Maa,² Su Chen,² Sung-Hwan Park,³ Dave Nicholls,⁴ Stefan Florentinus,⁵ Daniel Furtner,⁶ Josef S Smolen¹

Handling editor David S Pisetsky

► Additional material is published online only. To view please visit the journal online (<http://dx.doi.org/10.1136/annrheumdis-2018-214918>).

¹Department of Rheumatology, Medical University of Vienna, Vienna, Austria

²Data and Statistical Sciences, AbbVie Inc, North Chicago, Illinois, USA

³Department of Internal Medicine, Division of Rheumatology, Seoul St. Mary's Hospital of The Catholic University of Korea, Seoul, Republic of Korea

⁴Clinical Trials Centre, University of the Sunshine Coast, Maroochydore, Queensland, Australia

⁵Global Medical Affairs, AbbVie, Hoofddorp, The Netherlands

⁶Global Medical Affairs, AbbVie, Mascot, New South Wales, Australia

Correspondence to

Professor Daniel Aletaha, Department of Rheumatology, Medical University of Vienna, Vienna, Austria; daniel.aletaha@meduniwien.ac.at

Received 14 December 2018

Revised 1 July 2019

Accepted 25 July 2019

Published Online First

21 August 2019



© Author(s) (or their employer(s)) 2019. Re-use permitted under CC BY-NC. No commercial re-use. See rights and permissions. Published by BMJ.

To cite: Aletaha D, Maa J, Chen S, et al. *Ann Rheum Dis* 2019;**78**:1609–1615.

ABSTRACT

Objectives To determine if disease duration and number of prior disease-modifying antirheumatic drugs (DMARDs) affect response to therapy in patients with established rheumatoid arthritis (RA).

Methods Associations between disease duration or number of prior DMARDs and response to therapy were assessed using data from two randomised controlled trials in patients with established RA (mean duration, 11 years) receiving adalimumab+methotrexate. Response to therapy was assessed at week 24 using disease activity outcomes, including 28-joint Disease Activity Score based on C-reactive protein (DAS28(CRP)), Simplified Disease Activity Index (SDAI) and Health Assessment Questionnaire Disability Index (HAQ-DI), and proportions of patients with 20%/50%/70% improvement in American College of Rheumatology (ACR) responses.

Results In the larger study (N=207), a greater number of prior DMARDs (>2 vs 0–1) was associated with smaller improvements in DAS28(CRP) (–1.8 vs –2.2), SDAI (–22.1 vs –26.9) and HAQ-DI (–0.43 vs –0.64) from baseline to week 24. RA duration of >10 years versus <1 year was associated with higher HAQ-DI scores (1.1 vs 0.7) at week 24, but results on DAS28(CRP) and SDAI were mixed. A greater number of prior DMARDs and longer RA duration were associated with lower ACR response rates at week 24. Data from the second trial (N=67) generally confirmed these findings.

Conclusions Number of prior DMARDs and disease duration affect responses to therapy in patients with established RA. Furthermore, number of prior DMARDs, regardless of disease duration, has a limiting effect on the potential response to adalimumab therapy.

INTRODUCTION

A delay in initiating disease-modifying antirheumatic drugs (DMARDs) can negatively affect long-term outcomes and be associated with greater disease activity, more extensive joint damage and worsened physical disability in patients with rheumatoid arthritis (RA).^{1–2} Conversely, rapid implementation of conventional synthetic (cs) DMARDs or tumour necrosis factor inhibitors (TNFis) results in better disease control than delaying start of therapy.^{3–7}

However, longer disease duration is not necessarily associated with reduced clinical responsiveness based on observations that patients with different disease durations achieve similar outcomes in clinical trials.^{8–10} In contrast, patients with RA

Key messages

What is already known about this subject?

- Longer disease duration and delayed start of disease-modifying therapies (disease-modifying antirheumatic drugs, DMARDs) are associated with poorer disease control in patients with rheumatoid arthritis (RA).
- Prior DMARD use has also been shown to affect treatment outcomes in RA.

What does this study add?

- Our results demonstrated that the number of prior DMARDs and disease duration affect responses to adalimumab therapy in patients with established RA.
- Number of prior DMARDs appears to limit treatment response regardless of disease duration.

How might this impact on clinical practice or future developments?

- The use of multiple DMARDs prior to initiating therapy with tumour necrosis factor inhibitors (in this case, adalimumab) constitutes a poor prognostic factor and may also mediate the poor prognosis of longer disease duration.
- This should be taken into consideration for future clinical trial design when defining inclusion criteria, which currently limit patient access mostly by duration of disease but not by number of prior DMARDs.

who have failed methotrexate or TNFi therapy have much lower response rates than methotrexate-naïve patients,¹¹ although it is not clear if these differences are primarily related to having failed an increasing number of prior DMARD therapies or increasing disease duration.

A pooled analysis of 14 RA trials demonstrated that prior use of csDMARDs was associated with reduced likelihood of treatment response to a subsequent csDMARD independently of disease duration.¹² Similarly, the likelihood of achieving 28-joint Disease Activity Score (DAS28) response (reduction >1.2 points) increased as the number of prior biological therapies decreased (p=0.003).¹³ In line with this, a lower percentage of patients with ≥3 failed TNFi therapies achieved DAS28 remission compared with patients who failed

1–2 TNFi therapies in an abatacept study.¹⁴ However, it remains unknown if response to the first biologic DMARD, in particular a TNFi, depends on disease duration or prior numbers of failed csDMARDs.

To address this question, we assessed whether use of fewer prior csDMARDs, rather than disease duration, might be predictive of achievement of treatment response using data from a large, randomised, placebo-controlled clinical trial of adalimumab in patients with established RA who had active disease despite methotrexate. To confirm the findings, we analysed data from an additional smaller adalimumab trial.

PATIENTS AND METHODS

Study designs

This post hoc analysis included data from two trials, DE019 (NCT00195702) and ARMADA (conducted prior to trial registration requirement), of which the latter was used to confirm the results. The methods and primary results have been previously published for both trials.^{10 15} Briefly, both studies were randomised, placebo-controlled, double-blind clinical trials that evaluated the safety and efficacy of adalimumab versus placebo as an add-on therapy to background methotrexate in patients with established RA with active disease. Patients in DE019 were randomised (1:1:1) to receive 52 weeks of treatment with adalimumab 40 mg every other week (eow), adalimumab 20 mg every week (ew) or placebo ew+concomitant methotrexate ew.¹⁰ Patients in ARMADA were randomised to receive 24 weeks of adalimumab 20, 40 or 80 mg eow or placebo+concomitant methotrexate ew.¹⁵ Both studies were performed in accordance with the International Conference on Harmonisation Guidelines for Good Clinical Practice and the Declaration of Helsinki, and the study protocols were approved by ethics review boards of each study center. Written informed consent was obtained before the initiation of study procedures.

This analysis included only patients who received treatment with adalimumab 40 mg eow+methotrexate ew in the two trials. Data from other dosing regimen groups were excluded from this analysis because they are not in clinical use for RA. Patients had received prior csDMARDs (see online supplementary table S1); prior biological therapy was an exclusion criterion in both studies.

Outcomes

Treatment outcomes considered in this analysis included the following: American College of Rheumatology (ACR) response, defined as $\geq 20\%$ (ACR20), $\geq 50\%$ (ACR50) and $\geq 70\%$ (ACR70) improvement from baseline at week 24; mean DAS28 based on C-reactive protein (DAS28(CRP)); Simplified Disease Activity Index (SDAI); and Health Assessment Questionnaire Disability Index (HAQ-DI) at week 24. The mean changes from baseline to week 24 in DAS28(CRP), SDAI and HAQ-DI were also calculated; a reduction in each of these indices indicated improvement in disease activity.

The percentages of patients with HAQ-DI < 0.5 , DAS28(CRP) low disease activity (LDA, DAS28(CRP) ≤ 3.2) and SDAI LDA (SDAI ≤ 11) at week 24 were assessed in subgroups cross-tabulated for disease duration and number of prior DMARDs.

Statistical analysis

Patients were grouped according to the duration of RA, that is, time since diagnosis: ≤ 1 year, > 1 to 5 years, > 5 to 10 years and > 10 years for patients in DE019 and ≤ 5 years and > 5 to 10 years since the diagnosis of RA for patients in ARMADA.

Patients were also grouped according to the number of prior DMARDs received: methotrexate+0 or 1 prior DMARD, methotrexate+2 prior DMARDs and methotrexate+ > 2 prior DMARDs for patients in both trials. A separate sensitivity analysis was also conducted in the DE019 study for patient groups based on RA duration tertiles, where patients were divided into three equal-sized groups based on RA duration from shortest to longest.

The effect of RA duration and number of prior DMARDs was determined at week 24 for each treatment outcome in each subgroup. Associations between disease duration or extent of prior DMARD use variables and efficacy endpoints were modelled while controlling for the other variables using multivariate regression analysis. Logistic regression was used for dichotomous dependent variables, and linear regression was used for continuous dependent variables. Subgroups based on disease duration and number of prior DMARDs were assigned ordinal scores and treated as ordinal covariates. The estimate from the logistic model denotes the increase in the odds of ACR response per 1-DMARD category increase/1-duration category increase, while the estimate from the linear model denotes the increase in mean outcome value per 1-DMARD category increase/1-duration category increase. For regression models with mean changes from baseline in DAS28(CRP), SDAI or HAQ as the dependent variables, a positive regression coefficient indicates a smaller improvement.

RESULTS

Patient population

This analysis included 207 patients from DE019 and 67 patients from ARMADA who were treated with adalimumab 40 mg eow+methotrexate. In the DE019, RA duration was ≤ 1 year for 9 patients (4.3%), > 1 to 5 years for 62 patients (30.0%), > 5 to 10 years for 43 patients (20.8%) and > 10 years for 93 patients (44.9%). The mean numbers of prior DMARDs (including methotrexate) in these RA duration groups were 1.4, 2.0, 2.1 and 2.7, respectively (table 1). Of the 207 patients, 75 (36.2%), 62 (30.0%) and 70 patients (33.8%) had received methotrexate+0 or 1, 2 and > 2 prior DMARDs, respectively (table 1). All patients in the DE019 study had received prior csDMARDs; most common prior csDMARDs were methotrexate (all but one patient), hydroxychloroquine (45%) and sulfasalazine (26%; see online supplementary table S1).

In the cross-tabulation analysis, the highest percentage of patients had received > 2 prior DMARDs and had > 10 years of disease duration (19.8%) followed by those with two prior DMARDs and > 10 years of disease duration or 0–1 DMARDs and > 1 to 5 years of disease duration (both 14.0%; see online supplementary figure S1).

In ARMADA, the duration of RA was ≤ 5 years for 51 patients (76.1%) and > 5 to 10 years for 16 patients (23.9%). A total of 41 (61.2%), 13 (19.4%) and 13 patients (19.4%) had received methotrexate+0–1, 2 and > 2 prior DMARDs, respectively (table 2). Overall, 76% of patients in the ARMADA study had received prior csDMARDs; most common prior csDMARDs were gold and gold preparations (52%), sulfasalazine (33%) and methotrexate (24%; see online supplementary table S1). In the cross-tabulation analysis, the highest percentage of patients (50.7%) were in the methotrexate +0–1 prior DMARDs and ≤ 5 years of disease duration category (see online supplementary figure S1). Not surprisingly, as duration of disease increased, the number of prior DMARD treatments also tended to increase in both trials (tables 1 and 2).

Table 1 Baseline demographic and disease characteristics of patients receiving adalimumab+methotrexate in the DE019 study

Mean (SD)*	DE019 (N=207)						
	Disease duration				Prior DMARD treatment		
	≤1 year n=9	>1–5 years n=62	>5–10 years n=43	>10 years n=93	MTX+0–1 n=75	MTX+2 n=62	MTX+>2 n=70
Age, years	55.2 (18.0)	51.3 (15.7)	56.6 (12.3)	59.1 (11.1)	58.7 (2.8)	54.4 (14.7)	54.7 (12.9)
Sex, female, n (%)	5 (55.6)	48 (77.4)	33 (76.7)	72 (77.4)	58 (77.3)	50 (80.7)	50 (71.4)
RA duration, years	0.7 (0.2)	3.1 (1.3)	7.1 (1.3)	19.1 (8.0)	9.3 (10.4)	11.3 (9.3)	12.6 (7.5)
Prior DMARD treatments†	1.4 (0.5)	2.0 (1.2)	2.1 (1.3)	2.7 (1.6)	1.0 (0)	2.0 (0)	4.0 (1.1)
DAS28(CRP)	6.4 (1.1) n=8	5.6 (0.8) n=46	5.7 (0.9) n=29	5.8 (0.7) n=69	5.7 (0.9) n=54	5.8 (0.8) n=47	5.7 (0.8) n=51
SDAI	49.0 (17.2) n=8	38.5 (11.8) n=46	40.1 (13.1) n=29	41.6 (11.1) n=69	40.0 (12.1) n=54	41.9 (12.0) n=47	40.6 (12.5) n=51
HAQ-DI	1.6 (0.9) n=8	1.3 (0.7) n=46	1.3 (0.6) n=29	1.5 (0.6) n=69	1.4 (0.7) n=54	1.4 (0.6) n=47	1.4 (0.7) n=51

*Values are means (SD) unless specified otherwise.

†Including methotrexate.

DAS28(CRP), 28-joint Disease Activity Score based on C-reactive protein; DMARD, disease-modifying antirheumatic drug; HAQ-DI, Health Assessment Questionnaire Disability Index; MTX, methotrexate; RA, Rheumatoid arthritis; SDAI, Simplified Disease Activity Index.

Treatment outcomes

In the DE019 study, the proportion of patients with ACR20, ACR50 and ACR70 responses decreased linearly as the number of prior DMARDs increased (figure 1A). Although there was a general trend towards declining responsiveness with increases in disease duration, declines in ACR50 and ACR70 responses were primarily seen when comparing patients with a disease duration of >5 years versus ≤5 years.

The improvement from baseline in disease activity was highest among patients who had received methotrexate+0–1 prior DMARDs and numerically lowest among those who had previously received methotrexate+2 or more prior DMARDs (figure 2). In this context, it is noteworthy that baseline disease activity in the DE019 trial did not differ much between groups. Importantly, disease duration did not have an impact on improvement from baseline to week 24 in disease activity by DAS28(CRP) or SDAI. When assessed for physical function, the improvement in HAQ-DI from baseline to week 24 decreased with increasing number of DMARDs and disease duration (figure 2). Furthermore, mean disease activity (DAS28(CRP) and SDAI) and mean absolute HAQ-DI at week 24 showed a numerical increase with increasing numbers of prior DMARDs. Results were more varied with longer disease duration (see online supplementary figure S2A).

In the DE019 study cross-tabulation analysis, higher percentages of patients with fewer prior DMARDs and shorter disease

duration achieved ACR20, ACR50 and ACR70 responses compared with patients with higher numbers of prior DMARDs and/or longer disease duration (figure 3). This was also observed for achievement of DAS28(CRP) LDA, SDAI LDA and HAQ-DI <0.5 (figure 4).

These results were generally confirmed by the ARMADA trial; lower ACR20, ACR50 and ACR70 response rates at week 24 were observed among patients with >2 prior DMARDs+methotrexate versus patients with ≤2 prior DMARDs+methotrexate (figure 1B). Similar to observations in DE019, mean DAS28(CRP), SDAI and HAQ-DI at week 24 were higher in patients with higher number of prior DMARDs (see online supplementary figure S2B). Disease duration had no apparent impact on achievement of ACR responses in ARMADA (figure 1B) or mean disease activity or HAQ-DI at week 24 (see online supplementary figure S2B).

In the ARMADA cross-tabulation analysis, higher percentages of patients with fewer prior DMARDs, regardless of disease duration, generally achieved ACR20, ACR50 and ACR70 responses compared with patients with higher number of prior DMARDs (see online supplementary figure S3). Similar results were observed with achievement of DAS28(CRP) LDA, SDAI LDA and HAQ-DI <0.5 (see online supplementary figure S4).

Regression analysis

The multivariate regression analysis of DE019 showed that a greater number of prior DMARDs or longer disease duration

Table 2 Baseline demographic and disease characteristics of patients receiving adalimumab+methotrexate in the ARMADA study

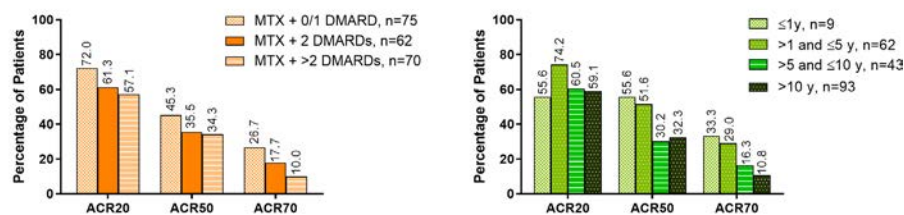
Mean (SD)*	ARMADA (N=67)				
	Disease duration		Prior DMARD treatment		
	≤5 years n=51	>5–10 years n=16	MTX+0–1 n=41	MTX+2 n=13	MTX+>2 n=13
Age, years	55.2 (10.4)	61.3 (13.6)	55.5 (10.0)	61.4 (14.6)	55.6 (12.0)
Sex, female, n (%)	38 (74.5)	12 (75.0)	32 (78.0)	10 (76.9)	8 (61.5)
RA duration, years	3.6 (1.2)	6.0 (0.0)	3.9 (1.4)	4.2 (1.7)	4.9 (1.2)
Prior DMARD treatments†	1.3 (1.2)	2.1 (1.5)	0.6 (0.5)	2.0 (0.0)	3.6 (1.0)
DAS28(CRP)	5.7 (0.8)	5.5 (0.9)	5.8 (0.7)	5.4 (0.9)	5.5 (0.8)
SDAI	40.1 (10.6)	37.4 (11.2)	41.5 (10.8)	36.8 (10.4)	35.7 (10.1)
HAQ-DI	1.5 (0.6)	1.6 (0.7)	1.5 (0.5)	1.3 (0.7)	2.0 (0.4)

*Values are means (SD) unless specified otherwise.

†Including methotrexate.

DAS28(CRP), 28-joint Disease Activity Score based on C-reactive protein; DMARD, disease-modifying antirheumatic drug; HAQ-DI, Health Assessment Questionnaire Disability Index; MTX, methotrexate; RA, rheumatoid arthritis; SDAI, Simplified Disease Activity Index.

A. DE019



B. ARMADA

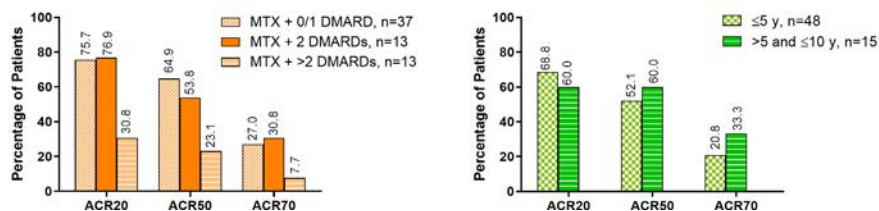


Figure 1 Percentage of patients with ACR20/50/70 response in subgroups based on prior exposure to DMARDs or prior disease duration in (A) DE019 and (B) ARMADA at week 24. ACR, American College of Rheumatology; DMARD, disease-modifying antirheumatic drug; MTX, methotrexate.

was associated with decreased odds of achieving ACR outcome criteria at week 24 with significantly decreased odds for achieving ACR70 (both with greater number of prior DMARDs or longer disease duration) and ACR50 (with longer disease duration only; online supplementary table S2). Longer disease duration was also associated with significantly smaller improvement from baseline to week 24 in HAQ-DI ($p < 0.05$; online supplementary table S2). No significant association was observed in the other disease activity measures or change in disease activity from baseline analyses.

Disease duration tertile sensitivity analysis

In the RA duration tertile analysis, 69 patients were allocated to each of the groups. The mean \pm SD RA duration was 2.8 ± 1.4 years in the first tertile, 8.6 ± 2.5 in the second tertile and 21.7 ± 7.7 in the third tertile (see online supplementary table S3). Patients in the third tertile were more likely to be older, to be women and to have used more DMARDs prior to study entry than patients in the first or second tertile. Disease activity and HAQ-DI were similar between the groups at baseline.

The proportions of patients with ACR responses were lower in the second and third tertiles versus the first tertile (see online supplementary figure S5). Similarly, patients in the first tertile had lower HAQ-DI at week 24 and greater improvement from baseline to week 24 in HAQ-DI versus the second and third tertiles. However, disease activity and changes in disease activity from baseline to week 24 were generally similar between the tertiles. Thus, the lack of association between disease duration and change in disease activity by SDAI or DAS28(CRP) was also seen when disease duration was categorised by tertiles rather than fixed cut-off points.

DISCUSSION

The results of this retrospective analysis of DE019, a large, randomised, double-blind multicentre clinical trial, showed that after 24 weeks of treatment, progressively lower proportions of patients achieved improvement of disease activity as the number of prior DMARDs increased. This was observed for the categorical ACR response rates as well as in reduction of continuous composite disease activity measures DAS28(CRP) and SDAI. Although a similar trend was observed with increasing disease duration, the results were more variable, suggesting that

number of prior DMARDs may have an independent effect on disease outcomes. These results were generally confirmed in the smaller ARMADA trial. The most marked differences were observed between patients who had received methotrexate + >2 prior DMARDs as compared with methotrexate with 0–1 prior DMARDs.

We have previously demonstrated that HAQ improvement decreases with increasing disease duration.^{16 17} In our current analysis, the change in HAQ-DI from baseline to week 24 decreased with greater number of prior DMARDs and increasing disease duration. Furthermore, longer disease duration was associated with a significantly smaller improvement from baseline in HAQ-DI, and attainment of HAQ-DI < 0.5 was also less frequent in those who had the most courses of prior DMARDs or longer disease duration based on the cross-tabulation analysis. This is in line with previous studies that showed that physical function has an activity-related and a damage-related component and with increasing damage (which accrues with increasing disease duration), improvement of HAQ-DI becomes more difficult.^{16 17}

Although we noticed the expected trend for increased number of DMARDs (from 1.4 to 2.7) with increasing disease duration (from < 1 year to > 10 years), disease duration did not differ much with increasing number of prior DMARDs (range from 9.3 years to 12.6 years). This contrasts with reported findings of longer disease duration associated with increased number of prior DMARDs in a previous study.¹⁸ The same study also demonstrated that longer disease duration and prior use of biologic DMARDs (TNFi), but not csDMARDs, was associated with significantly reduced likelihood of achieving sustained remission.¹⁸ Association between higher number of prior DMARDs and reduced likelihood of achieving treatment response has been demonstrated in a few other RA studies,^{14 19 20} including two certolizumab pegol studies.^{13 21} In our study, a greater number of prior DMARDs and longer disease duration were associated with significantly decreased odds of achieving improvement as measured by ACR response. This relationship for improvement in disease activity was also observed in the cross-tabulation analysis in the DE019 study but not in the ARMADA study, which demonstrated better disease outcomes with lower number of prior DMARDs irrespective of disease duration. Although a direct relationship between increasing disease duration and higher number of prior DMARDs to disease activity seems likely,

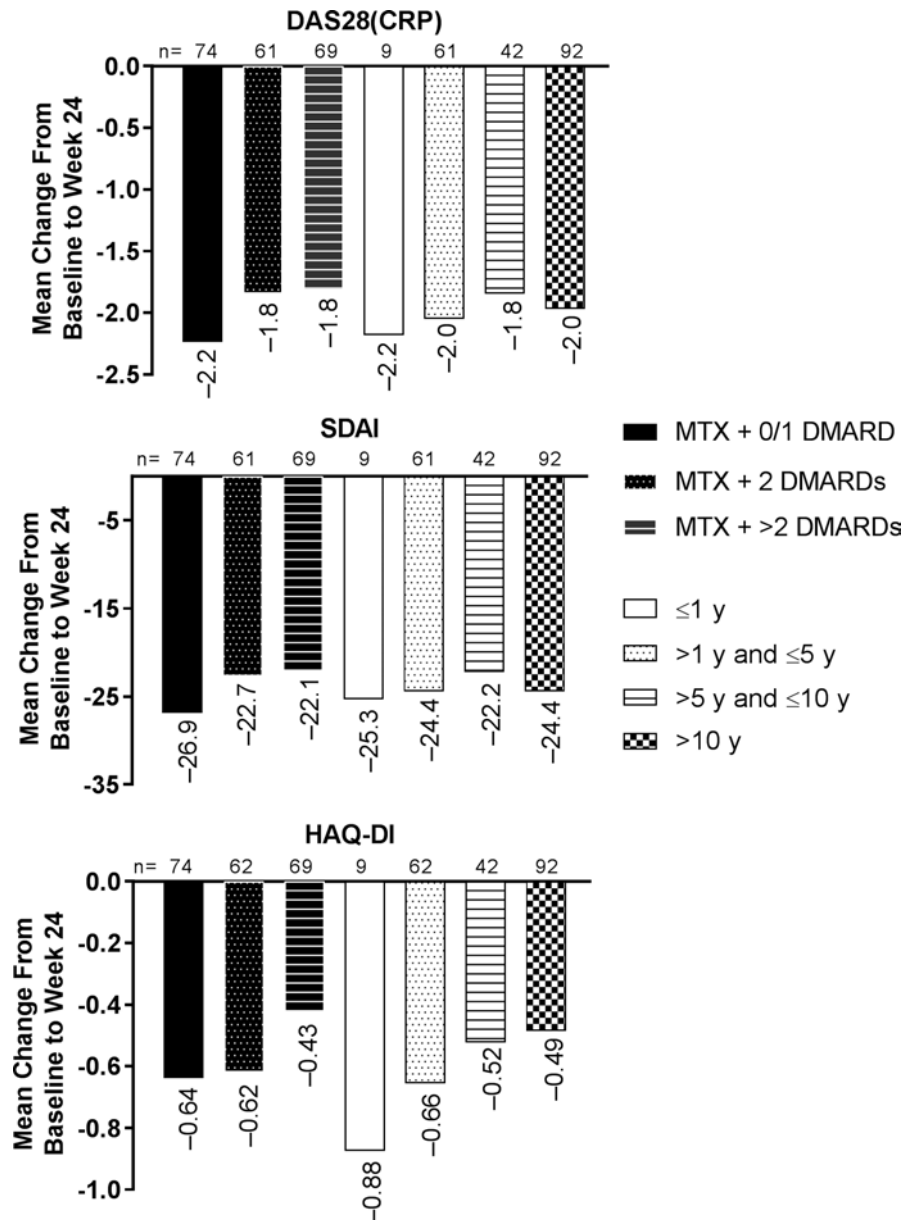


Figure 2 Change from baseline to week 24 in mean DAS28(CRP), SDAI and HAQ-DI in subgroups based on prior exposure to DMARDs or prior disease duration in DE019. DAS28(CRP), 28-joint Disease Activity Score based on C-reactive protein; DMARD, disease-modifying antirheumatic drug; HAQ-DI, Health Assessment Questionnaire Disability Index; MTX, methotrexate; SDAI, Simplified Disease Activity Index.

there also might be different mechanisms contributing to the effect. Thus, the current findings add to previous observations that a decreasing responsiveness is due to having failed more therapies¹³ rather than having longer disease duration, although there is an obvious overlap between these two. For example, more cycles of failing DMARDs might select a phenotype that is resistant to a new treatment because different pathogenetic pathways may have become ‘imprinted’.^{22,23} To this end, our analysis demonstrated that in patients with established RA, the number of prior DMARDs had an impact on disease outcomes, specifically changes in disease activity.

Overall, our results suggest that long delays and/or the use of multiple DMARDs prior to initiating therapy with a TNFi (in this case, adalimumab) may actually reduce the potential magnitude of the response to the TNFi. However, it must be noted that the present analyses only evaluated studies in which patients had been treated with prior csDMARD for prolonged periods of time rather than using them for only short term if a

low disease activity was not achieved.²⁴ Therefore, these findings pertain to these specific situations, and the impact of the prior number of csDMARDs may be different in studies that switched csDMARDs rapidly before introduction of biologic DMARDs.²⁵ Importantly, the European League Against Rheumatism has declared the failure of two csDMARDs as a poor prognostic marker,²⁶ which is generally in line with the present findings as well as other observations.²⁷ Thus, patients who do not respond to methotrexate therapy initiated early after a diagnosis of RA appear to benefit most from addition of adalimumab.²⁸ These analyses demonstrate the benefits of early therapeutic intervention and underscore the need for more standardised treatment guidelines for early RA, particularly in socioeconomic regions lacking rheumatologists, where patients are often managed or monitored by general practitioners or allied health workers. Furthermore, these findings should be considered in future trials when defining inclusion criteria not only by duration of disease but also by number of prior DMARDs.

Prior DMARDs	Disease duration			
	≤1 y (n=9)	>1–5 y (n=62)	>5–10 y (n=43)	>10 y (n=93)
ACR20				
MTX + 0/1 (n=75)	4/5 (80.0)	24/29 (82.8)	12/18 (66.7)	14/23 (60.9)
MTX + 2 (n=62)	1/4 (25.0)	13/19 (68.4)	7/10 (70.0)	17/29 (58.6)
MTX + >2 (n=70)	NA	9/14 (64.3)	7/15 (46.7)	24/41 (58.5)
ACR50				
MTX + 0/1 (n=75)	4/5 (80.0)	17/29 (58.6)	6/18 (33.3)	7/23 (30.4)
MTX + 2 (n=62)	1/4 (25.0)	9/19 (47.4)	2/10 (20.0)	10/29 (34.5)
MTX + >2 (n=70)	NA	6/14 (42.9)	5/15 (33.3)	13/41 (31.7)
ACR70				
MTX + 0/1 (n=75)	3/5 (60.0)	8/29 (27.6)	5/18 (27.8)	4/23 (17.4)
MTX + 2 (n=62)	0/4	6/19 (31.6)	1/10 (10.0)	4/29 (13.8)
MTX + >2 (n=70)	NA	4/14 (28.6)	1/15 (6.7)	2/41 (4.9)

■ ≥70%
 ■ ≥40% – <70%
 ■ ≥20% – <40%
 ■ <20%

Figure 3 Patients achieving ACR20, ACR50 and ACR70 responses in each disease duration and prior DMARD category at week 24 in the DE019 study. ACR, American College of Rheumatology; DMARD, disease-modifying antirheumatic drug; MTX, methotrexate; NA, not applicable.

This analysis has certain limitations, including its post hoc nature and restriction to adalimumab data; however, differences between TNFis are not expected.²⁹ The number of patients included in some prior treatment or disease duration stratum was small; thus, the analysis lacks sufficient statistical power to detect small but potentially statistically significant relationships between some prior treatment or treatment duration subgroups and treatment outcome. Although generally similar observations were made in the ARMADA trial, the confirmation of the results was limited by several factors, particularly the much smaller patient numbers, which did not provide sufficient power to confirm all analyses, and differences in maximum disease durations and standards of care.

In conclusion, the number of prior DMARDs and disease duration affect response to therapy in patients with established RA, although the effect of the number of prior DMARDs on

improvement in disease activity appears to be relevant regardless of disease duration. These results support recommendations that combination therapy with a biologic agent and methotrexate be initiated without delay in patients who do not have a satisfactory response to treatment with methotrexate alone.

Contributors AbbVie sponsored the studies, contributed to their design, and participated in the collection, analysis and interpretation of the data, and in the writing, reviewing and approval of the final version. Medical writing was provided by Blair Jarvis, MSc, ELS, and Maria Hovenden, PhD, of Complete Publication Solutions, LLC (North Wales, PA, USA) and was funded by AbbVie. This manuscript was based on work previously presented at the 2015 Annual Congress of the American College of Rheumatology and published as a conference abstract.

Funding This study was funded by AbbVie.

Competing interests DA has received grants and consulting fees from AbbVie, Janssen, Pfizer, and Roche and consulting fees from Amgen, Celgene, Eli Lilly, Merck, Novartis, Sandoz, Sanofi/Genzyme, and UCB. S-HP has nothing to disclose. DN has served on an advisory board for AbbVie and has clinical trial agreements

Prior DMARDs	Disease duration			
	≤1 y (n=9)	>1–5 y (n=62)	>5–10 y (n=43)	>10 y (n=93)
DAS28(CRP) LDA				
MTX + 0/1 (n=75)	2/5 (40.0)	14/29 (48.3)	7/18 (38.9)	7/23 (30.4)
MTX + 2 (n=62)	1/4 (25.0)	8/19 (42.1)	2/10 (20.0)	5/29 (17.2)
MTX + >2 (n=70)	NA	5/14 (35.7)	3/15 (20.0)	9/41 (22.0)
SDAI LDA				
MTX + 0/1 (n=75)	3/5 (60.0)	14/29 (48.3)	7/18 (38.9)	9/23 (39.1)
MTX + 2 (n=62)	1/4 (25.0)	8/19 (47.4)	2/10 (20.0)	8/29 (27.6)
MTX + >2 (n=70)	NA	6/14 (42.9)	3/15 (20.0)	11/41 (26.8)
HAQ-DI <0.5				
MTX + 0/1 (n=75)	3/5 (60.0)	12/29 (41.4)	7/18 (38.9)	3/23 (13.0)
MTX + 2 (n=62)	1/4 (25.0)	8/19 (42.1)	1/10 (10.0)	9/29 (31.0)
MTX + >2 (n=70)	NA	6/14 (42.9)	4/15 (26.7)	5/41 (12.2)

■ ≥70%
 ■ ≥40% – <70%
 ■ ≥20% – <40%
 ■ <20%

Figure 4 Patients achieving DAS28(CRP) LDA, SDAI LDA and HAQ-DI <0.5 responses in each disease duration and prior DMARD category at week 24 in the DE019. DAS28(CRP), 28-joint Disease Activity Score based on C-reactive protein; DMARD, disease-modifying antirheumatic drug; HAQ-DI, Health Assessment Questionnaire Disability Index; LDA, low disease activity; MTX, methotrexate; NA, not applicable; SDAI, Simplified Disease Activity Index.

with AbbVie, Bristol-Myers Squibb, Celgene, Eli Lilly, Gilead, Janssen-Cilag, Novartis, Pfizer, Regeneron, Sanofi-Aventis, UCB, and Zynherba. SC and SF are employees of AbbVie and may own stock/options. JM and DF are former employees of AbbVie and may own stock/options. JS has received grants and consulting fees from AbbVie Inc, AstraZeneca, Janssen, Lilly, Merck Sharpe & Dohme, Pfizer, and Roche and consulting fees from Amgen, Astro, Bristol-Myers Squibb, Celgene, Celltrion, Chugai, Gilead, Glaxo, ILTOO Pharma, Novartis-Sandoz, Samsung, Sanofi, and UCB.

Patient consent for publication Obtained.

Ethics approval Both studies were performed in accordance with the International Conference on Harmonisation Guidelines for Good Clinical Practice and the Declaration of Helsinki, and the study protocols were approved by ethics review boards of each study centre.

Provenance and peer review Not commissioned; externally peer reviewed.

Data availability statement AbbVie is committed to responsible data sharing regarding the clinical trials we sponsor. This includes access to anonymized, individual and trial-level data (analysis data sets), as well as other information (e.g., protocols and Clinical Study Reports), as long as the trials are not part of an ongoing or planned regulatory submission. This includes requests for clinical trial data for unlicensed products and indications. This clinical trial data can be requested by any qualified researchers who engage in rigorous, independent scientific research, and will be provided following review and approval of a research proposal and Statistical Analysis Plan (SAP) and execution of a Data Sharing Agreement (DSA). Data requests can be submitted at any time and the data will be accessible for 12 months, with possible extensions considered. For more information on the process, or to submit a request, visit the following link: <https://www.abbvie.com/our-science/clinical-trials/clinical-trials-data-and-information-sharing/data-and-information-sharing-with-qualified-researchers.html>.

Open access This is an open access article distributed in accordance with the Creative Commons Attribution Non Commercial (CC BY-NC 4.0) license, which permits others to distribute, remix, adapt, build upon this work non-commercially, and license their derivative works on different terms, provided the original work is properly cited, appropriate credit is given, any changes made indicated, and the use is non-commercial. See: <http://creativecommons.org/licenses/by-nc/4.0/>.

REFERENCES

- Molina E, Del Rincon I, Restrepo JF, et al. Association of socioeconomic status with treatment delays, disease activity, joint damage, and disability in rheumatoid arthritis. *Arthritis Care Res* 2015;67:940–6.
- van der Heide A, Jacobs JW, Bijlsma JW, et al. The effectiveness of early treatment with “second-line” antirheumatic drugs. A randomized, controlled trial. *Ann Intern Med* 1996;124:699–707.
- Lard LR, Visser H, Speyer I, et al. Early versus delayed treatment in patients with recent-onset rheumatoid arthritis: comparison of two cohorts who received different treatment strategies. *Am J Med* 2001;111:446–51.
- Gremese E, Salaffi F, Bosello SL, et al. Very early rheumatoid arthritis as a predictor of remission: a multicentre real life prospective study. *Ann Rheum Dis* 2013;72:858–62.
- Nell VP, Machold KP, Eberl G, et al. Benefit of very early referral and very early therapy with disease-modifying anti-rheumatic drugs in patients with early rheumatoid arthritis. *Rheumatology* 2004;43:906–14.
- Emery P, Kvien TK, Combe B, et al. Combination etanercept and methotrexate provides better disease control in very early (<=4 months) versus early rheumatoid arthritis (>4 months and <2 years): post hoc analyses from the COMET study. *Ann Rheum Dis* 2012;71:989–92.
- Detert J, Bastian H, Listing J, et al. Induction therapy with adalimumab plus methotrexate for 24 weeks followed by methotrexate monotherapy up to week 48 versus methotrexate therapy alone for DMARD-naïve patients with early rheumatoid arthritis: HIT HARD, an investigator-initiated study. *Ann Rheum Dis* 2013;72:844–50.
- Breedveld FC, Weisman MH, Kavanaugh AF, et al. The PREMIER study: a multicenter, randomized, double-blind clinical trial of combination therapy with adalimumab plus methotrexate versus methotrexate alone or adalimumab alone in patients with early, aggressive rheumatoid arthritis who had not had previous methotrexate treatment. *Arthritis Rheum* 2006;54:26–37.
- Smolen J, Collier D, Szumski A, et al. Effect of disease duration on clinical outcomes in moderate rheumatoid arthritis patients treated with etanercept plus methotrexate in the Preserve study. *Arthritis Rheumatol* 2014;66.
- Keystone EC, Kavanaugh AF, Sharp JT, et al. Radiographic, clinical, and functional outcomes of treatment with adalimumab (a human anti-tumor necrosis factor monoclonal antibody) in patients with active rheumatoid arthritis receiving concomitant methotrexate therapy: a randomized, placebo-controlled, 52-week trial. *Arthritis Rheum* 2004;50:1400–11.
- Smolen JS, Aletaha D, McInnes IB. Rheumatoid arthritis. *Lancet* 2016;388:2023–38.
- Anderson JJ, Wells G, Verhoeven AC, et al. Factors predicting response to treatment in rheumatoid arthritis: the importance of disease duration. *Arthritis Rheum* 2000;43:22–9.
- Soriano ER, Dellepiane A, Salvatierra G, et al. Certolizumab pegol in a heterogeneous population of patients with moderate-to-severe rheumatoid arthritis. *Future Sci OA* 2018;4.
- Schiff M, Zhou X, Kelly S, et al. FRI0160 efficacy of abatacept in RA patients with an inadequate response to anti-TNF therapy regardless of reason for failure, or type or number of prior anti-TNF therapy used. *Ann Rheum Dis* 2008;67(Suppl 2).
- Weinblatt ME, Keystone EC, Furst DE, et al. Adalimumab, a fully human anti-tumor necrosis factor alpha monoclonal antibody, for the treatment of rheumatoid arthritis in patients taking concomitant methotrexate: the ARMADA trial. *Arthritis Rheum* 2003;48:35–45.
- Aletaha D, Ward MM. Duration of rheumatoid arthritis influences the degree of functional improvement in clinical trials. *Ann Rheum Dis* 2006;65:227–33.
- Aletaha D, Strand V, Smolen JS, et al. Treatment-related improvement in physical function varies with duration of rheumatoid arthritis: a pooled analysis of clinical trial results. *Ann Rheum Dis* 2008;67:238–43.
- Furst DE, Pangan AL, Harrold LR, et al. Greater likelihood of remission in rheumatoid arthritis patients treated earlier in the disease course: results from the Consortium of Rheumatology Researchers of North America registry. *Arthritis Care Res* 2011;63:856–64.
- Andersson ML, Bergman S, Söderlin MK. The effect of socioeconomic class and immigrant status on disease activity in rheumatoid arthritis: data from BARFOT, a multi-centre study of early RA. *Open Rheumatol J* 2013;7:105–11.
- Narváez J, Magallares B, Díaz Torné C, et al. Predictive factors for induction of remission in patients with active rheumatoid arthritis treated with tocilizumab in clinical practice. *Semin Arthritis Rheum* 2016;45:386–90.
- Torrente-Segarra V, Urruticoechea Arana A, Sánchez-Andrade Fernández A, et al. RENACER study: assessment of 12-month efficacy and safety of 168 certolizumab PEG (PEGol) rheumatoid arthritis-treated patients from a Spanish multicenter national database. *Mod Rheumatol* 2016;26:336–41.
- van Nies JAB, Tsonaka R, Gaujoux-Viala C, et al. Evaluating relationships between symptom duration and persistence of rheumatoid arthritis: does a window of opportunity exist? Results on the Leiden early arthritis clinic and ESPOIR cohorts. *Ann Rheum Dis* 2015;74:806–12.
- Morgan C, Lunt M, Brightwell H, et al. Contribution of patient related differences to multidrug resistance in rheumatoid arthritis. *Ann Rheum Dis* 2003;62:15–19.
- Smolen JS, Aletaha D. Forget personalised medicine and focus on abating disease activity. *Ann Rheum Dis* 2013;72:3–6.
- Goekoop-Ruiterman YPM, de Vries-Bouwstra JK, Allaart CF, et al. Clinical and radiographic outcomes of four different treatment strategies in patients with early rheumatoid arthritis (the BeSt study): a randomized, controlled trial. *Arthritis Rheum* 2005;52:3381–90.
- Smolen JS, Landewé R, Bijlsma J, et al. EULAR recommendations for the management of rheumatoid arthritis with synthetic and biological disease-modifying antirheumatic drugs: 2016 update. *Ann Rheum Dis* 2017;76:960–77.
- Kiely P, Walsh D, Williams R, et al. Outcome in rheumatoid arthritis patients with continued conventional therapy for moderate disease activity—the early RA network (ERAN). *Rheumatology* 2011;50:926–31.
- Lau CS, Chia F, Harrison A, et al. APLAR rheumatoid arthritis treatment recommendations. *Int J Rheum Dis* 2015;18:685–713.
- Smolen JS, Burmester G-R, Combe B, et al. Head-to-head comparison of certolizumab pegol versus adalimumab in rheumatoid arthritis: 2-year efficacy and safety results from the randomised EXXELERATE study. *Lancet* 2016;388:2763–74.

CLINICAL SCIENCE

On the presence of HLA-SE alleles and ACPA-IgG variable domain glycosylation in the phase preceding the development of rheumatoid arthritis

Theresa Kissel ¹, Karin Anna van Schie,¹ Lise Hafkenscheid,¹ Anders Lundquist,² Heidi Kokkonen,³ Manfred Wuhrer,⁴ Tom WJ Huizinga,¹ Hans Ulrich Scherer,¹ René Toes ¹, Solbritt Rantapää-Dahlqvist ³

Handling editor Prof Josef S Smolen

► Additional material is published online only. To view please visit the journal online (<http://dx.doi.org/10.1136/annrheumdis-2019-215698>).

¹Rheumatology, Leiden University Medical Center, Leiden, The Netherlands
²Department of Statistics, Umeå University, Umeå, Sweden
³Department of Public Health and Clinical Medicine/ Rheumatology, Umeå University, Umeå, Sweden
⁴Center for Proteomics and Metabolomics, Leiden University Medical Center, Leiden, The Netherlands

Correspondence to

Theresa Kissel, Rheumatology, Leiden University Medical Center, Leiden 2300 RC, The Netherlands; T.kissel@lumc.nl

Received 10 May 2019
 Revised 16 August 2019
 Accepted 17 August 2019
 Published Online First
 30 August 2019



© Author(s) (or their employer(s)) 2019. No commercial re-use. See rights and permissions. Published by BMJ.

To cite: Kissel T, van Schie KA, Hafkenscheid L, et al. *Ann Rheum Dis* 2019;**78**:1616–1620.

ABSTRACT

Objective Anti-citrullinated protein antibodies (ACPA) in rheumatoid arthritis (RA) patients display a unique feature defined by the abundant presence of *N*-linked glycans within the variable domains (V-domains). Recently, we showed that *N*-glycosylation sites, which are required for the incorporation of V-domain glycans, are introduced following somatic hypermutation. However, it is currently unclear when V-domain glycosylation occurs. Further, it is unknown which factors might trigger the generation of V-domain glycans and whether such glycans are relevant for the transition towards RA. Here, we determined the presence of ACPA-IgG V-domain glycans in paired samples of pre-symptomatic individuals and RA patients.

Methods ACPA-IgG V-domain glycosylation was analysed using ultra-high performance liquid chromatography (UHPLC) in paired samples of pre-symptomatic individuals (median interquartile range (IQR) pre-dating time: 5.8 (5.9) years; n=201; 139 ACPA-positive and 62 ACPA-negative) and RA patients (n=99; 94 ACPA-positive and 5 ACPA-negative).

Results V-domain glycans on ACPA-IgG were already present up to 15 years before disease in pre-symptomatic individuals and their abundance increased closer to symptom onset. Noteworthy, human leucocyte antigen class II shared epitope (HLA-SE) alleles associated with the presence of V-domain glycans on ACPA-IgG.

Conclusion Our observations indicate that somatic hypermutation of ACPA, which results in the incorporation of *N*-linked glycosylation sites and consequently V-domain glycans, occurs already years before symptom onset in individuals that will develop RA later in life. Moreover, our findings provide first evidence that HLA-SE alleles associate with ACPA-IgG V-domain glycosylation in the pre-disease phase and thereby further refine the connection between HLA-SE and the development of ACPA-positive RA.

INTRODUCTION

Rheumatoid arthritis (RA) is hallmarked by the presence of autoantibodies, such as rheumatoid factor (RF) and anti-citrullinated protein antibodies (ACPA).^{1–3} Several genetic risk factors such as the human leucocyte antigen class II shared epitope (HLA-SE) alleles are associated with ACPA-positive RA. Noteworthy, an association with HLA-SE can only be found in ACPA-positive disease and is

Key messages

What is already known about this subject?

► IgG anti-citrullinated protein antibodies (ACPA) are abundantly *N*-glycosylated within their variable domains (V-domains).

What does this study add?

► ACPA-IgG V-domain glycosylation is already extensively present in pre-symptomatic individuals who developed rheumatoid arthritis later in life.
 ► ACPA-IgG V-domain glycosylation increases closer to symptom onset and associates with anti-CCP2 antibody levels pre-disease.
 ► Human leucocyte antigen class II shared epitope alleles (HLA-SE) associate with V-domain glycosylation and therefore predispose to the formation of *N*-linked glycosylation-sites in ACPA-IgG pre-disease.

mostly lost in ACPA-positive healthy individuals, indicating that HLA-SE-restricted T-helper cell activity is likely involved in the development of ACPA-positive disease and not the initial induction of auto-immunity. Presumably, these T-cells provide help to ACPA-expressing B-cells that have been activated in an earlier phase.^{4,5} ACPA-IgG are glycoproteins that harbour, like all IgG, *N*-linked glycans in the Fc-region located at Asn²⁹⁷.⁶ Remarkably, approximately 90% of ACPA-IgG molecules in sera from RA patients are also abundantly glycosylated within their variable domain (V-domain).⁷ Structural composition analysis revealed that these V-domain glycans are mostly biantennary complex-type glycans carrying sialic acids.^{7,8} To undergo *N*-linked glycosylation, a consensus sequence in the protein backbone is required (N-X-S/T, where X≠P).⁹ Previously, we have shown that *N*-linked glycosylation sites in ACPA-IgG V-domains are introduced during somatic hypermutation.¹⁰ Furthermore, in a cross-sectional study of indigenous North American individuals, we observed that ACPA-IgG V-domain glycosylation is largely absent in ACPA-positive subjects that did not transit to RA, while *N*-linked glycans were found on ACPA-positive healthy subjects that later developed RA.¹¹

On the basis of these and other observations, we hypothesise that V-domain glycosylation conveys a selective advantage to ACPA-expressing B-cells, which potentially plays a pivotal role in disease development.^{10 12} To investigate and understand the presence and acquisition of ACPA V-domain glycans in the phase preceding arthritis in more depth, we now aimed to analyse the presence of V-domain glycans on ACPA-IgG in paired samples of pre-symptomatic individuals and RA patients.

MATERIALS AND METHODS

Patient and public involvement

Patients were involved in this study by donating blood at the Medical Biobank of Northern Sweden, when attending population surveys.

Study cohort

Individuals, diagnosed with RA later in life, were sampled prior to symptom onset (median (IQR) pre-dating time: 5.8 (5.9) years; n=201; 139 ACPA-positive and 62 ACPA-negative) and after diagnosis of RA (n=99, 94 ACPA-positive and 5 ACPA-negative as specificity control). Further, randomly selected control samples (n=43, 3 ACPA-positive and 40 ACPA-negative) were included. The RA patients fulfilled the 1987 American Rheumatism Association (ARA) classification criteria.¹³ Descriptive cohort information is presented in online supplementary table 1.

ACPA-IgG isolation and V-domain glycan analysis

Experimental procedures for ACPA-IgG isolation, glycan release, labelling, UHPLC analysis as well as data processing and analysis are described in detail in the online supplementary materials and methods. Percentage ACPA-IgG V-domain glycosylation

was calculated based on the following formula: $((GP19+GP23+GP24)/(GP4+GP8+GP14)) \times 100$.^{11 14}

RESULTS

ACPA-IgG V-domain glycan profiles were detected in ACPA-positive pre-symptomatic individuals and RA patients

We analysed individuals who were sampled before symptom onset, after diagnosis of RA and randomly selected ACPA-positive and ACPA-negative control samples from the same population. Chromatographic glycosylation peaks (figure 1A) could be observed for captured ACPA-IgG of 94 out of 201 pre-symptomatic individuals (89 ACPA-positive), 80 out of 99 RA patients (78 ACPA-positive) and 2 out of 43 control samples (1 ACPA-positive and 1 with an anti-CCP2 antibody level <25 AU/mL). The results obtained strengthen the reliability of the method used, as from the samples displaying glycan profiles only 8 (4.5%) were derived from ACPA-negative individuals (anti-CCP2 antibody level below 25 AU/mL) compared with 168 glycan profiles (>95%) derived from samples obtained from ACPA-positive individuals (online supplementary table 2 and online supplementary figure 1). Of note, in 68 ACPA-positive samples (40.5%) no glycan profiles, including Fc-glycans (positive control), could be detected, indicating a limitation of assay sensitivity.

ACPA-IgG V-domain glycosylation rises towards symptom onset and is already present years before

To address the question when V-domain glycosylation first appears, matched paired individuals were sampled before symptom onset (between -15 and -0.5 years) as well as after diagnosis of RA (between +0.5 and +3 years) and analysed for ACPA-IgG V-domain glycosylation (figure 1A).⁷ The data

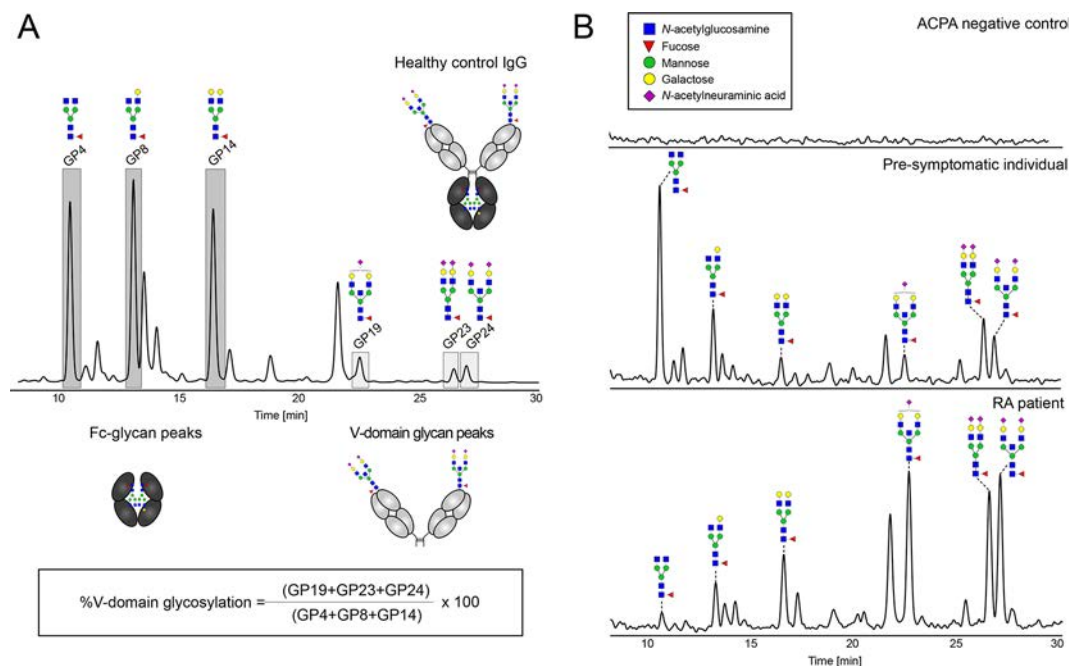


Figure 1 Representative UHPLC spectra of released *N*-glycans. (A) UHPLC chromatogram of healthy control IgG after IgG capturing and schematic representation of Fc-domain and variable domain (V-domain) derived glycosylation peaks. The six chromatographic peaks (alignment based on Pucic *et al*¹⁶) used for the calculation of %V-domain glycosylation are highlighted and the formula is visualised. (B) UHPLC spectra of released *N*-glycans after ACPA-IgG capturing from ACPA-IgG negative control sample (no detectable glycan peaks), ACPA-IgG positive pre-symptomatic individual (V-domain glycosylation of 55%) and ACPA-IgG positive rheumatoid arthritis sample (V-domain glycosylation of 324%). Assigned are the GP4, GP8, GP14, GP19, GP23 and GP24 chromatographic peaks of the IgG glycome based on literature.^{7 8} Blue square: *N*-acetylglucosamine, green circle: mannose, yellow circle: galactose, red triangle: fucose, pink diamond: α 2,6-linked *N*-acetylneuraminic acid. ACPA, anti-citrullinated protein antibodies.

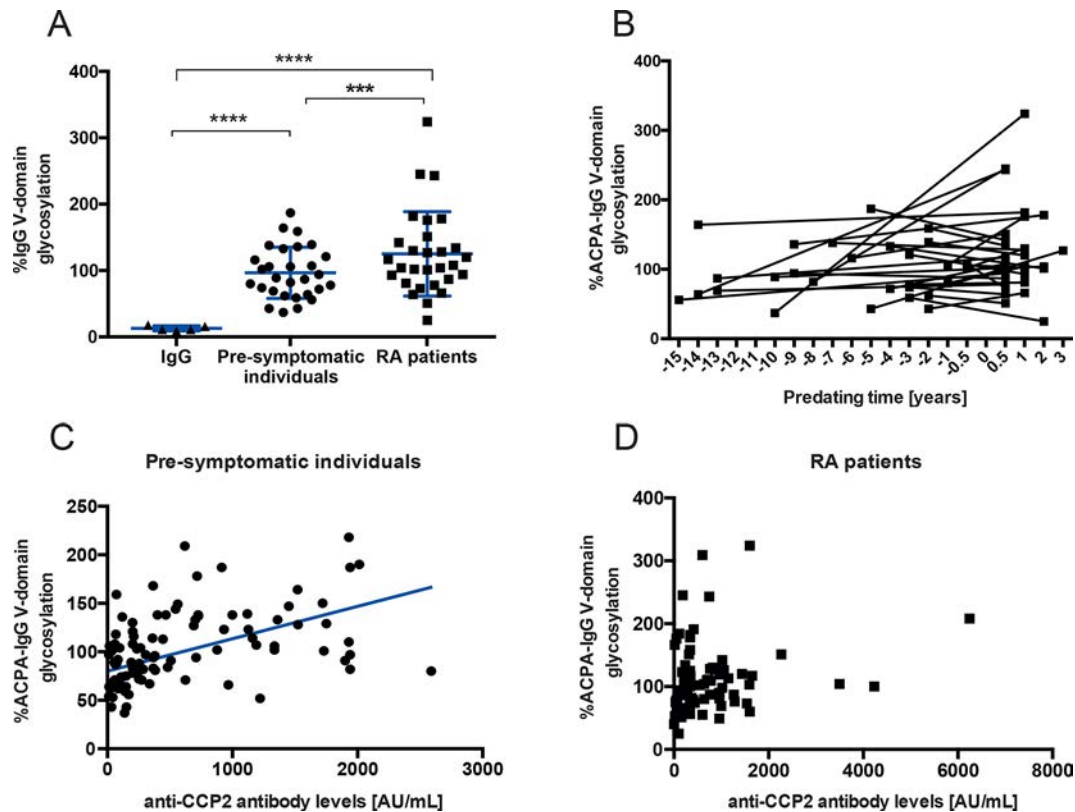


Figure 2 ACPA-IgG variable domain (V-domain) glycosylation levels of pre-symptomatic individuals and rheumatoid arthritis (RA) patients. (A) Percentage IgG V-domain glycosylation of healthy control IgG samples, captured ACPA-IgG from pre-symptomatic individuals and RA patients. (B) Percentage ACPA-IgG V-domain glycosylation followed over pre-dating time (–15 years before until +3 years after symptom onset) for 29 matched paired pre-symptomatic and RA samples that showed detectable V-domain glycan profiles. 0 indicates onset of RA. ACPA-IgG V-domain glycosylation increases towards disease onset ($p=0.043$, paired t-test). (C) Scatter plot of percentage ACPA-IgG V-domain glycosylation and anti-CCP2 antibody levels in pre-symptomatic individuals ($r_s=0.504$, $p<0.001$). (D) Scatter plot of percentage ACPA-IgG V-domain glycosylation and anti-CCP2 antibody levels in RA patients ($r_s=0.169$, $p=0.133$). Significant differences are indicated by *** $p<0.001$ and **** $p<0.0001$. The cut-off used for ACPA-IgG V-domain glycan peaks is defined as the average of the area under the curve (AUC) sum intensity of all blank sample peaks plus x standard deviation (x =value defined as such that all blank and ACPA-negative healthy donor control samples fall below the cut-off). ACPA, anti-citrullinated protein antibodies

obtained revealed that V-domain glycosylation was already present in pre-symptomatic individuals (figure 2A). Interestingly, ACPA-IgG V-domain glycosylation increased over time ($p<0.001$) reaching a mean of 111.4% at symptom onset, showing that, on average, more than one N-glycan is present within the V-domain of these ACPA-IgG. Likewise, also analyses of the 29 matched pairs, with detectable V-domain glycan peaks, showed an increase of ACPA-IgG V-domain glycosylation towards disease onset ($p=0.043$, paired t-test) (figure 2B). Furthermore, we observed that rising V-domain glycosylation levels in pre-symptomatic individuals correlated moderately with anti-CCP2 antibody levels ($r_s=0.504$, $p<0.001$) (figure 2C). This correlation could not be detected anymore after disease development (figure 2D).

ACPA-IgG V-domain glycosylation associates with HLA-SE

To investigate possible associations of ACPA-IgG V-domain glycosylation pre-disease and cohort characteristics, we performed a logistic regression analysis using detectable ACPA-IgG V-domain glycans versus non-detectable glycan profiles as an outcome. The statistical analysis showed no association between V-domain glycosylation and ‘sex’ or ‘ever smoking’. Interestingly, an association between ACPA-IgG V-domain glycosylation and HLA-SE was observed (OR=1.97, $p=0.043$). This association remained

significant after adjusting for anti-CCP2 antibody status, and pre-dating time (OR=2.46, $p=0.023$) as well as after adjusting for RF and pre-dating time (OR=2.54, $p=0.015$) (table 1). However, this association was non-significant after correcting for anti-CCP2 antibody levels although a clear trend remained (OR=2.06, $p=0.086$). In contrast, no association was found when a reciprocal analysis was performed addressing the question whether HLA-SE associates with anti-CCP2 antibody positivity pre-disease (OR=1.01, 95% CI 0.51–1.98).

DISCUSSION

In this study we have captured ACPA-IgG from pre-symptomatic individuals and RA patients and analysed their glycan profiles using UHPLC. The observed glycan profiles were derived from samples of ACPA-positive individuals in more than 95% of the cases. These results indicate the high reliability of the implemented methodology (online supplementary figure 1). Glycan profile detection in 8 out of 107 ACPA-negative samples may be explained by the presence of ACPA-levels slightly below the ELISA cut-off. In fact, three out of these eight subjects in whom ACPA V-domain glycans were detected, while displaying ACPA-negativity based on the ELISA cut-off, had been tested positive for reactivity towards other citrullinated-antigens, which could explain capturing by the CCP2-coated beads. A clear limitation

Table 1 Logistic regression analysis of samples from pre-symptomatic individuals with detectable versus non detectable ACPA-IgG glycan profiles

Variable	Simple			Multiple			Multiple			Multiple		
	OR	95% CI	P value	OR	95% CI	P value	OR	95% CI	P value	OR	95% CI	P value
Anti-CCP2 ab +/-	20.29	7.63 to 53.94	<0.001	32.13	10.54 to 97.91	<0.001	–	–	–	–	–	–
Anti-CCP2 ab levels	1.005	1.003 to 1.007	<0.001	–	–	–	1.005	1.003 to 1.008	<0.001	–	–	–
RF +/-	7.36	3.91 to 13.88	<0.001	–	–	–	–	–	–	7.59	3.85 to 14.96	<0.001
Sex m/f	0.78	0.44 to 1.38	0.393	–	–	–	–	–	–	–	–	–
Ever smoking y/n	0.72	0.394 to 1.317	0.286	–	–	–	–	–	–	–	–	–
HLA-SE +/-	1.97	1.022 to 3.806	0.043	2.46	1.13 to 5.33	0.023	2.06	0.90 to 4.70	0.086	2.54	1.20 to 5.36	0.015
Pre-dating time, years	1.077	0.999997 to 1.16	0.050008	0.94	0.85 to 1.04	0.206	0.98	0.89 to 1.08	0.747	1.01	0.93 to 1.10	0.804

ACPA, anti-citrullinated protein antibodies; HLA-SE, human leucocyte antigen class II shared epitope.

of the present study is that not all ACPA-positive samples could be analysed for the presence of V-domain glycans as not all glycan profiles, including Fc-glycans, could be detected. This is likely due to technical constraints such as low ACPA-levels or limited sample amounts.

At present ACPA-IgG is used as one of the most relevant biomarkers in RA. However, ACPA detection in subjects at risk does not always correlate with the progression to RA.¹⁵ Our data show that N-linked V-domain glycans are a specific feature of ACPA-IgG, which can be present already years before RA onset. These results are in line with a recent study indicating that the presence of V-domain glycans could potentially be used as a biomarker to identify ACPA-subjects at risk to develop RA.¹¹ Together our studies show that V-domain glycosylation occurs in almost all ACPA-positive subjects who will develop RA despite different ethnic and environmental backgrounds. Moreover, the current study shows that V-domain glycans appeared already up to 15 years before diagnosis (figure 2B). Furthermore, our data reveal that V-domain glycosylation increases towards disease onset, conceivably due to the generation of de novo N-glycosylation sites or the expansion of N-glycosylation site-bearing clones, and that this increase associates with higher ACPA-levels (figure 2C). These results are in line with the notion that ACPA-expressing B-cells gain a selective advantage through the generation of V-domain glycans.

Additionally, we did observe an association between ACPA-IgG V-domain glycosylation pre-disease and HLA-SE alleles. This association remains after including anti-CCP2-status into the model. Likewise, a clear, although non-significant trend remains after correcting for anti-CCP2 antibody levels.

Unfortunately, we could not study a possible correlation between V-domain glycosylation and epitope spreading of the ACPA-response as we did not have sufficient data on the citrullinated-epitope recognition profile of the samples available. Nonetheless, an association between HLA-SE status and ACPA-IgG V-domain glycosylation is intriguing as it suggests that HLA-SE predispose to the formation of N-linked glycosylation-sites in ACPA pre-disease and not to ACPA-positivity itself. This assumption is in line with findings indicating that the association between HLA-SE and ACPA-positivity is mostly lost in healthy individuals.^{4,5} However, although appealing, additional replication is warranted as the present study could have introduced bias due to for example, limited sample size or assay sensitivity. Nonetheless, we consider it highly relevant to perform such studies as it could provide novel insights into the role of HLA-SE-restricted T-cells on the development of ACPA-positive RA. HLA-SE T-cells might facilitate the introduction of N-linked glycosylation sites on ACPA-expressing B-cells allowing their expansion as conceivably explaining the rise in ACPA-levels pre-disease.

In summary, our data disclose that V-domain glycosylation precedes the development of ACPA-positive RA and may serve as aid to improve current algorithms predicting RA-development thereby allowing early treatment of high risk individuals. Noteworthy, our findings suggest that the action of HLA-SE could be explained by the contribution to facilitate the introduction of N-linked glycosylation sites into ACPA-IgG pre-disease.

Correction notice This article has been corrected since it published Online First. An error has been corrected in the abstract.

Acknowledgements The authors would like to thank the Department of Biobank Research at Umeå University, Västerbotten Intervention Programme, the Northern Sweden MONICA study and the County Council of Västerbotten for providing data and samples. We would like to thank Dr. Jan Wouter Drijfhout (LUMC, Leiden) for providing the CCP2 peptide.

Contributors TK: study concept and design, conducting experiments, acquisition of data, analysis and interpretation of the results, drafting and revising the manuscript, final approval of the manuscript. KAVS: study concept and design, conducting experiments, acquisition of data and interpretation of the results, critical revision and final approval of the manuscript. LH: study concept and design, methodology design, conducting experiments, acquisition of data, critical revision and final approval of the manuscript. AL: statistical analyses, interpretation of the results, critical revision and final approval of the manuscript. HK: statistical analyses, critical revision and final approval of the manuscript. MW: methodology design, critical revision and final approval of the manuscript. TWJH: interpretation of the results, critical revision and final approval of the manuscript. HUS: study concept and design, interpretation of the results, critical revision and final approval of the manuscript. RT: study concept and design, interpretation of the results, drafting and revising the manuscript critically, final approval of the manuscript. SR-D: study concept and design, statistical analyses, interpretation of the results, drafting and revising the manuscript critically, final approval of the manuscript. Department of Biobank Research at Umeå University: providing patient samples and data. Västerbotten Intervention Programme: providing patient samples and data. The Northern Sweden MONICA study: providing patient samples and data. The County Council of Västerbotten: providing patient samples and data. J.W. Drijfhout: providing the CCP2 peptides.

Funding This work has been financially supported by ReumaNederland (17-1-402), the IMI funded project RTCure (777357), ZonMw TOP (91214031), the Swedish Research Council (VR 2017-00650) as well as the King Gustaf V's 80-Year Fund, the King Gustaf V's and Queen Victoria's Fund and the Swedish Rheumatism Association.

Competing interests HUS, TWJH and REMT are mentioned inventors on a patent on ACPA-IgG V-domain glycosylation.

Patient consent for publication Not required.

Provenance and peer review Not commissioned; externally peer reviewed.

ORCID iDs

Theresa Kissel <http://orcid.org/0000-0002-5749-8087>

René Toes <http://orcid.org/0000-0002-9618-6414>

Solbritt Rantapää-Dahlqvist <http://orcid.org/0000-0001-8259-3863>

REFERENCES

- Schellekens GA, de Jong BA, van den Hoogen FH, et al. Citrulline is an essential constituent of antigenic determinants recognized by rheumatoid arthritis-specific autoantibodies. *J Clin Invest* 1998;101:273–81.
- Aletaha D, Neogi T, Silman AJ, et al. 2010 rheumatoid arthritis classification criteria: an American College of Rheumatology/European League against rheumatism collaborative initiative. *Arthritis Rheum* 2010;62:2569–81.

- 3 Aho K, Heliövaara M, Maatela J, *et al.* Rheumatoid factors antedating clinical rheumatoid arthritis. *J Rheumatol* 1991;18:1282–4.
- 4 Hensvold AH, Magnusson PKE, Joshua V, *et al.* Environmental and genetic factors in the development of anticitrullinated protein antibodies (ACPAs) and ACPA-positive rheumatoid arthritis: an epidemiological investigation in twins. *Ann Rheum Dis* 2015;74:375–80.
- 5 Terao C, Ohmura K, Ikari K, *et al.* Effects of smoking and shared epitope on the production of anti-citrullinated peptide antibody in a Japanese adult population. *Arthritis Care Res* 2014;66:1818–27.
- 6 Arnold JN, Wormald MR, Sim RB, *et al.* The impact of glycosylation on the biological function and structure of human immunoglobulins. *Annu Rev Immunol* 2007;25:21–50.
- 7 Hafkenschied L, Bondt A, Scherer HU, *et al.* Structural analysis of variable domain glycosylation of Anti-Citrullinated protein antibodies in rheumatoid arthritis reveals the presence of highly sialylated glycans. *Mol Cell Proteomics* 2017;16:278–87.
- 8 Rombouts Y, Willemze A, van Beers JJBC, *et al.* Extensive glycosylation of ACPA-IgG variable domains modulates binding to citrullinated antigens in rheumatoid arthritis. *Ann Rheum Dis* 2016;75:578–85.
- 9 Shakin-Eshleman SH, Spitalnik SL, Kasturi L. The amino acid at the X position of an Asn-X-Ser sequon is an important determinant of N-linked core-glycosylation efficiency. *J Biol Chem* 1996;271:6363–6.
- 10 Vergoesen RD, Slot LM, Hafkenschied L, *et al.* B-cell receptor sequencing of anti-citrullinated protein antibody (ACPA) IgG-expressing B cells indicates a selective advantage for the introduction of N-glycosylation sites during somatic hypermutation. *Ann Rheum Dis* 2018;77:956–8.
- 11 Hafkenschied L, de Moel E, Smolik I, *et al.* N-Linked glycans in the variable domain of ACPA-IgG predict the development of rheumatoid arthritis. *Arthritis Rheumatol* 2019. doi:10.1002/art.40920. [Epub ahead of print: 08 May 2019].
- 12 Scherer HU, Huizinga TWJ, Krönke G, *et al.* The B cell response to citrullinated antigens in the development of rheumatoid arthritis. *Nat Rev Rheumatol* 2018;14:157–69.
- 13 Arnett FC, Edworthy SM, Bloch DA, *et al.* The American rheumatism association 1987 revised criteria for the classification of rheumatoid arthritis. *Arthritis Rheum* 1988;31:315–24.
- 14 Jansen BC, Hafkenschied L, Bondt A, *et al.* HappyTools: a software for high-throughput HPLC data processing and quantitation. *PLoS One* 2018;13:e0200280.
- 15 van Beers JJBC, Willemze A, Jansen JJ, *et al.* ACPA fine-specificity profiles in early rheumatoid arthritis patients do not correlate with clinical features at baseline or with disease progression. *Arthritis Res Ther* 2013;15.
- 16 Pucić M, Knezević A, Vidic J, *et al.* High throughput isolation and glycosylation analysis of IgG-variability and heritability of the IgG glycome in three isolated human populations. *Mol Cell Proteomics* 2011;10:M111.010090–90.



OPEN ACCESS

TRANSLATIONAL SCIENCE

Anticitrullinated protein antibodies facilitate migration of synovial tissue-derived fibroblasts

Meng Sun ,¹ Bence Rethi,¹ Akilan Krishnamurthy,¹ Vijay Joshua,¹ Alexandra Circiumaru,¹ Aase Haj Hensvold,¹ Elena Ossipova,¹ Caroline Grönwall,¹ Yanying Liu,² Marianne Engstrom,¹ Sergiu Bogdan Catrina,³ Johanna Steen,¹ Vivianne Malmstrom,¹ Lars Klareskog ,¹ Camilla Svensson,⁴ Caroline Ospelt,⁵ Heidi Wähämaa,¹ Anca Irinel Catrina¹

Handling editor Josef S Smolen

► Additional material is published online only. To view, please visit the journal online (<http://dx.doi.org/10.1136/annrheumdis-2018-214967>).

¹Rheumatology Unit, Department of Medicine, Karolinska University Hospital, Karolinska Institutet, Stockholm, Sweden

²Department of Rheumatology and Immunology, Peking University People's Hospital, Beijing, China

³Molecular Medicine and Surgery, Karolinska University Hospital and Institutet, Stockholm, Sweden

⁴Physiology and Pharmacology, Karolinska Institutet, Stockholm, Sweden

⁵Center of Experimental Rheumatology, Zurich, Switzerland

Correspondence to

Dr Anca Irinel Catrina, Rheumatology Unit, Stockholm SE-17176, Sweden; anca.catrina@ki.se

Received 21 December 2018

Revised 21 August 2019

Accepted 22 August 2019

Published Online First

3 September 2019

ABSTRACT

Objectives Rheumatoid arthritis (RA)-specific anti-citrullinated protein/peptide antibodies (ACPAs) might contribute to bone loss and arthralgia before the onset of joint inflammation. We aimed to dissect additional mechanisms by which ACPAs might contribute to development of joint pathology.

Methods Fibroblast-like synoviocytes (FLS) were isolated from the synovial membrane of patients with RA. The FLS cultures were stimulated with polyclonal ACPAs (anti-CCP-2 antibodies) purified from the peripheral blood of patients with RA or with monoclonal ACPAs derived from single synovial fluid B cells. We analysed how ACPAs modulate FLS by measuring cell adhesion and mobility as well as cytokine production. Expression of protein arginine deiminase (PAD) enzymes and protein citrullination were analysed by immunofluorescence, and signal transduction was studied using immunoblotting.

Results Challenge of FLS by starvation-induced stress or by exposure to the chemokine interleukin-8 was essential to sensitise the cells to ACPAs. These challenges led to an increased PAD expression and protein citrullination and an ACPA-mediated induction of FLS migration through a mechanism involving phosphoinositide 3-kinase activation. Inhibition of the PAD enzymes or competition with soluble citrullinated proteins or peptides completely abolished the ACPA-induced FLS migration. Different monoclonal ACPAs triggered distinct cellular effects in either fibroblasts or osteoclasts, suggesting unique roles for individual ACPA clones in disease pathogenesis.

Conclusion We propose that transient synovial insults in the presence of a certain pre-existing ACPA repertoire might result in an ACPA-mediated increase of FLS migration.

INTRODUCTION

Anti-citrullinated protein antibodies (ACPAs) are present in a majority of patients with rheumatoid arthritis (RA) and are specific for this disease.¹ They consist of a group of antibodies with different specificities towards citrullinated antigens that might cross-react with other protein modifications but not with the native proteins^{2–4} and have been suggested to contribute to joint pain and bone loss already before onset of joint inflammation in RA.^{5–8} In line with this, we and others have shown that polyclonal ACPAs bind to the surface of developing osteoclasts (OC) and suggested that reactivity to citrullinated

Key messages**What is already known about this subject?**

- Anticitrullinated protein/peptide antibodies (ACPAs) exist prior to the onset of rheumatoid arthritis (RA), however, it is unclear how autoimmunity in some but not all cases translate into manifest joint inflammation.

What does this study add?

- Cellular stress and pro-inflammatory mediators (interleukin-8) can sensitise synovial fibroblasts to ACPAs by enhancing protein arginine deiminase enzyme expression and cellular citrullination.
- ACPAs promote synovial fibroblast migration through a phosphoinositide 3-kinase-mediated mechanism.
- Different monoclonal ACPAs have distinct cellular effects with three clones increasing migration of challenged fibroblasts, with no effect on osteoclasts and another clone increasing osteoclast differentiation with no effect on fibroblasts.

How might this impact on clinical practice or future developments?

- Our results suggest that unique ACPAs may be responsible for specific pathological features in ACPA+RA.
- Inducible protein citrullination could be a key event in the transition of a systemic humoral autoimmunity towards the inflammation of the joints.

targets increase OC differentiation and bone loss.^{9 10} Furthermore, experiments in mice have shown that polyclonal ACPAs (defined as anti-CCP-2 IgG antibodies) induces pain-related behaviours even though no joint inflammation develops,¹¹ similar to the predisease stage of pain described in ACPA-positive individuals. We originally proposed that this, as well as ACPA-induced bone loss in mice, occurred through an interleukin (IL)-8-dependent and citrulline-specific mechanisms.^{10 11} However, recent papers and corrections^{12 13} this year have led to a reconsideration and extension of the concept. As such also other RA-derived monoclonal antibodies



© Author(s) (or their employer(s)) 2019. Re-use permitted under CC BY. Published by BMJ.

To cite: Sun M, Rethi B, Krishnamurthy A, et al. *Ann Rheum Dis* 2019;**78**:1621–1631.

than those with citrulline reactivity and immune complexes are able to cause functional effects similar to those of polyclonal ACPAs, through different mechanisms that are potentially distinct between autoantibody subsets and might include both antigen-driven and Fc γ receptor activation-driven pathways.^{14–16} Taken together, these data suggest a new concept where different RA-associated antibodies with different reactivities contribute to bone loss and pain, potentially through different mechanisms, a complex scenario that requires additional investigations. The need for these investigations and the ways of performing them has been highlighted in a recent editorial.¹⁷

Previous studies have shown that in the presence of pre-existing joint inflammation in mice, transfer of a monoclonal ACPA may enhance synovial tissue injury,¹⁸ suggesting that additional local stimuli might be essential for sensitisation of the synovial compartment to effects of antibodies. In the synovial tissue, fibroblast-like synoviocytes (FLS) contribute to an inflammatory stroma that promote and amplify tissue-specific immune activation through the release of various cytokines and have the capacity to grow into the cartilage surface and create an erosive interface by producing tissue remodelling proteases, such as matrix metalloproteinases and cathepsins.¹⁹ RA-derived FLS have also an increased migration capacity, a feature that might contribute to disease propagation within and in between the joints.^{20 21}

In the present report, we investigated ACPA effects on FLS. We demonstrate that stimuli such as cellular stress and/or exposure to pro-inflammatory mediators are needed for the sensitisation of FLS to ACPAs. Furthermore, some but not all ACPAs are able to affect FLS. Our findings thereby suggest that transient synovial insults in the presence of certain pre-existing ACPA clones might act in concert to promote ACPA-mediated FLS migration.

MATERIALS AND METHODS

Additional detailed information is provided in online supplementary file.

Patient material

Polyclonal ACPA IgGs (anti-CCP2 antibodies) and non-ACPA control IgGs were purified from a pooled serum of patients with RA²² and from non-pooled sera of four ACPA-positive patients with RA (for details see online supplementary file). Using a similar method, polyclonal antiproteinase 3 (PR3) IgGs and non-anti-PR3 control IgGs were purified from the sera of a patient with PR3-associated vasculitis. Monoclonal antibodies were isolated from patients with RA as previously described^{2 4 15} and recombinantly expressed as IgG1. All IgG underwent extensive quality control testing including specificity evaluation, size exclusion chromatography aggregation test and limulus amoebocyte lysate (LAL) endotoxin test.²³ F(ab')₂ antibody fragments were generated and RF IgM antibody was purchased from Athens Research & Technology (Georgia, USA). RA-derived and osteoarthritis (OA)-derived synovial fibroblasts as well as human dermal fibroblasts were used in cell culture experiments. Synovial biopsies were obtained from four healthy volunteers and four patients with RA. Patients were enrolled at Karolinska University Hospital. Informed consent was obtained according to the protocol approved by the Ethical Review Committee North of Karolinska University Hospital.

Migration and adhesion assays

Fibroblast migration was assessed by IncuCyte Zoom live cell imaging system or by scratch assay. Adhesion assays were

performed using 16-well E-plates and the xCELLigence System Real-Time Cell Analyzer (ACEA Biosciences, USA). When indicated, the cells were washed with phosphate buffered saline and starved for 2 hours in medium without fetal bovine serum. Citrullinated or native human purified fibrinogen, recombinant vimentin, α -enolase and histone H4 were added as pretreatment to ACPA and control IgGs at 4°C overnight. Phosphoinositide 3-kinase (PI3K) was inhibited by wortmanin and phosphatase and tensin homolog (PTEN) by SF-1670 (Sigma-Aldrich, Stockholm, Sweden). PAD activity was inhibited by Cl-amidine (Cayman Chemical, Ann Arbor, Michigan, USA) or GSK199 (kind gift from Aaron Winkler, Pfizer) for 72 hours prior to scratching. Histone acetyltransferase or deacetylase enzymes were inhibited by anacardic acid or trichostatin A (Sigma-Aldrich, Stockholm, Sweden), respectively. Fibroblasts were cultured in the presence or absence of IL-8 (R&D Systems, Abingdon, UK) or tumour necrosis factor (TNF)- α (Peprotech, London, UK). Cytokine levels were analysed using the Cytometric Bead Array (BD Biosciences, San Diego, California, USA) and matrix metalloproteinases were measured by ELISA (R&D Systems, Abingdon, UK).

Immunohistochemistry and confocal microscopy

FLS were stained with indicated primary antibodies followed by horseradish peroxidase (HRP)-conjugated antibodies and developed by Vectastain Elite ABC and DAB (Vector Laboratories, Peterborough, UK) and then counterstained with Mayer's haematoxylin. For confocal microscopy, cells and tissues incubated with primary and secondary antibodies and then counterstained with 4,6-diamidino-2-phenylindole.

Mass spectrometry

Starved and non-starved FLS whole cell lysate were analysed by mass spectrometry for detection of citrullination.

Western blot analysis

Cells lysates were loaded an SDS-PAGE gel (Bio-Rad, Solna, Sweden), transferred to nitrocellulose membranes and incubated with primary antibodies and peroxidase-conjugated secondary antibodies.

Flow cytometry

Cells were collected using non-enzymatic detachment reagent (Sigma-Aldrich, Stockholm, Sweden), stained by fluorochrome-labelled antibodies and analysed by FACSVerse flow cytometer (BD Biosciences, San Jose, California, USA).

Statistical analysis

The data were analysed using either Kurskal-Wallis test followed by Dunn's multiple comparison test or two-way analysis of variance, followed by Tukey's post hoc test by using GraphPad Prism 6 software (GraphPad Software, San Diego, California, USA). P values <0.05 were considered to be statistically significant.

RESULTS

Polyclonal ACPAs enhance migration and adhesiveness in starved FLS

To test if FLS are or might be rendered sensitive to ACPAs, we compared the effects of polyclonal ACPA and non-ACPA control IgGs on FLS migration in both basal conditions and after challenging by a 2-hour serum starvation. Neither polyclonal ACPA IgGs nor non-ACPA control IgGs had any effect on the migration of non-starved FLS (figure 1A). In contrast, polyclonal ACPA IgGs, but not non-ACPA control IgGs, increased the migration

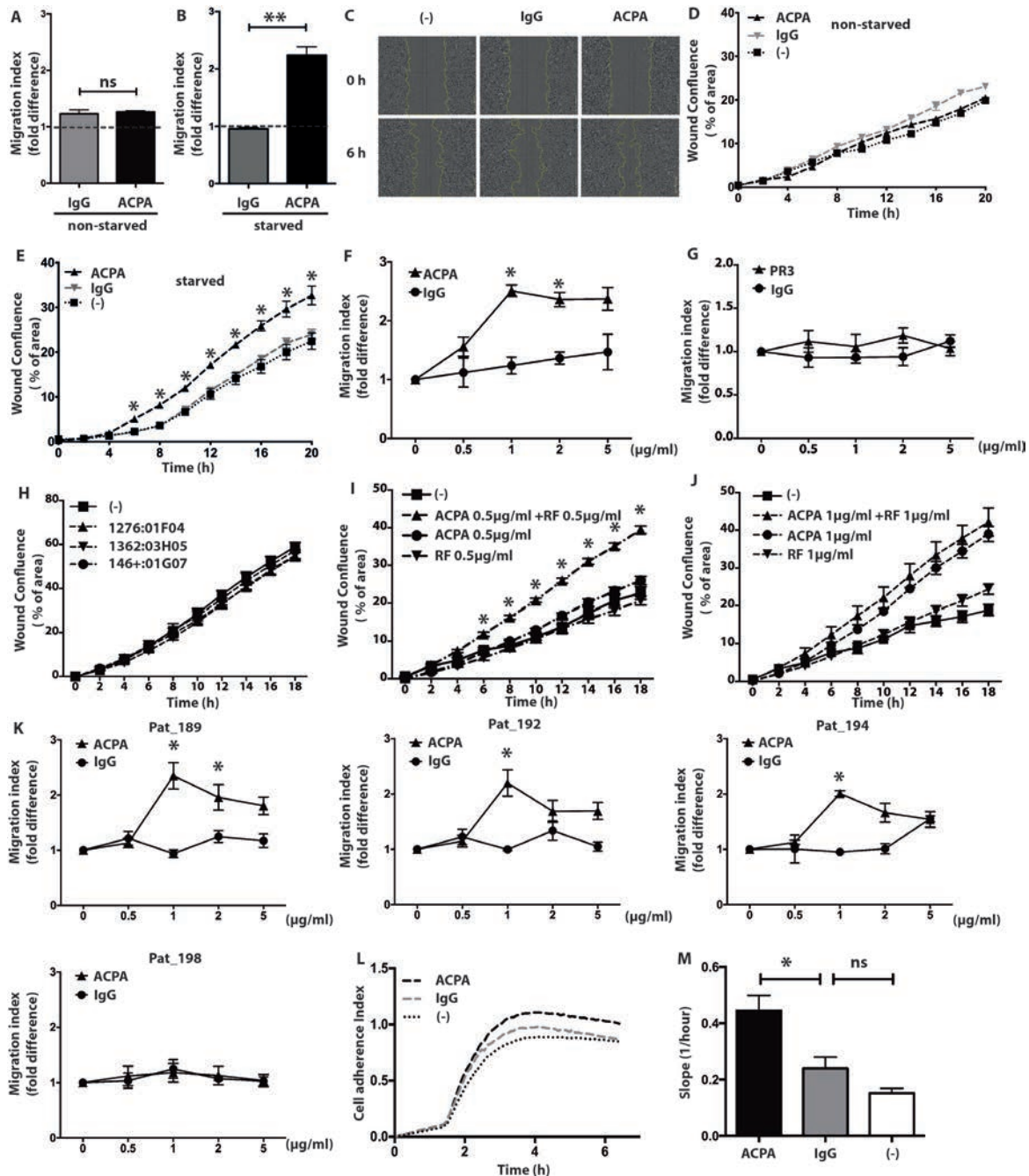


Figure 1 Increased mobility and adherence of synovial fibroblasts in presence of polyclonal ACPAs. Cell mobility was analysed during a period of 6 hours in the presence of 1 $\mu\text{g}/\text{mL}$ polyclonal ACPA IgGs (ACPA) or non-ACPA control IgGs (IgG) or without antibody treatment (-) in both non-starved (A) and starved (B) fibroblast cultures. The graphs represent mean \pm SD values obtained from 10 independent experiments, using cells of 10 different patients and 6 replicates for each treatment. Dot line indicate migration index of non-treated FLS. Image-based evaluation of cell migration in starved fibroblast cultures were performed using phase contrast microscopy with 10x magnification (C). Real-time cell migration was measured in the presence of 1 $\mu\text{g}/\text{mL}$ ACPA or control IgG or without any treatment in non-starved (D) and starved (E) fibroblast cultures using IncuCyte. The graphs represent mean \pm SD values obtained by using cells from 10 individuals patients and 6 replicates in 10 independent experiments. A titration experiment was performed on starved synovial fibroblasts with presence of ACPA (F) and anti-PR3 (G) with indicated concentrations. (H) Cell mobility were tested on starved FLS with presence of 1 $\mu\text{g}/\text{mL}$ anti-MDA antibodies (1276:01F04, 1362:03H05 and 146+:01G07). The graphs represent mean \pm SD values obtained from five replicates in three independent experiments for anti-PR3 titration and anti-MDA antibodies. Starved FLS mobility was analysed by combining 0.5 $\mu\text{g}/\text{mL}$ ACPA with 0.5 $\mu\text{g}/\text{mL}$ IgM RF (I) and 1 $\mu\text{g}/\text{mL}$ ACPA with 1 $\mu\text{g}/\text{mL}$ IgM RF (J). The graphs represent mean \pm SD values obtained from three different patients with six replicates in three independent experiments. Effect of ACPA IgGs fractions prepared from individual blood samples were tested on starved synovial fibroblasts using the indicated concentrations (K). The graphs represent results obtained from cells of three different patients, using six replicates in three independent experiment. Real-time cell adherence was monitored in the presence of 1 $\mu\text{g}/\text{mL}$ ACPA, control IgG or without antibody treatment in starved fibroblast cultures for up to 6 hours. The chart shows representative results in one experiment (L), whereas the graph indicates mean \pm SD values of slope during real-time cell adherence assay, calculated from five different patients with three replicates in five independent experiments (M). * $P < 0.05$. ACPA, anticitrullinated protein/peptide antibody; FLS, fibroblast-like synoviocytes; PR3, polyclonal antiproteinase 3; ns, not significant; RF, rheumatoid factor.

index of starved FLS with a mean±SD fold of 2.6 ± 0.3 for ACPA IgGs as compared with 0.95 ± 0.2 for non-ACPA control IgGs, $p<0.05$ (figure 1B,C). ACPA IgGs had no effect on cell viability and proliferation (online supplementary figure 1). Similar results were seen for OA-derived synovial fibroblasts and human dermal fibroblasts (online supplementary figure 2). The increase in cell mobility was observed as early as 6 hours and was stable up to 20 hours after ACPA exposure (figure 1D,E). Dose titration showed an optimal effect at $1\ \mu\text{g}/\text{mL}$ (figure 1F). In contrast, polyclonal anti-PR3 autoantibodies prepared in a similar way as ACPA showed no effect on starved FLS migration at doses as high as $5\ \mu\text{g}/\text{mL}$ (figure 1G). Furthermore, monoclonal anti-malondialdehyde(MDA) antibodies obtained through the same methodology as the monoclonal ACPAs had no effect on FLS migration (figure 1H). Interestingly, addition of IgM RF to the cultures significantly potentiated the effect of suboptimal (figure 1I) but not higher concentrations of the polyclonal ACPAs (figure 1J), while showing no effect when used alone (at doses as high as $5\ \mu\text{g}/\text{mL}$, online supplementary figure 3). Some but not all ACPA IgG fractions prepared from individual blood samples were able to recapitulate the effect observed with the ACPA IgGs prepared from pooled blood samples (figure 1K).

Besides migration, ACPA IgGs were able to increase adhesiveness of starved FLS (figure 1L), with an average slope increase of 0.44 ± 0.04 for polyclonal ACPA IgGs as compared with 0.24 ± 0.05 for non-ACPA control IgGs, $p<0.05$ (figure 1M). Notably, ACPAs did not influence either matrix invasion (data not shown), matrix metalloproteinases production or cytokine and chemokine levels (online supplementary figure 4).

Inducible protein citrullination is essential for the ACPAs effect on FLS migration

To investigate the mechanisms that render FLS sensitive to ACPAs, we analysed the expression of PAD-2 and PAD-4, two PAD enzymes known to be present in RA synovium,²⁴ and cellular citrullination following serum starvation. Non-starved FLS express low levels of intracellular PAD-2 and PAD-4 and do not bind polyclonal ACPA (figure 2A, upper panel). Cellular starvation significantly increased PAD-2 and PAD-4 enzymes expression in a majority of the cultured cells, as well as the amounts of citrullinated proteins labelled by polyclonal ACPA IgGs (figure 2A, lower panel and online supplementary figure 5). This was confirmed by mass spectrometry showing an increase in the number and the amount of citrullinated targets (estimated by label-free quantitative analysis) in starved as compared with non-starved FLS (online supplementary figure 6). Pre-incubation of the polyclonal ACPA with citrullinated (cit) but not native fibrinogen abolished FLS staining by ACPAs (figure 2B), as well as the ACPA-induced migration of starved FLS, an effect that titrated out at a protein:antibody ratio of 2:1 (figure 2C). Additional experiments demonstrated a similar effect for cit-vimentin and cit-enolase but not for cit-histone 4 (figure 2D). In line with this, inhibition of cellular citrullination by pretreatment with PAD inhibitors prevented both ACPA-staining (figure 2E) and the ACPA-induced migration of starved FLS (figure 2F), without affecting proliferation and cell viability (online supplementary figure 1). Furthermore, F(ab')₂ ACPA fragments had a similar capacity to induce migration of starved FLS (figure 2G), in line with lack of expression of Fcγ receptors by FLS (online supplementary figure 7).

PI3K activation is required for ACPA-induced FLS migration

To gain insight into the intracellular signals activated by ACPAs, we investigated two major regulators of FLS migration:

PI3K and mitogen-activated protein kinases (MAPK). Polyclonal ACPAs induced a transient but robust peak in Akt phosphorylation at the Thr308 residue linked to PI3K activation (figure 3A left and middle panels and figure 3B), whereas Akt phosphorylation at the Ser473 residue, linked to mammalian target of rapamycin activation, seemed to occur irrespectively of the presence of ACPAs (figure 3A left and middle panels). MAPK phosphorylation showed no differences between polyclonal ACPA and control IgGs. In contrast to the rather selective modulation of Akt by ACPAs, control treatment with TNF-α-induced prolonged and broad phosphorylation events (figure 3A, right panels). PI3K inhibition almost completely abolished the ACPA-induced migration of starved FLS (figure 3C). Furthermore, increased stimulation of PI3K by blocking PTEN led to higher cellular mobility with no further increment by ACPAs (figure 3D).

Inflammatory stimuli can substitute starvation and sensitise FLS to ACPAs

To identify additional factors that may render FLS sensitive to ACPAs, we investigated the potential contribution of pro-inflammatory stimuli, such as IL-8 and TNF-α. FLS express IL-8 receptors CXCR1 and CXCR2 (figure 4A) and produce low levels of IL-8, unaffected by ACPAs (online supplementary figure 4). Exogenously added IL-8 had no effect on the migration of non-starved (figure 4B) or starved (figure 4C) FLS, but significantly potentiated the effect of polyclonal ACPAs in both cultures. The synergistic effects were further demonstrated by combination of different concentrations of ACPAs with a fixed dose of IL-8 (figure 4D) or suboptimal concentration of ACPAs with increasing concentration of IL-8 (figure 4E). TNF-α triggered a significant increase in FLS migration both in the presence or absence of ACPAs, suggesting different mechanisms triggered by these two cytokines (figure 4F). Similar to cell starvation, exogenous IL-8 significantly increased PAD-2 and PAD-4 expression (figure 4G), as well as the amount of citrullinated proteins (figure 4H) in non-starved FLS (see also online supplementary figure 5).

Different ACPA clones induce FLS migration and osteoclast activation

Since polyclonal ACPA IgGs contain a wide spectrum of antibodies, we investigated whether monoclonal ACPAs differ in their capacity to affect distinct cellular functions such as FLS mobility and OC differentiation. Among eight monoclonal ACPAs, each with different patterns of antigen recognition, three of them (1325:01B09, 14CFCT2D09 and 14CFCT2H12), enhanced FLS migration significantly (figure 5A, for titration curves see online supplementary figure 8), while not having any effect on OC differentiation (figure 5B). Interestingly, clone 1325:01B09 but not 14CFCT2D09 and 14CFCT2H12 are cross-reactive with homo-citrullinated targets.^{4 25} In contrast, clone 1325:04C03, having no effect on FLS migration (figure 5A), significantly increased osteoclastogenesis (figure 5B) already at a concentration of $1\ \mu\text{g}/\text{mL}$. Selective cellular activation correlated with binding of clone 1325:01B09 to starved FLS and clone 1325:04C03 to OC (figure 5C). Binding of 1325:01B09 to FLS (figure 5D) was prevented by pre-incubation with cit-fibrinogen or cit-histone H4 but not by cit-vimentin or cit-enolase (figure 5E,F). As 1325:01B09 also cross-react with acetylated modified proteins,²⁵ we performed further experiments to show that altered citrullination but not acetylation could modulate 1325:01B09 effect on FLS (figure 5G). Furthermore, F(ab')₂

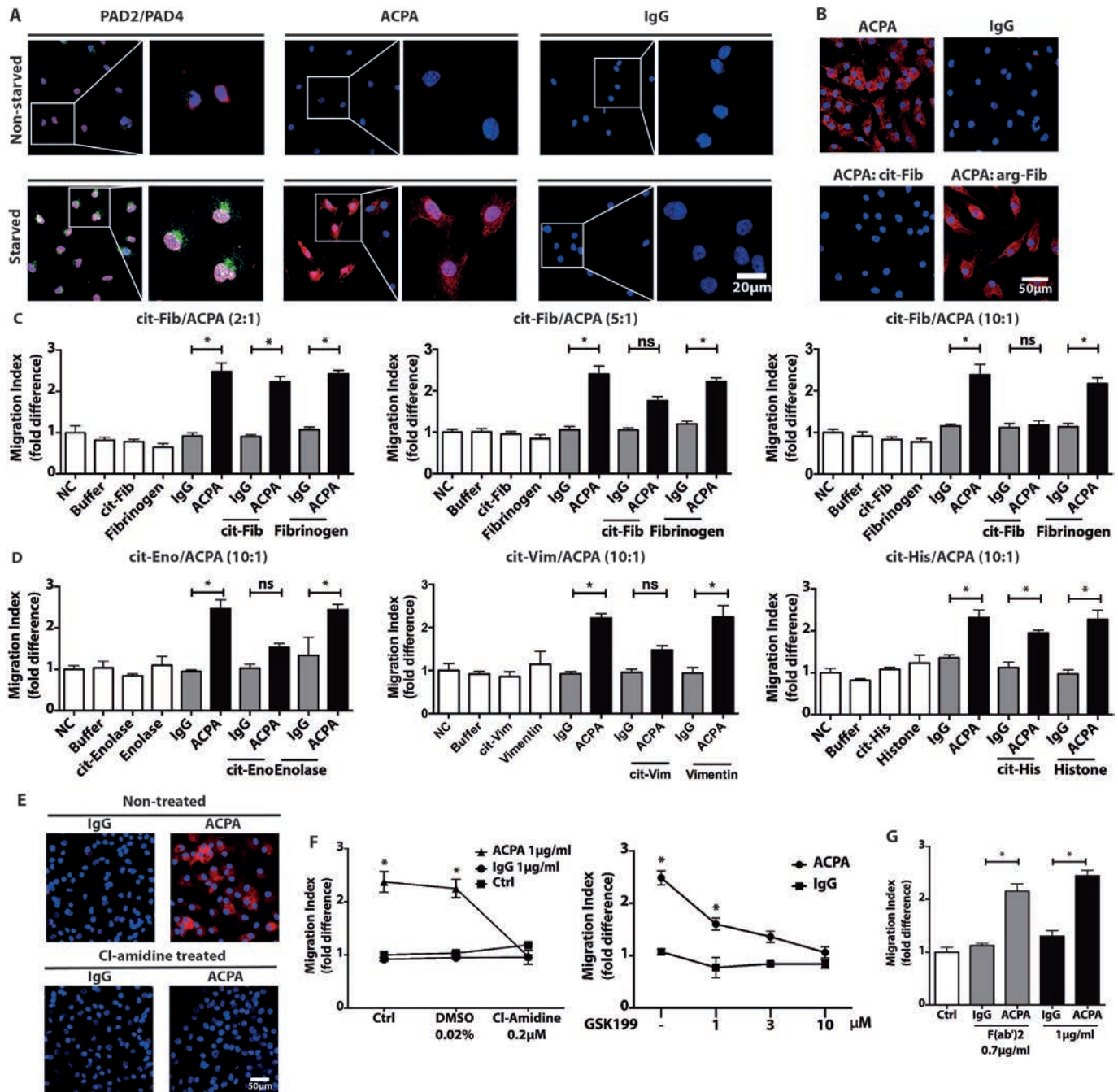


Figure 2 Starvation-induced protein citrullination is essential for synovial fibroblast migration induced by ACPAs. Confocal microscopy images visualise PAD-2 (green) and PAD-4 (red) expressions as well as polyclonal ACPA IgGs (ACPA) and non-ACPA control IgG (IgG) binding patterns in FLS cultures following serum withdrawal (starved) or in non-starved FLS, in the presence of 10% fetal bovine serum (A). An original magnification of 400x was used for all images obtained with confocal microscopy and nuclei are shown in blue. Starved FLS cultures were also stained with ACPAs (red colour) pre-incubated overnight with citrullinated (cit) or native fibrinogen with ratio of protein:antibody (10:1) (cit-Fib or Arg-Fib, respectively) or in the absence of fibrinogen (B). To block ACPA-induced migration, FLS migration was compared in the presence of 1 μg/mL polyclonal ACPAs and control IgG or with both antibodies pre-incubated with citrullinated or native fibrinogen in the indicated ratio overnight. Migration index was calculated from three independent experiments, using cells of three individual patients and six replicates for each treatment, mean±SD values are shown (C). Similar blocking experiments were performed with citrullinated vimentin (Vim), enolase (Eno) and histone 4 (His) using 10:1 decoy protein:antibody ratio. The graphs represent results obtained from three independent experiments, using cells of three individual patients and six replicates (D). To inhibit PAD enzymes, we exposed FLS cultures to 200 nM Cl-amidine for 72 hours. Confocal microscopy images show the inhibition of ACPA binding (red colour) to Cl-amidine pretreated FLS (E). Moreover, after pre-incubation of the cells with different PAD inhibitors, Cl-amidine and GSK199, we could not detect an increased FLS mobility in the presence of ACPAs (F). Migration index was calculated from three independent experiments, using cells of three individual patients and six sample-replicates, mean±SD values are shown. Furthermore, FLS migration were analysed in the presence of 0.7 μg/mL polyclonal ACPA F(ab')₂ and non-ACPA IgG F(ab')₂. The graph indicates results obtained from three independent experiments, using cells of three individual patients and six replicates (G). *P<0.05. ACPA, anticitrullinated protein/peptide antibody; DMSO, dimethyl sulfoxide; FLS, fibroblast-like synoviocytes; PAD, protein arginine deiminase; ns, not significant.

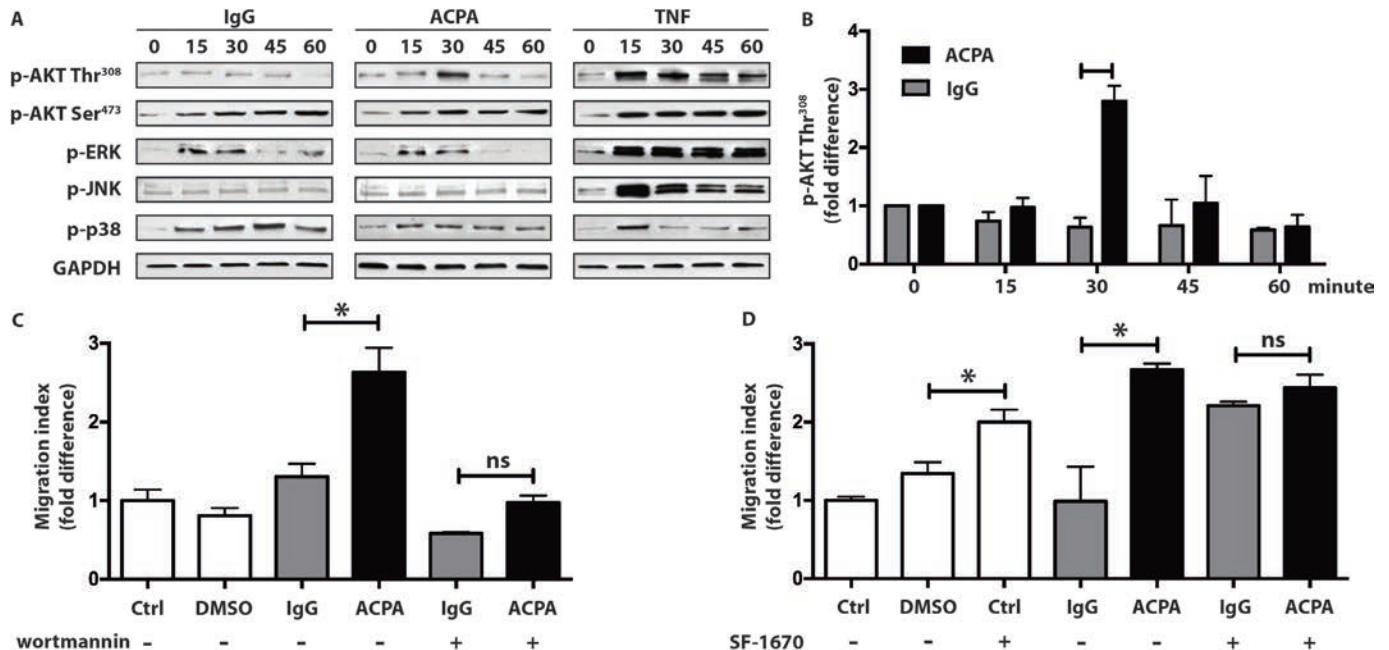


Figure 3 Role of PI3K in the ACPA-induced synovial fibroblast migration. Starved FLS were exposed to 1 µg/mL polyclonal ACPA IgG (ACPA) or non-ACPA control IgG (IgG) or to TNF 10 ng/mL. Immunoblot analysis of Akt (Thr308 or Ser473 residues), ERK1/2, JNK and p38 phosphorylation are shown, whereas GAPDH protein was detected as control. The presented data are representative for at least three independent experiments for all tested proteins (A). Change of Akt phosphorylation at the Thr308 residue is shown in response to 1 µg/mL ACPA or IgG treatments (B). The data were calculated following densitometry analysis in five independent experiments, levels were normalised to baseline intensities, mean±SD values are shown. FLS were pretreated with 200 nM of the PI3K inhibitor wortmannin (C) or 2 µg/mL of the PTEN inhibitor SF-1670 (D) for 2 hours prior to the analysis of cell migration in the presence of 1 µg/mL ACPA or control IgG. DMSO (0.01%) was used as solvent control. Graphs represent fold-change in cell mobility, mean±SD values were calculated from three independent experiments, *P<0.05. ACPA, anticitrullinated protein/peptide antibody; DMSO, dimethyl sulfoxide; FLS, fibroblast-like synoviocytes; PAD, protein arginine deiminase; PI3K, phosphoinositide 3-kinase; PTEN, phosphatase and tensin homolog; ns, not significant; TNF, tumour necrosis factor.

fragments of 1325:01B09 enhanced migration of (figure 5H) and bound to non-permeabilised (figure 5I) challenged FLS which was prevented by exogenously added cit-fibrinogen (figure 5J). Both whole and F(ab')₂ fragments of 1325:01B09 were able to promote migration of challenged FLS through a similar mechanism as for the polyclonal ACPA IgGs, as shown by activation of the PI3K pathway (figure 5K).

We further investigated cellular binding patterns in synovial biopsies obtained from both healthy volunteers and patients with RA. None of the ACPA clones labelled the uninfamed synovial tissues (figure 6A). In contrast, we detected 1325:01B09 binding to multiple cells from the dense layer of CD55 and podoplanin (PDPN)-positive fibroblasts in the synovial membrane of two out of the four tested inflamed RA synovial tissues, whereas virtually no binding of the clone 1325:04C03 was observed in the CD55 and/or PDPN-positive areas (figure 6B). No correlation was seen between the staining pattern and disease characteristics. The co-localisation of 1325:01B09 binding sites with CD55-positive (figure 6C) and PDPN-positive FLS (figure 6D), as well as co-localisation of the F(ab')₂ 1325:01B09 fragments with PDPN-positive FLS (figure 6E) was further confirmed in two additional inflamed RA synovial tissue using confocal microscopy.

DISCUSSION

In this report, we describe that steady-state FLS are unresponsive to ACPAs but can be rendered sensitive to these autoantibodies in the presence of additional stimuli. A key event in priming synovial fibroblasts to ACPA is an inducible PAD-2 and PAD-4 expression that is accompanied by increased protein citrullination. Importantly, individual monoclonal ACPAs exhibited

different capacities to induce migration of challenged FLS and activate OC. We provide novel insights into how different ACPA clones in concert might contribute to distinct pathogenic events in the RA development. Furthermore, PAD inhibition may be beneficial in targeting FLS during the development of ACPA-positive arthritis.

We demonstrated that polyclonal ACPA IgGs are able to induce migration and adhesiveness of challenged fibroblasts, independent of their tissue origin. This poses challenges in understanding the specific targeting of the synovial tissue in RA. While tissue-specific antibody-induced vascular changes²⁶ and site-specific differences in the responses to pro-inflammatory cytokine priming in skin versus synovial fibroblasts²⁷ might play a role, further research is needed to clarify this issue. The lack of effects of polyclonal ACPAs on steady-state fibroblasts is in accordance with the clinical observation that ACPAs alone are not sufficient for development of arthritis in seropositive individuals²⁸ and the fact that ACPA infusion in mice does not induce arthritis.¹¹ In contrast, challenging by transient cellular stress or exposure to pro-inflammatory signals render the FLS sensitive to ACPA effects. Furthermore, while not having a direct effect on FLS, RF is able to potentiate the ACPAs effects on the FcγR-negative FLS, potentially by forming complexes with the cell bound ACPAs and consequently recruiting more of the activated surface molecules, which are engaged in ACPA interactions, as well as their associated signalling components.²⁹⁻³³ Our findings provide support to the concept of a stepwise involvement of several molecular mechanisms in ACPA-mediated synovial pathology. Transient synovial events such as trauma³⁴⁻³⁸ or viral infections,^{39, 40} which often cause joint inflammation and

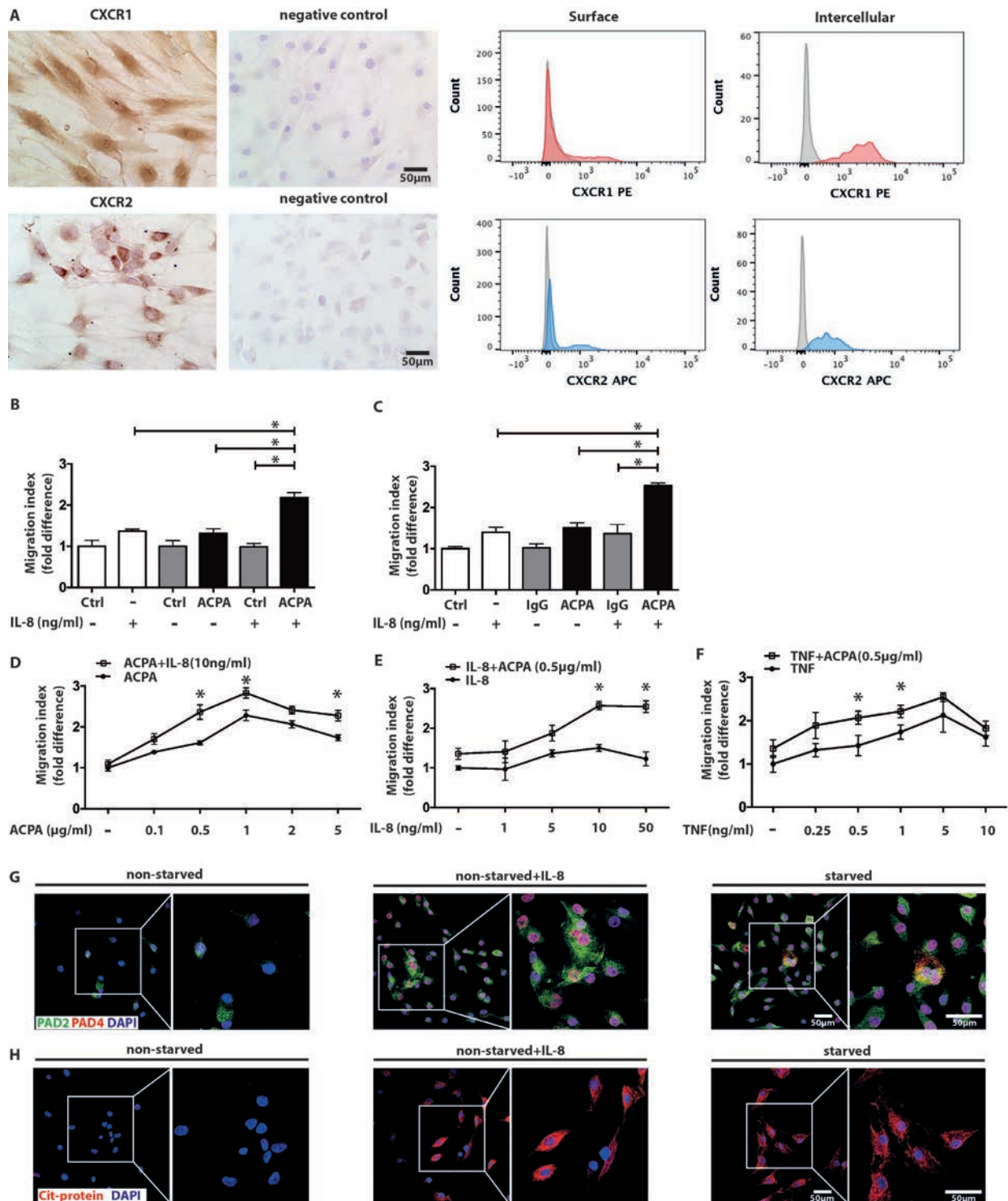


Figure 4 Collaboration of ACPA-mediated signals with the inflammatory cytokines IL-8 and TNF in inducing FLS migration. CXCR1 and CXCR2 expressions in FLS cultures were analysed with immunohistochemistry by light microscopy with the original magnification of 250x (left panel) and flow cytometry (right panel) (A). Migration of non-starved (B) and starved FLS (C) were assessed after exposing the cells to suboptimal (0.5 μg/mL) dose of ACPA or IgG in the presence or absence of 10 ng/mL recombinant human IL-8. Mean±SD values were calculated from three independent experiments, using cells of five individual patients and three replicates, **p*<0.05. Starved FLS mobility was analysed by combining high dose (10 ng/mL) of IL-8 with increasing ACPA concentrations (D) or suboptimal concentration of ACPA with increasing concentrations of IL-8 (E). On similar grounds, increasing concentrations of TNF were combined with ACPA applied at a suboptimal dose (F). Mean±SD values were calculated based on at three independent experiments, using cells of three different patients and six sample replicates, **p*<0.05 (G). Confocal microscopy images show increased PAD-4 (red colour) and PAD-2 (green colour) expression of non-starved FLS cultures stimulated by IL-8 (10 ng/mL). Nuclei are represented in blue colour. The effect of IL-8 (10 ng/mL) was also tested on ACPA binding to FLS cultures using confocal microscopy (H). Red colour represents antibody binding, nuclei are shown in blue. The original magnification was 400x. The right panels represent a zoomed area from the original images. ACPA, anticitrullinated protein/peptide antibody; DAPI, 4,6-diamidino-2-phenylindole; FLS, fibroblast-like synoviocytes; IL, interleukin; PAD, protein arginine deiminase; ns, not significant; SF, synovial fluid; TNF, tumour necrosis factor.

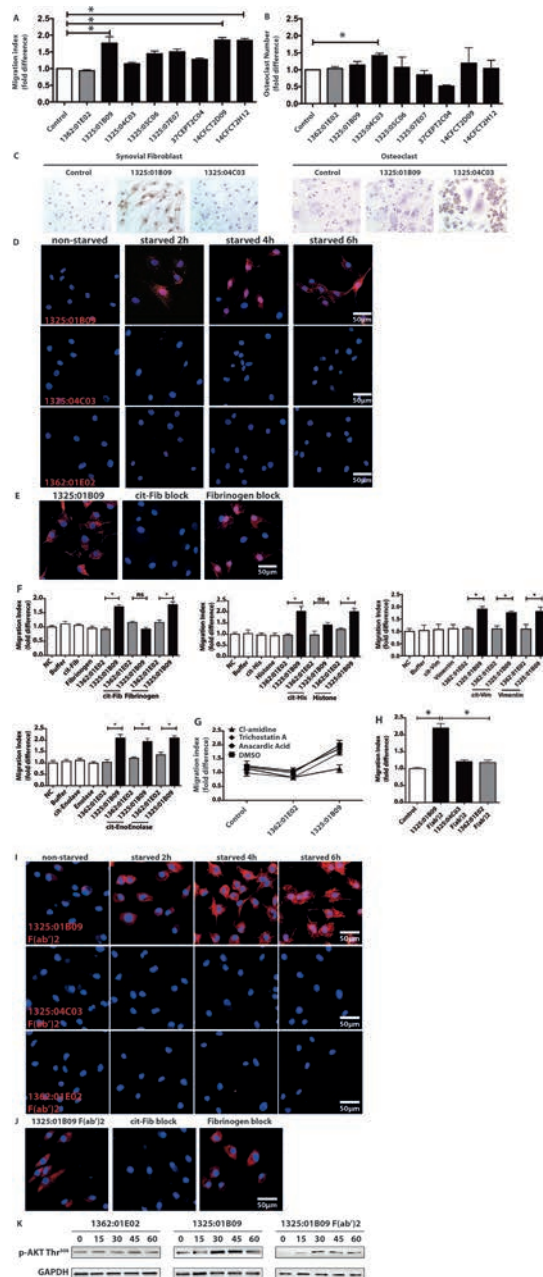


Figure 5 The monoclonal ACPAs 1325:01B09 and 1325:04C03 display selective binding and stimulatory capacities on FLS and osteoclasts. The effects of eight individual ACPA clones were tested in concentration of 1 µg/mL on fibroblast migration (A) and osteoclast differentiation (B) assays. The graphs represent migration index expressed as fold-difference normalised to untreated controls using data from three independent experiments, using cells of three different patients, all performed six replicate samples, *p<0.05. Osteoclast counts expressed in fold-difference normalised to untreated controls using data from two to five independent experiments, performed at least three replicates, *p<0.05. IHC stainings show binding capacity of individual ACPA clones, 1325:01B09 and 1325:04C03 to FLS and osteoclasts (C). Confocal microscopy images illustrate the binding of the ACPA clones (1325:01B09, 1325:04C03) and control (1362:01E02) monoclonal antibodies (red colour) to starved FLS (D). To block monoclonal ACPA binding, starved FLS were also stained with 1325:01B09 (red colour) pre-incubated with citrullinated (cit) or native fibrinogen (cit-Fib or Arg-Fib, respectively) or in the absence of fibrinogen (E). Blocking experiments were performed with cit vimentin (cit-Vim), cit enolase (cit-Eno) and cit histone H4 (cit-His) with 10:1 decoy protein:antibody ratio (F). Migration indexes were obtained from three independent experiments, using cells of three individual patients and six replicates. In addition, monoclonal ACPA-induced migration was blocked by PAD inhibitor (200 nM CI-amidine), but not by histone acetyltransferase or deacetylase inhibitors (10 µM anacardic acid, 0.2 µM trichostatin A) (G). FLS migration was also analysed in the presence of monoclonal ACPA or control IgG F(ab')₂ fragments at a concentration of 0.7 µg/mL. The graphs represent results from three independent experiments, using cells of three individual patients and six sample-replicates (H). Confocal images illustrate the binding of 1325:01B09, 1325:04C03 and 1362:01E02 F(ab')₂ fragments (red colour) to starved FLS (nuclei shown in blue, original magnification 400X (I)). Pre-incubation with citrullinated fibrinogen prevented 1325:01B09 F(ab')₂ fragments binding to starved FLS (nuclei shown in blue, original magnification 400X) (J). Nuclei are shown in blue. Original magnifications of 100x and 400x were used in light and confocal microscopy, respectively. Starved FLS were exposed to 1 µg/mL 1325:01B09, 1362:01E02 or 0.7 µg/mL 1325:01B09 F(ab')₂. Immunoblot analysis of Akt phosphorylation (Thr308 residues) is shown, GAPDH protein was detected as control (K). ACPA, anticitrullinated protein/peptide antibody; DMSO, dimethyl sulfoxide; FLS, fibroblast-like synoviocytes; IHC, immunohistochemistry; PAD, protein arginine deiminase; ns, not significant.

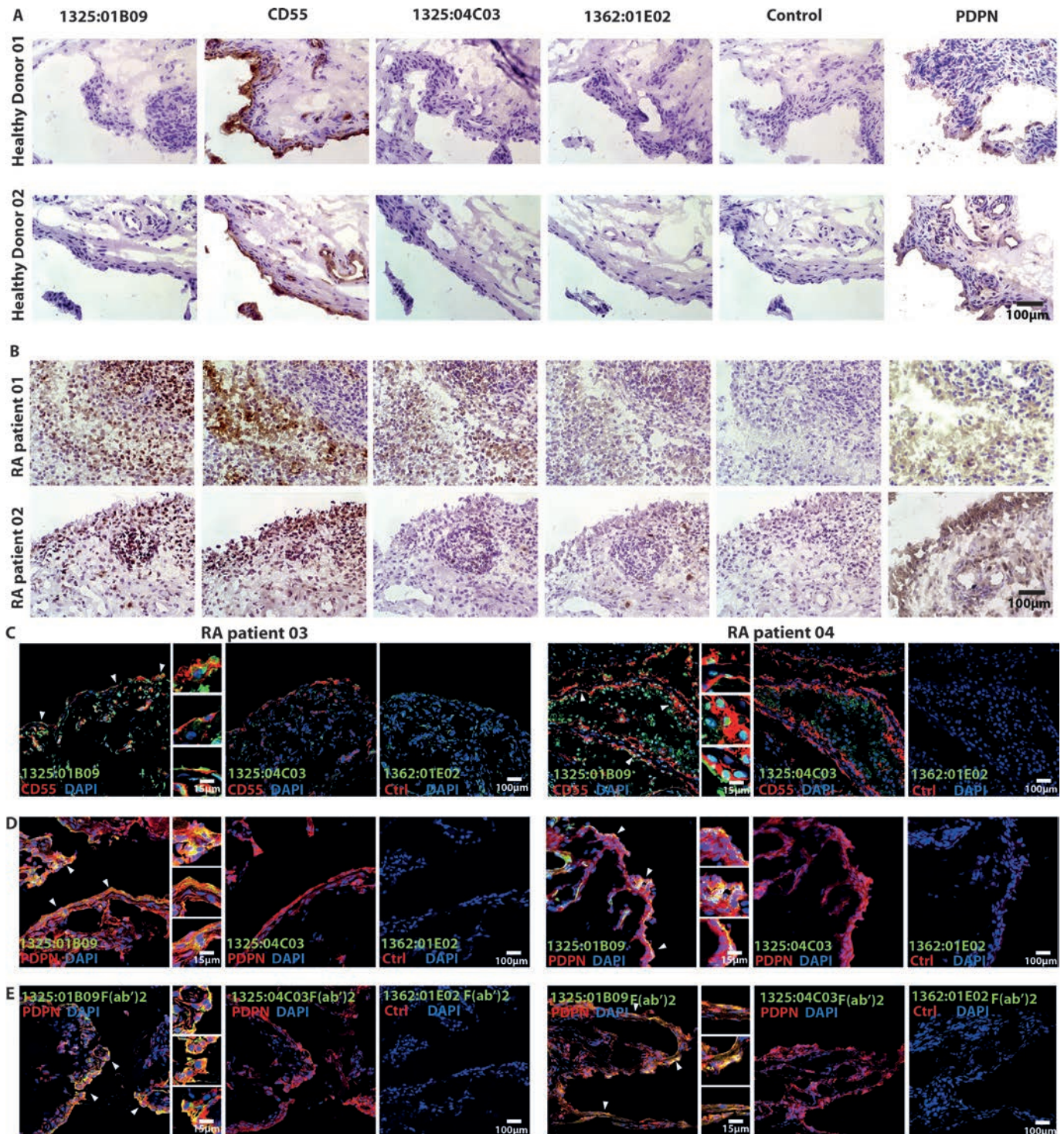


Figure 6 The monoclonal ACPA clones 1325:01B09 and 1325:04C03 bind to synovial targets in patients with RA but not in healthy controls. The immunohistochemistry images illustrate binding patterns of the monoclonal ACPA clones 1325:01B09 and 1325:04C03 to synovial tissues obtained from healthy donors (A) or patients with RA (B). Mouse IgG1 and the non-citrulline-specific 1362:01E02 (E02) monoclonal antibody were used as controls. CD55 and podoplanin (PDPN) stainings highlight FLS-rich areas of the synovial membrane. Immunohistochemistry stainings were analysed with light microscopy using 250x original magnification. (C) Confocal microscopy images illustrate a partial colocalisation of the ACPA clone 1325:01B09 with CD55 (C) and PDPN (D), highlighted by closed arrows. Stainings with the monoclonal ACPA 1325:04C03 and the control 1362:01E02 antibodies are also shown. Moreover, partially colocalisation of 1325:01B09 F(ab')₂ with PDPN were highlighted by arrows (E). An original magnification of 400x was used for confocal microscopy. ACPA, anticitrullinated protein/peptide antibody; DAPI, 4,6-diamidino-2-phenylindole; FLS, fibroblast-like synoviocytes; RA, rheumatoid arthritis.

have been associated with increased levels of pro-inflammatory cytokines and chemokines, including IL-8, as well as concomitant presence of the RF may contribute to synovial fibroblast

sensitisation. A majority but not all individual polyclonal ACPA preparations show a similar migration promoting effect with the polyclonal ACPA pool, suggesting that additional mechanisms

than the ones presented in the current study might be active in a minority of ACPA-positive RA and certainly in a majority of ACPA-negative RA. This remains to be further investigated.

In contrast to OCs, no others tested RA-derived antibodies but ACPAs had an effect on FLS migration, suggesting a citrullination dependency of the observed effect. As such, the paucity of citrullinated targets observed on steady-state FLS might explain the lack of ACPA effects in unchallenged conditions. Indeed, FLS that were challenged by either cellular stress or certain pro-inflammatory signals increased their expression of both PAD enzymes and citrullinated proteins, which sensitised the cells to ACPA effects. Cellular citrullination appears to be important for the ACPA-mediated FLS mobility, as PAD inhibition completely abolished this effect. While other cellular effects of these inhibitors cannot be completely excluded, the blocking experiments with soluble citrullinated proteins and the reproducibility of the effects when using the F(ab')₂ ACPA fragments further strengthens this observation. Importantly, MDA modification, acetylation and homo-citrullination do not appear to influence FLS migration, as demonstrated by the lack of effect of anti-MDA antibodies, the lack of influence of increased or decreased acetylation on the ACPA effects and the migration promoting effects of both homo-citrullinated cross-reactive and non-cross-reactive monoclonal ACPAs.

While citrullination appears to be central for the ACPA effects on FLS, precise identification of the exact cellular target(s) is still a challenge. Although citrullinated fibrinogen has been previously proposed as an interstitial tissue target able to generate immune complexes in the presence of ACPA,⁴¹ our current findings suggest an additional mechanism where ACPAs might interact with surface cellular targets. As individual ACPAs are cross-reactive with a wide range of citrullinated peptides and proteins through their consensus motifs,⁴ as also confirmed by our blocking experiments, it remains to be determined which of these antigens are relevant for the observed effect. It has been suggested that ACPAs are prone to bind minute amounts of LPS that might interfere with interpretation of the functional effects observed with different ACPA preparations.¹⁷ However, our LPS tests were negative and addition of different amounts of exogenous LPS to the FLS cultures with or without ACPAs had no effect on FLS migration (online supplementary figure 9).

FLS motility is governed by complex mechanisms, involving a large array of intracellular signalling pathways^{42–48} that mediate consecutive phases of this process: adhesion, migration and invasion, with PI3K and MAPK playing central roles. We describe here a role for PI3K/Akt but not for MAPK phosphorylation in regulating ACPA-induced migration of challenged FLS. PI3K modulates organisation of actin cytoskeleton and lamellipodium formation via Akt phosphorylation, which can result in cytoskeleton remodelling and increased motility.⁴⁹

A central finding of the current study resides in the selective cellular modulation by distinct monoclonal ACPAs. We show a selective increase of OC formation with the 1325:04C03 clone. This is in line with our previous reported increase of OC formation seen with the 1325:04C03 clone,⁴ that now reaches statistical significance at doses as low as 1 µg/mL, due to the larger number of replicates and the lower variability among the OC precursor cells donors. In spite of the typical cross-reactivity of ACPAs, this selective regulation suggests the targeting of non-overlapping cellular autoantigens. The lack of Fcγ receptors on FLS, the identical IgG1 Fc regions in ACPA clones with different functional effects and the positive effect of ACPA F(ab')₂ fragments on FLS migration suggest a role for specific-antigen binding in the observed ACPA effect. We

propose that unique ACPA clones/specificities might be responsible for specific pathological features in distinct stages of the development of ACPA+RA and some of these effects might be dependent on additional stress/inflammatory signals. Consequently, as ACPA fine-specificities are subjected to constant evolution and different ACPA combinations are present in different individuals,⁵⁰ the selective effects of individual ACPA clones could contribute to variability in the timing of arthritis development and in the symptoms present in seropositive individuals. Notably, this proposed role of ACPA is fully compatible with potential roles also of antibodies with other specificities in the generation of the various symptoms occurring before and during the course of RA.

In conclusion, we describe a novel potential pathogenic role for ACPAs in FLS migration. Our results also give further support for studies to investigate the early therapeutic and potentially preventive effect of drugs such as PAD enzymes inhibitors that affect the currently described mechanisms of FLS migration.

Acknowledgements The authors would like to thank Monika Hansson and Tina Ekenkrantz for rheumatoid factor analysis. The authors would also like to thank Khaled Amara and Iva Gunnarsson for providing phosphoinositide 3-kinase antibodies.

Contributors MS, BR and AIC designed the experiments, analysed the data and wrote the manuscript along with input from VM, HW, CS, AH, SBC and LK. MS designed and performed all fibroblast experiments with help from BR. MS and CO designed and performed adhesion assay. VJ, YL and HW measured chemokines and cytokines in supernatants. MS and ME performed all immunohistochemistry experiments with help from AC. EO performed and analysed mass spectrometry data. AK conducted osteoclast assays. AH recruited patients and characterised all clinical data. HW purified polyclonal ACPAs. JS, CG and VM produced and validated monoclonal ACPAs. AIC, MS, BR, AK, VJ, HW, AC, VM and LK discussed and developed the concept. All authors critically reviewed and approved the final form of the manuscript.

Funding This project has received funding from FOREUM, Foundation for Research in Rheumatology, from the European Research Council (ERC) under the European Union's Horizon 2020 research and innovation program (grant agreement CoG 2017—7722209_PREVENT RA and grant agreement 777357_RT Cure), from the Swedish Research Council and Konung Gustaf V:s och Drottning Victorias Frimurare Stiftelse.

Competing interests None declared.

Patient consent for publication Not required.

Ethics approval This study involves human participants with ethical permit listed in blow: (1) Kartläggning av prediktiva biomarkörer vid kronisk artrit ID: 2009-358-31-3; (2) Kartläggning av inflammatoriska mediators betydelse för sjukdomsforlopp vid kroniska ledsjukdomar ID:2009-1262-31-3.

Provenance and peer review Not commissioned; externally peer reviewed.

Data availability statement Data are available on reasonable request.

Open access This is an open access article distributed in accordance with the Creative Commons Attribution 4.0 Unported (CC BY 4.0) license, which permits others to copy, redistribute, remix, transform and build upon this work for any purpose, provided the original work is properly cited, a link to the licence is given, and indication of whether changes were made. See: <https://creativecommons.org/licenses/by/4.0/>.

ORCID iDs

Meng Sun <http://orcid.org/0000-0002-9301-0421>

Lars Klareskog <http://orcid.org/0000-0001-9601-6186>

REFERENCES

- Klareskog L, Catrina AI, Paget S. Rheumatoid arthritis. *Lancet* 2009;373:659–72.
- Titcombe PJ, Wigerblad G, Sippl N, et al. Pathogenic Citrulline-Multispecific B cell receptor clades in rheumatoid arthritis. *Arthritis Rheumatol* 2018;70:1933–45.
- Lloyd KA, Steen J, Amara K, et al. Variable domain N-linked glycosylation and negative surface charge are key features of monoclonal ACPA: implications for B-cell selection. *Eur J Immunol* 2018;48:1030–45.
- Steen J, Forsström B, Sahlström P, et al. Recognition of amino acid motifs, rather than specific proteins, by human plasma Cell-Derived monoclonal antibodies to posttranslationally modified proteins in rheumatoid arthritis. *Arthritis Rheumatol* 2019;71:196–209.

- 5 Bos WH, Wolbink GJ, Boers M, *et al.* Arthritis development in patients with arthralgia is strongly associated with anti-citrullinated protein antibody status: a prospective cohort study. *Ann Rheum Dis* 2010;69:490–4.
- 6 Kleyer A, Finzel S, Rech J, *et al.* Bone loss before the clinical onset of rheumatoid arthritis in subjects with anticitrullinated protein antibodies. *Ann Rheum Dis* 2014;73:854–60.
- 7 Krishnamurthy A, Ytterberg AJ, Sun M, *et al.* Citrullination controls dendritic cell transdifferentiation into osteoclasts. *Ji* 2019;202:3143–50.
- 8 Rantapää-Dahlqvist S, de Jong BAW, Berglin E, *et al.* Antibodies against cyclic citrullinated peptide and IgA rheumatoid factor predict the development of rheumatoid arthritis. *Arthritis Rheum* 2003;48:2741–9.
- 9 Harre U, Georgess D, Bang H, *et al.* Induction of osteoclastogenesis and bone loss by human autoantibodies against citrullinated vimentin. *J Clin Invest* 2012;122:1791–802.
- 10 Krishnamurthy A, Joshua V, Haj Hensvold A, *et al.* Identification of a novel chemokine-dependent molecular mechanism underlying rheumatoid arthritis-associated autoantibody-mediated bone loss. *Ann Rheum Dis* 2016;75:721–9.
- 11 Wigerblad G, Bas DB, Fernandes-Cerqueira C, *et al.* Autoantibodies to citrullinated proteins induce joint pain independent of inflammation via a chemokine-dependent mechanism. *Ann Rheum Dis* 2016;75:730–8.
- 12 Anon. Correction: Autoantibodies to citrullinated proteins induce joint pain independent of inflammation via a chemokine-dependent mechanism. *Ann Rheum Dis* 2019;78:865.
- 13 Anon. Correction: Identification of a novel chemokine-dependent molecular mechanism underlying rheumatoid arthritis-associated autoantibody-mediated bone loss. *Ann Rheum Dis* 2019;78:866.
- 14 Wang L, Jiang X, Zheng Q, *et al.* Neuronal FcγRI mediates acute and chronic joint pain. *J Clin Invest* 2019;130:128010.
- 15 Grönwall C, Amara K, Hardt U, *et al.* Autoreactivity to malondialdehyde-modifications in rheumatoid arthritis is linked to disease activity and synovial pathogenesis. *J Autoimmun* 2017;84:29–45.
- 16 Bersellini Farinotti A, Wigerblad G, Nascimento D, *et al.* Cartilage-binding antibodies induce pain through immune complex-mediated activation of neurons. *J Exp Med* 2019;216:1904–24.
- 17 Toes R, Pisetsky DS. Pathogenic effector functions of AcpA: where do we stand? *Ann Rheum Dis* 2019;78:716–21.
- 18 Kuhn KA, Kulik L, Tomooka B, *et al.* Antibodies against citrullinated proteins enhance tissue injury in experimental autoimmune arthritis. *J Clin Invest* 2006;116:961–73.
- 19 Dakin SG, Coles M, Sherlock JP, *et al.* Pathogenic stromal cells as therapeutic targets in joint inflammation. *Nat Rev Rheumatol* 2018;14:714–26.
- 20 Lefèvre S, Knedla A, Tennie C, *et al.* Synovial fibroblasts spread rheumatoid arthritis to unaffected joints. *Nat Med* 2009;15:1414–20.
- 21 Müller-Ladner U, Kriegsmann J, Franklin BN, *et al.* Synovial fibroblasts of patients with rheumatoid arthritis attach to and invade normal human cartilage when engrafted into SCID mice. *Am J Pathol* 1996;149:1607–15.
- 22 Ossipova E, Cerqueira C, Reed E, *et al.* Affinity purified anti-citrullinated protein/peptide antibodies target antigens expressed in the rheumatoid joint. *Arthritis Res Ther* 2014;16.
- 23 Amara K, Israelsson L, Stålesen R, *et al.* A refined protocol for identifying Citrulline-specific monoclonal antibodies from single human B cells from rheumatoid arthritis patient material. *Bio-protocol* 2019;9.
- 24 Foulquier C, Sebbag M, Clavel C, *et al.* Peptidyl arginine deiminase type 2 (PAD-2) and PAD-4 but not PAD-1, PAD-3, and PAD-6 are expressed in rheumatoid arthritis synovium in close association with tissue inflammation. *Arthritis Rheum* 2007;56:3541–53.
- 25 Lloyd KA, Wigerblad G, Sahlström P, *et al.* Differential AcpA binding to nuclear antigens reveals a PAD-independent pathway and a distinct subset of acetylation cross-reactive autoantibodies in rheumatoid arthritis. *Front Immunol* 2018;9:3033.
- 26 Binstadt BA, Patel PR, Alencar H, *et al.* Particularities of the vasculature can promote the organ specificity of autoimmune attack. *Nat Immunol* 2006;7:284–92.
- 27 Crowley T, O'Neil JD, Adams H, *et al.* Priming in response to pro-inflammatory cytokines is a feature of adult synovial but not dermal fibroblasts. *Arthritis Res Ther* 2017;19.
- 28 Arend WP, Firestein GS. Pre-rheumatoid arthritis: predisposition and transition to clinical synovitis. *Nat Rev Rheumatol* 2012;8:573–86.
- 29 Unanue ER, Perkins WD, Karnovsky MJ. Ligand-Induced movement of lymphocyte membrane macromolecules: I. Analysis by immunofluorescence and ultrastructural radioautography. *J Exp Med* 1972;136:885–906.
- 30 Taylor RB, Duffus WPH, Raff MC, *et al.* Redistribution and pinocytosis of lymphocyte surface immunoglobulin molecules induced by anti-immunoglobulin antibody. *Nat New Biol* 1971;233:225–9.
- 31 Wacholtz MC, Lipsky PE. Anti-Cd3-Stimulated Ca²⁺ signal in individual human peripheral T cells: activation correlates with a sustained increase in intracellular Ca²⁺. *J Immunol* 1993;150:5338–49.
- 32 Ghetie M-A, Podar EM, Ilgen A, *et al.* Homodimerization of tumor-reactive monoclonal antibodies markedly increases their ability to induce growth arrest or apoptosis of tumor cells. *Proc Natl Acad Sci U S A* 1997;94:7509–14.
- 33 Zhao Y, Kohler H. Enhancing tumor targeting and apoptosis using noncovalent antibody homodimers. *J Immunother* 2002;25:396–404.
- 34 Bigoni M, Turati M, Sacerdote P, *et al.* Characterization of synovial fluid cytokine profiles in chronic meniscal tear of the knee. *J Orthop Res* 2017;35:340–6.
- 35 Adams SB, Nettles DL, Jones LC, *et al.* Inflammatory cytokines and cellular metabolites as synovial fluid biomarkers of posttraumatic ankle arthritis. *Foot Ankle Int* 2014;35:1241–9.
- 36 Adams SB, Leimer EM, Setton LA, *et al.* Inflammatory microenvironment persists after bone healing in intra-articular ankle fractures. *Foot Ankle Int* 2017;38:479–84.
- 37 Irie K, Uchiyama E, Iwasa H. Intraarticular inflammatory cytokines in acute anterior cruciate ligament injured knee. *Knee* 2003;10:93–6.
- 38 Okamura K, Kobayashi T, Yamamoto A, *et al.* Shoulder pain and intra-articular interleukin-8 levels in patients with rotator cuff tears. *Int J Rheum Dis* 2017;20:177–81.
- 39 Mateo L, La Linn M, McColl SR, *et al.* An arthrogenic alphavirus induces monocyte chemoattractant protein-1 and interleukin-8. *Intervirology* 2000;43:55–60.
- 40 Theilacker C, Held J, Allering L, *et al.* Prolonged polyarthralgia in a German traveller with Mayaro virus infection without inflammatory correlates. *BMC Infect Dis* 2013;13:369.
- 41 Masson-Bessière C, Sebbag M, Girbal-Neuhaus E, *et al.* The major synovial targets of the rheumatoid arthritis-specific Antifilaggrin autoantibodies are deiminated forms of the α- and β-Chains of fibrin. *J Immunol* 2001;166:4177–84.
- 42 Choe J-Y, Hun Kim J, Park K-Y, *et al.* Activation of Dickkopf-1 and focal adhesion kinase pathway by tumour necrosis factor α induces enhanced migration of fibroblast-like synoviocytes in rheumatoid arthritis. *Rheumatology* 2016;55:928–38.
- 43 Gerarduzzi C, He Q, Zhai B, *et al.* Prostaglandin E2-dependent phosphorylation of Ras inhibition 1 (Rin1) at Ser 291 and 292 inhibits transforming growth factor-β-induced Ras activation pathway in human synovial fibroblasts: role in cell migration. *J Cell Physiol* 2017;232:202–15.
- 44 Grespan R, Fukada SY, Lemos HP, *et al.* CXCR2-specific chemokines mediate leukotriene B₄-dependent recruitment of neutrophils to inflamed joints in mice with antigen-induced arthritis. *Arthritis Rheum* 2008;58:2030–40.
- 45 Lv Q, Zhu XY, Xia YF, *et al.* Tetrandrine inhibits migration and invasion of rheumatoid arthritis fibroblast-like synoviocytes through down-regulating the expressions of Rac1, Cdc42, and RhoA GTPases and activation of the PI3K/Akt and JNK signaling pathways. *Chin J Nat Med* 2015;13:831–41.
- 46 Shelef MA, Bennis DA, Yasmin N, *et al.* Focal adhesion kinase is required for synovial fibroblast invasion, but not murine inflammatory arthritis. *Arthritis Res Ther* 2014;16.
- 47 Xue G, Hemmings BA. PKB/Akt-dependent regulation of cell motility. *J Natl Cancer Inst* 2013;105:393–404.
- 48 Yuan H, Yang P, Zhou D, *et al.* Knockdown of sphingosine kinase 1 inhibits the migration and invasion of human rheumatoid arthritis fibroblast-like synoviocytes by down-regulating the PI3K/Akt activation and MMP-2/9 production in vitro. *Mol Biol Rep* 2014;41:5157–65.
- 49 Kolsch V, Charest PG, Firtel RA. The regulation of cell motility and chemotaxis by phospholipid signaling. *J Cell Sci* 2008;121:551–9.
- 50 Brink M, Hansson M, Mathsson L, *et al.* Multiplex analyses of antibodies against citrullinated peptides in individuals prior to development of rheumatoid arthritis. *Arthritis Rheum* 2013;65:899–910.

TRANSLATIONAL SCIENCE

CD109 regulates the inflammatory response and is required for the pathogenesis of rheumatoid arthritis

Guanhua Song,¹ Tingting Feng,² Ru Zhao,² Qiqi Lu,³ Yutao Diao,¹ Qingwei Guo,⁴ Zhaoxia Wang,¹ Yuang Zhang,³ Luna Ge,⁵ Jihong Pan,⁵ Lin Wang ,⁵ Jinxiang Han⁵**Handling editor** Josef S Smolen

► Additional material is published online only. To view please visit the journal online (<http://dx.doi.org/10.1136/annrheumdis-2019-215473>).

For numbered affiliations see end of article.

Correspondence to

Dr Lin Wang, Key Laboratory for Rare and Uncommon Diseases of Shandong Province, Research Center for Medicinal Biotechnology, Shandong First Medical University & Shandong Academy of Medical Sciences, Jinan 250062, China; wanglin.83@163.com Professor Jinxiang Han; sams-h2016@163.com

Received 2 April 2019
Revised 31 July 2019
Accepted 6 August 2019
Published Online First
27 August 2019

ABSTRACT

Objective The aim of this study was to investigate the role of CD109 in rheumatoid arthritis (RA) fibroblast-like synoviocytes (FLSs) and to evaluate its potential as a therapeutic target.

Methods CD109 expression was examined in synovial tissues and FLSs from RA patients and collagen-induced arthritis (CIA) model mice. CD109-deficient mice were developed to evaluate the severity of CIA. Small interfering RNAs and a neutralising antibody against CD109 (anti-CD109) were designed for functional or treatment studies in RA FLSs and CIA.

Results CD109 was found to be abundantly expressed in the synovial tissues from RA patients and CIA mice. CD109 expression in RA FLSs was upregulated by inflammatory stimuli, such as interleukin-1 β and tumour necrosis factor- α . Silencing of CD109 or anti-CD109 treatment reduced proinflammatory factor production, cell migration, invasion, chemoattractive potential and osteoclast differentiation, thereby reducing the deleterious inflammatory response of RA FLSs in vitro. Mice lacking CD109 were protected against arthritis in the CIA model. Anti-CD109 treatment prevented the onset and ameliorated the severity of CIA lesions.

Conclusion Our study uncovers an antiarthritic role for CD109 and suggests that CD109 inhibition might serve as a promising novel therapeutic strategy for RA.

INTRODUCTION

Rheumatoid arthritis (RA) is a systemic autoimmune disease characterised by chronic inflammation and hyperplasia of fibroblast-like synoviocytes (FLSs).¹ RA FLSs display an aggressive phenotype and produce excessive amounts of proinflammatory cytokines and matrix-degrading enzymes, resulting in joint dysfunction and destruction.² Hence, identifying key factors that specifically target RA FLS-mediated inflammation may provide novel therapeutic targets for RA.

CD109 is a cell-surface antigen that belongs to the α 2-macroglobulin/C3, C4, C5 family of thioester-containing proteins.³ As a glycosylphosphatidylinositol-anchored protein,⁴ increased expression of CD109 in various tumours is indicative of a more aggressive phenotype and poor prognosis.^{5–7} Since RA FLSs exhibit tumour-like proliferation and invasion behaviours,² it is possible that CD109 may play a role in the aggressive phenotype of RA FLSs. It has been reported that CD109 interacts with glucose-regulated protein 78 (GRP78), a classical endoplasmic

Key message**What is already known about this subject?**

- CD109 regulates diverse pathogenic processes, including fibrosis, osteoporosis and tumour metastasis.
- CD109 inhibits transforming growth factor (TGF)- β signalling by enhancing SMAD7/Smurf2-dependent degradation of the TGF- β receptor.

What does this study add?

- CD109 is required to sustain rheumatoid arthritis (RA) fibroblast-like synoviocyte (FLS)-induced inflammation.
- CD109 interacts with and stabilises ENO1 to regulate the RA FLS-mediated inflammatory response.
- An anti-CD109 antibody shows both prophylactic and therapeutic effects in collagen-induced arthritis mice.

How might this impact on clinical practice or future developments?

- CD109 could be a promising treatment target for RA.

reticulum (ER) chaperone, to inhibit transforming growth factor (TGF- β) signalling in response to ER stress.⁸ Interestingly, GRP78 acts as a pathological factor that contributes to the severity of RA,⁹ suggesting that CD109 is likely involved in the pathological progression of RA.

A previous study demonstrated that CD109 inhibits TGF- β signalling by enhancing SMAD7/Smurf2-dependent degradation of the TGF- β receptor TGF β RI.^{10–11} More interestingly, although CD109 inactivates TGF- β signalling and subsequent fibrosis, fibroblasts with increased CD109 protein levels still produce excessive amounts of extracellular matrix (ECM).¹² It is thus believed that CD109 is insufficient to completely counteract the effect of TGF- β activation on fibrosis, and the exact role of elevated CD109 in fibroblasts remains unclear. Recently, CD109 has been shown to activate Jak-Stat3 signalling, which consequently leads to a metastatic phenotype in lung cancer cells.¹³ This evidence indicates that CD109 functions in a cell-specific manner, and it would be interesting to characterise the exact role of CD109 in RA FLSs.



© Author(s) (or their employer(s)) 2019. Re-use permitted under CC BY-NC. No commercial re-use. See rights and permissions. Published by BMJ.

To cite: Song G, Feng T, Zhao R, et al. *Ann Rheum Dis* 2019;**78**:1632–1641.

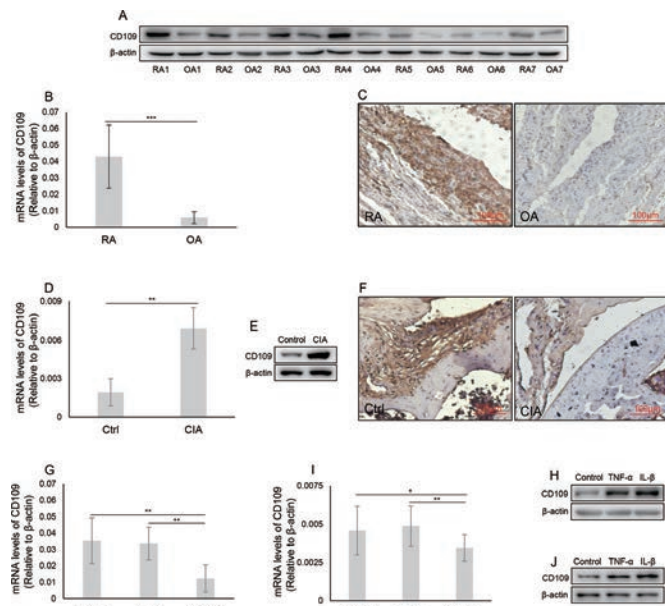


Figure 1 Expression of CD109 in synovial tissues extracted from RA patients and CIA model mice. (A) Western blot analysis of CD109 protein in synovial tissues from RA (n=7) and OA (n=7) patients. β -Actin was used as a loading control. (B) Quantitative real-time (qRT) PCR analysis of CD109 mRNA levels in FLSs from RA (n=7) and OA (n=7) patients. $***p < 0.001$. (C) Immunohistochemical staining of RA (n=16) and OA (n=7) synovial tissues using antibodies against CD109. Original magnification is 200 \times . FLSs were collected from DBA/1J mice immunised with collagen (CIA mice) or bovine serum albumin (BSA, referred to as Ctrl mice). qRT-PCR and Western blot assays were performed to assess the levels of CD109 mRNA (D) and protein (E). n=3 per group, $**p < 0.01$. (F) Immunohistochemical staining of CD109 from the hind paw in CIA and Ctrl mice. FLSs from RA patients (G and H) or CIA model mice (I and J) were stimulated with TNF- α or IL-1 β for 24 hours. Total RNA and protein levels were subjected to qRT-PCR and Western blotting for the analysis of CD109 mRNA (G and I) and protein (H and J) levels. qRT-PCR data in G and I are expressed as the mean of six samples (three male and three female) or three mice from two independent experiments. Western blot data in H and J represent two independent experiments from six samples (three males and three females) or three mice with similar results. $*p < 0.05$ and $**p < 0.01$ compared with vehicle. CIA, collagen-induced arthritis; FLSs, fibroblast-like synoviocytes; IL-1 β , interleukin-1 β ; OA, osteoarthritis; RA, rheumatoid arthritis; TNF- α , tumour necrosis factor- α .

The present study was conducted to investigate the role of CD109 in RA FLSs and collagen-induced arthritis (CIA) models and to assess the potential of CD109 inhibition as a treatment approach in RA.

MATERIALS AND METHODS

Detailed methods and sequence primers are described in the online supplementary materials and methods.

Reagent and cell stimulation

RA FLSs were plated in 24-well plates (3–5 \times 10⁵ cells/well) in Dulbecco's Modified Eagle's Medium and stimulated for the indicated time points with the following agents: tumour necrosis factor (TNF)- α (10 ng/mL, Abnova, Taiwan, China), interleukin (IL)-1 β (10 ng/mL, Abnova), cycloheximide (CHX, 10 μ g/mL, Calbiochem), galunisertib (10 μ M, Selleck), TGF- β 1 (1 ng/mL or 10 ng/mL, R&D), macrophage colony-stimulating

factor (M-CSF; 30 ng/mL, R&D) and RANKL (50 ng/mL, R&D). The dilution buffer, phosphate buffer saline, was applied as vehicle control.

RESULTS

CD109 is abundantly expressed in the synovial tissues of patients with RA

CD109 was first found to be abundantly expressed in all RA patient synovial tissues but dramatically reduced in osteoarthritis (OA) samples (figure 1A). In vitro, CD109 mRNA expression in RA FLSs was relatively higher than that in OA FLSs (figure 1B). Immunohistochemical staining showed that CD109 was expressed at higher levels in RA synovial tissues than in OA synovial tissues and mainly distributed in the lining layer of the RA synovial tissues (figure 1C). A similar increase in CD109 expression was also observed in FLSs (figure 1D,E) and synovial tissues (figure 1F) from CIA mice when compared with those from wild-type (WT) mice. In addition, CD109 expression was elevated at the mRNA (figure 1G,I) and protein (figure 1H,J) levels in FLSs from RA patients and CIA mice following TNF- α and IL-1 β stimulation, but not following IL-1 α , IL-6 and IL-17 stimulation (online supplementary figure 1).¹⁴

Effects of CD109 on the inflammatory phenotype of RA FLSs

RA FLSs can secrete IL-6, IL-8, matrix metalloproteinase (MMP)-1, MMP-3 and MMP-13 in response to IL-1 β and TNF- α stimulation, and these factors are implicated in the RA FLS-mediated inflammatory response.^{15–22} We next measured the levels of these proteins in the supernatant of siCD109-transfected or siCtrl-transfected RA FLS. The silencing efficiency of small interfering RNAs (siRNAs) against CD109 was confirmed by Western blot (figure 2A). The data showed that silencing of CD109 significantly reduced the levels of IL-6, IL-8, MMP-1 and MMP-3 (figure 2B–E), but not MMP-13 (data not shown), in the supernatants of RA FLSs with or without TNF- α and IL-1 β stimulation. Additionally, CD109 knockdown resulted in an obvious reduction in TNF- α -induced^{23–24} or IL-1 β -induced^{25–27} phosphorylation of AKT serine/threonine kinase (Akt), nuclear factor-kappa B (NF- κ B), signal transducer and activator of transcription 3 (Stat3) and p38 MAPK signalling proteins (figure 2F). CXCL9/10 modulates RA immune responses by activating and recruiting leucocytes.^{28–29} CD109 knockdown significantly reduced the production of CXCL9 and CXCL10 (figure 2G,H) in RA FLSs. The number of migrating leucocytes cultured with conditioned medium (CM) from siCD109-transfected RA FLSs also decreased significantly (figure 2I), suggesting decreased chemoattractive potential of RA FLSs. Furthermore, RA FLSs with CD109 downregulation displayed reduced levels of migration (figure 2J) and invasion (figure 2K). However, proliferation and apoptosis did not differ between siCD109-transfected RA FLSs and siCtrl-transfected RA FLSs (online supplementary figure 2A–B). Together, these data indicate the importance of CD109 inhibition in limiting the RA FLS-mediated inflammatory response.

CD109 acts as a negative regulator of TGF- β signalling by promoting the degradation of its receptor TGF β RI.^{10–12} However, CD109 is insensitive to TGF- β 1 in RA FLSs (online supplementary figure 3A). Blocking TGF- β signalling by treating cells with the specific inhibitor, galunisertib, did not attenuate the CD109 overexpression-induced increase in IL-6, IL-8, MMP-1, MMP-3, CXCL9 and CXCL10 expression in RA FLSs (online supplementary figure 3B–G). Our data suggest that CD109 regulates the RA FLS-mediated inflammation in a TGF- β signalling-independent manner.

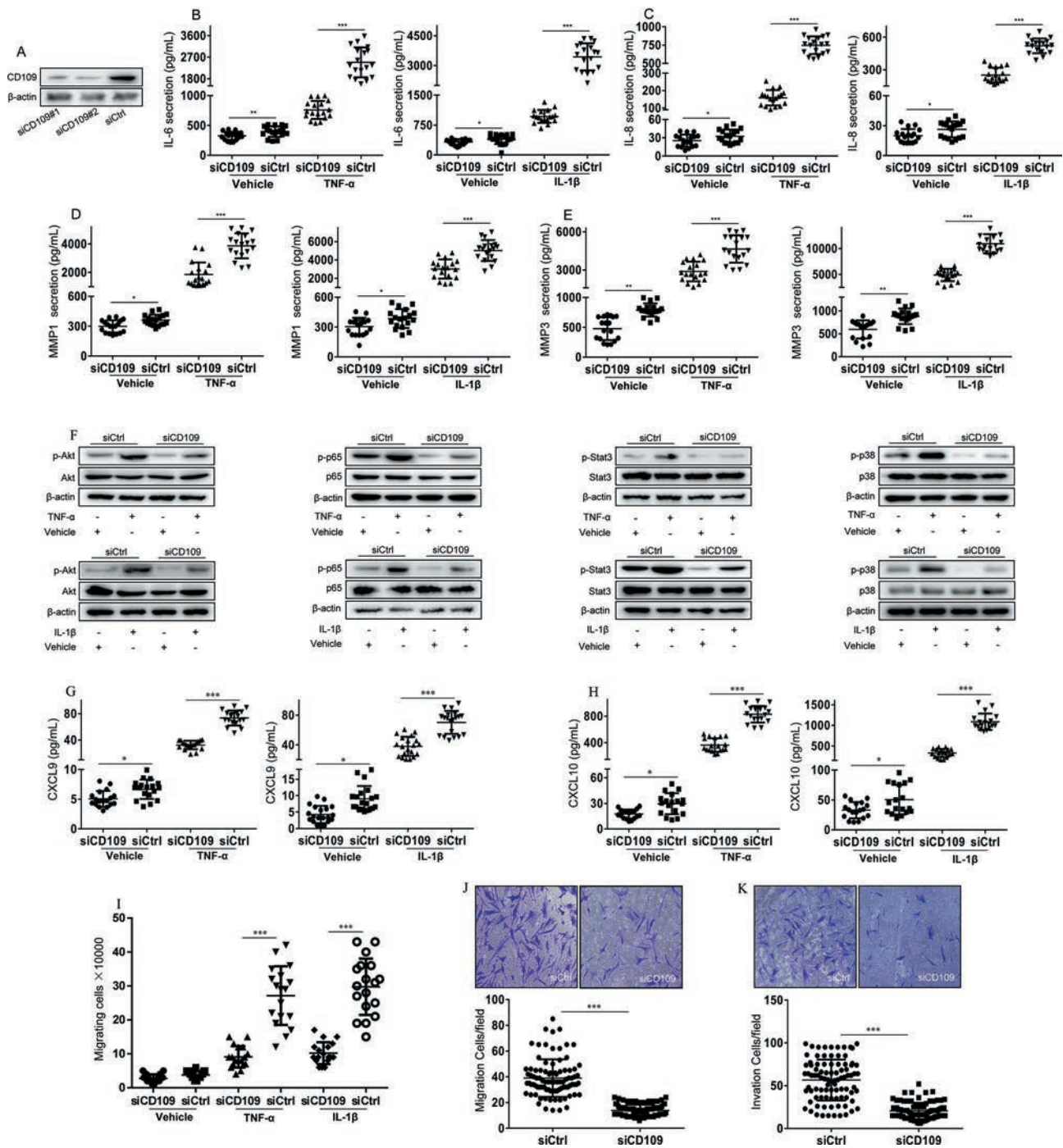


Figure 2 Effects of CD109 silencing on FLS in RA. (A) Silencing efficiency of siRNA targeting CD109 (siCD109) was detected by Western blot. The two siRNAs were combined at equal concentrations for the subsequent experiments. The negative control siRNA is referred to as siCtrl. The results are representative of two independent experiments with three different samples in each. (B–E) Following transfection with siCD109 or siCtrl for 12 hours, RA FLSs were stimulated with TNF-α and IL-1β for another 24 hours. IL-6 (B), IL-8 (C), MMP-1 (D) and MMP-3 (E) levels in the supernatant were analysed by ELISA. (F) Using similar treatments as B–E, total and phosphorylated levels of Akt, p65, Stat3 and p38 MAPK were analysed by Western blot. Western blot data are representative of two independent experiments from six different patients (three males and three females) with similar results. (G and H) RA FLSs were transfected with siCD109/siCtrl for 12 hours, followed by TNF-α or IL-1β stimulation for another 24 hours. CXCL9 (G) and CXCL10 (H) levels in the culture supernatant were measured by ELISA. Data in B–E, G and H are expressed as the mean of six samples (three males and three females) ± SD and represent three independent experiments. (I) After treatment as indicated in B–E, cell-free RA FLS supernatant was collected and used as a chemotactic source for healthy donor peripheral blood leucocytes (n=3) in a transwell migration system for 6 hours. The number of migrating leucocytes in the lower compartment was counted. The migration (J) and invasion (K) abilities were assessed in siCD109-transfected or siCtrl-transfected RA FLS from six different patients (three males and three females). Data represent independent experiments performed in triplicate, and five different fields were selected for cell counting (graph below). RA FLSs passing through the polycarbonate membrane with ECM coating show that cell invasion requires the ECM proteolysis step in addition to migration. *p<0.05, **p<0.01 and ***p<0.001 compared with siCtrl. ECM, extracellular matrix; FLSs, fibroblast-like synoviocytes; IL, interleukin; MMP, matrix metalloproteinase; RA, rheumatoid arthritis; siRNAs, small interfering RNAs; TNF-α, tumor necrosis factor-α.

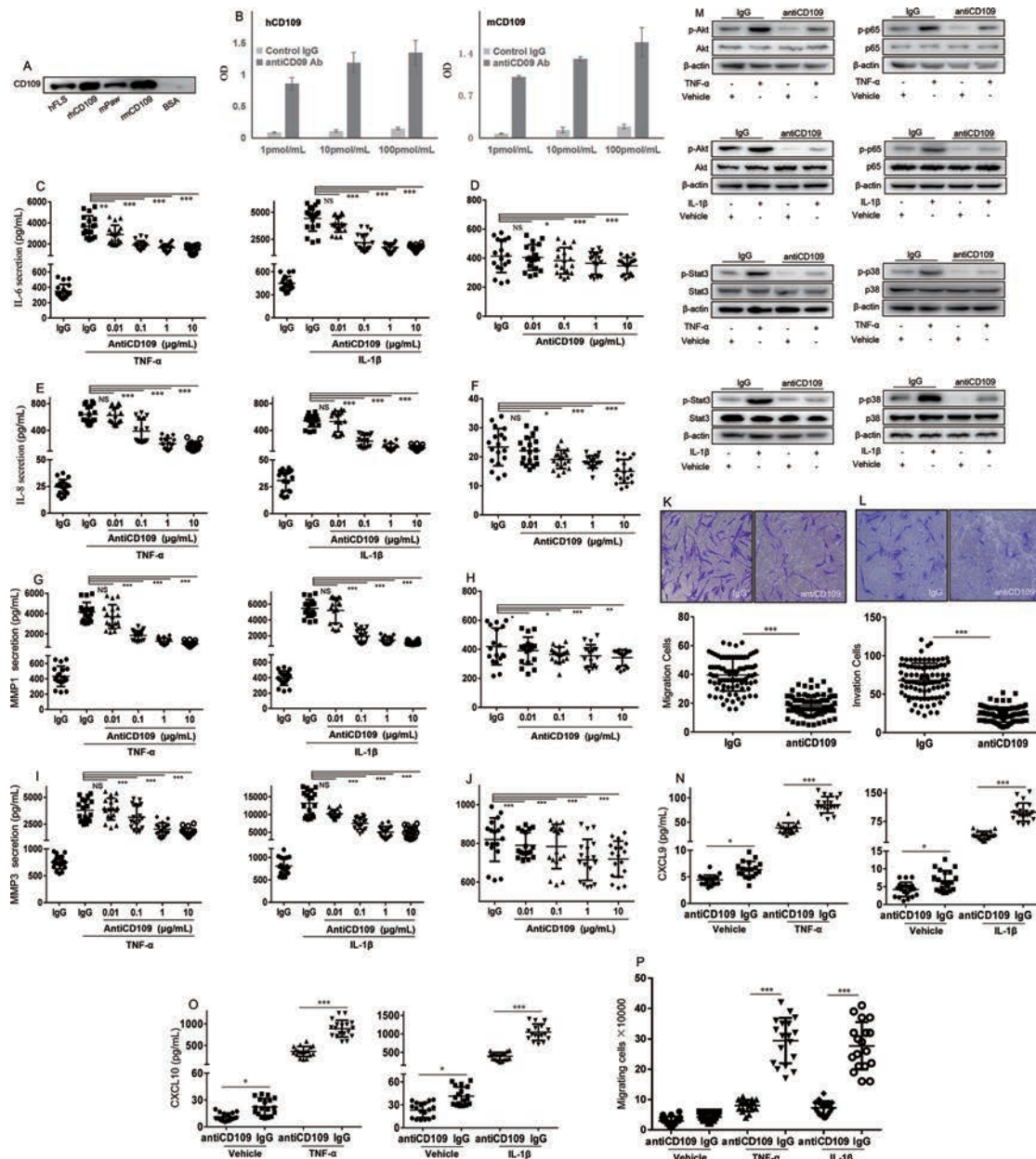


Figure 3 Effects of an antibody against CD109 (anti-CD109) on RA FLs. (A) Western blot analysis of anti-CD109 against human RA FLs (hFLS), recombinant human CD109 protein (rhCD109), mouse paw (mPaw), recombinant mouse CD109 (rmCD109) and BSA. Data are representative of three independent experiments. (B) ELISA analysis for the binding affinity of anti-CD109 towards human CD109 (hCD109, 1 µg) and mouse CD109 (mCD109, 1 µg) proteins at the indicated concentration. Anti-CD109 bound to both human and mouse recombinant CD109 protein dose dependently. The data are expressed as the mean±SD from three independent experiments. (C–J) Following stimulation with TNF-α and IL-1β or nothing for 12 hours, RA FLs were subsequently treated with anti-CD109 at the indicated concentration or IgG (10 µg/mL) for another 24 hours. IL-6 (C and D), IL-8 (E and F), MMP-1 (G and H) and MMP-3 (I and J) levels in the culture supernatant were measured by ELISA. The data are expressed as the mean±SD of six samples (three male and three female) and are representative of three independent experiments. **p*<0.05, ***p*<0.01 and ****p*<0.001 compared with IgG in the presence (C, E, G and I) or absence (D, F, H and J) of inflammatory stimuli. The migration (K) and invasion (L) of RA FLs from six different patients (three males and three females) were assessed and quantified (graph below) after the addition of anti-CD109 (10 µg/mL) or IgG (10 µg/mL) and incubation for 24 hours. ****p*<0.001 compared with IgG. (M) After exposure to TNF-α or IL-1β for 12 hours, RA FLs were treated with anti-CD109 (10 µg/mL) for another 24 hours. Total and phosphorylated levels of Akt, p65, Stat3 and p38 MAPK in RA FLs from six samples (three males and three females) were analysed by Western blot. Western blot data are representative of two independent experiments. RA FLs were incubated with anti-CD109/IgG (10 µg/mL) for 12 hours and treated with TNF-α or IL-1β for another 24 hours. CXCL9 (N) and CXCL10 (O) levels in the culture supernatant were measured by ELISA. Data are expressed as the mean±SD of six samples (three males and three females) and are representative of three independent experiments. **p*<0.05 and ****p*<0.001 compared with siCtrl or IgG. (P) After pretreatment with anti-CD109/IgG (10 µg/mL) for 12 hours, RA FLs from six different patients (three males and three females) were treated with inflammatory stimuli for another 24 hours. Cell-free supernatants were collected and used as a chemoattractant source for healthy donor peripheral blood leucocytes (n=3) in a transwell migration system for 6 hours. The number of migrating leucocytes in the lower compartment was counted. ****p*<0.001 compared with IgG. BSA, bovine serum albumin; FLs, fibroblast-like synoviocytes; IL, interleukin; IgG, immunoglobulin G; MMP, matrix metalloproteinase; NS, not significant; RA, rheumatoid arthritis; TNF-α, tumour necrosis factor-α.

Anti-CD109 treatment ameliorates the arthritis phenotype of RA FLSs

We next produced an anti-CD109 antibody (anti-CD109) and confirmed its specificity towards human and mouse CD109 by Western blot (figure 3A) and ELISA (figure 3B). The data showed that anti-CD109 treatment dose-dependently reduced the levels of IL-6 (figure 3C,D), IL-8 (figure 3E,F), MMP-1 (figure 3G,H) and MMP-3 (figure 3I,J) irrespective of TNF- α or IL-1 β stimulation. Furthermore, anti-CD109 treatment reduced the migration (figure 3K) and invasion (figure 3L) of RA FLSs. However, no obvious differences in the proliferation and apoptosis rates of RA FLSs were detected between anti-CD109 and IgG treatments (online supplementary figure 2C, D). In addition, the levels of phosphorylated Akt, NF- κ B, Stat3 and p38 MAPK in TNF- α -stimulated or IL-1 β -stimulated RA FLSs were all reduced by anti-CD109 treatment (figure 3M). Similarly, there was a strong reduction in CXCL9 and CXCL10 levels (figure 3N,O) in RA FLSs and migrating leucocytes (figure 3P) cultured with CM from anti-CD109-treated RA FLSs.

In addition, we analysed the effects of anti-CD109 on the TNF- α or IL-1 β response in FLSs from CD109-knockout (CD109 KO) and WT mice. Anti-CD109 addition did not reduce the TNF- α -induced or IL-1 β -induced increase in IL-6, MMP-3, CXCL9 and CXCL10 levels in CD109 KO FLSs, as it did in WT FLSs (online supplementary figure 4A-D). These results indicate the engagement of CD109 for anti-CD109.

CD109 interacts with and requires ENO1 to regulate the RA FLS-mediated inflammatory response

To explore the molecular mechanism of CD109 in RA FLSs, glutathione-S-transferase (GST) pull-down assay and mass spectrometry were used. The majority of the identified CD109-interacting partners are involved in processes such as metabolism, signalling pathways, protein processing and modification, and cell cycle and apoptosis (online supplementary table 2). ENO1 was selected for further investigation as it is also localised on the cell surface and regulates cytokine production and apoptotic resistance in RA FLSs.^{30–32} Co-immunoprecipitation (figure 4A) and immunofluorescence (figure 4B) analyses confirmed the specific association between CD109 and ENO1 on the surface of RA FLSs; the interaction was enhanced by TNF- α or IL-1 β treatment.

Then, we detected the intrinsic relationship between CD109 and ENO1 in RA FLSs. The overexpression or silencing efficiency of CD109 and ENO1 was first confirmed, as shown, respectively, in figure 4C and D. The overexpression of CD109 increased the level of ENO1 protein (figure 4E) as well as the proportion of ENO1 on the cell surface (figure 4F), irrespective of IL-1 β or TNF- α stimulation. In contrast, CD109 silencing or anti-CD109 treatment caused a significant reduction in ENO1 expression (figure 4G) and surface localisation (figure 4H,I). CHX chase assay results demonstrated that the degradation rate of ENO1 protein increased following CD109 inhibition with either siCD109 or anti-CD109 (figure 4J,K). Furthermore, we observed a marked increase in the levels of inflammatory factors (figure 4L–Q, IL-6, IL-8, MMP-1, MMP-9, CXCL9 and CXCL10), migration (figure 4R), invasion (figure 4S) and phosphorylation of proteins in the proinflammatory pathway (figure 4T) in CD109-overexpressing FLSs compared with control FLSs. However, ENO1 knock-down prevented these effects. These results suggest that ENO1 is required for CD109-mediated regulation of the FLS inflammatory response.

Reduced arthritis severity in CD109-deficient mice

To further demonstrate the function of CD109 in RA, CIA was induced in WT and CD109 KO mice. When endogenous CD109 was absent (figure 5A), the arthritis score and paw swelling were significantly ameliorated in CD109 KO mice compared with WT mice (figure 5B,C). Likewise, CD109 KO mice also developed a limited degree of inflammatory cell infiltration (granulocytes and T lymphocytes), synovial hyperplasia, cartilage degradation and bone destruction (figure 5D,E and online supplementary figure 5A–D), accompanied by a decrease in TNF- α , IL-1 β , IL-6 and IL-8 levels (figure 5F) in the paws. Inflammatory bone erosion and destruction are known features of RA.³³ Thus, we examined the effects of global CD109 deletion on bone destruction in CIA models by microcomputed tomography (micro-CT) analysis (figure 5G). The distal tibiae from CD109 KO CIA mice displayed an obvious increase in bone volume/tissue volume (BV/TV), total body bone mineral density (Tb BMD), trabecular thickness (Tb Th) and trabecular number (Tb N) but a decrease in trabecular spacing (Tb Sp) compared with those from the WT counterparts (figure 5H). Further evidence showed that bone marrow mononuclear cells (BMMCs) isolated from CD109 KO mice differentiated into osteoclasts *in vitro* less efficiently than those isolated from WT mice. Notably, this difference was increased between the CD109 KO and WT groups with CIA induction (online supplementary figure 6A). The receptor activator of NF- κ B ligand (RANKL) promotes osteoclast differentiation, while osteoprotegerin (OPG) attenuates osteoclastic bone destruction, and the OPG/RANKL ratio is critical for RA-induced bone destruction.³⁴ Serum from CIA mice was then examined by ELISA, which showed that the serum level of RANKL decreased while that of OPG remained unchanged. This imbalance finally led to an increase in the OPG/RANKL ratio but fewer osteoclasts in CD109 KO mice than WT mice (online supplementary figure 6B–D).

We also investigated whether CD109 regulates RANKL and OPG in FLS. CD109 ablation reduced the TNF- α and IL-1 β stimulation-induced increase in RANKL expression in FLS. As OPG levels remained unaffected, the OPG/RANKL ratio increased in CD109 KO FLSs compared with WT FLSs (online supplementary figure 6E–H). Subsequently, mouse BMMCs were cultured with CM from IL-1 β -activated or TNF- α -activated FLSs and stimulated with M-CSF. CD109 KO FLSs were less efficient at inducing tartrate-resistant acid phosphatase-positive multinucleated cells than WT cells (online supplementary figure S6I). Collectively, these findings indicate that ablation of the *CD109* gene sufficiently blocks the progression of experimental arthritis.

Effects of prophylactic anti-CD109 treatment

To evaluate the efficacy of anti-CD109 in the amelioration of CIA, the safety was first analysed. Neither physical and behavioural manifestations nor peripheral blood cell numbers appeared to be significantly affected (online supplementary figure 7). To mimic prophylactic intervention in human RA patients, anti-CD109 was administered on the day of first immunisation with type II collagen. Anti-CD109 treatment dose dependently reduced the arthritis score (figure 6A), hind paw thickness (figure 6B) and swelling (figure 6C) in CIA models. Histological analysis revealed reduced inflammatory cell infiltration (granulocytes and T lymphocytes), synovial hyperplasia, cartilage degradation and bone destruction in anti-CD109-treated mice (figure 6D,E and online supplementary figure 5E–H). The micro-CT showed that compared with immunoglobulin (Ig) G treatment, anti-CD109 treatment greatly reduced bone destruction (figure 6F), as quantitatively evidenced by the increased degree of Tb BMD,

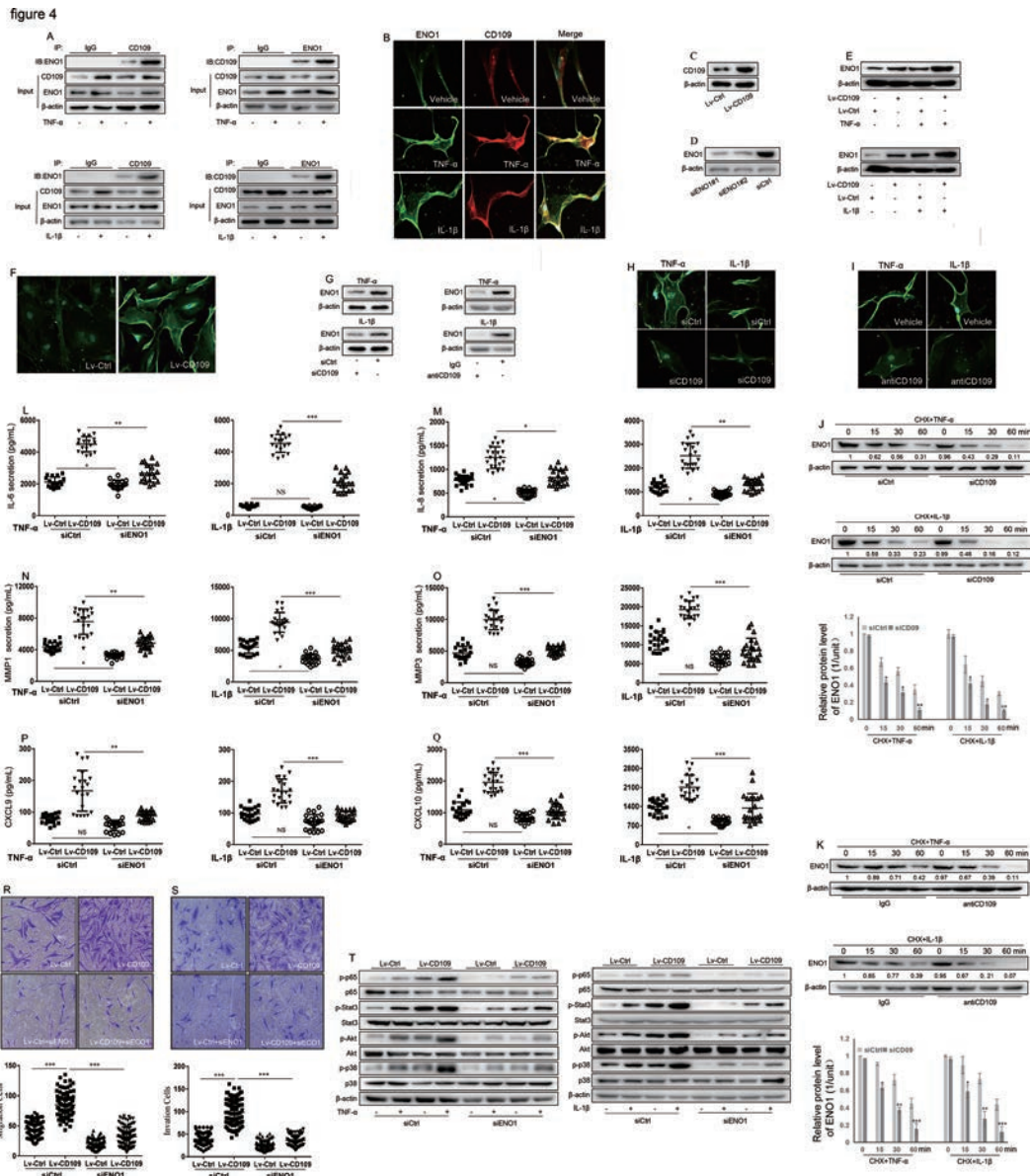


Figure 4 CD109 interacts with and stabilises ENO1. (A) RA FLSs were stimulated with TNF- α (upper) or IL-1 β (lower) for 24 hours. Immunoprecipitation and immunoblotting were performed on total protein with anti-CD109 or anti-ENO1 antibodies. The results are representative of four samples (two males and two females) from independent experiment. (B) After stimulation with TNF- α or IL-1 β for 24 hours, ENO1 (green) and CD109 (red) in RA FLSs were detected by immunofluorescence. (C) Western blot analysis of CD109 protein in RA FLSs following transfection of a lentiviral vector expressing CD109 (Lv-CD109) or its control (Lv-Ctrl). (D) Silencing efficiency of siENO1 was detected by Western blot. The two siRNAs were combined at equal concentrations for the subsequent experiments. Data in C and D are representative of two independent experiments with three different samples. (E) After Lv-CD109 or Lv-Ctrl transfection, RA FLSs were exposed to TNF- α or IL-1 β for 24 hours, and ENO1 protein levels were measured by Western blot. (F) Surface ENO1 was detected by immunofluorescence in Lv-CD109 or Lv-Ctrl-transfected RA FLSs. (G) After transfection of siCD109/siCtrl or treatment with anti-CD109/IgG for 24 hours, the ENO1 protein in TNF- α -activated or IL-1 β -activated RA FLSs was measured by Western blot. (H and I) TNF- α -stimulated or IL-1 β -stimulated RA FLSs were transfected with siCD109/siCtrl or treated with anti-CD109/IgG for 24 hours. ENO1 (green) in RA FLS was detected by immunofluorescence. (J and K) In the presence of TNF- α or IL-1 β , RA FLSs were exposed to CHX for different time periods, and the total protein was subjected to Western blotting to analyse ENO1 expression. Band intensities were measured using ImageJ software and are presented as fold change comparisons as indicated. * $p < 0.05$, ** $p < 0.01$ and *** $p < 0.001$ compared with siCtrl. CD109-overexpressing RA FLSs were transfected with siENO1 or siCtrl for 12 hours and subsequently stimulated with TNF- α and IL-1 β for another 24 hours. IL-6 (L), IL-8 (M), MMP-1 (N), MMP-3 (O), CXCL9 (P) and CXCL10 (Q) levels in the culture supernatant were measured by ELISA. Data are expressed as the mean \pm SD of six samples (three males and three females) and are representative of three independent experiments. * $p < 0.05$, ** $p < 0.01$ and *** $p < 0.001$ compared with Lv-Ctrl or Lv-CD109 in the siCtrl-transfected group. CD109-overexpressing RA FLSs were transfected with siENO1 or siCtrl for 24 hours. The migration (R) and invasion (S) abilities were assessed and counted (graph below) for RA FLSs from six different patients (three males and three females) and performed in triplicate. Five different fields were selected for cell counting. *** $p < 0.001$ compared with Lv-Ctrl. (T) CD109-overexpressing RA FLSs were transfected with siENO1 or siCtrl for 24 hours. Total and phosphorylated levels of Akt, p65, Stat3 and p38 MAPK were analysed by Western blot. Western blot data in A, E, G, J, K and T, and immunofluorescence data in B, F, H and I are representative of two independent experiments from six samples (three males and three females) with similar results. CHX, cycloheximide; FLSs, fibroblast-like synoviocytes; IL, interleukin; NS, not significant; RA, rheumatoid arthritis; siRNAs, small interfering RNAs; TNF- α , tumor necrosis factor- α .

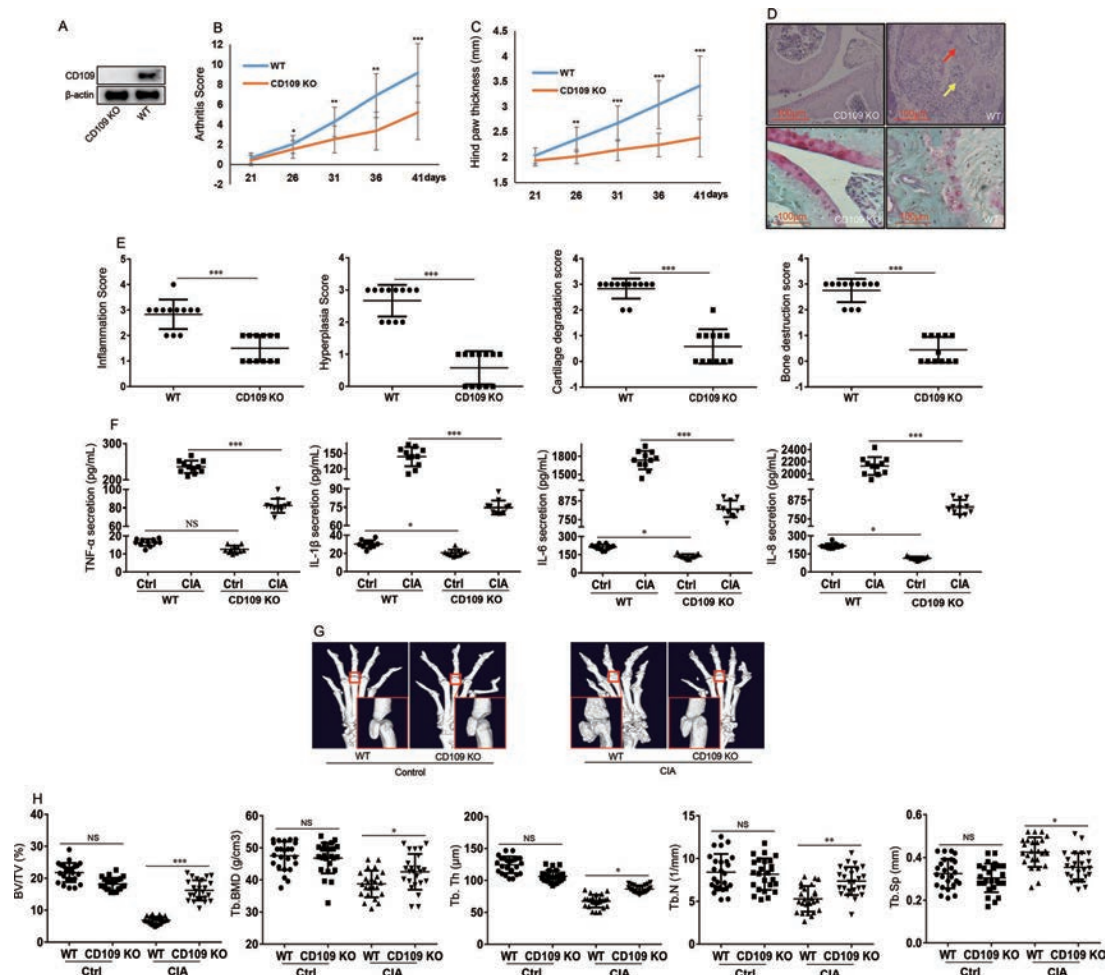


Figure 5 CD109 knockout (CD109 KO) prevents joint destruction in CIA mice. (A) The hind paws from CD109 KO and WT CIA mice at the resolution phase of arthritis were homogenised in cell lysis buffer for Western blot detection of CD109 (n=3 mice per group). (B, C) Arthritis in CD109 KO and WT mice was induced by bovine type II collagen injection (n=6 mice per group and per time point). After the second immunisation, the arthritis score (B) and hind paw thickness (C) were evaluated every 5 days. This experiment is representative of four independent experiments with similar results. *p<0.05, **p<0.01 and ***p<0.001 compared with WT. (D) Representative images of haematoxylin-eosin (H&E, upper) and Safranin O/ Fast green staining (lower) of the interphalangeal joint from CD109 KO and WT CIA mice on the 42nd day after the first immunisation. Pathological changes, including synovial proliferation (yellow arrowhead) and joint destruction (red arrowhead), are shown. (E) Inflammation, hyperplasia, cartilage degradation and bone destruction were evaluated using a scoring system (n=12 per group). ***p<0.001 compared with WT. (F) The hind paws from WT and CD109 KO CIA mice (n=6 mice per group) were homogenised in phosphate-buffered saline (PBS) for ELISA detection of TNF- α , IL-1 β , IL-6 and IL-8 on the 42nd day after the first immunisation. The data are representative of two independent experiments from six mice per group. *p<0.05 and ***p<0.001 compared with Ctrl or CIA in the WT group. (G) Representative micro-CT images of hind paws and interphalangeal joints (red square) on the 42nd day after the first immunisation (n=6 mice per group). (H) Bone volume fraction (BV/TV), trabecular bone mineral density (Tb BMD), trabecular thickness (Tb Th), trabecular number (Tb N) and trabecular separation (Tb Sp) in the distal tibia were assayed by micro-CT and 3D reconstruction. The data represent four independent experiments with similar results. *p<0.05, **p<0.01 and ***p<0.001 compared with WT. BMD, bone mineral density; CIA, collagen-induced arthritis; KO, knockout; NS, not significant; TNF- α , tumour necrosis factor- α ; WT, wild type.

BV/TV, Tb Th and Tb N but a lower degree of Tb Sp in the distal tibiae (figure 6G). Furthermore, anti-CD109 treatment effectively decreased the serum level of RANKL but had a minimal effect on the OPG level, thereby increasing the OPG/RANKL ratio and curtailing osteoclast numbers (online supplementary figure 8A-C) in CIA models.

Effects of therapeutic treatment with anti-CD109

We also analysed the therapeutic effects of anti-CD109. Compared with IgG-treated CIA model mice, anti-CD109-treated model mice showed dose-dependent amelioration with a marked decrease in arthritis score (figure 6H), thickness (figure 6I) and hind paw swelling (figure 6J). Histological

analysis of affected joints from anti-CD109-treated mice revealed reduced evidence of inflammation (granulocytes and T lymphocytes), synovial hyperplasia, cartilage degradation and bone destruction (figure 6K,L and online supplementary figure 5I-L). In addition, anti-CD109-treated CIA mice displayed reduced levels of bone erosion and destruction (figure 6M,N), as evidenced by the increase in BV/TV, Tb BMD, Tb Th and Tb N but decrease in Tb Sp in the distal tibia. Additionally, anti-CD109 treatment decreased the RANKL level, increased the OPG/RANKL ratio and led to a decline in the number of osteoclasts (online supplementary figure 8D-F). Therefore, anti-CD109 treatment alleviates RA progression in vivo.

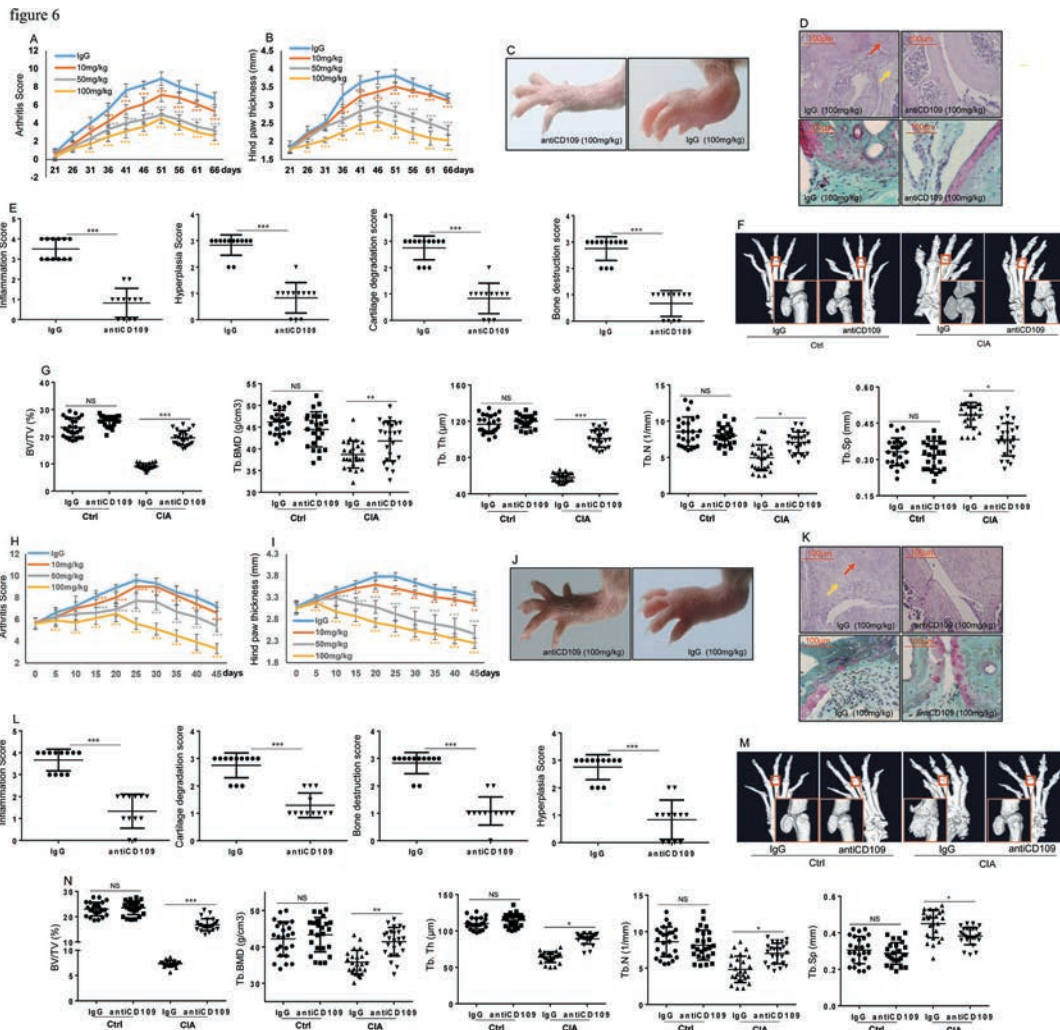


Figure 6 Antiarthritis effects of anti-CD109 on CIA. Mice immunised with CII were randomly divided into four groups ($n=6$ mice for each group and time point) and administered anti-CD109 or IgG at the indicated doses twice a week after the initial immunisation. The data are representative of four independent experiments with similar results. (A) Arthritis scores were monitored once per 5 days. (B) Hind paw thickness was calibrated from the 21st day following the first immunisation. (C) Paw photographs were obtained on day 42 from mice with CIA from the day of first immunisation. (D) Representative histology images by H&E (upper) and Safranin O/ Fast green staining (lower) were obtained on day 67 from mice with CIA with the indicated treatment. Pathological changes, including synovial proliferation (yellow arrowhead) and joint destruction (red arrowhead), are shown. (E) Inflammation, hyperplasia, cartilage degradation and bone destruction were measured through a scoring system ($n=12$ mice per group). (F) Representative micro-CT images of hind paws and interphalangeal joints (red square). (G) BV/TV, Tb BMD, Tb Th, Tb N and Tb Sp in the distal tibia were assayed by micro-CT and 3D reconstruction. Furthermore, mice immunised with CII were divided into four groups ($n=6$ mice per group and time point) equating to the mean arthritis score of individual groups. The mice were treated with anti-CD109 or IgG at the indicated doses twice a week from the point after the second immunisation when the arthritis scores reached 6 until day 45. (H) The arthritis severity was evaluated by the arthritis scores. (I) Paw swelling was measured every 5 days after anti-CD109 addition. (J) Paw photographs from mice with CIA captured on day 21 after starting anti-CD109 treatment. (K) Representative H&E (upper) and Safranin O/Fast green staining (lower) histology images of hind paws obtained on day 46 from anti-CD109 treatment. Synovial proliferation (yellow arrowhead) and joint destruction (red arrowhead) are shown. (L) Quantification of synovitis, hyperplasia, cartilage degradation and bone destruction according to the scoring system ($n=12$ mice per group). (M) Representative micro-CT images of hind paws and interphalangeal joints (red square). (N) BV/TV, Tb BMD, Tb Th, Tb N and Tb Sp in the distal tibia were assayed by micro-CT and 3D reconstruction. (A, B, E, H, I and L) $*p<0.05$, $**p<0.01$ and $***p<0.001$ compared with IgG. (G and N) $*p<0.05$, $**p<0.01$ and $***p<0.001$ compared with IgG in the Ctrl or CIA group. BMD, bone mineral density; BV/TV, bone volume fraction; CIA, collagen-induced arthritis; CII, type II collagen; NS, not significant; Tb BMD, trabecular bone mineral density; Tb N, trabecular number; Tb Sp, trabecular separation; Tb Th, trabecular thickness.

DISCUSSION

The inhibition of inflammatory reactions is an investigative focus for treating RA.³⁵ In this study, while confirming its roles in tumour progression and tissue fibrosis,^{7 12 36} we reveal a novel role for CD109 in the RA FLS-mediated immune response, such as in cytokine production, inflammatory signalling activation, migration, invasion and chemoattraction. As CD109

localises to the cell surface and exists mainly in the extracellular compartment, its activity can be effectively blocked by specific antibodies.^{3 37} Here, we found that anti-CD109 is as effective as siCD109 in attenuating the arthritis phenotype of RA FLSs. In addition, the anti-inflammatory effect of blocking CD109 in RA FLSs is equally efficient in male and female patients. More importantly, CD109 deficiency ameliorates the severity of

arthritis in a CIA model. Anti-CD109 addition in vivo demonstrates both prophylactic and therapeutic effects in a CIA model. Together, our results suggest that CD109 may represent a novel therapeutic target for RA.

ENO1 is a classical component of the glycolytic pathway and functions in multiple ways.^{38–40} A previous study showed that surface ENO1 activation on monocytes and macrophages from RA patients involves intracellular p38 MAPK and NF- κ B pathways and excessive levels of proinflammatory mediators.^{30–32} Furthermore, TNF- α -induced ENO1 contributes to RA FLS IL-6 production, proliferation and survival.³⁰ In addition, ENO1 increases plasminogen levels to enhance ECM degradation and the subsequent migration or invasion of monocytes and tumour cells.³⁹ Here, we found that CD109 forms a complex with ENO1 and stabilises ENO1 on the cell surface, thereby mediating the inflammatory response of RA FLSs. These findings further support the hypothesis that CD109 is a crucial factor in RA pathogenesis and that ENO1 is required for CD109-mediated RA FLS activation. Further analysis would be still needed to clarify the regulatory mechanism toward the expression and activity of CD109 in RA FLSs.

CD109 deficiency caused an osteoporosis-like phenotype in vivo, while the osteoclasts seemingly matured. However, there are contradictory results from in vitro experiments.^{41–42} Here, we found that CD109 loss or inhibition increased the OPG/RANKL ratio but reduced osteoclastogenesis and bone destruction in CIA model mice, suggesting that the effect of targeting CD109 on osteoclast differentiation is context-specific and needs further clarification for the potential treatment of RA. In addition, chronic inflammation-induced bone destruction is a critical pathological feature of RA.^{43–44} RA FLSs provide the necessary signals for osteoclasts and are the main resources of RANKL that promotes osteoclast differentiation.^{34–45–46} In this study, FLSs from CD109 KO mice were less capable than those from WT mice of supporting osteoclast differentiation in vitro, indicating that the CD109-mediated RA FLS inflammatory response towards osteoclasts also contributes to bone destruction in RA.

Based on previous studies showing that CD109 decreases excessive ECM production in systemic sclerosis fibroblasts,¹² we explored whether an anti-CD109 antibody could be applied in RA patients. Our study provides a vigorous analysis of bone metabolism and potential adverse effects in organ fibrosis. CD109 is expressed in activated platelets, T cells, endothelial cells and a subpopulation of CD34-expressing cells.^{4–5–11–36} Interestingly, these cells are important for RA progression, indicating that CD109 may contribute to RA via different routes and that the antiarthritic role of CD109 inhibition was achieved not only by RA FLSs but also by peripheral blood mononuclear cells and endothelial cells. To further benefit from CD109 as a treatment target in RA, the effects of CD109 inhibition and its underlying molecular mechanism in immune cells and endothelial cells require further investigation.

Taken together, our results uncover the proinflammatory properties of CD109. CD109 inhibition suppresses the inflammatory response and disease activity of inflammatory arthritis, and CD109 may serve as a suitable target for RA treatment.

Author affiliations

¹Institute of Basic Medicine, Shandong First Medical University & Shandong Academy of Medical Sciences, Jinan, China

²Department of Pathology, Shandong University Medical School, Jinan, China

³School of Medicine and Life Sciences, University of Jinan-Shandong Academy of Medical Sciences, Jinan, China

⁴Department of Hematology, Qilu Children's Hospital of Shandong University, Jinan, China

⁵Shandong Medicinal Biotechnology Centre, Key Laboratory for Rare and Uncommon Diseases of Shandong Province, Key Lab for Biotechnology Drugs of Ministry of Health, Shandong First Medical University & Shandong Academy of Medical Sciences, Jinan, China

Acknowledgements Transgenic founder CD109+/- mice (C57Bl6:129Sv background) was designed, constructed and identified by Dr Zhang Lianfeng's laboratory at The Institute of Laboratory Animal Science, Chinese Academy of Medical Sciences. Thanks for the critical review and helpful suggestion from Dr Gao Chengjiang (Shandong University School of Medicine).

Contributors GS, LW and JH designed the research. GS, TF, QL, QG, ZW, RZ, YZ and LG performed the research. GS, YD, JP, LW and JH analysed the data. RZ and LG helped in sample collection. All the authors contributed to writing the paper.

Funding This work was supported by the National Natural Science Foundation of China (grant nos. 81572544 and 81772760), The Shandong Taishan Scholarship (grant no. tsqn20161076) and The Innovation Project of Shandong Academy of Medical Sciences.

Competing interests None.

Patient consent for publication Obtained.

Ethics approval The studies were approved by the Institutional Review Board of Shandong Research Center for Medicinal Biotechnology.

Provenance and peer review Not commissioned; externally peer reviewed.

Data availability statement Data are available upon reasonable request. All data relevant to the study are included in the article or uploaded as supplementary information.

Open access This is an open access article distributed in accordance with the Creative Commons Attribution Non Commercial (CC BY-NC 4.0) license, which permits others to distribute, remix, adapt, build upon this work non-commercially, and license their derivative works on different terms, provided the original work is properly cited, appropriate credit is given, any changes made indicated, and the use is non-commercial. See: <http://creativecommons.org/licenses/by-nc/4.0/>.

ORCID iD

Lin Wang <http://orcid.org/0000-0003-3489-4383>

REFERENCES

- Bottini N, Firestein GS. Duality of fibroblast-like synoviocytes in RA: passive responders and imprinted aggressors. *Nat Rev Rheumatol* 2013;9:24–33.10.1038/nrrheum.2012.190
- Bartok B, Firestein GS. Fibroblast-Like synoviocytes: key effector cells in rheumatoid arthritis. *Immunol Rev* 2010;233:233–55.
- Lin M, Sutherland DR, Horsfall W, et al. Cell surface antigen CD109 is a novel member of the alpha(2) macroglobulin/C3, C4, C5 family of thioester-containing proteins. *Blood* 2002;99:1683–91.
- Solomon KR, Sharma P, Chan M, et al. Cd109 represents a novel branch of the α 2-macroglobulin/complement gene family. *Gene* 2004;327:171–83.
- Hagiwara S, Murakumo Y, Mii S, et al. Processing of CD109 by furin and its role in the regulation of TGF- β signaling. *Oncogene* 2010;29:2181–91.
- Shiraki Y, Mii S, Enomoto A, et al. Significance of perivascular tumour cells defined by CD109 expression in progression of glioma. *J Pathol* 2017;243:468–80.
- Hashimoto M, Ichihara M, Watanabe T, et al. Expression of CD109 in human cancer. *Oncogene* 2004;23:3716–20.
- Tsai Y-L, Ha DP, Zhao H, et al. Endoplasmic reticulum stress activates Src, relocating chaperones to the cell surface where GRP78/CD109 blocks TGF- β signaling. *Proc Natl Acad Sci U S A* 2018;115:E4245–E4254.
- Yoo S-A, You S, Yoon H-J, et al. A novel pathogenic role of the ER chaperone GRP78/BiP in rheumatoid arthritis. *J Exp Med* 2012;209:871–86.
- Bizet AA, Liu K, Tran-Khanh N, et al. The TGF-beta co-receptor, CD109, promotes internalization and degradation of TGF-beta receptors. *Biochim Biophys Acta* 2011;1813:742–53.
- Bizet AA, Tran-Khanh N, Saksena A, et al. CD109-mediated degradation of TGF- β receptors and inhibition of TGF- β responses involve regulation of Smad7 and Smurf2 localization and function. *J Cell Biochem* 2012;113:238–46.
- Man X-Y, Finsson KW, Baron M, et al. Cd109, a TGF- β co-receptor, attenuates extracellular matrix production in scleroderma skin fibroblasts. *Arthritis Res Ther* 2012;14.
- Chuang C-H, Greenside PG, Rogers ZN, et al. Molecular definition of a metastatic lung cancer state reveals a targetable CD109–Janus kinase–Stat axis. *Nat Med* 2017;23:291–300.
- Aletaha D, Neogi T, Silman AJ, et al. 2010 rheumatoid arthritis classification criteria: an American College of Rheumatology/European League against rheumatism collaborative initiative. *Arthritis Rheum* 2010;62:2569–81.
- McInnes IB, Schett G. Cytokines in the pathogenesis of rheumatoid arthritis. *Nat Rev Immunol* 2007;7:429–42.

16. Alam J, Jantan I, Bukhari SNA. Rheumatoid arthritis: recent advances on its etiology, role of cytokines and pharmacotherapy. *Biomed Pharmacother* 2017;92:615–33.
17. Klein K, Kabala PA, Grabiec AM, et al. The bromodomain protein inhibitor I-BET151 suppresses expression of inflammatory genes and matrix degrading enzymes in rheumatoid arthritis synovial fibroblasts. *Ann Rheum Dis* 2016;75:422–9.
18. Burrage PS, Mix KS, Brinckerhoff CE. Matrix metalloproteinases: role in arthritis. *Front Biosci* 2006;11:529–43.
19. Li N, Xu Q, Liu Q, et al. Leonurine attenuates fibroblast-like synoviocyte-mediated synovial inflammation and joint destruction in rheumatoid arthritis. *Rheumatology* 2017;56:1417–27.
20. Xiao Y, Liang L, Huang M, et al. Bromodomain and extra-terminal domain bromodomain inhibition prevents synovial inflammation via blocking I κ B kinase-dependent NF- κ B activation in rheumatoid fibroblast-like synoviocytes. *Rheumatology* 2016;55:173–84.
21. Mu N, Gu J, Huang T, et al. A novel NF- κ B/YY1/microRNA-10a regulatory circuit in fibroblast-like synoviocytes regulates inflammation in rheumatoid arthritis. *Sci Rep* 2016;6:20059.
22. Tagoe CE, Marjanovic N, Park JY, et al. Annexin-1 mediates TNF- α -stimulated matrix metalloproteinase secretion from rheumatoid arthritis synovial fibroblasts. *J Immunol* 2008;181:2813–20.
23. Akhtar N, Singh AK, Ahmed S. MicroRNA-17 suppresses TNF- α signaling by interfering with TRAF2 and cIAP2 association in rheumatoid arthritis synovial fibroblasts. *Ji* 2016;197:2219–28.
24. Xu H, He Y, Yang X, et al. Anti-Malarial agent artesunate inhibits TNF- α -induced production of proinflammatory cytokines via inhibition of NF- κ B and PI3 kinase/Akt signal pathway in human rheumatoid arthritis fibroblast-like synoviocytes. *Rheumatology* 2007;46:920–6.
25. Singh AK, Fechtner S, Chourasia M, et al. Critical role of IL-1 α in IL-1 β -induced inflammatory responses: cooperation with NF- κ Bp65 in transcriptional regulation. *The FASEB Journal* 2019;33:2526–36.
26. Mori T, Miyamoto T, Yoshida H, et al. IL-1 β and TNF α -initiated IL-6-STAT3 pathway is critical in mediating inflammatory cytokines and RANKL expression in inflammatory arthritis. *Int Immunol* 2011;23:701–12.
27. Meng Q, Du X, Wang H, et al. Astragalus polysaccharides inhibits cell growth and pro-inflammatory response in IL-1 β -stimulated fibroblast-like synoviocytes by enhancement of autophagy via PI3K/Akt/mTOR inhibition. *Apoptosis* 2017;22:1138–46.
28. Kuan WP, Tam L-S, Wong C-K, et al. Cxcl 9 and CXCL 10 as sensitive markers of disease activity in patients with rheumatoid arthritis. *J Rheumatol* 2010;37:257–64.
29. Ruschpler P, Lorenz P, Eichler W, et al. High CXCR3 expression in synovial mast cells associated with CXCL9 and CXCL10 expression in inflammatory synovial tissues of patients with rheumatoid arthritis. *Arthritis Res Ther* 2003;5:R241–52.
30. Bae S, Kim H, Lee N, et al. α -Enolase expressed on the surfaces of monocytes and macrophages induces robust synovial inflammation in rheumatoid arthritis. *Ji* 2012;189:365–72.
31. Fan SS, Zong M, Zhang H, et al. Decreased expression of alpha-enolase inhibits the proliferation of hypoxia-induced rheumatoid arthritis fibroblasts-like synoviocytes. *Mod Rheumatol* 2015;25:701–7.
32. Lee JY, Kang MJ, Choi JY, et al. Apolipoprotein B binds to enolase-1 and aggravates inflammation in rheumatoid arthritis. *Ann Rheum Dis* 2018;77:1480–9.
33. Choi Y, Arron JR, Townsend MJ. Promising bone-related therapeutic targets for rheumatoid arthritis. *Nat Rev Rheumatol* 2009;5:543–8.
34. Tanaka Y, Ohira T. Mechanisms and therapeutic targets for bone damage in rheumatoid arthritis, in particular the RANK-RANKL system. *Curr Opin Pharmacol* 2018;40:110–9.
35. McInnes IB, Schett G. Pathogenetic insights from the treatment of rheumatoid arthritis. *The Lancet* 2017;389:2328–37.
36. Winocour S, Vorstenbosch J, Trzeciak A, et al. CD109, a novel TGF- β antagonist, decreases fibrotic responses in a hypoxic wound model. *Exp Dermatol* 2014;23:475–9.
37. Litvinov IV, Bizet AA, Binamer Y, et al. Cd109 release from the cell surface in human keratinocytes regulates TGF- β receptor expression, TGF- β signalling and STAT3 activation: relevance to psoriasis. *Exp Dermatol* 2011;20:627–32.
38. Capello M, Ferri-Borgogno S, Cappello P, et al. α -enolase: a promising therapeutic and diagnostic tumor target. *Febs j* 2011;278:1064–74.
39. Wygrecka M, Marsh LM, Morty RE, et al. Enolase-1 promotes plasminogen-mediated recruitment of monocytes to the acutely inflamed lung. *Blood* 2009;113:5588–98.
40. Giallongo A, Feo S, Showe LC, et al. Isolation and partial characterization of a 48-kDa protein which is induced in normal lymphocytes upon mitogenic stimulation. *Biochem Biophys Res Commun* 1986;134:1238–44.
41. Mii S, Hoshino A, Enomoto A, et al. Cd109 deficiency induces osteopenia with an osteoporosis-like phenotype in vivo. *Genes Cells* 2018;23:590–8.
42. Wang Y, Inger M, Jiang H, et al. Cd109 plays a role in osteoclastogenesis. *PLoS One* 2013;8:e61213.
43. Harre U, Schett G. Cellular and molecular pathways of structural damage in rheumatoid arthritis. *Semin Immunopathol* 2017;39:355–63.
44. Tanaka Y, Nakayamada S, Okada Y. Osteoblasts and osteoclasts in bone remodeling and inflammation. *Curr Drug Targets Inflamm Allergy* 2005;4:325–8.
45. Tanaka S, Tanaka Y, Ishiguro N, et al. RANKL: a therapeutic target for bone destruction in rheumatoid arthritis. *Modern Rheumatology* 2018;28:9–16.
46. Danks L, Komatsu N, Guerrini MM, et al. RANKL expressed on synovial fibroblasts is primarily responsible for bone erosions during joint inflammation. *Ann Rheum Dis* 2016;75:1187–95.

Synovial tissue signatures enhance clinical classification and prognostic/treatment response algorithms in early inflammatory arthritis and predict requirement for subsequent biological therapy: results from the pathobiology of early arthritis cohort (PEAC)

Gloria Lliso-Ribera,¹ Frances Humby ,² Myles Lewis ,³ Alessandra Nerviani ,¹ Daniele Mauro,¹ Felice Rivellese ,¹ Stephen Kelly,⁴ Rebecca Hands,⁵ Fabiola Bene,³ Nandhini Ramamoorthi,⁶ Jason A Hackney,⁷ Alberto Cauli,⁸ Ernest H Choy,⁹ Andrew Filer,¹⁰ Peter C Taylor ,¹¹ Iain McInnes,¹² Michael J Townsend,⁷ Costantino Pitzalis ¹³

Handling editor Josef S Smolen

For numbered affiliations see end of article.

Correspondence to

Professor Costantino Pitzalis, Experimental Medicine and Rheumatology, William Harvey Research Institute, London EC1M 6BQ, UK; c.pitzalis@qmul.ac.uk

GL-R and FH contributed equally.

Received 20 May 2019
Revised 26 August 2019
Accepted 27 August 2019
Published Online First
2 October 2019

ABSTRACT

Objective To establish whether synovial pathobiology improves current clinical classification and prognostic algorithms in early inflammatory arthritis and identify predictors of subsequent biological therapy requirement.

Methods 200 treatment-naïve patients with early arthritis were classified as fulfilling RA1987 American College of Rheumatology (ACR) criteria (RA1987) or as undifferentiated arthritis (UA) and patients with UA further classified into those fulfilling RA2010 ACR/European League Against Rheumatism (EULAR) criteria. Treatment requirements at 12 months (Conventional Synthetic Disease Modifying Antirheumatic Drugs (csDMARDs) vs biologics vs no-csDMARDs treatment) were determined. Synovial tissue was retrieved by minimally invasive, ultrasound-guided biopsy and underwent processing for immunohistochemical (IHC) and molecular characterisation. Samples were analysed for macrophage, plasma-cell and B-cells and T-cells markers, pathotype classification (lympho-myeloid, diffuse-myeloid or pauci-immune) by IHC and gene expression profiling by Nanostring.

Results 128/200 patients were classified as RA1987, 25 as RA2010 and 47 as UA. Patients classified as RA1987 criteria had significantly higher levels of disease activity, histological synovitis, degree of immune cell infiltration and differential upregulation of genes involved in B and T cell activation/function compared with RA2010 or UA, which shared similar clinical and pathobiological features. At 12-month follow-up, a significantly higher proportion of patients classified as lympho-myeloid pathotype required biological therapy. Performance of a clinical prediction model for biological therapy requirement was improved by the integration of synovial pathobiological markers from 78.8% to 89%–90%.

Conclusion The capacity to refine early clinical classification criteria through synovial pathobiological markers offers the potential to predict disease outcome and stratify therapeutic intervention to patients most in need.

Key messages

What is already known about this subject?

► The introduction of ACR/EULAR rheumatoid arthritis (RA) classification criteria has impacted positively on early diagnosis and treatment of RA leading to better outcomes. By the same token, broader criteria have led to the inclusion of patients with milder and more heterogeneous disease. This, together with the inability to precisely predict disease prognosis and treatment response at the individual patient levels, emphasise the need to identify patients at risk of accelerated structural damage progression and fast-track aggressive/biological therapies to patients with poor prognosis.

INTRODUCTION

The introduction of new classification criteria for rheumatoid arthritis (RA) in 2010¹ has been demonstrated to be clinically useful with enhanced diagnostic sensitivity in early disease compared with 1987 criteria²; however, this is balanced by a lower specificity.^{3,4} This is of particular importance, as data suggest that approximately 40% of patients with early inflammatory arthritis, not fulfilling 1987 criteria, may spontaneously remit while approximately 30% will progress to RA.⁵ Critically, the mechanisms underlying the transition from undifferentiated arthritis (UA) to RA remain unknown though it has been suggested that qualitative or quantitative difference within synovial tissue may contribute to diverse disease evolution and/or treatment response.^{6,7} Thus, pretreatment stratification of early inflammatory arthritis is important in order to target therapy to poor prognosis patients. Previous data suggest that stratifying early arthritis according to RA2010 versus RA1987 classification criteria reveals significant clinical heterogeneity in diagnosis at 2-year



© Author(s) (or their employer(s)) 2019. Re-use permitted under CC BY-NC. No commercial re-use. See rights and permissions. Published by BMJ.

To cite: Lliso-Ribera G, Humby F, Lewis M, et al. *Ann Rheum Dis* 2019;**78**:1642–1652.

Key messages

What does this study add?

► This study analyses the largest biopsy-driven early inflammatory arthritis cohort to date (200 patients) and, through a detailed synovial cellular and molecular characterisation refines ACR/EULAR disease classification. In addition, the study identifies synovial pathobiological markers associated with the lympho-myeloid pathotype and the requirement of biological therapy at 12 months, reinforcing recently published data that indicate that these patients are affected by highly aggressive disease and worse radiographic outcome. Notably, these findings are independent from the time of diagnosis within the first 12 months of symptoms initiation, suggesting that the so-called 'window of opportunity' is wider than 6 months and early stratification of biological therapies according to poor prognostic synovial pathobiological subtypes at disease onset may improve the outcome of these patients. The integration of synovial pathobiological markers into a logistic regression model improves the prediction accuracy from 78.8% (clinical) to 89%–90% (clinical +molecular) and enables the identification at disease onset of patients who subsequently require biological therapy. Thus, this study provides support to the notion that biological therapies should be started early in patients with poor prognosis.

How might this impact on clinical practice or future developments?

► The identification at disease onset of patients who are unlikely to respond to csDMARDs remains a major unmet need. The capacity to refine early clinical classification criteria through the application of synovial pathobiological markers and the ability to identify patients who subsequently require biological therapy at disease onset offer the opportunity to stratify therapeutic intervention to the patients most in need. This present study adds weight to the need to change current therapeutic algorithms and start biological therapies at disease onset in patients with poor prognosis. This is likely to have a major impact on disease control/remission and long-term disability, as notionally supported by numerous early intervention studies using biological therapies.

follow-up⁸ although subsequent analysis of synovial tissue did not suggest that such clinical heterogeneity translated to significant differences in synovial pathobiology.⁹ However, recently published data from a cohort of 144 patients with early RA have demonstrated that synovial cellular and molecular signatures define prognostic and treatment response phenotypes.¹⁰ Importantly, whether clinical heterogeneity associated with the introduction of the 2010 ACR/EULAR criteria can be explained by synovial pathobiological signatures and whether they associate with subsequent disease outcome, up to now, remain unknown.

Therefore, the aim of this study was to investigate whether in patients with early inflammatory arthritis synovial cellular and molecular signatures: (1) segregate according to clinical classification (RA1987 vs RA2010 vs UA), (2) change depending on symptom duration and (3) determine prognosis including subsequent requirement for biological therapy.

PATIENTS AND METHODS

Patients

Two hundred consecutive patients with inflammatory arthritis recruited at Barts Health NHS Trust as part of the multicentre pathobiology of early arthritis cohort (<http://www.peac-mrc.mds.qmul.ac.uk>) were included within the study. Patients were treatment naïve (csDMARD and steroid) and had <1 year symptoms.

At baseline, patients underwent collection of routine demographic data and were categorised according to the following criteria: (1) RA1987² or (2) UA. 2010 ACR/EULAR criteria for RA¹ were then applied to further classify patients with UA, resulting in three groups: (1) RA1987 (RA1987+/RA2010+), (2) RA2010 (RA1987–/RA2010+) and (3) UA (RA1987–/RA2010–). An ultrasound-guided synovial biopsy of a clinically active joint was performed.¹¹ Patients were then given standard conventional synthetic csDMARD therapy with a treat-to-target approach to treatment escalation (Disease Activity Score 28 joints (DAS28) <3.2). Patients failing csDMARD therapy were given biological therapy (anti-tumour necrosis factor (TNF), tocilizumab or rituximab) according to the prevailing UK National Institute for Clinical Excellence (NICE) prescribing algorithm if they continued to have a DAS28 >5.1 following 6 months of therapy.¹² At 12-month, follow-up patients were categorised as follows: (1) self-limiting (SL) disease (DAS28 <3.2 and off csDMARD/steroid therapy) versus persistent disease (PD) (DAS28 >3.2 and/or csDMARD) and (2) symptomatic treatment (non-steroidal anti-inflammatories) versus csDMARD therapy versus biological ±csDMARD therapy.

Synovial biopsy collection and processing

A minimum of six biopsies per patient were collected for paraffin embedding and if intact lining layer identified underwent histopathological assessment. Synovitis score was determined using a previously validated scoring system.¹³ Following immunohistochemical staining of sequentially cut slides using previously reported protocols for B cells (CD20), T cells (CD3), macrophages (CD68) and plasma cells (CD138), the degree of immune cell infiltration was assessed semiquantitatively (0–4).¹⁴ Biopsies were stratified into one of three synovial pathotypes according to the following criteria: (1) lympho-myeloid presence of grade 2–3 CD20 +aggregates, (CD20 ≥2) and/or CD138 >2, (2) diffuse-myeloid CD68 SL ≥2, CD20 ≤1 and/or CD3 ≥1, CD138 ≤2 and (3) pauci-immune CD68 SL <2 and CD3, CD20, CD138 <1.

Nanostring analysis

A minimum of six synovial samples per patient were immediately immersed in RNA-Later and RNA extraction performed as previously described.¹⁰ RNA samples then underwent profiling for the expression of 238 genes preselected based on previous microarray analyses of synovial tissue from patients with established RA¹⁵ and/or relevance to RA pathogenesis. Raw NanoString counts were processed using the NanoStringQCPro package in R V.3.2.0. Counts were normalised for RNA content by global gene count normalisation and then log transformed (base 2). The validity of normalisation was then checked via box plot and scatter plot of normalised counts. Benjamini-Hochberg method was used to adjust for multiple testing, and genes were considered to be differentially expressed if they demonstrated an false discovery rate (FDR)-adjusted $p < 0.01$.

Statistical analysis

Statistical analyses were run using R V.3.0.2. For three-way comparisons, the Kruskal-Wallis test was used for continuous and χ^2 or Fisher's exact test used for categorical variables as appropriate. A $p < 0.05$ was considered statistically significant. Post hoc comparison tests were performed using the Dunn test or Bonferroni correction as appropriate.

Linear regression models

Logistic regression using forward, backward and bidirectional stepwise selection was employed using the glm function in R.

Gene expression predictors were selected by L1 (LASSO) sparse logistic regression using R package glmnet. The penalty parameter λ was optimised using 10-fold cross validation. λ corresponding to the minimum mean cross-validated error was retained as final penalty parameter in the model.

Predictive performance evaluation

Predictive performance of the final prediction model was assessed by computing the area under the receiver operating characteristic curve (AUC), using both apparent and internal validation with 95% CI. Internal validation using a bootstrap method^{16 17} (performed with R package boot version 1.3-18) was employed to correct for overfitting, to generate unbiased optimism-adjusted estimates of the C statistic (AUC) with low absolute error. Bootstrap estimate of the AUC statistic was computed by random sampling with replacement 500 times to enable estimation of the optimism corrected AUC.

RESULTS

Patient demographics and clinical correlations

Two hundred pathobiology of early arthritis cohort patients were included: 128/200 (64%) patients were classified as RA1987 (RA1987+/RA2010+) and 72/200 (36%) as UA. Of the patients with UA, 25 were further classified as RA2010 (RA1987-/RA2010+) (25/200, 12.5%) and 47 remained as UA (RA1987-/RA2010-) (47/200, 23.5%) (figure 1A). No significant difference in mean age, disease duration or erythrocyte sedimentation rate (ESR) between groups was demonstrated. However, the RA1987 group had significantly higher levels of C reactive protein (CRP), tender joint count (TJC), swollen joint count (SJC), DAS28, rheumatoid factor (RF), anticitrullinated protein antibody (ACPA) and Visual Analogue Score (VAS) and significantly higher numbers of patients seropositive for RF and ACPA compared with either the RA2010 or UA groups (figure 1B). SJC and ACPA titres were the only clinical parameters with significant differences between the RA2010 and UA groups, indicating that in terms of clinical measures of disease activity these two groups are relatively homogenous.

Synovial pathotypes distinguish clinical phenotypes regardless of disease duration

Synovial biopsies were obtained predominantly from small joints (81.5%) (figure 2A). Patients with synovial tissue suitable for histological analysis (166/200) were segregated according to baseline synovial pathotype (figure 2B) and differences in clinical parameters evaluated. We demonstrated significantly higher mean DAS28 within the lympho-myeloid compared with either the diffuse-myeloid or pauci-immune group (5.82 vs 4.93 vs 4.86, $p < 0.001$). Mean CRP was significantly higher in the lympho-myeloid and diffuse-myeloid versus pauci-immune groups (16.86 vs 15.52 vs 9.55, $p < 0.001$) and a significantly higher number of patients were seropositive for either RF ($p = 0.012$) or ACPA ($p = 0.011$) within the lympho-myeloid group (figure 2C). To evaluate whether disease duration influenced prevalence of

synovial pathotype, patients were stratified into four groups according to disease duration at baseline (1–3 m, 4–6 m, 7–9 m and 10–12 m) and frequency of synovial pathotype determined. No significant differences in synovial pathotype frequency at each timepoint were demonstrated ($p = 0.65$) (figure 2D).

RA1987 patients display significantly higher levels of synovial immune cell infiltration compared to RA2010 and UA patients

Patients were segregated according to pathotype and further into RA1987, RA2010 and UA categories. A higher proportion of patients within the RA1987 group were categorised as lympho-myeloid (vs diffuse myeloid or pauci-immune) (43.5% vs 33% vs 23.5%) (figure 3A). We also demonstrated a significantly higher mean synovitis, CD3 +T cell, CD20 +B cell, CD138 +plasma cell and CD68 +SL/L macrophage score between the RA1987 group and both the RA2010 and UA groups ($p < 0.001$) (figure 3B). We saw no significant differences in synovitis score, mean CD3 +T, CD20 +B, CD68 +L or SL macrophage or CD138 +plasma cell number between the RA2010 and UA group (figure 3B), indicating that these two groups are relatively homogenous in terms of tissue pathology.

Synovial genes regulating B cell activation and function are significantly upregulated in RA1987 patients compared to the RA2010/UA groups

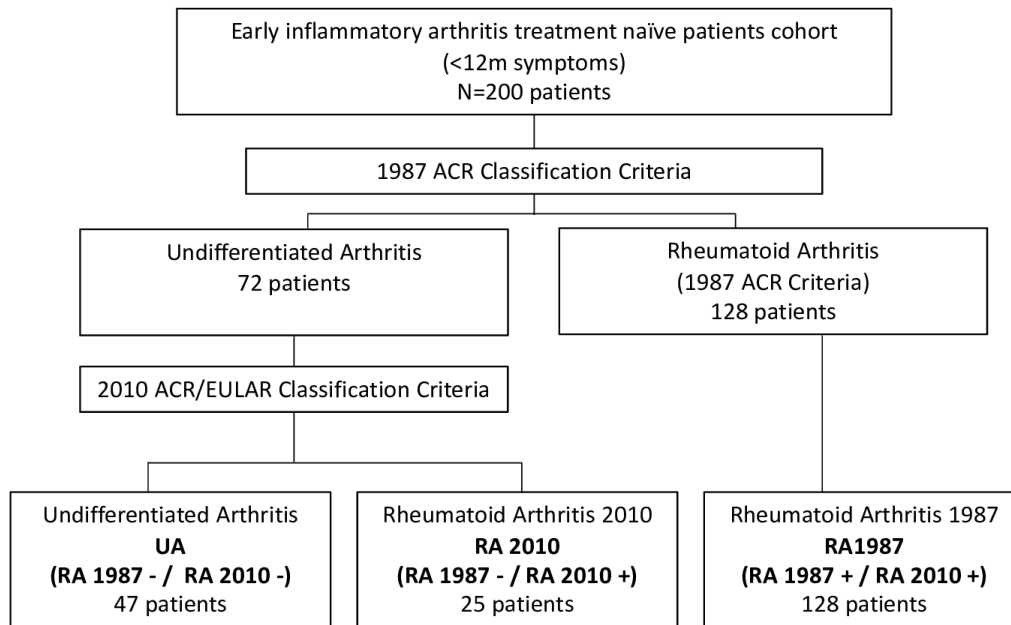
Of 200 patients, 145 had RNA available for Nanostring analysis (95/128 RA1987 patients, 12/25 RA2010 patients and 38/47 patients with UA) and were analysed for differential gene expression (238 genes) between groups.

Comparing RA1987 versus RA2010 groups, we demonstrated a significant differential expression of 53 genes (figure 3C). In line with the histological analysis, a number of differentially upregulated genes within the RA1987 cohort were involved in mediating B cell activation/function (eg, *CD79A*, *CD38*, *IGJ*, *CXCL13*, *IRF4*, *CCL19*, *CD38*, *TNFA* and *IL6*). When evaluating gene expression between RA1987 and UA groups, we found a similar trend with differential upregulation of a number of genes within the RA1987 cohort mediating B cell activation/function although only *CXCL13* remained significant following correction for multiple comparisons (figure 3D). Conversely, when evaluating gene expression between the RA2010 and UA cohorts, only seven genes appeared as significant with a preponderance of differentially upregulated genes within the RA2010 cohort mediating cartilage biology (*COMP*, *DKK3*, *INHBA*) and none remaining significant after correction for multiple comparisons (figure 3E).

Classification as RA1987 criteria at disease onset predicts PD at 12 months

Of 200 patients, 190 had 12-month follow-up data available; we examined whether baseline synovial pathotype was associated with disease evolution. 119/121 (99%) RA1987 patients and 19/22 (90%) RA2010 had PD (figure 4A). Within the UA cohort, 11/47 (23%) had other diagnoses. Of the remaining 36 patients, 26/36 (72.2%) had PD, and 10/36 (27.8%) SL. Of the patients with UA with PD, 4/26 (15.3%) progressed to fulfil 2010 ACR/EULAR criteria RA at 12 months. Results demonstrated a significantly higher proportion of patients with SL disease in the UA group compared with the RA2010 or RA1987 groups and a significantly higher number of patients within the RA1987 group with PD (figure 4B). When evaluating the effect of baseline pathotype, we demonstrated a higher proportion of patients with a lympho-myeloid versus diffuse-myeloid or pauci-immune pathotype (39% vs 32% vs 13%) with PD and a higher number of patients with a diffuse-myeloid versus

A



B

N 200	RA 1987 (RA 1987 + / RA 2010 +) N 128	RA 2010 (RA 1987 - / RA 2010 +) N 25	UA (RA1987 - / RA2010-) N 47	p-value	p-value (post-hoc) RA 1987- UA	p-value (post-hoc) RA1987- RA2010	p-value (post-hoc) RA2010- UA
Age (years). Mean (SD)	52.64 (16.02)	52.25 (12.54)	52.76 (15.33)	0.98			
Disease duration (months). Mean (SD)	5.64 (4.48)	10.47 (25.28)	6.11 (3.51)	0.91			
ESR. Mean (SD)	39.05 (19.69)	30.64 (30.06)	10.63 (21.51)	0.56			
CRP. Mean (SD)	17.82 (13.89)	14.6 (20.36)	7.21 (12.35)	0.03 *	<0.001 *	0.12	0.071
28 TJC. Mean (SD)	11.98 (7.29)	6.88 (5.72)	6.80 (6.79)	<0.001 *	<0.001 *	0.0012 *	0.74
28 SJC. Mean (SD)	7.68 (5.62)	5.68 (4.91)	3.10 (2.82)	<0.001 *	<0.001 *	0.042 *	0.031 *
Das 28. Mean (SD)	5.76 (1.35)	4.73 (1.56)	4.001 (1.51)	<0.001 *	<0.001 *	0.002 *	0.13
Vas global disease activity. Mean (SD)	64.82 (24.80)	45.36 (28.78)	34.55 (29.27)	<0.001 *	<0.001 *	0.0043 *	0.17
RF titre. Mean (SD)	25.53 (22.49)	2.68 (2.95)	1.27 (1.42)	<0.001 *	<0.001 *	<0.001 *	0.21
ACPA titre. Mean (SD)	26.16 (18.42)	75.24 (175.40)	1.68 (10.56)	<0.001 *	<0.001 *	<0.001 *	0.01 *
RF +ve. N (%)	84 (65%)	7 (28%)	1 (2%)	<0.001 *			
ACPA +ve. N (%)	87 (68%)	6 (24%)	2 (4%)	<0.001 *			

Figure 1 Baseline patient demographics. (A) Baseline classification of patients. Two hundred patients were classified into RA1987 versus UA. RA2010 ACR/EULAR criteria were then applied to patients with UA. Final 3 groups obtained showed 47 patients UA (RA1987–/RA2010–), RA2010 (RA1987–/RA2010+), RA1987 (RA1987+/RA2010+). (B) Demographics according to classification criteria. Data are presented as mean (SD) for continue variables and frequency and percentages for categorical variables. Baseline characteristics between the three groups were compared using the Kruskal-Wallis or Fisher's exact test as appropriate. For post hoc comparison, Dunn tests were run and p value from pairwise comparison reported in the last three columns of the table. ACPA titre, anticitrullinated protein antibody titre (IU/L); ACPA +ve, anticitrullinated protein antibody (>20 IU/L); CRP, C reactive protein; DAS28, Disease Activity Score 28 joints; ESR, erythrocyte sedimentation rate; RF titre, rheumatoid factor titre (IU/mL); RF +ve, rheumatoid factor serum positive (>15 IU/L); 28TJC, 28 tender joint count; 28SJC, 28 swollen joint count.

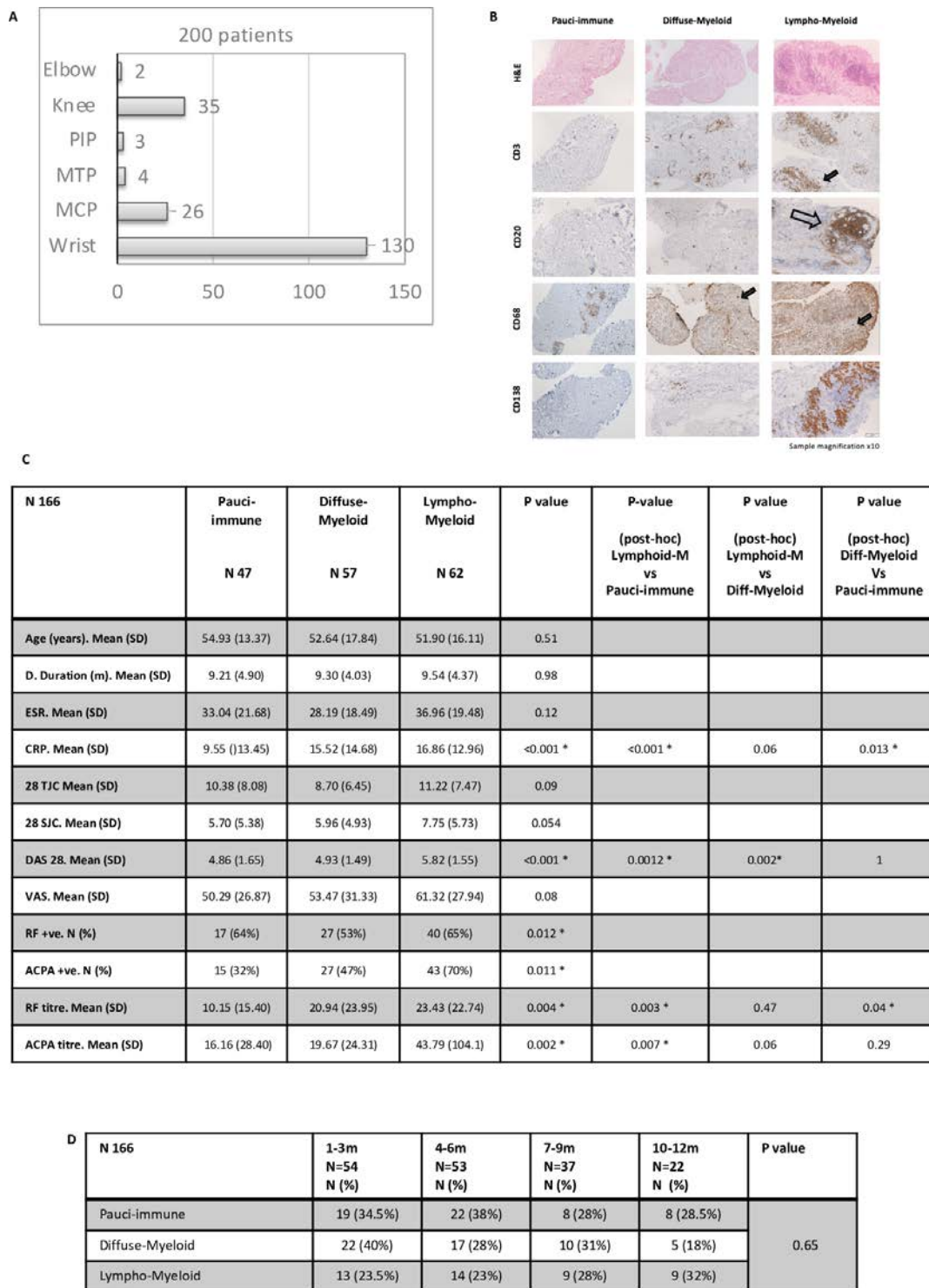


Figure 2 Patient demographics and disease activity: comparison between pathotypes. (A) Number of biopsy procedures per joint. MCP, metacarpophalangeal; MTP, metatarsophalangeal; PIP, proximal interphalangeal. (B) Representative images of synovial pathotypes. Sections underwent immunohistochemical staining and semiquantitative scoring (0–4) to determine the degree of CD20 +B cells, CD3 +T cells, CD68 +lining) and sublining macrophage and CD138 +plasma cell infiltration. Sections were categorised into three pathotypes: (1) pauci-immune (CD68 SL <2 and or CD3, CD20, CD138 <1), (2) diffuse myeloid: (CD68SL >2, CD20 <1 and or CD3 >1) and (3) lymphomyeloid: (grade 2–3 CD20 +aggregates, CD20 >2). Arrow heads indicate positive stain cells. Empty arrows indicate B cell aggregates. (C) Demographic analysis by pathotype. Data are presented as mean and SD for numerical variables and frequency and percentage for categorical variables. Baseline characteristics between the three pathotypes were compared using a Kruskal-Wallis test and Fisher test (RF and ACPA positivity) as appropriate. Post hoc analysis for significant differences using the Dunn test for multiple comparison. A p value of <0.05 was considered statistically significant. (D) Pathotype according to disease duration (months) at diagnosis. Absolute values (N) and percentage. A p value of <0.05 was considered statistically significant. ACPA titre, anticitrullinated protein antibody titre (IU/L); ACPA +ve, anticitrullinated protein antibody (>20 IU/L); CRP, C reactive protein; DAS28, Disease Activity Score 28 joints; ESR, erythrocyte sedimentation rate; RF titre, rheumatoid factor titre (IU/mL); RF +ve, rheumatoid factor serum positive (>15 IU/L); 28TJC, 28 tender joint count; 28SJC, 28 swollen joint count.

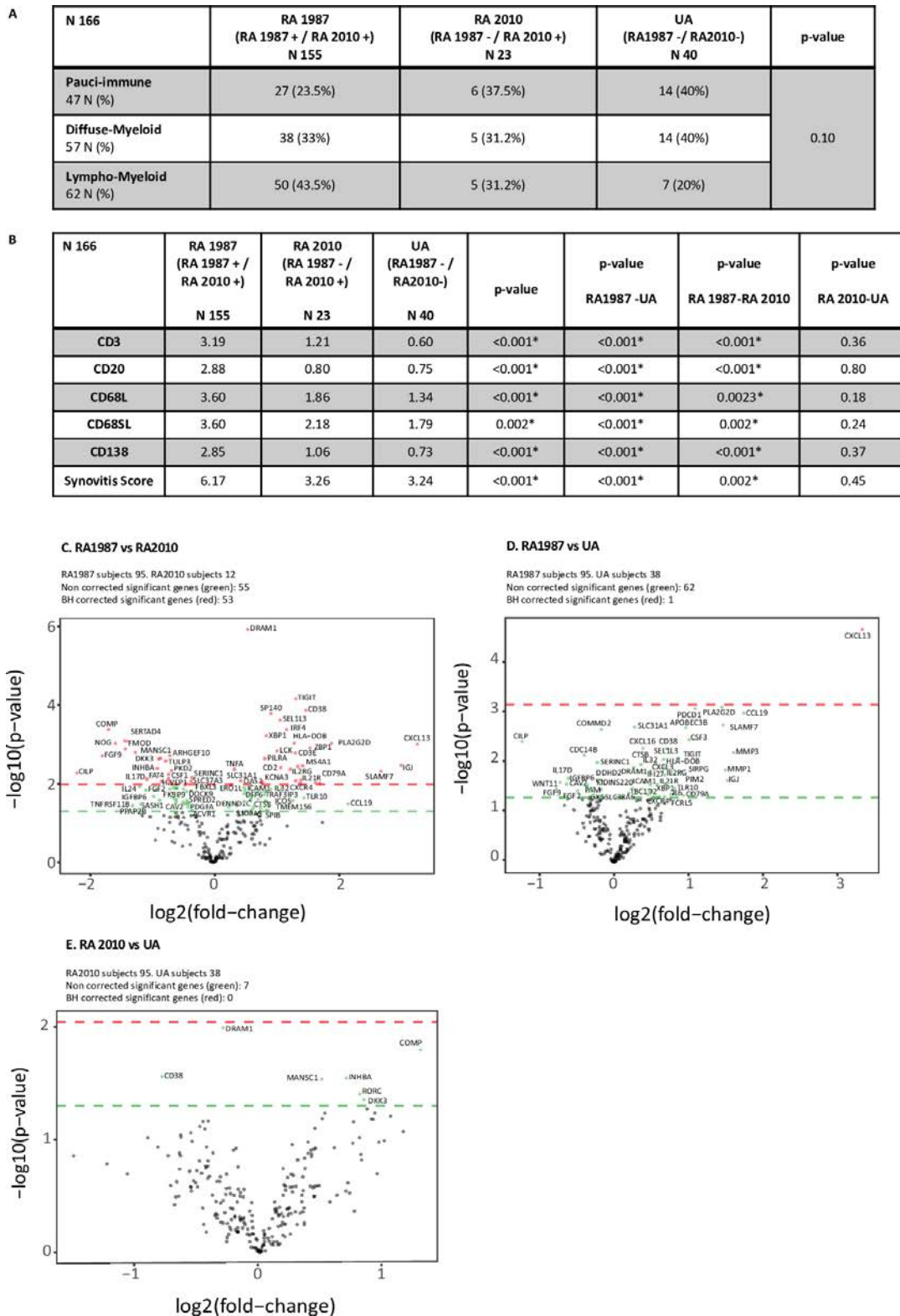


Figure 3 Variation in synovial pathobiology according to clinical classification of patients. (A) Baseline clinical classification compared with pathotype. Baseline subgroups (RA1987, RA2010 and UA) were compared with pathotype. Fisher test used for analysis. (B) Immune cell infiltration for each clinical subgroup. Kruskal-Wallis test for comparison between three groups. Post hoc analysis for significant differences using the Dunn test for multiple comparison. (C)–(E) Gene expression analysis for comparison between subgroups. t-Test for comparison and volcano plot for representative image. Positive values represent upregulation and negative values downregulation. Green circles above green horizontal line represents non-corrected for multiple analysis expressed genes between groups. Red circles above red line represents corrected p values (Benjamini-Hochberg (BH) method) for multiple analysis. (C) Volcano plot RA1987 versus RA2010: difference in gene expression between patient fulfilling RA 1987 ACR criteria and RA 2010 ACR/EULAR criteria. (D) Volcano plot RA1987 versus UA: difference in gene expression between patient fulfilling RA 1987 ACR criteria and UA. (E) Volcano plot RA 2010 versus UA: differences in gene expression between patient fulfilling RA 2010 ACR/EULAR criteria and UA. RA, rheumatoid arthritis; UA, undifferentiated arthritis.

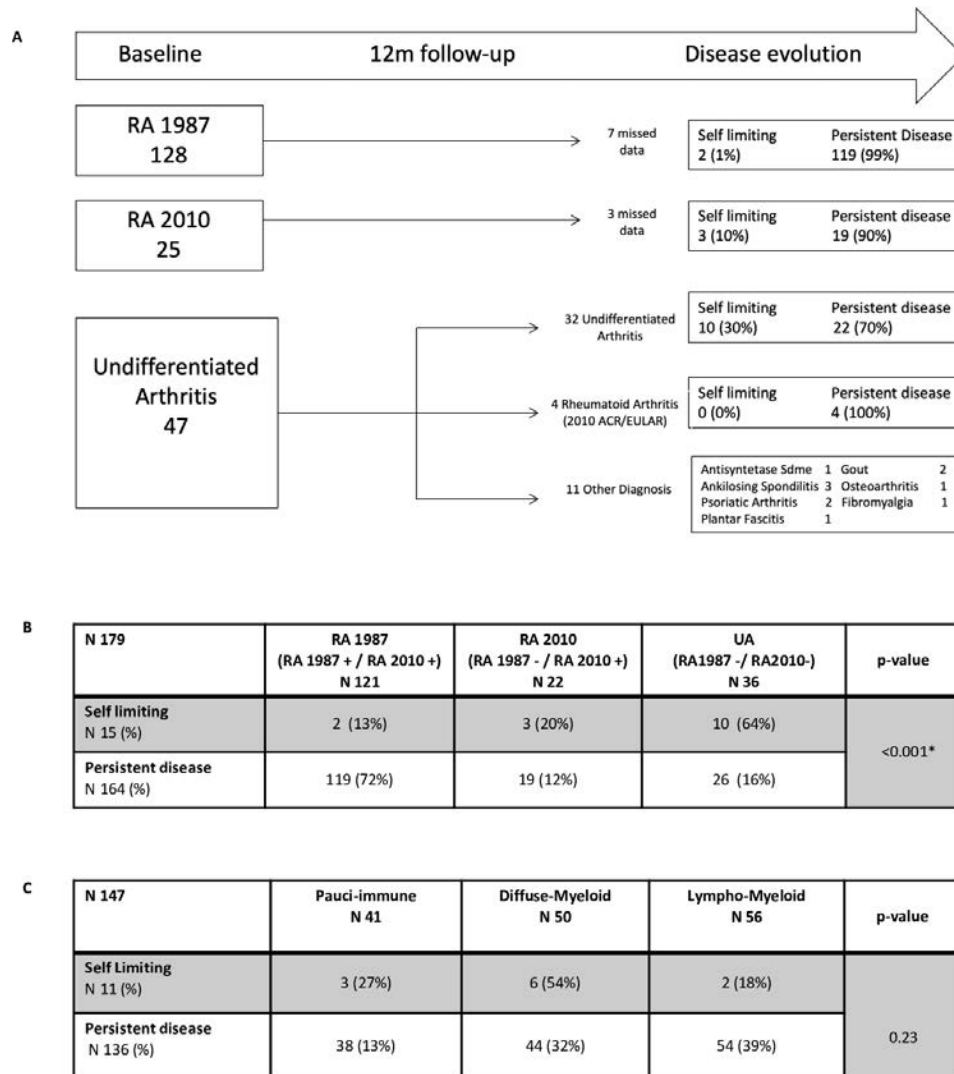


Figure 4 Disease evolution. (A) Patient classification after 12-month follow-up. Disease outcome after 12 months of follow-up for each of the initial baseline subgroups (RA1987/RA2010/UA). Disease evolution classified as self-limiting or persistent disease. Other diagnosis as described for those who were reclassified after 1 year from UA cohort. (B) Disease evolution by subgroups. Disease evolution was compared with baseline subgroups (RA1987, RA2010 and UA). Fisher test used for analysis. (C) Disease evolution by pathotype. Disease evolution was compared with pathotype (pauci-immune vs diffuse myeloid vs lymphomyeloid). Fisher test used for analysis. A p value of <0.05 was considered statistically significant. RA, rheumatoid arthritis; UA, undifferentiated arthritis.

lympho-myeloid or pauci-immune pathotype (54% vs 18% vs 27%) with SL (figure 4C).

A baseline lympho-myeloid pathotype significantly associates with 12-month requirement for biological therapy

Patients stratified according to diagnostic group or pathotype were further classified according to 12-month treatment requirement: (1) symptomatic treatment, (2) csDMARDs or (3) biologics±csDMARDs. A significantly higher proportion of RA1987 patients required biologic compared with RA2010 and UA (27.82% vs 20.83% vs 10.63%) (p<0.001) (figure 5A) and importantly, lympho-myeloid (vs diffuse-myeloid or pauci-immune) pathotype significantly associated with 12-month requirement for biological therapy (57% vs 21% vs 21% p=0.02) (figure 5B).

We then compared expression of the 238 genes in the Nanospring panel between patients requiring biological therapy (n=34) or not (n=106) and found 119 differentially expressed genes. Patients requiring biological therapy had significantly higher

differential upregulation of genes regulating B and T cell proliferation, differentiation and activation (eg, *TNFRSF13C*, *CD79A*, *CD2*, *CD3E* and *CD38*), genes involved in matrix metalloproteinase production/regulation (eg, *MMP1* and *TIMP1*), genes involved in cytokine-mediated cellular activation (*TNFA*, *TRAF3IP3*, *IFNA1*) and osteoclastogenesis inhibition (*DEF6*). Patients who did not require biological therapy expressed some B and T cell regulation genes and B proliferation markers but mostly markers of fibroblast proliferation and cartilage turnover (figure 5C).

To determine whether disease duration influenced outcome, we segregated patients according to 12-month treatment (biological therapy or not) and further into disease duration quartiles (figure 5D) and demonstrated no significant differences in terms of disease duration at diagnosis. Next, we segregated patients treated with biological therapy (n=39) according to quartiles of disease duration and then synovial pathotype. We found no significant differences in patient number in each quartile (p=0.3) (figure 5E). These results strongly suggest that synovial

A

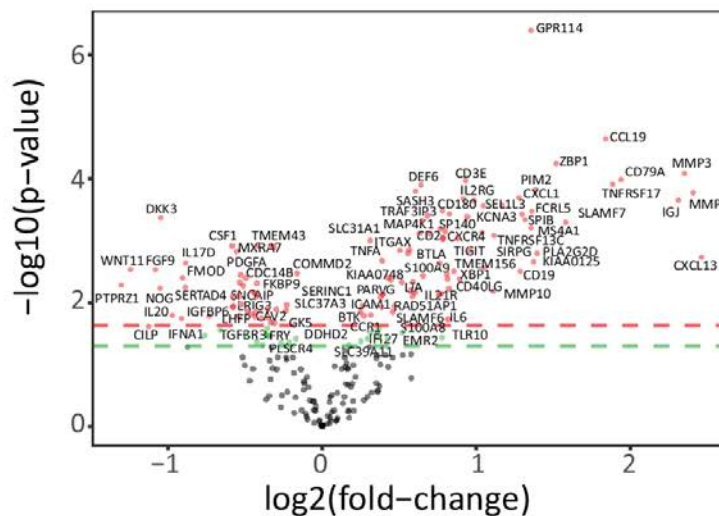
N 186	RA 1987 (RA 1987 + / RA 2010 +) N 115	RA 2010 (RA 1987 - / RA 2010 +) N 24	UA (RA1987 - / RA2010-) N 47	p-value
Symptomatic treatment N 23	2 (1.7%)	4 (16.66%)	17 (36,17%)	<0.001*
csDMARDs N 121	81 (70.43%)	15 (62.50%)	25 (53,19%)	
Biologics +/- csDMARDs N 42	32 (27.82%)	5 (20,83%)	5 (10.63%)	

B

N 153	Pauci-immune N 44	Diffuse-Myeloid N 52	Lympho-Myeloid N 57	p-value
Symptomatic Treatment N 14	6 (42%)	6 (42%)	2 (14%)	<0.02*
csDMARDs N 101	30 (29%)	38 (37%)	33 (33%)	
Biologics +/- csDMARDs N 38	8 (21%)	8 (21%)	22 (57%)	

C. Biologic vs NonBiologic

Biologic subjects 34. NonBiologic subjects 106
Non corrected significant genes (green): 23
BH corrected significant genes (red): 119



D

N 176	1-3m N 55	4-6m N 61	7-9m N 32	10-12m N 28	p-value
csDMARDs n 137	43 (30%)	43 (30%)	26 (18%)	25 (17%)	0.23
Biologics +/- csDMARDs n 39	12 (29%)	18 (43%)	6 (14%)	3 (7%)	

E

N 39 Biologic cohort	1-3m N 12	4-6m N 18	7-9m N 6	10-12m N 3	p-value
Pauci-immune	1 (58%)	5 (27%)	0 (0%)	2 (66%)	0.30
Diffuse - Myeloid	3 (25%)	1 (5%)	3 (50%)	0 (0%)	
Lympho - Myeloid	7 (58%)	9 (50%)	3 (50%)	1 (33%)	

Figure 5 (A) Comparison between diagnostic subgroups and treatment outcome at 12-month follow-up. Treatment required was divided in three groups: (1) no treatment; (2) csDMARDs only, and (3) csDMARDs ±biologics. Fisher test for analysis. (B) Comparison between pathotype and treatment outcome at 12 months. (C) Gene expression analysis, represented in a volcano plot comparison between patient requiring biologics versus non-biological group. t-Test comparison for gene difference expression between groups. Positive values represent upregulation and negative values downregulation. An adjusted (Benjamini-Hochberg) (BH) correction for multiple analysis) p value of <0.01 was considered statistically significant, represented as dots above red line. Green dots above green line for gene expression significance when no correction applied for multiple analysis (p<0.05). (D) Treatment outcome according to baseline disease duration. Fisher test for analysis. (E) Pathotype according to baseline disease duration for biological patient cohort. Fisher test for analysis. A p value of <0.05 was considered statistically significant unless otherwise stated. RA, rheumatoid arthritis; UA, undifferentiated arthritis.

pathotype rather than disease duration influences 12-month treatment outcome.

Synovial gene expression signatures enhance the performance of clinical prediction models for biological requirement

To determine whether baseline clinical and gene expression data could be combined into a model for predicting requirement for biological therapy, we used two complementary approaches: a logistic regression model to identify predictive clinical covariates, and a penalised method based on logistic regression with an L1 regularisation penalty (LASSO) to identify genes improving the clinical model.

Nine baseline clinical covariates were considered as candidates in the regression model: disease duration, ESR, CRP, RF, ACPA, TJC, SJC, DAS28 and pathotype (two categories, lympho-myeloid vs pauci-immune/diffuse-myeloid). Logistic regression models using backward forward and bidirectional stepwise selection resulted in the selection of the same set of clinical covariates: DAS28, pathotype, CRP and TJC. The apparent predictive performance of the model evaluated by AUC was 0.78 (95% CI 0.70 to 0.87).

Genes were selected to improve the clinical model using logistic regression with an L1 regularisation penalty (LASSO) applied on the four clinical covariates selected by the previous logistic regression and the 119 genes identified as being significantly differentially expressed between the biological and non-biological groups. Models in which clinical predictors were penalised or subject to forced inclusion were compared. When all predictors were penalised, 11 predictors were retained in the final model and when the clinical covariates were not penalised, 13 predictors were retained (figure 6A). In both the penalised and unpenalised clinical model, the apparent prediction performance was improved (apparent AUC=0.89, 95% CI 0.83 to 0.95 and AUC=0.90, 95% CI 0.84 to 0.95) (figure 6B). We additionally performed internal validation to correct the AUC performance measure for overfitting by calculating the optimism of the AUC for each model by bootstrapped sampling with replacement from the original dataset. The optimism corrected AUC was 0.75 for the pure clinical model and 0.81 for the clinical and gene model (LASSO) (figure 6C and D) suggesting that including both clinical covariates and genes in the model results in an improvement of the predictive ability of the model.

DISCUSSION

These results present a number of novel findings: first, they strongly suggest that patients with early inflammatory arthritis not fulfilling RA1987 criteria display similar clinical, synovial histological and molecular features irrespective of further classification according to RA2010 or UA criteria. Second, these data also suggest that a lympho-myeloid pathotype at disease onset predicts poor outcome with patients subsequently requiring biological therapy irrespective of clinical classification, and finally that the integration of histological and molecular signatures into a clinical prediction model enhances sensitivity/specificity for predicting whether patients will require biological therapy.

To the best of our knowledge, these results emerge from the largest synovial tissue treatment-naïve early arthritis cohort reported to date and support previous data from early RA cohorts suggesting that a synovial immune cell infiltrate characterised by a predominant infiltrate of B cells associates with more active disease¹⁸ and seropositivity for RF and ACPA.¹⁰ The results

suggest that this effect also extends to patients within the UA cohort. The clinical similarities between RA2010+/RA1987– patients and those with UA have been reported previously⁸ and the data presented herein provide a pathophysiological explanation for this with the demonstration of homogeneous synovial cellular and molecular signatures among the two groups. The data show a lower percentage of patients requiring biological therapy in RA2010+/RA1987– group, in line with the expectation that the ACR/EULAR 2010 criteria enable an earlier diagnosis and thus efficacious treatment. However, it is also possible that this group has a milder pathology from the beginning.

Although synovial pathotypes per se do not appear to distinguish between patients at risk of developing PD rather than SL disease, this is not surprising given the early and treat-to-target approach pursued in the study rather than observing untreated natural disease evolution. However, when applying 12-month biological requirement as a prognostic outcome, we demonstrated that patients with a lympho-myeloid pathotype with a dense synovial infiltrate enriched in B cells and significant upregulation of T/B cell genes at disease onset predicted requirement for subsequent biological therapy and critically that this was independent of disease duration. These results are consistent with recently published data in early RA which reports that the lympho-myeloid pathotype is associated with highly aggressive disease and worse radiographic outcomes.¹⁰ The current study reinforces these findings demonstrating that, at 12-month follow-up, a significantly higher proportion of patients classified as lympho-myeloid pathotype required biological therapy. The study also calls into question the current dogma surrounding ‘an early window of opportunity’ for all patients with RA,^{19–21} suggesting that pathotype rather than simply disease duration influences outcome and that intensive therapeutic regimens should be targeted to poor prognostic pathotypes. This notion is supported by the demonstration that the integration of synovial histological and molecular markers into a clinical prediction model for biologics use improves sensitivity/specificity from 78.8% to 89%–90% independently from disease duration.

Discrepancy with previously reported data suggesting that synovial heterogeneity does not relate to clinical phenotypes⁹ maybe explained by the fact that in our study the majority of biopsies were performed on small joints while in that cohort arthroscopic biopsy was restricted to patients with mainly large joint involvement and, thus, a potential selection bias.²² Additionally, the paired histological and molecular data in the largest biopsy-driven early arthritis cohort reported to date ensured internal validation and high classification accuracy.

Our study does have limitations however, for example, the real-life nature of the study did not permit the true evaluation of the natural history of the disease or outcome, as no patients were left untreated and therapy was not actively withdrawn. Also, a treat-to-target approach, treatment escalation and initiation of biological therapy, was determined by treating physicians according to NICE guidelines rather than study protocol.

Within these limitations, our results are robust and suggest that the introduction of the new RA2010 classification criteria brings additional clinical and biological heterogeneity into early patient classification compared with the 1987 criteria with limited ability of RA2010 criteria alone to predict poor outcome. The demonstration that the integration of synovial pathobiological markers into clinical algorithms predicting poor outcome (requirement for biological therapy) independent of disease duration suggests that the ‘window of opportunity’ is wider than 6 months and early stratification of biological therapies

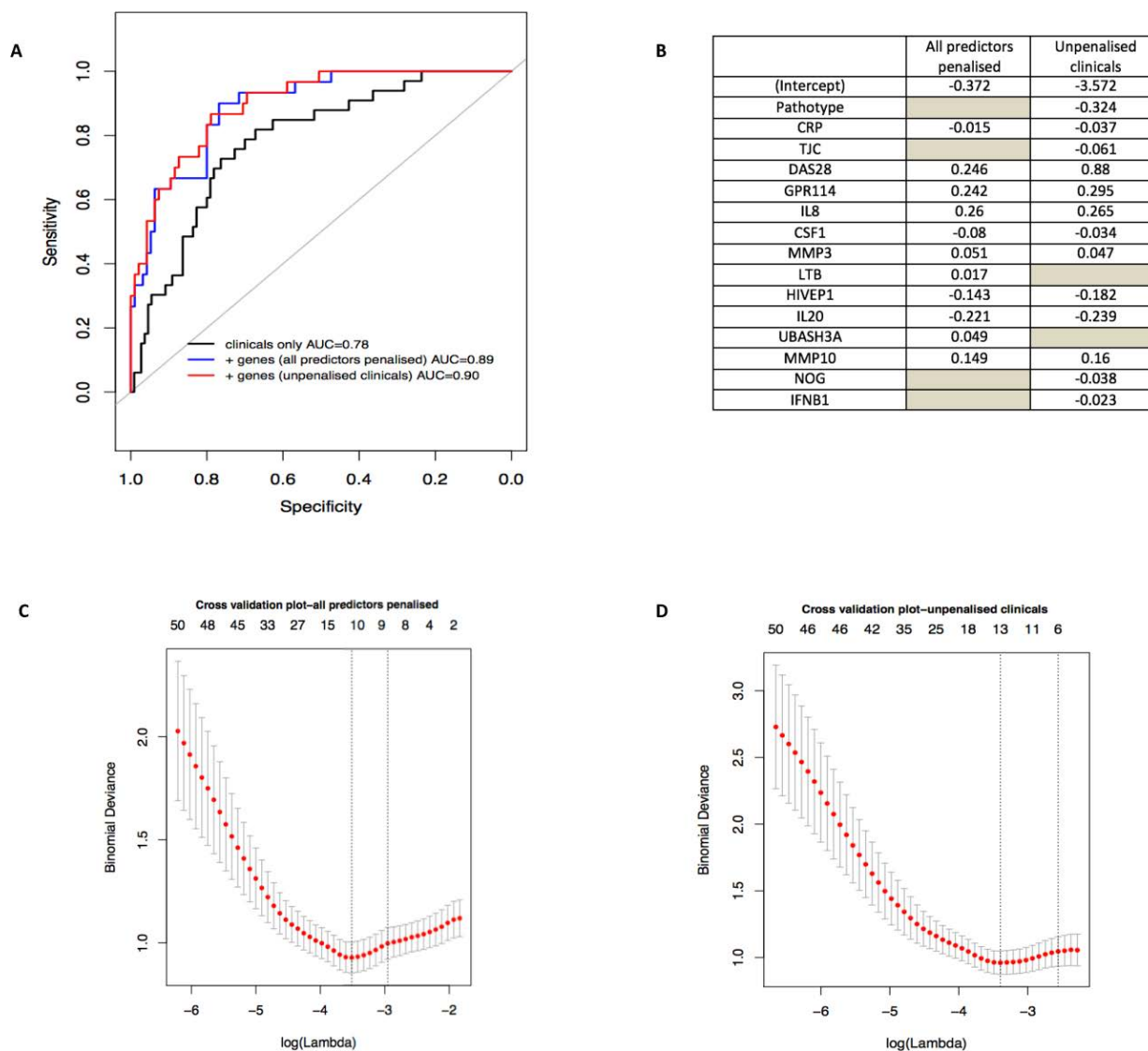


Figure 6 Prediction model. (A) and (B) Identification of clinical and gene expression features predictive of biological therapy use at 1 year. Logistic regression, coupled with backward and stepwise model selection, was applied to baseline clinical parameters against a dependent variable of biological therapy use or not at 12 months to select which clinical covariate contributed the most to the prediction. Selected covariates (119 genes+4 clinical covariates) were entered simultaneously into a logistic model with an L1 regularisation penalty (LASSO) in order to determine the optimal sparse prediction model. A similar predictive performance of the model when clinical was seen when results were penalised (blue-dashed line, A) than when they were not penalised (red-dotted line, A) with a slightly different set of selected covariates (B). (B) Non-zero weights associated with the final variables selected by the LASSO regression. The grey spaces represent the variables that were not selected by the model. (C) and (D) Lambda training curve from the final glmnet fitted model. The red dots represent mean binomial deviance using 10-fold cross validation. The error bars represent SE of binomial deviance. The vertical dotted lines indicate minimum binomial deviance (λ_{\min}) and a more regularised model for which the binomial deviance error is within one SE of the minimum binomial deviance (λ_{1se}). λ_{\min} was selected, corresponding to 11 non-zero coefficients in the final model for the LASSO where clinical were penalised (C) and 13 non-zero coefficients in the final model for the LASSO where clinical were not penalised (D). AUC, area under the receiver operating characteristic curve; CRP, C reactive protein; DAS28, Disease Activity Score 28 joints; TJC, tender joint count.

according to poor prognostic synovial pathobiological subtypes at disease onset may improve the outcome of these patients.

Author affiliations

¹Centre of Experimental Medicine and Rheumatology, William Harvey Research Institute, London, UK

²Centre for Experimental Medicine and Rheumatology, Barts and the London School of Medicine and Dentistry, London, UK

³Queen Mary University of London—Charterhouse Square Campus, London, UK

⁴Rheumatology, Barts Health NHS Trust, London, UK

⁵Experimental Medicine and Rheumatology, Queen Marys University of London, London, UK

⁶Biomarker Discovery OMNI, Genentech Research & Early Development, San Francisco, California, USA

⁷ITGR Biomarker Discovery Group, Genentech, South San Francisco, California, USA

⁸Rheumatology and Rheumatology Unit, University of Cagliari and AOI University Clinic of Cagliari, Monserrato, Italy

⁹Institute of Infection and Immunity, Cardiff University School of Medicine, Cardiff, UK

¹⁰Institute of Inflammation and Ageing, University of Birmingham, Birmingham, UK

¹¹Nuffield Department of Orthopaedics, Rheumatology and Musculoskeletal Sciences, University of Oxford, Oxford, UK

¹²Institute of Infection, Immunity and Inflammation, University of Glasgow, Glasgow, UK

¹³Experimental Medicine and Rheumatology, William Harvey Research Institute, London, UK

Acknowledgements The authors thank all study participants.

Contributors GL-R and FH contributed equally to this manuscript. All authors have contributed to different degrees to patients recruitment and or data generation and or data analysis and or writing the manuscript and or revising data and or manuscript.

Funding Funding for PEAC MRC: Grant code 36661. Funding Infrastructure support to EMR, Arthritis Research UK Experimental Treatment Centre: Grant code 20022.

Competing interests None declared.

Patient consent for publication Not required.

Ethics approval The study received local ethical approval (REC 05/Q0703/198).

Provenance and peer review Not commissioned; externally peer reviewed.

Data availability statement Data are available upon reasonable request.

Open access This is an open access article distributed in accordance with the Creative Commons Attribution Non Commercial (CC BY-NC 4.0) license, which permits others to distribute, remix, adapt, build upon this work non-commercially, and license their derivative works on different terms, provided the original work is properly cited, appropriate credit is given, any changes made indicated, and the use is non-commercial. See: <http://creativecommons.org/licenses/by-nc/4.0/>.

ORCID iDs

Frances Humby <http://orcid.org/0000-0003-1280-9133>

Myles Lewis <http://orcid.org/0000-0001-9365-5345>

Alessandra Nerviani <http://orcid.org/0000-0003-4064-4014>

Felice Rivellese <http://orcid.org/0000-0002-6759-7521>

Peter C Taylor <http://orcid.org/0000-0001-7766-6167>

Costantino Pitzalis <http://orcid.org/0000-0003-1326-5051>

REFERENCES

- Aletaha D, Neogi T, Silman AJ, et al. 2010 rheumatoid arthritis classification criteria: an American College of Rheumatology/European League against rheumatism collaborative initiative. *Arthritis Rheum* 2010;62:2569–81.
- Arnett FC, Edworthy SM, Bloch DA, et al. The American rheumatism association 1987 revised criteria for the classification of rheumatoid arthritis. *Arthritis & Rheumatism* 1988;31:315–24.
- van Nies JAB, Brouwer E, van Gaalen FA, et al. Improved early identification of arthritis: evaluating the efficacy of Early Arthritis Recognition Clinics. *Ann Rheum Dis* 2013;72:1295–301.
- Sakellariou G, Scirè CA, Zambon A, et al. Performance of the 2010 classification criteria for rheumatoid arthritis: a systematic literature review and a meta-analysis. *PLoS One* 2013;8:1–10.
- van der Helm-vanMil AHM, le Cessie S, van Dongen H, et al. A prediction rule for disease outcome in patients with recent-onset undifferentiated arthritis: how to guide individual treatment decisions. *Arthritis Rheum* 2007;56:433–40.
- Raza K, Falciani F, Curnow SJ, et al. Early rheumatoid arthritis is characterized by a distinct and transient synovial fluid cytokine profile of T cell and stromal cell origin. *Arthritis Res Ther* 2005;7:R784–95.
- Raza K. The Michael Mason prize: early rheumatoid arthritis—the window narrows. *Rheumatology* 2010;49:406–10.
- de Hair MJH, Lehmann KA, van de Sande MGH, et al. The clinical picture of rheumatoid arthritis according to the 2010 American College of Rheumatology/European League against rheumatism criteria: is this still the same disease? *Arthritis Rheum* 2012;64:389–93.
- van de Sande MGH, de Hair MJH, Schuller Y, et al. The features of the synovium in early rheumatoid arthritis according to the 2010 ACR/EULAR classification criteria. *PLoS One* 2012;7:1–7.
- Humby F, Lewis M, Ramamoorthi N, et al. Synovial cellular and molecular signatures stratify clinical response to csDMARD therapy and predict radiographic progression in early rheumatoid arthritis patients. *Ann Rheum Dis* 2019;78:761–72.
- Kelly S, Humby F, Filer A, et al. Ultrasound-guided synovial biopsy: a safe, well-tolerated and reliable technique for obtaining high-quality synovial tissue from both large and small joints in early arthritis patients. *Ann Rheum Dis* 2015;74:611–7.
- NICE. Overview | rheumatoid arthritis in adults: management | guidance. Available: <https://www.nice.org.uk/guidance/ng100> [Accessed 2 Jul 2019].
- Krenn V, Morawietz L, Burmester G-R, et al. Synovitis score: discrimination between chronic low-grade and high-grade synovitis. *Histopathology* 2006;49:358–64.
- Humby F, Bombardieri M, Manzo A, et al. Ectopic lymphoid structures support ongoing production of class-switched autoantibodies in rheumatoid synovium. *PLoS Med* 2009;6:e1–75.
- Dennis G, Holweg CTJ, Kummerfeld SK, et al. Synovial phenotypes in rheumatoid arthritis correlate with response to biologic therapeutics. *Arthritis Res Ther* 2014;16.
- Smith GCS, Seaman SR, Wood AM, et al. Correcting for optimistic prediction in small data sets. *Am J Epidemiol* 2014;180:318–24.
- Efron B, Tibshirani R. *An introduction to the bootstrap*. Chapman & Hall, 1994. <https://www.crcpress.com/An-Introduction-to-the-Bootstrap/Efron-Tibshirani/p/book/9780412042317>
- Bugatti S, Manzo A, Vitolo B, et al. High expression levels of the B cell chemoattractant CXCL13 in rheumatoid synovium are a marker of severe disease. *Rheumatology* 2014;53:1886–95.
- Lard LR, Visser H, Speyer I, et al. Early versus delayed treatment in patients with recent-onset rheumatoid arthritis: comparison of two cohorts who received different treatment strategies. *Am J Med* 2001;111:446–51.
- Finckh A, Liang MH, van Herckenrode CM, et al. Long-Term impact of early treatment on radiographic progression in rheumatoid arthritis: a meta-analysis. *Arthritis Rheum* 2006;55:864–72.
- Greisen SR, Schelde KK, Rasmussen TK, et al. CXCL13 predicts disease activity in early rheumatoid arthritis and could be an indicator of the therapeutic 'window of opportunity'. *Arthritis Res Ther* 2014;16.
- Linn-Rasker SP, van der Helm-van Mil AHM, Breedveld FC, et al. Arthritis of the large joints—in particular, the knee—at first presentation is predictive for a high level of radiological destruction of the small joints in rheumatoid arthritis. *Ann Rheum Dis* 2007;66:646–50.

TRANSLATIONAL SCIENCE

HLA-B27 alters BMP/TGF β signalling in *Drosophila*, revealing putative pathogenic mechanism for spondyloarthritis

Benjamin Grandon,^{1,2} Aurore Rincheval-Arnold,¹ Nadège Jah,² Jean-Marc Corsi,¹ Luiza M Araujo,² Simon Glatigny,² Erwann Prevost,^{1,2} Delphine Roche,¹ Gilles Chiochia,² Isabelle Guéna,¹ Sébastien Gaumer,¹ Maxime Breban ^{2,3}

Handling editor Josef S Smolen

► Additional material is published online only. To view please visit the journal online (<http://dx.doi.org/10.1136/annrheumdis-2019-215832>).

¹LGBC, EA4589, UVSQ/ Université Paris-Saclay, EPHE/ PSL Research University, Montigny-le-Bretonneux, France
²Infection & Inflammation, UMR 1173, Inserm, UVSQ/ Université Paris Saclay, Montigny-le-Bretonneux, France
³Rheumatology, Ambroise Paré Hospital, Boulogne Billancourt, France

Correspondence to

Professor Maxime Breban, Rheumatology, Ambroise Paré Hospital, Boulogne Billancourt, France; maxime.breban@aphp.fr

IG, SG and MB are joint senior authors.

This work has been presented at the 2019 EULAR Congress (Abstract FRI0353; Madrid, Spain, June 2019).

Received 4 June 2019
Revised 8 September 2019
Accepted 9 September 2019
Published Online First
28 September 2019



© Author(s) (or their employer(s)) 2019. No commercial re-use. See rights and permissions. Published by BMJ.

To cite: Grandon B, Rincheval-Arnold A, Jah N, et al. *Ann Rheum Dis* 2019;**78**:1653–1662.

ABSTRACT

Objectives The human leucocyte antigen (HLA)-B27 confers an increased risk of spondyloarthritis (SpA) by unknown mechanism. The objective of this work was to uncover HLA-B27 non-canonical properties that could explain its pathogenicity, using a new *Drosophila* model.

Methods We produced transgenic *Drosophila* expressing the SpA-associated HLA-B*27:04 or HLA-B*27:05 subtypes, or the non-associated HLA-B*07:02 allele, alone or in combination with human β 2-microglobulin (h β 2m), under tissue-specific drivers. Consequences of transgenes expression in *Drosophila* were examined and affected pathways were investigated by the genetic interaction experiments. Predictions of the model were further tested in immune cells from patients with SpA.

Results Loss of crossveins in the wings and a reduced eye phenotype were observed after expression of HLA-B*27:04 or HLA-B*27:05 in *Drosophila* but not in fruit flies expressing the non-associated HLA-B*07:02 allele. These HLA-B27-induced phenotypes required the presence of h β 2m that allowed expression of well-folded HLA-B conformers at the cell surface. Loss of crossveins resulted from a dominant negative effect of HLA-B27 on the type I bone morphogenetic protein (BMP) receptor saxophone (Sax) with which it interacted, resulting in elevated mothers against decapentaplegic (Mad, a *Drosophila* receptor-mediated Smad) phosphorylation. Likewise, in immune cells from patients with SpA, HLA-B27 specifically interacted with activin receptor-like kinase-2 (ALK2), the mammalian Sax ortholog, at the cell surface and elevated Smad phosphorylation was observed in response to activin A and transforming growth factor β (TGF β).

Conclusions Antagonistic interaction of HLA-B27 with ALK2, which exerts inhibitory functions on the TGF β /BMP signalling pathway at the cross-road between inflammation and ossification, could adequately explain SpA development.

INTRODUCTION

The class I major histocompatibility complex (MHC-I) allele encoding human leucocyte antigen (HLA)-B27 is the main genetic factor predisposing to ankylosing spondylitis (AS) and the related spondyloarthritis (SpA). This is a group of frequent disabling diseases primarily characterised by chronic inflammation of the axial skeleton, leading to bony

Key messages

What is already known about this subject?

► The HLA-B27 allele is strongly associated with spondyloarthritis (SpA) risk by unknown mechanism.

What does this study add?

- In this study, a new model of *Drosophila* transgenic for HLA-B27 was investigated, showing a wing phenotype, not observed in control HLA-B7 transgenic *Drosophila*.
- This phenotype was due to a dominant negative effect of HLA-B27 on the *Drosophila* type I bone morphogenetic protein receptor, saxophone (Sax) with which it interacted specifically.
- In immune cells from SpA patients, a specific interaction was also shown between HLA-B27 and the mammalian Sax ortholog, activin receptor-like kinase-2 (ALK2) and, as predicted if HLA-B27 antagonised ALK2, an increased response to Activin A and transforming growth factor β (TGF β).

How might this impact on clinical practice or future developments?

► This study implicates a misregulation of the BMP/TGF β pathway as a putative pathogenic mechanism of HLA-B27 for SpA development.

ankylosis of the sacroiliac and vertebral joints.¹ Strong association between AS and HLA-B27 was first described 46 years ago² but still remains largely unexplained.

On synthesis, MHC-I heavy chain enters the endoplasmic reticulum (ER) where it associates non-covalently with both the invariant human β 2-microglobulin (h β 2m) chain and an 8 to 10-mer peptide before being exported to the cell surface via the Golgi apparatus.³ The canonical function of HLA-B molecules is to present antigenic peptides derived from cytosolic proteins to CD8+ T cells, leading to a cytotoxic response.⁴ Accordingly, one of the oldest theories that was proposed to explain HLA-B27 pathogenicity, also designated as the ‘arthritogenic peptide’ hypothesis, speculates on the capacity of this molecule to specifically present as yet undetermined antigenic peptide(s) derived from

the joint, thereby triggering a harmful CD8+ T cell-mediated response.⁵ However, convincing evidence supporting the implication of such mechanism is still lacking. Other theories have emerged more recently, based on non-canonical biological features of HLA-B27. These include the formation of homodimers of HLA-B27 heavy chains at the cell surface, interacting with killer immunoglobulin-like receptors expressed on CD4+ T cells and natural killer cells.⁴ Alternatively, failure of HLA-B27 to fold properly during its assembly may lead to an ER stress response, thereby fostering chronic inflammation.⁶ However, none of these hypotheses has been fully proven yet.

Drosophila melanogaster is an invaluable system to understand complex molecular mechanisms.⁷ Indeed, many cellular signaling pathways and functions are conserved between mammals and *Drosophila*. Here, we speculated that this simple experimental live system could be suitable to unravel aberrant functional consequences of HLA-B27/h β 2m expression, which could contribute to its pathogenicity.

METHODS

Drosophila lines

Drosophila were cultured using standard corn-agar medium. Crosses were performed at 25°C. Various GAL4 drivers used to induce transgenes expression and origin of the stocks are described in online supplementary table 1.

Transgenic lines constructs

Flies carrying the cDNA of either HLA-B*27:04, HLA-B*27:05, HLA-B*07:02 or h β 2m, under control of UAS regulatory sequences that can be bound by the yeast GAL4 transcription factor to direct tissue-specific expression were generated by P-element transgenesis.⁸ Human cDNAs containing the full-length coding region have been previously described.⁹ They were ligated in the pUASg-attB vector (Gateway Technology). The resulting plasmids were purified with Qiagen tips and sent for injection into w¹¹¹⁸ embryos (BestGene, California, USA). UAS-HLA-B*07:02, UAS-HLA-B*27:05 and UAS-HLA-B*27:04 transgenes were all inserted as single copy in the same predefined site (68A4 of chromosome 3) allowing to control for the non-specific consequence of the insertion, when comparing different HLA-B transgenes. UAS-h β 2m was inserted in 89E11 of chromosome 3. At least two independent transgenic lines were studied for each single or recombined transgene, leading to identical phenotype. Effective expression of the transgenes was observed at the transcription and protein levels by real-time quantitative PCR (RT-q-PCR) and Western-blot, respectively (online supplementary file 1a-c).

Genetic interaction tests

The effect of HLA-B*27:05/h β 2m expression driven by nub-Gal4 was assayed in different genetic backgrounds to test for the interaction of HLA-B*27:05 with different candidate genes. nub-Gal4 >UAS-HLA-B*27:05, UAS-h β 2m *Drosophila* females were crossed with males bearing a loss of function or overexpressing mutant alleles of these genes. Each test was done thrice in independent experiments. For wing phenotype analysis, all the progeny was analysed for each cross, including 40–100 flies. The phenotype of each cross was fully penetrant. About 10 adult wings were dissected from random adult flies in phosphate-buffered saline (PBS) and mounted with 50% glycerol. Images were obtained with an LEICA MZFLIII microscope and an Olympus DP20 digital colour camera (Olympus, Hamburg, Germany). Scale information was recorded in the image. For

wing imaginal discs, the number of imaginal discs analysed was indicated on the corresponding graph.

RNA extraction and RT-q-PCR

Forty wing imaginal discs were dissected in the RNA XS NucleoSpin kit's lysis buffer (Macherey-Nagel, Düren, Germany) on ice for each genotype to extract total RNAs. RNA concentration was determined by NanoDrop 1000 (ThermoScientific, Wilmington, USA). Reverse transcription was performed using 500 ng of total RNA following the protocol of M-MLV Reverse Transcriptase (ThermoScientific). RT-q-PCR was performed using the CFX96 Touch RT-PCR Detection System. Reaction mix preparation is composed of iTaq Universal SYBRGreen Supermix (BIORAD, Hercules, USA) and 11 ng of cDNA as described in Biorad reaction mix preparation protocol. Three independent RT-q-PCR experiments were performed and data were normalised against *uba2* mRNA levels. Forward and reverse primer sequences (Invitrogen, Life Technologies) used for RT-q-PCR are shown in online supplementary table 2.

Immunostaining and microscopy

Wing discs of third-instar larvae were dissected and immunostained as previously described.¹⁰ The following primary antibodies (Abs) were used: rabbit anti-death caspase-1 (Asp216, Cell Signaling, Danvers, Massachusetts, USA, 1:50)¹¹; rabbit anti-phosphorylated (p)-Smad1/5 to detect p-mothers against Dpp (p-Mad, S463/465, Cell Signaling, 1:100)¹²; rabbit anti-GFP (A-11122, ThermoFisher Scientific, Massachusetts, USA, 1:500); rabbit anti-HA tag (Y-11, Santa Cruz, Dallas Texas, USA, 1:500); HC-10, a mouse IgG₂a monoclonal Ab (mAb) recognising unfolded HLA-B heavy chains¹³; ME1, a mouse IgG1 mAb that is specific for properly folded HLA-B27, HLA-B7 and HLA-B22 proteins¹⁴; w6/32, a mouse IgG₂a mAb uniformly recognising a monomorphic determinant of all folded HLA-A, HLA-B and HLA-C proteins (ab22432, Abcam)¹⁵ and BBM1 a mouse anti-h β 2m IgG₂b mAb.¹⁶ Secondary Abs conjugated to Alexa Fluor 488, 568 or 647 were purchased from Molecular Probes (Eugen, Oregon, USA 1:400). Discs were mounted in Citifluor (Biovalley, Marne-La-Vallée, France). Images were captured using a Leica SPE confocal laser-scanning microscope (Leica, Wetzlar, Germany). Images were stacked and mean intensity was quantified with the ImageJ software.

Eye size measurement

Adult flies of 2–3 days were immobilised by freezing at –80°C and mounted on a Petri dish before being imaged at 3.2X magnification using a LEICA MZFLIII microscope and an Olympus DP20 Digital colour camera (Olympus). Eye size was measured with the ImageJ pixel area function.

Imaginal disc cell preparation for flow cytometry

Thirty wing discs were dissected in PBS and transferred to siliconized tubes for trypsinization during 1.5 hours at 25°C (90% Trypsin in PBS, Thermofisher). Transgene expressing cells were also expressing GFP. Dissociated cells were left 2.5 hours in Schneider medium at 25°C and incubated with the primary Ab diluted in PBS+ bovine serum albumin 0.1% for 30 min at room temperature (RT). Cells were then rinsed and incubated with the secondary Ab and propidium iodide (PI) for 30 min at RT. PI-negative and GFP+ cells were characterised with a FACS-Canto II system (FORTESSA, BD Biosciences) and analysed thanks to the Flowjo software (Tree Star).

Proximity ligation assay

Proximity ligation assay (PLA) was performed using the Duolink In Situ Red Starter Kit Mouse/Rabbit (Sigma-Aldrich), following the manufacturer's protocol. For *Drosophila* experiments, 20 wing imaginal discs for each genotype were dissected in PBS, fixed in 3.7% formaldehyde for 20 min at RT and permeabilised in PBS+Tween 0.3%. Primary anti-HA, and w6/32 Abs were used overnight at 4°C. For B-lymphoblastoid cell line (B-LCL) experiments, anti-activin receptor-like kinase-2 (ALK2) (Sigma-Aldrich, 1:100), anti-CD45 (mouse, 2B11+PD7/26, Dako, California, USA, 1:100), ME1 and w6/32 Abs were used. Ten random 40x images per condition were acquired using the DAPI (blue nuclei) and Cy5 (red PLA signals) filters. Z-stack confocal images were collected and maximum intensity projections were generated by ImageJ. Automatic counting of the PLA dots using the 'Find Maxima' function in ImageJ software were performed.

Human cells

B-LCLs 10 151 (HLA-A*02, *31; B*27:05, *15; C*02, *03), 6370 (HLA-A*02, *68; B*27:05, *44; C*02, *07) and 13 617 (HLA-A*02, *03; B*27:05, *18; C*02, *07) were established from AS patients and have been previously described.^{17,18} B-LCLs 9435 (HLA-A*02, *03; B*07, *44; C*05, *07), 9953 (HLA-A*03, *30; B*07, *49; C*06, *07) and 6908 (HLA-A*02, *11; B*22, *44; C*03, *05) were established from Epstein-Barr virus-transformed lymphocytes from healthy controls according to standard protocol and grown at 37°C in RPMI 1640 medium supplemented with 10% heat inactivated fetal bovine serum, 100 U/mL penicillin and 100 µg/mL streptomycin. Peripheral blood mononuclear cells (PBMC) were isolated from HLA-B27+ SpA patients and HLA-B27 negative healthy controls, having signed informed consent, by Ficoll (GE Healthcare) density gradient centrifugation. CD14+ cells were first removed from PBMC by positive magnetic selection, using anti-CD14 microbeads and AutoMacs Pro Separator (Miltenyi Biotec). The characteristics of SpA and controls are shown in online supplementary table 3.

Analysis of Smad2/3 phosphorylation by flow cytometry

CD14-negative PBMC (10⁶ cells/tube in PBS) from pairs of patients SpA and healthy controls were stimulated with recombinant human (rh) transforming growth factor β (TGFβ) (10 ng/mL; R&D Systems) or rhActivin A (20 ng/mL; R&D Systems) or not for 30 min at 37°C. After staining with anti-CD3 mAb (clone-UCHT1; BD Biosciences) and fixation during 20 min at 37°C with cytoFix Buffer (BD Biosciences), cells were permeabilised with perm buffer and stained with anti-p-Smad2 (pS465/pS467)/p-Smad3 (pS423/pS425) PhosFlow Ab according to the manufacturer's instructions (BD Biosciences) and analysed using an LSRIII Fortessa flow cytometer (BD Biosciences). Results were expressed as staining index calculated as the ratio between samples and fluorescence-minus-one staining control.

Western blotting

Forty wing discs of third-instar larvae were dissected in PBS and crushed in 400 µl of lysis buffer (Tris-HCl pH 8.2, 1M; NaCl 25 mM; Nonidet P40 1%, protease inhibitor (complete Mini ethylenediaminetetraacetic acid (EDTA) free, Roche, Boulogne-Billancourt, France)). Total protein extract was completed by Laemmli 4X, DTT 0.5M and heated to 95°C for 5 min. Three independent samples of total protein were analysed by Western-blot following a standard protocol, using rabbit anti-GRP78 (BiP) (ab21685, abcam),¹⁹ HC-10,

BBM1 and mouse anti-Lamin C (LC28.26, DSHB, Iowa, USA)²⁰ and peroxidase-conjugated goat antimouse Ig or rabbit Ig (Dakocytomation, Carpinteria, California, USA) for 1.5 hours. CD14-negative PBMC (1–2 10⁶ cells) were lysed in lysis buffer (Tris-HCl pH 7.5 20 mM; NaCl 20 mM; Triton 100×1%, EDTA 10 mM, protease inhibitor (complete Mini EDTA free, Roche), phosphatase inhibitor (PhosSTOP, Roche, 04906837001), Na3VO4 (1 mM)). A total of 2 µg of proteins were separated in 4%–12% gradient gel and transferred on a polyvinylidene fluoride membrane. Blot was revealed following a standard protocol using rabbit anti-p-Smad2 (Cell Signaling #3108), rabbit anti-Smad2/3 (Cell Signaling #8685) and rabbit anti-actin (Sigma #A2066).

Statistical analysis

Quantitative data are shown as the mean±SEM. Unpaired Student's t-test was used for comparisons between two groups, unless otherwise stated. Analysis of variance (ANOVA) was used for comparison of more than two groups, followed by unpaired Student's t-test after Bonferroni correction. Normality and homoscedasticity were, respectively, verified by Shapiro-Wilk and F tests before unpaired t-tests with n<30 or ANOVA. When data were not normal or homoscedastic, ANOVA was replaced by the Kruskal-Wallis test, followed by Dunn's multiple comparisons tests comparing each condition to the control. Wilcoxon matched-pairs test was used for comparison of matched groups. P values inferior to 0.05 were considered significant. The effect size was measured by Cohen's d.

Data availability

The authors declare that the main data supporting the findings of this study are available within the article and its online supplementary information files.

RESULTS

AS-associated HLA-B27 alleles induce-specific wing and eye phenotypes in *Drosophila*

Transgenic flies, carrying SpA-associated HLA-B*27:04 or HLA-B*27:05 alleles in combination with *hβ2m* developed abnormal phenotypes. The adult fly wing contains five longitudinal veins (from the most anterior L1 to the posterior L5) spanning the length of the wing and the anterior (ACV) and posterior (PCV) crossveins that connect L3–L4 and L4–L5, respectively (figure 1A). Neither expression of single transgenes (figure 1B,C,E,G), nor expression of HLA-B*07:02 with *hβ2m* (figure 1D and online supplementary Fig. 1d) induced any phenotype in the adult fly. However, expression of HLA-B*27:04 or HLA-B*27:05 with *hβ2m* induced a loss of ACV and/or PCV, when driven in the wing by nub-GAL4 or en-GAL4 (figure 1F,H, and online supplementary file 1d). Moreover, expression of HLA-B27 alleles with *hβ2m*—but not of single transgenes nor of HLA-B*07:02 with *hβ2m*—caused a significant reduction of the eye size, when driven by the eye-specific driver ey-GAL4 (figure 1I–L). We focused further studies on the crossveinless phenotype that was fully penetrant, in contrast to the eye phenotype.

The crossveinless phenotype is neither associated with ER stress nor cell death induction

Efficient MHC-I folding in the ER depends on the peptide-loading complex,²¹ which lacks some components in *Drosophila*. Therefore, HLA-B*27:05/*hβ2m* expression in such organism could lead to ER stress and unfolded protein

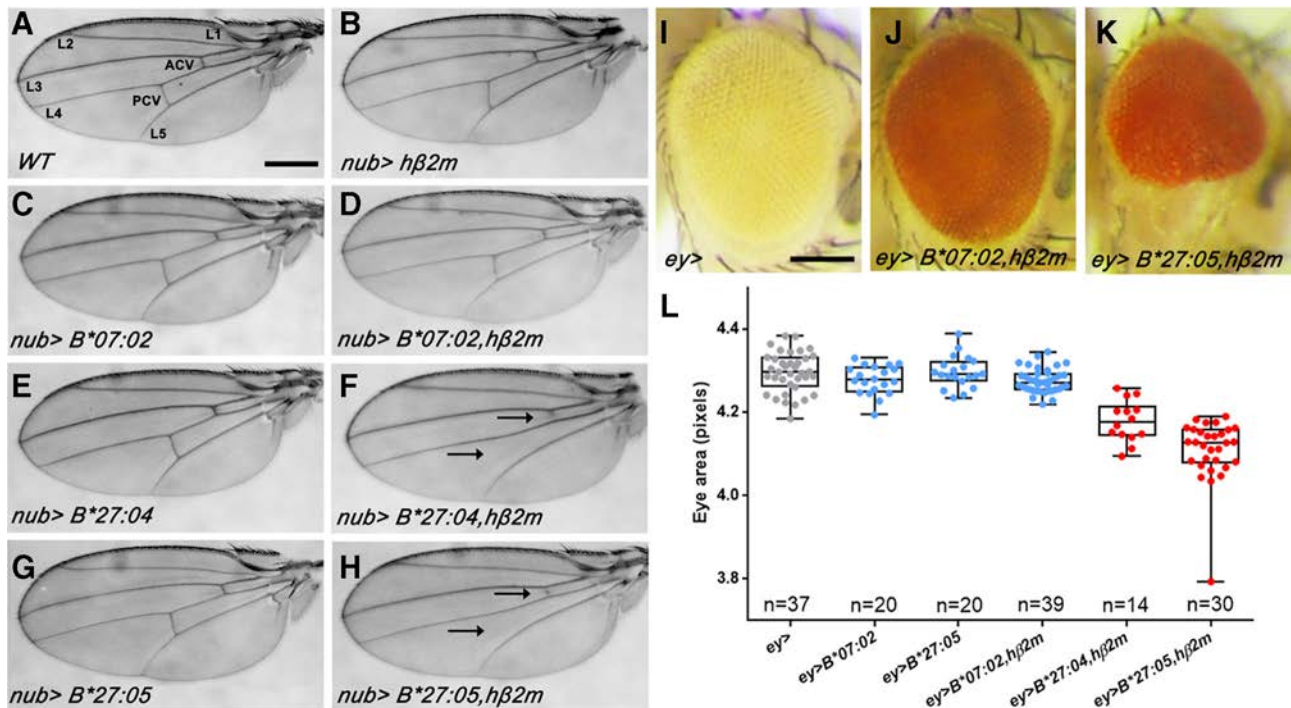


Figure 1 Specific crossveinless and small-eye phenotypes in *Drosophila* coexpressing AS-associated HLA-B27 with hβ2m. (A–H) Nub-GAL4 was used to drive transgenes expression in the wing. Scale bar: 200 μm. Wild-type (WT) adult wing (A) and wings of flies expressing hβ2m alone (nub-GAL4/+; UAS-hβ2m/+ (B), non-AS-associated HLA-B*07:02 (nub-GAL4/+; UAS-HLA-B*07:02/+ and nub-GAL4/+; UAS-HLA-B*07:02,UAS-hβ2m/+ (C,D), AS-associated HLA-B*27:04 (nub-GAL4/+; UAS-HLA-B*27:04/+ and nub-GAL4/+; UAS-HLA-B*27:04,UAS-hβ2m/+ (E,F), AS-associated HLA-B*27:05 (nub-GAL4/+; UAS-HLA-B*27:05/+ and nub-GAL4/+; UAS-HLA-B*27:05,UAS-hβ2m/+ (G,H) alone (C,E,G) or together with hβ2m (D,F,H). Coexpression of HLA-B*27:04 (F) or HLA-B*27:05 (H) with hβ2m transgenes resulted in the complete or partial disappearance of both crossveins (arrows). (I–K) ey-GAL4 was used to drive transgenes expression in the eye. Scale bar: 200 μm. Eye aspect of an ey-GAL4/+ control (I). Eye coexpressing HLA-B*07:02 (J) or HLA-B*27:05 (K) with hβ2m, the latest showing a reduced size. (L) Quantification of male *Drosophila* eye size (red box indicates flies expressing both an AS-associated HLA-B27 allele and hβ2m). Box-and-whisker graphs show the median, range and IQR of the data; Kruskal-Wallis: $p < 10^{-4}$, followed by Dunn's multiple comparisons test showing significant difference with the control, only for B*27:04/hβ2m and B*27:05/hβ2m ($p < 10^{-4}$ for both comparisons). AS, ankylosing spondylitis; HLA, human leucocyte antigen; hβ2m, human β2-microglobulin.

response (UPR), a mechanism that has been proposed to mediate HLA-B27 pathogenicity.⁶ However, ER stress (online supplementary file 2a-c, 2f-g) and apoptosis (online supplementary file 2h-j) markers revealed no effect of HLA-B*27:05/hβ2m expression. Additionally, reducing putative ER stress (online supplementary file 2d-e) or apoptosis (online supplementary file 2k-l) did not modify the crossveinless phenotype, ruling out a role of ER stress or apoptosis in the HLA-B*27:05/hβ2m-induced phenotype.

HLA-B*2705/hβ2m expression misregulates bone morphogenetic protein signalling

Another hypothesis that may explain the crossveinless wings relies on the misregulation of the Notch, epidermal growth factor (EGF) or bone morphogenetic protein (BMP) pathways during development.²² Notch signalling is activated in the wing intervein cells and is required to prevent ectopic vein formation. Expression of HLA-B*2705/hβ2m transgenes in intervein cells under the control of bs-GAL4 did not induce the crossveinless phenotype, whereas driving their expression in vein cells with shv-GAL4 led to loss of ACV and PCV, arguing against involvement of Notch pathway (online supplementary file 3a-c). To test if HLA-B*2705/hβ2m could interfere with EGF signalling, we quantified transcript levels of four EGF signalling target genes involved in wing development. None was modified, excluding the involvement of this pathway (online supplementary file 3d-g).

The crossveinless wing phenotype induced by expression of HLA-B27/hβ2m in *Drosophila* phenocopies mutations of genes involved in BMP signalling.^{23 24} During wing development, the BMP pathway induces the proveins position.^{23 25 26} BMP signalling requires the formation of a hetero or homodimer composed of the decapentaplegic (Dpp) and/or glass bottom boat (Gbb) ligands (figure 2A). Dimeric ligand binds to a heterotetramer composed of a hetero or homodimer of BMP type I receptors (BMPR1, ie, thickveins (Tkv) and saxophone (Sax)) and a hetero or homodimer of the BMP type II receptors (BMPR2, ie, Punt and Wishful thinking). Activated receptors phosphorylate the transcription factor Mad that associates with Medea for its import into the nucleus, where it induces transcription of optomotor-blind (omb), spalt-major (spalm) and daughters against Dpp (dad).^{25 26}

Expression of a dominant negative mutant of Gbb or depletion of Dpp in the wing, resulted in a reduction of wing size and/or an alteration of venation, which were worse in the presence of HLA-B*27:05/hβ2m, demonstrating interaction between HLA-B*27:05/hβ2m and the BMP pathway (figure 2B–E). Overexpression of Gbb or Dpp induces the formation of a blistered wing (figure 2F,H). Interestingly, coexpression of HLA-B*27:05/hβ2m dramatically suppressed the Gbb overexpression phenotype and reciprocally crossveins were restored by Gbb overexpression (figure 2G). In contrast, coexpression of HLA-B*27:05/hβ2m suppressed very moderately the phenotype induced by Dpp overexpression (figure 2I). These results showed that

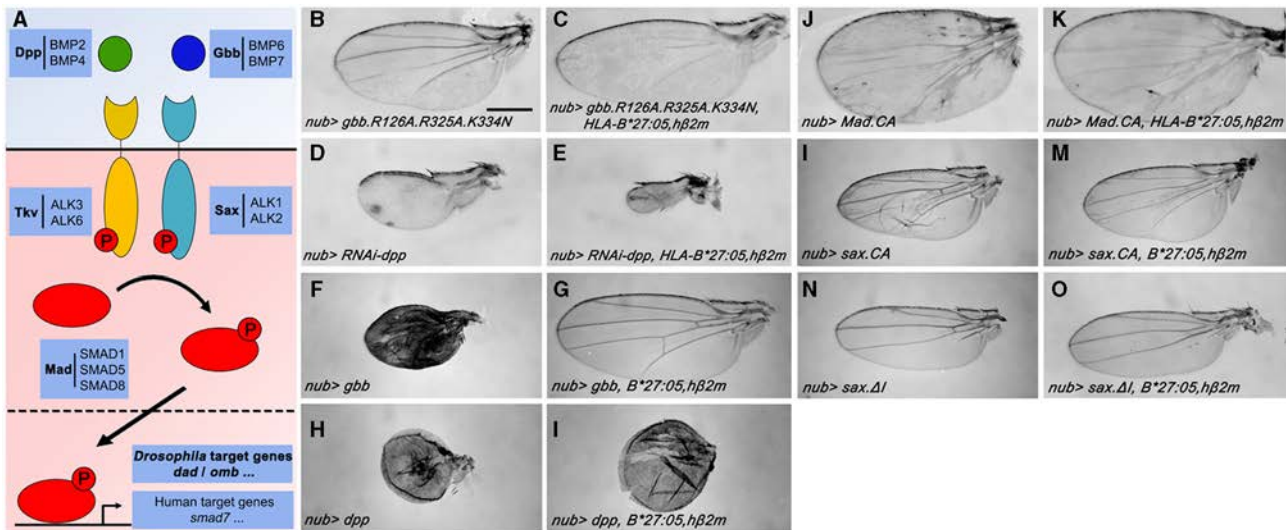


Figure 2 HLA-B27:05/hβ2m genetically interacts with BMP signalling components in *Drosophila* wings. (A) Schematic representation of BMP signalling pathway components (ie, ligands, BMPR1s, transcription factor and target genes) in *Drosophila* (BOLD) and their corresponding orthologs in human. (B) Overexpression of a loss-of-function mutant targeting the cleavage site of Gbb induces a crossveinless phenotype and a partial loss of posterior longitudinal veins (*nub/+; UAS-Gbb.R126A.R325A.K334N/+*). (C) Genetic interaction with HLA-B*27:05/hβ2m further deletes the longitudinal wing veins (*nub/+; UAS-Gbb.R126A.R325A.K334N/UAS-HLA-B*27:05,UAS-hβ2m*). (D) Depletion of DPP results in a reduction of wing size and the absence of wing venation (*nub/+; UAS-RNAi-Dpp/+*). scale bar: 200 μm. (E) Genetic interaction with HLA-B*27:05/hβ2m worsens Dpp-depletion phenotype (*nub/+; UAS-RNAi-Dpp/UAS-HLA-B*27:05,UAS-hβ2m*). (F) Overexpression of Gbb results in a blistered and pigmented adult wing (*nub-GAL4/+; UAS-Gbb/+*). (G) Genetic interaction between HLA-B*27:05/hβ2m and Gbb overexpression results in suppression of Gbb- and HLA-B*27:05/hβ2m-induced phenotypes (*nub-GAL4/+; UAS-Gbb/UAS-HLA-B*27:05,UAS-hβ2m*). (H) Overexpression of Dpp phenocopies gbb overexpression (*nub-GAL4/+; UAS-Dpp/+*). (I) Genetic interaction with HLA-B*27:05/hβ2m, reverses only partially Dpp-induced phenotype (*nub-GAL4/+; UAS-Dpp/UAS-HLA-B*27:05,UAS-hβ2m*). (J) Overexpression of a constitutively active form of Mad induces extravein formation (*nub/+; UAS-Mad.CA/+*). (K) HLA-B*27:05/hβ2m does not significantly modify the extravein phenotype (*nub/+; UAS-Mad.CA/UAS-HLA-B*27:05,UAS-hβ2m*). (L) A constitutively active form of Sax provokes minor vein defects and blisters (*nub-GAL4/+; UAS-sax.CA/+*). (M) Genetic interaction with HLA-B*27:05/hβ2m partially suppresses this phenotype (*nub-GAL4/+; UAS-sax.CA/UAS-HLA-B*27:05,UAS-hβ2m*). (N) Expression of a sax depleted of its kinase domain results in a narrowed adult wing with defects in the formation of L2 and L5 veins (*nub-GAL4/+; UAS-saxΔI/+*). (O) Genetic interaction with HLA-B*27:05/hβ2m does not modify the SaxΔI-induced phenotype (*nub-GAL4/+; UAS-saxΔI/UAS-HLA-B*27:05,UAS-hβ2m*). ALK, activin receptor-like kinase; BMP, bone morphogenetic protein; BMPR1, BMP type I receptor; Dpp, decapentaplegic; Gbb, glass bottom boat; HLA, human leucocyte antigen; hβ2m, human β2-microglobulin; Mad, Mothers against Dpp; Mad.CA, constitutively active form of Mad; Sax.CA, constitutively active form of Sax.

interaction between BMP signalling and HLA-B27 expression resulted in Gbb-mediated signalling dampening.

HLA-B*27:05/hβ2m expression inhibits BMPR1 Sax function

To identify the level of interaction of HLA-B*27:05/hβ2m with the BMP signalling pathway, we tested the effect of HLA-B*27:05/hβ2m expression in a Mad-misregulated background. Interestingly, it had no significant effect on a constitutively active form of Mad (Mad.CA)-induced phenotype (figure 2J,K), indicating that HLA-B27/hβ2m likely interacted upstream of the transcription factor Mad and potentially with BMP receptors. Since Gbb preferentially binds to Sax and Dpp to Tkv, we further investigated the interaction between HLA-B*27:05/hβ2m and Sax.^{22,27} Sax can either promote BMP signalling by forming a heterodimer with Tkv, or, as a homodimer, limit the availability of Gbb and thereby antagonise signalling (figure 3A).²⁸ Overexpression of a CA form of Sax alters the formation of wings, which was suppressed by HLA-B*27:05/hβ2m, showing that HLA-B*27:05/hβ2m genetically repressed Sax activity (figure 2L,M). As expected, if HLA-B*27:05/hβ2m repressed Sax, HLA-B*27:05/hβ2m had no effect on wing vein defects induced by a negative dominant mutant of Sax (*Sax.ΔI*) (figure 2N,O).

Loss of function of Sax is known to widen the p-Mad gradient, which results in an increase of its target genes

expression.²⁸ Consistently, HLA-B*27:05/hβ2m behaved as Sax.ΔI: both induced a widening of pMad gradient in wing imaginal discs (figure 4A–D). HLA-B*27:05/hβ2m also increased the transcript levels of BMP signalling targets *dad* and *omb* (figure 4E–F). Altogether, those results supported an antagonistic interaction between HLA-B*27:05/hβ2m and Sax. The alternative hypothesis that HLA-B*27:05/hβ2m increased Tkv activity could be excluded, as genetic interaction between HLA-B*27:05/hβ2m and a CA form of Tkv (Tkv.CA) decreased the p-Mad and attenuated the Tkv.CA phenotype in adult wings (online supplementary file 4a–e). Suppression of Tkv.CA-induced phenotype by HLA-B*27:05/hβ2m is readily explained by HLA-B*27:05/hβ2m reducing Sax availability and the formation of Tkv-Sax heterodimers, thereby dampening BMP signalling (figure 3B).

HLA-B*27:05 folds and localizes to the plasma membrane in *Drosophila*

HLA-B27 and HLA-B7 were previously observed at the surface of transfected *Drosophila* cells in a well-folded conformation and hβ2m-dependent manner.²⁹ Consistently, well-folded HLA-B*27:05 or HLA-B*07:02 was detected by immunostaining performed on wing imaginal discs using w6/32 and ME1 Abs, only when hβ2m was present (online supplementary file 5a–h

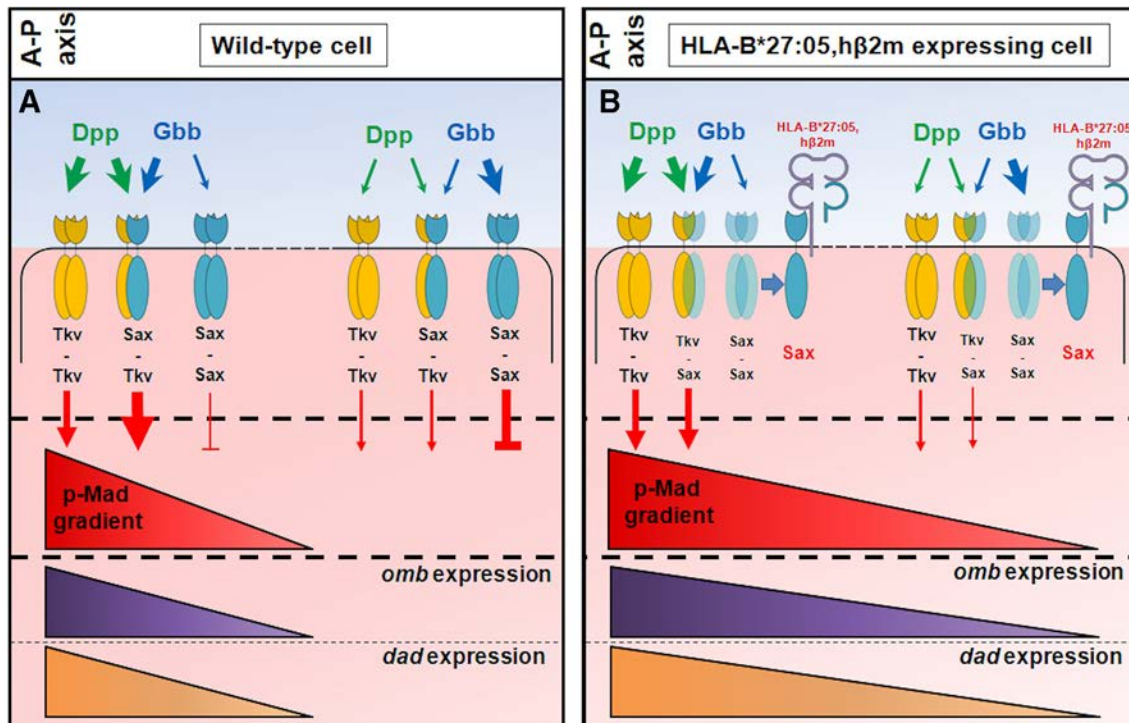


Figure 3 Proposed model of interaction between HLA-B*27:05/hβ2m and the BMP pathway. Representation of *Drosophila* BMP signalling pathway in wild type cells (A) and in HLA-B*27:05/hβ2m-expressing cells (B) of wing imaginal discs. Three different forms of BMPRI dimers exist: Tkv-Tkv and Sax-Sax homodimers, and Tkv-Sax heterodimers. Gbb (blue) and DPP (green) ligands of the BMP pathway show distinct binding preferences. Thicker arrows indicate preponderant signalling because of ligand and receptor availability as well as affinity differences. Signalling in the cells close to the antero–posterior frontier (A-P axis) is shown on the left, signalling in the cells distant from this frontier is represented on the right. (A) The Tkv-Sax heterodimeric receptor is the main complex that mediates BMP signalling. Tkv-Tkv homodimers also activate BMP signalling but less. Sax-Sax homodimers do not activate BMP signalling but limit the range of Gbb diffusion, restricting p-Mad gradient from the A-P frontier. omb (purple) and dad (orange) are target genes of BMP signalling. (B) Ectopic HLA-B*27:05/hβ2m in the wing pouch induces a widening of p-Mad gradient, resulting in an increase of omb and dad expressing cells. We show that HLA-B*27:05/hβ2m interacts with Sax, which may reduce Sax-Sax homodimer and Tkv-Sax heterodimer formation (pale blue Sax). Sax receptor sequestration by HLA-B*27:05/hβ2m would result in an expansion of the Gbb gradient, disrupting BMP signalling. BMP, bone morphogenetic protein; dad, daughters against Dpp; Dpp, decapentaplegic; Gbb, glass bottom boat; HLA, human leucocyte antigen; hβ2m, human β2-microglobulin; omb, optomotor-blind; p-MAD, phosphorylated Mad; Sax, saxophone; Tkv, thickveins;

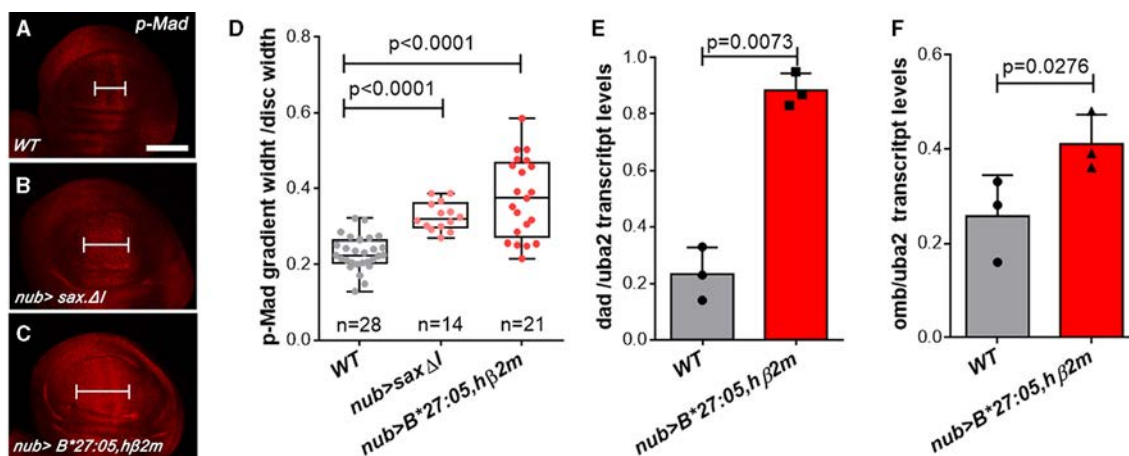


Figure 4 HLA-B27:05/hβ2m misregulates BMP signalling similar to a Sax loss of function. (A–C) projections from confocal stacks of third-instar larval wing imaginal discs stained with an anti-p-Mad antibody of wild-type (WT) (A), nub-GAL4/+; UAS-saxΔ1 (B) and nub-GAL4/+; UAS-HLA-B*27:05,UAS-hβ2m/+ (C) discs. Scale bar: 200 μm. (D) Quantification of p-Mad staining reported to imaginal discs width in the foregoing genotypes. Box-and-whisker graphs show the median, range and IQR of the data; the p values correspond to Dunn’s multiple comparisons test following significant Kruskal-Wallis test. (E,F) Quantification of dad and omb transcripts expression (three independent experiments; the p values of paired t-tests are shown; dad: Cohen’s d=8.17 and omb: Cohen’s d=1.94). BMP, bone morphogenetic protein; dad, daughters against Dpp; HLA, human leucocyte antigen; hβ2m, human β2-microglobulin; omb, optomotor-blind; p-Mad, phosphorylated Mothers against Dpp; Sax, saxophone.

and Supplementary 6a-d), indicating that h β 2m is essential to the HLA-B complex formation, as in mammals. Interestingly, HLA-B*27:05/h β 2m resulted in a more intense staining than HLA-B*07:02/h β 2m (online supplementary file 5a-h), although the amount of h β 2m in wing discs was similar between both conditions (online supplementary file 6e-g). Using flow cytometry on non-permeabilised cells from wing imaginal discs, we also detected a greater amount of well-folded HLA-B*27:05/h β 2m than HLA-B*07:02/h β 2m on the cell surface (online supplementary file 5i, j). Those results show that HLA-B*27:05 had a better folding capacity than HLA-B*07:02 when combined with h β 2m in the *Drosophila* context.

HLA-B*27:05 interacts with Sax in *Drosophila* and with ALK2 in AS patient's cells

We next investigated whether HLA-B*27:05/h β 2m and Sax could interact physically using PLA. Unlike the irrelevant human HA-tagged membrane protein hPen2-HA (figure 5A,C), CA HA-tagged Sax was indeed revealed in very close proximity (ie, less than 40 nm) of HLA-B*27:05/h β 2m in the *Drosophila* wing imaginal disc, (figure 5B,D). Moreover, the human Sax ortholog ALK2 and HLA-B27 were also found in close vicinity of each other at the surface of B-LCLs from AS patients. This interaction was specific for both proteins, since ALK2 neither

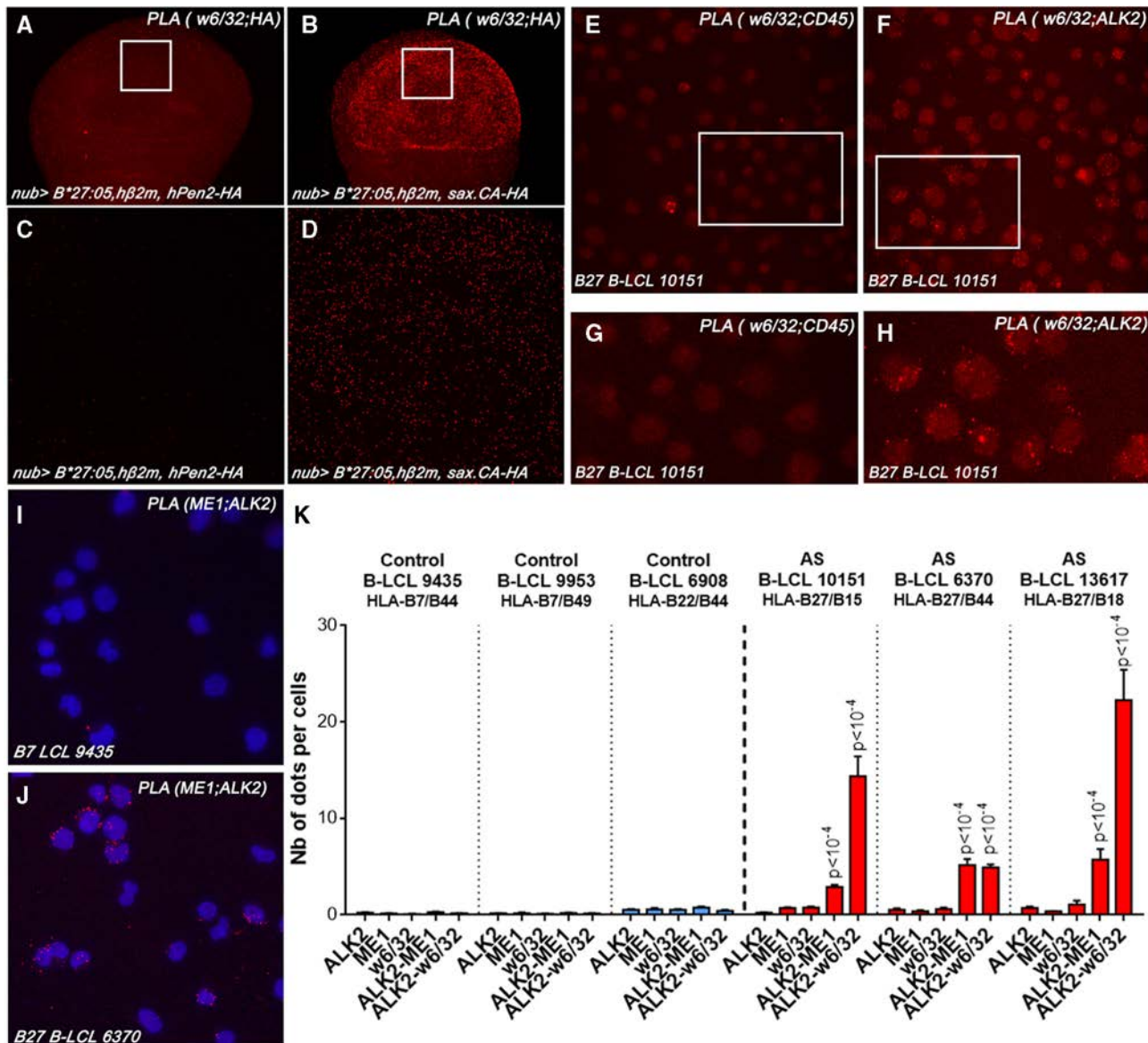


Figure 5 HLA-B27 interacts with Sax and ALK2. (A–D) PLA performed with w6/32 and anti-HA Abs on the wing pouch cells expressing HLA-B*27:05/h β 2m and HA-tagged-hPen2 (negative control) (a, c) or HLA-B*27:05/h β 2m and HA-tagged Sax.CA with nub-GAL4 driver (B, D). (E–H) PLA conducted in B-LCL 10151 from an HLA-B*27:05/B*15 as patient with w6/32 and either anti-CD45 (negative control) (E, G) or anti-ALK2 Abs (F, H). (C), (D), (G) and (H) are zoomed in details of boxed areas from (A), (B), (E) and (F), respectively. (I–J) PLA conducted on B-LCLs 9435 from an HLA-B*7/B*44 healthy control (I) or 6370 from an HLA-B*27:05/B*44 as patient (J) with ME1 and anti-ALK2 antibodies. (K) Average number of PLA staining dots/cell showing an interaction between ALK2 and HLA-A/B/C (ALK2-w6/32) or HLA-B*27/B*7/B*22 (ALK2-ME1) in B-LCLs from 3 controls and 3 AS patients. No signal was detected with ALK2, ME1 or w6/32 antibodies alone. Ten random 40x images per condition were acquired using the DAPI (grey nuclei) and Cy5 (white PLA signals) filters. Two-way ANOVA (factors: Ab and cell line) followed by Bonferroni's multiple-comparisons test: $p < 10^{-4}$. Abs, antibodies; ALK2, activin receptor-like kinase-2; AS, ankylosing spondylitis; ANOVA, analysis of variance; B-LCL, B-lymphoblastoid cell line; HLA, human leucocyte antigen; h β 2m, human β 2-microglobulin; PLA, proximity ligation assay; Sax.CA, constitutively active form of Sax.

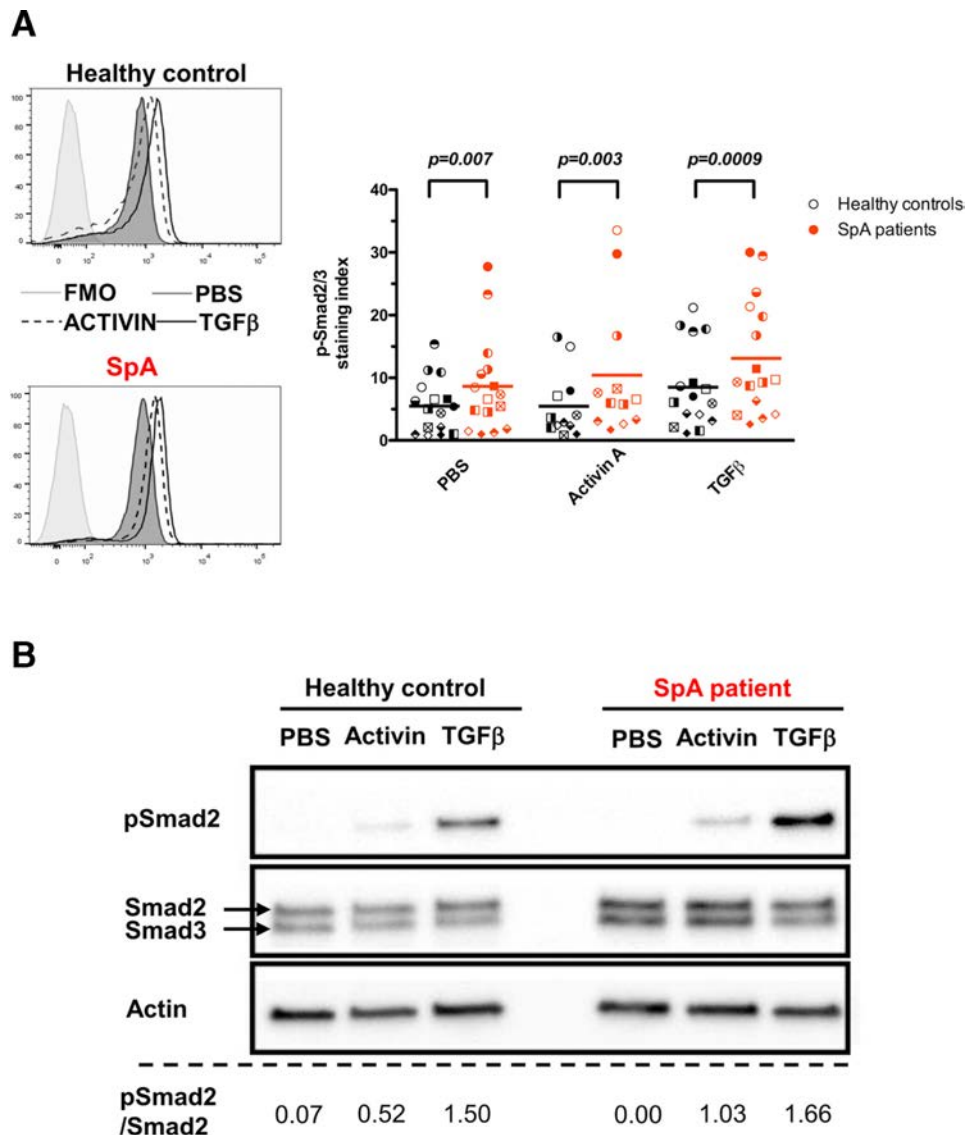


Figure 6 p-Smad2/3 is increased in immune cells from HLA-B27+ SpA patients in response to Activin A or TGFβ. (A) Intracellular p-Smad2/3 was quantified in T cells from paired HLA-B27+ SpA patients and HLA-B27 negative healthy controls, after exposure to PBS, Activin A or TGFβ. Left: representative expression histograms. Right: scatter graph of staining index calculated as the ratio between samples and fluorescence-minus-one (FMO). Similar symbols indicate paired conditions. Horizontal bars show the mean values (12–16 independent experiments). Of note, statistical analysis performed after excluding the three case–control pairs corresponding to the most extreme outliers from the SpA group yielded significant *p* values (PBS: *p*=0.01; activin: *p*=0.012; TGFβ: *p*=0.002). (B) Western blot showing p-Smad2, Smad2 and Smad3 in CD14-negative PBMC from HLA-B27 negative control and HLA-B27+ SpA patients. Values beneath the blots indicate the relative intensity of p-Smad2/Smad2 bands (representative of 2 independent experiments). HLA, human leucocyte antigen; PBS, phosphate-buffered saline; PBMC, peripheral blood mononuclear cells; pSmad, phosphorylated small Mothers against Dpp; SpA, spondyloarthritis; TGFβ, transforming growth factorβ.

colocalised with CD45, nor with any other HLA-B allotypes (figure 5E–K).

TGFβ superfamily ligands Activin A and TGFβ induce elevated Smad2/3 phosphorylation in T cells from HLA-B27+ SpA patients

ALK2, which is widely expressed in mammalian cells, binds several TGFβ superfamily ligands, including Activins and TGFβ and may antagonise their signalling that proceeds *via* Smad2/3 phosphorylation.^{30–32} Thus, to determine if HLA-B27 would disturb TGFβ/BMP pathway signalling in SpA, we examined the phosphorylation of Smad2/3 in peripheral blood T lymphocytes from SpA patients (figure 6). Indeed, we observed elevated phosphorylation of Smad2/3 in those cells, as compared with T cells from healthy controls. The difference was detectable in resting

cells by PhosFlow but was exacerbated after exposure to TGFβ superfamily ligands (ie, Activin A and TGFβ) consistent with a repression of the antagonistic activity of ALK2 by HLA-B27, similar to its effect on Sax function in *Drosophila*.

DISCUSSION

We used *Drosophila* to uncover non-canonical effects that might underlie the as yet unexplained association of HLA-B27 with AS. Strikingly, flies transgenic for AS-associated HLA-B*27:04 and HLA-B*27:05, in combination with hβ2m, exhibited crossveinless and small-eye phenotypes. In contrast, coexpression of HLA-B*07:02 allele (which is known to be protective from AS)³³ with hβ2m, used as a control condition, did not affect fly development. These results underscore HLA-B27-expressing *Drosophila* as a new promising model to investigate HLA-B27 pathogenic

effects, even if it bears some limitations owing to the lack of adaptive immune system.

In mammalian cells, HLA-B27 exhibits slow-folding capacity and a tendency to misfold, which was proposed as putative mechanism for its pathogenicity, by triggering ER stress and UPR.⁶ This could have been the case in *Drosophila* that lacks tapasin and transporters associated with antigen processing, required for optimal folding of MHC-I molecules.²¹ However, given that MHC-I misfolding is reduced in the presence of h β 2m,³⁴ and that neither expression of HLA-B alone nor its coexpression with h β 2m induced ER stress in transgenic *Drosophila*, it is unlikely that MHC-I misfolding would account for the observed phenotypes. Moreover, the level of folded HLA-B molecules at the cell surface was greater in HLA-B27/h β 2m than HLA-B7/h β 2m transgenic wing imaginal discs. Thus, well-folded conformers were likely responsible for the phenotypes occurring in flies coexpressing HLA-B27 and h β 2m.

In *Drosophila*, the formation of crossveins involves a cross-talk between BMP, EGF and Notch pathways.²² To identify which pathway was implicated in the phenotype induced by HLA-B27/h β 2m, their alteration was systematically examined. BMP signalling disruption appeared to be primarily responsible for the crossveinless phenotype. Indeed, HLA-B27/h β 2m expression in the wing imaginal disc mimicked a Sax dominant negative mutant effect. BMP signalling balance in the wing was modified by HLA-B27/h β 2m, resulting in widening of p-Mad gradient and overall increased expression of p-Mad target genes, that is, *omb* and *dad*, indicating a loss of the antagonistic function of Sax.²⁸ These results appear to be highly relevant to SpA as the BMP pathway also happens to be misregulated in patients with SpA. For instance, *Smad7* was upregulated as its *Drosophila* ortholog *dad* in our model.³⁵ Moreover, the p-Mad gradient widening seen in our model could fit with p-Smad1/5/8 detection in bony outgrowth of SpA patients, which is consistent with ectopic BMP signalling.³⁶ We interpreted this result by hypothesising a repression of Sax function by the MHC-I molecule. Consistently, we showed that HLA-B27/h β 2m physically interacted with Sax in the wing tissue.

The mammalian orthologs of Sax are the BMPR1s ALK1 and ALK2, encoded by *ACVRL1* and *ACVR1* genes, respectively.³² ALK1 is predominantly present on endothelial cells and involved in angiogenesis, whereas ALK2 is more widely expressed and exerts an essential role in cartilage development and endochondral ossification, particularly in the axial skeleton.^{37 38} Both of them bind several TGF β superfamily ligands, including BMPs, Activins and TGF β , and like Sax, form heterotetrameric complexes with BMPR2s, including BMPRII and Activin receptor type 2A and 2B (ActRIIA and ActRIIB).^{39 40}

Similar to Sax, ALK1 and 2 play either a positive or a negative role in signalling, depending on the ligand and BMPR2 binding. They transduce signal in response to BMPs via Smad1/5/8 phosphorylation, whereas they antagonise signalling mediated by Activin and TGF β via Smad2/3 phosphorylation or even BMP-mediated signalling in some circumstances.^{30–32 39 41–43} For instance, Activin A, is a ligand secreted by innate immune system cells during inflammation that primarily uses ALK4 and ALK7 as BMPR1s to initiate signalling via Smad2/3.^{39 44 45} However, Activin A may also compete with BMPs to bind to ALK2, forming inactive complexes with ActRIIA and ActRIIB that inhibit Smad2/3-mediated Activin signalling and prevent Smad1/5/8-mediated BMP signalling.^{31 46 47} Moreover, ALK2 can inhibit osteogenic BMP2- and BMP4-induced signalling by competing with their ALK3/ALK6 functional BMPR1s and recruiting BMPR2s into non-competent complexes.⁴¹ Interestingly, loss of

the inhibitory effect of ALK2 on BMP signalling in response to Activin A, due to mutations in *ACVR1* gene, leads to fibrodysplasia ossificans progressiva, a rare genetic disorder characterised by episodic heterotopic ossification of soft connective tissue, including tendons, ligaments, fascia, that may sometime bear similarities with AS.^{48–51}

Interestingly, when expressed in *Drosophila*, ALK2 inhibited endogenous BMP signalling in wing discs like Sax did, suggesting that HLA-B27/h β 2m may interfere with ALK2 in mammals in a way similar to Sax in *Drosophila*.³² Indeed, we observed that well-folded HLA-B27/h β 2m physically interacted with ALK2 at the surface of B-LCLs from AS patients and that this was not the case for the non-AS-associated HLA-B7 or HLA-B22 alleles that were also recognised by ME1 Ab. Characteristics of HLA-B27 explaining specific interaction with BMPR1s Sax/ALK2 remain to be determined. Interestingly, however, one of the distinctive features common to all HLA-B27 alleles is an unpaired free cysteine at position 67 that could potentially interact with the cysteine-rich extracellular binding domain of Sax and ALK2.⁵²

This prompted us to examine whether the presence of HLA-B27 would affect the response of immune cells from patients with SpA to Activin A and TGF β , two ligands known to bind ALK2 and that could be implicated in the disease process. Most interestingly, as predicted if the presence of HLA-B27/h β 2m released a brake on Activin A/TGF β signalling, we observed elevated Smad2/3 phosphorylation that was detected in resting cells and exacerbated in response to both ligands in T cells from patients with SpA.

Based on our findings, we propose a mechanism for HLA-B27 implication in SpA, whereby HLA-B27/h β 2m antagonising the inhibitory function of ALK2 would potentiate Activin A, TGF β and/or BMP signalling in context-dependent fashion. A shift towards Smad2/3-mediated signalling in a context of inflammatory stimulus could notably contribute to the T-helper 17 differentiation bias⁵³ that has been shown in SpA.^{6 54} Complementarily, release of the brake normally held by ALK2 on BMP-mediated endochondral ossification, in inflammatory context, could account for increased ossification, which is another striking hallmark of SpA - although this study does not address other factors that may contribute to AS in HLA-B27-negative cases.^{55 56} This fits one of the oldest hypotheses proposed to account for HLA-B27 pathogenicity, that is, that HLA-B27 itself might confer an enhanced sensitivity to an inflammatory mediator.⁵⁷

Correction notice This article has been corrected since it published Online First. The senior authorship statement has been added and the sixth author's name has been corrected as well as affiliations one and two.

Acknowledgements We thank Bernard Mignotte (Laboratoire de Génétique et Biologie Cellulaire, UVSQ, Université Paris-Saclay, EPHE, PSL Research University, Montigny-le-Bretonneux, France) for suggestions on the manuscript.

Contributors BG, AR-A and NJ designed and performed all *Drosophila* experiments and analysed the data. J-MC, EP and DR performed PLA and Western blot on human cells. LMA and SG designed and performed human cells experiments. BG, AR-A, IG, SG and MB wrote the manuscript with input from all the coauthors. GC, IG, SG and MB supervised the research and contributed to experimental design.

Funding This work was supported by a grant from Société Française de Rhumatologie (SFR). NJ was in part supported by grant ING20130526783 from the French 'Fondation pour la Recherche Médicale' (FRM). We thank the genomics and CYMAGES imaging facilities of the Simone Veil faculty (University of Versailles Saint-Quentin and Paris-Saclay) for its logistic and technical support.

Competing interests None declared.

Patient consent for publication Not required.

Ethics approval This study was approved by the institutional ethical committee of Ile-de-France XI (Saint-Germain-en-Laye France).

Provenance and peer review Not commissioned; externally peer reviewed.

Data availability statement All data relevant to the study are included in the article or uploaded as online supplementary information.

ORCID iD

Maxime Breban <http://orcid.org/0000-0002-6932-9395>

REFERENCES

- Taurog JD, Chhabra A, Colbert RA. Ankylosing spondylitis and axial spondyloarthritis. *N Engl J Med* 2016;375:1303.
- Caffrey MF, James DC. Human lymphocyte antigen association in ankylosing spondylitis. *Nature* 1973;242:121.
- Rock KL, Reits E, Neefjes J. Present yourself! by MHC class I and MHC class II molecules. *Trends Immunol* 2016;37:724–37.
- Bowness P. HLA-B27. *Annu Rev Immunol* 2015;33:29–48.
- Benjamin RJ, Madrigal JA, Parham P. Peptide binding to empty HLA-B27 molecules of viable human cells. *Nature* 1991;351:74–7.
- Colbert RA, Tran TM, Layh-Schmitt G. HLA-B27 misfolding and ankylosing spondylitis. *Mol Immunol* 2014;57:44–51.
- Chao H-T, Liu L, Bellen HJ. Building dialogues between clinical and biomedical research through cross-species collaborations. *Semin Cell Dev Biol* 2017;70:49–57.
- Brand AH, Perrimon N. Targeted gene expression as a means of altering cell fates and generating dominant phenotypes. *Development* 1993;118:401–15.
- Jeanty C, Sourisse A, Noteuil A, et al. HLA-B27 subtype oligomerization and intracellular accumulation patterns correlate with predisposition to spondyloarthritis. *Arthritis Rheumatol* 2014;66:2113–23.
- Demay Y, Perochon J, Szuplewski S, et al. The PERK pathway independently triggers apoptosis and a Rac1/S1pr/JNK/Dilp8 signaling favoring tissue homeostasis in a chronic ER stress Drosophila model. *Cell Death Dis* 2014;5:e1452.
- Florentin A, Arama E. Caspase levels and execution efficiencies determine the apoptotic potential of the cell. *J Cell Biol* 2012;196:513–27.
- Wong JT, Akhbar F, Ng AYE, et al. Dip1 modulates stem cell homeostasis in Drosophila through regulation of sisR-1. *Nat Commun* 2017;8:759.
- Stam NJ, Spits H, Ploegh HL. Monoclonal antibodies raised against denatured HLA-B locus heavy chains permit biochemical characterization of certain HLA-C locus products. *J Immunol* 1986;137:2299–306.
- Ellis SA, Taylor C, McMichael A. Recognition of HLA-B27 and related antigen by a monoclonal antibody. *Hum Immunol* 1982;5:49–59.
- Barnstable C et al. Production of monoclonal antibodies to group A erythrocytes, HLA and other human cell surface antigens—new tools for genetic analysis. *Cell* 1978;14:9–20.
- Brodsky FM, Parham P. Monomorphic anti-HLA-A,B,C monoclonal antibodies detecting molecular subunits and combinatorial determinants. *J Immunol* 1982;128:129–35.
- Costantino F, Talpin A, Evnouchidou I, et al. ERAP1 Gene Expression Is Influenced by Nonsynonymous Polymorphisms Associated With Predisposition to Spondyloarthritis. *Arthritis Rheumatol* 2015;67:1525–34.
- Martin-Esteban A, Guasp P, Barnea E, et al. Functional interaction of the ankylosing spondylitis-associated endoplasmic reticulum aminopeptidase 2 with the HLA-B*27 peptidome in human cells. *Arthritis Rheumatol* 2016;68:2466–75.
- Sanchez-Martinez A, Beavan M, Gegg ME, et al. Parkinson disease-linked GBA mutation effects reversed by molecular chaperones in human cell and fly models. *Sci Rep* 2016;6:31380.
- Schulze SR, Curio-Penny B, Li Y, et al. Molecular Genetic Analysis of the Nested *Drosophila melanogaster* Lamin C Gene. *Genetics* 2005;171:185–96.
- Blees A, Janulienė D, Hofmann T, et al. Structure of the human MHC-I peptide-loading complex. *Nature* 2017;551:525–8.
- Sotillos S, De Celis JF. Interactions between the Notch, EGFR, and decapentaplegic signaling pathways regulate vein differentiation during Drosophila pupal wing development. *Dev Dyn*. 2005;232:738–52.
- Ralston A, Blair SS. Long-Range DPP signaling is regulated to restrict BMP signaling to a crossvein competent zone. *Dev Biol* 2005;280:187–200.
- Matsuda S, Yoshiyama N, Künnappu-Vulli J, et al. Dpp/Bmp transport mechanism is required for wing venation in the sawfly *Athalia rosae*. *Insect Biochem Mol Biol* 2013;43:466–73.
- Crozatier M, Glise B, Vincent A. Patterns in evolution: veins of the Drosophila wing. *Trends in Genetics* 2004;20:498–505.
- Raftery LA, Umulis DM. Regulation of BMP activity and range in Drosophila wing development. *Curr Opin Cell Biol* 2012;24:158–65.
- Haerry TE. The interaction between two TGF- β type I receptors plays important roles in ligand binding, Smad activation, and gradient formation. *Mech Dev* 2010;127:358–70.
- Bangi E. Dual function of the Drosophila Alk1/Alk2 ortholog saxophone shapes the BMP activity gradient in the wing imaginal disc. *Development* 2006;133:3295–303.
- Jackson MR, Song ES, Yang Y, et al. Empty and peptide-containing conformers of class I major histocompatibility complex molecules expressed in Drosophila melanogaster cells. *Proc Natl Acad Sci U S A* 1992;89:12117–21.
- SP O, Seki T, Goss KA, et al. Activin receptor-like kinase 1 modulates transforming growth factor-beta 1 signaling in the regulation of angiogenesis. *Proc Natl Acad Sci USA* 2000;97:2626–31.
- Renlund N, O'Neill FH, Zhang L, et al. Activin receptor-like kinase-2 inhibits activin signaling by blocking the binding of activin to its type II receptor. *J Endocrinol* 2007;195:95–103.
- Le V, Anderson E, Akiyama T, et al. Drosophila models of FOP provide mechanistic insight. *Bone* 2018;109:192–200.
- Costantino F, Breban M, Garchon H-J. Genetics and functional genomics of spondyloarthritis. *Front Immunol* 2018;9:2933.
- Tran TM, Dorris ML, Satumtira N, et al. Additional human β 2-microglobulin curbs HLA-B27 misfolding and promotes arthritis and spondylitis without colitis in male HLA-B27-transgenic rats. *Arthritis Rheum* 2006;54:1317–27.
- Lee YH, Song GG. Meta-Analysis of differentially expressed genes in ankylosing spondylitis. *Genet Mol Res* 2015;14:5161–70.
- Lories RJU, Derese I, Luyten FP. Modulation of bone morphogenetic protein signaling inhibits the onset and progression of ankylosing enthesitis. *J Clin Invest* 2005;115:1571–9.
- Salazar VS, Gamer LW, Rosen V. Bmp signalling in skeletal development, disease and repair. *Nat Rev Endocrinol* 2016;12:203–21.
- Roman BL, Hinck AP. Alk1 signaling in development and disease: new paradigms. *Cell Mol Life Sci* 2017;74:4539–60.
- Yadin D, Knaus P, Mueller TD. Structural insights into BMP receptors: specificity, activation and inhibition. *Cytokine Growth Factor Rev* 2016;27:13–34.
- ten Dijke P, Yamashita H, Ichijo H, et al. Characterization of type I receptors for transforming growth factor-beta and activin. *Science* 1994;264:101–4.
- Hildebrand L, Stange K, Deichsel A, et al. The fibrodysplasia ossificans progressiva (FOP) mutation p.R206H in ACVR1 confers an altered ligand response. *Cell Signal* 2017;29:23–30.
- Goumans M-J, Valdimarsdottir G, Itoh S, et al. Activin Receptor-like Kinase (ALK) 1 is an Antagonistic Mediator of Lateral TGF β /ALK5 Signaling. *Mol Cell* 2003;12:817–28.
- Ebner R, Chen R, Shum L, et al. Cloning of a type I TGF-beta receptor and its effect on TGF-beta binding to the type II receptor. *Science* 1993;260:1344–8.
- Phillips DJ, de Kretser DM, Hedger MP. Activin and related proteins in inflammation: not just interested bystanders. *Cytokine Growth Factor Rev* 2009;20:153–64.
- de Kretser DM, O'Hehir RE, Hardy CL, et al. The roles of activin A and its binding protein, follistatin, in inflammation and tissue repair. *Mol Cell Endocrinol* 2012;359:101–6.
- Alessi Wolken DM, Idone V, Hatsell SJ, et al. The obligatory role of activin A in the formation of heterotopic bone in fibrodysplasia ossificans progressiva. *Bone* 2018;109:210–7.
- Olsen OE, Wader KF, Hella H, et al. Activin A inhibits BMP-signaling by binding ACVR2A and ACVR2B. *Cell Commun Signal* 2015;13.
- Fukuda T, Kohda M, Kanomata K, et al. Constitutively activated ALK2 and increased SMAD1/5 cooperatively induce bone morphogenetic protein signaling in fibrodysplasia ossificans progressiva. *J Biol Chem*. 2009;284:7149–56.
- Shore EM, Xu M, Feldman GJ, et al. A recurrent mutation in the BMP type I receptor ACVR1 causes inherited and sporadic fibrodysplasia ossificans progressiva. *Nat Genet* 2006;38:525–7.
- Bridges AJ, Hsu K-C, Singh A, et al. Fibrodysplasia (myositis) ossificans progressiva. *Semin Arthritis Rheum* 1994;24:155–64.
- Dugar M, Limaye V, Cleland LG, et al. Fibrodysplasia ossificans progressiva presenting as ankylosing spondylitis. *Intern Med J* 2010;40:862–4.
- Massagué J. Tgf-Beta signal transduction. *Annu Rev Biochem* 1998;67:753–91.
- Zhang S. The role of transforming growth factor β in T helper 17 differentiation. *Immunology* 2018;155:24–35.
- Glatigny S, Fert J, Blaton MA, et al. Proinflammatory Th17 cells are expanded and induced by dendritic cells in spondylarthritis-prone HLA-B27-transgenic rats. *Arthritis & Rheumatism* 2012;64:110–20.
- Bennett AN, McGonagle D, O'Connor P, et al. Severity of baseline magnetic resonance imaging-evident sacroiliitis and HLA-B27 status in early inflammatory back pain predict radiographically evident ankylosing spondylitis at eight years. *Arthritis Rheum* 2008;58:3413–8.
- Dougados M, Sepriano A, Molto A, et al. Sacroiliac radiographic progression in recent onset axial spondyloarthritis: the 5-year data of the DESIR cohort. *Ann Rheum Dis* 2017;76:1823–8.
- Rosenbaum JT. Why HLA-B27: an analysis based on two animal models. *Ann Intern Med* 1981;94:261–3.

CLINICAL SCIENCE

Safety and immune response of a live-attenuated herpes zoster vaccine in patients with systemic lupus erythematosus: a randomised placebo-controlled trial

Chi Chiu Mok ,¹ Kwok Hung Chan,² Ling Yin Ho,¹ Yim Fong Fung,² Wai Fong Fung,² Patrick Chiu Yat Woo²

Handling editor Josef S Smolen

¹Department of Medicine, Tuen Mun Hospital, Hong Kong, SAR China

²Department of Microbiology, University of Hong Kong, Hong Kong, SAR China

Correspondence to

Dr Chi Chiu Mok, Medicine, Tuen Mun Hospital, Hong Kong, SAR China; ccmok2005@yahoo.com

Received 24 June 2019

Revised 29 August 2019

Accepted 1 September 2019

Published Online First

17 September 2019

ABSTRACT

Objectives To study the safety and immunogenicity of a live-attenuated herpes zoster (HZ) vaccine in patients with systemic lupus erythematosus (SLE).

Methods Adult SLE patients having a SLEDAI <6 and stable immunosuppressive treatment for ≥6 months were recruited. Participants were randomly assigned to receive HZ vaccine (Zostavax) or placebo injection. Anti-varicella zoster virus (VZV) IgG reactivity (baseline and week 6) was measured by an enzyme-linked fluorescence assay. Cell-mediated response was assessed by a VZV-stimulated interferon-gamma (IFN-γ) enzyme-linked ELISPOT assay. Adverse events and immune responses of the two groups were compared.

Results 90 SLE patients were recruited (age 45.6±14.1 years; 93% women) and assigned to Zostavax or placebo (in 1:1 ratio). Baseline clinical parameters were similar between the two groups. The change in anti-VZV IgG from week 0 to 6 was +59.8% in the vaccine and -2.1% in the placebo group. Week 6 anti-VZV IgG was significantly higher in vaccinated than placebo-treated patients, after adjustment for baseline (4.16±1.26 vs 3.32±1.01; p<0.001). The number of IFN-γ secreting T-cell spots decreased in the placebo-treated patients (-17%) but increased in vaccinated patients (+42%). The T-cell spots number at week 6 was significantly higher in vaccine—than placebo-treated patients after adjustment for baseline (38.1±78.2 vs 23.1±47.9; p=0.02). Significantly more vaccinated patients reported self-limiting injection site reaction than controls (31% vs 7%; p<0.01). Two vaccinated patients (4.4%) and one (2.2%) placebo-treated patient had mild/moderate SLE flares but no patients developed HZ eruption within 6 weeks postvaccination.

Conclusions In patients with stable SLE not receiving intensive immunosuppression, Zostavax was well-tolerated and provoked an immune response.

Trial registration number US ClinicalTrials.gov registry (NCT02477150).

INTRODUCTION

Herpes zoster (HZ) (shingles) is a painful condition caused by reactivation of varicella zoster virus (VZV) that remains dormant after primary infection. Key risk factors for HZ reactivation are increasing age, immunosuppressive therapies, HIV infection, malignancies and postchemotherapy.¹ Shingles may cause significant morbidity such as postherpetic neuralgia (PHN) and even mortality

Key messages

What is already known about this subject?

- ▶ Herpes zoster (HZ) reactivation is common in patients with systemic lupus erythematosus (SLE).
- ▶ There is very limited information on the safety and immunogenicity of the live-attenuated HZ vaccine in SLE patients. As a result, the rate of HZ vaccination is low in SLE patients.

What does this study add?

- ▶ This first randomised placebo-controlled trial demonstrates that the live HZ vaccine is well-tolerated and provokes a humoral and cell-mediated response in stable SLE patients not receiving intensive immunosuppressive therapies.

How might this impact on clinical practice or future developments?

- ▶ HZ vaccine should be given to SLE patients during periods of disease quiescence and minimal immunosuppression to maximise its efficacy in reducing the risk of HZ reactivation.

for disseminated infection, particularly in immunocompromised subjects.²

The live-attenuated HZ vaccine (Zostavax) is essentially a larger-than-normal dose of the chick-enpox vaccine, which contains the Oka strain of live-attenuated VZV.³ Zostavax has been shown by randomised controlled trials (RCTs) to be safe and protective in immunocompetent subjects >60 years and between 50 and 59 years of age in reducing HZ reactivation and PHN by two-third.^{4,5} However, as the vaccine is live-attenuated, it is relatively contraindicated in immunocompromised persons.

HZ reactivation is fairly common in patients with systemic lupus erythematosus (SLE).⁶⁻⁹ The prevalence of HZ reactivation in SLE ranges from 6.4 to 91.4 cases per 1000 patient-year.⁸ A recent longitudinal study reported that SLE patients had more HZ infection at all ages, with an age-adjusted incidence of 12.0/1000 person-years compared with controls (8.7/1000 person-years) (HR 1.7).⁹ Risk factors associated with HZ infection in SLE included immunosuppressive therapies, renal and major organ disease, lymphopenia, malignancies and other comorbidities, as well as certain



© Author(s) (or their employer(s)) 2019. No commercial re-use. See rights and permissions. Published by BMJ.

To cite: Mok CC, Chan KH, Ho LY, et al. *Ann Rheum Dis* 2019;**78**:1663–1668.

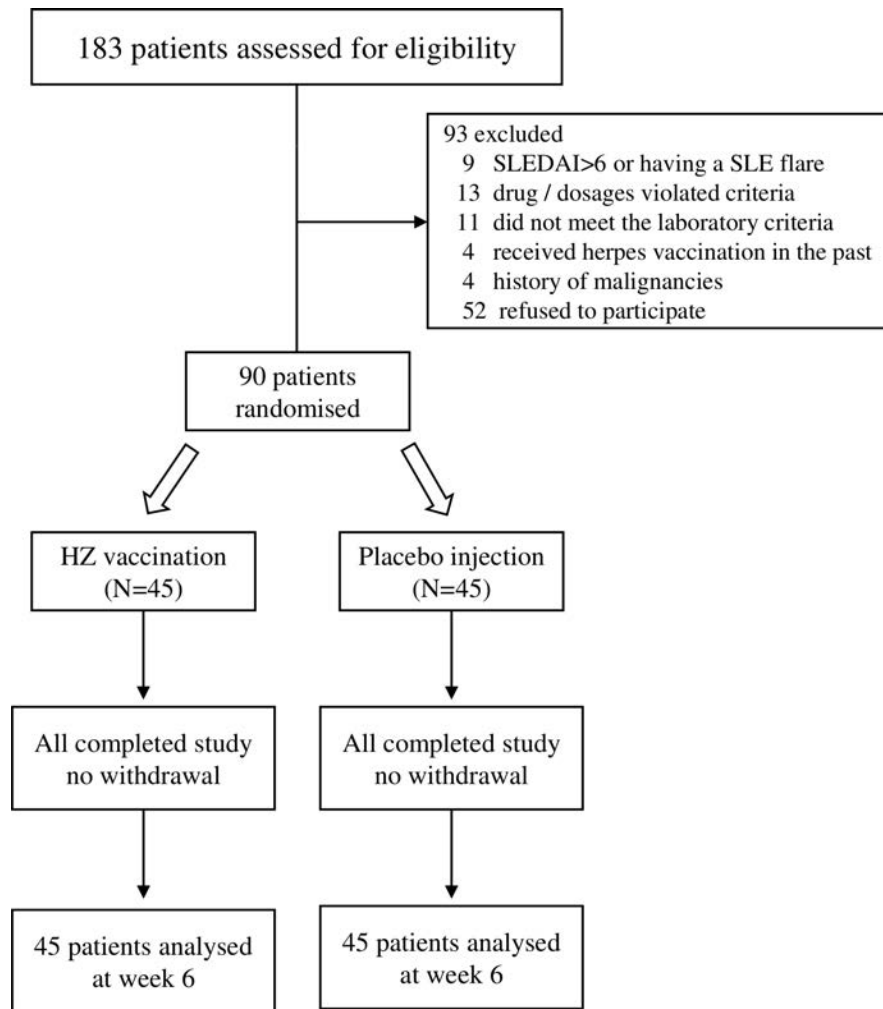


Figure 1 Disposition of patients. HZ, herpes zoster.

autoantibodies.¹⁰ However, these factors are inconsistent across studies, probably because of small samples and the difference in patient selection.

An observational study of 463 541 US patients with inflammatory arthritis reported efficacy of Zostavax in reducing HZ reactivation after 2 years (HR 0.61).¹¹ Among 633 patients exposed to biologics at the time of vaccination, no cases of HZ or varicella infection occurred in the subsequent 42 days. However, there is little information regarding the safety of the live-attenuated HZ vaccine in SLE. A small pilot case-control study did not observe any episodes of HZ reactivation, serious adverse events (SAEs) or disease flares in 10 SLE patients after HZ vaccination.¹² In view of the paucity of data, this RCT was carried out to evaluate the safety and immunogenicity of a live-attenuated HZ vaccine in patients with SLE.

PATIENTS AND METHODS

Study population

The inclusion criteria of this study were: (1) patients fulfilling ≥ 4 of the 1997 ACR¹³ or the 2012 SLICC/ACR criteria for SLE¹⁴ and were followed in the rheumatology clinics of Tuen Mun Hospital; (2) age ≥ 18 years; (3) clinically stable disease with a Safety of Estrogens in Lupus Erythematosus National Assessment—SLE Disease Activity Index (SELENA-SLEDAI) score < 6 ^{15 16} and receiving stable doses of immunosuppressive agents for ≥ 6 months; and (4) a previous history of chickenpox

or HZ infection. Exclusion criteria were: (1) active infection, including tuberculosis and HIV; (2) lymphocyte count $< 500/\text{mm}^3$; (3) reduced serum IgG/IgA/IgM level; (4) serum creatinine $> 200 \mu\text{mol/L}$; (5) history of haematological malignancies or solid tumours; (6) current immunosuppressive therapies with doses exceeding the following: prednisolone ($> 15 \text{ mg}$); azathioprine ($> 100 \text{ mg/day}$); mycophenolate mofetil (MMF) ($> 1000 \text{ mg/day}$); ciclosporin A ($> 100 \text{ mg/day}$); tacrolimus ($> 3 \text{ mg/day}$); methotrexate ($> 15 \text{ mg/week}$); cyclophosphamide; or biological agents; and (7) patients who were pregnant or planned for pregnancy within 1 year of study entry.

Ten healthy controls (≥ 50 years of age without medical illnesses) with a previous history of chickenpox or HZ infection were also recruited for HZ vaccination. The humoral and cell-mediated immune responses before and 6 weeks after vaccination were compared with SLE patients.

Written consent was obtained from all participants. This study was supported by the Health and Medical Research Fund of the Research Fund Secretariat of Hong Kong. Patients and the public was not involved in the design, conduct or reporting of this research.

Study procedures

SLE patients recruited were randomised by computer-generated blocks of four to receive either one dose of Zostavax (0.65 mL) or placebo (same volume of normal saline) injection subcutaneously.

Table 1 Clinical characteristics of the SLE patients studied

	HZ vaccinated group (n=45)	Placebo group (n=45)	P value
	N (%), mean±SD		
Age at study entry, years	45.9±15.4	45.2±12.7	0.81
SLE duration, years	13.2±8.6	14.2±8.9	0.58
Women	40 (89)	44 (98)	0.2
Cumulative clinical manifestations			
Arthritis	32 (71)	34 (76)	0.63
Facial rash	19 (42)	23 (51)	0.4
Discoid rash	7 (16)	6 (13)	0.76
Mucosal ulceration	6 (13)	6 (13)	1
Photosensitivity	11 (24)	13 (29)	0.63
Hemolytic anaemia	14 (31)	10 (22)	0.34
Leucopenia (<4×10 ⁹ /L)	13 (29)	19 (42)	0.19
Thrombocytopenia (<100×10 ⁹ /L)	11 (24)	12 (27)	0.81
Lymphopenia (<1.5×10 ⁹ /L)	30 (67)	30 (67)	1
Lymphadenopathy	10 (22)	7 (16)	0.42
Renal	22 (49)	26 (58)	0.4
Serositis	6 (13)	10 (22)	0.27
*Neuropsychiatric	3 (6.7)	4 (8.9)	1
Cutaneous vasculitis	10 (22)	7 (16)	0.42
Myositis	2 (4.4)	3 (6.7)	1
Gastrointestinal	1 (2.2)	2 (4.4)	1
Autoantibodies			
Anti-dsDNA	33 (73)	34 (76)	0.81
Anti-Sm	10 (22)	4 (8.9)	0.14
Anti-Ro	27 (60)	26 (58)	0.83
Anti-La	8 (18)	8 (18)	1
Anti-nRNP	17 (38)	13 (29)	0.37
Anticardiolipin (IgG)	11 (24)	10 (22)	0.8
Lupus anticoagulant	9 (20)	7 (16)	0.58

*Referred to those which required immunosuppressive therapies, for example, psychosis, acute confusional state, demyelinating disease, myelitis, peripheral and cranial neuropathy, myasthenia gravis, aseptic meningitis.
HZ, herpes zoster; SLE, systemic lupus erythematosus.

Injection was performed by a designated nurse blinded for the study details. Investigators and patients were also blinded for the identity of the assigned injection.

Participants were assessed at baseline and at 6 weeks postvaccination for immunogenicity and adverse events, including SLE activity and flares. Blood was taken for serum anti-VZV IgG and ELISPOT assay for the humoral and cell-mediated responses to vaccination.

The primary outcome of this study was the difference between the two groups in the rise in IgG to VZV at week 6 postvaccination compared with baseline. Secondary outcomes included: (1) safety of the HZ vaccine within 6 weeks of injection; (2) change in cell-mediated immune response to VZV; and (3) change in SLE disease activity and clinical flares.

Assessment of disease activity and flares of SLE

Disease activity of SLE was assessed by the SELENA-SLEDAI, a validated instrument employed in the SELENA-SLE trials.^{15 16} The physician's global assessment of disease activity (score 0–3) was also performed to grade disease activity.¹⁷ Flares of SLE (mild/moderate or severe) were assessed by the SELENA flare instrument^{15 16} according to the clinical status of the patients with reference to the preceding clinic visit.

Cellular and humoral immune response to HZ vaccination

The humoral response to HZ vaccination was studied by the VIDAS VZV-IgG assay, which is an automated test on the VIDAS instruments (Biomerieux) for the detection of IgG antibodies to VZV in human serum using a two-step enzyme linked fluorescence assay. According to the manufacturer's instructions, strip and the solid phase receptacle were loaded to the instrument with 100µL specimen from study subjects. At the end of the assay, a test value (TV) was generated by a ratio of the relative fluorescence against that of a standard. TVs were interpreted as follows: <0.60 negative; 0.6 to <0.9 equivocal; and ≥0.9 positive for anti-VZV IgG. Higher index values reflected higher anti-VZV IgG titers semiquantitatively.

The cell-mediated response to HZ vaccination was studied by an IFN-γ ELISPOT assay for VZV (BD Biosciences) according to manufacturer's instructions. The VZV antigen was derived from clarified cell culture supernatants in VZV-infected human fetal lung fibroblast cells (HEL). Control antigen was obtained by the same process using uninfected HEL cells. Peripheral blood mononuclear cells were isolated by Ficoll-Hypaque (GE Healthcare Bio-Sciences) and stored in liquid nitrogen until use. Briefly, 100µL of VZV antigen, control antigen or 50µg/mL of phytohaemagglutinin-M (Thermo Fisher) (positive control) were added to the wells precoated with antihuman IFN-γ monoclonal antibody together with 100µL of the 1×10⁶/mL cell suspension. All samples were run in duplicate. The plate was incubated at 37°C in 5% CO₂ for 18 hours. Detection antibody was added after washing and incubated for 2 hours at room temperature. Streptavidin-HRP solution was added for 1 hour at room temperature, followed by addition of ACE substrate solution after washing. Spots developed after 5–60 min and were enumerated using an ELISPOT plate reader. The number of spots represented the number of IFN-γ secreting CD4+ T cell colonies.

Sample size calculation

In immunocompetent subjects aged 50–59 years, the mean fold rise of IgG to VZV was 2.31 (95% CI 2.20 to 2.43), that is, >95% of patients could achieve a twofold rise in IgG titer.¹⁸ As SLE patients are receiving immunosuppressive treatment, we anticipate 40% of patients could achieve a twofold rise in IgG. Assuming only 10% of patients would have increase in IgG titer by twofold in the placebo group, a sample size of 84 patients is needed to detect the difference between the vaccinated and unvaccinated group with an alpha error of 5% and a study power of 90%. Taking a drop-out rate of 10%, 90 patients are required.

Statistical analyses

Clinical data of the two groups were compared by the independent sample Student's t-test (for continuous variables) and χ² test (for categorical variables). Within group comparison of the IgG VZV titers and the number of IFN-γ secreting T-cell colonies from baseline and week 6 was performed by the non-parametric Wilcoxon's matched pair analysis. The IgG anti-VZV reactivity and the number of T-cell colonies at week 6 of the two groups were compared by analysis of covariance with adjustment of baseline values.

Statistical significance was defined as a two-tailed p value of <0.05. All analyses were performed by the SPSS programme V.17.0 for Windows 10.

RESULTS

Clinical characteristics of the participants

Between March 2016 and October 2017, 183 SLE patients were assessed for eligibility. Ninety patients were recruited (93.3%

women) and assigned to vaccine or placebo in a 1:1 ratio. Figure 1 shows the disposition of patients. The mean age of patients was 45.6±14.1 years and SLE duration was 13.7±8.7 years. All except two patients (chickenpox infection in childhood) had a history of HZ infection. Table 1 shows the clinical characteristics of the patients. No significant differences in the prevalence of clinical manifestations and autoantibodies were observed between the vaccinated and placebo groups.

Table 2 shows the laboratory parameters and medications of the participants at study entry. The levels of IgG/IgA/IgM, serum creatinine, C3 and anti-dsDNA were similar between the two groups. There were also no significant differences in the SLEDAI or damage scores. Three patients in the vaccinated group and two patients in the placebo group had baseline clinical SLE activity (all mild thrombocytopenia that did not require change in therapy). All patients were receiving low-dose maintenance immunosuppressive therapies (table 2). No significant difference was observed in the medication use between the two groups except for a higher mean daily dose of azathioprine in the vaccinated group. No patients received combination therapies with more than one non-glucocorticoid immunosuppressive drugs (except hydroxychloroquine).

Humoral immune response to HZ vaccine

All participants completed the study. The baseline and week 6 anti-VZV IgG reactivity is shown in figure 2. All except one SLE patients had positive IgG anti-VZV test at baseline and there was no significant difference in the IgG anti-VZV values between the two groups (p=0.48). The anti-VZV IgG dropped from baseline to week 6 (3.45±1.07 to 3.32±1.01 (-2.1%); p=0.08)

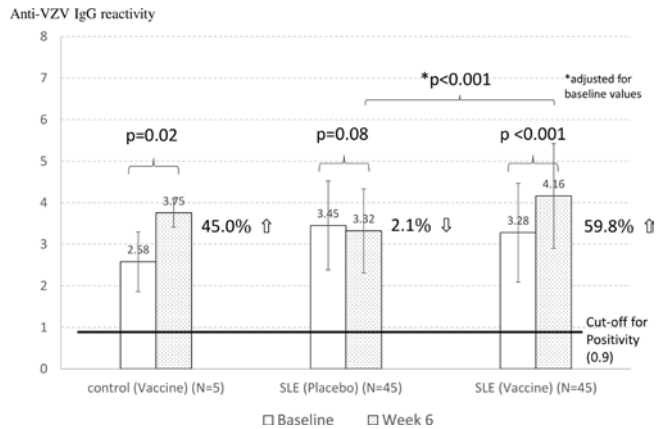


Figure 2 Change in anti-VZV IgG from baseline to week 6 after herpes zoster vaccination. SLE, systemic lupus erythematosus; VZV, varicella zoster virus.

in the placebo-treated patients. In contrast, the anti-VZV IgG increased significantly from week 0 to 6 in HZ-vaccinated patients (3.28±1.19 to 4.16±1.26 (+59.8%); p<0.001). The increment in IgG in vaccinated patients was similar in magnitude to healthy controls in whom the anti-VZV IgG titers increased from 2.58±0.72 to 3.75±0.34 (+45%); p=0.02) after HZ vaccination. The difference in IgG anti-VZV at week 6 between the vaccine and placebo-treated patients was statistically significant after adjustment for baseline values (p<0.001).

Cell-mediated immune response to HZ vaccine

The number of IFN-γ secreting CD4+ T cell spots (per 5×10⁵ cells) was similar between the two groups of patients at baseline (p=0.92). T-cell spots decreased in the placebo-treated patients from week 0 to 6 (27.8±44.5 to 23.1±47.9 (-17%); p=0.17), whereas they increased in the vaccine-treated patients (26.9±45.9 to 38.1±78.2 (+42%); p=0.24) (figure 3). The percentage increase in T-cell spots in vaccinated SLE patients was similar to that of healthy controls after HZ vaccination (32.9±35.8 to 48.7±24.6 (+48%); p=0.05). The number of T-cell spots at week 6 was significantly higher in vaccine than placebo-treated patients after adjustment for baseline values (38.1±78.2 vs 23.1±47.9; p=0.02).

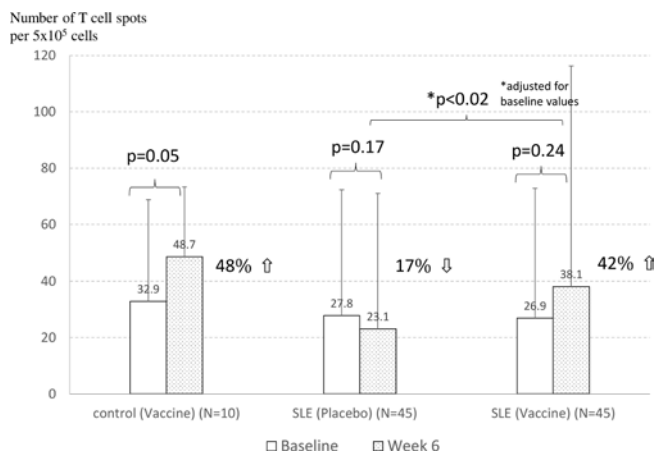


Figure 3 Change in VZV-stimulated T cell colonies (spots) from baseline to week 6 after herpes zoster vaccination. SLE, systemic lupus erythematosus; VZV, varicella zoster virus.

Table 2 Disease activity, serological results and medications of the SLE patients at study entry

	HZ vaccinated group (n=45)	Placebo group (n=45)	P value
	N (%), mean±SD		
SELENA-SLEDAI score	1.53±1.66	1.33±1.58	0.56
PGA score	0.25±0.14	0.25±0.13	1
Damage score (SDI)	0.84±1.07	0.77±1.16	0.76
Serological results			
IgG level, g/L	16.9±5.4	16.8±5.7	0.93
IgA level, g/L	3.4±1.6	3.1±1.1	0.24
IgM level, g/L	1.4±2.1	0.95±0.7	0.14
Lymphocyte count, x10 ⁹ /L	1.40±0.60	1.28±0.62	0.37
Serum creatinine, µmol/L	70.9±18.9	75.7±25.4	0.31
Complement C3 level, g/L	0.96±0.30	1.02±0.29	0.32
Anti-dsDNA titer, IU/mL	63.5±83.1	60.4±85.9	0.86
Medications at entry			
Prednisolone	23 (51)	29 (64)	0.2
Daily dose, mg	4.2±1.2	5.0±2.1	0.1
Azathioprine	11 (24)	11 (24)	1
Daily dose, mg	70.4±18.8	47.7±17.5	0.008
Mycophenolate mofetil	17 (38)	18 (40)	0.83
Daily dose, g	0.88±0.22	0.93±0.12	0.11
Hydroxychloroquine	25 (56)	33 (73)	0.08
Daily dose, mg	209±92	194±74	0.53
Tacrolimus	0 (0)	2 (4.4)	0.49
Ciclosporin A	2 (4.4)	0 (0)	0.49

HZ, herpes zoster; PGA, physician's global assessment; SDI, ACR/SLICC damage index; SELENA-SLEDAI, Safety of Estrogens in Lupus Erythematosus National Assessment—SLE Disease Activity Index; SLE, systemic lupus erythematosus.

Table 3 Unsolicited adverse events at week 6

	HZ vaccinated group (n=45)	Placebo group (n=45)	P value
Adverse events	N (%), mean±SD		
Conjunctivitis	0 (0)	1 (2.2)	1
Subjective fever	2 (4.4)	1 (2.2)	1
Injection site erythema and pain	14 (31)	3 (6.7)	0.006
Dizziness	1 (2.2)	0 (0)	1
Muscle cramps	1 (2.2)	0 (0)	1
Arthralgia	1 (2.2)	0 (0)	1
*SLE flares	2 (4.4)	1 (2.2)	1

*Two patients in the vaccinated group had mild SLE flares (dermatological); one patient in the placebo had mild renal flare (increase in proteinuria). SLE, systemic lupus erythematosus.

Factors affecting the cell-mediated and humoral response to HZ vaccination

Among SLE patients who were treated with the HZ vaccine, no correlation could be found between the increase in T-cell spots or anti-VZV IgG and age, sex, baseline lymphocyte counts, SLEDAI scores, complements, anti-dsDNA levels and the serum immunoglobulin levels (data not shown). Compared with patients not using prednisolone at baseline, those treated with prednisolone had lower increase in T-cell spots (3.2 ± 28.3 vs 19.6 ± 102 ; $p=0.47$) and anti-VZV IgG reactivity (31.5 ± 67.0 vs 90.8 ± 217 ; $p=0.24$) postvaccination, but the difference was not statistically significant. Patients using MMF also showed a non-significantly lower increase in T-cell spots than those not using the drug postvaccination.

Adverse events

None of the participants had SAEs that led to study withdrawal. Table 3 summarises the adverse events reported by the patients at week 6. Injection site erythema and pain was the most common symptoms reported and was significantly more common in the vaccinated than placebo-treated patients. In all cases, the symptoms were mild and self-limiting after a few days. Two vaccinated patients had mild/moderate SLE flares (dermatological) while one patient in the placebo group had mild/moderate SLE flare (increase in proteinuria).

We further evaluated whether injection site reactivity to the HZ vaccine was associated with its immunogenicity. However, we did not find any significant relationship. In fact, those vaccinated SLE patients who developed injection site reaction had a slightly lower percentage increase in IgG anti-VZV and T-cell spots (data not shown). There was also no association between injection site reaction and other clinical variables that included age, sex, SLE duration, disease activity, baseline immunoglobulin levels, lymphocyte counts and dosages of immunosuppressive drugs.

DISCUSSION

This is the first RCT on the safety and immune response of a live-attenuated HZ vaccine in patients with SLE. We demonstrated that the vaccine was safe and well-tolerated in stable patients not receiving intensive immunosuppression. The only unsolicited adverse event that occurred at a higher frequency in vaccinated patients was transient injection site reaction. Flares of SLE did not increase after HZ vaccination. No patients developed clinical HZ eruption within 6 weeks of vaccination.

Our results showed that the humoral response in terms of IgG reactivity against VZV increased significantly after vaccination in SLE patients. The percentage increase of anti-VZV IgG in patients was comparable to healthy controls after administration of the same vaccine, although the absolute increase in values was lower. In immunocompetent subjects, a more than twofold increase in anti-VZV titers after vaccination was reported.¹⁸ However, our data showed that the increase in IgG anti-VZV was lower than expected in both SLE patients and controls postvaccination. While the reason is not apparent, one contributing factor is the high rate of previous exposure to VZV infection in most participants, which could have led to a higher baseline anti-IgG anti-VZV value that limited its rise after vaccination. As SLE patients recruited in our study had stable disease and received minimal immunosuppression, their baseline IgG anti-VZV reactivity could be increased because of the higher frequency of previous HZ reactivation as compared with controls.

An IFN- γ ELISPOT assay was used in our study to assess the cell-mediated response to HZ vaccination, which was indirectly reflected by the number of T-cell colonies (spots) on VZV stimulation. However, there is still no benchmark of the degree of increase in the T spots to define an adequate immune response. Our data demonstrated that T-cell spots increased in vaccinated SLE patients from baseline to week 6. The percentage increase was comparable to that of healthy controls. In contrast, there was a reduction in the number of T-cell spots in SLE patients treated with placebo. The difference in T-cell spots at week 6 between the vaccinated and placebo-treated patients was statistically significant after adjustment for baseline values. These indicated an immune response to the HZ vaccine in SLE patients. However, we were unable to reveal any factors significantly associated with the cell-mediated response to vaccination except a trend of lower response in those using prednisolone or MMF at study entry. This could be the result of recruitment of SLE patients with stable disease using minimal immunosuppression and the limited sample size of the study.

A recent study showed that SLE patients had reduced cellular immune response to VZV, as evidenced by a reduced number of IFN- γ spot-forming cells and impaired proliferation of CD4+ T cells on VZV stimulation.¹⁹ However, the anti-VZV IgG titer was increased as compared with healthy controls, which was unrelated to subclinical HZ reactivation or disease activity.²⁰ Results of this study¹⁹ are consistent with ours which showed that the baseline anti-VZV IgG reactivity was higher but the number of T spots on VZV stimulation was lower in SLE patients than healthy controls. Although the percentage increase in IgG anti-VZV and T spots in SLE patients was similar to healthy controls postvaccination, the absolute increase in the respective numbers was lower in our patients.

The safety of Zostavax in SLE was reported in only one previous study of 10 SLE patients aged >50 years.¹² Similar to ours, this study also reported a comparable percentage increase of the VZV-stimulated T spots postvaccination in SLE patients with controls but the absolute increase was lower. Another study showed that a live-attenuated varicella-zoster vaccine was well-tolerated in 28 paediatric SLE patients with a history of chickenpox.²¹ However, the cell-mediated response to vaccination was lower in patients than controls.

Despite the increased risk of HZ infection, SLE had the lowest HZ vaccination rates among age-eligible subjects,⁹ probably because of the concern of vaccine safety, the principle of contraindication to live-attenuated vaccines in immunocompromised hosts, as well as the current ambiguous guidelines for HZ vaccination in SLE.¹⁰ The US Centers for Disease Control and

Prevention only recommends the live-attenuated HZ vaccine in patients receiving low-to-moderate immunosuppression such as short-term corticosteroid therapy (<14 days), low to moderate doses of corticosteroid (<20 mg/day prednisolone), methotrexate (<0.4 mg/kg/week) and azathioprine (<3 mg/kg/day).²² The cut-off dosages of various drugs to differentiate between heavy and non-heavy immunosuppression are based on expert opinions and not all SLE medications are included. The EULAR recommendation suggests that the live-attenuated HZ vaccine may be considered in patients with rheumatic diseases who are less seriously immunosuppressed.²³ However, the definition of 'less serious' immunosuppression is not explicit. The recent availability of the non-live subunit and inactivated HZ vaccines might provide more opportunities for SLE patients to be protected against HZ reactivation as they do not contain the live virus that may cause disseminated infection in patients on heavy immunosuppression.¹⁰ Despite the lack of head-to-head comparative studies, a recent network meta-analysis showed that the recombinant adjuvant subunit vaccine may be more effective than the live vaccine in preventing HZ reactivation in older healthy individuals.²⁴ However, the subunit HZ vaccine requires two injections and the incidence of injection site reactivity was significantly higher.²⁴ The subunit HZ vaccine provokes a strong immune response regardless of previous vaccination with live HZ vaccine²⁵ and is a suitable option to revaccinate prior live HZ vaccine recipients. However, the subunit HZ vaccines are not yet tested in SLE patients or available in all localities.

There are a few limitations of the study. First, during sample calculation, we had assumed a greater humoral immune response to the HZ vaccine in SLE patients. The actual results, however, showed that the immune responses to vaccination in both SLE patients and controls were lower and exhibited a great individual variation. As a result, the sample size of the study might be insufficient to detect a difference in the immune response to vaccination, particularly the cell-mediated response. Second, the safety and immunogenicity of Zostavax derived from our results does not apply to patients with active SLE or those receiving more intensive immunosuppression. Finally, the persistence of immunogenicity of the HZ vaccine and its clinical efficacy in reducing HZ reactivation in the long-run has yet to be seen. In fact, we have collected samples for the humoral response to the HZ vaccine at 1 year and extended our study to 3 years for repeat assessment of the vaccine immunogenicity.

In conclusion, our study has demonstrated safety and immunogenicity of a live-attenuated HZ vaccine in stable SLE patients with a previous history of HZ or varicella infection. HZ vaccine should best be administered during periods of SLE quiescence to maximise its efficacy. Longer-term surveillance is necessary to evaluate the immunogenicity of the vaccine and its correlation with clinical efficacy in reducing HZ reactivation.

Contributors CCM and LYH: study design, patients' assessment, data collection and analysis. KHC, YFF, WFF and PCYW: laboratory assay, data collection and analysis.

Funding This work was funded by the Health and Medical Research Fund from the Hong Kong Research Fund Secretariat.

Competing interests None declared.

Patient consent for publication Not required.

Ethics approval The study protocol was approved by the Research and Ethics Committee of Tuen Mun Hospital and registered in ClinicalTrials.gov (NCT02477150).

Provenance and peer review Not commissioned; externally peer reviewed.

Data availability statement All data relevant to the study are included in the article or uploaded as supplementary information.

ORCID iD

Chi Chiu Mok <http://orcid.org/0000-0003-3696-1228>

REFERENCES

- O'Connor KM, Paauw DS. Herpes zoster. *Med Clin North Am* 2013;97:503–22.
- Wilson JF. Herpes zoster. *Ann Intern Med* 2011;154:ITC31–15.
- Freer G, Pistello M. Varicella-Zoster virus infection: natural history, clinical manifestations, immunity and current and future vaccination strategies. *New Microbiol* 2018;41:95–105.
- Oxman MN, Levin MJ, Johnson GR, et al. A vaccine to prevent herpes zoster and postherpetic neuralgia in older adults. *N Engl J Med* 2005;352:2271–84.
- Schmader KE, Levin MJ, Gnann JW, et al. Efficacy, safety, and tolerability of herpes zoster vaccine in persons aged 50–59 years. *Clin Infect Dis* 2012;54:922–8.
- SC H, Lin CL, YW L, et al. Lymphopaenia, anti-Ro/anti-RNP autoantibodies, renal involvement and cyclophosphamide use correlate with increased risk of herpes zoster in patients with systemic lupus erythematosus. *Acta Derm Venereol* 2013;93:314–8.
- Borba EF, Ribeiro ACM, Martin P, et al. Incidence, risk factors, and outcome of herpes zoster in systemic lupus erythematosus. *J Clin Rheumatol* 2010;16:119–22.
- Cogman AR, Chakravarty EF. The case for Zostavax vaccination in systemic lupus erythematosus. *Vaccine* 2013;31:3640–3.
- Chakravarty EF, Michaud K, Katz R, et al. Increased incidence of herpes zoster among patients with systemic lupus erythematosus. *Lupus* 2013;22:238–44.
- Mok CC. Herpes zoster vaccination in systemic lupus erythematosus: the current status. *Hum Vaccin Immunother* 2019;15:45–8.
- Zhang J, Xie F, Delzell E, et al. Association between vaccination for herpes zoster and risk of herpes zoster infection among older patients with selected immune-mediated diseases. *JAMA* 2012;308:43–9.
- Guthridge JM, Cogman A, Merrill JT, et al. Herpes zoster vaccination in SLE: a pilot study of immunogenicity. *J Rheumatol* 2013;40:1875–80.
- Hochberg MC. Updating the American College of rheumatology revised criteria for the classification of systemic lupus erythematosus. *Arthritis Rheum* 1997;40:1725.
- Petri M, Orbai A-M, Alarcón GS, et al. Derivation and validation of the systemic lupus international collaborating clinics classification criteria for systemic lupus erythematosus. *Arthritis Rheum* 2012;64:2677–86.
- Buyon JP, Petri MA, Kim MY, et al. The effect of combined estrogen and progesterone hormone replacement therapy on disease activity in systemic lupus erythematosus: a randomized trial. *Ann Intern Med* 2005;142:953–62.
- Petri M, Kim MY, Kalunian KC, et al. Combined oral contraceptives in women with systemic lupus erythematosus. *N Engl J Med* 2005;353:2550–8.
- Petri M, Hellmann D, Hochberg M. Validity and reliability of lupus activity measures in the routine clinic setting. *J Rheumatol* 1992;19:53–9.
- Gilbert PB, Gabriel EE, Miao X, et al. Fold rise in antibody titers by measured by glycoprotein-based enzyme-linked immunosorbent assay is an excellent correlate of protection for a herpes zoster vaccine, demonstrated via the vaccine efficacy curve. *J Infect Dis* 2014;210:1573–81.
- Rondaan C, de Haan A, Horst G, et al. Altered cellular and humoral immunity to varicella-zoster virus in patients with autoimmune diseases. *Arthritis Rheumatol* 2014;66:3122–8.
- Rondaan C, van Leer CC, van Assen S, et al. Longitudinal analysis of varicella-zoster virus-specific antibodies in systemic lupus erythematosus: no association with subclinical viral reactivations or lupus disease activity. *Lupus* 2018;27:1271–8.
- Barbosa CMPL, Terreri MTRA, Rosário PO, et al. Immune response and tolerability of varicella vaccine in children and adolescents with systemic lupus erythematosus previously exposed to varicella-zoster virus. *Clin Exp Rheumatol* 2012;30:791–8.
- Harpaz R, Ortega-Sanchez IR, Seward JF. Advisory Committee on immunization practices (ACIP) centers for disease control and prevention (CDC). prevention of herpes zoster: recommendations of the Advisory Committee on immunization practices (ACIP). *MMWR Recomm Rep* 2008;57:1–30.
- van Assen S, Agmon-Levin N, Elkayam O, et al. EULAR recommendations for vaccination in adult patients with autoimmune inflammatory rheumatic diseases. *Ann Rheum Dis* 2011;70:414–22.
- Tricco AC, Zarin W, Cardoso R, et al. Efficacy, effectiveness, and safety of herpes zoster vaccines in adults aged 50 and older: systematic review and network meta-analysis. *BMJ* 2018;30.
- Gruppung K, Campora L, Douha M, et al. Immunogenicity and safety of the HZ/su adjuvanted herpes zoster subunit vaccine in adults previously vaccinated with a live attenuated herpes zoster vaccine. *J Infect Dis* 2017;216:1343–51.

CLINICAL SCIENCE

Ultrasensitive serum interferon- α quantification during SLE remission identifies patients at risk for relapse

Alexis Mathian ,¹ Suzanne Mouries-Martin,² Karim Dorgham,³ Hervé Devilliers,⁴ Hans Yssel,³ Laura Garrido Castillo,³ Fleur Cohen-Aubart,¹ Julien Haroche,¹ Miguel Hié,¹ Marc Pineton de Chambrun,¹ Makoto Miyara,³ Micheline Pha,¹ Flore Rozenberg,⁵ Guy Gorochoy,³ Zahir Amoura¹

Handling editor Josef S Smolen

► Additional material is published online only. To view please visit the journal online (<http://dx.doi.org/10.1136/annrheumdis-2019-215571>).

For numbered affiliations see end of article.

Correspondence to

Dr Alexis Mathian, Internal Medicine, Pitié-Salpêtrière Hospital, Paris 75013, France; alexis.mathian@aphp.fr

AM, SM-M and KD contributed equally.
GG and ZA contributed equally.

Received 18 April 2019
Revised 3 September 2019
Accepted 4 September 2019
Published Online First
30 September 2019

ABSTRACT

Objectives Maintenance of remission has become central in the management of systemic lupus erythematosus (SLE). The importance of interferon-alpha (IFN- α) in the pathogenesis of SLE notwithstanding, its expression in remission has been poorly studied as yet. To study its expression in remission and its prognostic value in the prediction of a disease relapse, serum IFN- α levels were determined using an ultrasensitive single-molecule array digital immunoassay which enables the measurement of cytokines at physiological concentrations.

Methods A total of 254 SLE patients in remission, according to the Definition of Remission in SLE classification, were included in the study. Serum IFN- α concentrations were determined at baseline and patients were followed up for 1 year. Lupus flares were defined according to the Safety of Estrogens in Lupus Erythematosus: National Assessment version of the Systemic Lupus Erythematosus Disease Activity Index Flare Index, whereas the Kaplan-Meier analysis and Cox regression analysis were used to estimate the time to relapse and to identify baseline factors associated with time to relapse, respectively.

Results Of all patients in remission, 26% displayed abnormally high IFN- α serum levels that were associated with the presence of antibodies specific for ribonucleoprotein (RNP), double stranded (ds)DNA and Ro/SSA60, as well as young age. Importantly, elevated-baseline IFN- α serum levels and remission duration were associated in an independent fashion, with shorter time to relapse, while low serum levels of complement component 3 and anti-dsDNA Abs were not.

Conclusion Direct serum IFN- α assessment with highly sensitive digital immunoassay permits clinicians to identify a subgroup of SLE patients, clinically in remission, but at higher risk of relapse.

INTRODUCTION

Systemic lupus erythematosus (SLE) is a chronic autoimmune disease of incompletely known aetiology characterised by the presence of anti-nuclear autoantibodies and inflammation in a wide spectrum of organs.¹ Despite the improvement of SLE prognosis in the last decades, SLE patients are still at high risk of disease-related complications and premature death.^{2,3} Several authors have

Key messages

What is already known about this subject?

- Serum interferon-alpha (IFN- α) levels have been poorly studied in systemic lupus erythematosus (SLE) patients in remission so far.
- The single-molecule array assay is an ultrasensitive assay that quantifies directly IFN- α at attomolar concentrations.

What does this study add?

- A quarter of SLE patients in remission display elevated serum IFN- α levels.
- Elevated serum IFN- α levels constitute an independent predictive biomarker of lupus flares.

How might this impact on clinical practice or future developments?

- Including serum IFN- α in the routine laboratory assessments in patients in remission will assist clinicians in identifying SLE patients at higher risk of relapse.

shown that remission defined as the elimination of disease activity predicted a better disease outcome with a lower burden of damage and a lower risk of relapse.^{4,5} Thus, remission achievement and its maintenance have become central in the management of SLE patients.^{6,7} Many definitions have been used to better characterise remission states, but a single one has recently made consensus, the DORIS (Definitions of Remission in SLE). For defining remission, the DORIS uses a clinical index, such as the clinical SLE disease activity index (SLEDAI)=0 with routine laboratory assessments including anti-double stranded DNA (anti-dsDNA) antibodies (Abs) and complement.⁷ Serologically active patients, that is, patients with an increase in serum anti-dsDNA Abs and/or a complement consumption, are much more likely to experience subsequent flares, as compared with those who are serologically inactive.⁷ However, these two markers fail to reliably predict a lupus flare.^{8,9} Consequently, no consensus has yet been reached by the DORIS working group as



© Author(s) (or their employer(s)) 2019. No commercial re-use. See rights and permissions. Published by BMJ.

To cite: Mathian A, Mouries-Martin S, Dorgham K, et al. *Ann Rheum Dis* 2019;**78**:1669–1676.

to a reliable definition that enables the distinction of patients who are serologically active from those who are serologically inactive.⁷

Many authors consider the dysregulation of interferons (IFNs), especially interferon-alpha (IFN- α), to be a central cause of the immunological abnormalities observed in SLE.^{10–16} Transcriptome analysis using microarray technology revealed upregulation of the expression of numerous IFN-stimulated genes (ISGs) in SLE patients' peripheral blood mononuclear cells, constituting an overall 'IFN signature'.^{17–18} Many reports showed patients' elevated serum-IFN- α levels to be associated with SLE activity and severity, suggesting that monitoring this cytokine might help physicians to better evaluate disease activity,^{17–35} although, unexpectedly, some clinically inactive patients have persistently elevated serum IFN- α levels.^{19–23 25 35} Since serum concentrations of IFN- α are usually very low and often not detectable by classic immunoassays, monitoring the expression of ISGs is used to evaluate IFN serological activity. The resulting 'IFN scores' are calculated based on the expression of several representative ISGs.^{29 36 37} However, the low availability and high complexity of transcriptome-microarray technology implies that IFN scores are not standardised and therefore cannot be easily used in clinical practice. At present, IFN- α overexpression has been poorly studied in patients in remission.

The single-molecule array (Simoa) assay, or digital immunoassay, is an ultrasensitive assay based on enumeration of individual enzyme-labelled immunocomplexes of proteins captured on beads in single-molecule arrays. It enables direct IFN- α quantification at attomolar concentrations,^{35 38–40} corresponding to a 5000-fold—increased sensitivity over classic ELISAs. We and others have shown that, at physiological concentrations, the digital immunoassay is as sensitive as ISG expression as a means to quantify IFN- α levels and simpler to perform and standardise.^{35 40} We thus conducted a study to determine the magnitude of serum IFN- α concentrations in SLE patients in remission using the DORIS criteria.⁷ Additionally, in order to improve the definition of remission, we determined the clinical and biological features associated with elevated IFN- α levels in patients experiencing a remission and we investigated whether high serum IFN- α levels at baseline in patients in remission were predictive of a flare in the ensuing year.

PATIENTS, MATERIALS AND METHODS

Study design and patients

The longitudinal study reported here was conducted between September 2014 and September 2017 at the National Referral Center for SLE, Paris, France. Serum samples were obtained at day 0 (=baseline) from consecutive patients diagnosed with SLE according to the 1997 American College of Rheumatology criteria for SLE classification, regardless of the activity of the disease.⁴¹ Exclusion criteria were: (1) known or suspected infection or malignancy on the day blood was drawn; (2) increased hydroxychloroquine (HCQ), prednisone and/or immunosuppressant (IS) during the 4 weeks preceding day 0. SLE clinical characteristics (see online supplementary file), SELENA-SLEDAI,^{42–44} SLEDAI-2K,⁴⁵ class of lupus nephritis according to ISN/RPS-2003,⁴⁶ and therapeutic regimen were recorded on day 0. Lupus flares were defined according to the SELENA-SLEDAI Flare Index.^{43 44} The term 'clinical' SLEDAI (cSLEDAI) refers to symptoms, signs and routine laboratory testing and disregards only the points that can be given for the presence of anti-dsDNA Abs and/or low complement.⁷ Five exclusive disease activity statuses were defined, according to the DORIS⁷ and following

Wilhelm *et al*⁴⁷ and Ugarte-Gil *et al*⁴⁸ without physician global assessment (PGA) and serum C4 analysis:

- ▶ *Complete remission off treatment*: cSELENA-SLEDAI=0, no corticosteroids, no IS, no anti-dsDNA Abs and no complement component 3 (C3) decrease.
- ▶ *Clinical remission off treatment*: cSELENA-SLEDAI=0, no corticosteroids, no IS. Anti-dsDNA Abs and/or C3 decrease present.
- ▶ *Complete remission on treatment*: cSELENA-SLEDAI=0, prednisone 1–5 mg/day, IS allowed, no anti-dsDNA Abs and no C3 decrease
- ▶ *Clinical remission on treatment*: cSELENA-SLEDAI=0, prednisone 1–5 mg/day, IS allowed. Anti-dsDNA Abs and/or C3 decrease present.
- ▶ *Not in remission*: cSELENA-SLEDAI >0 and/or prednisone >5 mg/day.

HCQ was allowed in all groups. Duration of remission was recorded. Over a consecutive 5-year period of remission, the patient was considered in 'prolonged remission', as proposed by Steiman *et al*,⁴⁹ and treated in the statistical analysis as a 5-year remission. Alternatively, patients not in remission but fulfilling Lupus Low Disease Activity State (LLDAS)^{48 50} were included in the 'LLDAS without remission' subgroup (see online supplementary file). Sera from age-matched and gender-matched healthy donors (n=68) were collected (Établissement Français du Sang, Île-de-France, Pitié-Salpêtrière Hospital, Paris, France) during the same time period.

Patient follow-up

Patients in remission at day 0 were followed for 1 year (see online supplementary file).

IFN- α digital immunoassay

Serum IFN- α concentrations, expressed in fg/mL, were determined at day 0 with digital immunoassay technology (IFN- α Reagent Kit, Quanterix Simoa, Lexington, Massachusetts, USA), based on a three-step protocol (see online supplementary file) using the HD-1 Analyzer (Quanterix).³⁸ The IFN- α digital ELISA positivity threshold (defining elevated IFN- α) was 136 fg/mL, which is three SD above the mean serum IFN- α concentration calculated from the sera samples from the 68 healthy blood donors.

Statistical analysis

Statistical analyses were performed using GraphPad Prism, V.5.0 software (GraphPad Software, San Diego, California, USA) and SAS V.9.4 software (see online supplementary file).

RESULTS

Patient characteristics and distribution according to disease activity

A total of 407 patients were included in the study, with 254 patients in remission (ie, cSELENA-SLEDAI=0 and prednisone equal or less than 5 mg/day) and 153 not in remission. Patients' baseline characteristics are described in table 1. From the 254 patients in remission, 86 (33.9%) were in complete remission off treatment, 59 (23.2%) in complete remission on treatment, 47 (18.5%) in clinical remission off treatment and 62 (24.4%) in clinical remission on treatment. Sixty-seven (26.3%) patients were in remission for less than 1 year, 101 (39.8%) for 1–5 years, and 86 (33.9%) for more than 5 years. The median (range) of remission duration was 5 years (0–5) for patients in complete remission off treatment, 1.6 years (0–5) for patients in complete

Table 1 Disease characteristics in SLE patients at baseline

	Patients in remission (n=254)	Patients not in remission (n=153)
Women	226 (89)	139 (91)
Age, years, mean±SD	42.4±12.9	36.3±12.0
Disease duration, years, mean±SD	12.6±9.7	8.9±8.5
SELENA-SLEDAI score, median (range)	0 (0–4)	6 (0–41)
SELENA-SLEDAI score ≥4	21 (8)	110 (72)
Mild/moderate flare*	0 (0)	31 (20)
Severe flare*	0 (0)	76 (50)
Clinical involvement		
Fever	0 (0)	37 (24)
Weight loss or anorexia	0 (0)	21 (14)
Lymphadenopathy	1 (0)	24 (16)
Any constitutional signs	0 (0)	46 (30)
Active cutaneous lupus	0 (0)	48 (31)
Active lupus serositis	0 (0)	23 (15)
Active lupus arthritis	0 (0)	67 (44)
Active lupus nephropathy	0 (0)	31 (20)
Proliferative nephropathy	0 (0)	15 (10)
Membranous nephropathy	0 (0)	16 (10)
Active neuropsychiatric lupus	0 (0)	8 (5)
Cytopenia	0 (0)	34 (22)
Treatment regimen		
Hydroxychloroquine use	228 (90)	119 (78)
Prednisone use	100 (39)	105 (69)
Prednisone ≥10 mg/j	0 (0)	56 (37)
Immunosuppressive agent use†	46 (18)	50 (33)
Biological tests		
Positive Farr test	101 (40)	97 (63)
Positive anti-RNP Abs	50 (20)	68 (44)
Positive anti-Sm Abs	18 (7)	33 (22)
Positive anti-Ro/SSA 52 Abs	56 (22)	41 (27)
Positive anti-Ro/SSA 60 Abs	83 (33)	68 (44)
Positive anti-La/SSB Abs	22 (9)	20 (13)
Low C3	30/248‡ (12)	68/150‡ (45)

Values are expressed as n (%), unless stated otherwise.

*Defined using SELENA flare index^{43,44}

†Excluding antimalarials and prednisone. Immunosuppressant therapy was mycophenolate mofetil (MMF) for 43 (44%) patients, methotrexate (MTX) for 39 (41%), azathioprine for 13 (14%) and cyclophosphamide for 1 (1%). Two patients were receiving calcineurin inhibitor in addition to MMF and three patients were receiving belimumab in addition to MTX.

‡Positive assay/number of patients assessed.

Abs, antibodies; SELENA-SLEDAI, Safety of Estrogens in Lupus Erythematosus: National Assessment version of the Systemic Lupus Erythematosus Disease Activity Index; SLE, systemic lupus erythematosus.

remission on treatment, 4.2 years (0.1–5) for clinical remission off treatment and 1.6 years (0–5) for clinical remission on treatment. Among the 153 patients not in remission, 19 (12.4%) fulfilled the LLDAS criteria, defining the ‘LLDAS without remission’ subgroup.

Serum IFN- α in remission and LLDAS

The serum IFN- α levels according to the different states of remission are presented in table 2. A total of 26.0% of patients in remission had still detectable serum IFN- α levels exceeding the positivity threshold. Patients in ‘clinical remission’ had the highest rate of elevated serum IFN- α : 41.9% for ‘clinical remission on treatment’ and 38.3% for ‘clinical remission off treatment’ (vs 16.3% for ‘complete remission off treatment’, $p=0.0007$ and 0.006 , respectively). Among patients

in remission, patients in ‘clinical remission on treatment’ had the highest concentration of IFN- α with a median (quartiles) of 109 fg/mL (12–378) (vs 11 fg/mL (0–81) in patients in ‘complete remission off treatment’, $p=0.0002$). Alternatively, we assessed serum IFN- α levels in different states of remission according to the definition of Zen *et al*,⁵ a definition of remission in which the role of corticosteroids is highlighted in comparison to immunosuppressive treatment. As shown in online supplementary file 1, we found similar results: patients in ‘clinical remission on or off corticosteroids’ had the highest rate of abnormal serum IFN- α levels, as compared with those of patients in ‘complete remission’. Thus, a significant number of patients in remission had increased IFN- α levels in their serum. Eight (42.1%) patients of the ‘LLDAS without remission’ subgroup displayed abnormal IFN- α serum concentrations (OR 3.7 (95% CI 1.3 to 11.0) and a mean IFN- α level of 111 fg/mL (0–1647), $p=0.02$ and $p=0.07$, respectively, as compared with patients in ‘complete remission off treatment’).

SLE characteristics associated with abnormal serum IFN- α levels in remission

Elevated IFN- α serum levels of patients in remission were significantly associated, in multivariable analysis, with the presence of serum Abs specific for RNP, dsDNA and Ro/SSA60, young age and lower granulocyte counts (table 3). In contrast, disease and remission duration, prednisone intake, IS therapy, HCQ and low C3 serum levels did not show a significant association with IFN- α serum levels.

Elevated IFN- α serum levels in SLE patients in remission predict a lupus flare

Of the 254 patients in remission at day 0, 250 were followed for 1 year. Twenty-four (9.6%) patients experienced a flare. The median (range) time of the flare occurrence was 141 (25–349) days. The type and severity of the flares are reported in online supplementary table 3. A total of 37.5% of the flares were severe. The most frequent type of relapses was arthritis ($n=15$) followed by cutaneous flare ($n=7$) and serositis ($n=4$). Unadjusted cox regression showed a significantly higher risk of relapse in patients who displayed at baseline elevated IFN- α (HR 5.5 (95% CI 2.4 to 12.5), $p<0.0001$) or decreased C3 (HR 3.7 (95% CI 1.6 to 9.1), $p=0.003$) serum levels, respectively, but not in patients who had a positive Farr assay (HR 1.5 (95% CI 0.7 to 3.4), $p=0.3$) (figure 1). The highest concentrations of IFN- α at baseline were associated with the greatest frequencies of relapse (online supplementary figure 1). Other factors at baseline associated with the risk of relapse were prednisone intake 1–5 mg/day (HR 3.2 (95% CI 1.4 to 7.5), $p=0.007$), positive anti-RNP Abs (HR 3.1 (1.4 to 7.0), $p=0.006$), age <40 years (HR 0.4 (95% CI 0.2 to 0.9), $p=0.02$) and disease duration <10 years (HR 0.2 (95% CI 0.1 to 0.6), $p=0.003$). The remission duration was a protective factor for the probability of flare (HR 0.6 (95% CI 0.5 to 0.8) for each consecutive year of remission completed, $p=0.0002$).

Finally, in multivariable analysis, the factors independently associated with the risk of flare were abnormal serum IFN- α levels at baseline (HR 4.0 (95% CI 1.7 to 9.6), $p=0.002$) and remission duration (HR 0.7 (95% CI 0.5 to 0.9), $p=0.02$, for each year in remission). Low C3 (HR 2.4 (95% CI 0.9 to 6.2), $p=0.07$) and prednisone intake (HR 2.4 (95% CI 0.9 to 5.9), $p=0.06$) were also kept in the model as associated with a higher risk of flare but these associations were not statistically significant. We performed a sensitivity analysis using a lower concentration of IFN- α as the threshold of elevated IFN- α levels and found similar results (data not shown).

Additionally, the risks of relapse according to combined SLE biomarkers (low C3, positive Farr assay and elevated IFN- α serum

Table 2 Serum IFN- α levels at baseline in SLE patients in remission or not in remission (according to Wilhelm *et al*⁴⁷ modified)

	Abnormal serum IFN- α level	OR (95% CI)	P value*	Serum IFN- α fg/mL, median (Q1, Q3)	P value†
Remission (n=254)	66 (26.0)				
Complete remission off treatment (n=86)‡	14 (16.3)	1 (Ref.)	Ref.	11 (0–81)	Ref.
Complete remission on treatment (n=59)	8 (13.6)	0.8 (0.3 to 2.1)	NS	15 (0–51)	NS
Clinical remission off treatment (n=47)	18 (38.3)	3.2 (1.4 to 7.2)	0.006	18 (0–314)	NS
Clinical remission on treatment (n=62)	26 (41.9)	3.7 (1.7 to 8.0)	0.0007	109 (12–378)	0.0002
Not in remission (n=153)	97 (63.4)				
Prednisone >5 mg/day (n=33)	10 (30.3)	2.2 (0.9 to 5.7)	NS	78 (0–296)	0.04
cSLEDAI >0 (n=74)	51 (68.9)	11.4 (5.4 to 24.3)	<0.0001	519 (68–3,087)	<0.0001
Prednisone >5 mg/day and cSLEDAI >0 (n=46)	36 (78.3)	18.5 (7.5 to 45.8)	<0.0001	2,054 (455–8,751)	<0.0001

Values are expressed as n (%), unless stated otherwise.

*Bivariable analysis using Mann-Whitney U test compared with 'complete remission off treatment' as the reference.

†Bivariable comparison using Fisher's exact test compared with patients in 'complete remission off treatment' as the reference.

‡Reference group for statistical analysis.

cSLEDAI, clinicalSLEDAI; IFN- α , interferon alpha; NS, non-significant; SLE, systemic lupus erythematosus; SLEDAI, Systemic Lupus Erythematosus Disease Activity Index.

levels) were independently analysed with a proportional risk Cox model (online supplementary table 4). In this model, isolated elevated IFN- α levels were a predictive factor of lupus flare (HR of 5.5 (95% CI 1.7 to 18.1), $p=0.005$). In contrast, isolated positive Farr assay and isolated low C3 levels had no predictive value of lupus flare.

Potentiality of the digital immunoassay, C3 and Farr assay performances to predict a flare

The time-dependent receiver operating characteristics (ROC) area under the curve (AUC) (figure 2) estimates for the IFN- α digital immunoassay to predict a flare was 0.73, better than

that of anti-dsDNA Abs (0.60, $p=0.055$), and C3 serum levels (0.56, $p=0.2$). The time-dependent ROC AUCs for the three biomarkers were highest around day 90.

DISCUSSION

The significance of monitoring IFN- α serum levels in SLE for the assessment of remission and the risk to develop flares has been poorly documented as yet. In the present study, we show that a significant proportion of patients despite being in remission have high serum IFN- α levels that were found to independently predict the risk of subsequent SLE flares, thereby emphasising

Table 3 Disease characteristics associated with serum IFN- α levels at baseline in SLE patients in remission

	IFN- α		Bivariable P value*	Multivariable P value†	Adjusted OR† (95% CI)
	Normal n=188	Elevated n=66			
Women	165 (88)	61 (92)	0.30	ND	
Age, years, mean \pm SD	44.0 \pm 13.3	37.5 \pm 10.8	<0.001	0.002	0.96 (0.93 to 0.98)
Disease duration, years, mean \pm SD	13.4 \pm 10.0	10.4 \pm 8.3	0.029	NS	
Remission duration, years, median (Q1–Q3)	3.4 (1.1–5.0)	1.8 (0.5–5.0)	0.024	NS	
Hydroxychloroquine use	165 (88)	63 (95)	0.08	ND	
Prednisone use	72 (38)	28 (42)	0.55	ND	
Prednisone use, mg/d, median (Q1–Q3)	0 (0–5)	0 (0–5)	0.65	ND	
Immunosuppressive agent use‡	31 (16)	15 (23)	0.26	ND	
Positive Farr test	59 (31)	42 (64)	<0.001	0.02	2.3 (1.1 to 4.6)
Positive anti-RNP Abs	21 (11)	29 (44)	<0.001	0.0002	4.6 (2.1 to 10.2)
Positive anti-Ro/SSA 52 Abs	34 (18)	22 (33)	0.01	NS	
Positive anti-Ro/SSA 60 Abs	52 (28)	31 (47)	0.004	0.01	2.6 (1.3 to 5.4)
Positive anti-La/SSB Abs	14 (7)	8 (12)	0.25	ND	
Positive anti-Sm Abs	5 (3)	13 (20)	<0.001	NS	
Low C3	14/184§ (8)	16 (24)	<0.001	NS	
Lymphocytes, G/L, median (Q1–Q3)	1.5 (1.2–2.1)	1.2 (0.9–1.5)	0.0001	NS	
Granulocytes, G/L, median (Q1–Q3)	3.9 (2.9–5.5)	3.1 (2.4–3.7)	<0.001	0.001	0.7 (0.5 to 0.8)
Thrombocytes, G/L, median (Q1–Q3)	249 (215–284)	232 (205–282)	0.5	ND	
Haemoglobin, g/dL, median (Q1–Q3)	13.3 (12.6–14.1)	12.6 (11.8–13.7)	<0.001	NS	

Values are expressed as n (%), unless stated otherwise.

*Estimated by Mann-Whitney test, Fisher's exact or χ^2 test.

†Evaluated by multivariable logistic regression.

‡Excluding antimalarials and prednisone.

§Positive assay/number of patients assessed.

Abs, antibodies; IFN- α , interferon-alpha; ND, not done; NS, non-significant; SLE, systemic lupus erythematosus.

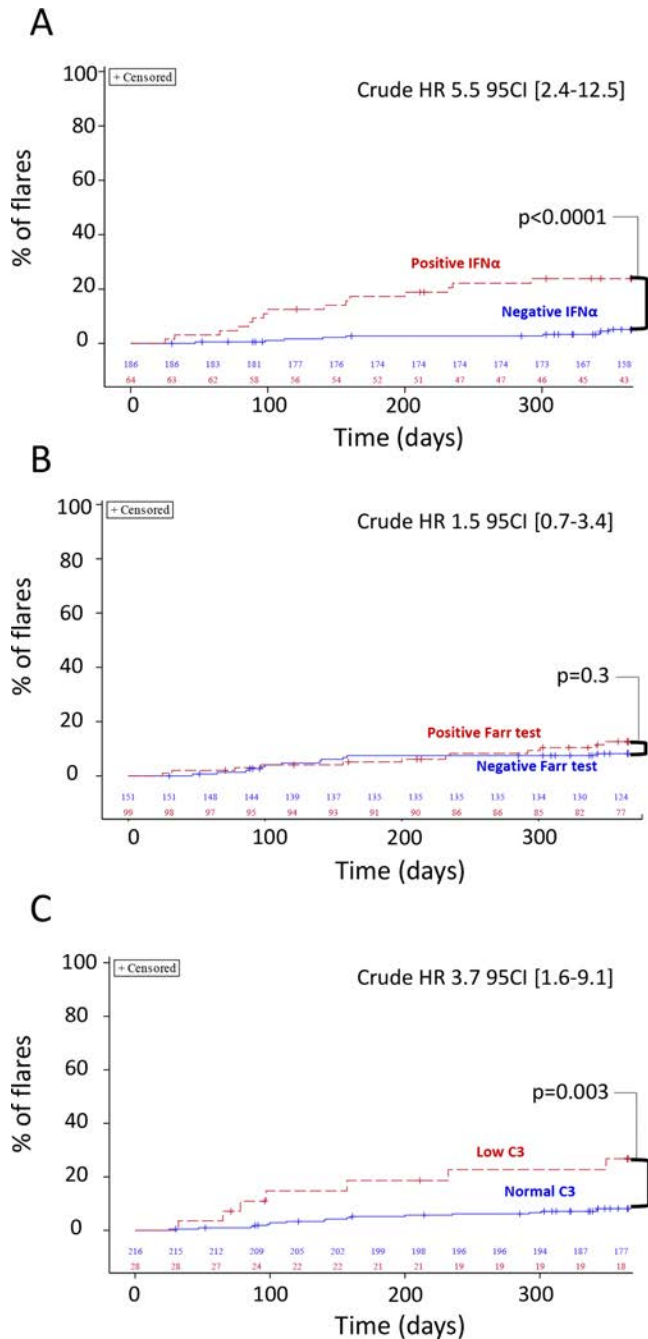


Figure 1 Baseline elevated serum interferon-alpha (IFN- α) and low C3 levels identify patients with elevated risk for future systemic lupus erythematosus flares. Kaplan-Meier curves. Serum IFN- α (positivity threshold of 136 fg/mL), anti-double stranded DNA (anti-dsDNA) antibodies by Farr assay (cut-off value: 9.0 IU/mL) and C3 levels (cut-off value: 0.78 g/L) were assessed at day 0. Kaplan-Meier plots show the percentage of patients who flared in any organ system. Vertical tick marks along each curve represent patients who remained flare-free but did not have a full year of clinical follow-up (censored data). Curves were compared using Log-Rank tests. Crude HRs were calculated using proportional risk cox model. (A) The red dashed line represents the 64 patients with elevated IFN- α serum level at day 0. The continuous blue line represents the 186 patients with negative IFN- α serum level at day 0. (B) The red dashed line represents the 99 patients with positive Farr assay at day 0. The continuous blue line represents the 151 patients with negative Farr assay at day 0. (C) The red dashed line represents the 28 patients with low C3 level at day 0. The continuous blue line represents the 216 patients with normal C3 level at day 0.

the interest of measuring the production of this cytokine to monitor the course of disease.

Earlier publications have reported that between 3% and 32% of SLE patients without active disease present elevated IFN- α serum levels depending on the type of assay used to determine the presence of this cytokine.^{19-23 25 35} However, because different definitions of disease inactivity were used in these studies, the results cannot directly be compared with our study that takes into account the recently formulated consensual definition of disease remission.^{5 7 47} Contrary to the results of a previously published report,⁵¹ we noted that serum concentrations of IFN- α above the positive threshold values varied between different remission subgroups. Patients in clinical remission, that is, with serological activity, presented more frequently elevated serum levels of IFN- α than patients in complete remission. The presence of serum Abs specific for RNP, dsDNA and Ro/SSA60 were found to be independently associated with the magnitude of serum IFN- α levels. These associations have previously been shown in SLE^{29-31 52-57} but, to the best of our knowledge, never been reported for patients in remission. Our data are in accordance with those from previous studies that showed a key role of DNA/RNA-associated immune complexes through the activation of TLR7 and TLR9 for the induction of type I IFN production.^{58 59}

The DORIS group has recently agreed that the subsequent occurrence of flares is among the most appropriate outcome variables for defining the prognostic value of remission and furthermore suggested the inclusion of serological criteria for this definition.⁷ Results from previous reports on smaller SLE patient cohorts, based on the analysis of expression of ISGs in peripheral blood cells by microarray, failed to demonstrate an association between IFN scores and the longitudinal risk of relapse.^{30 31} It is to be noted however that type I and type II IFNs largely overlap in the genes that they control, making it difficult to distinguish the signatures of IFN-gamma (IFN- γ) from IFN- α and IFN-beta (IFN- β). Indeed, the results from a modular repertoire analysis have emphasised that IFN signatures in SLE are not restricted to IFN- α , but also involve IFN- β and IFN- γ , thus underscoring the non-specific nature of IFN scores.⁶⁰ Therefore, in a disease like SLE in which IFN- α appears to be central in the pathogenesis, it is likely that clinical activity better correlates with the values of IFN- α serum levels, directly measured by a highly specific digital ELISA, than with the less specific expression of IGSs. Moreover, the IFN scores are likely to be rather poorly sensitive to changes in IFN- α serum concentrations and therefore of little use in monitoring the risk of relapse of disease. The results of our study suggest that the measurement of additional interferons, including IFN- β , IFN- γ and IFN- λ with the ultrasensitive digital immunoassay, might help to determine whether the expression of other IFN members also correlates with disease activity or specific characteristics of the disease.^{34 61 62} Nonetheless, our results corroborate those from an earlier study showing the usefulness of monitoring expression levels of certain IFN-regulated chemokines to predict future flares: serum levels of CXCL10, CCL2 and CCL19 chemokines were found to be linked with SLE activity and performed better than other laboratory tests to predict a flare over the following year.⁶³ Yet, these chemokines can be induced by other SLE-associated cytokines beyond IFN- α , such as IFN- γ and their monitoring remains difficult in routine practice. As reported by others, we did not find an association between the presence of anti-dsDNA Abs and the risk of flare. Not surprisingly, the duration of remission was significantly associated with a poor

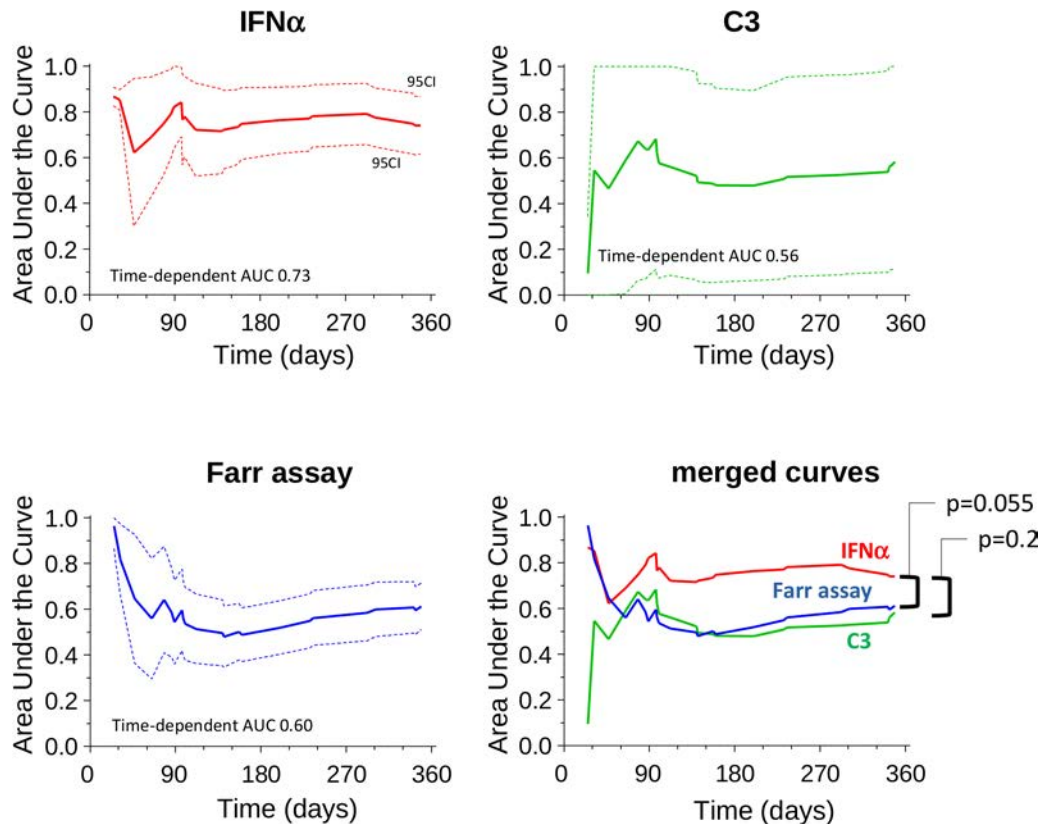


Figure 2 Cumulative time-dependent receiver operating characteristics (ROC) curves. Serum interferon-alpha (IFN- α) digital immunoassay, anti-double stranded DNA (anti-dsDNA) antibodies by Farr assay and C3 levels were assessed at baseline (day 0). Systemic lupus erythematosus (SLE) patients in remission were followed for 1 year. Lupus flares were defined using the Safety of Estrogens in Lupus Erythematosus: National Assessment version of the Systemic Lupus Erythematosus Disease Activity Index Flare Index. Patients who had a flare in any organ system were recorded. The diagnostic performances of the baseline serum-IFN- α digital immunoassay (red line), Farr assay (blue line) and C3 (green line) to predict SLE flare were investigated by computing cumulative time-dependent ROC curves, with lupus flares serving as the gold standard for those analyses. The dashed line represents the upper and the lower 95% CI. The cumulative time-dependent ROC area under the curve estimated to predict a flare are given and were compared based on Uno *et al.*⁷¹

risk of flare in the following year, thus identifying a subgroup of patients in prolonged remission with less risk of relapse and for whom clinical monitoring can probably be lightened.

The sustained presence of IFN- α in serum of SLE patients in remission may have pathological consequences by itself. IFN- α overexpression could be an explanation of chronic fatigue, depression and reduction of sleep secondary to the stimulation of the dopamine metabolism by IFN- α in the central neurological system.^{64–66} IFN- α plays also a prominent role in endothelial cell damage and up-regulation of the expression of scavenger receptors in monocyte and macrophages, leading to increased lipid uptake and foam cell formation, a process that may be at the origin of the accelerated atherosclerosis observed in SLE.^{67–69} These data suggest that for patients in clinical remission, return of serum IFN- α to normal values could become one of the objectives of the treatment.

Our study has some limitations. It unfortunately lacks data on patients' ethnicity, which is known to bias serum IFN- α levels.⁵⁵ We also used a definition of remission and LLDAS in the absence of PGA that has not been assessed in our cohort. However, other teams have already adapted the definition of remission and LLDAS arguing that in the SLE Response Index, the SLEDAI is the variable with the highest impact on the definition of response and that, even without PGA, a modified definition of remission or LLDAS is still entirely valid.^{48–70} Finally, serum IFN- α concentrations were not assessed during the longitudinal part of the

study and therefore information with respect to intra-individual variability of serum IFN- α levels over time is lacking. This aspect will be subject to further studies.

In conclusion, our data confirm that a large number of SLE patients in remission display elevated serum IFN- α concentrations, especially in the presence of anti-dsDNA and anti-ribonucleoprotein Abs (ie, anti-Ro/SSA 60, anti-RNP), as well as young age. This overexpression is an independent predictive biomarker of lupus flare in the following year. Including serum IFN- α measurements in the routine laboratory assessments in patients in remission could help clinicians to identify a subgroup of SLE patients clinically in remission but who still overexpress IFN- α and are at higher risk of relapse. These data suggest that the return of normalcy of serum IFN- α could become one of the objectives of the treatment. Our results are to be validated in other independent cohorts.

Author affiliations

¹Sorbonne Université, Assistance Publique–Hôpitaux de Paris, Groupement Hospitalier Pitié–Salpêtrière, French National Referral Center for Systemic Lupus Erythematosus, Antiphospholipid Antibody Syndrome and Other Autoimmune Disorders, Service de Médecine Interne 2, Institut E3M, Inserm UMRS, Centre d'Immunologie et des Maladies Infectieuses (CIMI-Paris), Paris, France
²Centre Hospitalier Universitaire de Dijon, Hôpital François-Mitterrand, service de médecine interne et maladies systémiques (médecine interne 2), Dijon, France

³Sorbonne Université, Inserm UMRS, Centre d'Immunologie et des Maladies Infectieuses (CIMI-Paris), Assistance Publique–Hôpitaux de Paris, Groupement Hospitalier Pitié–Salpêtrière, Département d'Immunologie, Paris, France
⁴Centre Hospitalier Universitaire de Dijon, Hôpital François-Mitterrand, service de médecine interne et maladies systémiques (médecine interne 2) et Centre d'Investigation Clinique, Inserm CIC 1432, Dijon, France
⁵Université de Paris, Assistance Publique–Hôpitaux de Paris, Hôpital Cochin, Service de Virologie, Paris, France

Correction notice This article has been corrected since it published Online First. Figure one has been corrected.

Acknowledgements We thank the patients, the healthy donors, the nurses and the Department of Internal Medicine two staff who participated in this study. We thank Professor Jean-Christophe Lega for its advices.

Contributors SM-M, AM, HD, KD, HY, GG, FR and ZA contributed to the conception and design of the study; SM-M, AM, KD, FC-A, JH, MH, MM, MP, FR and ZA were involved in the acquisition of data; SM-M, AM, HD, KD, HY, MPdC, GG, FR and ZA contributed to the analysis and interpretation of data. All authors contributed to drafting and/or revising the manuscript.

Funding Assistance Publique–Hôpitaux de Paris, Institut National de la Santé et de la Recherche Médicale (Inserm), Sorbonne Université, the French Arthritis Foundation, the Société Nationale Française de Médecine Interne and The Fondation pour la Recherche Médicale.

Competing interests None declared.

Patient consent for publication Informed consent was obtained from all the participants.

Ethics approval The local Ethics Committee of the Pitié–Salpêtrière Hospital approved this study.

Provenance and peer review Not commissioned; externally peer reviewed.

Data availability statement Data are available upon reasonable request.

ORCID iD

Alexis Mathian <http://orcid.org/0000-0002-7653-6528>

REFERENCES

- Lisnevskaja L, Murphy G, Isenberg D. Systemic lupus erythematosus. *The Lancet* 2014;384:1878–88.
- Bernatsky S, Boivin J-F, Joseph L, et al. Mortality in systemic lupus erythematosus. *Arthritis Rheum* 2006;54:2550–7.
- Tektonidou MG, Lewandowski LB, Hu J, et al. Survival in adults and children with systemic lupus erythematosus: a systematic review and Bayesian meta-analysis of studies from 1950 to 2016. *Ann Rheum Dis* 2017;76:2009–16.
- Nossent J, Kiss E, Rozman B, et al. Disease activity and damage accrual during the early disease course in a multinational inception cohort of patients with systemic lupus erythematosus. *Lupus* 2010;19:949–56.
- Zen M, Iaccarino L, Gatto M, et al. Prolonged remission in Caucasian patients with SLE: prevalence and outcomes. *Ann Rheum Dis* 2015;74:2117–22.
- van Vollenhoven RF, Mosca M, Bertias G, et al. Treat-to-target in systemic lupus erythematosus: recommendations from an international task force. *Ann Rheum Dis* 2014;73:958–67.
- van Vollenhoven R, Voskuyl A, Bertias G, et al. A framework for remission in SLE: consensus findings from a large international task force on definitions of remission in SLE (DORIS). *Ann Rheum Dis* 2017;76:554–61.
- Steiman AJ, Gladman DD, Ibañez D, et al. Prolonged serologically active clinically quiescent systemic lupus erythematosus: frequency and outcome. *J Rheumatol* 2010;37:1822–7.
- Gensous N, Marti A, Barnette T, et al. Predictive biological markers of systemic lupus erythematosus flares: a systematic literature review. *Arthritis Res Ther* 2017;19.
- Theofilopoulos AN, Baccala R, Beutler B, et al. Type I interferons (alpha/beta) in immunity and autoimmunity. *Annu Rev Immunol* 2005;23:307–35.
- Obermoser G, Pascual V. The interferon-alpha signature of systemic lupus erythematosus. *Lupus* 2010;19:1012–9.
- Rönblom L, Elkon KB. Cytokines as therapeutic targets in SLE. *Nat Rev Rheumatol* 2010;6:339–47.
- Niewold TB. Interferon alpha as a primary pathogenic factor in human lupus. *J Interferon Cytokine Res* 2011;31:887–92.
- Rönblom L, Alm GV, Eloranta M-L. The type I interferon system in the development of lupus. *Semin Immunol* 2011;23:113–21.
- Lauwerys BR, Ducreux J, Houssiau FA. Type I interferon blockade in systemic lupus erythematosus: where do we stand? *Rheumatology* 2014;53:1369–76.
- Kirou KA, Gkrouzman E. Anti-Interferon alpha treatment in SLE. *Clin Immunol* 2013;148:303–12.
- Bennett L, Palucka AK, Arce E, et al. Interferon and granulopoiesis signatures in systemic lupus erythematosus blood. *J Exp Med* 2003;197:711–23.
- Baechler EC, Batliwalla FM, Karypis G, et al. Interferon-Inducible gene expression signature in peripheral blood cells of patients with severe lupus. *Proc Natl Acad Sci U S A* 2003;100:2610–5.
- Hooks JJ, Moutsopoulos HM, Geis SA, et al. Immune interferon in the circulation of patients with autoimmune disease. *N Engl J Med Overseas Ed* 1979;301:5–8.
- Preble OT, Black RJ, Friedman RM, et al. Systemic lupus erythematosus: presence in human serum of an unusual acid-labile leukocyte interferon. *Science* 1982;216:429–31.
- Ytterberg SR, Schnitzer TJ. Serum interferon levels in patients with systemic lupus erythematosus. *Arthritis Rheum* 1982;25:401–6.
- Friedman RM, Preble O, Black R, et al. Interferon production in patients with systemic lupus erythematosus. *Arthritis Rheum* 1982;25:802–3.
- Shi SN, Feng SF, Wen YM, et al. Serum interferon in systemic lupus erythematosus. *Br J Dermatol* 1987;117:155–9.
- Kanayama Y, Kim T, Inariba H, et al. Possible involvement of interferon alfa in the pathogenesis of fever in systemic lupus erythematosus. *Ann Rheum Dis* 1989;48:861–3.
- Vallin H, Blomberg S, Alm GV, et al. Patients with systemic lupus erythematosus (SLE) have a circulating inducer of interferon-alpha (IFN-alpha) production acting on leucocytes resembling immature dendritic cells. *Clin Exp Immunol* 1999;115:196–202.
- Bengtsson AA, Sturfelt G, Truedsson L, et al. Activation of type I interferon system in systemic lupus erythematosus correlates with disease activity but not with antiretroviral antibodies. *Lupus* 2000;9:664–71.
- Dall'era MC, Cardarelli PM, Preston BT, et al. Type I interferon correlates with serological and clinical manifestations of SLE. *Ann Rheum Dis* 2005;64:1692–7.
- Kirou KA, Lee C, George S, et al. Activation of the interferon-alpha pathway identifies a subgroup of systemic lupus erythematosus patients with distinct serologic features and active disease. *Arthritis Rheum* 2005;52:1491–503.
- Feng X, Wu H, Grossman JM, et al. Association of increased interferon-inducible gene expression with disease activity and lupus nephritis in patients with systemic lupus erythematosus. *Arthritis Rheum* 2006;54:2951–62.
- Petri M, Singh S, Tesfayone H, et al. Longitudinal expression of type I interferon responsive genes in systemic lupus erythematosus. *Lupus* 2009;18:980–9.
- Landolt-Marticorena C, Bonventi G, Lubovich A, et al. Lack of association between the interferon-alpha signature and longitudinal changes in disease activity in systemic lupus erythematosus. *Ann Rheum Dis* 2009;68:1440–6.
- Rose T, Grützka A, Hirsland H, et al. IFN α and its response proteins, IP-10 and SIGLEC-1, are biomarkers of disease activity in systemic lupus erythematosus. *Ann Rheum Dis* 2013;72:1639–45.
- Rose T, Grützka A, Klotsche J, et al. Are interferon-related biomarkers advantageous for monitoring disease activity in systemic lupus erythematosus? A longitudinal benchmark study. *Rheumatology* 2017;56:1618–26.
- Oke V, Brauner S, Larsson A, et al. IFN- λ 1 with Th17 axis cytokines and IFN- α define different subsets in systemic lupus erythematosus (SLE). *Arthritis Res Ther* 2017;19.
- Mathian A, Mouries-Martin S, Dorgham K, et al. Monitoring disease activity in systemic lupus erythematosus with single-molecule array digital enzyme-linked immunosorbent assay quantification of serum interferon- α . *Arthritis Rheumatol* 2019;71:756–65.
- Yao Y, Higgs BW, Morehouse C, et al. Development of potential pharmacodynamic and diagnostic markers for Anti-IFN- α monoclonal antibody trials in systemic lupus erythematosus. *Hum Genomics Proteomics* 2009;1.
- Yao Y, Higgs BW, Richman L, et al. Use of type I interferon-inducible mRNAs as pharmacodynamic markers and potential diagnostic markers in trials with sifalimumab, an anti-IFN α antibody, in systemic lupus erythematosus. *Arthritis Res Ther* 2010;12(Suppl 1).
- Rissin DM, Kan CW, Campbell TG, et al. Single-molecule enzyme-linked immunosorbent assay detects serum proteins at subfemtomolar concentrations. *Nat Biotechnol* 2010;28:595–9.
- Wilson DH, Rissin DM, Kan CW, et al. The simoa HD-1 analyzer: a novel fully automated digital immunoassay analyzer with single-molecule sensitivity and multiplexing. *J Lab Autom* 2016;21:533–47.
- Rodero MP, Decalf J, Bondet V, et al. Detection of interferon alpha protein reveals differential levels and cellular sources in disease. *J Exp Med* 2017;214:1547–55.
- Hochberg MC. Updating the American College of rheumatology revised criteria for the classification of systemic lupus erythematosus. *Arthritis Rheum* 1997;40:1725.
- Bombardier C, Gladman DD, Urowitz MB, et al. Derivation of the SLEDAI. A disease activity index for lupus patients. The Committee on prognosis studies in SLE. *Arthritis Rheum* 1992;35:630–40.
- Buyon JP, Petri MA, Kim MY, et al. The effect of combined estrogen and progesterone hormone replacement therapy on disease activity in systemic lupus erythematosus: a randomized trial. *Ann Intern Med* 2005;142:953–62.
- Petri M, Kim MY, Kalunian KC, et al. Combined oral contraceptives in women with systemic lupus erythematosus. *N Engl J Med* 2005;353:2550–8.
- Gladman DD, Ibañez D, Urowitz MB. Systemic lupus erythematosus disease activity index 2000. *J Rheumatol* 2002;29:288–91.
- Weening JJ, D'Agati VD, Schwartz MM, et al. The classification of glomerulonephritis in systemic lupus erythematosus revisited. *Kidney Int* 2004;65:521–30.

- 47 Wilhelm TR, Magder LS, Petri M. Remission in systemic lupus erythematosus: durable remission is rare. *Ann Rheum Dis* 2017;76:547–53.
- 48 Ugarte-Gil MF, Wojdyla D, Pons-Estel GJ, et al. Remission and low disease activity status (LDAS) protect lupus patients from damage occurrence: data from a multiethnic, multinational Latin American lupus cohort (GLADEL). *Ann Rheum Dis* 2017;76:2071–4.
- 49 Steiman AJ, Urowitz MB, Ibañez D, et al. Prolonged clinical remission in patients with systemic lupus erythematosus. *J Rheumatol* 2014;41:1808–16.
- 50 Franklyn K, Lau CS, Navarra SV, et al. Definition and initial validation of a lupus low disease activity state (LLDAS). *Ann Rheum Dis* 2016;75:1615–21.
- 51 Steiman AJ, Gladman DD, Ibañez D, et al. Lack of interferon and proinflammatory Cytokines in serologically active clinically quiescent systemic lupus erythematosus. *J Rheumatol* 2015;42:2318–26.
- 52 Hua J, Kirou K, Lee C, et al. Functional assay of type I interferon in systemic lupus erythematosus plasma and association with anti-RNA binding protein autoantibodies. *Arthritis Rheum* 2006;54:1906–16.
- 53 Niewold TB, Hua J, Lehman TJA, et al. High serum IFN-alpha activity is a heritable risk factor for systemic lupus erythematosus. *Genes Immun* 2007;8:492–502.
- 54 Niewold TB, Kelly JA, Flesch MH, et al. Association of the IRF5 risk haplotype with high serum interferon-alpha activity in systemic lupus erythematosus patients. *Arthritis Rheum* 2008;58:2481–7.
- 55 Weckerle CE, Franek BS, Kelly JA, et al. Network analysis of associations between serum interferon- α activity, autoantibodies, and clinical features in systemic lupus erythematosus. *Arthritis Rheum* 2011;63:1044–53.
- 56 Ko K, Koldobskaya Y, Rosenzweig E, et al. Activation of the interferon pathway is dependent upon autoantibodies in African-American SLE patients, but not in European-American SLE patients. *Front Immunol* 2013;4:309.
- 57 Connelly KL, Kandane-Rathnayake R, Hoi A, et al. Association of MIF, but not type I interferon-induced chemokines, with increased disease activity in Asian patients with systemic lupus erythematosus. *Sci Rep* 2016;6:29909.
- 58 Banchereau J, Pascual V. Type I interferon in systemic lupus erythematosus and other autoimmune diseases. *Immunity* 2006;25:383–92.
- 59 Bengtsson AA, Rönblom L. Role of interferons in SLE. *Best Pract Res Clin Rheumatol* 2017;31:415–28.
- 60 Chiche L, Jourde-Chiche N, Whalen E, et al. Modular transcriptional repertoire analyses of adults with systemic lupus erythematosus reveal distinct type I and type II interferon signatures. *Arthritis Rheumatol* 2014;66:1583–95.
- 61 Munroe ME, Lu R, Zhao YD, et al. Altered type II interferon precedes autoantibody accrual and elevated type I interferon activity prior to systemic lupus erythematosus classification. *Ann Rheum Dis* 2016;75:2014–21.
- 62 Oke V, Gunnarsson I, Dorschner J, et al. High levels of circulating interferons type I, type II and type III associate with distinct clinical features of active systemic lupus erythematosus. *Arthritis Res Ther* 2019;21.
- 63 Bauer JW, Petri M, Batliwalla FM, et al. Interferon-regulated chemokines as biomarkers of systemic lupus erythematosus disease activity: a validation study. *Arthritis Rheum* 2009;60:3098–107.
- 64 Raison CL, Borisov AS, Broadwell SD, et al. Depression during PEGylated interferon-alpha plus ribavirin therapy: prevalence and prediction. *J Clin Psychiatry* 2005;66:41–8.
- 65 Raison CL, Rye DB, Woolwine BJ, et al. Chronic interferon-alpha administration disrupts sleep continuity and depth in patients with hepatitis C: association with fatigue, motor slowing, and increased evening cortisol. *Biol Psychiatry* 2010;68:942–9.
- 66 Felger JC, Li L, Marvar PJ, et al. Tyrosine metabolism during interferon-alpha administration: association with fatigue and CSF dopamine concentrations. *Brain Behav Immun* 2013;31:153–60.
- 67 Kaplan MJ, Salmon JE. How does interferon- α insult the vasculature? let me count the ways. *Arthritis Rheum* 2011;63:334–6.
- 68 Denny MF, Thacker S, Mehta H, et al. Interferon-Alpha promotes abnormal vasculogenesis in lupus: a potential pathway for premature atherosclerosis. *Blood* 2007;110:2907–15.
- 69 Li J, Fu Q, Cui H, et al. Interferon- α priming promotes lipid uptake and macrophage-derived foam cell formation: a novel link between interferon- α and atherosclerosis in lupus. *Arthritis Rheum* 2011;63:492–502.
- 70 Navarra SV, Guzmán RM, Gallacher AE, et al. Efficacy and safety of belimumab in patients with active systemic lupus erythematosus: a randomised, placebo-controlled, phase 3 trial. *The Lancet* 2011;377:721–31.
- 71 Uno H, Cai T, Pencina MJ, et al. On the C-statistics for evaluating overall adequacy of risk prediction procedures with censored survival data. *Stat Med* 2011;30:1105–17.

CLINICAL SCIENCE

A WHO Reference Reagent for lupus (anti-dsDNA) antibodies: international collaborative study to evaluate a candidate preparation

Bernard J Fox ¹, Jason Hockley,² Peter Rigsby,² Carl Dolman,¹ Pier Luigi Meroni,³ Johan Rönnelid ⁴

Handling editor Josef S Smolen

► Additional material is published online only. To view please visit the journal online (<http://dx.doi.org/10.1136/annrheumdis-2019-215845>).

¹Division of Biotherapeutics, National Institute for Biological Standards and Control, Potters Bar, UK

²Division of Analytical & Biological Sciences, National Institute for Biological Standards and Control, Potters Bar, UK

³Immunorheumatology Research Laboratory, Istituto Auxologico Italiano, Milanino, Italy

⁴Department of Immunology, Genetics and Pathology, Uppsala University, Uppsala, Sweden

Correspondence to

Bernard J Fox, Division of Biotherapeutics, National Institute for Biological Standards and Control, Potters Bar EN6 3QG, UK; bernard.fox@nibsc.org

Received 5 June 2019
Revised 24 July 2019
Accepted 25 July 2019
Published Online First 5 September 2019



© Author(s) (or their employer(s)) 2019. Re-use permitted under CC BY-NC. No commercial re-use. See rights and permissions. Published by BMJ.

To cite: Fox BJ, Hockley J, Rigsby P, et al. *Ann Rheum Dis* 2019;**78**:1677–1680.

ABSTRACT

Introduction Antibodies against double-stranded DNA (anti-dsDNA) are a specific biomarker for systemic lupus erythematosus (SLE). The first WHO International Standard (IS) for anti-dsDNA (established in 1985), which was used to assign units to diagnostic tests, was exhausted over a decade ago.

Methods Plasma from a patient with SLE was first evaluated in 42 European laboratories. The plasma was thereafter used by the National Institute for Biological Standards and Control to prepare a candidate WHO reference preparation for lupus (anti-dsDNA) antibodies. That preparation, coded 15/174, was subjected to an international collaborative study, including 36 laboratories from 17 countries.

Results The plasma mainly contained anti-dsDNA, other anti-chromatin antibodies and anti-Ku. The international collaborative study showed that the field would benefit from 15/174 as a common reference reagent improving differences in performance between different assays. However, no statistically meaningful overall potency or assay parallelism and commutability could be shown.

Conclusion 15/174 cannot be considered equivalent to the first IS for anti-dsDNA (Wo/80) and was established as a WHO Reference Reagent for lupus (oligo-specific) anti-dsDNA antibodies with a nominal value of 100 units/ampoule. This preparation is intended to be used to align test methods quantifying levels of anti-dsDNA antibodies.

INTRODUCTION

Antibodies against double-stranded DNA (anti-dsDNA) are biomarkers for systemic lupus erythematosus (SLE).^{1–2} As a result, measurement of anti-dsDNA is widely used as a diagnostic and prognostic test for SLE, and there are a range of kits and tests available.³

The first WHO International Standard (IS) for anti-dsDNA denoted Wo/80 was established in 1985 to assign International Units (IU) to diagnostic tests.⁴ Wo/80 was exhausted over a decade ago and requires replacement.

MATERIALS AND METHODS

Raw material characterisation by 42 European laboratories

Plasmapheresis plasma from a female patient with SLE diagnosed according to the 1997 classification criteria^{5–6} was evaluated blindly by 42 European laboratories in the European Consensus Finding

Key messages

What is already known about this subject?

- Autoantibody reference reagents improve comparability between laboratories using different assays.
- The First International Standard for anti-double-stranded DNA (dsDNA) is no longer available.

What does this study add?

- This report describes the validation of 15/174, a new WHO Reference Reagent for anti-dsDNA.

How might this impact on clinical practice or future developments?

- 15/174 can be used to align test methods quantifying anti-dsDNA.

Study Group on autoantibodies, a.k.a. the EULAR Autoantibody Study Group (https://www.eular.org/investigative_rheumatology_study_groups.cfm). Sampling was approved by the local Institutional Review Board, and the patient had given written informed consent.

Treatment of the candidate standard (15/174) and commutability samples (S1–S3)

2.4 L of plasma, evaluated above, and three patient samples with SLE coded 15/174, S1, S2 and S3, respectively, were thrombin-treated,⁷ clarified, 0.5 mL filled into glass ampoules and lyophilised at the National Institute for Biological Standards and Control (NIBSC).^{7,8} Accelerated stability studies on 15/174 showed a reduction in activity of 0.09%/year at –20°C (online supplementary table S1).⁹

Participants and assays used in the international collaborative study

In an international collaborative study (36 laboratories from 17 countries; online supplementary table S2), 15/174 was compared with local standards and S1–S3 to evaluate commutability. Each laboratory is referred to by an arbitrarily assigned number (1–36). For a laboratory performing more than one method, each method is treated as if performed by separate laboratories. A total of 26 different methods were used (table 1). Participants were requested to contribute full dilution comparisons and content estimates of 15/174 with local

Table 1 Laboratory methods

Laboratory code	Method
1,4,5,6,8,9,11,13,14,16,18,20,3,20.4,21,22,26,28,30,33,35,36	<i>Crithidia luciliae</i> immunofluorescence test (CLIFT)
Enzyme-linked immunosorbent assays (ELISA), chemiluminescence immunoassays (CIA) and fluoroenzyme immunoassays (FEIA)	
2,4,6,7,10,11,22,23,25,28,30	Phadia EliA FEIA
3	Eurodiagnostica ELISA
9.2	Trinity Biotech Captia ELISA
9.3	Immco ELISA
12,17, 33	Orgentec ELISA
13	Immunoconcepts ELISA
14	Phadia Varelisa ELISA
16	In-house fluoroimmuno assay (binding ratio)
18.1	Therdiag ELISA
19, 29.4	Innova Quanta Flash CIA 701178
20.1	Euroimmun anti-dsDNA ELISA
20.2	Euroimmun anti-dsDNA NcX ELISA
26	Orgentec Alegria ELISA
27.2	Bio-Rad Kallestad EIA
27.3, 34.1	Bio-Rad ELISA
29.1	Inova Quanta Lite ELISA 708510
29.2	Inova Quanta Lite HA ELISA 704615
29.3	Inova Quanta Lite dsDNAC ELISA 704650
31	Alpha Diagnostica ELISA
Addressable laser bead immunoassays	
1, 8, 27.1, 32, 35	Bioplex 2200
18.2	Therdiag FIDIS dsDNA MX005
18.3, 21	Therdiag FIDIS Connective Profile MX117
24	Zeus Athena
Farr immunoassays	
15	IBL International dsDNA Farr RIA
9.1, 34.2, 36	Trinity Farr RIA

standards, and assay replicate dilution series in duplicate. Three independent assays were requested, on separate days, with dilutions from freshly reconstituted ampoules.

Study participants were recruited separately to the European and international studies and both were run independently of each other.

Statistical analyses

At NIBSC, estimates in IU/mL at each sample dilution as reported by participants were used directly in the analysis to calculate the potency of 15/174 and S1–S3. A geometric mean (GM) of results corrected for dilution was calculated for each sample in each assay run, excluding dilutions not on a linear section. Parallelism^{10 11} with standards supplied with commercial assay kits was concluded if a linear relationship with a fitted slope between 0.80 and 1.25 was observed for log estimated concentration against log dilution. Outside this range, no calculated estimate relative to kit standard was reported. Where fewer than half of the assays performed by a laboratory gave valid results for a sample, no laboratory mean result is reported for that sample. GM was used to combine results from individual assays of 15/174 and S1–S3 for each laboratory.

Relative potencies for S1–S3 to 15/174 were calculated using a parallel-line model¹⁰ with log estimated concentration as assay

response. Where the ratio of fitted slopes for the samples was outside 0.80 to 1.25, no relative potency was reported.

Results from all valid assay runs were combined to generate unweighted GMs for each laboratory and used to calculate overall unweighted GM potency estimates. Variability between laboratories has been expressed using geometric coefficients of variation ($GCV = \{10^s - 1\} \times 100\%$ where s is the SD of the \log_{10} transformed estimates). Outliers were defined as results more than $(1.5 \times IQR)$ higher than the upper quartile or $(1.5 \times IQR)$ lower than the lower quartile.

Patient involvement

There was no patient involvement in this study.

RESULTS

Characterisation of the raw material by 42 European laboratories

Homogeneous antinuclear antibody or AC-1 pattern was detected in all laboratories (figure 1A).⁵ All laboratories reported anti-dsDNA (figure 1B). Anti-histone antibodies were reported from 24/25, anti-nucleosome in 18/19 and anti-Ku by 18/18 laboratories. Other autoantibodies were rarely reported (online supplementary table S3).

Assay validity for the international collaborative study

Individual assay estimates and instances of non-parallelism (with commercial kit standards or 15/174) are shown in online supplementary table S4 (calculated from reported results) and online supplementary table S5 (calculated relative to 15/174 by parallel line analysis). A summary of the extent of non-parallelism is shown in table 2.

Statistically valid estimates for 15/174 in terms of commercial kit standards or for S1–S3 in terms of kit standards or relative to 15/174 tended to be highly variable. Estimates of 15/174 against kit standards, for example, ranged from 56 IU/mL to a high of 847 IU/mL, although most estimates fell in the 100–200 IU/mL range (figure 1C). Similar variability for S1–S3 was also observed (online supplementary figure S1A–J). Endpoint titres for the *Crithidia luciliae* immunofluorescence test (CLIFT) were also highly variable, ranging from 50 to 1000 for 15/174 (figure 1D and online supplementary figure S2A–C).

Intra-laboratory and inter-laboratory variability for the international collaborative study

Calculation of estimates in terms of a common candidate standard invariably produced a reduction in %GCV, most noticeable for CLIFT results when comparing the estimates in terms of absolute titres with those obtained relative to 15/174 (table 2). For quantitative immunoassays, comparing estimates reported in terms of kit standards against those calculated in terms of 15/174 showed reductions in %GCV for S1&S2, but not S3, based on results after exclusion of outliers (table 2).

DISCUSSION

In all laboratories and test methods, 15/174 exhibited anti-dsDNA reactivity. In approximately half of the laboratories, the material behaved in an apparently similar way to local standards, and by inference to the first IS (Wo/80). In a similar number of laboratories, there was observable non-parallelism and no quantitative traceability to Wo/80 could be established. Moreover, across the entire study, it was not possible to establish commutability, as a consistent ranking order for the three patient samples was not obtained. In this context, it is important to mention that

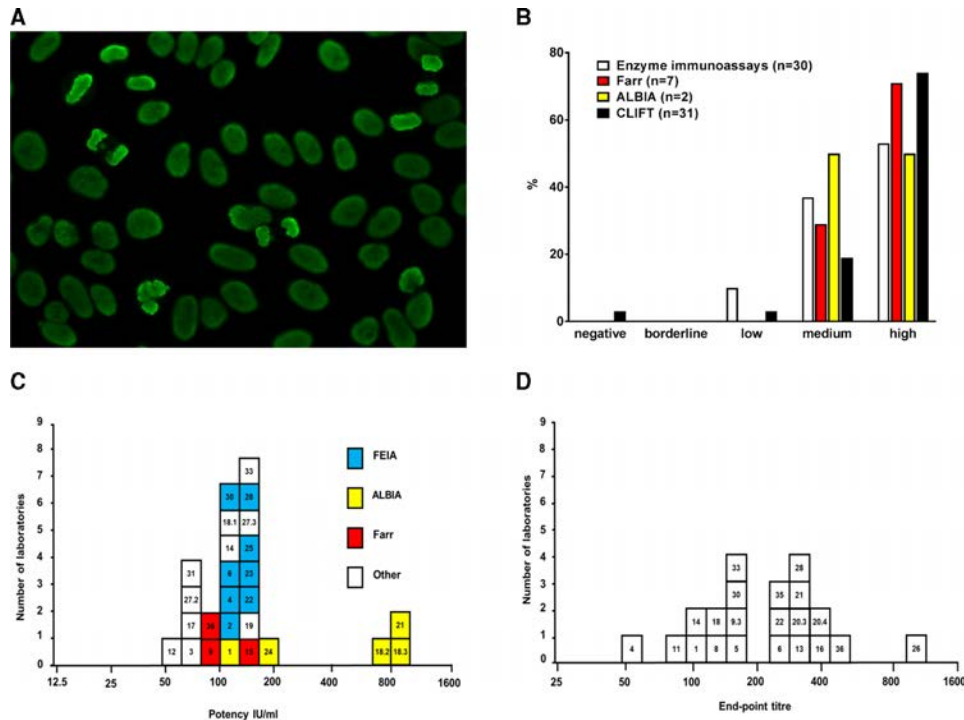


Figure 1 Evaluation of SLE plasma subjected to a European study and anti-dsDNA levels for 15/174 from an international collaborative study. (A) Indirect immune fluorescence staining on HEp-2 cells using the raw material used to prepare 15/174. Photo Dr Stephan Regenass. (B) Distribution of test results for anti-dsDNA levels among the 42 European laboratories in relation to laboratory techniques used. Some laboratories performed more than one type of analysis. Levels were evaluated as negative, borderline, low, medium or high by the laboratories performing the analysis. (C) GM potency estimates (IU/mL) of 15/174 from the international collaborative study for statistically valid immunoassay results. (D) GM endpoint titres of 15/174 from the international collaborative study for the CLIFT. The numbers in the squares denote the laboratory codes. Each square represents the unweighted GM from the laboratory. ALBIA, addressable laser bead immunoassay; CLIFT, *Crithidia luciliae* immunofluorescent test; dsDNA, double-stranded DNA; ELISA, enzyme-linked immunosorbent assay; FEIA, fluoroenzyme immunoassay; GM, geometric mean; SLE, systemic lupus erythematosus.

anti-dsDNA levels in S1 and S2 were very similar (table 2). It is also of interest to note that laboratories 18.2, 18.3 and 21 used high sensitivity addressable laser bead immunoassay kits and the

higher potency results reported were probably due to detection of low affinity antibodies (figure 1C). However, as shown in table 2, alignment to 15/174 reduced variability and minimised batch-to-batch variability of a test kit, rather than obtaining an absolute value, should be considered most important in clinical diagnosis and monitoring disease progression and/or the effect of treatment over time.

The range of available anti-dsDNA assays has increased considerably during the 30 years since Wo/80 was described.⁴ The 36 laboratories participating in the collaborative study for 15/174 all employed the assays routinely used to quantify anti-dsDNA in their routine clinical settings.⁸ This setting differs appreciably from the setup employed in the evaluation of Wo/80 when eight laboratories with special expertise in anti-dsDNA testing all obtained identical centrally prepared reagents and then performed CLIFT and Farr assays according to fixed protocols.

The first IS for anti-dsDNA, Wo/80, is exhausted and has been unavailable for more than a decade. Some methods included in this study can provide a historical linkage to the unitage assigned to Wo/80 through earlier calibration exercises, although many cannot, and none can be confirmed due to the unavailability of Wo/80. Thus, the typical replacement paradigm is not applicable when introducing 15/174. Another problem in exchanging autoantibody standards based on patient's samples is that the candidate replacement is unlikely to be identical to the original. This is particularly significant in the case of anti-dsDNA where autoantibody avidity might differ between patients. SLE sera also contain many different autoantibodies against a range of

Table 2 Overall results for the international collaborative study

Sample	Calculations from reported results	
	Relative to 15/174	
	Percentage of labs with non-parallelism (n)*	
15/174	33% (39)	n/a
S1	38% (26)	14% (28)
S2	17% (23)	14% (28)
S3	22% (23)	18% (28)
	CLIFT endpoint titre GM†/%GCV‡ (n)	
S1	268/153 (10)	1.14/47 (10)
S2	266/143 (9)	1.03/46 (9)
S3	1376/259 (10)	5.84/88 (10)
	Immunoassay potencies (IU/mL) GM†/%GCV‡ (n)	
S1	200/123 (30)	1.32/86 (24)
S2	199/184 (27)	1.57/42 (20)
S3	1406/93 (27)	8.2/117 (23)

* (n): number of laboratories (when a laboratory performed more than one method, each method is treated as if performed by separate laboratories).

†GM: geometric mean (overall combined unweighted GM estimates).

‡%GCV: geometric coefficient of variation between laboratories.

CLIFT, *Crithidia luciliae* immunofluorescent test.

antigens, including dsDNA. Although 15/174 cannot be regarded as monospecific for anti-dsDNA, we found the raw material for 15/174 to be rather specific for anti-chromatin reactivities and antibodies against Ku, a DNA binding protein.^{12–14} It is known that different methods may detect different populations of anti-dsDNA³ so there are discrepancies in antibody levels depending on the type of test when applied to individual patients.

Given the presumed different binding characteristics resulting in an apparent lack of comparability of this candidate standard with the previous IS, it is considered that it would be unwise to establish this material as a replacement IS, with a defined unitage in IU. Notwithstanding this discontinuity, this study showed that the field would benefit from the availability of an international reference reagent, and that the current situation, with manifest differences in performance between different assays supposedly measuring the same thing, would be improved. The preparation 15/174 is intended to be used to align test methods quantifying levels of anti-dsDNA to a common standard.

Based on the results presented here, the WHO Expert Committee on Biological Standardisation endorsed preparation 15/174 as the WHO Reference Reagent for lupus (oligo-specific) anti-dsDNA antibodies with a nominal potency of 100 units per ampoule.¹⁵ The name intentionally emphasises the non-continuity with the first IS for anti-dsDNA. The Reference Reagent 15/174 is available from the NIBSC (https://www.nibsc.org/products/brm_product_catalogue/detail_page.aspx?catid=15/174).

Acknowledgements We thank Drs Susan Thorpe and Adrian Bristow for their respective contributions in initiating the WHO project and drafting the WHO report. The study organisers thank Drs Charlotte Dahle and Anders Bengtsson for donating clinical samples, and Dr Stephan Regenass for the permission to use his photo of the HEp-2 staining. We thank the staff of the Centre for Biological Reference Materials, NIBSC, for lyophilising the candidate IS and clinical samples. We are extremely grateful to the study participants for contributing data. Johan Rönnelid is the chairman of the EULAR European Consensus Finding Study Group on Autoantibodies, performing the immunological characterisation of the raw material for 15/174. The preliminary results from this study were presented at the 3rd International Autoantibody Standardization (IAS) Workshop, Dresden.

Contributors PLM, JR, CD and BJF evaluated the suitability of the proposed candidate material; JH and PR carried out the statistical analysis; BJF and JR drafted the manuscript, which was critically reviewed and approved by all the authors.

Funding The authors have not declared a specific grant for this research from any funding agency in the public, commercial or not-for-profit sectors.

Competing interests None declared.

Patient consent for publication Not required.

Ethics approval Ethical approval was granted by the Institutional Review Board of the Istituto Auxologico Italiano (date: 1-02-2000).

Provenance and peer review Not commissioned; externally peer reviewed.

Data availability statement All data relevant to the study are included in the article or uploaded as supplementary information.

Open access This is an open access article distributed in accordance with the Creative Commons Attribution Non Commercial (CC BY-NC 4.0) license, which permits others to distribute, remix, adapt, build upon this work non-commercially, and license their derivative works on different terms, provided the original work is properly cited, appropriate credit is given, any changes made indicated, and the use is non-commercial. See: <http://creativecommons.org/licenses/by-nc/4.0/>.

ORCID iDs

Bernard J Fox <http://orcid.org/0000-0001-6362-5196>

Johan Rönnelid <http://orcid.org/0000-0003-1186-3226>

REFERENCES

- 1 Kavanaugh AF, Solomon DH. American College of rheumatology AD hoc Committee on immunologic testing G. guidelines for immunologic laboratory testing in the rheumatic diseases: anti-DNA antibody tests. *Arthritis Rheum* 2002;47:546–55.
- 2 Cozzani E, Drosera M, Gasparini G, et al. Serology of lupus erythematosus: correlation between immunopathological features and clinical aspects. *Autoimmune Dis* 2014;2014:1–13.
- 3 Pisetsky DS. Standardization of anti-DNA antibody assays. *Immunol Res* 2013;56:420–4.
- 4 Feltkamp TE, Kirkwood TB, Maini RN, et al. The first international standard for antibodies to double stranded DNA. *Ann Rheum Dis* 1988;47:740–6.
- 5 Chan EKL, Damoiseaux J, Carballo OG, et al. Report of the first international consensus on standardized Nomenclature of antinuclear antibody HEp-2 cell patterns 2014–2015. *Front Immunol* 2015;6:412.
- 6 Hochberg MC. Updating the American College of rheumatology revised criteria for the classification of systemic lupus erythematosus. *Arthritis Rheum* 1972;15:197.
- 7 Thorpe SJ, Heath A, Fox B, et al. The 3rd international standard for serum IgE: international collaborative study to evaluate a candidate preparation. *Clin Chem Lab Med* 2014;52:1283–9.
- 8 World Health O. Recommendations for the preparation, characterization and establishment of international and other biological reference standards (revised 2004). *World Health Organ Tech Rep Ser* 2006;932:1–137.
- 9 Kirkwood TB. Predicting the stability of biological standards and products. *Biometrics* 1977;33:736–42.
- 10 Council of Europe. CombiStats. Available: www.edqm.eu/en/combistats
- 11 Finney DJ. *Statistical method in biological assay*. 3th edn. London: Griffin, 1978.
- 12 Mimori T, Hardin JA. Mechanism of interaction between Ku protein and DNA. *J Biol Chem* 1986;261:10375–9.
- 13 Suwa A, Hirakata M, Takeda Y, et al. Dna-Dependent protein kinase (Ku protein-p350 complex) assembles on double-stranded DNA. *Proc Natl Acad Sci U S A* 1994;91:6904–8.
- 14 Mimori T, Hardin JA, Steitz JA. Characterization of the DNA-binding protein antigen Ku recognized by autoantibodies from patients with rheumatic disorders. *J Biol Chem* 1986;261:2274–8.
- 15 World Health O. *Who expert Committee on biological standardization: sixty-eighth report*. World Health Organ Tech Rep Ser, 2018;1011:48–9.

CLINICAL SCIENCE

Revised European Scleroderma Trials and Research Group Activity Index is the best predictor of short-term severity accrual

Serena Fasano ¹, Antonella Riccardi,¹ Valentina Messiniti,¹ Paola Caramaschi,² Edoardo Rosato ³, Britta Maurer ⁴, Vanessa Smith,⁵ Elise Siegert,⁶ Ellen De Langhe,⁷ Valeria Riccieri,⁸ Paolo Airó,⁹ Carina Mihai,¹⁰ Jerome Avouac,¹¹ Elisabetta Zanatta,¹² Ulrich A Walker,¹³ Florenzo Iannone ¹⁴, Paloma García De la Peña Lefebvre,¹⁵ Jörg H W Distler ¹⁶, Alessandra Vacca,¹⁷ Oliver Distler ¹⁸, Otylia Kowal-Bielecka,¹⁹ Yannick Allanore,¹¹ Gabriele Valentini ¹

Handling editor Josef S Smolen

► Additional material is published online only. To view please visit the journal online (<http://dx.doi.org/10.1136/annrheumdis-2019-215787>).

For numbered affiliations see end of article.

Correspondence to

Dr Serena Fasano, Università degli Studi della Campania Luigi Vanvitelli, Napoli 80131, Italy; serena.fasano@unicampania.it

Received 28 May 2019
Revised 12 July 2019
Accepted 19 July 2019
Published Online First
17 August 2019

ABSTRACT

Background The European Scleroderma Trials and Research Group (EUSTAR) recently developed a preliminarily revised activity index (AI) that performed better than the European Scleroderma Study Group Activity Index (EScSG-AI) in systemic sclerosis (SSc). **Objective** To assess the predictive value for short-term disease severity accrual of the EUSTAR-AI, as compared with those of the EScSG-AI and of known adverse prognostic factors.

Methods Patients with SSc from the EUSTAR database with a disease duration from the onset of the first non-Raynaud sign/symptom ≤ 5 years and a baseline visit between 2003 and 2014 were first extracted. To capture the disease activity variations over time, EUSTAR-AI and EScSG-AI adjusted means were calculated. The primary outcome was disease progression defined as a $\Delta \geq 1$ in the Medsger's severity score and in distinct items at the 2-year follow-up visit. Logistic regression analysis was carried out to identify predictive factors.

Results 549 patients were enrolled. At multivariate analysis, the EUSTAR-AI adjusted mean was the only predictor of any severity accrual and of that of lung and heart, skin and peripheral vascular disease over 2 years.

Conclusion The adjusted mean EUSTAR-AI has the best predictive value for disease progression and development of severe organ involvement over time in SSc.

INTRODUCTION

Systemic sclerosis (SSc) is a multisystem autoimmune disease with the highest case-specific mortality among rheumatic diseases.^{1,2} Predicting outcome and tailoring treatment and surveillance in patients with a potentially unfavourable evolution may improve quality of life and survival.³ In that regard, a number of adverse prognostic features as assessed at presentation and predictive of shortened survival have been identified.⁴⁻⁹ However, predicting severity accrual in the short term is still a poorly accomplished task. Recently, the Canadian Scleroderma Study Group has pointed out a role of the adjusted mean European Scleroderma Study Group Activity Index (EScSG-AI)¹⁰ in predicting internal organ involvement and disease progression in an early scleroderma cohort.¹¹ Because of

Key messages

What is already known about this subject?

- The European Scleroderma Trial and Research (EUSTAR) group task force recently succeeded in constructing a revised activity index (AI).
- The predictive value of EUSTAR-AI for disease severity accrual has not been evaluated.

What does this study add?

- The adjusted mean EUSTAR-AI reliably captured all variations in disease activity during the observation period in patients with SSc and has the best predictive value for short-term disease progression and development of severe internal organ involvement over time.

How might this impact on clinical practice?

- Identifying patients at risk has important implications for clinical care, because it helps the clinician in managing patients with SSc, monitoring disease state with rapid adjustments in treatment to prevent irreversible organ damage.

the limitation of the EScSG-AI (ie, high number of missing values and a cohort with a long-standing disease), in 2017, a European Scleroderma Trial and Research (EUSTAR) group task force succeeded in constructing a revised AI that performed better than the EScSG-AI in identifying patients with active disease.¹²

This study aimed to test the performance of the adjusted mean European Scleroderma Trial and Research Activity Index (EUSTAR-AI) in predicting patient disease course as compared with the EScSG-AI and to investigate the role on short-term disease progression of other prognostic factors known to affect survival.

PATIENTS AND METHODS

Study design

The study was based on the analysis of the EUSTAR database in which clinical information on patient visits are recorded prospectively using standardised



© Author(s) (or their employer(s)) 2019. No commercial re-use. See rights and permissions. Published by BMJ.

To cite: Fasano S, Riccardi A, Messiniti V, et al. *Ann Rheum Dis* 2019;**78**:1681–1685.

data collection forms. The database structure has been described previously.¹³ The whole EUSTAR data set, consisting of 14 755 patients at the time of the data export (30 October 2017), was considered. Predictors with $\geq 50\%$ missing values were not considered for inclusion (online supplementary table S1).

Patients classified with SSc according to American College of Rheumatology/European League Against Rheumatism classification criteria,¹⁴ with a disease duration from the onset of the first non-Raynaud sign/symptom ≤ 5 years at first visit recorded and a baseline visit between 2003 and 2014 were first extracted. Patients were considered for the study if they presented the following predefined features: (1) availability of all the items included in the EScSG-AI and in the EUSTAR-AI at baseline and yearly for at least two consecutive years (within the first 2 years of observation and with a time frame between consecutive visits not exceeding 18 months); (2) availability of items included in the Medsger's severity scale¹⁵ at entry and after 2 years of observation and (3) availability of vital status at the last observation.

Potentially predictive features

Disease activity

Disease activity was measured by EUSTAR-AI and EScSG-AI. To capture the disease activity variations over time, we calculated the EUSTAR-AI and EScSG-AI adjusted mean (see online supplementary text).

Features predictive of shortened survival

We also investigated the predictive role in the short term of variables detectable at admission and reported to be predictive of the subsequent 5-year mortality⁴⁻⁹: age at disease onset, male sex, erythrocyte sedimentation rate (ESR) >25 mm/hour, haemoglobin <12 g/L, anti-RNA polymerase III antibody positivity, tendon friction rubs, the presence of proteinuria (positive level of urine protein more than trace), baseline severity in any major organ/system.

Primary and secondary outcomes

Given the current lack of a validated SSc damage index,¹⁶ we selected as primary outcome the disease severity progression using the Medsger's severity scale.¹⁵ In particular, disease progression was defined as accrual of a new ($\Delta \geq 1$) severity score at the 2-year follow-up visit compared with the initial visit. The secondary outcome was the progression in any organ/system domains of the Medsger's severity scale analysed separately, defined as an increase of at least one point in severity grade ($\Delta \geq 1$).

Statistical analysis

Continuous variables are presented as the mean \pm SD if normally distributed or as median and quartiles if distribution was skewed. Comparisons were performed using the χ^2 or Fisher's test for categorical variables and using the Student's test for continuous variables, as appropriate. To explore specific determinants of disease progression, logistic regression analysis was carried out. Analyses were performed with Medcalc software, V.15.4.

RESULTS

Patients

A total of 549 patients with SSc were included in the analysis. The main epidemiological, serological and clinical features of the cohort at baseline are listed in table 1. There were 445 (81%) women; mean age (SD) at entry was 51.9 (± 13.6). One hundred and seventy-nine (32.6%) patients were classified as

Table 1 Epidemiological, serological and clinical features at baseline (n=549)

Sex, F/M	445/104
Age at entry in the registry, years, mean (SD)	51.9 (± 13.6)
Age at Raynaud's onset, years, mean (SD)	46.5 (± 14.3)
Age at first non-Raynaud's feature, years, mean (SD)	49.8 (± 13.7)
ANA positive (n, %)	529 (96.3)
Anti-Scl-70 positive (n, %)	217 (39.5)
Anticentromere positive (n, %)	178 (32.4)
Anti-PmScl positive (n, %)	10 (1.8)
Anti-U1RNP positive (n, %)	10 (1.8)
Anti-RNA polymerase III positive (n, %)	10 (1.8)
Limited SSc (n, %)	370 (67.3)
Diffuse SSc (n, %)	179 (32.6)

ANA, antinuclear antibody; SSc, systemic sclerosis.

having diffuse SSc. During the observation period, most patients (55.2%) developed a progression of organ involvement, that is, $\Delta \geq 1$ in any of the evaluated organ systems according to Medsger's severity scale, along the 2-year follow-up visit.

Univariate and multivariate logistic regression

At univariate analysis (online supplementary table S2), the adjusted mean EUSTAR-AI (OR 1.43, $p < 0.0001$), the adjusted mean EScSG-AI (OR 1.41, $p < 0.0001$), diffuse subset (OR 1.46, $p = 0.040$), anti-Scl-70 antibodies positivity (OR 1.72, $p = 0.003$), ESR >25 mm/hour at baseline (OR 1.58, $p = 0.04$), age at disease onset (OR 1.01, $p = 0.01$) predicted any increase in severity progression. No predictive role emerged for other baseline variables, that is, male gender, tendon friction rubs, anti-RNA polymerase III antibodies positivity, the presence of urine proteins, haemoglobin <12 g/L and general, gut, peripheral vascular, muscle, joint/tendon, skin, lung, heart and kidney involvement. At multivariate analysis (table 2), the adjusted mean EUSTAR-AI (OR 1.43; 95% CI 1.23 to 1.66) was the only covariate retained in the model for the prediction of disease progression. Moreover, the adjusted mean EUSTAR-AI predicted any increase ≥ 1 in the severity score of skin, heart, lung and peripheral vascular system. However, activity indices were not able to predict general, kidney, muscle, gastrointestinal tract, joint/tendon severity accrual (table 2 and online supplementary table S2).

A subanalysis confirmed that the adjusted mean EUSTAR-AI was the best predictor of severity progression at 2-year follow-up visit in both diffuse and limited subsets (OR 1.28; 95% CI 1.05 to 1.57, $p = 0.01$ and OR 1.62; 95% CI 1.30 to 2.01, $p < 0.0001$, respectively).

DISCUSSION

SSc is a challenging disease to manage with significant damage accrual that occurs early in the disease course and results in end-organ dysfunction and high mortality.^{17 18}

A previous study has demonstrated that disease activity quantified by the adjusted mean EScSG-AI predicted the risk of disease progression in an early diffuse cutaneous SSc cohort over 3 years.¹¹ In particular, in multivariate analysis, the adjusted mean EScSG-AI was the best predictor of progression of lung disease but did not play a significant role in the prediction of heart and renal disease severity. In the current study, we tried to assess the predictive validity of the 2017 EUSTAR-AI and to compare it with EScSG-AI. We demonstrated that the adjusted mean EUSTAR-AI had better predictive value for damage accrual

Table 2 Multivariate logistic regression analysis for organ severity accrual

Features	OR (95% CI)	Organ/system severity accrual	P value	z score
Adjusted mean EUSTAR-AI	1.43 (1.23 to 1.66)	Δ Medsger's severity score ≥ 1	0.002	9.49
Adjusted mean ESScG-AI	0.98(0.75 to 1.28)		0.92	0.007
Age	1.00 (0.99 to1.02)		0.32	0.95
ESR >25	1.01 (0.59 to 1.73)		0.95	0.003
Anti-Scl-70 Ab	1.51 (0.94 to2.44)		0.08	2.96
Subset diffuse	0.80 (0.48 to 1.31)		0.38	0.76
Adjusted mean EUSTAR-AI	1.23 (1.06 to 1.42)	Δ Lung severity score ≥ 1	0.006	7.45
Adjusted mean ESScG-AI	1.09 (0.83 to 1.43)		0.11	0.44
Basal lung severity	0.57 (0.35 to 0.92)		0.01	0,006
Anti-Scl-70 Ab	1.27(0.75 to 2.15)		0.35	0.84
Subset diffuse	0.79 (0.46 to 1.36)		0.40	0.69
Adjusted mean EUSTAR-AI	1.96(1.10 to 3.50)	Δ Heart severity score ≥ 1	0.02	5.20
Adjusted mean ESScG-AI	0.52 (0.24 to 1.12)		0.09	2.75
Age	1.02 (0.98 to 1.07)		0.26	1.24
RNA polymerase III Ab	5.56 (0.65 to 6.98)		0.11	2.48
Subset diffuse	0.24 (0.04 to 1.42)		0.11	2.45
Basal vascular severity	1.08 (0.28 to 4.16)		0.90	0.01
Basal joint severity	2.71 (0.69 to 10.70)		0.15	2.04
Basal lung severity	1.04 (0.26 to 4.01)		0.95	3
Adjusted mean EUSTAR-AI	1.48 (1.21to1.82)	Δ Skin severity score ≥ 1	0,0002	14.29
Age	0.97 (0.95 to 0.99)		0.003	4.40
Baseline skin severity	0.21 (0.09 to 0.47)		0.0002	14.27
Adjusted mean ESScG-AI	1.34 (0.90 to 2.00)		0.13	2.17
Anti-Scl-70 Ab	2.16 (0.85 to 5.50)		0.10	2.65
Adjusted mean EUSTAR-AI	1.31 (1.13 to 1.52)	Δ Peripheral vascular severity score ≥ 1	0.0002	5.18
Adjusted mean ESScG-AI	1.02 (0.76 to 1.37)		0.87	0.02
Basal lung severity	1.94 (1.03 to 3.64)		0.03	4.26
Basal vascular severity	0.23 (0.13 to 0.39)		<0.0001	29.61
Anti-Scl-70 Ab	1.46 (0.75 to 2.48)		0.26	1.24
Subset diffuse	1.36 (0.74 to 2.48)		0.30	1.02
Adjusted mean EUSTAR-AI	0.86 (0.45 to 1.64)	Δ Muscle severity score ≥ 1	0.66	0.19
Adjusted mean ESScG-AI	1.49 (0.66 to 3.34)		0.33	0.94
Subset diffuse	0.69 (0.12 to 3.81)		0.67	0.17
RNA polymerase III Ab	8.32 (1.21 to 6.88)		0.03	4.66
Adjusted mean EUSTAR-AI	1.21 (0.15 to 9.32)	Δ Kidney severity score ≥ 1	0.85	0.03
Adjusted mean ESScG-AI	1.24 (0.19 to 7.89)		0.59	0.28
Adjusted mean EUSTAR-AI	1.20 (0.40 to 3.53)	Δ GI tract severity score ≥ 1	0.73	0.11
Adjusted mean ESScG-AI	1.37 (0.32 to 5.76)		0.66	0.18

ESR, erythrocyte sedimentation rate; ESScG-AI, European Scleroderma Study Group Activity Index; EUSTAR-AI, European Scleroderma Trials and Research Group Activity Index; GI, gastrointestinal.

and development of severe internal organ involvement over 2 years as compared with ESScG-AI. In particular, the adjusted mean EUSTAR-AI predicted the development of a higher total severity score and in the following distinct severity domains: heart, peripheral vascular, skin and lung. A protective role of baseline skin severity grade ≥ 1 was pointed out but is likely to depend on the natural disease course characterised by skin sclerosis reaching its maximal grade in the early 2–3 years.¹⁹

Nevskaya *et al*¹¹ did not investigate the role on short-time severity accrual of baseline features demonstrated to predict mortality in SSc, as ESR >25 mm/hour, tendon friction rubs, anti-RNA polymerase III antibodies positivity, the presence of urine proteins, haemoglobin <12 g/L, diffuse subset and internal organ involvement.^{4–9} We failed to point out any role of these features. These data suggest that variables predicting survival in

the medium - long term differ from those associated with disease deterioration in the short period.

Our study has some limitations. First, we were not able to assess damage accrual and we measured disease severity as primary outcome, which might reflect both activity and damage. Second, data were obtained from scleroderma tertiary centres, meaning that we might fail to include patients with milder disease who are not referred. Nevertheless, a EUSTAR-AI predictive role of organ/system severity accrual in the short term has emerged, indicating that measuring this parameter can help the clinician in adjusting treatment in such time frame.

Author affiliations

¹Department of Precision Medicine, Section of Rheumatology, University of Campania Luigi Vanvitelli, Naples, Italy

²Department of Rheumatology, University of Verona, Verona, Italy

³Dipartimento di Medicina Traslationale e di Precisione, Sapienza University of Rome, Roma, Italy

⁴Department of Rheumatology, University Hospital Zurich, Zurich, Switzerland

⁵Department of Rheumatology, University Hospital Ghent, Ghent, Belgium

⁶Department of Rheumatology, Charit University Hospital, Berlin, Germany

⁷Department of Development and Regeneration, Laboratory of Tissue Homeostasis and Disease, Skeletal Biology and Engineering Research Center, KU Leuven, Leuven, Belgium

⁸Clinical Medicine and Therapy, Sapienza University of Rome, Rome, Italy

⁹Rheumatology and Clinical Immunology Department, Spedali Civili di Brescia, Brescia, Italy

¹⁰Department of Rheumatology, Carol Davila University of Medicine and Pharmacy, Bucarest, Romania

¹¹Department of Rheumatology, Paris Descartes University, Rheumatology A and INSER U1016, Cochin Hospital, Paris, France

¹²Dipartimento di Medicina, DIMED, Università degli Studi di Padova, Padova, Italy

¹³Department of Rheumatology, Basel University, Basel, Switzerland

¹⁴Department of Rheumatology, University of Bari, Bari, Italy

¹⁵Department of Rheumatology, Ramon y Cajal University Hospital, Madrid, Spain

¹⁶Department of Internal Medicine III, University of Erlangen, Erlangen, Germany

¹⁷Chair and Rheumatology Unit, University Clinic AOU Cagliari, Monserrato, Italy

¹⁸Department of Rheumatology, University Hospital Zurich, Zurich, Switzerland

¹⁹Department of Rheumatology and Internal Medicine, Medical University of Bialystok, Bialystok, Poland

Acknowledgements EUSTAR collaborators: Marco Matucci-Cerinic and Silvia Bellando Randone, University of Florence, Italy; Veronika Jaeger and Bettina Bannert, Department of Rheumatology, University Hospital Basel, Basel, Switzerland; Fabio Cacciapaglia, Rheumatology Unit-DiMIMP School of Medicine, University of Bari, Italy; Suzana Jordan, Rucsandra Dobrota and Mike Becker, Department of Rheumatology, University Hospital Zürich, Switzerland; Radim Becvarare and Michal Tomčík, 1st Medical School, Charles University, Prague, Czech Republic; Ewa Gindzienska-Sieskiewicz and Katarzyna Karaszewska, Department of Rheumatology and Internal Diseases, Medical University of Bialystok, Poland; Maurizio Cutolo, Carmen Pizzorni, Sabrina Paolino, Alberto Sulli, Barbara Ruaro and Elisa Alessandri, University of Genova, Italy; Veronica Giacco and Rosaria Itrace, Rheumatology Section, Department of Precision Medicine, University of Campania L. Vanvitelli, Naples, Italy; Claudia Kedor, Vincent Casteleyn, Julia Hilger and Jakob Hoepfner, Department of Rheumatology, Charité University Hospital, Berlin, Germany; Simona Rednic, Iulia Szabo and Ana Petcu, University of Medicine and Pharmacy, 'Iuliu Hatieganu' Cluj, Cluj-napoca, Romania; Frantz Camelia and Carole Desbas, Rheumatology, University Cochin Hospital, Paris, France; P Vlachoyiannopoulos, Department of Pathophysiology Medical School, National University of Athens, Athens, Greece; C Montecucco, Roberto Caporali and Lorenzo Cavagna, IRCCS Policlinico s Matteo, Pavia, Italy; Jiri Stork, Department of Dermatology, the First Faculty of Medicine, Charles University, Prague, Czech Republic; Murat Inanc, Division of Rheumatology, Department of Internal Medicine, Istanbul Medical Faculty, Istanbul, Turkey; Patricia e Carreira and Beatriz E Joven, Hospital 12 de Octubre, Madrid, Spain; Srdan Novak and Felina Anic, KBC Rijeka, Croatia; Iásló Cziráj, Cecília Varju and Tunde Minier, University of Pécs, Hungary; Carlo Chizzolini and Daniela Allai, University Hospital Geneva, Switzerland; Eugene J Kucharz, Anna Kotulska, Magdalena Kopec-Medrek and Malgorzata Widuchowska, Medical University of Silesia, Katowice, Poland; Andrea Doria, Rheumatology Unit, Department of Medicine, Padova University Hospital, Padova, Italy; Alenka Sipek Dolnicar, Department of Rheumatology, University Medical Center Ljubljana, Slovenia; Bernard Coleiro, 'Stella Maris', Balzan, Malta; Armando Gabrielli, Lucia Manfredi, Devis Benfaremo and Alessia Ferrarini, Istituto Di Clinica Medica Generale, Ematologia Ed Immunologia Clinica, Università Politecnica Delle Marche Polo Didattico, University of Ancona, Italy; Dominique Farge Bancel, Adrian Hij and Pauline Lansiaux, Hôpital Saint-Louis, Paris, France; Maria Grazia Lazzaroni, Spedali Civili di Brescia, Servizio di Reumatologia Allergologia e Immunologia Clinica, Brescia, Italy; Roger Hesselstrand, Dirk Wuttge and Kristofer Andréasson, Lund University Hospital, Sweden; Duska Martinovic, Ivona Bozic, Mislav Radic, Clinical Hospital of Split, Croatia; Alexandra Balbir-Gurman and Yolanda Braun-Moscovici, B. Shine Rheumatology Institute, Rambam Health Care Campus, Haifa, Israel; Andrea Lo Monaco and Federica Furini, Department of Clinical and Experimental Medicine, Rheumatology Unit, University of Ferrara, Italy; Nicolas Hunzelmann and Pia Moinzadeh, Universitätsklinik Köln, Germany; Raffaele Pellerito, Ospedale Mauriziano, Torino, Italy; Dr Cristian Caimm and Eugenia Bertoldo, Reumatologia-Medicina Interna Università degli Studi di Verona, Italy; Dr Jadranka Morovic-Vergle and Ivana Melanie Culo, Division of Clinical Immunology and Rheumatology, Department of Internal Medicine, Dubrava University Hospital, Zagreb, Croatia; Christopher Denton, Royal Free And University College London Medical School, London, UK; Nemanja Damjanov, Institute Of Rheumatology Belgrade, Serbia and Montenegro; Jörg Henes and Ann-Christian Pecher, Medizinische Universitätsklinik Abt. II, Tübingen, Germany; Vera Ortiz Santamaria, Rheumatology Granollers General Hospital, Barcelona, Spain; Stefan Heitmann, Medeleine Codagnone and Johannes Pflugfelder, Marienhospital Stuttgart, Germany; Dorota Krasowska and Malgorzata Michalska-Jakubus, Department of Dermatology, Venereology and Pediatric Dermatology, Medical University of Lublin, Poland; Paul Hasler and Samuel Kretzschmar, Kantonsspital Aarau, Rheumaklinik und Institut für Physikalische Medizin und Rehabilitation Kantonsspital Aarau, Switzerland; Michaela Kohm, Klinikum der Johann Wolfgang Goethe Universität Medizinische Klinik III, Frankfurt am Main, Germany; Ivan Foeldvari Matthias Seidel and Nicola Helmus, Medizinische Universitäts-Poliklinik, Bonn, Germany; Gianluigi Bajocchi, Arcispedale Santa Maria Nuova Dipartimento Area Medica I, U.O. di Reumatologia, Reggio Emilia, Italy; Dr Maria João Salvador and José Antonio Pereira Da Silva, Da Universidade, Coimbra, Portugal; Bojana Stamenkovic and Aleksandra Stankovic, Institute For Prevention, Treatment and Rehabilitation Rheumatic and Cardiovascular Disease niska Banja, Serbia and Montenegro; Carlo Francesco Selmi, Maria De Santis and Angela Ceribelli, University of Milan, Italy; Mohammed Tikly, Chris Hani Baragwanath Hospital and University of the Witwatersrand, Johannesburg, South Africa; Lidia P Ananieva, Ludmila Garzanova, Olga Koneva and Maya Starovoytova, Vanasonova Institute of Rheumatology, Moscow, Russia; Ariane Herrick, Hope/Hospital University of Manchester, Rheumatic Diseases Centre, Clinical Sciences Building, Scott Lane, Salford, UK; Ulf Müller-ladner, Kerckhoff Clinic Bad nauheim, Germany; Francesco Puppo, Simone Negri and Giuseppe Murdaca, Università di Genova, Italy; Merete Engelhart, University Hospital of Gentofte, Hellerup, Denmark; Gabriela Szücs and Szilvia Szamosi, University of Debrecen, Hungary; Carlos de la Puente, Cristina Sobrino Grande and Maria Jesus Garcia Villanueva, Hospital Ramon Y Cajal, Madrid, Spain; Øyvind Midtvedt and Anna-Maria Hoffmann-Vold, Rikshospitalet University Hospital, Oslo, Norway; Eric Hachulla, David Launay and Vincent Sobanski, Hôpital Claude Huriez, Lille, France; Massimiliano Vasile and Katia Stefanoni, 'sapienza' Università di Roma, Italy; Ruxandra Maria Ionescu, Daniela Opris and Laura Groseanu, St. Maria Hospital, Carol Davila University of Medicine and Pharmacy, Bucharest, Romania; Ami Sha and Adrienne Woods, Johns Hopkins School of Medicine, Baltimore, USA; Ana Maria Gheorghiu and Mihai Bojinca, Ion Cantacuzino Clinical Hospital, Bucharest, Romania; Cord Sunderkötter and Jan Ehrchen, University of Münster, Germany; Francesca Ingegnoli, Istituto Gaetano Pini, University of Milano, Italy; Luc Mouthon, Bertrand Dunogue, Benjamin Chaigne and Paul Legendre, Hôpital Cochin, Paris, France; Vanessa Smith, University of Ghent, Belgium; Francesco Paolo Cantatore, Ada Corrado, U.O. Reumatologia-Università degli studi di Foggia, Ospedale 'Col. D'Avanzo', Foggia, Italy; Susanne Ullman, University Hospital of Copenhagen, Denmark; Carlos Alberto von Mühlen Rheuma Clinic, Porto Alegre, Brazil; Maria Rosa Pozzi, Ospedale san Gerardo, Monza, Italy; Kilian Eyerich and Felix Lauffer, TU Munich, Germany; Piotr Wiland, Magdalena szmyrka-Kaczmarek, Renata sokolik, Ewa Morgiel and Marta Madej, Wrocław University of Medicine, Poland; Marie Vanthuyne and Houssiau Frédéric, Université Catholique de Louvain Bruxelles, Belgium; Juan Jose Alegre-sancho, Hospital Universitario Dr Peset, Valencia, Spain; Martin Aringer and Claudia Günther, University Medical Center, Carl Gustav Carus, Technical University of Dresden, Germany; Rene Westhovens and Jan Lenaerts, University Hospital Leuven, Skeletal Biology and Engineering Research Center, Leuven, Belgium; Branimir Anic, Marko Baresic and Miroslav Mayer, University Hospital Center Zagreb, Croatia; Maria Úprus and Kati Otsa, East-Tallin Central Hospital, Tallin, Estonia; Sule Yavuz, University of Marmara, Altunizade, Istanbul, Turkey; Brigitte Granel, Hôpital Nord de Marseille, France; Carolina de souza Müller, Sebastião Cezar Radominski and Valderilio Feijó Azevedo, Hospital de Clinicas da Universidade Federal do Paraná, Curitiba, Brazil; Fabian Mendoza and Joanna Busquets, Thomas Jefferson Scleroderma Center, Philadelphia, USA; Svetlana Agachi, Sergei Popa, Svetlana Agachi, Liliana Groppa, Lealea Chiaburu and Eugen Russu, Republican Clinical Hospital, Chisinau, Republic of Moldova; Thierry Zenone, Unit of Internal Medicine, Valence, France; Margarita Pileckyte, Kaunas University of Medicine Hospital Kaunas, Lithuania; Simon Stebbings, Sarah Jordan, Dunedin school of Medicine, New Zealand; Alessandro Mathieu, II Chair of Rheumatology, University of Cagliari-Policlinico Universitario, Cagliari, Italy; Lisa Stamp, University of Otago, Christchurch, New Zealand; Kamal Solanki, Cherumi Silva, Joanne Schollum and Helen Barns-Graham, Waikato University Hospital, Hamilton, New Zealand; Douglas Veale, St. Vincent's University Hospital, Dublin, Ireland; Esthela Loyo, Carmen Tineo Glenny Paulino, Hospital Regional Universitario Jose Ma Cabral y Baez, Clinica Corominas, Santiago, Dominican Republic; Sergio Toledo, Hospital San Juan Batista, Catamarca, Argentina; Mengtao Li, Peking Union Medical College Hospital (West Campus), Beijing, China; Antonietta Gigante, Sapienza Università di Roma, Università la sapienza, Policlinico Umberto I, Roma, Italy; Fahrettin Oksel and Figen Yargucu, Ege University, Bornova, Izmir, Turkey; Cristina-Mihaela Tanaseanu, Monica Popescu, Alina Dumitrascu and Isabela Tiglea, Clinical Emergency Hospital, St. Pantelimon, Bucharest, Romania; Rosario Foti, Elisa Visalli, Alessia Benenati and Giorgio Amato, a.O.U. Policlinico Vittorio emanuele la U.O. Di Reumatologia, a.O.U. Policlinico V.e. Catania Centro di Riferimento Regionale Malattie Rare Reumatologiche, Catania, Italy; Codrina Ancuta and Rodica Chiriac, GRF Popa Center for Biomedical Research, European Center for Translational Research, University of Medicine and Pharmacy, Rehabilitation Hospital, Iasi, Romania; Peter Villiger, Sabine Adler and Johannes Fröhlich, University of Bern, Switzerland; Cristiane Kayser and Andrade Luis Eduardo C, Universidade Federal de São Paulo, Brazil; Dr Nihal Fathi, Safa Alii, Marrow Ahmed, Samar Hasaneen and Eman El Hakeem, Rheumatology Department Assiut University Hospital, Egypt; Jorge Juan Gonzalez Martin, Hospital Universitario Sanchinarro, Madrid, Spain; Patrick Carpentier and Bernard Imbert, Centre Hospitalier

Universitaire de Grenoble, France; Camille Francès and Patricia Senet, Hôpital Tenon, Paris, France; Jean Sibilia, Emmanuel Chatelus, Jacques Eric Gottenberg and Hélène Chiffrot, University Hospital of Strasbourg, Hôpital de Haute-pierre, Strasbourg, France; Ira Iltinsky, Tel Aviv Sourasky Medical Center, Israel; Jean Luc Senécal, Martial Koenig, France Joval and Grodzicky Tamara, University of Montréal, Canada; Francesco Del Galdo, Giuseppina Abignano and Sookhoe Eng, University of Leeds, Chapel Allerton Hospital, Leeds, UK; Goda Seskute, Irena Butrimiene, Rita Ruginiene and Diana Karpec, State Research Institute for Innovative Medicine, Vilnius University, Lithuania; Lesley Ann Saketkoo, Melanie Pascal and Joseph Alasky, Tulane/University Medical Center, Scleroderma and Sarcoidosis Patient Care and Research Center, New Orleans, Louisiana, USA; Eduardo Kerzberg, Osteoarticular Diseases and Osteoporosis Centre, Pharmacology and Clinical Pharmacological Research Centre, School of Medicine, University of Buenos Aires, Ramos Mejia Hospital, Buenos Aires, Argentina; Washington Bianchi, Breno Valdetaro Bianchi, Dante Valdetaro Bianchi and Yeda Barcellos, Department of Rheumatology-Santa Casa da Misericórdia do Rio de Janeiro, Brasil; Ivan Castellví and Milena Millan, Hospital de la Santa Creu i Sant Pau, Barcelona, Spain; Jasminka Milas-Ahic, Roberta Visevic Clinical Hospital Center Osijek, Croatia; Massimiliano Iimonta, USSD Reumatologia, Ospedali Riuniti di Bergamo, Italy; Doron Rimar, Itzhak Rosner and Gleb Slobodin, Rheumatology Unit Bnai Zion Medical Center, Haifa, Israel; Maura Couto Unidade de Reumatologia de Viseu, Portugal; François Spertini, Camillo Ribi and Guillaume Buss, Department of Rheumatology, Clinical Immunology and Allergy, Lausanne, Switzerland; Antonella Marcocchia, Francesco Bondanini, Aldo Ciani and Sandro Pertini, Hospital Roma, Italy; Sarah Kahl, Universitätsklinikum Schleswig-Holstein, Bad Bramstedt, Germany; Ivien M Hsu, Clinical Research Center, Robert Wood Johnson Medical School, New Brunswick, USA; Thierry Martin, Vincent Poindron and Kilifa Meghit, Nouvel Hôpital Civil, Strasbourg, France; Sergey Moiseev and Pavel Novikov, Clinic of Nephrology, Internal and Occupational Diseases, Moscow, Russia; Lorinda Chung, Kathleen Kolstad and Marianna Stark, Stanford University, School of Medicine, California, USA; Tim Schmeiser, Astrid Tiele, Krankenhaus St. Josef, Wuppertal-elberfeld, Germany; Dominik Majewski Poznan, University of Medical Sciences, Poland; Zbigniew Zdrojewski, Smolenska Zaneta and Karol Wierzba, University Clinical Centre, Medical University of Gdansk. Dębinki 7, Gdansk, Poland; Julia Martínez-Barrio, Francisco Javier López-Longo, Department of Rheumatology, Gregorio Marañón University Hospital Madrid, Spain; Dinesh Khanna, Elena Schiopu and April Marquardt, University of Michigan Scleroderma Program, Academic Offices, USA; Vera Bernardino, Maria Francisca Moraes-Fontes and Ana Catarina Rodrigues, Unidade de Doenças Autoimunes-Hospital Curry Cabral, Centro Hospitalar Lisboa Central, Lisbon, Portugal; Gabriela Riemekasten, Sabine Sommerlatte, Sebastian Jendreck and Sabrina Arnold, Universitätsklinik Lübeck, Germany; Lelita Santo, Manuel Gomes and Catarina Canha, Serviço de Medicina Interna, Centro Hospitalar e Universitário de Coimbra, Portugal; Yair Levy, Meir Medical Centre, Kfar-saba, Israel; Elena Rezus, Anca Cardoneanu, Alexandra Maria Burlui, University of Medicine and Pharmacy 'G.R.T.Popa' Iasi, Rehabilitation Hospital, Iasi, Romania; Dr Omer Nuri Pamuk, Rakya University Medical Faculty, Department of Internal Medicine, Division of Rheumatology, Edirne, Turkey; Dr Daniel Brito de Araujo Universidade Federal de Pelotas, Brazil; Piercarlo Sarzi Puttini, Rossella Talotta and Sara Bongiovanni, University Hospital Luigi Sacco, Milan, Italy; Marek Brzosko, Beata Trzcinska-Butkiewicz and Marcin Milchert, University in Szczecin, Poland; Hadi Poormoghim, Elham Andalib and Simin Almasi, Firoozgar Hospital Tehran, Iran; Marta Maman and Priscilla Marcáida Fernando Melo, Department of Rheumatology, Buenos Aires, Argentina; Ina Kötter and Martin Krusche, Asklepios Clinic Altona, Medical Department 4, Rheumatology, Immunology, Nephrology, Hamburg, Germany; Giovanna Cuomo, Fiammetta Danzo and Francesco Masini, UOC Medicina Interna, Università della Campania, Napoli, Italy; Francis Gaches, Martin Michaud and Florian Cartos, Hôpital Joseph Ducuing Toulouse, France; Laura Belloli, Cinzia Casu, Ospedale Niguarda, Milano, Italy; Petros Sfikakis and Maria Tektonidou, Athens University Medical School, Greece; Juliana Markus and Roberto Ranza, Universidade Federal de Uberlândia, Brazil; Daniel Furst and Gary R Feldman, Arthritis Association of Southern California, Los Angeles, USA; Ana-Maria Ramazan, Emel Nurmambet, Amalia Miroto and Cristina Suta, Lulia Andronache Constanta City, Romania; Tom WJ Huizinga, Jeska de Vries-Bouwstra and H U Scherer, Department of Rheumatology, Leiden University Medical Center, The Netherlands; Marie-Elise Truchetet, Rheumatology Department, Bordeaux, France; Patrick Jegou and A Lescoat, Service de Médecine Interne Hôpital Sud, Rennes, France; Lorenzo Dagna, Giacomo De Luca and Corrado Campochiaro, Unit of Immunology, Rheumatology, Allergy and Rare Diseases (UnIRAR), San Raffaele Hospital, Milan, Italy; J M van Laar, Julia Spierings, Evelien Ton and Tim Radstake, University Medical Center, Utrecht, The Netherlands; Lidia Rudnicka, Malgorzata Olszewska and Anna Stochmal, Department of Dermatology, Medical University of Warsaw, Poland; Susana Oliveira, Joana Caetano and Marta Amaral, Systemic Immunomediated Diseases Unit, Department of Medicine IV, Fernando Fonseca Hospital Amadora, Portugal; Fabiola Atzeni and Donatella Sangari, Francesca Marino Rheumatology Unit, University of Messina, Italy; Masataka Kuwana and Yuichiro Shirai, Nippon Medical School Hospital Sendagi, Tokyo, Japan; Arsene Mekinian, Sebastien Riviere Internal Medicine Saint Antoine, Paris, France.

Contributors GV contributed to the study conception and design, acquisition of data, analysis and design of the study. SF and GV contributed to the data

interpretation and analysis. All authors contributed to the acquisition of data; drafting and revising the manuscript and have critically reviewed and approved the final submitted version to be published.

Funding This study was funded by European Scleroderma Trials and Research group (EUSTAR).

Competing interests None declared.

Patient consent for publication Not required.

Ethics approval All contributing EUSTAR centres have obtained approval from their respective local ethics committee for including patients' data in the EUSTAR database and written informed consent was obtained in those centres, where required by the ethics committee.

Provenance and peer review Not commissioned; externally peer reviewed.

ORCID iDs

Serena Fasano <http://orcid.org/0000-0002-4718-4551>
 Edoardo Rosato <http://orcid.org/0000-0002-7417-8093>
 Britta Maurer <http://orcid.org/0000-0001-9385-8097>
 Florenzo Iannone <http://orcid.org/0000-0003-0474-5344>
 Jörg H W Distler <http://orcid.org/0000-0001-7408-9333>
 Oliver Distler <http://orcid.org/0000-0002-0546-8310>
 Gabriele Valentini <http://orcid.org/0000-0002-7852-9137>

REFERENCES

- Bryan C, Howard Y, Brennan P, *et al*. Survival following the onset of scleroderma: results from a retrospective inception cohort study of the UK patient population. *Br J Rheumatol* 1996;35:1122–6.
- Elhai M, Meune C, Boubaya M, *et al*. Mapping and predicting mortality from systemic sclerosis. *Ann Rheum Dis* 2017;76:1897–905.
- Kowal-Bielecka O, Fransen J, Avouac J, *et al*. Update of EULAR recommendations for the treatment of systemic sclerosis. *Ann Rheum Dis* 2017;76:1327–39.
- Bryan C, Knight C, Black CM, *et al*. Prediction of five-year survival following presentation with scleroderma: development of a simple model using three disease factors at first visit. *Arthritis Rheum* 1999;42:2660–5.
- Medsger TA, Masi AT, Rodnan GP, *et al*. Survival with systemic sclerosis (scleroderma). A life-table analysis of clinical and demographic factors in 309 patients. *Ann Intern Med* 1971;75:369–76.
- Giordano M, Valentini G, Migliaresi S, *et al*. Different antibody patterns and different prognoses in patients with scleroderma with various extent of skin sclerosis. *J Rheumatol* 1986;13:911–6.
- Ferri C, Valentini G, Cozzi F, *et al*. Systemic sclerosis: demographic, clinical, and serologic features and survival in 1,012 Italian patients. *Medicine* 2002;81:139–53.
- Fransen J, Popa-Diaconu D, Hesselstrand R, *et al*. Clinical prediction of 5-year survival in systemic sclerosis: validation of a simple prognostic model in EUSTAR centres. *Ann Rheum Dis* 2011;70:1788–92.
- Domsic RT, Nihtyanova SI, Wisniewski SR, *et al*. Derivation and external validation of a prediction rule for five-year mortality in patients with early diffuse cutaneous systemic sclerosis. *Arthritis Rheumatol* 2016;68:993–1003.
- Valentini G *et al*. European scleroderma Study Group to define disease activity criteria for systemic sclerosis. III. assessment of the construct validity of the preliminary activity criteria. *Ann Rheum Dis* 2003;62:901–3.
- Nevskaya T, Baron M, Pope JE, *et al*. Predictive value of European scleroderma group activity index in an early scleroderma cohort. *Rheumatology* 2017;56:1111–22.
- Valentini G, Iudici M, Walker UA, *et al*. The European scleroderma trials and research Group (EUSTAR) Task force for the development of revised activity criteria for systemic sclerosis: derivation and validation of a preliminarily revised EUSTAR activity index. *Ann Rheum Dis* 2017;76:270–6.
- Walker UA, Tyndall A, Cziráková L, *et al*. Clinical risk assessment of organ manifestations in systemic sclerosis: a report from the EULAR scleroderma trials and research Group database. *Ann Rheum Dis* 2007;66:754–63.
- van den Hoogen F, Khanna D, Fransen J, *et al*. 2013 classification criteria for systemic sclerosis: an American College of rheumatology/European League against rheumatism collaborative initiative. *Ann Rheum Dis* 2013;72:1747–55.
- Medsger TA, Silman AJ, Steen VD, *et al*. A disease severity scale for systemic sclerosis: development and testing. *J Rheumatol* 1999;26:2159–67.
- Ferdowsi N, Huq M, Stevens W, *et al*. Development and validation of the scleroderma clinical trials Consortium damage index (SCTC-DI): a novel instrument to quantify organ damage in systemic sclerosis. *Ann Rheum Dis* 2019.
- Steen VD, Medsger TA. Severe organ involvement in systemic sclerosis with diffuse scleroderma. *Arthritis Rheum* 2000;43:2437–44.
- Hao Y, Hudson M, Baron M, *et al*. Early mortality in a multinational systemic sclerosis inception cohort. *Arthritis Rheumatol* 2017;69:1067–77.
- Walker JG, Steele RJ, SCHNITZER M, *et al*. The association between disease activity and duration in systemic sclerosis. *J Rheumatol* 2010;37:2299–306.

TRANSLATIONAL SCIENCE

Vascularised human skin equivalents as a novel in vitro model of skin fibrosis and platform for testing of antifibrotic drugs

Alexandru-Emil Matei ¹, Chih-Wei Chen,¹ Lisa Kiesewetter,² Andrea-Hermina Györfi,¹ Yi-Nan Li,¹ Thuong Trinh-Minh,¹ Xiaohan Xu,¹ Cuong Tran Manh,¹ Toin van Kuppevelt,³ Jan Hansmann,^{2,4} Astrid Jüngel,⁵ Georg Schett ¹, Florian Groeber-Becker,^{2,6} Jörg H W Distler ¹

Handling editor Josef S Smolen

► Additional material is published online only. To view please visit the journal online (<http://dx.doi.org/10.1136/annrheumdis-2019-216108>).

For numbered affiliations see end of article.

Correspondence to

Dr Jörg H W Distler, Department of Internal Medicine 3 – Rheumatology and Immunology, Friedrich-Alexander-University Erlangen-Nürnberg (FAU) and University Hospital Erlangen, Erlangen D-91054, Germany; joerg.distler@uk-erlangen.de

A-EM, C-WC, FG-B and JHWD contributed equally.

Received 30 July 2019
Revised 12 September 2019
Accepted 13 September 2019
Published Online First
20 September 2019

ABSTRACT

Objectives Fibrosis is a complex pathophysiological process involving interplay between multiple cell types. Experimental modelling of fibrosis is essential for the understanding of its pathogenesis and for testing of putative antifibrotic drugs. However, most current models employ either phylogenetically distant species or rely on human cells cultured in an artificial environment. Here we evaluated the potential of vascularised in vitro human skin equivalents as a novel model of skin fibrosis and a platform for the evaluation of antifibrotic drugs.

Methods Skin equivalents were assembled on a three-dimensional extracellular matrix by sequential seeding of endothelial cells, fibroblasts and keratinocytes. Fibrotic transformation on exposure to transforming growth factor- β (TGF β) and response to treatment with nintedanib as an established antifibrotic agent were evaluated by quantitative polymerase chain reaction (qPCR), capillary Western immunoassay, immunostaining and histology.

Results Skin equivalents perfused at a physiological pressure formed a mature, polarised epidermis, a stratified dermis and a functional vessel system. Exposure of these models to TGF β recapitulated key features of SSc skin with activation of TGF β pathways, fibroblast to myofibroblast transition, increased release of collagen and excessive deposition of extracellular matrix. Treatment with the antifibrotic agent nintedanib ameliorated this fibrotic transformation.

Conclusion Our data provide evidence that vascularised skin equivalents can replicate key features of fibrotic skin and may serve as a platform for evaluation of antifibrotic drugs in a pathophysiologically relevant human setting.

INTRODUCTION

Fibrotic disorders such as systemic sclerosis (SSc) are complex multifactorial diseases that develop as interplay of different cell types with each other and with their local microenvironment.¹ Preclinical model systems are essential to improve our understanding of the underlying pathophysiology of fibrotic diseases and to test novel therapeutic approaches. The most frequent approaches are simulating fibrotic conditions either in vitro with human cell culture systems or in vivo with mouse models. Most of the current cell culture systems

Key messages

What is already known about this subject?

- Many current model systems of skin fibrosis are of limited predictive value as they rely either on phylogenetically distant species or oversimplified culture conditions that deprive the cells of a three-dimensional matrix and of interactions with other cell types.
- These limitations provide major challenges to preclinical development and may contribute to the significant rate of negative clinical trials in systemic sclerosis (SSc).

What does this study add?

- We describe vascularised skin equivalents as an advanced model of human skin with a fully polarised epidermal layer, a stratified dermis and a functional vascular system with physiological perfusion pressures.
- Human skin equivalents can be induced to undergo fibrotic transformation and resemble key features of SSc skin with accumulation of extracellular matrix, fibroblast to myofibroblast transition and aberrant activation of transforming growth factor- β (TGF β) signalling.
- Vascularised skin equivalents can predict response to antifibrotic therapies as shown by inhibition of fibroblast activation and of extracellular matrix deposition in response to nintedanib.

How might this impact on clinical practice or future developments?

- Vascularised skin equivalents may serve as a novel model to better mimic the complex interplay of different cells in fibrotic skin and may also provide a platform for the evaluation of antifibrotic drugs in a pathophysiologically relevant human setting with improved predictive value.

are two dimensional (2D), where cells are cultured on stiff, flat plastic surfaces.² Although studies in 2D cell culture systems have provided important insights into cellular responses of individual cell types to defined stimuli, they have several



© Author(s) (or their employer(s)) 2019. No commercial re-use. See rights and permissions. Published by BMJ.

To cite: Matei A-E, Chen C-W, Kiesewetter L, et al. *Ann Rheum Dis* 2019;**78**:1686–1692.

important limitations: they cannot mimic (patho)physiologically relevant cell–matrix interactions, interactions between different cell types, presence of nutrient gradients and signalling pathways related to these processes.^{3–5} Moreover, culture of adherent cell types on plastic surfaces exposes them to an unphysiologically stiff environment, which alters central cellular responses such as response to cytokines, organisation of the cytoskeleton, migration and proliferation.^{6,7} Cellular responses in 2D culture models may thus not always reliably predict the pathological processes in fibrotic tissues. Mouse models overcome several of these limitations, such as lack of cell–cell and cell–matrix interactions, absence of gradients and excessive tissue stiffness, but contain other potential pitfalls. There are many differences between murine and human immune systems—dendritic epidermal T cells, for example, are only found in mouse.^{8,9} Moreover, not all pathways are conserved between mice and men and individual molecules may exert different functions in those signalling cascades.¹⁰ Pathophysiological studies and preclinical test programmes for novel antifibrotic approaches may thus benefit from novel in vitro test systems with primary human cells to overcome some of the limitations of conventional 2D cell culture systems and mouse models.

Here, we report an in vitro test system for skin fibrosis, generated by adapting a previously described vascularised skin equivalent.¹¹ This model employs primary human fibroblasts, keratinocytes and endothelial cells that resemble all functional skin layers affected by fibrosis in a three-dimensional (3D) environment and provides a functional vascular system with

physiological perfusion. We demonstrate that this engineered human skin equivalent can be converted into fibrotic skin by exposure to transforming growth factor- β (TGF β). The induction of fibrosis is prevented by nintedanib, demonstrating that this model is a suitable test system for candidate antifibrotic drugs. This vascularised in vitro human skin equivalent may thus be an interesting addition to the arsenal of preclinical models of skin fibrosis.

MATERIALS AND METHODS

Materials and methods are described in the online supplementary information file.

RESULTS

Vascularised human skin equivalents reproduce main characteristics of human skin relevant for the pathogenesis of skin fibrosis

We generated vascularised human skin equivalent models and evaluated their suitability as a test system for generation and prevention of skin fibrosis by exposing them to TGF β and/or nintedanib (figure 1A).¹¹

For this, we refined a previously described bioreactor design to ensure higher reproducibility and throughput. We modified the bioreactor body from a round to a rectangular shape, while adapting its inner dimensions to allow easy access to the cannulas of the artery and vein of the skin equivalent during culture (figure 1B,C,E). The polydimethylsiloxane (PDMS) lid of the

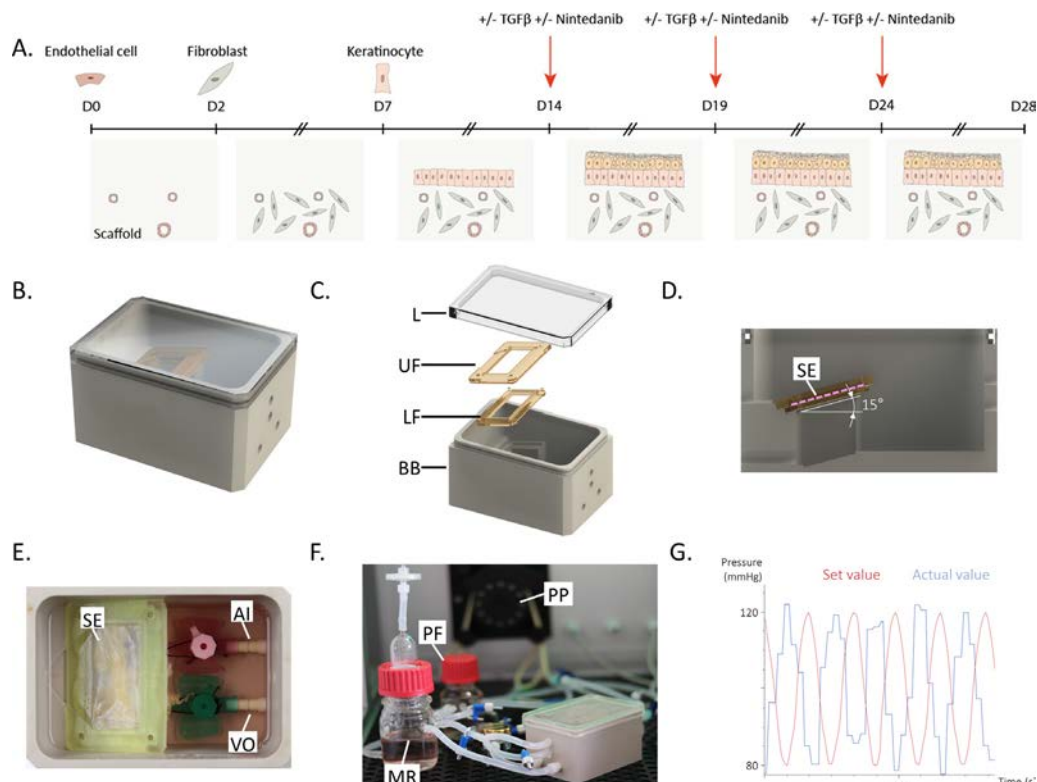


Figure 1 Assembly of the vascularised human skin equivalent and characterisation of the optimised bioreactor system. (A) Schematic overview of the generation of the human skin equivalent and its conversion to fibrotic skin. (B–D): Schematic representation of the optimised bioreactor and its contents (B, C), with the matrix at a 15° angle (D). (E) Picture illustrating the bioreactor contents: the human skin equivalent with cannulated supplying artery (red cannula) and vein (green cannula) connected to the perfusion system. (F) Picture illustrating the perfusion system and the bioreactor containing the human skin equivalent. (G) Pressure curves measured at the arterial end of the human skin equivalent (blue) following the set values (red) and resembling the physiological human systemic blood pressure. AI, arterial; BB, bioreactor body; L, lid; LF, lower frame; MR, medium reservoir; PF, pressure balance flask; PP, peristaltic pump; SE, skin equivalent; TGF β , transforming growth factor- β ; UF, upper frame; VO, venous outlet.

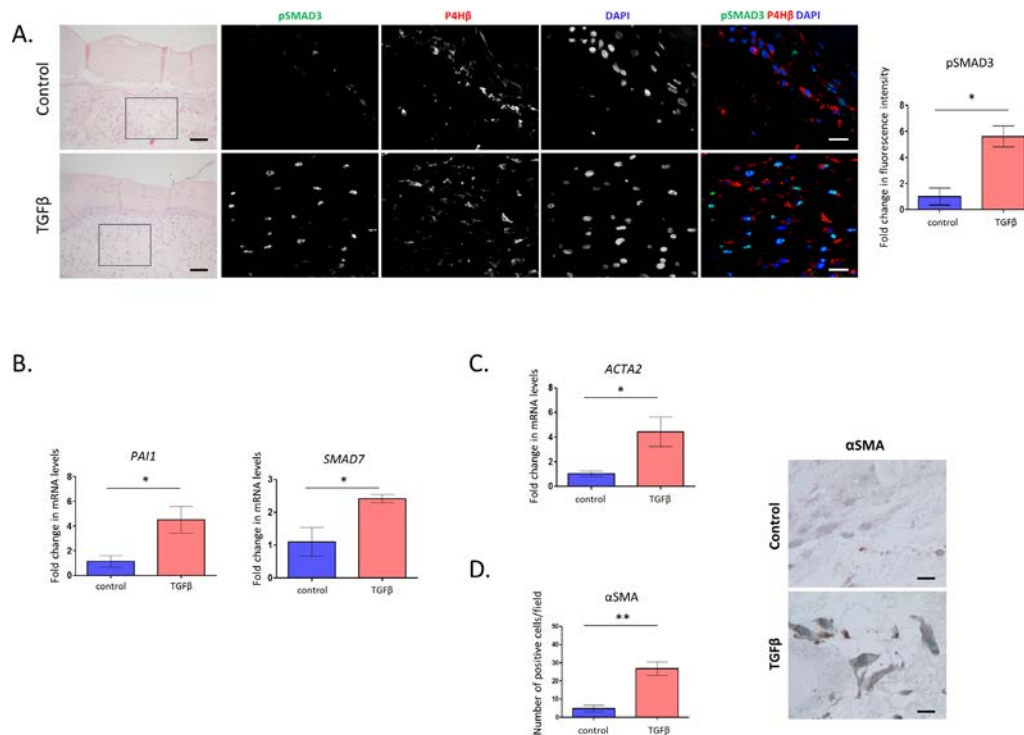


Figure 2 Systematic evaluation of TGF β signalling in vascularised human skin equivalent models. (A) Activation of Smad signalling as shown by immunofluorescence staining for pSMAD3 (green) and costaining with prolyl-4-hydroxylase- β (red) and DAPI (blue), at 600-fold magnification (scale bars=25 μ m). Quantification of pSMAD3 signal intensity and HE stainings (200-fold magnification, scale bars=100 μ m) is included. (B) mRNA levels of the prototypical TGF β /SMAD target genes PAI-1 and Smad7. (C) mRNA levels of ACTA2 (which encodes for α SMA). (D) Quantification of myofibroblast counts and representative α -SMA stainings counterstained with haematoxylin at 1000-fold magnification (scale bars=20 μ m). α -SMA, α -smooth muscle actin; DAPI, 4',6-diamidino-2-phenylindole; TGF β , transforming growth factor- β .

bioreactor provided a tight sealing while allowing direct macroscopic inspection of the skin model and its vessels during culture, which permits rapid detection of technical problems (figure 1C). Furthermore, we introduced an angled orientation of the skin equivalent to prevent entrapment of air bubbles underneath the matrix that would lead to uneven medium supply (figure 1D).

Perfusion at the arterial end was ensured by connecting the bioreactor system containing the skin models to a fluidic circuit; a peristaltic pump and a pressure sensor ensured pressure generation and control that resemble the physiological systemic blood pressure (figure 1F,G).

After 1 month of in vitro culture, the microscopic structure of the vascularised skin equivalent resembled that of human skin (online supplementary figure 1A). The keratinocytes had fully differentiated to form a polarised human epidermis with physiological location of cytokeratin-14 in the basal layer and cytokeratin-10 in the suprabasal layers and presence of a corneous layer (online supplementary figure 1B). Laminin-5 staining demonstrated that the epidermis is separated from the underlying dermis by a continuous basal membrane in our model as it is in human skin (online supplementary figure 1B). Fibroblasts migrated in the scaffold and distributed uniformly to form a dermal equivalent, while the superficial fibroblasts remain in close proximity to the epidermis.

Endothelial cells lined the pre-existent vessel structures, as shown by the positive staining for CD31 in the dermis (online supplementary figure 1C). Fibroblasts identified as vimentin-positive or P4H β -positive cells migrated in close proximity to the endothelial cells, facilitating interactions (online supplementary figure 1C). The vessel density in skin equivalent models, although lower than in human skin from

healthy donors, was similar to the density in skin from patients with SSc (online supplementary figure 2). Podoplanin-positive lymphatic endothelial cells formed lymphatic vessels in vascularised skin equivalents that persisted until the end of the experiment (online supplementary figure 3).

Exposure to TGF β induces fibroblast to myfibroblast transition and deposition of extracellular matrix (ECM) in vascularised human skin equivalents

Aberrant TGF β signalling is both sufficient and required to induce fibrosis in various organs including skin.¹² We thus evaluated whether exposure to pathophysiologically relevant concentrations of TGF β would convert normal skin equivalents to fibrotic skin equivalents.

We first aimed to confirm that incubation with TGF β activates the transcription of common downstream targets of TGF β . Indeed, we observed increased phosphorylation and nuclear translocation of Smad3 in P4H β -positive cells in the dermis of vascularised human skin equivalents (figure 2A). Moreover, the TGF- β target genes *PAI1* and *SMAD7* were upregulated in tissue homogenates from fibrotic skin equivalents as compared with the control (figure 2B).

We further analysed fibroblast to myfibroblast transition in the vascularised skin models exposed to TGF β . The mRNA levels of *ACTA2* and the number of α -smooth muscle actin (α -SMA)-positive cells were significantly higher in the TGF β -stimulated skin equivalents than in controls (figure 2C,D), thus reproducing the activated state of fibroblasts observed in fibrotic skin.¹³

We next investigated the deposition of ECM components in TGF β -exposed human skin equivalents. The mRNA levels of *COL1A1*, *COL1A2* and fibronectin were significantly increased

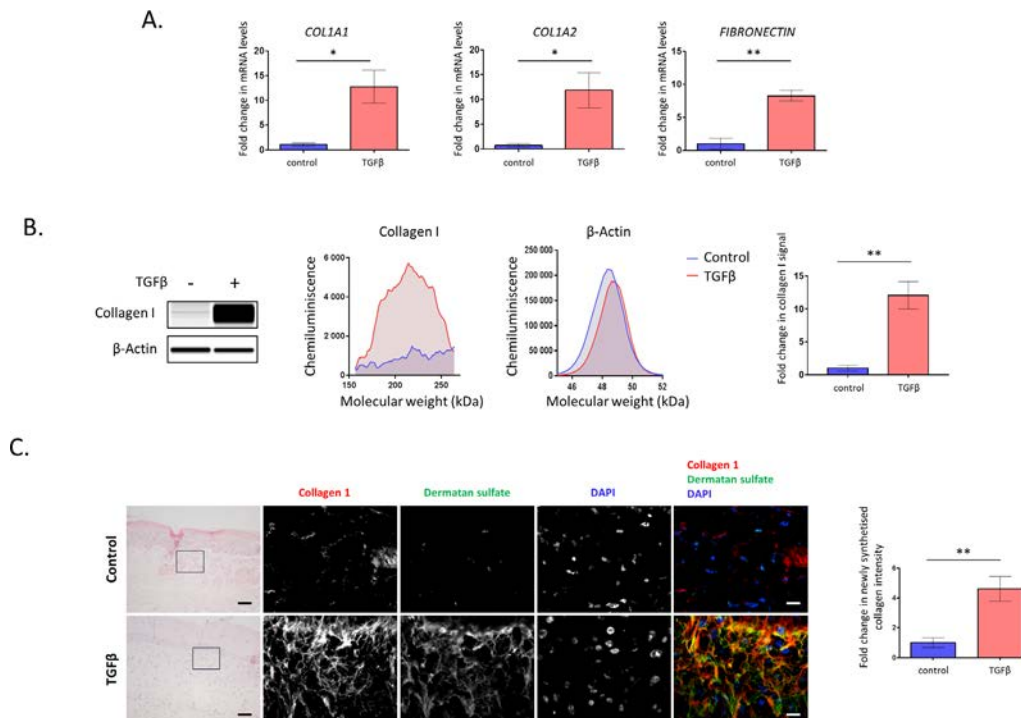


Figure 3 Fibrotic remodelling of the vascularised human skin equivalent in response to TGFβ. (A) Upregulation of the mRNA levels of *COL1A1*, *COL1A2* and fibronectin as major ECM proteins in the skin. (B) Representative western blot for type I collagen, with β-actin as housekeeping gene. Chemiluminescence versus molecular weight plots and quantification are included. (C) Immunofluorescence stainings of dermatan sulfate to identify human type I collagen in the vascularised human skin equivalent, at 1000-fold magnification (scale bars=20 μm), counterstained with DAPI. HE stainings (200-fold magnification, scale bars=100 μm) and quantification of collagen type I signal colocalising with dermatan sulfate are included. DAPI, 4',6-diamidino-2-phenylindole; ECM, extracellular matrix; TGFβ, transforming growth factor-β.

in the TGFβ-stimulated skin equivalents (figure 3A). Moreover, the levels of type 1 collagen protein, evaluated by capillary Western immunoassay, were highly upregulated in the TGFβ-exposed human skin equivalent (figure 3B).

However, all antibodies directed against collagen type 1 that we tested could not reliably discriminate between human (newly synthesised) and porcine (pre-existent) collagen, since collagen type 1 protein is evolutionarily highly conserved (data not shown). To identify the newly synthesised collagen type 1 and determine its relative contribution to the collagen levels in the two experimental conditions, we used an indirect approach. Dermatan sulfate was previously shown to be an excellent surrogate readout for de novo deposition of type 1 collagen, due to its association with newly formed collagen fibrils and its absence from the matrices.¹⁴ We confirmed the specificity of this approach in our setting by showing with immunofluorescence staining that collagen type 1 of porcine origin could be detected in the acellular matrix by western blot, while the dermatan sulfate signal was absent (online supplementary figure 4). The dermatan sulfate and collagen type I double positive signal highlighted the organisation of newly synthesised collagen as prominent fibres in the TGFβ group, whereas in the control group double positive signals were minimal. The intensity of collagen type I signal colocalising with dermatan sulfate was much stronger in the TGFβ group than in control, proving the increased de novo synthesis and deposition of collagen in TGFβ-exposed skin equivalents (figure 3C).

Nintedanib ameliorates fibrosis in the vascularised human skin equivalent

To evaluate its potential use as a platform to test candidate antifibrotic drugs, we analysed whether TGFβ-induced fibrosis could

be reduced by treatment with nintedanib, a multiple tyrosine kinases inhibitor with proven antifibrotic effects.^{15–17}

We first evaluated whether nintedanib can inhibit TGFβ downstream signalling and TGFβ-induced fibroblast to myfibroblast transition. In the dermis of TGFβ-exposed, nintedanib-treated skin equivalents, phosphorylation and nuclear translocation of Smad3 in P4Hβ-positive cells was decreased, and the TGFβ target genes *PAI1* and *SMAD7* were downregulated as compared with TGFβ-stimulated and untreated skin models (figure 4A,B). Nintedanib treatment also inhibited the TGFβ-induced upregulation of *ACTA2* mRNA levels and led to lower numbers of α-SMA-positive cells (figure 4C,D).

We subsequently analysed the deposition of ECM components in TGFβ-exposed, nintedanib-treated skin models in comparison with stimulated and vehicle-treated equivalents. TGFβ-induced upregulation of *COL1A1*, *COL1A2* and fibronectin mRNA levels and total collagen type I protein were significantly decreased by nintedanib treatment (figure 5A,B). In the TGFβ-stimulated, nintedanib-treated group, the signal intensity of newly synthesised collagen was reduced in comparison to the TGFβ-stimulated, vehicle-treated group (figure 5C).

DISCUSSION

Vascularised human skin equivalents resemble key features of human skin. The keratinocytes in the epidermal layer are polarised, and dermis and epidermis are separated by a basal membrane. Fibroblasts are located as single cells in the dermal layer, embedded into a physiological matrix. Endothelial cells form a functional, perfused vascular network comprising both blood and lymphatic vessels. This model thus includes all major resident cell types of human skin in typical topographic order

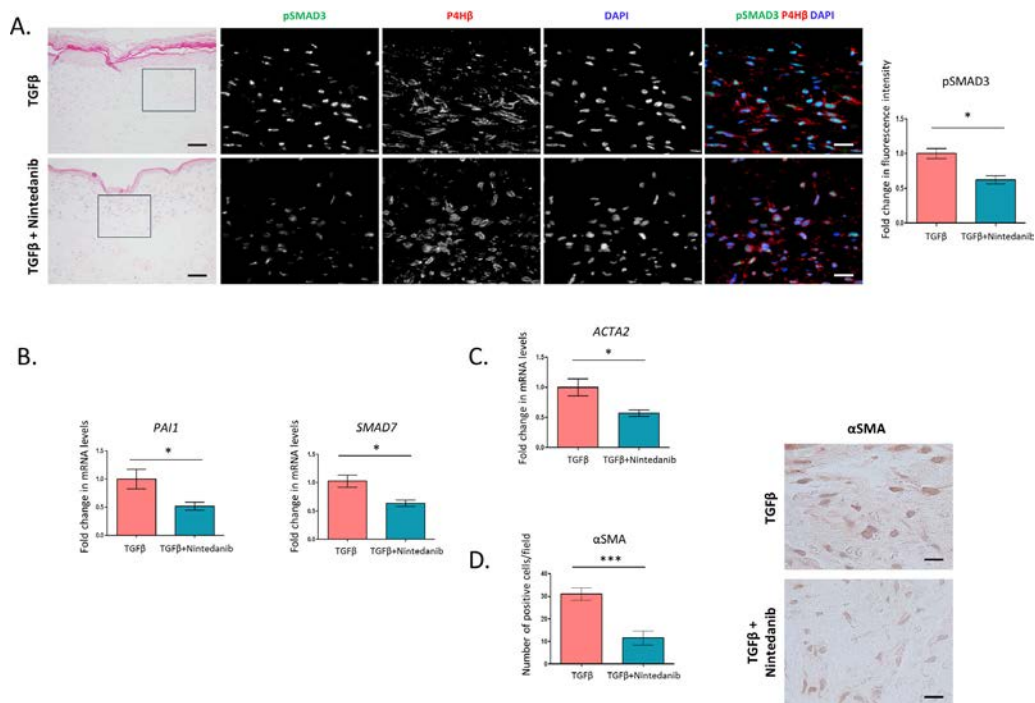


Figure 4 Inhibition of TGFβ signalling by nintedanib treatment in vascularised skin equivalent models. (A) Decreased activation of TGFβ-induced SMAD signalling on nintedanib treatment as shown by immunofluorescence staining for pSMAD3 (green) and costaining with prolyl-4-hydroxylase-β (red) and DAPI (blue), at 600-fold magnification (scale bars=25 μm). Quantification of pSMAD3 signal intensity and HE stainings (200-fold magnification, scale bars=100 μm) is included. (B) mRNA levels of the prototypical TGFβ/SMAD target genes *PAI-1* and *Smad7*. (C) mRNA levels of *ACTA2* (which encodes for α-SMA). (D) Quantification of myofibroblast counts and representative α-SMA stainings counterstained with haematoxylin at 1000-fold magnification (scale bars=20 μm). α-SMA, α-smooth muscle actin; DAPI, 4',6-diamidino-2-phenylindole; TGFβ, transforming growth factor-β.

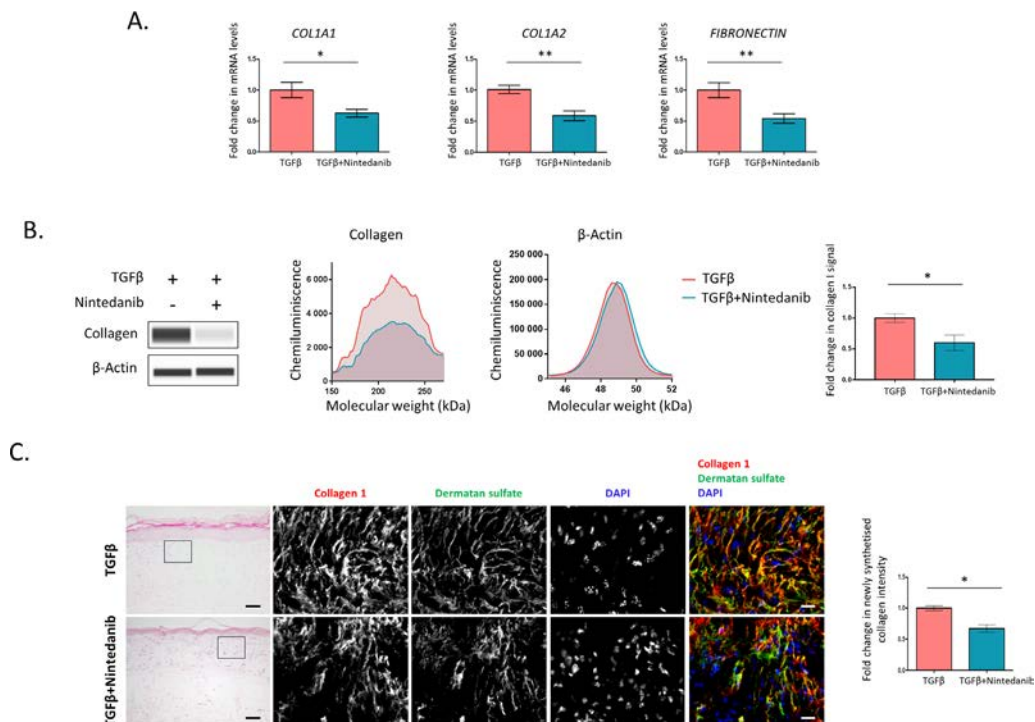


Figure 5 Antifibrotic effects of nintedanib treatment in vascularised skin equivalent models. (A) Inhibition of TGFβ-induced upregulation of *COL1A1*, *COL1A2* and fibronectin mRNA levels by nintedanib treatment. (B) Representative western blot for type I collagen, with β-actin as housekeeping gene. Chemiluminescence versus molecular weight plots and quantification are included. (C) Immunofluorescence stainings of dermatan sulfate to identify human type I collagen in the vascularised human skin equivalent, at 1000-fold magnification (scale bars=20 μm), counterstained with DAPI. HE stainings (200-fold magnification, scale bars=100 μm) and quantification of collagen type I signal colocalising with dermatan sulfate are included. DAPI, 4',6-diamidino-2-phenylindole; TGFβ, transforming growth factor-β.

and enables studies of interactions between fibroblasts, endothelial cells and keratinocytes. The interplay between these cell types is a critical feature of fibrotic skin diseases like SSc. Keratinocytes are a major source of proinflammatory and profibrotic cytokines in SSc, such as interleukin (IL)-1 α , IL-6, connective tissue growth factor (CTGF), oncostatin M and vascular endothelial growth factor (VEGF), and are involved in bidirectional double paracrine signalling with fibroblasts, thereby promoting fibroblast activation.^{18–21} Endothelial cells are thought to be the primary site of injury in SSc and modulate fibroblast activation by release of factors such as endothelin 1 and nitric oxide. Moreover, endothelial cells can undergo endothelial to mesenchymal transition to acquire a myofibroblast phenotype and may thus directly contribute to matrix deposition.²² Such interactions can be reproduced in vascularised skin equivalents.

We demonstrate that exposure to TGF β induces fibrotic transformation of vascularised skin equivalents. Stimulation with TGF β induces activation of classical profibrotic downstream mediators such as SMAD signalling and transcription of prototypical target genes. This promotes fibroblast to myofibroblast transition and ECM deposition in vascularised skin equivalents, key features of fibrotic skin in SSc.^{23–24} Fibroblasts in vascularised skin equivalents can therefore acquire an activated phenotype that reproduces their aberrant activation in SSc skin.

Of particular interest, we provide first evidence that vascularised skin equivalents can serve as a platform for the evaluation of antifibrotic drugs. We used nintedanib for formal proof, as nintedanib is the first targeted antifibrotic drug that awaits approval in SSc.^{15–17} Treatment with nintedanib in a pharmacologically relevant dose exerted antifibrotic effects in vascularised human skin equivalents: nintedanib attenuated TGF β signalling, reduced fibroblast to myofibroblast transition and decreased ECM deposition.

A potential alternative approach to the generation of vascularised skin equivalents from mature cell types as in our current study is the use of induced pluripotent stem cells (iPSCs). iPSCs can be rapidly expanded and can subsequently differentiated with specific protocols into the individual cell types found in human skin.^{25–30}

Although vascularised human skin equivalents may offer novel opportunities for translational studies and drug testing, the model also has important limitations: (1) The generation of vascularised skin equivalents requires specific equipment such as an incubator with adjustable perfusion pressure, bioreactors and specific material such as decellularised porcine intestinal matrices. Since adjustable perfusion pressure is an essential feature of this model, the custom incubator is indispensable; however, matrices generated by 3D bioprinters are currently evaluated as alternatives to decellularised porcine matrices and may eventually overcome the need for them.³¹ (2) Generation of vascularised skin equivalents is work and time intensive, which limits the potential for high-throughput drug screening. They thus serve as confirmatory rather than as screening models. (3) Our current version of the model aims to analyse the interaction of resident cells in the skin, but omits circulating cells such as leucocytes. However, peripheral blood mononuclear cells or selected leucocyte populations of interest can be added to the circulation of vascularised skin equivalents to study crosstalk between resident cells and circulating inflammatory cells. Experiments to study the efflux of circulating leucocytes into vascularised skin equivalents are currently in preparation.

Aside from vascularised skin equivalents, alternative *in vitro* approaches to mimic the complex interaction in human skin and model skin fibrosis are currently developed. Most of them

are lacking a functional vascular system.³² Given the importance of vascular cells in the pathogenesis of SSc, this may be an important limitation. Full-thickness skin models are 3D cell cultures that have an epidermal and a dermal component and reproduce the interaction between fibroblasts and keratinocytes. Such 3D models composed exclusively of fibroblasts and keratinocytes have been successfully used to study skin pathologies including fibrosis.^{33–34} Modifications of this approach that include monocytes as other pathophysiologically relevant cell types have recently been described.³⁵

In skin-on-chip models, selected skin cells are cultured in a 3D microsystem. These chips can theoretically reproduce physiological structures of different complexities up to multiorgan-on-chip.³⁶ Some of these systems include perfusion of a microfluidic channel lined by endothelial cells. However, even in these more complex skin-on-chip models, a microvascular network is lacking, thereby minimising crosstalk between endothelial cells and fibroblasts, and the physiological undulation of blood perfusion pressure cannot be reproduced.^{37–38}

Another alternative approach to *in vitro* generated skin models is the *ex vivo* culture of skin samples. In this approach, human skin samples are taken into culture directly after the biopsies have been obtained. A major advantage of this approach is that all the cellular components including immune cells and skin structures including vessels and skin appendages are preserved in their native form.^{39–41} However, the biopsies can only be kept for short period in culture, before cells lose their phenotype and undergo apoptosis. Moreover, experimental manipulation such as knockdown is challenging in this setting. In addition, standardised access to human skin samples is limited, often disabling systematic larger scale studies.

We describe herein a novel human *in vitro* model of skin fibrosis. Decisive features of these vascularised skin equivalents include a functional vascular perfusion system; interaction with a physiological matrix; crosstalk between the major resident cells of human skin, such as fibroblasts, keratinocytes and endothelial cells; and the option to further expand cellular interactions by the addition of leucocytes. Vascularised skin equivalents thus resemble many of the key features of fibrotic skin and may not only provide novel pathophysiological insights but also serve as an advanced platform for drug testing.

Author affiliations

¹Department of Internal Medicine 3 – Rheumatology and Immunology, Friedrich-Alexander-University Erlangen-Nürnberg (FAU) and University Hospital Erlangen, Erlangen, Germany

²Translational Center Würzburg, Fraunhofer Translational Center Regenerative Therapies, Fraunhofer Institute for Silicate Research (ISC), Würzburg, Germany

³Radboud Institute for Molecular Life Sciences, Department of Biochemistry, Radboud University Medical Center, Nijmegen, The Netherlands

⁴University for Applied Sciences Würzburg-Schweinfurt, Würzburg, Germany

⁵Center of Experimental Rheumatology, University Hospital Zurich/Zurich Center of Integrative Human Physiology (ZIHP), Zurich, Switzerland

⁶Department for Tissue Engineering and Regenerative Medicine, Würzburg University Medical Center, Würzburg, Germany

Contributors A-EM, C-WC, FG-B and JHWD designed the study. A-EM, C-WC, LK, A-HG, Y-NL, TT-M., XX, CTM were involved in acquisition of data. A-EM, C-WC, A-HG, LK, AJ, GS, FG-B and JHWD were involved in interpretation of data. A-EM and JHWD were involved in manuscript preparation. THvK, JH and FG-B provided essential materials.

Funding Grants DI 1537/9-1 and DI 1537/9-2, DI 1537/11-1, DI 1537/12-1, DI 1537/13-1, DI 1537/14-1 and RA 2506/3-1 of the German Research Foundation, SFB CRC1181 (project C01) and SFB TR221/ project number 324392634 (B04) of the German Research Foundation; grants J40 and A64 of the IZKF in Erlangen; grants 2014_A47 and 2014_A184 of the Else-Kröner-Fresenius-Foundation; grant 14-12-17-1-Bergmann of the ELAN-Foundation Erlangen and a Career Support Award of Medicine of the Ernst Jung Foundation. AJ is a member of the SKINTEGRITY consortium at University Medicine Zürich/Hochschulmedizin Zürich.

Competing interests JHWD has consultancy relationships and/or has received research funding from Actelion, BMS, Celgene, Bayer Pharma, Boehringer Ingelheim, JB Therapeutics, Sanofi-Aventis, Novartis, UCB, GSK, Array Biopharma and Active Biotech in the area of potential treatments of SSc and is stock owner of 4D Science GmbH.

Patient consent for publication Not required.

Provenance and peer review Not commissioned; externally peer reviewed.

Data availability statement Data are available on reasonable request.

ORCID iDs

Alexandru-Emil Matei <http://orcid.org/0000-0003-1248-3145>

Georg Schett <http://orcid.org/0000-0001-8740-9615>

Jörg H W Distler <http://orcid.org/0000-0001-7408-9333>

REFERENCES

- Distler JH, Györfi AH, Ramanujam M, *et al.* Shared and distinct mechanisms of fibrosis. *nature reviews rheumatology* in press.
- Garrett SM, Baker Frost D, Feghali-Bostwick C. The mighty fibroblast and its utility in scleroderma research. *J Scleroderma Relat Disord* 2017;2:100–7.
- Hinz B, Gabbiani G. Cell-Matrix and cell-cell contacts of myofibroblasts: role in connective tissue remodeling. *Thromb Haemost* 2003;90:993–1002.
- Pakshir P, Hinz B. The big five in fibrosis: macrophages, myofibroblasts, matrix, mechanics, and miscommunication. *Matrix Biol* 2018;68-69:81–93.
- Grinnell F. Fibroblast biology in three-dimensional collagen matrices. *Trends Cell Biol* 2003;13:264–9.
- Rhee S. Fibroblasts in three dimensional matrices: cell migration and matrix remodeling. *Exp Mol Med* 2009;41:858–65.
- Randall MJ, Jünger A, Rimann M, *et al.* Advances in the Biofabrication of 3D Skin *in vitro*: Healthy and Pathological Models. *Front Bioeng Biotechnol* 2018;6.
- Mestas J, Hughes CCW. Of mice and not men: differences between mouse and human immunology. *J Immunol* 2004;172:2731–8.
- Sutoh Y, Mohamed RH, Kasahara M. Origin and evolution of dendritic epidermal T cells. *Front Immunol* 2018;9:1059.
- Yue F, Cheng Y, Breschi A, *et al.* A comparative encyclopedia of DNA elements in the mouse genome. *Nature* 2014;515:355–64.
- Groeber F, Engelhardt L, Lange J, *et al.* A first vascularized skin equivalent as an alternative to animal experimentation. *ALTEX* 2016;33:415–22.
- Györfi AH, Matei A-E, Distler JHW. Targeting TGF- β signaling for the treatment of fibrosis. *Matrix Biology* 2018;68-69:8–27.
- Chakraborty D, Šumová B, Mallano T, *et al.* Activation of STAT3 integrates common profibrotic pathways to promote fibroblast activation and tissue fibrosis. *Nat Commun* 2017;8:1130.
- Oostendorp C, Uijtendewilligen PJE, Versteeg EM, *et al.* Visualisation of newly synthesised collagen *in vitro* and *in vivo*. *Sci Rep* 2016;6:18780.
- Huang J, Beyer C, Palumbo-Zerr K, *et al.* Nintedanib inhibits fibroblast activation and ameliorates fibrosis in preclinical models of systemic sclerosis. *Ann Rheum Dis* 2016;75:883–90.
- Huang J, Maier C, Zhang Y, *et al.* Nintedanib inhibits macrophage activation and ameliorates vascular and fibrotic manifestations in the Fra2 mouse model of systemic sclerosis. *Ann Rheum Dis* 2017;76:1941–8.
- Distler O, Highland KB, Gahlemann M, *et al.* Nintedanib for systemic sclerosis-associated interstitial lung disease. *N Engl J Med* 2019;380:2518–28.
- Distler O, Distler Jörg HW, Scheid A, *et al.* Uncontrolled expression of vascular endothelial growth factor and its receptors leads to insufficient skin angiogenesis in patients with systemic sclerosis. *Circ Res* 2004;95:109–16.
- Aden N, Nuttall A, Shiwen X, *et al.* Epithelial cells promote fibroblast activation via IL-1 α in systemic sclerosis. *J Invest Dermatol* 2010;130:2191–200.
- McCoy SS, Reed TJ, Berthier CC, *et al.* Scleroderma keratinocytes promote fibroblast activation independent of transforming growth factor beta. *Rheumatology* 2017;56:1970–81.
- Canady J, Arndt S, Karrer S, *et al.* Increased KGF expression promotes fibroblast activation in a double paracrine manner resulting in cutaneous fibrosis. *J Invest Dermatol* 2013;133:647–57.
- Manetti M, Romano E, Rosa I, *et al.* Endothelial-To-Mesenchymal transition contributes to endothelial dysfunction and dermal fibrosis in systemic sclerosis. *Ann Rheum Dis* 2017;76:924–34.
- Distler JHW, Feghali-Bostwick C, Soare A, *et al.* Review: frontiers of antifibrotic therapy in systemic sclerosis. *Arthritis Rheumatol* 2017;69:257–67.
- Beyer C, Distler O, Distler JHW. Innovative antifibrotic therapies in systemic sclerosis. *Curr Opin Rheumatol* 2012;24:274–80.
- Itoh M, Umegaki-Arao N, Guo Z, *et al.* Generation of 3D skin equivalents fully reconstituted from human induced pluripotent stem cells (iPSCs). *PLoS One* 2013;8:e77673.
- Kim Y, Park N, Rim YA, *et al.* Establishment of a complex skin structure via layered co-culture of keratinocytes and fibroblasts derived from induced pluripotent stem cells. *Stem Cell Res Ther* 2018;9.
- Wang Z, Nakamura K, Jinnin M, *et al.* Establishment and gene expression analysis of disease-derived induced pluripotent stem cells of scleroderma. *J Dermatol Sci* 2016;84:186–96.
- Kim J-W, Kim Y, Kim J, *et al.* AB0189 3d skin organoid mimicking systemic sclerosis generated by patient-derived induced pluripotent stem cells: 'disease in a dish' and development of animal model. *Ann Rheum Dis* 2018;77:1281.2–1.
- Takagi R, Ishimaru J, Sugawara A, *et al.* Bioengineering a 3D integumentary organ system from iPSC cells using an *in vivo* transplantation model. *Sci Adv* 2016;2:e1500887.
- Wimmer RA, Leopoldi A, Aichinger M, *et al.* Human blood vessel organoids as a model of diabetic vasculopathy. *Nature* 2019;565:505–10.
- Ng WL, Wang S, Yeong WY, *et al.* Skin Bioprinting: impending reality or fantasy? *Trends Biotechnol* 2016;34:689–99.
- van den Broek LJ, Bergers LIJ, Reijnders CMA, *et al.* Progress and future perspectives in Skin-on-Chip development with emphasis on the use of different cell types and technical challenges. *Stem Cell Rev Rep* 2017;13:418–29.
- Wohlfahrt T, Rauber S, Uebe S, *et al.* Pu.1 controls fibroblast polarization and tissue fibrosis. *Nature* 2019;566:344–9.
- Rossi A, Appelt-Menzel A, Kurdyn S, *et al.* Generation of a three-dimensional full thickness skin equivalent and automated wounding. *Jove* 2015;(96).
- Toledo DM, Huang M, Wang Y, *et al.* Molecular Analysis of a Skin Equivalent Tissue Culture Model System of Systemic Sclerosis Using RNA Sequencing, Epigenetic Assays, Histology, and Immunoassays [abstract]. *Arthritis Rheumatol* 2018;70(suppl 10).
- Maschmeyer I, Lorenz AK, Schimek K, *et al.* A four-organ-chip for interconnected long-term co-culture of human intestine, liver, skin and kidney equivalents. *Lab Chip* 2015;15:2688–99.
- Abaci HE, Guo Z, Coffman A, *et al.* Human skin constructs with spatially controlled vasculature using primary and iPSC-derived endothelial cells. *Adv Healthc Mater* 2016;5:1800–7.
- Mori N, Morimoto Y, Takeuchi S. Skin integrated with perfusable vascular channels on a CHIP. *Biomaterials* 2017;116:48–56.
- Yasuoka H, Larregina AT, Yamaguchi Y, *et al.* Human skin culture as an *ex vivo* model for assessing the fibrotic effects of insulin-like growth factor binding proteins. *Open Rheumatol J* 2008;2:17–22.
- Yamaguchi Y, Takihara T, Chambers RA, *et al.* A peptide derived from endostatin ameliorates organ fibrosis. *Sci Transl Med* 2012;4:136ra71.
- Watanabe T, Frost DB, Mlakar L, *et al.* A human skin model recapitulates systemic sclerosis dermal fibrosis and identifies COL22A1 as a TGF β early response gene that mediates fibroblast to myofibroblast transition. *Genes* 2019;10:75.

EPIDEMIOLOGICAL SCIENCE

Knee osteoarthritis risk in non-industrial societies undergoing an energy balance transition: evidence from the indigenous Tarahumara of Mexico

Ian J Wallace,¹ David T Felson,^{2,3} Steven Worthington,⁴ Jeffrey Duryea,⁵ Margaret Clancy,² Piran Aliabadi,⁵ Geeta N Eick,⁶ J Josh Snodgrass,⁶ Aaron L Baggish,⁷ Daniel E Lieberman¹

Handling editor Josef S Smolen

► Additional material is published online only. To view please visit the journal online (<http://dx.doi.org/10.1136/annrheumdis-2019-215886>).

For numbered affiliations see end of article.

Correspondence to

Ian J Wallace;
iwallace@fas.harvard.edu
Daniel E Lieberman;
danlieb@fas.harvard.edu

Received 12 June 2019

Revised 29 August 2019

Accepted 30 August 2019

Published Online First

13 September 2019

ABSTRACT

Non-industrial societies with low energy balance levels are expected to be less vulnerable than industrial societies to diseases associated with obesity including knee osteoarthritis. However, as non-industrial societies undergo rapid lifestyle changes that promote positive energy balance, individuals whose metabolisms are adapted to energetic scarcity are encountering greater energy abundance, increasing their propensity to accumulate abdominal adipose tissue and thus potentially their sensitivity to obesity-related diseases. **Objectives** Here, we propose that knee osteoarthritis is one such disease for which susceptibility is amplified by this energy balance transition.

Methods Support for our hypothesis comes from comparisons of knee radiographs, knee pain and anthropometry among men aged ≥ 40 years in two populations: Tarahumara subsistence farmers in Mexico undergoing the energy balance transition and urban Americans from Framingham, Massachusetts.

Results We show that despite having markedly lower obesity levels than the Americans, the Tarahumara appear predisposed to accrue greater abdominal adiposity (ie, larger abdomens) for a given body weight, and are more vulnerable to radiographic and symptomatic knee osteoarthritis at lower levels of body mass index. Also, proportionate increases in abdomen size in the two groups are associated with greater increases in radiographic knee osteoarthritis risk among the Tarahumara than the Americans, implying that the abdominal adipose tissue of the Tarahumara is a more potent stimulus for knee degeneration.

Conclusions Heightened vulnerability to knee osteoarthritis among non-industrial societies experiencing rapid lifestyle changes is a concern that warrants further investigation since such groups represent a large but understudied fraction of the global population.

INTRODUCTION

Knee osteoarthritis (OA) is a major public health concern in developed and newly industrialised countries,¹ yet relatively little is known about the disease's prevalence in non-industrial societies including hunter-gatherers and subsistence farmers.² Although risk of knee OA is influenced by numerous factors including age, sex and certain genes, multiple lines of evidence indicate that the

Key messages

What is already known about this subject?

► Non-industrial societies worldwide are experiencing rapid lifestyle changes that promote chronic positive energy balance, but the impact of such changes on knee osteoarthritis risk is unknown.

What does this study add?

► Based on data from Tarahumara subsistence farmers in Mexico, we propose that individuals in non-industrial societies undergoing an energy balance transition have a heightened sensitivity to knee osteoarthritis.
► Specifically, individuals born under conditions of energetic scarcity who later encounter greater energy abundance are predisposed to accumulate abdominal adipose tissue, making them susceptible to knee osteoarthritis at lower levels of body mass index.

How might this impact on clinical practice or future developments?

► Our findings suggest that the burden of knee osteoarthritis among non-industrial societies undergoing lifestyle changes is likely greater than realised and warrants increased attention.

high burden of the disease in industrialised nations is due in large part to the obesity epidemic.³ Obesity, defined as having a body mass index (BMI) of 30 kg/m² or higher, has the potential to contribute to knee OA pathogenesis by promoting chronic low-grade systemic inflammation, mechanically induced damage to joint tissues and local inflammation secondary to this damage, all of which may interact to weaken and degrade joint tissues.³ Thus, populations with a relatively low prevalence of obesity, as has been reported for many non-industrial societies,^{4,5} might be expected to exhibit proportionately low levels of knee OA.

In recent decades, however, non-industrial populations worldwide have been experiencing varying degrees of lifestyle change, including an energy balance transition characterised by shifts in diet and physical activity that have led to increases in BMI.^{6,7} Moreover, studies of groups undergoing this energy



© Author(s) (or their employer(s)) 2019. No commercial re-use. See rights and permissions. Published by BMJ.

To cite: Wallace IJ, Felson DT, Worthington S, et al. *Ann Rheum Dis* 2019;**78**:1693–1698.

balance transition have frequently documented a heightened sensitivity to obesity-related diseases for a given BMI relative to individuals in developed countries.^{8,9} The mechanisms underlying this amplified disease risk are complex and not fully understood, but early-life environmental conditions play an important role.^{10,11} Early development in energy-limited environments adapts individuals' metabolic phenotype to conditions of energetic scarcity, which may be beneficial in terms of short-term survival but potentially comes at the cost of increased susceptibility to metabolic dysregulation later in life if energy becomes more abundant.^{12,13} As a result of this 'thrifty phenotype',¹⁴ numerous populations undergoing the energy balance transition are experiencing rapidly rising rates of cardiometabolic disorders such as type 2 diabetes, hypertension and coronary heart disease,^{15,16} all of which are often comorbid with knee OA,³ implying that the threat of knee OA in non-industrial societies could be higher than perhaps expected.

Among the most salient characteristics of the metabolic phenotype of individuals born in energy-limited environments but later exposed to greater energy abundance is a propensity to preferentially accumulate and maintain visceral adipose tissue,^{17,18} typically resulting in a relatively large abdomen circumference for a given body weight.¹⁹ Excess visceral adipose tissue is a potent source of adipokines that promote chronic low-grade systemic inflammation,²⁰ including IL-6, TNF- α , leptin and others that may contribute to knee OA pathogenesis.²¹ Moreover, experimental evidence suggests that individuals whose metabolic phenotype is adapted to energetic scarcity are not only more prone to possessing large amounts of visceral adipose tissue under conditions of energetic abundance, but their adipocytes also secrete higher concentrations of pro-inflammatory adipokines.^{22,23} Therefore, it is reasonable to hypothesise that non-industrial populations experiencing the energy balance transition may not only have an enhanced susceptibility to knee OA for a given BMI, but also that abdomen size among such

groups is a stronger determinant of knee OA risk than in industrialised countries.

Here, we test this model of heightened knee OA risk among non-industrial societies undergoing the energy balance transition by comparing the probability of knee OA and its association with BMI and abdomen size in two groups: the Tarahumara, an indigenous population of subsistence farmers living in the Sierra Madre Occidental of Mexico (figure 1); and a well-studied urban population of Americans from Framingham, Massachusetts.^{24,25} The Tarahumara grow and eat mostly maize and beans and tend to be very physically active due to their non-mechanised farming methods, lack of motorised vehicles and the mountainous terrain in which they typically walk long daily distances to collect water, firewood and other resources.^{26,27} Notwithstanding, few Tarahumara remain isolated from outside economic and cultural influences. In particular, recent expansion of the market economy in the Sierra Madre Occidental has increased the availability of inexpensive processed foods and drinks, which the Tarahumara afford by supplementing their farming with temporary paid work and government aid. As a result, Tarahumara diets have been shifting to include more high-fat, high-sugar processed foods,²⁸ and food preparation increasingly involves frying rather than using the more traditional methods of roasting or boiling.²⁹ Consequently, while anthropometric data from decades ago indicate that obesity used to be extremely rare among the Tarahumara,^{30,31} recent surveys suggest it is now a growing health concern.^{27,32}

This study tested four predictions: First, because the Tarahumara are still in the early stages of the energy balance transition, we predicted that they would have lower average BMIs and obesity levels than individuals from Framingham. However, second, due to early-life exposure to energy limitation, we predicted that Tarahumara experiencing the energy balance transition would tend to grow larger abdomen sizes for a given body weight compared with Framingham individuals. Third, as



Figure 1 Tarahumara subsistence farming. *Top, left:* clearing a field with a machete. *Top, right:* tilling a field with a donkey-drawn plough. *Bottom, left:* weeding a field by hand. *Bottom, right:* carrying harvested stalks of chia. Photos by David Ramos and used here with permission.

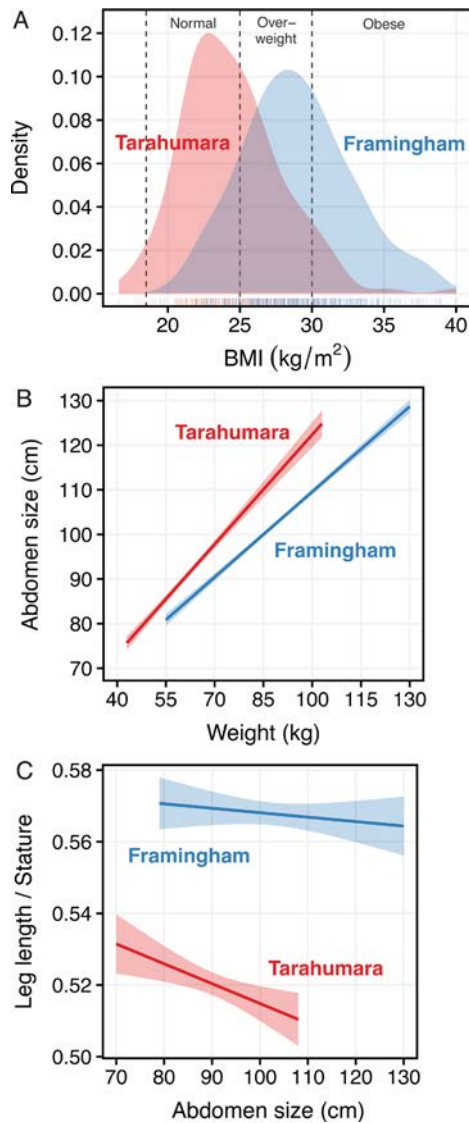


Figure 2 Anthropometric comparisons of the Tarahumara and Framingham individuals. (A) Density plot of body mass index (BMI) with thresholds for overweight and obesity indicated. (B) Association between body weight and abdomen size controlling for age. (C) Association between abdomen size and relative leg length (leg length/stature) controlling for age. Note that in (C), leg length was measured slightly differently among Tarahumara and Framingham individuals, so the difference in y-intercepts does not accurately reflect a group difference in relative leg length. Shading in (B) and (C) represents 95% CIs.

a result of this mismatch between metabolic phenotypes adapted to energetic scarcity and later-life greater energy availability, we predicted that the Tarahumara would have a higher risk of knee OA for a given BMI than Framingham individuals. Fourth and finally, we predicted that abdomen size would be a stronger predictor of knee OA risk among the Tarahumara than individuals from Framingham.

METHODS

Participants

The Tarahumara sample consists of 157 men aged 40–92 years (average \pm SD: 62 \pm 12 years) from the regions around the Sinfarosa and Urique Canyons in the southwestern portion of the Mexican state of Chihuahua. Participants were recruited in

2015 and 2016 by word of mouth with the help of local residents and transported to clinics in the towns of Guachochi and Cerocahui where they were examined. Although our model of heightened knee OA risk among groups experiencing the energy balance transition applies as much to women as men, we were unable to collect data from Tarahumara women because of their inability to devote sufficient time to travelling to and from the clinics. To maximise participation, our research was scheduled during seasons when time devoted to farming was at a minimum, but seasonal downturns in farming activity had a greater impact on male than female workloads. The Framingham sample includes 565 white men who were members of the Offspring Cohort of the Framingham Osteoarthritis Study,^{24,25} aged 40–94 years (average \pm SD: 66 \pm 9 years), who were examined at local clinics between 2002 and 2005. All participants were recruited without respect to knee pain or other health complaints. Basic information about participants' lifestyles obtained from questionnaires is provided in online supplementary material 1.

Anthropometry, knee radiographs and pain assessment

Each participant's stature, body weight and abdomen circumference were measured. In addition, measurements of leg length from a subset of participants in each group (n=101 Tarahumara; n=88 Framingham individuals) were available from prior research.^{33,34} Leg length was measured as greater trochanter height and umbilical height among the Tarahumara and Framingham individuals, respectively. Relative leg length, calculated as the ratio of leg length to stature, is a well-established surrogate measure of an individual's energy availability during prenatal and early postnatal development, with a short relative leg length being indicative of an energetically limited early-life environment.^{35,36}

A single weight-bearing posteroanterior fixed-flexion radiograph of both knees was obtained from all participants using a SynaFlexer x-ray positioning frame following a standardised protocol.³⁷ Radiographic features of the knees were assessed using the Kellgren/Lawrence scale³⁸ of 0–4 based on the presence of osteophytes, joint space narrowing, sclerosis and cysts. Presence of radiographic knee OA was defined as having a Kellgren/Lawrence score of 2 or greater in one or both knees.

All participants were asked in Rarámuri (the native language of the Tarahumara), Spanish or English the following question: "On most days, do you have pain in your knee?" Individuals were considered to have symptomatic knee OA if they had both knee pain and radiographic knee OA in one or both knees.

Statistical analyses

Data from Tarahumara and Framingham participants were compared using generalised linear models, from which we report unstandardised point estimates and 95% confidence intervals (CIs). An alpha level of 0.05 was set for statistical significance and all tests were two-tailed. Analyses were performed in R v 3.5.1. Further details on the statistical models, results of model goodness-of-fit tests and summary statistics for raw data are reported in online supplementary material 2.

RESULTS

Across all participants (n=722), after controlling for age, Tarahumara BMIs (adjusted mean, 24.3 kg/m²; 95% CI 23.8 to 24.9 kg/m²) were, on average, 17% lower (95% CI 15% to 20%; $p < 0.0001$) than those of Framingham individuals (adjusted mean, 29.4 kg/m²; 95% CI 29.0 to 29.8 kg/m²) (figure 2A). After controlling for age, the probability of obesity (BMI \geq 30) among

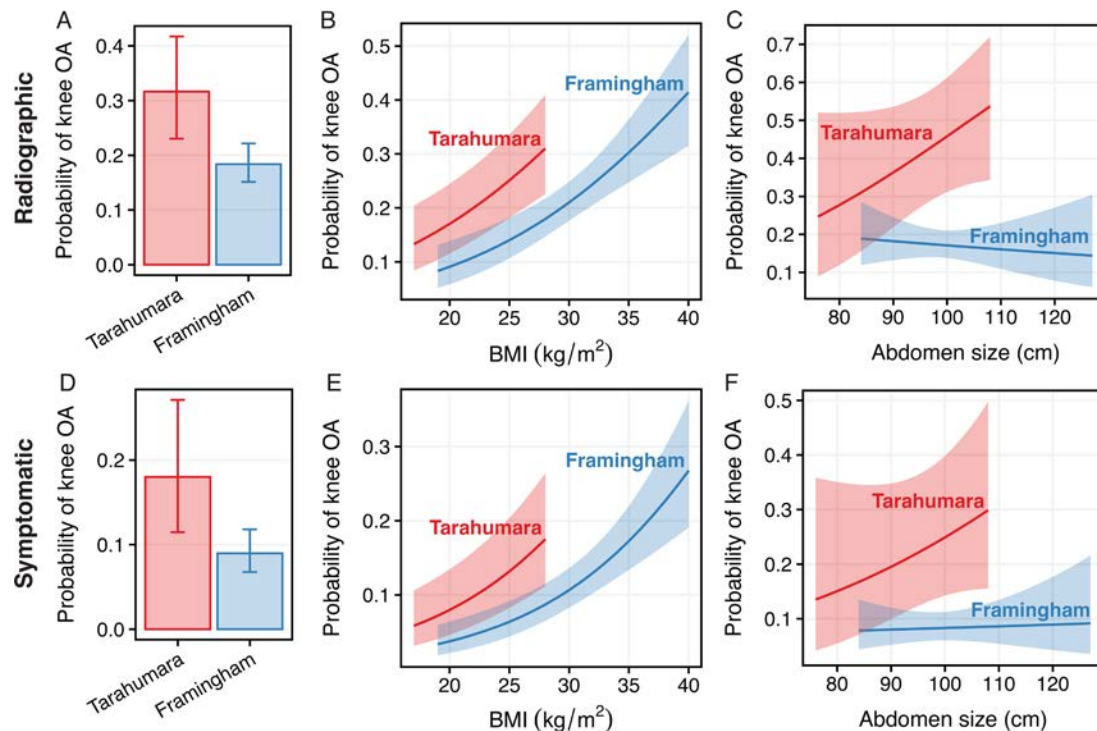


Figure 3 Comparison of knee osteoarthritis (OA) probability and its association with body mass index (BMI) and abdomen size among the Tarahumara and Framingham individuals. (A) Probability of radiographic knee OA controlling for BMI and age. (B) Association between radiographic knee OA probability and BMI controlling for age. (C) Association between radiographic knee OA probability and abdomen size controlling for age and body weight. (D) Probability of symptomatic knee OA controlling for BMI and age. (E) Association between symptomatic knee OA probability and BMI controlling for age. (F) Association between symptomatic knee OA probability and abdomen size controlling for age and body weight. Whiskers in (A) and (D) and shading in (B), (C), (E) and (F) represent 95% CIs.

the Tarahumara (6%; 95%CI 3% to 11%) was 35% lower (95%CI 26% to 41%; $p < 0.0001$) than among Framingham individuals (41%; 95%CI 37% to 45%). The probability of being overweight ($25 \leq \text{BMI} < 30$) was 13% lower (95%CI 1% to 24%; $p = 0.023$) among the Tarahumara (32%; 95%CI 25% to 39%) than Framingham individuals (45%; 95%CI 41% to 49%) after controlling for age. However, controlling for body weight and age, Tarahumara abdomen circumferences (adjusted mean, 109.3 cm; 95%CI 107.6 to 111.0 cm) were larger ($p < 0.0001$) than those of Framingham individuals (adjusted mean, 99.4 cm; 95%CI 98.8 to 99.9 cm) (figure 2B; see also online supplementary material 3). Controlling for age, abdomen size was negatively associated with relative leg length among the Tarahumara ($p = 0.0042$) but not among Framingham individuals ($p = 0.38$) (figure 2C).

Radiographic knee OA was present in 24% (38/157) of the Tarahumara participants and 24% (135/565) of Framingham individuals. The probability of having radiographic knee OA increased with BMI and age across all participants ($p < 0.0001$ for both variables), but after controlling for BMI and age, radiographic knee OA probability among the Tarahumara (32%; 95%CI 23% to 42%) was 13% higher (95%CI 1% to 27%; $p = 0.0057$) than among Framingham individuals (18%; 95%CI 15% to 22%) (figure 3A,B). Among the Tarahumara, the probability of radiographic knee OA increased more markedly with greater abdomen circumference than among Framingham individuals (group \times abdomen size interaction: $p = 0.041$) after controlling for age and body weight (figure 3C).

Symptomatic knee OA was diagnosed in 13% (21/157) and 13% (71/565) of the Tarahumara and Framingham participants, respectively. BMI and age were positively associated

with symptomatic knee OA probability ($p < 0.0001$ for both variables across all participants), but after adjusting for BMI and age, symptomatic knee OA probability among the Tarahumara (18%; 95%CI 11% to 27%) was 9% higher (95%CI 0% to 20%; $p = 0.0092$) than among Framingham individuals (9%; 95%CI 7% to 12%) (figure 3D,E). Controlling for age and body weight, symptomatic knee OA probability tended to increase more markedly with greater abdomen size among Tarahumara than Framingham individuals (figure 3F), but not significantly so (group \times abdomen size interaction: $p = 0.27$).

DISCUSSION

Previous research has demonstrated that individuals born in energy-limited environments who are later exposed to greater energy abundance often have a heightened sensitivity to obesity-related diseases including type 2 diabetes, hypertension and coronary heart disease.^{10–13} Building on this work, we have proposed a model of heightened knee OA risk among non-industrial societies undergoing the energy balance transition and tested predictions of this model by comparing the probability of the disease and its association with BMI and abdomen size among an indigenous group of subsistence farmers in Mexico, the Tarahumara, relative to urban Americans from Framingham, Massachusetts. Overall, the results support four key predictions of our model. First, as expected for a population still in the early stages of the energy balance transition, the Tarahumara were found to have lower average BMIs and obesity levels than individuals from Framingham. Nevertheless, second, the Tarahumara tended to have larger abdomens for a given body weight than Framingham individuals, indicating relatively greater abdominal adiposity,

a potent source of adipokines that promote chronic low-grade systemic inflammation.^{20 21} Moreover, abdomen size among the Tarahumara was negatively associated with relative leg length, an established biomarker of early-life nutritional environment,^{35 36} suggesting that larger abdomen sizes among the Tarahumara derived from the interaction between scarcity-adapted metabolisms and later-life energy abundance. Third, in association with this relatively low-BMI, large-abdomen phenotype, the Tarahumara exhibited a heightened susceptibility to radiographic and symptomatic knee OA for a given BMI compared with Framingham individuals. In addition, fourth, proportionate increases in abdomen size in the two groups were associated with greater increases in radiographic knee OA risk among the Tarahumara than individuals from Framingham, implying that the abdominal adipose tissue of the Tarahumara was a more potent stimulus for knee tissue degeneration. These findings suggest that risk of knee OA among non-industrial populations undergoing the energy balance transition is likely greater than would be expected based on the prevalence of obesity alone. Instead, our findings suggest that knee OA is yet another obesity-related disease to which risk is enhanced by mismatches between early-life and later-life energy availability.

Although our model emphasises the contribution of chronic low-grade systemic inflammation to knee OA pathogenesis, another factor that often plays an important role is mechanically induced joint tissue damage.³⁹ Since physical activity is the most common source of knee loading, it is important to consider to what extent the Tarahumara's relatively high activity levels might have affected their risk of knee OA. Routine activity engendering knee loads within the normal physiological range is not inherently harmful to knee tissues,³ as illustrated by the fact that habitual long-distance runners are not more prone to knee OA than non-runners.^{40 41} Nevertheless, activities that expose knees to abnormal, supraphysiological loads undoubtedly have the potential to damage joint tissues, explaining the strong association between traumatic injuries and knee OA.³⁹ It is thus notable that during examinations, all participants in this study were asked whether they had ever experienced a knee injury that limited their ability to walk for more than 3 days, and only 18% (7/38) of the Tarahumara with radiographic knee OA reported ever having had such an injury, compared with 30% (40/135) of Framingham individuals with radiographic disease (Fisher's exact test: $p=0.22$). Also, among Tarahumara and Framingham participants who were not diagnosed with knee OA, we measured knee joint space width (a proxy for cartilage thickness) from radiographs using an established protocol⁴² and found that while joint space width declined with age in both groups (online supplementary material 4), age-related joint space thinning was not more rapid among the Tarahumara than Framingham individuals (general linear model, group \times age interaction: $p=0.98$). Therefore, the Tarahumara's active lifestyles do not appear to have distinctly predisposed them to either injury-related knee OA or generally greater joint tissue degeneration throughout life. Ultimately, based on available evidence, if Tarahumara activity patterns influenced susceptibility to knee OA, we speculate that it was not primarily because the loads their knees sustained were abnormally high, but that due to the energy balance transition, knee loading in many individuals occurred in the context of chronic low-grade systemic inflammation that weakened their joint tissues.

This study has important limitations. First, we were able to collect data only from a relatively small sample of Tarahumara men and no women, and thus the degree to which the vulnerability to knee OA of the participants in this study is representative

of the overall Tarahumara population is unclear. Second, our model assumes that the effect of the energy balance transition on abdominal adiposity (and hence knee OA risk) depends on an individual's energy status during early development, yet we lack direct information on this. Nevertheless, our finding that relative leg length was negatively associated with abdomen size among the Tarahumara provides indirect support for our model.^{35 36} Third, while our model assumes that the primary pathway by which greater abdominal adiposity affects knee OA risk is through higher levels of chronic low-grade systemic inflammation, logistical difficulties prevented us from collecting data on most biomarkers of inflammation from the Tarahumara. We were able, however, to measure C-reactive protein (CRP) levels from dried blood spots using an established protocol⁴³ in a subset of the Tarahumara, and as would be expected, CRP levels were found to be positively associated with abdomen size (general linear model, $p=0.013$) after controlling for age and body weight (online supplementary material 5). Although CRP is a non-specific marker of inflammation that is associated with knee OA pain but not radiographic disease,⁴⁴ these data underscore the link between abdomen size and systemic inflammation levels. Fourth, differences in anthropometry and knee OA risk between Tarahumara and Framingham individuals are interpreted as being primarily due to environmental factors, but we cannot rule out that genetic variation was partly responsible for some of the patterns detected between groups. Even so, at least in terms of knee OA risk, we would expect any influence of genetics to have been limited given that alleles affecting disease susceptibility have relatively small effect sizes.⁴⁵ Moreover, the vast majority of genetic diversity among humans is accounted for within populations,⁴⁶ and there is currently little evidence that alleles affecting knee OA risk are biased towards the small fraction of genetic diversity that exists between populations.

Finally, the results of this study provide further evidence supporting the hypothesis that knee OA represents an example of a 'mismatch disease' that is caused in part by human bodies being inadequately or imperfectly adapted to novel features of modern environments.² However, whereas prior discussions of this hypothesis have focused on the extent to which knee OA stems from deleterious interactions between modern environments and the genes we inherited from ancient ancestors who evolved in markedly different environments,^{2 3} this study highlights the potential contribution to knee OA risk by another form of mismatch, one which reflects processes operating on a much shorter timescale, within just a single generation.^{12 13} Ultimately, more data are needed from the Tarahumara and other non-industrial groups to determine more precisely the magnitude and mechanisms of heightened knee OA risk faced by individuals born in energy-limited environments who later experience greater energy abundance. In all likelihood, both evolutionary and developmental mismatches play important roles in the growing burden of knee OA worldwide, yet the potential impact of mismatches between early-life and later-life energy availability is especially alarming and warrants special attention, as non-industrial societies undergoing the energy balance transition comprise a large fraction of the global population⁴⁷ and typically receive little attention from health and prevention services.⁴⁸

Author affiliations

¹Department of Human Evolutionary Biology, Peabody Museum, Harvard University, Cambridge, Massachusetts, USA

²Rheumatology Section, Boston University School of Medicine, Boston, Massachusetts, USA

³NIHR Manchester Musculoskeletal Biomedical Research Centre, Manchester University Hospitals NHS Foundation Trust, Manchester, UK

⁴Institute for Quantitative Social Science, Harvard University, Cambridge, Massachusetts, USA

⁵Department of Radiology, Brigham and Women's Hospital, Harvard Medical School, Boston, Massachusetts, USA

⁶Department of Anthropology, University of Oregon, Eugene, Oregon, USA

⁷Cardiovascular Performance Program, Massachusetts General Hospital, Harvard Medical School, Boston, Massachusetts, USA

Correction notice This article has been corrected since it published Online First. The author details have been updated.

Acknowledgements For help with research in Mexico, we are especially grateful to Mickey Mahaffey and Silvano Cubesare, as well as Christine Aguilar, Marcel Brown, Nicholas Holowka, David Ramos, Humberto Ramos and Gabriela Yañez. For additional help with the study, we thank Carrie Brown, Shane Emmett, Marian Hannan, Chris Kuzawa, John Lynch, Douglas Kiel, Jonathan Stieglitz and Xianbang Sun.

Contributors IJW, DTF, SW and DEL designed research. IJW, DTF, JD, MC, PA, GNE, JJS, ALB and DEL performed research. IJW and SW analysed data. IJW, DTF, SW and DEL wrote the paper.

Funding Supported by the Hintze Family Charitable Foundation, the American School of Prehistoric Research (Harvard University) and the National Institute of Arthritis and Musculoskeletal and Skin Diseases (National Institutes of Health).

Competing interests None declared.

Patient and public involvement statement During fieldwork in Mexico, local Tarahumara community leaders were consulted regarding the study design and conduct, but study participants were not involved in the work.

Patient consent for publication Not required.

Ethics approval Approved by the institutional review boards of Boston University Medical Center, Harvard University and Massachusetts General Hospital.

Provenance and peer review Not commissioned; externally peer reviewed.

Data availability statement Data from the Tarahumara are available on reasonable request to IJW or DEL. Data from the Framingham individuals may be obtained from a third party (www.framinghamheartstudy.org).

REFERENCES

- Vos T, Flaxman AD, Naghavi M, *et al*. Years lived with disability (YLDs) for 1160 sequelae of 289 diseases and injuries 1990–2010: a systematic analysis for the Global Burden of Disease Study 2010. *Lancet* 2012;380:2163–96.
- Wallace IJ, Worthington S, Felson DT, *et al*. Knee osteoarthritis has doubled in prevalence since the mid-20th century. *Proc Natl Acad Sci U S A* 2017;114:9332–6.
- Berenbaum F, Wallace IJ, Lieberman DE, *et al*. Modern-day environmental factors in the pathogenesis of osteoarthritis. *Nat Rev Rheumatol* 2018;14:674–81.
- Walker R, Gurven M, Hill K, *et al*. Growth rates and life histories in twenty-two small-scale societies. *Am J Hum Biol* 2006;18:295–311.
- Pontzer H, Wood BM, Raichlen DA. Hunter-gatherers as models in public health. *Obes Rev* 2018;19(Suppl 1):24–35.
- Popkin BM. The nutrition transition in the developing world. *Dev Policy Rev* 2003;21:581–97.
- Kraft TS, Stieglitz J, Trumble BC, *et al*. Nutrition transition in 2 lowland Bolivian subsistence populations. *Am J Clin Nutr* 2018;108:1183–95.
- Huxley R, James WPT, Barzi F, *et al*. Ethnic comparisons of the cross-sectional relationships between measures of body size with diabetes and hypertension. *Obes Rev* 2008;9(Suppl 1):53–61.
- Chan JCN, Malik V, Jia W, *et al*. Diabetes in Asia: epidemiology, risk factors, and pathophysiology. *JAMA* 2009;301:2129–40.
- McMillen IC, Robinson JS. Developmental origins of the metabolic syndrome: prediction, plasticity, and programming. *Physiol Rev* 2005;85:571–633.
- Rinaudo P, Wang E. Fetal programming and metabolic syndrome. *Annu Rev Physiol* 2012;74:107–30.
- Gluckman PD, Hanson MA, Cooper C, *et al*. Effect of in utero and early-life conditions on adult health and disease. *N Engl J Med* 2008;359:61–73.
- Kuzawa CW, Gluckman PD, Hanson MA. Evolution, developmental plasticity, and metabolic disease. In: Stearns SC, Koella JC, eds. *Evolution in health and disease*. Oxford: Oxford Univ Press, 2008: 253–64.
- Hales CN, Barker DJP. The thrifty phenotype hypothesis. *Br Med Bull* 2001;60:5–20.
- Zhou B, Lu Y, Hajifathalian K, *et al*. Worldwide trends in diabetes since 1980: a pooled analysis of 751 population-based studies with 4.4 million participants. *Lancet* 2016;387:1513–30.
- Forouzanfar MH, Liu P, Roth GA, *et al*. Global burden of hypertension and systolic blood pressure of at least 110 to 115 mm Hg, 1990–2015. *JAMA* 2017;317:165–82.
- Wells JCK. The thrifty phenotype: an adaptation in growth or metabolism? *Am J Hum Biol* 2011;23:65–75.
- West-Eberhard MJ. Nutrition, the visceral immune system, and the evolutionary origins of pathogenic obesity. *Proc Natl Acad Sci U S A* 2019;116:723–31.
- Yajnik CS. Early life origins of insulin resistance and type 2 diabetes in India and other Asian countries. *J Nutr* 2004;134:205–10.
- Ouchi N, Parker JJ, Lugus JJ, *et al*. Adipokines in inflammation and metabolic disease. *Nat Rev Immunol* 2011;11:85–97.
- Robinson WH, Lepus CM, Wang Q, *et al*. Low-grade inflammation as a key mediator of the pathogenesis of osteoarthritis. *Nat Rev Rheumatol* 2016;12:580–92.
- Symonds ME, Pope M, Sharkey D, *et al*. Adipose tissue and fetal programming. *Diabetologia* 2012;55:1597–606.
- Khanal P, Nielsen MO. Maternal undernutrition and visceral adiposity. In: Rajendram R, Preedy VR, Patel VB, eds. *Diet, nutrition, and fetal programming*. New York: Humana Press, 2017: 91–105.
- Nguyen U-SDT, Zhang Y, Zhu Y, *et al*. Increasing prevalence of knee pain and symptomatic knee osteoarthritis: survey and cohort data. *Ann Intern Med* 2011;155:725–32.
- Niu J, Clancy M, Aliabadi P, *et al*. Metabolic syndrome, its components, and knee osteoarthritis: the Framingham Osteoarthritis Study. *Arthritis Rheumatol* 2017;69:1194–203.
- Cerqueira MT, Fry MM, Connor WE. The food and nutrient intakes of the Tarahumara Indians of Mexico. *Am J Clin Nutr* 1979;32:905–15.
- Christensen DL, Alcalá-Sánchez I, Leal-Berumen I, *et al*. Physical activity, cardio-respiratory fitness, and metabolic traits in rural Mexican Tarahumara. *Am J Hum Biol* 2012;24:558–61.
- Monárrez-Espino J, Greiner T, Hoyos RC. Perception of food and body shape as dimensions of Western acculturation potentially linked to overweight in Tarahumara women of Mexico. *Ecol Food Nutr* 2004;43:193–212.
- Monárrez-Espino J, Greiner T. Anthropometry in Tarahumara Indian women of reproductive age in northern Mexico: is overweight becoming a problem? *Ecol Food Nutr* 2000;39:437–57.
- Basauri C. *Monografía de los Tarahumaras*. Mexico: Talleres Graficos de la Nacion, 1929.
- Connor WE, Cerqueira MT, Connor RW, *et al*. The plasma lipids, lipoproteins, and diet of the Tarahumara Indians of Mexico. *Am J Clin Nutr* 1978;31:1131–42.
- Moreno-Ulloa J, Moreno-Ulloa A, Martínez-Tapia M, *et al*. Comparison of the prevalence of metabolic syndrome and risk factors in urban and rural Mexican Tarahumara-foot runners. *Diabetes Res Clin Pract* 2018;143:79–87.
- Hagedorn TJ, Dufour AB, Riskowski JL, *et al*. Foot disorders, foot posture, and foot function: the Framingham Foot Study. *PLoS One* 2013;8:e74364.
- Wallace IJ, Koch E, Holowka NB, *et al*. Heel impact forces during barefoot versus minimally shod walking among Tarahumara subsistence farmers and urban Americans. *R Soc Open Sci* 2018;5.
- Bogin B, Varela-Silva MI. Leg length, body proportion, and health: a review with a note on beauty. *Int J Environ Res Public Health* 2010;7:1047–75.
- Lelijveld N, Seal A, Wells JC, *et al*. Chronic disease outcomes after severe acute malnutrition in Malawian children (ChroSAM): a cohort study. *Lancet Glob Health* 2016;4:e654–62.
- Peterfy C, Li J, Zaim S, *et al*. Comparison of fixed-flexion positioning with fluoroscopic semi-flexed positioning for quantifying radiographic joint-space width in the knee: test–retest reproducibility. *Skeletal Radiol* 2003;32:128–32.
- Kellgren JH, Lawrence JS. Radiological assessment of osteo-arthrosis. *Ann Rheum Dis* 1957;16:494–502.
- Felson DT. Osteoarthritis as a disease of mechanics. *Osteoarthritis Cartilage* 2013;21:10–5.
- Lo GH, Driban JB, Kriska AM, *et al*. History of running is not associated with higher risk of symptomatic knee osteoarthritis: a cross-sectional study from the osteoarthritis initiative. *Arthritis Care Res* 2017;69:183–91.
- Timmins KA, Leech RD, Batt ME, *et al*. Running and knee osteoarthritis: a systematic review and meta-analysis. *Am J Sports Med* 2017;45:1447–57.
- Duryea J, Li J, Peterfy CG, *et al*. Trainable rule-based algorithm for the measurement of joint space width in digital radiographic images of the knee. *Med Phys* 2000;27:580–91.
- Urlacher SS, Ellison PT, Sugiyama LS, *et al*. Tradeoffs between immune function and childhood growth among Amazonian forager-horticulturalists. *Proc Natl Acad Sci U S A* 2018;115:E3914–21.
- Jin X, Beguerie JR, Zhang W, *et al*. Circulating C reactive protein in osteoarthritis: a systematic review and meta-analysis. *Ann Rheum Dis* 2015;74:703–10.
- Panoutsopoulou K, Zeggini E. Advances in osteoarthritis genetics. *J Med Genet* 2013;50:715–24.
- Li JZ, Absher DM, Tang H, *et al*. Worldwide human relationships inferred from genome-wide patterns of variation. *Science* 2008;319:1100–4.
- Bixby H, Benthham J, Zhou B, *et al*. Rising rural body-mass index is the main driver of the global obesity epidemic in adults. *Nature* 2019;569:260–4.
- Stephens C, Nettleton C, Porter J, *et al*. Indigenous peoples' health—why are they behind everyone, everywhere? *Lancet* 2005;366:10–3.

TRANSLATIONAL SCIENCE

Discovery of an autoantibody signature for the early diagnosis of knee osteoarthritis: data from the Osteoarthritis Initiative

María Camacho-Encina,¹ Vanesa Balboa-Barreiro,² Ignacio Rego-Perez,³ Florencia Picchi,¹ Jennifer VanDuin,⁴ Ji Qiu,⁴ Manuel Fuentes,⁵ Natividad Oreiro,⁶ Joshua LaBaer,⁴ Cristina Ruiz-Romero ,¹ Francisco J Blanco ⁷

Handling editor Josef S Smolen

► Additional material is published online only. To view please visit the journal online (<http://dx.doi.org/10.1136/annrheumdis-2019-215325>).

For numbered affiliations see end of article.

Correspondence to

Dr Francisco J Blanco, Servicio de Reumatología, INIBIC-Hospital Universitario A Coruña, A Coruña 15006, Spain; fblagar@sergas.es
Dr Cristina Ruiz-Romero; cristina.ruiz.romero@sergas.es

Received 11 March 2019

Revised 23 July 2019

Accepted 22 August 2019

Published Online First

30 August 2019

ABSTRACT

Objective To find autoantibodies (AABs) in serum that could be useful to predict incidence of radiographic knee osteoarthritis (KOA).

Design A Nucleic-acid Programmable Protein Arrays (NAPPA) platform was used to screen AABs against 2125 human proteins in sera at baseline from participants free of radiographic KOA belonging to the incidence and non-exposed subcohorts of the Osteoarthritis Initiative (OAI) who developed or not, radiographic KOA during a follow-up period of 96 months. NAPPA-ELISA were performed to analyse reactivity against methionine adenosyltransferase two beta (MAT2 β) and verify the results in 327 participants from the same subcohorts. The association of MAT2 β -AAB levels with KOA incidence was assessed by combining several robust biostatistics analysis (logistic regression, Receiver Operating Characteristic and Kaplan-Meier curves). The proposed prognostic model was replicated in samples from the progression subcohort of the OAI.

Results In the screening phase, six AABs were found significantly different at baseline in samples from incident compared with non-incident participants. In the verification phase, high levels of MAT2 β -AAB were significantly associated with the future incidence of KOA and with an earlier development of the disease. The incorporation of this AAB in a clinical model for the prognosis of incident radiographic KOA significantly improved the identification/classification of patients who will develop the disorder. The usefulness of the model to predict radiographic KOA was confirmed on a different OAI subcohort.

Conclusions The measurement of AABs against MAT2 β in serum might be highly useful to improve the prediction of OA development, and also to estimate the time to incidence.

INTRODUCTION

Osteoarthritis (OA) is the most common arthritic disease involving movable joints and it is increasingly important in current ageing populations, leading to patient chronic disability.^{1,2} The current diagnostic methods are insensitive to detect the small changes occurring at early stages, when OA is characterised as an asymptomatic disease.¹ To solve this problem, a molecular level of interrogation is hypothesised as the only alternative to detect the earliest phases of the disease process.²

Key messages

What is already known about this subject?

- Autoantibodies (AABs) are used as biomarkers in autoimmune diseases such as rheumatoid arthritis or systemic lupus erythematosus. In these and other plethora of disorders, they can be detected at asymptomatic stages.
- Although the presence of AABs has been reported in the serum of patients with osteoarthritis (OA), they had not been previously associated with the incidence or progression of this disease.

What does this study add?

- A specific panel of AABs has been detected at baseline in individuals developing incident radiographic knee OA (KOA) during a 96-month follow-up period, compared with those who remained healthy.
- Reactivity levels of AABs against the beta subunit of the methionine adenosyltransferase (MAT2 β -AAB) II enzyme are positively correlated with the time to OA incidence.

How might this impact on clinical practice or future developments?

- The addition of MAT2 β -Aab to a prognostic clinical model of incident radiographic KOA might significantly improve the identification at baseline of those individuals who will develop the disorder during a follow-up period of 96 months.

Although OA is not considered an autoimmune disease, cell stress and extracellular matrix degradation may activate maladaptive repair responses, including pro-inflammatory pathways of innate immunity.³ Activation of the immune response usually involves the production of immunoglobulins against self-proteins or autoantibodies (AABs), which can be detected in sera and used as biomarkers for early diagnosis.^{4,5} In this field, the Nucleic-Acid Programmable Protein Array (NAPPA) strategy has been widely used to detect AABs in a high-throughput manner in many diseases,^{6,7} and has been employed in an exploratory study on sera from patients with OA.⁸ The NAPPA arrays are



© Author(s) (or their employer(s)) 2019. Re-use permitted under CC BY-NC. No commercial re-use. See rights and permissions. Published by BMJ.

To cite: Camacho-Encina M, Balboa-Barreiro V, Rego-Perez I, et al. *Ann Rheum Dis* 2019;**78**:1699–1705.

generated by printing full-length cDNAs encoding the target proteins with a tag on the surface of the array.⁹ Proteins are then transcribed and translated by a mammalian cell-free system and captured in situ by immobilised antibodies specific for the tag encoded at the carboxy-terminus of the amino acid sequence.¹⁰

The Osteoarthritis Initiative (OAI) is an ideal target population to detect relevant biomarker characteristics of earlier stages of the disease. It is a multi-centre, longitudinal and observational cohort study that has enrolled 4796 individuals which have been followed during 96 months.^{11 12} Among all these subjects, the OAI comprises participants without clinically significant knee osteoarthritis (KOA) at baseline, but selected on the basis of having specific characteristics that give them an increased risk of developing incident symptomatic KOA (incidence subcohort), and a reference control group whose participants did not have neither symptomatic KOA nor risk factors at baseline (non-exposed subcohort).

In the present study, serum samples at baseline from the incidence and non-exposed subcohorts of the OAI were analysed using NAPPA technology for the discovery of an AAb profile that could be associated with an early and asymptomatic stage of the disease. The objective was to detect AABs useful to identify those asymptomatic individuals who will develop radiographic KOA before 96 months, and examine the putative relationship between their levels in serum and the time for OA incidence.

MATERIALS AND METHODS

Definition of incident radiographic KOA

In this case-control study, two main outcomes group, with one study knee per subject (target knee), were defined: the incident (n=146) and the non-incident group (n=181), both without clinically relevant radiographic KOA at baseline (Kellgren and Lawrence (KL) grade=0–1) in at least one knee (target knee). Incident radiographic KOA was defined by KL grade ≥ 2 in the target knee at some point between 12 and 96 months of follow-up.

Study design

A two-stage discovery approach (screening and verification) was designed to analyse the presence and putative usefulness of KOA-associated AABs to predict the incidence of the disorder. The sera were blindly analysed and belonged to Caucasian participants from the incidence and non-exposed subcohorts of the OAI at the baseline visit (181 non-incidents and 146 incidents at 96 months). The prognostic clinical model generated to predict KOA development was later replicated in a total of 108 participants (65 non-incidents and 43 incidents at 96 months) from the progression subcohort of the OAI at the baseline visit. Detailed information about the workflow of the study is summarised and illustrated in figure 1.

NAPPA profiling of serum AABs

The NAPPA core Centre for Personalised Diagnostics (CPD) at the Biodesign Institute (Arizona State University, USA) had all human genes from the DNASU (www.dnasu.org) on six different array sets: HC1–HC6. The HC5 set was selected for the screening on the basis of having the greatest number of genes that could be related with OA pathogenesis according to bibliography (listed in online supplementary table S1). The quality of DNA printing, protein expression and detection of the NAPPA slides were performed using the standard procedure of CPD,¹³ but incubating the expressed slides overnight with 150 μ L of 1:20 (v/v) diluted serum. A titration assay was performed using

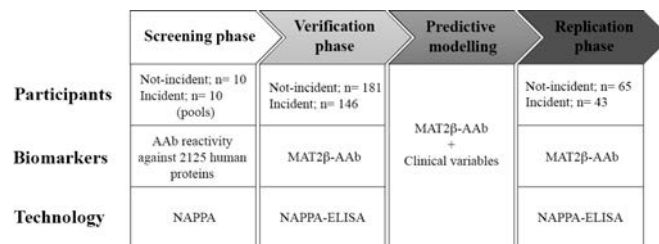


Figure 1 Study design. A two-stage discovery approach (screening and verification) was designed to investigate the putative utility of AABs to predict OA development. Sera from the non-exposed and incidence OAI subcohorts at baseline without radiographic KOA (KL=0–1) in at least one knee (target knee) were analysed in these two phases. Incident radiographic KOA was defined by KL ≥ 2 at 12–96 months of follow-up. In the *screening phase*, reactivity levels of AABs against 2125 proteins were evaluated in 10 pooled serum samples at baseline per Study Group (incident and non-incident) using the NAPPA platform. Each pool was prepared by mixing equal volumes of 10 individual sera. In the *verification phase*, the sensitivity and specificity of the baseline levels of MAT2 β -AAb to predict KOA incidence was confirmed by applying the NAPPA-ELISA technique on a total of 327 individual sera at baseline, which included the 200 samples used at the screening. Then, a logistic regression model was developed combining different clinical variables and MAT2 β -AAb levels. The clinical variables selected as covariates are listed in table 2. Finally, the proposed prognostic model was replicated in 108 individual sera at baseline from participants of the progression subcohort of the OAI without radiographic KOA. AABs, autoantibodies; KOA, knee osteoarthritis; KL, Kellgren and Lawrence; MAT2 β , methionine adenosyltransferase two beta; NAPPA, Nucleic-acid Programmable Protein Array; OA, osteoarthritis; OAI, Osteoarthritis Initiative.

serum dilutions from 1:20 down to 1:200 to identify an optimal dilution factor that provided an acceptable background without overwhelming the true signals.

The signal intensities obtained in the assay were normalised as described.¹⁴ To determine positive AAb response, a cut-off level was calculated by median intensity absolute deviation rule from all the spots through all the serum pools. The mean and SD of the mean were obtained for the incident and non-incident groups. The antigens that did not exhibit intensities over the cut-off were eliminated. A differential spot analysis was performed with the remaining antigens by Wilcoxon Rank-Sum test (p value < 0.05) and the area under the curve (AUC) at 95% specificity were calculated using the pROC package in R. In addition, AAb candidates were qualitatively examined by visual analysis through all the slides by adjusting in identical black and full colour threshold scale.

NAPPA-ELISA assay

In all, 500 ng of full-length methionine adenosyltransferase two beta (MAT2 β) human recombinant protein fused to glutathione S-transferase (GST) were synthesised in vitro using the HeLa cell lysate-based protein in vitro transcription/translation (IVTT) system (Thermo Fisher Scientific). NAPPA-ELISA assay was performed as previously described⁸ with some variations. 96-well plates coated with 40 ng of anti-GST antibody were blocked 4 hours at room temperature with 5% milk-1 \times phosphate-buffered saline with tween (PBST) (0.02% Tween20). 50 μ L of the IVTT-expressed recombinant human protein was transferred to each well and incubated at 4°C overnight on shaker. Plates were then washed and incubated with 1:20 (v/v) diluted sera. The presence of specific MAT2 β -AAb was detected by

incubation with horseradish peroxidase (HRP)-linked anti-Human IgG (Jackson ImmunoResearch Laboratories) diluted 1:1000 (v/v) in blocking buffer. After addition of tetramethylbenzidine substrate, the absorbance signals at 450 nm were read on a Biotek Synergy four plate reader (Winooski, VT, USA). Levels of MAT2 β -AAb were expressed in arbitrary units (a.u.) of absorbance.

Data analysis

The biological context network of MAT2 β was analysed with the STRING (<https://string-db.org/>) bioinformatics webtool, using the K-means clustering method. Differences in the baseline reactivity levels of MAT2 β -AAb were assessed by the Mann-Whitney U test and the association of this potential biomarker with OA incidence was evaluated with the OR. In addition, after assessment of cut-off values (tertiles) for MAT2 β -AAb, patients with OA were categorised into high-level, medium-level and low-levels groups. Kaplan-Meier (KM) analyses were used to estimate and represent the survival probability, explained as the probability of not developing KOA in specific periods of time (12, 24, 36, 48, 72 and 96 months) depending on the tertiles of MAT2 β -AAb reactivity levels of the participants.

To define prognostic models of OA, clinical data at baseline were obtained from the OAI database (<https://data-archive.nimh.nih.gov/oai>). Candidate non-radiographic clinical variables that may have prognostic value were selected based on the specific eligibility risk factor criteria for the incident subcohort of the OAI and prior published evidence suggesting a risk factor role in KOA incidence (online supplementary table S2). For all variables concerning the joint, knee-value predictors were recoded to indicate they were for the target knee. When neither or both knees have incident KOA, one of them was randomly selected and used in the analysis. In a primary step, univariable logistic regression analyses were employed to assess association between each variable with incident radiographic KOA. In a secondary step, a stepwise multivariable logistic regression analysis was performed to define a prognostic model of incident radiographic KOA.

The capacity of the models to predict OA incidence was evaluated using the AUC. The utility of the measurement of the reactivity levels of the potential biomarker was assessed by comparing the AUC of the covariates-only model with the AUC of the biomarker plus covariates model. Sensitivity, specificity and positive predictive value and negative predictive value were also estimated by the Youden Index to determine the validity and security of the models, and receiver operating characteristic (ROC) curves were evaluated. A nomogram was developed to facilitate application of the proposed prognostic model in a clinical setting. Finally, the validity of the proposed biomarker plus covariates model was evaluated by a replication analysis in a different set of participants from the OAI progression subcohort.

All regression analyses and KM curves were carried out using SPSS V.25 for Mac. Metrics were calculated using the pROC package in R.

Patient and public involvement

This research was done without patient involvement. Patients were not invited to comment on the study design and were not consulted to develop patient relevant outcomes or interpret the results. Patients were not invited to contribute to the writing or editing of this document for readability or accuracy.

RESULTS

Identification of AAbs associated with the incidence of KOA

To search for AAbs in the serum that could be associated with a future development of KOA, a comprehensive AAb profiling against 2125 full-length proteins was performed by NAPPA. It was carried out comparing pools of serum samples at baseline from two groups: the incident group, which contains participants belonging to the incidence subcohort of the OAI who did develop radiographic KOA during the 96-month follow-up (n=100, 10 pools), and the non-incident group, which contains participants from the non-exposed subcohort that remained radiographically healthy (n=100, 10 pools).

A signal cut-off >1.1 was employed to assure a sufficient margin between positive and negative AAbs reactivities. Among the 2125 screened proteins, a total of 1031 proteins showed positive immunoreactivity (online supplementary table S3). Mean and SD values for all the proteins expressed on the array for the incident and non-incident groups are summarised in online supplementary table S3. From all the proteins over the cut-off, the Wilcoxon Rank-Sum test identified a total of six AAbs that reacted with six different proteins on the array (online supplementary table S4). Furthermore, as shown in online supplementary figure S1, visually discernible differences demonstrated that the normalisation criteria employed did neither create signal differences that do not exist, nor destroy true signal differences.

Verification of MAT2 β -AAb levels as potential prognosis marker of OA incidence

To confirm the putative ability of any of these AAbs to predict the incidence of OA, anti-MAT2 β was selected to be technically verified by NAPPA-ELISA in 327 individual serum samples, 200 of which (100 incidents and 100 non-incidents) were previously used at the screening phase. This selection was based on the role of MAT2 β as negative regulatory subunit of the production of S-adenosylmethionine (SAMe), a main methyl donor in the human body and a widely used dietary supplement for OA management (AdoMet). In addition, its biological context network (online supplementary figure S2) suggests a bottleneck role of this protein in metabolic pathways that are known to be related with OA pathogenesis. After the subtraction of the negative control, we found positive reactivity against MAT2 β in all the analysed sera. The higher baseline reactivity levels of MAT2 β -AAb found in the incident group (0.58 ± 0.22 vs 0.49 ± 0.23 a.u., $p=3.140E-04$) verified our previous findings. The association of this potential biomarker with the clinical outcome and its ability to predict incidence of radiographic KOA were assessed and are summarised in table 1.

Furthermore, we detected a significant decrease in anti-MAT2 β reactivity levels with the time to KOA onset (p value=0.002), as it is shown in online supplementary figure S3. The association between the baseline reactivity levels of MAT2 β -AAb in sera and

Table 1 MAT2 β -AAb model assessment in the verification phase

	Estimate	95% CI	
OR (p value)	5.99 (1.000E-03)	2.16	16.63
AUC	0.62	0.56	0.68
Sensitivity (%)	86	80	91
Specificity (%)	39	31	46
PPV (%)	53	50	57
NPV (%)	78	70	85

AUC, area under the curve; MAT2 β -AAb, methionine adenosyltransferase two beta-autoantibody; NPV, negative predictive value; PPV, positive predictive value.

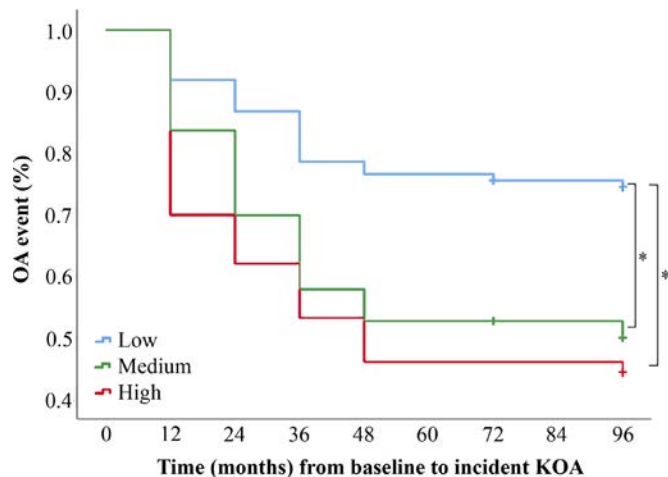


Figure 2 Association of biomarker levels with the time to KOA incidence. Kaplan-Meier reliability analysis for MAT2β-AAb in the OAI participants included in this work, classified into three groups (low level, medium level and high level) after the calculation of a cut-off value (MAT2β-AAb tertiles). *Level of significance below 0.05 by the Log-Rank test. KOA, knee osteoarthritis; MAT2β-AAb, methionine adenosyltransferase two beta-autonitbody; OAI, Osteoarthritis Initiative.

the time to OA incidence were inferred by KM curves (figure 2). Individuals with low AAb levels at baseline (range=2.00E-3–0.39 a.u.) had a significant lower risk to develop KOA sooner in time than those with high (range=0.60–1.58 a.u., $p=2.440E-04$) or medium (range=0.39–0.60 a.u., $p=5.000E-06$) baseline levels. There were no significant differences in the time to KOA incidence when the high-level and medium-levels groups were compared ($p=0.267$).

Predictive modelling of KOA incidence with the combination of clinical variables and MAT2β-AAb levels

A unique covariates-only model including age, sex, body mass index (BMI), frequent knee bending activity, history of knee injury and the Western Ontario and McMaster Universities Osteoarthritis Index pain score was defined by stepwise multivariable logistic regression analysis. The clinical characteristics finally included in the model of the selected participants are presented in table 2. The results from the univariable logistic regression model of all the clinical variables analysed are shown in online supplementary table S5.

The clinical model defined herein yielded an AUC (95% CI) of 0.81 (0.76–0.86). The addition of MAT2β-AAb to this model significantly improved the capacity to predict radiographic KOA development in the target knee ($p=0.048$), yielding an AUC of 0.83 (0.78–0.87). Figure 3A,B shows the results from this regression analysis, together with the metrics and the ROC curves

obtained when comparing the covariates-only model with the MAT2β-AAb plus covariates model.

To facilitate the use of the proposed prognostic model in a clinical routine, a nomogram was developed (figure 3C) to determine the probability of a certain individual to develop KOA in the next 96 months.

Replication analysis in an independent OAI subcohort

The proposed MAT2β-AAb plus covariates model was replicated in an independent set of sera at baseline from participants without KOA belonging to the progression subcohort of the OAI. The clinical characteristics of this population are summarised in table 2. The AUC observed in this replication analysis was 0.76 (table 3), showing no significant differences with that obtained in the verification phase ($p=0.218$). In addition, the sensitivity, specificity and predictive values remained very similar in both verification and replication cohorts.

DISCUSSION

One of the features of a prognostic marker is the ability to predict the future occurrence of a certain disease among people who do not have it.¹⁵ The production of antibodies against self-proteins is a characteristic feature of many diseases.¹⁶ Considering the fact that AAbs can often be detected at asymptomatic stages,⁴ they might have the potential to identify susceptible individuals or populations and facilitate prognosis. The idea that AAbs can be used to predict a disease state has been extensively studied in different disorders, such as cancer^{17–19} or type 1 diabetes.^{20,21} In the field of rheumatic diseases, AAbs have a fundamental value in the diagnosis of those with an autoimmune pathogenesis, such as systemic lupus erythematosus²² and rheumatoid arthritis.²³

Although OA is not considered an autoimmune disorder, the immune system is highly related with early disease.²⁴ However, existing literature related to the presence of AAbs in patients with OA is limited.^{8,25–27} Indeed, this is the first study that evaluates the usefulness of AAbs to stratify patients with asymptomatic OA. The use of a large-scale approach (NAPPA) enabled the search of a massive number of putative AAbs, which is the largest screening performed to date in the OA field. With this approach, we have identified significant levels of reactivity from AAbs against six different proteins that are associated with the future incidence of the disease. At this point, a characteristic of this approach should be taken into consideration when interpreting the findings presented herein: The low sera dilutions employed in this work lead to the primary detection of class M immunoglobulins (IgM), which, in contrast to IgGs, have no immune memory. However, IgMs are not subjected to immunoregulation²⁸ and are formed early in the immune response. Therefore, specific antibodies of the IgM class might be important in the diagnosis of chronic diseases.²⁹

Table 2 Characteristics at baseline of the study participants in the verification and replication phases

Covariates	Verification phase		Replication phase	
	Incident OA (n=146)	Non-incident OA (n=181)	Incident OA (n=65)	Non-incident OA (n=43)
Age, mean years (SD)	60.65 (8.51)	56.61 (8.57)	58.26 (9.40)	59.86 (8.50)
Sex, n (%) female	98 (67.1)	102 (56.4)	26 (60.5)	25 (38.5)
BMI, mean kg/m ² (SD)	28.93 (4.59)	25.88 (4.14)	29.75 (4.94)	28.29 (3.69)
Frequent knee bending activity, n (%) yes	110 (75.3)	106 (58.6)	30 (71.4)	27 (41.5)
History of knee injury, n (%) yes	39 (26.7)	23 (12.7)	9 (21.4)	7 (10.9)
WOMAC pain score	1.63 (2.36)	0.61 (1.63)	3.21 (3.58)	1.68 (2.43)

BMI, body mass index; WOMAC, Western Ontario and McMaster Universities Osteoarthritis Index.

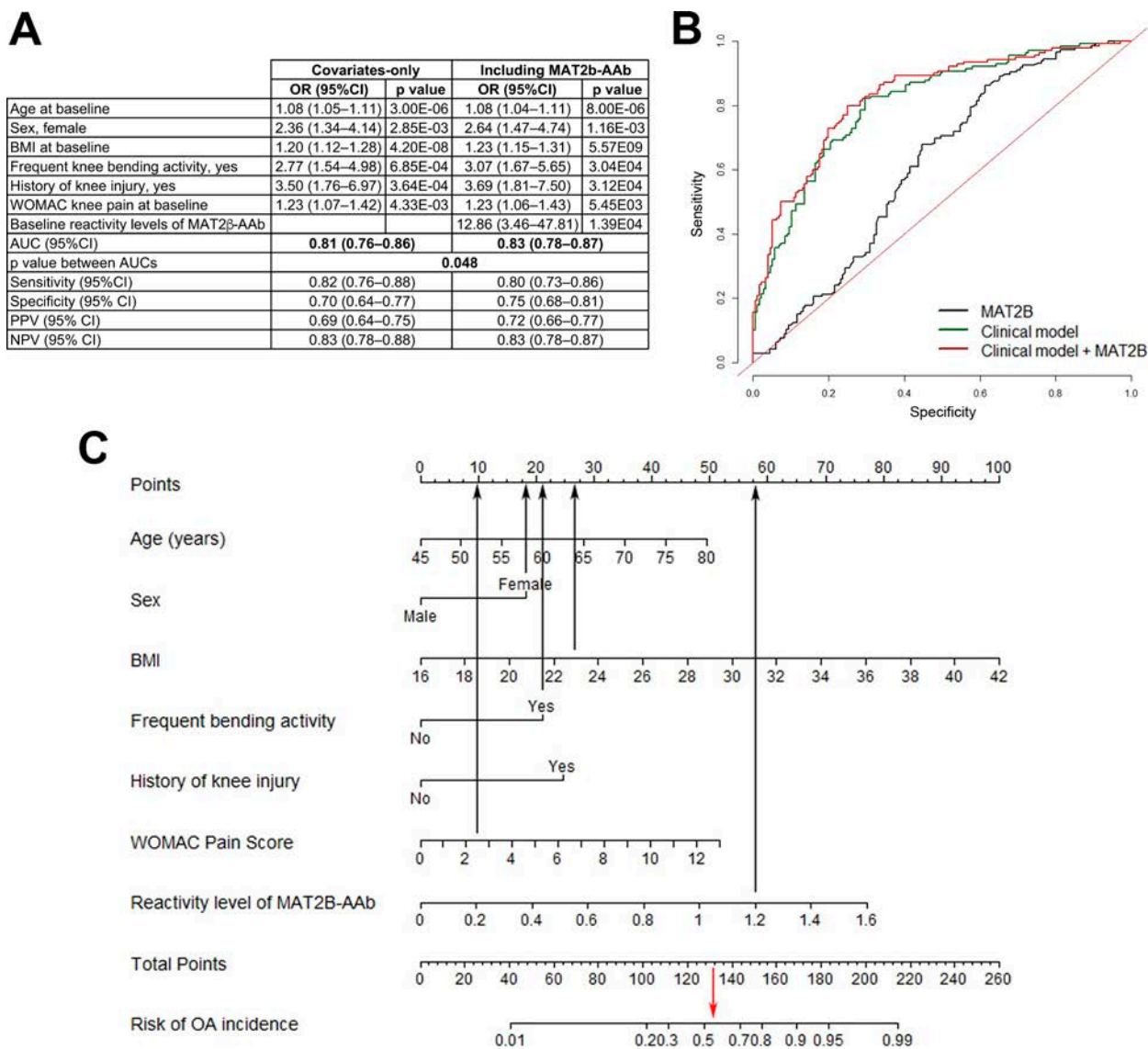


Figure 3 Prognostic model for incident radiographic KOA. (A) Metrics comparing the covariates-only model with the biomarker plus covariates model. (B) ROC curve for the models. (C) Nomogram of the biomarker plus covariates prognostic model. To use the nomogram, a straight edge on the top of the figure identifies the value on the points scale that corresponds to the score for each predictor (black arrows pointing up). In addition, the straight edge is aligned with the total points to determine probability at the bottom of the nomogram, once all the points for each predictor are summed. For example, a woman (18 points) of 45-year old (0 points), with a BMI of 23 kg/m² (27 points), who is involved in an activity with frequent knee bending (21 points), with no history of injury (0 points), a WOMAC pain score of 2.5 (10 points), and whose reactivity levels of MAT2 β -AAb in serum were 1.2 a.u. (57.5 points) renders a total of 133.5 points. This value gives her a probability of 55.5% to develop radiographic KOA within a period of 96 months (red arrow pointing down). a.u., arbitrary units; AUC, area under the curve; BMI, body mass index; KOA, knee osteoarthritis; MAT2 β -AAb, methionine adenosyltransferase two beta-autontibody; NPV, negative predictive value; OA, osteoarthritis; PPV, positive predictive value; ROC, receiver operating characteristic; WOMAC, Western Ontario and McMaster Universities Osteoarthritis Index.

Table 3 Predictive capacity of the MAT2 β -AAb plus covariates model in the verification and replication phases

	Verification phase	Replication phase	P value between AUCs
AUC (95% CI)	0.83 (0.78 to 0.87)	0.76 (0.66 to 0.86)	0.218
Sensitivity % (95% CI)	80 (73 to 86)	71 (56 to 83)	
Specificity % (95% CI)	75 (68 to 81)	81 (70 to 91)	
PPV % (95% CI)	72 (66 to 77)	71 (60 to 83)	
NPV % (95% CI)	83 (77 to 87)	81 (74 to 89)	

AUC, area under the curve; MAT2 β -AAb, methionine adenosyltransferase two beta-autontibody; NPV, negative predictive value; PPV, positive predictive value.

The results for MAT2 β -AAb have been verified on 327 individual samples at baseline from the OAI cohort, which provides a robust evaluation of its ability to classify patients at baseline as incident or non-incident during a 96-month period. Moreover, KM curves showed a significant association of the baseline reactivity levels of MAT2 β -AAb with the time of KOA appearance. This statistical approach has been widely used in cancer biomarkers^{30–32} and it has been recently introduced in the rheumatology field.^{33,34} Interestingly, our results showed that higher baseline reactivity levels of this AAb result in a sooner development of radiographic KOA.

MAT2 β is the regulatory subunit responsible of enhancing or inhibiting the synthesis of SAME. This latter compound plays

a vital role in methylation, transsulfuration and aminopropylation pathways,³⁵ and it has been employed as dietary supplement for OA management.^{35–38} Although there is no evidence of the direct involvement of MAT2 β in OA, its fundamental role in key biological processes for the pathogenesis of this disease (online supplementary figure S2) turns it into a potential marker of interest. Curiously, this protein was not included in either the planar arrays or the NPPA developed previously by our group for the screening of OA-associated AAb.⁸

The MAT2 β -AAb-only model showed a modest ability to predict radiographic KOA development, yielding an AUC of 0.62 with 39% specificity and 86% sensitivity. In the OA field, this modest predictive capacity is in agreement with that obtained for different biomarkers that have been evaluated in the last years to predict relevant OA progression. For example, Eckstein and collaborators examined the relationship of 15 molecular markers with structural progression based on femorotibial cartilage loss.³⁹ The strongest predictors of longitudinal thinning were serum C-terminal telopeptide of collagen type I (CTX-I) and plasma N-terminal propeptide of type II procollagen, yielding AUCs of 0.65 and 0.64, respectively, but all the remaining biomarkers showed AUCs < 0.60. Furthermore, in the meta-analysis published by Valdes and collaborators,⁴⁰ urine CTX-II also showed a limited predictive capacity (AUC \leq 0.63). Recently, Kraus and collaborators have investigated a target set of 18 biochemical markers (baseline and time-integrated concentrations (TICs) over 12 and 24 months) as predictors of symptomatic and radiographic KOA progression.⁴¹ Among all of them, the best single biomarker was the 24 M TIC CTX-II measured in urine, yielding an AUC = 0.58.

With the aim of defining a useful non-radiographic prognostic model focused on KOA, different non-radiographic clinical factors related with risk of incident KOA in the literature^{42–44} have been analysed in this study by univariable logistic regression analysis to look for significant predictors. It is important to specify that this study is based on a Caucasian US population, which may not comprise all the factors that enhance predisposition to OA. Among the clinical variables finally included in the model, the history of knee injury showed the highest OR, which was markedly lower than the reactivity levels of MAT2 β -AAb (OR 2.57 vs 5.99) for being incident. As shown herein, the use of stepwise multivariable regression analysis resulted in one prognostic model of KOA incidence with an AUC = 0.81. Using data from individuals in the Rotterdam study, a prediction model using clinical factors that yields an AUC of 0.66 was defined.⁴⁵ In another study, Zhang and collaborators defined a model of incidence of radiographic KOA with data from the Nottingham cohort, the OAI cohort and the Genetics of Osteoarthritis and Lifestyle (GOAL) study.⁴⁶ This model, including variables such as age, gender, BMI, occupational risk, family history and knee injury yielded the greatest AUC (0.74) in the GOAL population, compared with the OAI (AUC = 0.60) and the Nottingham (AUC = 0.69). In our case, the remarkably high ability to predict the appearance of radiographic KOA using this covariates-only model could be due to the high prevalence of the disease in our verification cohort (45% of incident participants). Indeed, the application of this model into the whole OAI database yielded a lower AUC (AUC < 0.70 (data not shown)).

Despite the rather low AUC of MAT2 β -AAb, the addition of this potential biomarker to the prognostic covariates-only model led to an increase in its discriminative ability (AUC = 0.83), being this increase statistically significant ($p = 0.048$). A similar improvement, but in this case not significant, was previously reported by including uCTX-II levels in a clinical prediction

model for KOA.⁴⁵ At this point, it is important to take into account that among all the patients involved in this study, 42.5% of them had already developed radiographic OA in the off-target knee (KL \geq 2). Nevertheless, we observed that the prognostic ability of MAT2 β -AAb levels is maintained after removing subjects with contralateral OA at baseline (AUC = 0.61 (0.54–0.68)). In addition, the inclusion of the presence of contralateral OA to the proposed MAT2 β -AAb plus covariates model did not improve its predictive capacity ($p = 0.093$). This strengthens the utility of this biomarker to predict incidence of KOA without the need of any radiographical information from the patients, avoiding their exposure to harmful radiation. Finally, the prognostic model combining baseline levels of MAT2 β -AAb with clinical variables was replicated in an independent population, which confirms its putative utility to predict the appearance of radiographic KOA and strongly suggests it can be generalisable to the wider population.

In summary, the present study shows that a high antibody reactivity against MAT2 β protein in serum is associated at baseline with individuals who will develop incident radiographic KOA, and also with an earlier appearance of the disease. Our results suggest that the inclusion of MAT2 β -AAb in a clinical prognostic model for radiographic KOA could improve the identification of individuals who will develop the disease before 96 months.

Author affiliations

¹Grupo de Investigación de Reumatología, Unidad de Proteómica, INIBIC-Complejo Hospitalario Universitario A Coruña, SERGAS, Universidad de A Coruña, A Coruña, Spain

²Grupo de Epidemiología Clínica y Bioestadística, INIBIC-Complejo Hospitalario Universitario A Coruña, SERGAS, Universidad de A Coruña, A Coruña, Spain

³Grupo de Investigación de Reumatología, Unidad de Genómica, INIBIC-Complejo Hospitalario Universitario de A Coruña, SERGAS, Universidad de A Coruña, A Coruña, Spain

⁴Virginia G. Piper Center for Personalized Diagnostics, Biodesign Institute-Arizona State University, Tempe, Arizona, USA

⁵Department of Medicine and General Cytometry Service-Nucleus. Proteomics Unit. CIBER-ONC, Cancer Research Center (IBMCC/CSIC/USAL/IBSAL), Salamanca, Spain

⁶Grupo de Investigación Reumatología, Unidad de Investigación Clínica, INIBIC-Complejo Hospitalario Universitario A Coruña, SERGAS, Universidad de A Coruña, A Coruña, Spain

⁷Grupo de Investigación de Reumatología, INIBIC-Complejo Hospitalario Universitario A Coruña, SERGAS, Departamento de Medicina, Universidad de A Coruña, A Coruña, Spain

Acknowledgements The authors acknowledge the sample and data set provided from the OAI, a public-private partnership comprised of five contracts (N01-AR-2-2258; N01-AR-2-2259; N01-AR-2-2260; N01-AR-2-2261 and N01-AR-2-2262) funded by the NIH.

Contributors Conception and design: MC-E, JvD, JQ, JLB, CR-R and FJB. Acquisition, analysis and interpretation of data: MC-E, VB-B, FP, IR-P, JvD, JQ, MF, JLB, CR-R and FJB. Drafting the article: MC-E, VB-B, IR-P, CR-R and FJB. Final approval of the article: All authors.

Funding The Proteomics Unit belongs to ProteoRed, PRB3- ISCIII, supported by grant PT17/0019/0014. This work has been funded by grants from Fondo Investigación Sanitaria-Spain (PI14/01707, PI16/02124, PI17/00404, DTS17/00200, CIBER-BBN CB06/01/0040, CIBER-ONC CB16/12/00400, RETIC-RIER-RD12/0009/0018), a part of the National Plan for Scientific Program Development and Technological Innovation 2013-2016, funded by the ISCIII-General Subdirection of Assessment and Promotion of Research - European Regional Development Fund (FEDER) "A way of making Europe". MC-E is supported by the Xunta de Galicia and the European Union (European Social Fund – ESF) through a predoctoral fellowship (IN606A-2016/012). IR-P and CR-R were supported by the Miguel Servet II programme from Fondo Investigación Sanitaria-Spain (CPII17/0026 and CPII15/00013, respectively).

Competing interests None declared.

Patient consent for publication Not required.

Provenance and peer review Not commissioned; externally peer reviewed.

Data availability statement All data relevant to the study are included in the article or uploaded as supplementary information.

Open access This is an open access article distributed in accordance with the Creative Commons Attribution Non Commercial (CC BY-NC 4.0) license, which permits others to distribute, remix, adapt, build upon this work non-commercially, and license their derivative works on different terms, provided the original work is properly cited, appropriate credit is given, any changes made indicated, and the use is non-commercial. See: <http://creativecommons.org/licenses/by-nc/4.0/>.

ORCID iDs

Cristina Ruiz-Romero <http://orcid.org/0000-0001-7649-9803>

Francisco J Blanco <http://orcid.org/0000-0001-9821-7635>

REFERENCES

- Sen R, Hurley JA. Osteoarthritis. *StatPearls* 2018.
- Kraus VB, Blanco FJ, Englund M, et al. Call for standardized definitions of osteoarthritis and risk stratification for clinical trials and clinical use. *Osteoarthritis Cartilage* 2015;23:1233–41.
- Geurts J, Jurić D, Müller M, et al. Novel ex vivo human osteochondral explant model of knee and spine osteoarthritis enables assessment of inflammatory and drug treatment responses. *Int J Mol Sci* 2018;19:1314.
- Leslie D, Lipsky P, Notkins AL. Autoantibodies as predictors of disease. *J Clin Invest* 2001;108:1417–22.
- Macdonald IK, Parsy-Kowalska CB, Chapman CJ. Autoantibodies: opportunities for early cancer detection. *Trends Cancer* 2017;3:198–213.
- Katchman BA, Chowell D, Wallstrom G, et al. Autoantibody biomarkers for the detection of serous ovarian cancer. *Gynecol Oncol* 2017;146:129–36.
- Wang H, Demirkan G, Bian X, et al. Identification of Antibody Against SNRNP, Small Nuclear Ribonucleoprotein-Associated Proteins B and B', as an Autoantibody Marker in Crohn's Disease using an Immunoproteomics Approach. *J Crohns Colitis* 2017;11:848–56.
- Henjes F, Lourido L, Ruiz-Romero C, et al. Analysis of autoantibody profiles in osteoarthritis using comprehensive protein array concepts. *J Proteome Res* 2014;13:5218–29.
- Anderson KS, Sibani S, Wallstrom G, et al. Protein microarray signature of autoantibody biomarkers for the early detection of breast cancer. *J Proteome Res* 2011;10:85–96.
- Ramachandran N, Raphael JV, Hainsworth E, et al. Next-Generation high-density self-assembling functional protein arrays. *Nat Methods* 2008;5:535–8.
- Rego-Pérez I, Blanco FJ, Roemer FW, et al. Mitochondrial DNA haplogroups associated with MRI-detected structural damage in early knee osteoarthritis. *Osteoarthritis Cartilage* 2018;26:1562–9.
- Halilaj E, Le Y, Hicks JL, et al. Modeling and predicting osteoarthritis progression: data from the osteoarthritis initiative. *Osteoarthritis Cartilage* 2018;26:1643–50.
- Bian X, Wallstrom G, Davis A, et al. Immunoproteomic profiling of antiviral antibodies in new-onset type 1 diabetes using protein arrays. *Diabetes* 2016;65:285–96.
- Wang J, Barker K, Steel J, et al. A versatile protein microarray platform enabling antibody profiling against denatured proteins. *Proteomics Clin Appl* 2013;7:378–83.
- Matson E, Baliog C, Reginato AM. Papel de Los biomarcadores en La artrosis. in: *Artrosis Fisiopatología, diagnóstico Y tratamiento. Editorial Médica Panamericana; Madrid* 2010;21:327–53.
- Gibson DS, Qiu J, Mendoza EA, et al. Circulating and synovial antibody profiling of juvenile arthritis patients by nucleic acid programmable protein arrays. *Arthritis Res Ther* 2012;14.
- Qi S, Huang M, Teng H, et al. Autoantibodies to chromogranin A are potential diagnostic biomarkers for non-small cell lung cancer. *Tumor Biol* 2015;36:9979–85.
- Chen H, Werner S, Tao S, et al. Blood autoantibodies against tumor-associated antigens as biomarkers in early detection of colorectal cancer. *Cancer Lett* 2014;346:178–87.
- Kunizaki M, Hamasaki K, Wakata K, et al. Clinical value of serum p53 antibody in the diagnosis and prognosis of esophageal squamous cell carcinoma. *Anticancer Res* 2018;38:1807–13.
- Bonifacio E, Genovese S, Braghi S, et al. Islet autoantibody markers in IDDM: risk assessment strategies yielding high sensitivity. *Diabetologia* 1995;38:816–22.
- Fabris M, Zago S, Liguori M, et al. Anti-zinc transporter protein 8 autoantibodies significantly improve the diagnostic approach to type 1 diabetes: an Italian multicentre study on paediatric patients. *Autoimmun Highlights* 2015;6:17–22.
- Putterman C, Wu A, Reiner-Benaim A, et al. SLE-key® rule-out serologic test for excluding the diagnosis of systemic lupus erythematosus: developing the ImmunArray iCHIP®. *J Immunol Methods* 2016;429:1–6.
- Aletaha D, Neogi T, Silman AJ, et al. 2010 rheumatoid arthritis classification criteria: an American College of Rheumatology/European League against rheumatism collaborative initiative. *Arthritis Rheum* 2010;62:2569–81.
- Ene R, Sinescu RD, Ene P, et al. Synovial inflammation in patients with different stages of knee osteoarthritis. *Rom J Morphol Embryol* 2015;56:169–73.
- Janin HE. Autoantibody specificities of immune complexes sequestered in articular cartilage of patients with rheumatoid arthritis and osteoarthritis. *Arthritis Rheum* 1985;28:241–8.
- Du H, Masuko-Hongo K, Nakamura H, et al. The prevalence of autoantibodies against cartilage intermediate layer protein, YKL-39, osteopontin, and cyclic citrullinated peptide in patients with early-stage knee osteoarthritis: evidence of a variety of autoimmune processes. *Rheumatol Int* 2005;26:35–41.
- Ruthard J, Hermes G, Hartmann U, et al. Identification of antibodies against extracellular matrix proteins in human osteoarthritis. *Biochem Biophys Res Commun* 2018;503:1273–7.
- Diaz-Zaragoza M, Hernandez-Avila R, Viedma-Rodríguez R, et al. Natural and adaptive IgM antibodies in the recognition of tumor-associated antigens of breast cancer (review). *Oncol Rep* 2015;34:1106–14.
- Burrell CJ, Howard CR, Murphy FA. Adaptive Immune Responses to Infection. In: *Fenner and White's Medical Virology*. 5th edn. Academic Press (ELSEVIER), 2017: 65–76.
- Albertus DL, Seder CW, Chen G, et al. AZGP1 autoantibody predicts survival and histone deacetylase inhibitors increase expression in lung adenocarcinoma. *J Thorac Oncol* 2008;3:1236–44.
- Aguirre-Gamboa R, Gomez-Rueda H, Martínez-Ledesma E, et al. SurvExpress: an online biomarker validation tool and database for cancer gene expression data using survival analysis. *PLoS One* 2013;8:e74250.
- Rinaldetti S, Wirtz R, Worst TS, et al. Foxm1 predicts disease progression in non-muscle invasive bladder cancer. *J Cancer Res Clin Oncol* 2018;144:1701–9.
- Lezcano-Valverde JM, Salazar F, León L, et al. Development and validation of a multivariate predictive model for rheumatoid arthritis mortality using a machine learning approach. *Sci Rep* 2017;7.
- van Wulfften Palthe AFY, Clement ND, Temmerman OPP, et al. Survival and functional outcome of high tibial osteotomy for medial knee osteoarthritis: a 10–20-year cohort study. *Eur J Orthop Surg Traumatol* 2018;28:1381–9.
- Hosea Blewett HJ. Exploring the mechanisms behind S-adenosylmethionine (same) in the treatment of osteoarthritis. *Crit Rev Food Sci Nutr* 2008;48:458–63.
- Soeken KL, Lee WL, Bausell RB, et al. Safety and efficacy of S-adenosylmethionine (same) for osteoarthritis. *J Fam Pr* 2002;51:425–30.
- Najm WI, Reinsch S, Hoehler F, et al. S-adenosyl methionine (SAME) versus celecoxib for the treatment of osteoarthritis symptoms: a double-blind cross-over trial. [ISRCTN36233495]. *BMC Musculoskelet Disord* 2004;5:6.
- Kim J, Lee EY, Koh E-M, et al. Comparative clinical trial of S-adenosylmethionine versus nabumetone for the treatment of knee osteoarthritis: an 8-week, multicenter, randomized, double-blind, double-dummy, phase IV study in Korean patients. *Clin Ther* 2009;31:2860–72.
- Eckstein F, Le Graverand MPH, Charles HC, et al. Clinical, radiographic, molecular and MRI-based predictors of cartilage loss in knee osteoarthritis. *Ann Rheum Dis* 2011;70:1223–30.
- Valdes AM, Meulenbelt I, Chassaing E, et al. Large scale meta-analysis of urinary C-terminal telopeptide, serum cartilage oligomeric protein and matrix metalloprotease degraded type II collagen and their role in prevalence, incidence and progression of osteoarthritis. *Osteoarthritis and Cartilage* 2014;22:683–9.
- Kraus VB, Collins JE, Hargrove D, et al. Predictive validity of biochemical biomarkers in knee osteoarthritis: data from the FNIH oa biomarkers Consortium. *Ann Rheum Dis* 2017;76:186–95.
- Nevitt M, Felson DT, Lester G. The osteoarthritis initiative, protocol for the cohort study. Available: <https://oai.epi-ucsf.org/datarelease/docs/studydesignprotocol.pdf>
- Johnson VL, Hunter DJ. The epidemiology of osteoarthritis. *Best Pract Res Clin Rheumatol* 2014;28:5–15.
- Sharma L, Hochberg M, Nevitt M, et al. Knee tissue lesions and prediction of incident knee osteoarthritis over 7 years in a cohort of persons at higher risk. *Osteoarthritis Cartilage* 2017;25:1068–75.
- Kerkhof HJM, Bierma-Zeinstra SMA, Arden NK, et al. Prediction model for knee osteoarthritis incidence, including clinical, genetic and biochemical risk factors. *Ann Rheum Dis* 2014;73:2116–21.
- Zhang W, McWilliams DF, Ingham SL, et al. Nottingham knee osteoarthritis risk prediction models. *Ann Rheum Dis* 2011;70:1599–604.

CLINICAL SCIENCE

Diagnosis of osteoporosis in statin-treated patients is dose-dependent

Michael Leutner,¹ Caspar Matzhold,^{2,3} Luise Bellach,¹ Carola Deischinger,¹ Jürgen Harreiter,¹ Stefan Thurner,^{2,3,4,5} Peter Klimek,^{2,3} Alexandra Kautzky-Willer ¹

Handling editor Francis Berenbaum

► Additional material is published online only. To view please visit the journal online (<http://dx.doi.org/10.1136/annrheumdis-2019-215714>).

¹Department of Internal Medicine III, Clinical Division of Endocrinology and Metabolism, Unit of Gender Medicine, Medical University of Vienna, Vienna, Austria

²Section for Science of Complex Systems, CeMSIS, Medical University of Vienna, Vienna, Austria

³Complexity Science Hub Vienna, Vienna, Austria

⁴Santa Fe Institute, Santa Fe, New Mexico, USA

⁵IIASA, Laxenburg, Austria

Correspondence to

Professor Alexandra Kautzky-Willer, Internal Medicine III, Division of Endocrinology and Metabolism, Medical University of Vienna, Vienna 1090, Austria; alexandra.kautzky-willer@meduniwien.ac.at

Received 16 May 2019

Revised 27 August 2019

Accepted 12 September 2019

Published Online First

26 September 2019

ABSTRACT

Objective Whether HMG-CoA-reductase inhibition, the main mechanism of statins, plays a role in the pathogenesis of osteoporosis, is not entirely known so far. Consequently, this study was set out to investigate the relationship of different kinds and dosages of statins with osteoporosis, hypothesising that the inhibition of the synthesis of cholesterol could influence sex-hormones and therefore the diagnosis of osteoporosis.

Methods Medical claims data of all Austrians from 2006 to 2007 was used to identify all patients treated with statins to compute their daily defined dose averages of six different types of statins. We applied multiple logistic regression to analyse the dose-dependent risks of being diagnosed with osteoporosis for each statin individually.

Results In the general study population, statin treatment was associated with an overrepresentation of diagnosed osteoporosis compared with controls (OR: 3.62, 95% CI 3.55 to 3.69, $p < 0.01$). There was a highly non-trivial dependence of statin dosage with the ORs of osteoporosis. Osteoporosis was underrepresented in low-dose statin treatment (0–10 mg per day), including lovastatin (OR: 0.39, CI 0.18 to 0.84, $p < 0.05$), pravastatin (OR: 0.68, 95% CI 0.52 to 0.89, $p < 0.01$), simvastatin (OR: 0.70, 95% CI 0.56 to 0.86, $p < 0.01$) and rosuvastatin (OR: 0.69, 95% CI 0.55 to 0.87, $p < 0.01$). However, the exceeding of the 40 mg threshold for simvastatin (OR: 1.64, 95% CI 1.31 to 2.07, $p < 0.01$), and the exceeding of a 20 mg threshold for atorvastatin (OR: 1.78, 95% CI 1.41 to 2.23, $p < 0.01$) and for rosuvastatin (OR: 2.04, 95% CI 1.31 to 3.18, $p < 0.01$) was related to an overrepresentation of osteoporosis.

Conclusion Our results show that the diagnosis of osteoporosis in statin-treated patients is dose-dependent. Thus, osteoporosis is underrepresented in low-dose and overrepresented in high-dose statin treatment, demonstrating the importance of future studies' taking dose-dependency into account when investigating the relationship between statins and osteoporosis.

INTRODUCTION

Osteoporosis is a chronic disease characterised by a reduced bone mineral density (BMD) induced by an imbalance in osteoblastic and osteoclastic bone formation and resorption.¹ Due to the elevated fracture risk, osteoporosis can have detrimental effects on a patient's quality of life and is associated with a higher mortality and morbidity as well as being an economic burden.² By now, numerous studies about osteoporosis and its treatment have

Key messages

What is already known about this subject?

► There is a relationship between statins and osteoporosis.

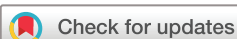
What does this study add?

► Osteoporosis is underrepresented in low-dose statin treatment.
► There is an overrepresentation of osteoporosis in high-dose statin treatment.

How might this impact on clinical practice or future developments?

► In clinical practice, high-risk patients for osteoporosis under high-dose statin treatment should be monitored more frequently.

been conducted—many of which revolve around the question whether statins affect bone metabolism.^{3–10} Statins play a crucial role in the management of hypercholesterolemia, which makes them a commonly used drug.¹¹ Actual guidelines for the treatment of hypercholesterolemia in high-risk patients suffering from cardiovascular disease (CVD) or diabetes have been issued, recommending cholesterol levels to be as low as possible.¹² Therefore, due to the sheer number of patients under statin therapy, research on the connection between statin usage and osteoporosis risk is of great importance. In particular, the underlying pathophysiological mechanisms of a possible osteoprotective effect of statins have yet to be fully established.^{3 13 14} Although many observational studies report positive effects of statin use on BMD and/or fracture risk, existing data do not sufficiently support the use of statins as osteoporosis prophylaxis. This is mainly due to the heterogeneity of the data concerning the effect of statin therapy on bone formation markers, BMD in females and overall BMD and fracture risk,³ as well as the lack of data regarding the relationship between different kinds and dosages of statins and diagnosis of osteoporosis. Another topic causing controversy is the question whether statins affect sex hormone levels such as testosterone or oestrogen.^{15–17} Statins act by inhibiting the endogenous synthesis of cholesterol, the main substrate for the synthesis of sex hormones, and thus we cannot disregard the possibility of a negative effect of statins on bone health, especially in higher dosages. However, data on the dosage-dependency of statins in the diagnosis of



© Author(s) (or their employer(s)) 2019. Re-use permitted under CC BY-NC. No commercial re-use. See rights and permissions. Published by BMJ.

To cite: Leutner M, Matzhold C, Bellach L, et al. *Ann Rheum Dis* 2019;**78**:1706–1711.

osteoporosis are sparse. Consequently, the present study seeks to investigate the relationship between different kinds and dosages of statins and osteoporosis and to shed light on the controversy regarding the relationship between statin treatment and the diagnosis of osteoporosis in a nationwide population-based study.

STUDY DESIGN AND METHODS

We conducted a cross-sectional retrospective analysis of the entire Austrian population using a consolidated administrative research data base.¹⁸

Patient population

Our data include all Austrians with health claims (roughly 97% of the population) for which data on all main and side diagnoses from hospital stays and all prescriptions of drugs with costs that exceed a prescription charge of EUR 4.70 is available. We included patients with uniquely identifiable age and sex who were alive during the entire observation period from January 2006 to December 2007 (n=7 945 775). Patients born in these years or with age >90 years were excluded to gain a more homogenous group of patients. The obtained cohort consisted of 7 897 449 patients (male=3 702 572; female=4 194 877). Information on prescriptions was available in the Anatomical Therapeutic Chemical (ATC) Classification System codes; to identify patients being diagnosed with osteoporosis, main and side diagnoses from hospital stays were extracted as International Classification of Diseases, 10th revision (ICD10) codes. Patients with a main or side diagnosis from the range M80–M82 (including M80: ‘Osteoporosis with current pathological fracture’, M81: ‘Osteoporosis without current pathological fracture’ and M82: ‘Osteoporosis in diseases classified elsewhere’ (defined as osteoporosis in multiple myelomatosis or endocrine disorders) were classified as osteoporosis patients. We additionally conducted a sensitivity analysis to control for occurrences of rheumatoid arthritis (ICD10 code M06), ischaemic heart diseases (any code from the range I20–I25), diseases of arteries including arterioles and capillaries (I70–I79), stroke (I63, I64), diabetes (E10, E11), chronic renal insufficiency (N17–N19), nicotine dependency (F17), overweight and obesity (E65–E68), chronic obstructive pulmonary disease (J44), asthma (J45) and Crohn’s disease (K50).

Identifying patients with statin treatment

We identified all patients who had at least one prescription of any of the seven statins available on the market during the observation period: Simvastatin (ATC-code: C10AA01), Lovastatin (ATC-code: C10AA02), Pravastatin (ATC-code: C10AA03), Fluvastatin (ATC-code: C10AA04), Atorvastatin (ATC-code: C10AA05), Cerivastatin (ATC-code: A10AA06) and Rosuvastatin (ATC-code: C10AA07). For these patients, we additionally controlled for possible effects of other prescribed drugs including 49 different kinds of insulin-sparing or providing medication (all ATC-codes starting with A10) and 3 fibrates (ATC-code: C10AB02, C10B05, C10A×09).

For each medication, we tested if the patient was a regular drug user or not. Only if a patient had a minimum of four different prescription entries for a given drug, we identified him/her as a valid drug user. As most health claims are filed on a quarterly basis, four different prescription entries are equivalent to a treatment regularly applied over 1 year. Medications with less than 35 valid patients were excluded. The control group was made up of all patients not treated with statins.

Average daily doses

The average daily dose of a given drug for each patient was calculated as the amount of the drug (converted from defined daily dose to mg¹) divided by the number of treatment days that the patient did not spend in a hospital. Patients were then grouped according to their average daily dose for each statin in groups of >0–10 mg, >10–20 mg, >20–40 mg, >40–60 mg and >60–80 mg.

Patient and public involvement

Patients were not involved in the study design. Details of the ethical approval are provided in the online supplementary material.

Statistical analyses

We computed age-specific and sex-specific ORs between statin use and being diagnosed with osteoporosis. Multiple logistic regression was used to investigate this association while controlling for age, sex, dosage and prescription of other medications (drugs used in diabetes and fibrates). Next to age and sex, the independent variables in the regression included the dosage category for each type of statin or other medication as a categorical variable. Patients were assigned a categorical variable for each statin according to their average daily dose in milligrams. We controlled for other medications (20 glucose lowering drugs, including metformin; 3 fibrates) by introducing binary dummy variables for whether the patient fulfilled all criteria to be considered a valid drug user or not (see above). Goodness of fit of the regression models was evaluated by the adjusted R-squared statistic; the variance inflation factor (VIF) was used to test for multicollinearity.

RESULTS

Baseline characteristics

We identified 353 502 statin-treated patients (175 506 males, 177 996 females) out of which 11 701 patients (1765 males, 9936 females) were diagnosed with osteoporosis (for a detailed description of the osteoporotic population, see also online supplementary tables S1 and S2). The control group (no statin exposure) consisted of 7 543 947 patients (3 527 066 males, 4 016 881 females), including 68 699 patients (10 410 males, 58 289 females) diagnosed with osteoporosis. Table 1 presents the results of a sex-matched and age-matched cohort analysis of statin users in comparison to non-statin users and shows that statin users presented more often with a diagnosis of CVD, renal failure, nicotine dependency, overweight and obesity and were treated more often with antidiabetics.

Sex-specific comparison of the diagnosis of osteoporosis

Within the whole study population, our results show that women are at a higher risk of being diagnosed with osteoporosis when compared with men (OR: 5.08, 95% CI 4.98 to 5.18, p<0.01; see also online supplementary table S3).

Comparison of the diagnosis of osteoporosis between patients with and without statin treatment

In the present analysis, the diagnosis of osteoporosis was more prevalent in patients of any age treated with statins when compared with control subjects without statin treatment (OR: 3.62, 95% CI 3.55 to 3.69, p<0.01). In a sex-specific analysis, the diagnosis of osteoporosis was overrepresented in both statin-treated females (OR(f): 3.90, 95% CI 3.81 to 3.98, p<0.01) and males (OR(m): 3.35, 95% CI 3.18 to 3.52, p<0.01). Therefore,

Table 1 Baseline characteristics of the study population matched for age and sex

	Statin		Matched control	
	Male	Female	Male	Female
N	175 506	177 996	526 518	533 988
Age (mean±SD)	65.02±10.89	69.02±10.46	65.02±10.89	69.02±10.46
Osteoporosis (M80–M82)	1765 (1.01%)	9936 (5.58%)	5.264 (1.00%)	26.903 (5.04%)**
Insulin	11 690 (6.66%)	12 332 (6.93%)	8603** (1.63%)	8617** (1.61%)
Oral antidiabetics	34 511 (19.66%)	32 514 (18.27%)	32 569** (6.19%)	31 237** (5.85%)
Fibrates	3667 (2.09%)	1993 (1.12%)	6470** (1.23%)	8131** (1.52%)
Arthritis (M06)	359 (0.20%)	991 (0.56%)	988 (0.19%)	2.703* (0.51%)
CVD (I20–I25)	36 970 (21.06%)	23 998 (13.48%)	33 971 (6.45%)	27 814** (5.21%)
Stroke (I63, I64)	5164 (2.94%)	4429 (2.49%)	8250** (1.57%)	7875** (1.47%)
Diseases of arteries (I70–I79)	12 513 (7.13%)	9058 (5.09%)	17 621** (3.35%)	13 605** (2.55%)
Renal failure (N17–N19)	8148 (4.64%)	6684 (3.76%)	15 774** (3.00%)	14 039** (2.63%)
Overweight and obesity (E66)	8314 (4.74%)	8290 (4.66%)	10 913** (2.07%)	13 526** (2.53%)
Nicotine dependency (F17)	4.215 (2.40%)	1766 (0.99%)	6925** (1.32%)	2422** (0.45%)

We give group size, age and the absolute and relative frequencies of osteoporosis, use of other medications (insulin, metformin, fibrates) and comorbid conditions for males and females in the statin-treated and control group, respectively.

** $p < 0.01$; * $p < 0.05$.

CVD, cardiovascular disease.

the ORs for females were significantly increased with respect to males ($p < 0.01$; see also online supplementary table S3). After stratifying the patients by their age in 10-year-intervals, we obtained similar results (osteoporosis being overrepresented in statin-treated individuals with significantly stronger effects in females than males) (see figure 1 and online supplementary table S3). In addition, figure 1 presents that in the age-class of 40–50 years, the relationship between statin treatment and increased odds of osteoporosis is stronger than in all other age groups.

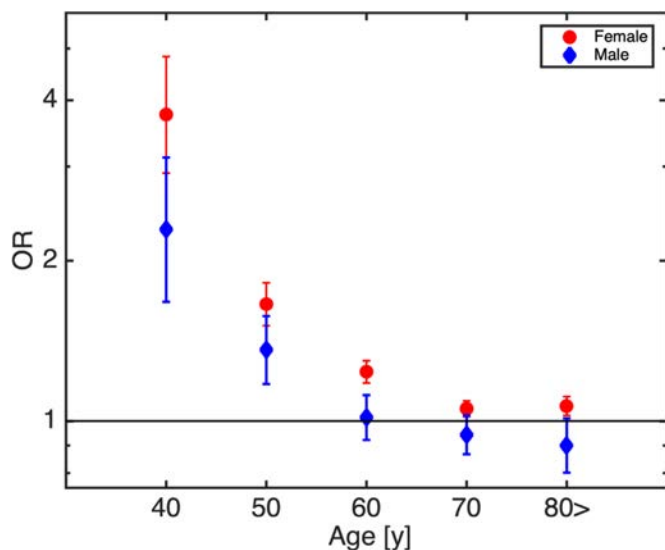


Figure 1 Age-dependent, sex-specific ORs for osteoporosis and statin use. Statin-related osteoporosis risks increase with younger age and female sex.

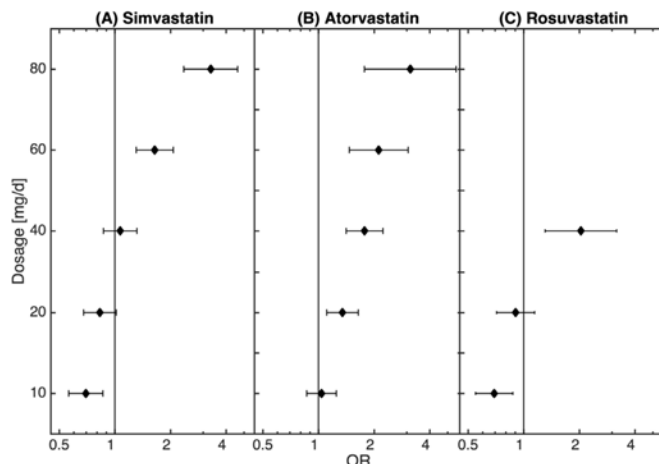


Figure 2 Dosage dependency of the statin—osteoporosis association. While low doses of statin can even be related to decreased osteoporosis risks, the disease risk clearly increases for higher doses.

Comparison of the different dosages of statins in the diagnosis of osteoporosis

There is a highly non-trivial dependence of statin dosage with the odds of osteoporosis. For low dose statin treatment (0–10 mg) osteoporosis is underrepresented in simvastatin (OR: 0.70, 95% CI 0.56 to 0.86, $p < 0.01$), lovastatin (OR: 0.39, 95% CI 0.18 to 0.84, $p < 0.05$), pravastatin (OR: 0.68, 95% CI 0.52 to 0.89, $p < 0.01$) and rosuvastatin (OR: 0.69, 95% CI 0.55 to 0.87, $p < 0.01$). However, the relationship between statin treatment and osteoporosis reverses with increased dosages. Particularly, this is the case for simvastatin, atorvastatin and rosuvastatin (note that for the remaining types of statin the patient numbers were too low to reliably estimate dosage-dependence) (see figure 2 and table 2). There we show that the diagnosis of osteoporosis was overrepresented in the group treated with >40–60 mg of simvastatin per day (OR: 1.64, 95% CI 1.31 to 2.07, $p < 0.01$) and further increased with the increase of the daily dosage (>60–80 mg simvastatin: OR: 3.30, 95% CI 2.36 to 4.62, $p < 0.01$). The fact that the diagnosis of osteoporosis was overrepresented in higher dosages of statin treatment could be also observed for atorvastatin (>10–20 mg: OR: 1.35, 95% CI 1.11 to 1.64, $p < 0.01$; >20–40 mg: OR: 1.78, 95% CI 1.41 to 2.23, $p < 0.01$; >40–60 mg: OR: 2.12, 95% CI 1.47 to 3.06, $p < 0.01$; >60–80 mg: OR: 3.14, 95% CI 1.77 to 5.56, $p < 0.01$) and for rosuvastatin (>20–40 mg: OR: 2.04, 95% CI 1.31 to 3.18, $p < 0.01$); the detailed description of the relationship of the dosages of statins with the diagnosis of osteoporosis with fracture is presented in online supplementary table S4. As demonstrated in online supplementary table S6, age was homogenous distributed over the different groups of statins.

To investigate whether the dosage-dependent relationship between statin use and osteoporosis risk as shown in figure 2 might be confounded by comorbidities such as arthritis, CVD, diseases of the arteries, stroke, diabetes, renal failure, nicotine dependence, overweight and obesity, and diseases possibly treated with corticosteroids such as asthma, Crohn’s disease or chronic obstructive pulmonary disease, we repeated the logistic regression analysis while excluding all patients with the given comorbidity, see online supplementary files (baseline tests, including online supplementary figures S2–S7). We find that the exclusion of these patients does not change the results qualitatively. All considered regression models have adjusted

Table 2 Individual statin dosage-dependent ORs of osteoporosis (95% CI) obtained from the logistic regression model

All	Lovastatin	Fluvastatin	Pravastatin	Simvastatin	Atorvastatin	Rosuvastatin
0–10 mg	0.39*	1.00	0.68**	0.70**	1.04	0.69**
CI	0.18 to 0.84	1.00 to 1.00	0.52 to 0.89	0.56 to 0.86	0.86 to 1.25	0.55 to 0.87
10–20 mg	1.06	0.59**	0.87	0.83	1.35**	0.90
CI	0.68 to 1.64	0.42 to 0.82	0.70 to 1.07	0.68 to 1.02	1.11 to 1.64	0.71 to 1.15
20–40 mg	1.59	0.85	1.01	1.07	1.78**	2.04**
CI	0.83 to 3.07	0.69 to 1.04	0.81 to 1.26	0.87 to 1.32	1.41 to 2.23	1.31 to 3.18
40–60 mg		0.91		1.64**	2.12**	
CI		0.74 to 1.11		1.31 to 2.07	1.47 to 3.06	
60–80 mg		1.09		3.30**	3.14**	
CI		0.87 to 1.35		2.36 to 4.62	1.77 to 5.56	
Adj. R ²	0.94	0.94	0.94	0.93	0.95	0.94
Max. VIF	4.21	3.26	3.04	2.74	2.87	3.29

**P<0.01; *p<0.05.

The bold values represent the significant results.

VIF, variance inflation factor.

R-squared statistics from the range 0.71–0.96 (see table 2 and online supplementary table S5). To test for multicollinearity, we considered the VIF for each variable and found the maximum value to be 4.21, indicating that multicollinearity is not an issue in the data (see table 2 and online supplementary table S5).

Sex-specific analysis

In a sex-specific analysis, the obtained results could be confirmed with slight differences as described in detail in the online supplementary material (see online supplementary table S5 and figure S1).

DISCUSSION

The aim of the present study was to investigate the relationship of statin therapy with osteoporosis. Our results showed that osteoporosis was overrepresented in statin-treated patients in the general study population. Thus, by splitting the study cohort in the different kinds of statins and dosages, there was a dose-dependent relationship with a diagnosed osteoporosis. Therefore, our results which showed that the diagnosis of osteoporosis was overrepresented in high-dose and underrepresented in low-dose statin treatment seem to be of great importance as they first show that it is important to analyse the different dosages and substances of statins.

Several studies have investigated whether HMG-CoA reductase inhibition, the main mechanism of statins, affects BMD. However, one of the main limitations of existing studies is that they did not investigate the relationship between the different kinds of statins (including potency and dosages) and the occurrence of osteoporosis in detail. A recent meta-analysis concluded that statin treatment had a tendency towards a positive effect on the reduction of fracture risk and marked improvement of BMD in statin-treated patients.³ A large meta-analysis conducted in Taiwan, including 45 342 patients in the statin cohort and 115 594 patients in the control cohort, stated that statin therapy correlates with a decreased risk of osteoporosis when taken daily over a longer period of time, however, also not accounting for the different types of statins and their dosages.⁷ In the present study, there was an increased risk of being diagnosed with osteoporosis in the general study population of statin-treated patients when compared with controls. However, the risk of being diagnosed with osteoporosis under statin-treatment decreased as a function of age, which could indicate that a longer statin

treatment could be related to a lower occurrence of the diagnosis of osteoporosis. To the best of our knowledge, this is the first study which shows that it is important to consider the different kinds of substances and dosages when investigating the relationship of osteoporosis and statin therapy. Therefore, we could show that low-dose statin treatment with daily dosages lower or equal to 10 mg of pravastatin, lovastatin, simvastatin and rosuvastatin was related to an underrepresentation of osteoporosis. Lin *et al* also compared different types of statins but did not investigate the effects of different daily dosages of the statins on the prevalence rate of osteoporosis. Thus, in their study, they investigated the effect of statins on the probability of developing new-onset osteoporotic fractures (NOFs) and concluded that a therapy with rosuvastatin and atorvastatin was related to a risk reduction of NOFs, significantly stronger when compared with simvastatin treatment.⁸ However, our results demonstrate that it is important to analyse the different kinds and dosages of statins. Rejnmark *et al* compared 124 655 fracture cases with 373 962 controls and found out that patients who had a fracture were less likely to use statins than the controls.¹⁹ In accordance with these findings, the present study also demonstrates an underrepresentation of osteoporosis in statin-treated patients, but only in patients on low dose statin therapy and not on high dose treatment of at least 1 year. Therefore, the increase of the dosage of statins was related to an overrepresentation of osteoporosis. A retrospective cohort study by Ward *et al* also omitted specifying the type of statin when comparing the fracture incidence of 6967 patients taking statins vs an equal number of controls. About one third of the patients received maximum dosages for simvastatin, pravastatin and atorvastatin, which were defined as 80 mg, and 40 mg for rosuvastatin. Although statins seem to decrease the risk of femoral neck fractures, there was no difference in the overall fracture risk when compared with the controls.²⁰ In light of numerous publications presenting rather heterogenous results while pursuing the same research question, we attempted to propose additional explanations for the observed discrepancies. Likely causes for different conclusions about whether or not statins are beneficial for bone health among various studies might be genetic determinants concerning CYP19A1/aromatase levels²¹ as this enzyme is responsible for the peripheral conversion of testosterone to oestrogen. It is a well-known fact that females are more commonly diagnosed with osteoporosis when compared with males, which was also the case in the present study. Furthermore, it is also known that the risk of osteoporosis, including

a higher risk of bone fractures, is especially high in postmenopausal women.²² In the postmenopausal state, oestradiol plays a crucial role in the maintenance of BMD²³ and, thus, one has to keep in mind that oestrogens are cholesterol derivatives²⁴ and play a significant role in bone metabolism by inhibiting bone resorption.²⁵ Thus, whether higher dosages of statins could inhibit the synthesis of sex hormones, via HMG-CoA-reductase inhibition, is of special interest, as we could show that an increase in the dosages of statins was related to an exaggerated increase and overrepresentation of diagnosed osteoporosis cases in the whole study population, and additionally significantly stronger in women than when compared with men. Women, especially due to lower oestrogen levels in the post menopause, are more likely to have an insufficient BMD.^{26 27} In men, free testosterone levels are positively associated with higher levels of BMD and inversely related to bone turnover markers.²⁸ The sex-specific differences in the pathogenesis of osteoporosis, a decreased activity of osteoblasts in men and an increased bone resorption due to a lack of oestrogen in women, would support the theory posed above.³ In mice models, statins have been shown to reduce plasma levels of testosterone, oestradiol and progesterone, while raising levels of follicle stimulating hormone and luteinising hormone at the same time;²⁹ similar results have also been presented in cell lines.³⁰ In the Rotterdam study, the effect of statins in 4166 men on sexual hormones was investigated and the authors could prove that statin treatment was related to lower serum total and non-sexual hormone-binding globulin (SHBG)-bound testosterone levels.³¹ Lower testosterone levels under statin therapy were also observed in other studies.^{15–17} Another study has shown that higher levels of SHBG are associated with a decrease in BMD.²⁸ Taken together, these findings suggest a connection between sex hormone levels and statins in the pathogenesis of osteoporosis.

There are limitations and strengths in the present study which have to be discussed. Limitations of our study include that the data extracted from the patient contingent only show the current dosage the patients are taking. However, only patients who had a statin treatment for a minimum of 1 year were included. Another limitation is that we could not confirm the diagnosis of osteoporosis, for example, with bone densitometry data, and that we had no access to relevant treatments such as corticosteroids, hormonal replacement therapy or bisphosphonates. Additionally, one has to keep in mind that diseases such as CVD, which are commonly treated with statins, are related to other diseases and conditions such as diabetes, physical inactivity, nicotine abuse or lack of hormone treatment in the menopause, all factors directly related to osteoporosis. A strength is that the compliance of the patients could be evaluated due to the data about the prescriptions of statins per year. Another strength is that the study investigated the general Austrian population and, therefore, the number of statin-treated patients is high.

CONCLUSION

In conclusion, our data suggest that osteoporosis is overrepresented in high-dosage, but underrepresented in low-dosage statin treatment. Guidelines for cholesterol lowering therapies for prevention of cardiovascular complications advise to reduce plasma low-density lipoprotein (LDL-cholesterol) levels as low as 70 mg/dL in high risk populations.¹² We propose that monitoring high-risk patients, that is, postmenopausal female patients under high-dosage statin therapy, might be useful in order to offer an individual therapy to prevent or treat osteoporosis. Thus, larger and prospective studies with a focus on dosages of

statins should be conducted in order to clarify the relationship with osteoporosis.

Acknowledgements We acknowledge to Dr Gottfried Endel for helping with data assessment.

Contributors Study design: ML, CM, ST, PK and AK-W. Data analysis: ML, CM, PK. Manuscript writing: ML, CM, PK. All authors read, reviewed and approved the final manuscript.

Funding This study was funded by the WWTF (MA16-045).

Competing interests None declared.

Patient consent for publication Obtained.

Provenance and peer review Not commissioned; externally peer reviewed.

Data availability statement Data are available on reasonable request. All data relevant to the study are included in the article or uploaded as supplementary information.

Open access This is an open access article distributed in accordance with the Creative Commons Attribution Non Commercial (CC BY-NC 4.0) license, which permits others to distribute, remix, adapt, build upon this work non-commercially, and license their derivative works on different terms, provided the original work is properly cited, appropriate credit is given, any changes made indicated, and the use is non-commercial. See: <http://creativecommons.org/licenses/by-nc/4.0/>.

ORCID iD

Alexandra Kautzky-Willer <http://orcid.org/0000-0002-3520-4105>

REFERENCES

1. Stone MD, Hosking DJ. Treatment of osteoporosis: current and future. *Ann Rheum Dis* 1991;50:663–5.
2. Zethraeus N, Borgström F, Ström O, *et al*. Cost-effectiveness of the treatment and prevention of osteoporosis—a review of the literature and a reference model. *Osteoporos Int* 2007;18:9–23.
3. An T, Hao J, Sun S, *et al*. Efficacy of statins for osteoporosis: a systematic review and meta-analysis. *Osteoporos Int* 2017;28:47–57.
4. Chan KA, Andrade SE, Boles M, *et al*. Inhibitors of hydroxymethylglutaryl-coenzyme A reductase and risk of fracture among older women. *Lancet* 2000;355:2185–8.
5. Hippisley-Cox J, Coupland C. Unintended effects of statins in men and women in England and Wales: population based cohort study using the QResearch database. *BMJ* 2010;340:c2197.
6. Larsson BAM, Sundh D, Mellström D, *et al*. Association between cortical bone microstructure and statin use in older women. *J Clin Endocrinol Metab* 2019;104:250–7.
7. Lin T-K, Chou P, Lin C-H, *et al*. Long-Term effect of statins on the risk of new-onset osteoporosis: a nationwide population-based cohort study. *PLoS One* 2018;13:e0196713.
8. Lin T-K, Liou Y-S, Lin C-H, *et al*. High-Potency statins but not all statins decrease the risk of new-onset osteoporotic fractures: a nationwide population-based longitudinal cohort study. *Clin Epidemiol* 2018;10:159–65.
9. Meier CR, Schlienger RG, Kraenzlin ME, *et al*. Hmg-Coa reductase inhibitors and the risk of fractures. *JAMA* 2000;283:3205–10.
10. van Staa TP, Wegman S, de Vries F, *et al*. Use of statins and risk of fractures. *JAMA* 2001;285:1850–5.
11. Johansen ME, Green LA, Sen A, *et al*. Cardiovascular risk and statin use in the United States. *Ann Fam Med* 2014;12:215–23.
12. Catapano AL, Graham I, De Backer G, *et al*. 2016 ESC/EAS guidelines for the management of Dyslipidaemias. *Eur Heart J* 2016;37:2999–3058.
13. Sugiyama M, Kodama T, Konishi K, *et al*. Compactin and simvastatin, but not pravastatin, induce bone morphogenetic protein-2 in human osteosarcoma cells. *Biochem Biophys Res Commun* 2000;271:688–92.
14. Wei W, Schwaid AG, Wang X, *et al*. Ligand activation of ERR α by cholesterol mediates statin and bisphosphonate effects. *Cell Metab* 2016;23:479–91.
15. Corona G, Boddi V, Balercia G, *et al*. The effect of statin therapy on testosterone levels in subjects consulting for erectile dysfunction. *J Sex Med* 2010;7:1547–56.
16. Schooling CM, Au Yeung SL, Freeman G, *et al*. The effect of statins on testosterone in men and women, a systematic review and meta-analysis of randomized controlled trials. *BMC Med* 2013;11:57.
17. Stanworth RD, Kapoor D, Channer KS, *et al*. Statin therapy is associated with lower total but not bioavailable or free testosterone in men with type 2 diabetes. *Diabetes Care* 2009;32:541–6.
18. Kautzky-Willer A, Thurner S, Klimek P. Use of statins offsets insulin-related cancer risk. *J Intern Med* 2017;281:206–16.
19. Rejnmark L, Vestergaard P, Mosekilde L. Statin but not non-statin lipid-lowering drugs decrease fracture risk: a nation-wide case-control study. *Calcif Tissue Int* 2006;79:27–36.

20. Ward IM, Mortensen EM, Battafarano DF, *et al.* Association of statins and risk of fractures in a military health system: a propensity score-matched analysis. *Ann Pharmacother* 2014;48:1406–14.
21. Eriksson AL, Perry JRB, Coviello AD, *et al.* Genetic determinants of circulating estrogen levels and evidence of a causal effect of estradiol on bone density in men. *J Clin Endocrinol Metab* 2018;103:991–1004.
22. Lane NE, Epidemiology LNE. Epidemiology, etiology, and diagnosis of osteoporosis. *Am J Obstet Gynecol* 2006;194(2 Suppl):S3–11.
23. Bone HG, Greenspan SL, McKeever C, *et al.* Alendronate and estrogen effects in postmenopausal women with low bone mineral density. Alendronate/Estrogen Study Group. *J Clin Endocrinol Metab* 2000;85:720–6.
24. Jefcoate C. High-Flux mitochondrial cholesterol trafficking, a specialized function of the adrenal cortex. *J Clin Invest* 2002;110:881–90.
25. Kameda T, Mano H, Yuasa T, *et al.* Estrogen inhibits bone resorption by directly inducing apoptosis of the bone-resorbing osteoclasts. *J Exp Med* 1997;186:489–95.
26. Cole ZA, Dennison EM, Cooper C. Osteoporosis epidemiology update. *Curr Rheumatol Rep* 2008;10:92–6.
27. Pinheiro MM, Reis Neto ETdos, Machado FS, *et al.* Risk factors for osteoporotic fractures and low bone density in pre and postmenopausal women. *Rev Saude Publica* 2010;44:479–85.
28. Kim H-J, Koo HS, Kim Y-S, *et al.* The association of testosterone, sex hormone-binding globulin, and insulin-like growth factor-1 with bone parameters in Korean men aged 50 years or older. *J Bone Miner Metab* 2017;35:659–65.
29. Zhang X, Li J, Zhou X, *et al.* Simvastatin decreases sex hormone levels in male rats. *Endocr Pract* 2017;23:175–81.
30. Guldvang A, Hansen CH, Weisser JJ, *et al.* Simvastatin decreases steroid production in the H295R cell line and decreases steroids and FSH in female rats. *Reprod Toxicol* 2015;58:174–83.
31. de Keyser CE, de Lima FV, de Jong FH, *et al.* Use of statins is associated with lower serum total and non-sex hormone-binding globulin-bound testosterone levels in male participants of the Rotterdam study. *Eur J Endocrinol* 2015;173:155–65.

TRANSLATIONAL SCIENCE

Immunome perturbation is present in patients with juvenile idiopathic arthritis who are in remission and will relapse upon anti-TNF α withdrawal

Jing Yao Leong ,¹ Phyllis Chen,¹ Joo Guan Yeo,^{1,2} Fauziah Ally,¹ Camillus Chua,¹ Sharifah Nur Hazirah,¹ Su Li Poh,¹ Lu Pan,¹ Liyun Lai,¹ Elene Seck Choon Lee,² Loshinidevi D/O Thana Bathi,¹ Thaschawee Arkachaisri,^{1,2} Daniel Lovell,^{3,4} Salvatore Albani,¹ Pediatric Rheumatology Collaborative Study Group

Handling editor Josef S Smolen

► Additional material is published online only. To view, please visit the journal online (<http://dx.doi.org/10.1136/annrheumdis-2019-216059>).

¹Translational Immunology Institute, Singhealth/Duke-NUS Academic Medical Centre, Singapore Health Service, Singapore, Singapore

²Division of Medicine, KK Women's and Children's Hospital, Singapore, Singapore

³Division of Rheumatology, Cincinnati Children's Hospital Medical Center, Cincinnati, Ohio, USA

⁴Department of Paediatrics, University of Cincinnati College of Medicine, Cincinnati, Ohio, USA

Correspondence to

Dr Jing Yao Leong, Translational Immunology Institute, Singhealth/Duke-NUS Academic Medical Centre, Singapore Health Service, Singapore, Singapore; leong.jing.yao@singhealth.com.sg

Received 21 July 2019

Revised 26 August 2019

Accepted 13 September 2019

Published Online First

20 September 2019



© Author(s) (or their employer(s)) 2019. Re-use permitted under CC BY. Published by BMJ.

To cite: Leong JY, Chen P, Yeo JG, et al. *Ann Rheum Dis* 2019;**78**:1712–1721.

ABSTRACT

Objectives Biologics treatment with antitumour necrosis factor alpha (TNF α) is efficacious in patients with juvenile idiopathic arthritis (JIA). Despite displaying clinical inactivity during treatment, many patients will flare on cessation of therapy. The inability to definitively discriminate patients who will relapse or continue to remain in remission after therapy withdrawal is currently a major unmet medical need. CD4 T cells have been implicated in active disease, yet how they contribute to disease persistence despite treatment is unknown.

Methods We interrogated the circulatory reservoir of CD4⁺ immune subsets at the single-cell resolution with mass cytometry (cytometry by time of flight) of patients with JIA (n=20) who displayed continuous clinical inactivity for at least 6 months with anti-TNF α and were subsequently withdrawn from therapy for 8 months, and scored as relapse or remission. These patients were examined prior to therapy withdrawal for putative subsets that could discriminate relapse from remission. We verified on a separate JIA cohort (n=16) the dysregulation of these circulatory subsets 8 months into therapy withdrawal. The immunological transcriptomic signature of CD4 memory in relapse/remission patients was examined with NanoString.

Results An inflammatory memory subset of CD3⁺CD4⁺CD45RA⁻TNF α ⁺ T cells deficient in immune checkpoints (PD1⁻CD152⁻) was present in relapse patients prior to therapy withdrawal. Transcriptomic profiling reveals divergence between relapse and remission patients in disease-centric pathways involving (1) T-cell receptor activation, (2) apoptosis, (3) TNF α , (4) nuclear factor-kappa B and (5) mitogen-activated protein kinase signalling.

Conclusions A unique discriminatory immunomic and transcriptomic signature is associated with relapse patients and may explain how relapse occurs.

INTRODUCTION

Targeted therapy of juvenile idiopathic arthritis (JIA) with antitumour necrosis factor alpha (TNF α) biologics is efficacious, with 70%–80% responders and up to 50% achieving clinical inactivity on long-term treatment.^{1,2} While sustained immune suppression through anti-TNF α is generally well tolerated, clinicians seek to achieve clinical remission off medication to reduce risk of general infection, adverse

Key messages

What is already known about this subject?

- Biologics treatment with tumour necrosis factor alpha inhibitors is efficacious in patients with juvenile idiopathic arthritis, though many patients flare upon cessation of therapy despite achieving clinical inactivity.
- There is lack of scientific understanding and definitive biological markers to discriminate patients who will relapse from those who will remain in stable remission after therapy withdrawal.

What does this study add?

- This study demonstrates that an inflammatory subset of CD4 memory cells deficient in immune checkpoint receptors is present in patients who will relapse.
- T-effector diversification occurs during overt flare in relapse patients.

How might this impact on clinical practice or future developments?

- Tracking of these dysregulated CD4 memory subsets may aid in clinical therapeutic management of patients under therapy, and understanding its mechanisms may provide an avenue for future precision therapeutic developments.

events and financial burden.² Drug withdrawal in patients who attain clinical inactivity is complicated by the fact that 50%–80% of patients relapse on therapy discontinuation.^{3,4} This phenomenon indicates that relapse patients who have attained clinical inactivity on medication, as defined by the Wallace criteria,⁵ continue to experience subclinical inflammation and persistence of disease without overt presentation of clinical symptoms. Conversely, patients who achieve clinical remission off medication could be spared long-term drug effects. As such, there is a clinical need to address how discontinuing anti-TNF α therapy can be safely implemented, as well as a scientific need to understand the immune mechanisms related to relapse.

The pathogenesis of JIA remains widely debated.⁶ Unsupervised genome-wide association studies and pathway analysis have highlighted the role of CD4 T-helper cell populations in autoimmune disease progression.⁷ CD4 T cells were shown to infiltrate the synovium microenvironment,^{8–11} and corresponding pathogenic CD4 HLA-DR⁺ T-effector and regulatory subsets possessing strong immune phenotypic and T-cell receptor (TCR) activation correlation with synovial T cells have been found recirculating in the blood during active inflammation.^{12,13} Furthermore, epigenetic histone modifications associated with enhancer functions have been detected in CD4 T cells of patients with JIA.¹⁴ Using network analysis of DNA CpG methylation sites in total CD4 T cells, we have previously demonstrated that T-cell activation pathways are associated with clinical fate on anti-TNF α withdrawal.¹⁵ However, the identity of the specific pathogenic CD4 subset that maintains subclinical disease persistence remains elusive.

In this study, we exploited the high-dimensional single-cell resolution capabilities of cytometry by time of flight (CyTOF) and patient samples from a well-defined clinical cohort with the objective of uncovering CD4 T-cell subsets responsible for disease persistence. Patients with JIA who maintained clinical inactivity under anti-TNF α for at least 6 months were subsequently withdrawn from therapy. These patients were rigorously scored for their disease activity across 8 months, and their clinical outcome was defined as relapse or remission. We investigated the circulatory immunome of these patients with JIA to determine the immunological differences at the core of the dichotomic clinical fates. These differences may help provide a framework for understanding the mechanisms of disease relapse on drug withdrawal, thus enabling a knowledge-based guidance for clinical management while proposing some potential new targets for intervention.

MATERIALS AND METHODS

Samples

Peripheral blood mononuclear cells (PBMCs) were obtained from patients with polyarticular JIA recruited through the “Determining Predictors of Safe Discontinuation of Anti-TNF treatment in JIA” trial (ID: NCT00792233).¹⁶ Patients treated with anti-TNF α biologics and shown to be in an inactive disease state for 6 months were enrolled into the study. Clinical inactivity was defined by Wallace *et al* criteria⁵: (1) absence of active joints; (2) lack of fever, rash and serositis attributable to JIA; (3) no active uveitis; (4) within normal range of erythrocyte sedimentation rate (ESR) unless attributable to JIA; (5) physician global disease activity of ≤ 0.5 (Likert-like scale); and (6) duration of morning stiffness of ≤ 15 min. On enrolment, patients are withdrawn from anti-TNF α therapy and accessed through monthly clinical visits for a study period of 8 months. Clinical outcome is designated as relapse or remission depending on six core JIA parameters: (1) number of active joints, (2) number of joints with loss of motion, (3) medical doctor global assessment of current disease activity (Likert-like scale), (4) patient/parent global assessment of overall disease severity in the prior week (Likert-like scale), (5) a validated measure of physical function childhood health assessment questionnaire (CHAQ) and (f) ESR. A patient was considered to be experiencing a relapse if there was $\geq 30\%$ worsening in more than three of the six JIA core parameters, with no more than one parameter improving by $>30\%$.¹⁷ For remission individuals, they would have achieved ≥ 14 months of clinical inactivity from prior recruitment to study end. PBMCs were interrogated by CyTOF from patients (n=20)

prior to withdrawal and were designated as (T₀), and separately from another batch (n=16) at the end of 8 months after withdrawal were designated as (T_{end}). Patient PBMCs (n=12) were also sorted for CD3⁺CD4⁺CD45RO⁺CD45RA⁻ for NanoString analysis. The demographics/medication history profile of patients with JIA withdrawn from therapy and sample usage breakdown is shown in online supplementary table S1.

Age-matched healthy controls (n=69) were recruited through the Precision Rheumatology International Platform (PRIP) study conducted at the KK Women’s and Children’s Hospital (KKH). These controls have no indication of inflammation and PBMCs were isolated pre-operatively from patients scheduled for day surgeries. Healthy PBMCs were examined with CyTOF (n=10), NanoString (n=3) or age-matched strata cross validation for receiver operating characteristic (ROC) curve (n=56).

Paired treatment naive/post-treatment patients with JIA (n=4) were also recruited through the study “A Precision Medicine Approach to Understand and Predict Responsiveness to Therapy in Human Arthritis” conducted in KKH for NanoString analysis. These patients with active JIA were initially treatment naive to anti-TNF α and, after a 6-month drug course, exhibited treatment susceptibility determined by complete absence of active joints. The demographics/medication history profile of patients with JIA is shown in online supplementary table S2.

Additional methodological details are available as online supplementary information.

RESULTS

CD4⁺CD45RA⁻TNF α ⁺ T cells were present in patients with JIA prior to relapse

Dysregulated CD4 T cells are thought to contribute to JIA pathogenesis.^{8–13} We interrogated the circulatory CD4 landscape of patients with JIA (n=20) prior to therapy withdrawal to understand why certain individuals relapse. At this stage, the patients were clinically scored to be inactive for 6 months; thus, patients who will relapse or remain in remission were clinically indistinguishable prior to withdrawal. We assessed the PBMCs with a CyTOF panel consisting of 31 functional, 6 lineage markers (online supplementary table S3) and CD45 barcoding to facilitate pooling of individuals.¹⁸ Batch variability in staining was monitored through an internal biological control (online supplementary figure S1). The debarcoded CD3⁺CD4⁺ T cells were exported and normalised for cell events, and the 31 markers were dimensionally reduced with MarVis onto a bivariate X–Y axis through t-distributed stochastic neighbour embedding (t-SNE) (online supplementary figure S2). Clustering with k-means segregated the CD4 cells into distinct nodes (figure 1A), and we detected an enrichment ($p < 0.01$) in node 22 for patients who will relapse that represents CD4⁺CD45RA⁻TNF α ⁺IFN γ ⁻CD152⁻PD1⁻ T cells (figure 1A–C). This was further verified with a separate clustering method, FlowSoM (online supplementary figure S3). To ensure the results were not due to clustering artefacts, we manually gated the preclustering flow cytometry standard (FCS) files (figure 1D, gating strategy in online supplementary figure S4) and determined significant ($p < 0.05$) upregulation in CD4⁺CD45RA⁻ memory subsets that was restricted within the TNF α ⁺ compartment. In particular, relapse patients were enriched for CD4⁺CD45RA⁻TNF α ⁺ T cells, which were absent for IFN γ expression, and were notably deficient in immune checkpoints (PD1/CD152). We investigated the relationship of the dysregulated T effectors and immune checkpoint expression within the memory compartment (figure 1E). There was a stronger positive correlation of

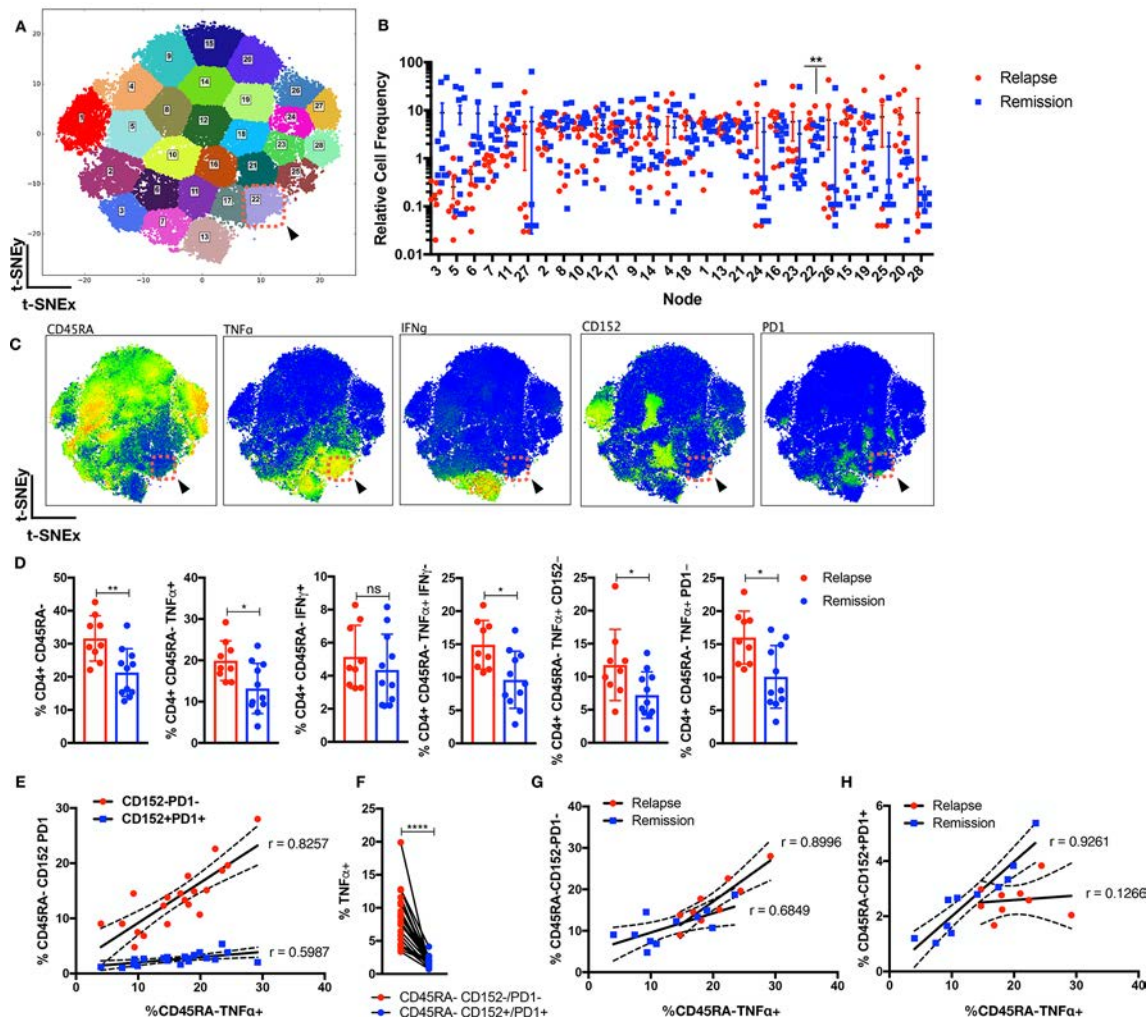


Figure 1 Perturbation in CD4 landscape in patients with JIA who will relapse. Circulatory CD3⁺CD4⁺ cells from patients with JIA (n=20; relapse=9, remission=11) prior to therapy withdrawal were stained with 31 functional markers in cytometry by time of flight and were dimensionally reduced onto a bivariate X–Y axis scale with t-SNE. (A) The t-SNE map is segregated into 28 distinct nodes with k-means, and node 22 is highlighted (red-dotted box). (B) The distribution of relative cell frequency in relapse or remission patients across the nodes is shown, with node 22 significantly higher ($p < 0.01$) in relapse individuals. (C) The phenotypic expression of markers is shown for node 22 (red-dotted box). (D) Supervised gating of the preclustering FCS files validates the relevant CD4 memory cellular subsets in relapse versus remission individuals. (E) Correlation analysis of CD45RA[−]TNF α ⁺ versus CD45RA[−]CD152[−]/PD1[−] or CD45RA[−]CD152⁺/PD1⁺ as percentage of CD3⁺CD4⁺ cells across patients with JIA. (F) Percentage of TNF α ⁺ cells in CD45RA[−]CD152[−]/PD1[−] or CD45RA[−]CD152⁺/PD1⁺ compartment. Correlation analysis of CD45RA[−]TNF α ⁺ versus (G) CD45RA[−]CD152[−]/PD1[−] or (H) CD45RA[−]CD152⁺/PD1⁺ as percentage of CD3⁺CD4⁺ cells across relapse or remission patients. Comparison of cellular subsets performed with Mann-Whitney U, unpaired or paired two-tailed test, means \pm SD. * $p < 0.05$, ** $p < 0.01$, **** $p < 0.0001$. Correlation analysis performed with Pearson correlation, two-tailed test. IFN, interferon; TNF α , tumour necrosis factor alpha; t-SNE, t-distributed stochastic neighbour embedding.

CD45RA[−]TNF α ⁺ with CD45RA[−]CD152[−]PD1[−] ($r = 0.8257$) as opposed to CD45RA[−]CD152⁺PD1⁺ ($r = 0.5987$) cells across the patients. The percentage of TNF α ⁺ cells was significantly higher ($p < 0.0001$) in CD45RA[−]CD152[−]/PD1[−] cells (figure 1F). While relapse patients showed a perceptible increase in T effectors in the absence CD152/PD1, there was a marked drop to upregulate CD152/PD1 as compared with remission patients (figure 1G,H).

Analysis of the CD4⁺TNF α ⁺ healthy landscape unveils subclinical T-effector diversification in relapse patients

To validate the previously mentioned findings and to investigate the possibility of disease-centric CD4⁺ cellular subsets that are masked by comparing JIA relapse/remission individuals, we included age-matched paediatric healthy controls. CD4⁺TNF α ⁺ T cells from JIA relapse/remission (n=20) prior to withdrawal or healthy individuals (n=10) were compared

with further delineated key differences within the T-effector compartment. Patients with JIA who will relapse were enriched ($p < 0.05$) for node 17 against remission individuals (figure 2A,B) and additionally for nodes 17, 13 and 18 against healthy controls ($p < 0.05$) (figure 2C,D). Node 17 reaffirms relapse individuals are enriched for CD4⁺CD45RA[−]TNF α ⁺IFN γ [−]CD152[−]PD1[−] T cells (figure 2E,F) as compared with remission or healthy individuals. Additionally, node 13 (figure 2E) represents CD4⁺CD45RA[−]TNF α ⁺IFN γ [−]CD152[−]PD1[−] T cells that are also interleukin (IL)-6⁺. Supervised gating (figure 2G gating strategy in online supplementary figure S4) validated that relapse individuals are enriched ($p < 0.001$) with CD4⁺CD45RA[−]TNF α ⁺IL-6⁺ as compared with healthy individuals. The intensity of TNF α was significantly higher ($p < 0.0001$) in CD45RA[−]IL-6⁺ as opposed to IL-6[−] cells (figure 2H), and relapse individuals had a higher fold increase ($p < 0.05$) in

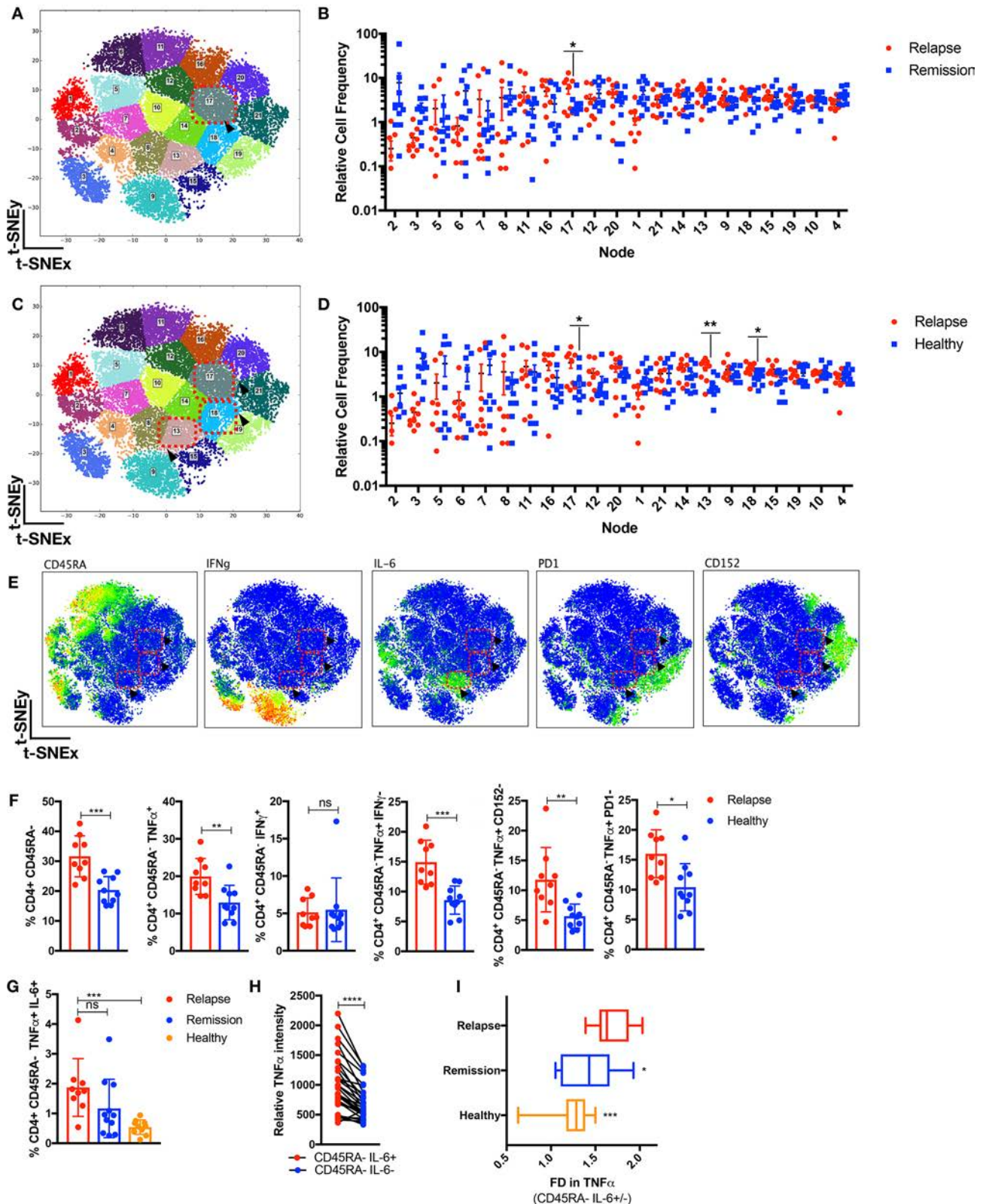


Figure 2 Subclinical T-effector diversification in relapse individuals. CD4⁺TNFα⁺ cells from patients with JIA (n=20; relapse=9, remission=11) prior to therapy withdrawal and healthy paediatric controls (n=10) were analysed through t-SNE. (A) The CD4⁺TNFα⁺ t-SNE MAP is segregated into 21 nodes with enrichment in (B) node 17 (p<0.05) for relapse as compared with remission individuals and (C,D) node 17, 18 and 13 (p<0.05) for relapse as compared with healthy individuals. (E) The phenotype expression is shown for node 17, 18 and 13 (red-dotted boxes and arrowheads). (F) Supervised gating of preclustering FCS files validates the relevant CD4 memory cellular subsets in relapse versus healthy individuals. (G) Supervised gating of CD4⁺CD45RA⁻TNFα⁺IL-6⁺ cells in relapse/remission/healthy individuals. (H) Relative TNFα intensity in CD45RA⁻IL-6⁺ or CD45RA⁻IL-6⁻ cells. (I) Fold difference (FD) in TNFα intensity in CD45RA⁻IL-6⁺ over CD45RA⁻IL-6⁻ cells in relapse/remission/healthy individuals. Comparison of cellular subsets performed with Mann-Whitney U, unpaired or paired two-tailed test, means±SD. *p<0.05, **p<0.01, ***p<0.001, ****p<0.0001. IFN, interferon; IL, interleukin; ns, not significant; TNFα, tumour necrosis factor alpha; t-SNE, t-distributed stochastic neighbour embedding.

TNF α in CD45RA⁻IL-6⁺ cells as compared with remission or healthy individuals.

Overt T-effector diversification during flare manifestation and quiescence in stable remission

We have observed the presence of CD4 memory T cells in patients prior to relapse. To examine this phenomenon further, we interrogated the CD4 landscape of an independent batch of JIA individuals (n=16) withdrawn from therapy for 8 months that either developed flare or remained in stable remission. Relapse (in flare) patients exhibited the emergence of a previously subclinical CD4⁺CD45RA⁻TNF α ⁺IL-6⁺ subset (figure 3A–D, node 7) as compared with patients who remained in remission after 8 months of withdrawal. To determine the state of immunological quiescence in remission (T₀: prior withdrawal, T_{end}: 8 months' withdrawal) patients, we gated for the relevant dysregulated CD4⁺CD45RA⁻TNF α ⁺ subsets and found no difference as compared with healthy individuals (figure 3E). The CD4 landscape of remission patients (T₀/T_{end}) as compared with healthy individuals revealed mostly similar profiles (figure 3F) except for nodes 17 and 1 enriched in remission T₀ or T_{end} patients, respectively. Both nodes were absent for TNF α , with node 17 exhibiting CD45RA⁺ and node 1 expressing the CD45RA^{-/+}CXCR3⁺CCR6⁺ phenotype (figure 3G).

Corresponding increase of memory Tregs and CD45RA⁻TNF α ⁺ prior to relapse

As Tregs have been previously implicated in JIA pathogenesis,^{11 13 19–21} we examined their role in patients with JIA prior/after therapy withdrawal (figure 4A,B; gating strategy in online supplementary figure S4). While no differential total Treg frequencies was detected, we observed higher levels of CD45RA⁻Treg (p<0.0001) in patients with JIA prior to relapse. We further verified this with t-SNE analysis of Tregs from relapse/remission patients prior to withdrawal and determined an enrichment for CD45RA⁻CD152⁺CD127⁻Tregs for relapse individuals (figure 4C,D). While no correlation (r=0.1532) with total Tregs was observed for CD45RA⁻TNF α ⁺ cells (figure 4E), there was a positive correlation (r=0.6017) with CD45RA⁻Treg.

Transcriptomic divergence in disease-centric pathways that persists despite therapy

We have previously shown that patients with JIA who developed active disease on therapy withdrawal have stable epigenetic DNA CpG modifications in CD4 T cells that predisposed towards T-cell activation and TCR signalling.¹⁵ We wanted to investigate if CD4 memory T cells from JIA relapse/remission patients were differential in transcriptomic profile when their TCR is activated. We sorted for CD3⁺CD4⁺CD45RA⁻CD45RO⁺ T cells (online supplementary figure S5), stimulated 24 hours with anti-CD3/CD28, and profiled 579 immunological genes through NanoString. Functional gene enrichment analysis (DAVID) of JIA relapse (n=6) or remission (n=6) patients versus healthy individuals (n=3) identified five common disease-centric pathways that persisted from prior to after withdrawal of therapy (online supplementary figure S6 and tables S4 and S5). Dysregulation in *UBE2L3*, *IL-6*, *STAT4*, *TYK2*, *TNFAIP3* and *PTPN2* were found in both relapse and remission individuals, have been previously associated with JIA.^{22 23} We examined through Cytoscape and Reactome database for the gene associations involved in the five pathways (figure 5A–E): (1) TCR activation, (2) apoptosis, (3) TNF α , (4) nuclear factor-kappa B (NF- κ B) and (5) mitogen-activated protein kinase (MAPK) signalling,

and found a considerable overlap between relapse and remission individuals. This overlap of pathways in patients with relapse/remission JIA may arise from their shared susceptibility to clinical control with continued anti-TNF α therapy. Indeed, we observe a similar disease-centric pathway persistence in a separate cohort of patients with JIA (n=4) that are responsive to anti-TNF α therapy, from the point of pretreatment (active) until post-treatment (recent clinical inactivity) (online supplementary figures S7 and S8 and table S3 and S6). Despite this overlap, we detected selective divergence within these pathways (figure 5A–E), with remission individuals expressing higher levels of *FYN*, *TNFRSF9*, *CASP1*, *TRAF1* and *IKBKE*, which are involved in the termination or resolution of these pathways.^{24–33}

CD4⁺CD45RA⁻TNF α ⁺ discriminates clinical fate prior to withdrawal of therapy

We explored whether disease or remission duration of patients with JIA (n=39) prior to study enrolment could differentiate clinical fate, and found no significant difference between patients with relapse JIA or patients with remission JIA (figure 6A–D). As we have shown that an inflammatory memory subset of CD4⁺CD45RA⁻TNF α ⁺ is present in relapse individuals prior to therapy withdrawal, we tested whether this could afford for discrimination in clinical fate. There was a significant difference (p<0.001) in the ratio of CD45RA⁻TNF α ⁺/CD45RA⁺TNF α ⁺ cells in relapse as compared with remission individuals prior to therapy withdrawal, allowing for an ROC curve of area under the curve (AUC)=0.9394 (figure 6E,F). As age could be a serious potential cofounder for immunological memory, we determined that, in the relevant age groups (7–14 years), there was no significant difference in CD45RA⁻ or CD45RA⁻TNF α ⁺ cells among healthy individuals (n=56) (figure 6G,H). Relapse individuals had significantly higher CD45RA⁻TNF α ⁺ cells as compared across all the relevant age groups in healthy individuals (figure 6H).

DISCUSSION

With a large proportion of patients with JIA achieving clinical inactivity as a result of efficacious treatment with anti-TNF α biologics,² it becomes increasingly pertinent to address the lack of definitive withdrawal guidelines. Here, we investigated with CyTOF the heterogenous CD4 landscape of patients who achieved clinical inactivity prior to therapy withdrawal. We have identified for the first time an inflammatory CD4 memory subset (CD3⁺CD4⁺CD45RA⁻TNF α ⁺) that remains elevated in patients with JIA prior to relapse, and could notably discriminate clinical fate prior to therapy withdrawal (AUC=0.939).

Remarkably, the presence of this inflammatory subset, despite therapy, was associated with a deficit in immune checkpoint (PD1⁻CD152⁻). This is consistent with the phenomenon of rheumatic immune-related adverse events, where the application of immune checkpoint therapy (anti-PD1/anti-CD152) in cancer results in rheumatic diseases.³⁴ The presence of this inflammatory subset was further verified when we separately compared relapse against healthy non-JIA individuals. The CD4⁺TNF α ⁺ healthy landscape helped reveal the subclinical diversification of T-effector mechanisms in relapse individuals, with the emergence of CD3⁺CD4⁺CD45RA⁻TNF α ⁺PD1⁻CD152⁻ T cells that are IL-6⁺. Particularly, CD4⁺CD45RA⁻ T cells that are IL-6⁺ express higher levels of TNF α . Recently, a case series of three patients with cancer and developed severe polyarthritis following immune blockade therapy, reported successful treatment with tocilizumab (anti-IL-6).³⁵ This reflects a level of

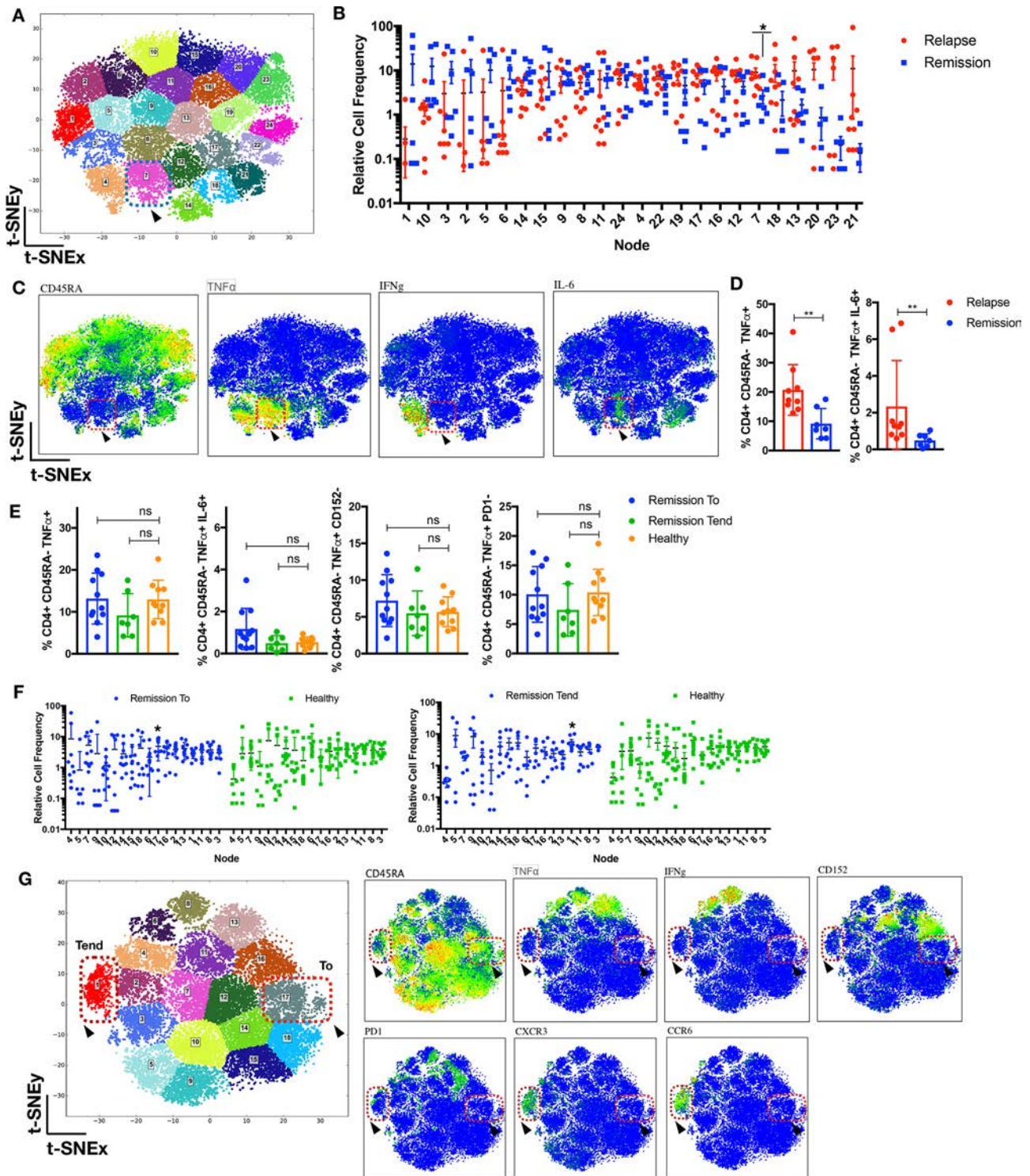


Figure 3 Emergence of T-effector diversification in flare manifestation and quiescence in stable remission. (A–D) CD4⁺ T cells from patients with JIA (n=16; relapse=9, remission=7) withdrawn from therapy for 8 months were analysed with t-SNE. (A) The t-SNE MAP is segregated into 24 nodes; node 7 is highlighted (blue-dotted box). (B) The distribution of relative cell frequency across the nodes is shown, with node 7 enriched (p<0.05) in relapse individuals, exhibiting (C) the CD4⁺CD45RA⁻ TNF α ⁺ IL-6⁺ IFN γ ⁻ phenotype (node7: red-dotted box and arrowhead). (D) Supervised gating of preclustering FCS files for CD4⁺CD45RA⁻ TNF α ⁺ IL-6⁺ in relapse and remission patients. (E) Supervised gating of relevant CD4⁺CD45RA⁻ TNF α ⁺ subsets in remission patients (t₀: prior to withdrawal or t_{end}: 8 months after withdrawal) or healthy individuals. (F,G) CD4⁺ T cells from JIA remission patients (n=18; T₀=11, T_{end}=7) and healthy controls (n=10) were analysed with t-SNE. (F) The distribution of relative cell frequency across the nodes is shown, with node 17 enriched (p<0.05) in remission t₀ and node 1 enriched (p<0.05) in remission t_{end} as compared with healthy individuals. (G) Nodes 1 and 17 phenotypes are depicted. Comparison of cellular subsets performed with Mann-Whitney U, two-tailed test, means \pm SD. *p<0.05, **p<0.01. IFN, interferon; IL, interleukin; ns, not significant; TNF α , tumour necrosis factor alpha; t-SNE, t-distributed stochastic neighbour embedding.

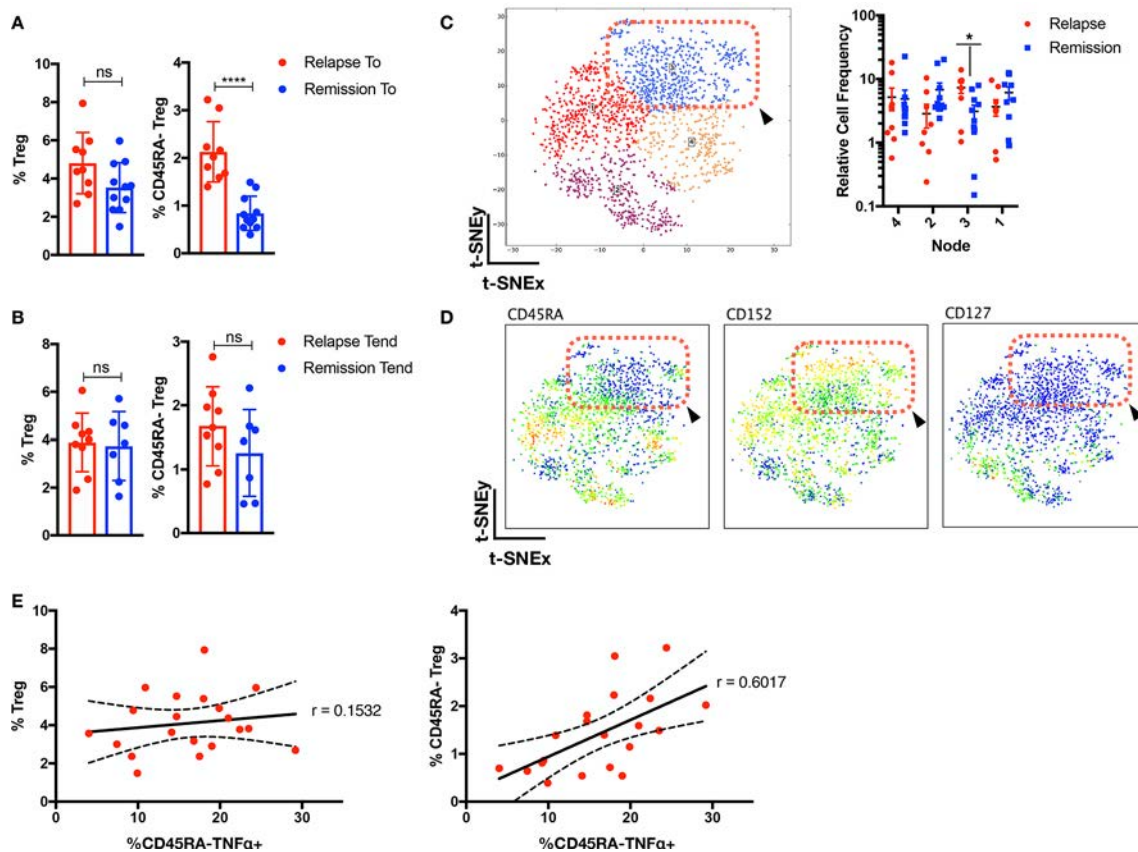


Figure 4 Corresponding increase of memory Tregs and CD45RA⁺ TNF α ⁺ prior to relapse. Supervised gating of Tregs and CD45RA⁺ Tregs in patients with JIA (A) prior (n=20) and (B) after withdrawal (n=16) of therapy. (C–D) Tregs cells from patients with JIA (n=20; relapse=9, remission=11) prior to withdrawal were analysed with t-SNE and (C) segregated into four nodes, with node 3 (p<0.05) enriched in relapse individuals. (D) Phenotype of node 3 is depicted (red-dotted box and arrowhead). (E) Correlation analysis of frequency of Tregs or CD45RA⁺ Tregs with CD45RA⁺ TNF α ⁺. Comparison of cellular subsets performed with Mann-Whitney U, two-tailed test, means \pm SD. *p<0.05, ****p<0.0001. Correlation analysis performed with Pearson correlation, two-tailed test. ns, not significant; TNF α , tumour necrosis factor alpha; t-SNE, t-distributed stochastic neighbour embedding.

commonality between inflammatory and disease resolution mechanisms operating in autoimmune disorders and cancer.

We further examined a separate cohort of patients with JIA who developed flare or remained in remission 8 months into withdrawal of therapy, and verified the overt presence of T-effector diversification (CD45RA⁺ TNF α ⁺ IL-6⁺) during flare. Whereas in patients who continued to remain in remission 8 months into withdrawal, there was no differential display of any CD45RA⁺ TNF α ⁺ subsets as compared with the healthy CD4 landscape, though a CD4⁺ CXCR3⁺ CCR6⁺ subset was detected. It remains speculative if the CD4⁺ CXCR3⁺ CCR6⁺ subset seen in remission patients is an early disease-driven subset or side effect of therapy as it extends beyond the scope of the study and will require a longer follow-up duration. In rheumatoid arthritis, the CD4⁺ CXCR3⁺ CCR6⁺ subset is known to express high levels of IFN γ with poor secretion of IL-17A,³⁶ though we did not observe any associated cytokine profile in our remission patients.

In patients prior to relapse, the prevalence of the inflammatory CD4⁺ CD45RA⁺ TNF α ⁺ T cells within the T-effector compartment is parallel by a corresponding increase in CD4⁺ CD45RA⁺ CD152⁺ Tregs in the regulatory arm. This suggests there is a compensatory regulatory response towards subclinical inflammation prior to relapse, though it remains to be seen whether the suppression suffices or is defective. Others have shown that synovium T effectors are resistant to Treg suppression,²⁰ which can be alleviated in patients with JIA undergoing

anti-TNF α therapy.³⁷ Though it is noted that in a subset of patients, in vitro blockade of IL-6⁺ additionally alleviated T-effector resistance to Treg suppression.³⁷

Transcriptomic profiling of immunological genes in response to TCR signalling reveals five common disease-centric pathways (TCR activation, apoptosis, TNF α , NF- κ B and MAPK signalling) in relapse/remission patients as compared with healthy controls. Separately, the same dysregulated pathways were also detected in patients with JIA that are treatment naive and later responsive to anti-TNF α therapy. This suggests that the disease pathways affected are likely an indication of susceptibility to anti-TNF α treatment rather than an artefact of prolonged medication. As the afflicted pathways remain dysregulated prior and after therapy withdrawal in both relapse and remission patients, exogenous therapy by sequestration of TNF α may accomplish little to re-establish healthy physiological TCR response. Despite this, we detected selective divergence in certain genes (eg, *TRAF1*) with these pathways that may aid in termination or resolution of TCR-induced signalling for remission individuals. Notably, disease association within the *TRAF1*-C5 locus^{38–40} and epigenetic dysregulation within the *TRAF1* locus of CD4 T cells have been detected in patients with JIA.⁴¹ Studies using *TRAF1*^{-/-} mice revealed a TRAF1 negative regulatory role in T-cell response to TCR and TNF α signalling.²⁵ *TRAF1*^{-/-} T cells show enhanced proliferation in response to TCR and TNF α stimulation resulting in NF- κ B and AP-1 activation.²⁵

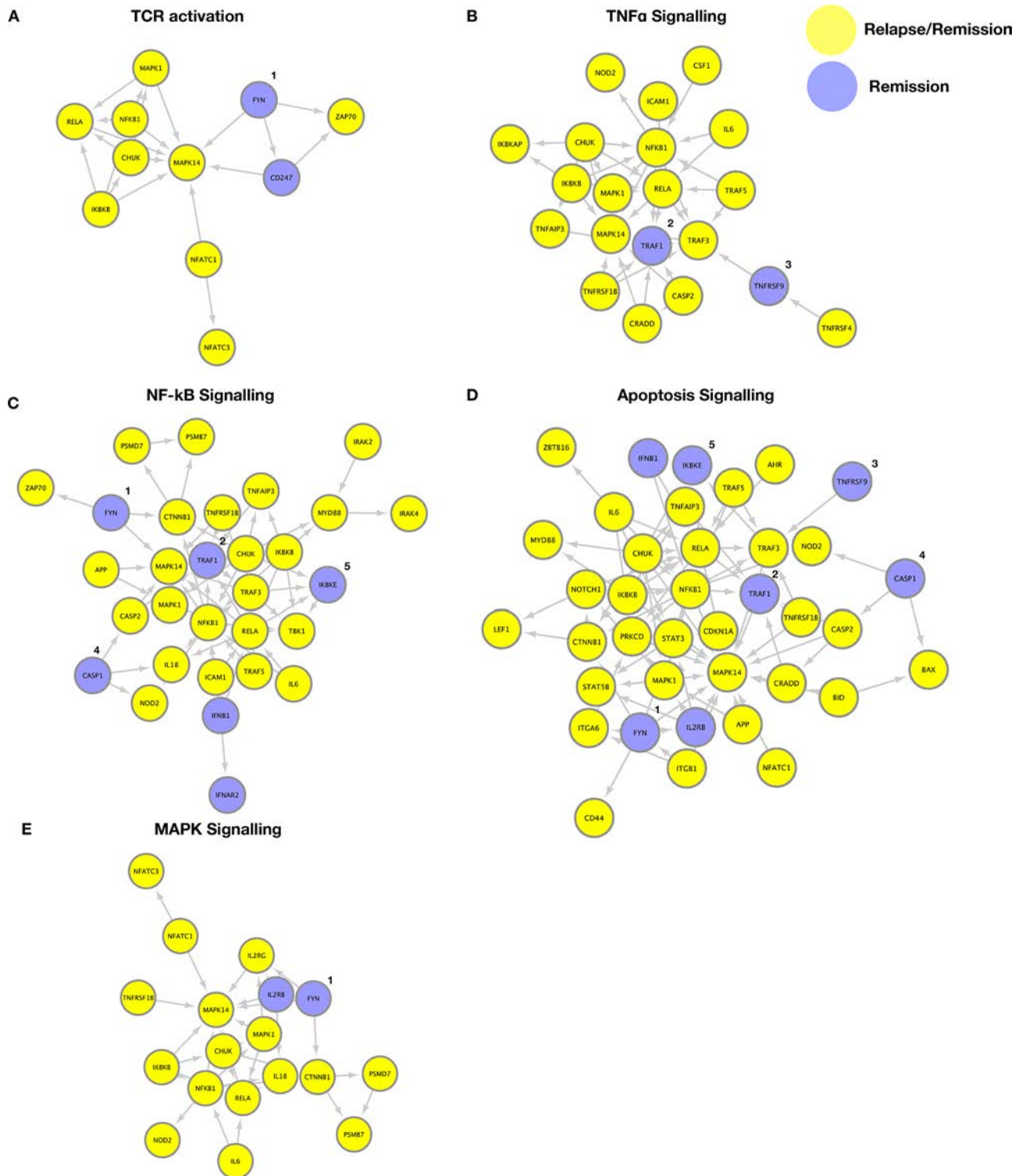


Figure 5 Transcriptomic divergence in disease-centric pathways that persist despite therapy. Genes enriched ($p < 0.05$, fold difference > 1.5) in patients with JIA ($n = 6$ relapse or $n = 6$ remission) that were persistent from prior to after therapy withdrawal, as compared with healthy individuals, were exported to David for functional gene-set enrichment, and gene associations were constructed with Cytoscape using the Reactome database. Five major pathways were dysregulated in relapse and remission patients with JIA compared with healthy controls: (A) TCR activation, (B) $\text{TNF}\alpha$ signalling, (C) NF- κ B signalling, (D) apoptosis, (E) MAPK signalling (yellow=relapse/remission, blue=remission only). Genes enriched in remission individuals include 1, *Fyn*; 2, *TRAF1*; 3, *TNFRSF9*; 4, *CASP1*; and 5, *IKBE*. MAPK, mitogen-activated protein kinase; NF- κ B, nuclear factor-kappa B; TCR, T-cell receptor; $\text{TNF}\alpha$, tumour necrosis factor alpha.

In summary, by applying a combination of high-dimensionality technologies, we have identified functional perturbations of the immune in patients with arthritis who will relapse on withdrawal for anti- $\text{TNF}\alpha$ therapy. These aberrations show that

relapse of clinical disease relies on a foundation of complex and diverse interlacing immune mechanisms, which affect both the effector and regulatory arms of adaptive T-cell immunity. Our findings have an immediate translational valency. Indeed, there

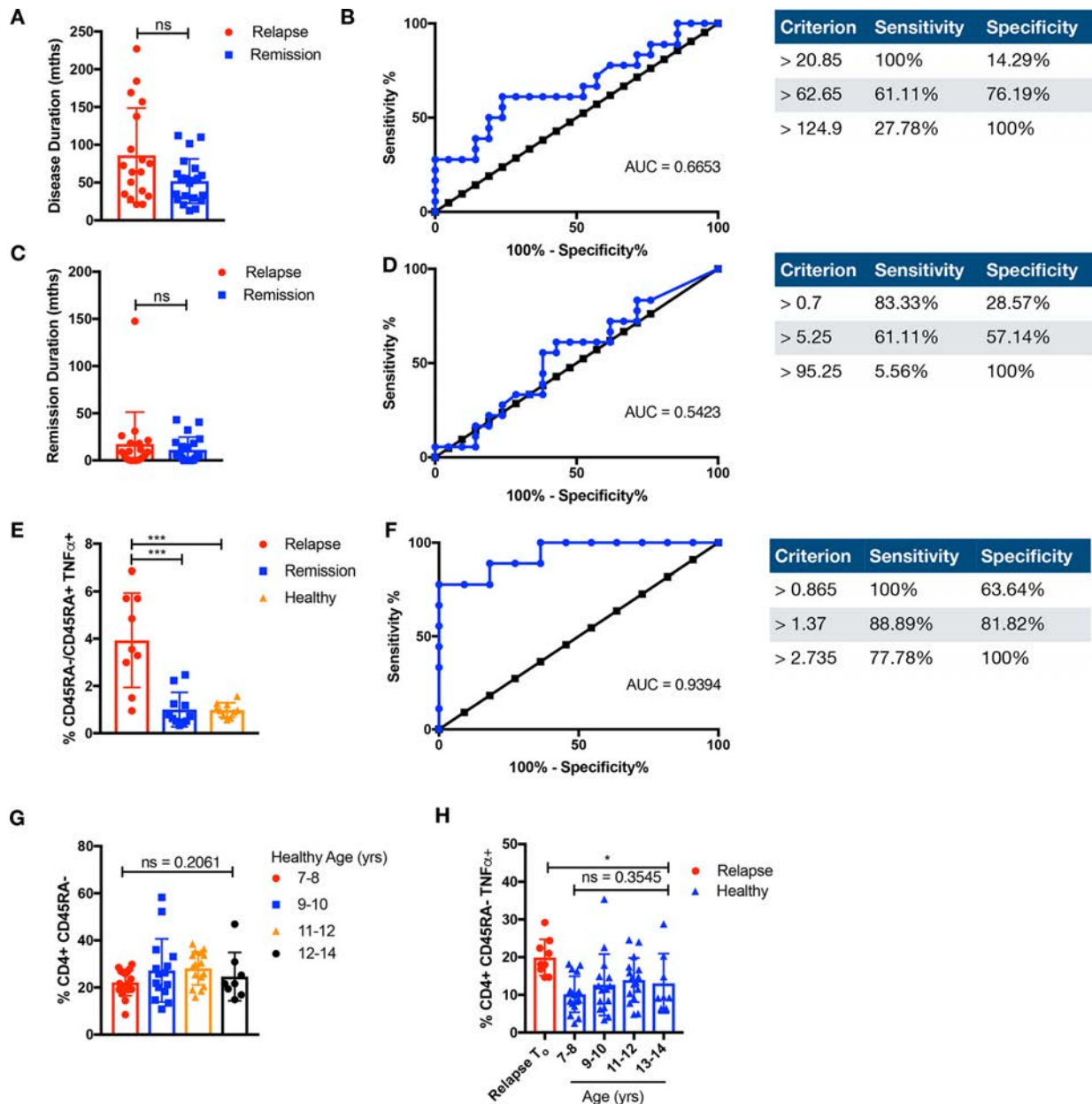


Figure 6 CD4⁺CD45RA⁻ TNFα⁺ discriminates clinical fate. Duration and ROC of (A,B) disease (months) or (C,D) remission (months) prior to study enrolment is compared among relapse (n=18) or remission (n=21) individuals. (E) The ratio of memory CD4⁺CD45RA⁻ TNFα⁺ over naive CD4⁺CD45RA⁺ TNFα⁺ of relapse or remission prior to withdrawal and healthy individuals is compared. Comparison of cellular subsets performed with Mann-Whitney U, two-tailed test, means±SD. *p<0.05. (F) ROC of ratio of CD4⁺CD45RA⁻ TNFα⁺ over CD4⁺CD45RA⁺ TNFα⁺ of relapse or remission prior to withdrawal. (G) CD3⁺CD4⁺CD45RA⁻ CD45RO⁺ T cells were compared in healthy paediatric controls (n=56) across the relevant age groups of 7–8 years (n=17), 9–10 years (n=15), 11–12 years (n=16) and 12–14 years (n=8) or (H) against relapse (n=9) prior to therapy withdrawal for CD3⁺CD4⁺CD45RA⁻ TNFα⁺. Comparison of cellular subsets performed with Kruskal-Wallis test, means±SD. AUC, area under the curve; ns, not significant; ROC, receiver operating characteristic; TNFα, tumour necrosis factor alpha.

is a potential diagnostic advantage⁴² in tracking these dysregulated CD4 subsets to affect clinical management of therapy withdrawal. Also, the occurrence of T-effector diversification in relapse patients and insights into key divergence in disease-centric pathways for remission patients are mechanistically relevant as, altogether, they define a cluster of deranged mechanisms that can be target of focused intervention.

Collaborators PRCSGPediatric Rheumatology Collaborative Study Group (PRCSG): Daniel J. Lovell, Anne L. Johnson, Steven J. Spalding, Beth S. Gottlieb, Paula W. Morris, Yukiko Kimura, Karen Onel, Suzanne C. Li, Alexei A. Grom, Janalee Taylor, Hermine I. Brunner, Jennifer L. Huggins, James J. Nocton, Kathleen A. Haines, Barbara S. Edelheit, Michael Shishov, Lawrence K. Jung, Calvin B. Williams, Melissa S. Teshler,

Denise M. Costanzo, Lawrence S. Zemel, Jason A. Dare, Murray H. Passo, Kaleo C. Ede, Judyann C. Olson, Elaine A. Cassidy, Thomas A. Griffin, Linda Wagner-Weiner, Jennifer E. Weiss, Larry B. Vogler, Kelly A. Rouster-Stevens, Timothy Beukelman, Randy Q. Cron, Daniel Kietz, Kenneth Schikler, Jay Mehta, Tracy V. Ting, James W. Verbsky, B. Anne Eberhard, Bin Huang, Chen Chen, Edward H. Giannini. Authors involved in the clinical trial are listed in the Acknowledgement and affiliations in the online supplementary. (The position of this study group in the author list is shown in the main document)

Contributors JYL performed the mass cytometry (cytometry by time of flight(CyTOF)), sorting and NanoString experiments and analysis. PC and SLP helped with the CyTOF and NanoString runs. FA, CC and SNH helped with mRNA processing and NanoString. LP helped write the R scripts for the CyTOF analysis. LL helped with the CyToF. LTB helped with sample processing. DL, JGY,

ESCL, TA and PRSCG helped with patient recruitment. SA was the lead principal investigator.

Funding Grant support from the National Medical Research Council (NMRC) (NMRC/STaR/020/2013, NMRC/MOHAFACAT2/2/08, MOHAFACAT2/0001/2014, NMRC MOHAFACAT1-6003, centre grants, TCR15Jun006, NMRC/CIRG/1460/2016, MH 095:003/016-0002), Duke-NUS, A*STAR-BMRC (IAF311020), BMRC (SPF2014/005) is gratefully acknowledged.

Competing interests None declared.

Patient and public involvement statement This research was done without patient involvement. Patients were not invited to comment on the study design and were not consulted to develop patient relevant outcomes or interpret the results. Patients were not invited to contribute to the writing or editing of this document for readability or accuracy.

Patient consent for publication Not required.

Ethics approval All samples were collected upon informed consent. All experiments were conducted according to the principles expressed in the Declaration of Helsinki, and institutional review board approved by the Sanford-Burnham or KK Women's and Children's Hospital IRB Committee.

Provenance and peer review Not commissioned; externally peer reviewed.

Data availability statement Data are available upon reasonable request.

Open access This is an open access article distributed in accordance with the Creative Commons Attribution 4.0 Unported (CC BY 4.0) license, which permits others to copy, redistribute, remix, transform and build upon this work for any purpose, provided the original work is properly cited, a link to the licence is given, and indication of whether changes were made. See: <https://creativecommons.org/licenses/by/4.0/>.

ORCID iD

Jing Yao Leong <http://orcid.org/0000-0002-8651-9801>

REFERENCES

- Lovell DJ, Giannini EH, Reiff A, *et al.* Etanercept in children with polyarticular juvenile rheumatoid arthritis. pediatric rheumatology collaborative Study Group. *N Engl J Med* 2000;342:763–9.
- Taddio A, Cattalini M, Simonini G, *et al.* Recent advances in the use of Anti-TNF α therapy for the treatment of juvenile idiopathic arthritis. *Expert Rev Clin Immunol* 2016;12:641–9.
- Baszic K, Garbutt J, Toib D, *et al.* Clinical outcomes after withdrawal of anti-tumor necrosis factor α therapy in patients with juvenile idiopathic arthritis: a twelve-year experience. *Arthritis Rheum* 2011;63:3163–8.
- Iglesias E, Torrente-Segarra V, Bou R, *et al.* Non-Systemic juvenile idiopathic arthritis outcome after reaching clinical remission with anti-TNF- α therapy: a clinical practice observational study of patients who discontinued treatment. *Rheumatol Int* 2014;34:1053–7.
- Wallace CA, Giannini EH, Huang B, *et al.* American College of rheumatology provisional criteria for defining clinical inactive disease in select categories of juvenile idiopathic arthritis. *Arthritis Care Res* 2011;63:929–36.
- Leong JY, Guan YJ, Albani S, *et al.* Recent advances in our understanding of the pathogenesis of juvenile idiopathic arthritis and their potential clinical implications. *Expert Rev Clin Immunol* 2018;14:933–44.
- Eyre S, Orozco G, Worthington J. The genetics revolution in rheumatology: large scale genomic arrays and genetic mapping. *Nat Rev Rheumatol* 2017;13:421–32.
- Hunter PJ, Nistala K, Jina N, *et al.* Biologic predictors of extension of oligoarticular juvenile idiopathic arthritis as determined from synovial fluid cellular composition and gene expression. *Arthritis Rheum* 2010;62:896–907.
- Cosmi L, Cimaz R, Maggi L, *et al.* Evidence of the transient nature of the Th17 phenotype of CD4+CD161+ T cells in the synovial fluid of patients with juvenile idiopathic arthritis. *Arthritis Rheum* 2011;63:2504–15.
- Issekutz AC, Quinn PJ, Lang B, *et al.* Coexpression of chemokine receptors CCR5, CXCR3, and CCR4 and ligands for P- and E-selectin on T lymphocytes of patients with juvenile idiopathic arthritis. *Arthritis Rheum* 2011;63:3467–76.
- Prakken B, Albani S, Martini A. Juvenile idiopathic arthritis. *Lancet* 2011;377:2138–49.
- Spreafico R, Rossetti M, van Loosdregt J, *et al.* A circulating reservoir of pathogenic-like CD4+ T cells shares a genetic and phenotypic signature with the inflamed synovial micro-environment. *Ann Rheum Dis* 2016;75:459–65.
- Rossetti M, Spreafico R, Consolaro A, *et al.* Tcr repertoire sequencing identifies synovial Treg cell clonotypes in the bloodstream during active inflammation in human arthritis. *Ann Rheum Dis* 2017;76:435–41.
- Jiang K, Zhu L, Buck MJ, *et al.* Disease-Associated single-nucleotide polymorphisms from noncoding regions in juvenile idiopathic arthritis are located within or adjacent to functional genomic elements of human neutrophils and CD4+ T cells. *Arthritis Rheumatol* 2015;67:1966–77.
- Spreafico R, Rossetti M, Whitaker JW, *et al.* Epipolymorphisms associated with the clinical outcome of autoimmune arthritis affect CD4+ T cell activation pathways. *Proc Natl Acad Sci U S A* 2016;113:13845–50.
- Determining predictors of safe discontinuation of anti-TNF treatment in JIA. Available: <https://clinicaltrials.gov/show/NCT00792233>
- Brunner HI, Lovell DJ, Finck BK, *et al.* Preliminary definition of disease flare in juvenile rheumatoid arthritis. *J Rheumatol* 2002;29:1058–64.
- Lai L, Ong R, Li J, *et al.* A CD45-based barcoding approach to multiplex mass-cytometry (CyTOF). *Cytometry A* 2015;87:369–74.
- Collison J. Paediatric rheumatology: novel Treg cell subset discovered in JIA. *Nat Rev Rheumatol* 2016;12:436–7.
- Haufe S, Haug M, Schepp C, *et al.* Impaired suppression of synovial fluid CD4+CD25- T cells from patients with juvenile idiopathic arthritis by CD4+CD25+ Treg cells. *Arthritis Rheum* 2011;63:3153–62.
- Henderson LA, Volpi S, Frugoni F, *et al.* Next-Generation sequencing reveals restriction and clonotypic expansion of Treg cells in juvenile idiopathic arthritis. *Arthritis Rheumatol* 2016;68:1758–68.
- Hinks A, Cobb J, Marion MC, *et al.* Dense genotyping of immune-related disease regions identifies 14 new susceptibility loci for juvenile idiopathic arthritis. *Nat Genet* 2013;45:664–9.
- Hersh AO, Prahalad S. Immunogenetics of juvenile idiopathic arthritis: a comprehensive review. *J Autoimmun* 2015;64:113–24.
- Ebata T, Mogi S, Hata Y, *et al.* Rapid induction of CD95 ligand and CD4+ T cell-mediated apoptosis by CD137 (4-1BB) costimulation. *Eur J Immunol* 2001;31:1410–6.
- Tsitsikov EN, Laouini D, Dunn IF, *et al.* Traf1 is a negative regulator of TNF signaling. enhanced TNF signaling in TRAF1-deficient mice. *Immunity* 2001;15:647–57.
- Filby A, Seddon B, Kleczkowska J, *et al.* Fyn regulates the duration of TCR engagement needed for commitment to effector function. *J Immunol* 2007;179:4635–44.
- Salmond RJ, Filby A, Qureshi I, *et al.* T-Cell receptor proximal signaling via the Src-family kinases, Lck and Fyn, influences T-cell activation, differentiation, and tolerance. *Immunol Rev* 2009;228:9–22.
- Harr MW, McColl KS, Zhong F, *et al.* Glucocorticoids downregulate Fyn and inhibit IP(3)-mediated calcium signaling to promote autophagy in T lymphocytes. *Autophagy* 2010;6:912–21.
- Nagila A, Netsawang J, Suttitheptumrong A, *et al.* Inhibition of p38MAPK and CD137 signaling reduce dengue virus-induced TNF- α secretion and apoptosis. *Virology* 2013;10:105.
- Doitsh G, Galloway NLK, Geng X, *et al.* Cell death by pyroptosis drives CD4 T-cell depletion in HIV-1 infection. *Nature* 2014;505:509–14.
- Nishimoto T, Seta N, Anan R, *et al.* A single nucleotide polymorphism of TRAF1 predicts the clinical response to anti-TNF treatment in Japanese patients with rheumatoid arthritis. *Clin Exp Rheumatol* 2014;32:211–7.
- Lee D-J, Du F, Chen S-W, *et al.* Regulation and function of the caspase-1 in an inflammatory microenvironment. *J Invest Dermatol* 2015;135:2012–20.
- Zhang J, Feng H, Zhao J, *et al.* Ikb kinase ϵ is an NFATc1 kinase that inhibits T cell immune response. *Cell Rep* 2016;16:405–18.
- Calabrese L, Mariette X. The evolving role of the rheumatologist in the management of immune-related adverse events (irAEs) caused by cancer immunotherapy. *Ann Rheum Dis* 2018;77:162–4.
- Kim ST, Tayar J, Trinh VA, *et al.* Successful treatment of arthritis induced by checkpoint inhibitors with tocilizumab: a case series. *Ann Rheum Dis* 2017;76:2061–4.
- Mellado M, Martínez-Muñoz L, Cascio G, *et al.* T cell migration in rheumatoid arthritis. *Front Immunol* 2015;6:384.
- Wehrens EJ, Vastert SJ, Mijnheer G, *et al.* Anti-Tumor necrosis factor α targets protein kinase B/c-Akt-induced resistance of effector cells to suppression in juvenile idiopathic arthritis. *Arthritis Rheum* 2013;65:3279–84.
- Albers HM, Kurreeman FAS, Houwing-Duistermaat JJ, *et al.* The TRAF1/C5 region is a risk factor for polyarthritis in juvenile idiopathic arthritis. *Ann Rheum Dis* 2008;67:1578–80.
- Behrens EM, Finkel TH, Bradfield JP, *et al.* Association of the TRAF1-C5 locus on chromosome 9 with juvenile idiopathic arthritis. *Arthritis Rheum* 2008;58:2206–7.
- Pers Y-M, Le Blay P, Ludwig C, *et al.* Association of TRAF1-C5 with risk of uveitis in juvenile idiopathic arthritis. *Joint Bone Spine* 2017;84:305–8.
- Zhu L, Jiang K, Webber K, *et al.* Chromatin landscapes and genetic risk for juvenile idiopathic arthritis. *Arthritis Res Ther* 2017;19.
- Leong JY, Albani S. Using a theragnostic approach in juvenile idiopathic arthritis. *Expert Opin Orphan Drugs* 2016;4:269–80.

Emergent high fatality lung disease in systemic juvenile arthritis

Vivian E Saper,¹ Guangbo Chen,² Gail H Deutsch,^{3,4} R Paul Guillerman,⁵ Johannes Birgmeier,⁶ Karthik Jagadeesh,⁶ Scott Canna,⁷ Grant Schulert,^{8,9} Robin Deterding,^{10,11} Jianpeng Xu,¹ Ann N Leung,¹² Layla Bouzoubaa,¹³ Khalid Abulaban,^{14,15} Kevin Baszis,¹⁶ Edward M Behrens,^{17,18} James Birmingham,^{19,20} Alicia Casey,^{21,22} Michal Cidon,^{23,24} Randy Q Cron,^{25,26} Aliva De,²⁷ Fabrizio De Benedetti,²⁸ Ian Ferguson,²⁹ Martha P Fishman,^{21,22} Steven I Goodman,³⁰ T Brent Graham,³¹ Alexei A Grom,^{8,9} Kathleen Haines,^{32,33} Melissa Hazen,^{21,22} Lauren A Henderson,^{21,22} Assunta Ho,^{34,35} Maria Ibarra,^{36,37} Christi J Inman,³⁸ Rita Jerath,^{39,40} Khulood Khawaja,⁴¹ Daniel J Kingsbury,⁴² Marisa Klein-Gitelman,⁴³ Khanh Lai,³⁸ Sivia Lapidus,^{32,33} Clara Lin,^{10,11} Jenny Lin,^{44,45} Deborah R Liptzin,^{10,11} Diana Milojevic,⁴⁶ Joy Mombourquette,⁴⁷ Karen Onel,^{48,49} Seza Ozen,⁵⁰ Maria Perez,⁵¹ Kathryn Phillippi,^{52,53} Sampath Prahalad,^{54,55} Suhas Radhakrishna,^{56,57} Adam Reinhardt,⁵⁸ Mona Riskalla,^{59,60} Natalie Rosenwasser,^{48,49} Johannes Roth,⁶¹ Rayfel Schneider,^{62,63} Dieneke Schonenberg-Meinema,^{64,65} Susan Shenoj,^{4,66} Judith A Smith,⁶⁷ Hafize Emine Sönmez,⁵⁰ Matthew L Stoll,^{25,26} Christopher Towe,^{8,9} Sara O Vargas,^{22,68} Richard K Vehe,^{59,60} Lisa R Young,^{17,18} Jacqueline Yang,² Tushar Desai,⁶⁹ Raymond Balise,¹³ Ying Lu,⁷⁰ Lu Tian,⁷⁰ Gill Bejerano,⁶ Mark M Davis,⁷¹ Purvesh Khatri,² Elizabeth D Mellins ,¹ the Childhood Arthritis and Rheumatology Research Alliance Registry Investigators

Handling editor Josef S Smolen

► Additional material is published online only. To view please visit the journal online (<http://dx.doi.org/10.1136/annrheumdis-2019-216040>).

For numbered affiliations see end of article.

Correspondence to

Dr Elizabeth D Mellins, Pediatrics, Stanford University, Stanford, CA 94305, USA; mellins@stanford.edu

GHD and RPG contributed equally.
JoB and KJ contributed equally.
SC and GS contributed equally.

VES and GC are joint first authors.
PK and EDM are joint senior authors.

Received 17 July 2019
Revised 11 September 2019
Accepted 13 September 2019
Published Online First 27 September 2019



© Author(s) (or their employer(s)) 2019. No commercial re-use. See rights and permissions. Published by BMJ.

To cite: Saper VE, Chen G, Deutsch GH, *et al.* *Ann Rheum Dis* 2019;**78**:1722–1731.

ABSTRACT

Objective To investigate the characteristics and risk factors of a novel parenchymal lung disease (LD), increasingly detected in systemic juvenile idiopathic arthritis (sJIA).

Methods In a multicentre retrospective study, 61 cases were investigated using physician-reported clinical information and centralised analyses of radiological, pathological and genetic data.

Results LD was associated with distinctive features, including acute erythematous clubbing and a high frequency of anaphylactic reactions to the interleukin (IL)-6 inhibitor, tocilizumab. Serum ferritin elevation and/or significant lymphopaenia preceded LD detection. The most prevalent chest CT pattern was septal thickening, involving the periphery of multiple lobes ± ground-glass opacities. The predominant pathology (23 of 36) was pulmonary alveolar proteinosis and/or endogenous lipoid pneumonia (PAP/ELP), with atypical features including regional involvement and concomitant vascular changes. Apparent severe delayed drug hypersensitivity occurred in some cases. The 5-year survival was 42%. Whole exome sequencing (20 of 61) did not identify a novel monogenic defect or likely causal PAP-related or macrophage activation syndrome (MAS)-related mutations. Trisomy 21 and young sJIA onset increased LD risk. Exposure to IL-1 and IL-6 inhibitors (46 of 61) was associated with multiple LD features. By several indicators, severity of sJIA was comparable in drug-exposed subjects and published sJIA cohorts. MAS at

Key messages

What is already known about this subject?

► Pleuritis is common in systemic-onset juvenile idiopathic arthritis (sJIA), but parenchymal lung disease (LD) is very rare, with sporadic reports and one multicentre series of 25 cases (Kimura *et al*, 2013) in the literature.

sJIA onset was increased in the drug-exposed, but was not associated with LD features.

Conclusions A rare, life-threatening lung disease in sJIA is defined by a constellation of unusual clinical characteristics. The pathology, a PAP/ELP variant, suggests macrophage dysfunction. Inhibitor exposure may promote LD, independent of sJIA severity, in a small subset of treated patients. Treatment/prevention strategies are needed.

INTRODUCTION

Systemic juvenile idiopathic arthritis (sJIA) is a chronic, inflammatory disease of childhood, observed worldwide, with an incidence of 0.4–0.9/100 000 in North America and Europe.¹ A similar disease occurs in adults (adult-onset Still's disease (AOSD); incidence: 0.2–0.4/100 000).² sJIA is characterised by a combination of arthritis,

Key messages

What does this study add?

- ▶ In the last decade, increasing numbers of cases of high fatality, parenchymal LD are being detected worldwide, with a majority characterised by unusual clinical and radiological features, in association with a variant of pulmonary alveolar proteinosis/endogenous lipoid pneumonia.
- ▶ Children with trisomy 21 and sJIA or with sJIA onset at <5 years are at increased risk of LD, and an unexplained association with anaphylaxis to tocilizumab is observed.
- ▶ Prodromal features can include lymphopaenia, rising serum ferritin and evidence of drug hypersensitivity (peripheral eosinophilia, extensive atypical rash).

How might this impact on clinical practice or future developments?

- ▶ This study highlights risk factors, prodromal features and clinical characteristics that should raise suspicion of LD, which otherwise can remain subclinical until severe and life-threatening.
- ▶ Clinician awareness of delayed drug hypersensitivity to interleukin (IL)-1 and IL-6 inhibitors could lead to earlier recognition and management, including cessation of the implicated drug.
- ▶ Pneumocystis pneumonia may complicate LD in sJIA; consideration of prophylaxis is warranted.

which can be destructive, and systemic inflammation, including daily fever spikes, evanescent macular rash and serositis. A life-threatening complication (mortality rate: 8%–17% in sJIA)³ is overt macrophage activation syndrome (MAS). MAS is a form of secondary haemophagocytic lymphohistiocytosis (HLH) that manifests as a cytokine storm with very high serum ferritin and, in severe cases, organ failure. Therapies that antagonise cytokines interleukin (IL)-1 and IL-6 were introduced into management of sJIA ~15 years ago. This approach is rapidly effective in >65% of patients, implicating these inflammatory mediators as key drivers of sJIA.^{4–6}

The usual pulmonary complications of sJIA are pleuritis and pleural effusion.^{1,7} Scattered case reports of other lung diseases (LDs) in sJIA have appeared.^{8–12} However, in the last decade, paediatric rheumatologists have increasingly detected cases with types of LDs rarely seen in sJIA previously. Kimura *et al*¹³ described 25 cases that occurred before February 2011; diagnoses included pulmonary arterial hypertension (64%), interstitial LD (28%) and pulmonary alveolar proteinosis (PAP) (20%). sJIA course was considered severe, with MAS in 80%.

Here, we performed a multicentre, retrospective study of 61 cases with centralised analyses of radiographic, pathological and genetic data to provide current characterisation of LD in sJIA or sJIA-like disease, search for early indicators and investigate risk factors.

METHODS

Case definition and comparators

We used an operational sJIA case definition, developed by expert consensus as a modification of the International League of Associations for Rheumatology sJIA classification criteria.¹⁴ Cases failing to meet the case definition but managed clinically like sJIA were classified as sJIA-like. We identified 61 patients with sJIA or sJIA-like disease and parenchymal LD through

the Childhood Arthritis and Rheumatology Research Alliance (CARRA) network and the international paediatric rheumatology listserv (administered by McMaster University, Ontario). Inclusion required verification of sJIA or sJIA-like illness, data at LD diagnosis, and parenchymal LD by chest CT and/or lung tissue, available for expert review. Comparator data were from physician-classified patients with sJIA without known LD enrolled in the CARRA registry (CR)¹⁵ between 2015 and 2018, or in the PharmaChild pharmacovigilance registry.¹⁶ See online supplementary figures S1A–B and S2 and online supplementary information for additional details.

Data collection

Data included demographics, medical history, and clinical features at sJIA onset, at LD diagnosis and at defined time points (visits) before and after LD diagnosis. RegiSCAR score for drug-related eosinophilic systemic syndrome (DRess) was calculated from clinical data.¹⁷ Online supplementary information includes details and definitions (online supplementary table S1).

Data analysis

Centralised analyses were performed for chest CT scans from 58 of 61 subjects, histopathology from 36 of 61 subjects and whole exome sequence (WES) data from 20 subjects. R V.3.5.1 program was used for all statistical analyses. Additional methods are in online supplementary information.

RESULTS

Disease characterisation: features unusual for sJIA

The cohort included 45 cases of sJIA and 16 cases of sJIA-like disease; demographics (table 1) and findings prior to or associated with LD did not differ systematically between these two groups (online supplementary tables S2–S4). Demographics of the LD cohort are mostly similar to subjects with sJIA in the CR, with the notable exceptions of significantly lower median age at sJIA onset and significantly higher prevalence of trisomy 21 (T21) (table 1). These findings are discussed further in the Candidate risk factors for parenchymal LD section.

Clinical features prior to LD and associated with LD are summarised in online supplementary tables S2 and S3, respectively. At LD diagnosis, respiratory signs and symptoms were typically absent or subtle, although hypoxia was reported in 43% and clinical pulmonary hypertension (PH) in 30%. Strikingly, 61% of patients developed acute clubbing, sometimes as the first indicator of LD. In over half of these, digital erythema occurred (figure 1A–C). Other atypical features were pruritic, non-evanescent rashes in 56% (figure 1D–F), eosinophilia in 37%, and unexplained, severe abdominal pain in 16% (likely underestimated as this was not directly queried). Anaphylaxis to tocilizumab was unusually common, occurring in 38% of those exposed (14 of 37; see online supplementary table S3, footnote 6), compared with 0.6% (1 of 159) in the CR and 0.9% (1 of 110) in the tocilizumab trial in sJIA.⁵ Overall, the LD cohort manifested clinical features that are unusual for sJIA¹⁸ or pulmonary disease.

Candidate early indicators of LD in sJIA: ferritin and lymphopaenia

The median time to LD diagnosis after sJIA onset was 1.6 years (IQR 0.8–3.3 years), excluding 6 of 61 cases with LD at systemic disease onset. To identify candidate early signs of LD, we analysed laboratory values commonly followed in sJIA. We matched cases to sJIA controls from the CR (1:1) for factors including

Table 1 Demographic characteristics

	sJIA-lung disease cohort vs CR† control			sJIA-lung disease cohort by subgroup‡		
	sJIA-lung disease	sJIA (CR)	P value§	sJIA-like	sJIA-ILAR+	OR (95% CI)¶
Sex (female, %)	66% (40/61)	59% (278/471)	0.41	81% (13/16)	60% (27/45)	0.35 (0.056 to 1.5)
Age, median years (IQR)	2.8 (1.2–6.3)	5.2 (2.8–9.8)	1.7×10 ⁻⁵ ***	2.3 (0.9–7.8)	3.1 (1.5–6.2)	0.43 (0.13 to 1.45)
Race			0.53			
White	62% (38/61)	66% (308/466)		50% (8/16)	67% (30/45)	2 (0.53 to 7.4)
Black	8.2% (5/61)	11% (50/466)		6.2% (1/16)	8.9% (4/45)	1.5 (0.13 to 77)
Other††	30% (18/61)	23% (108/466)		44% (7/16)	24% (11/45)	0.42 (0.11 to 1.7)
Region (only USA)‡‡			0.02*			
Northeast	19% (10/53)	28% (123/442)		27% (4/15)	16% (6/38)	0.5 (0.12 to 2.17)
Midwest	25% (13/53)	29% (129/442)		20% (3/15)	26% (10/38)	1.43 (0.33 to 6.1)
South	17% (9/53)	23% (101/442)		20% (3/15)	16% (6/38)	1.25 (0.29 to 5.3)
West	40% (21/53)	20% (89/442)		33% (5/15)	42% (16/38)	1.45 (0.42 to 5.1)
Genetics						
Trisomy 21	9.8% (6/61)	0.2% (1/471)	0.04*¶¶	12% (2/16)	8.9% (4/45)	0.69 (0.087 to 8.4)
Familial HLH	7.1% (2/28)§§	–	–	22% (2/9)	0% (0/19)	0 (0 to 2.4)

*P<0.05, **p<0.01, ***p<0.001. For OR, 95% CI is shown.

†CR, CARRA registry. Diagnosed as sJIA per physician report without specific verification of ILAR features.

‡sJIA-ILAR+ or sJIA-like classification verified (see the Methods section). sJIA-like had no arthritis (13) or failed modified fever criteria (3).

§For categorical items, Fisher's exact tests (including the multicategory form) were performed. For age, a Wilcoxon rank-sum test was performed.

¶OR showed no significant difference with the exception of trisomy 21 vs CR (OR=50).

††Other: Hispanic (5), Middle Eastern (1), Asian (2), multiethnic (8) and other (2).

‡‡Based on US Census Bureau population-balanced regions: www2.census.gov/geo/pdfs/maps-data/maps/reference/us_regdiv.pdf.

§§Diagnosed by clinical testing; one with 2 UNC13D mutations and one with UNC13D/PRF1 mutations; both sJIA-like.

HLH, haemophagocytic lymphohistiocytosis; ILAR, International League of Associations for Rheumatology; sJIA, systemic juvenile idiopathic arthritis.

laboratory test timing relative to sJIA onset, overall drug exposure, sex and sJIA onset age (online supplementary figure S3). We then assessed serum ferritin as an indicator of inflammation. The mean serum ferritin level in cases 1 year prior to LD diagnosis was not distinguishable from that of propensity-matched patients with sJIA in the CR. However, the level rose substantially within the 12 months before LD diagnosis in the cohort (figure 1G, online supplementary figure S4).

Another finding that preceded LD detection was significant lymphopaenia (absolute lymphocyte count <60% of age-adjusted, lower limit of normal).¹⁹ This degree of lymphopaenia, without concurrent MAS, was documented between the 6-month and 1-month visit prior to LD diagnosis in 42% of cases (excluding those with LD at sJIA onset; online supplementary table S3). We were unable to compare this with CR controls due to lack of information. However, this degree of lymphopaenia is not a known feature of active sJIA.¹⁸ Increased ferritin and lymphopaenia before LD diagnosis suggest a possibly extended incubation phase associated with smouldering inflammation and/or delayed recognition of LD.

Radiological features

As a step towards determining the nature of the LD, chest CT scans from 58 of 61 patients, most obtained at diagnosis, were systematically reviewed (RPG). Most exhibited one or more of five patterns (figure 2A–E). Pattern A (septal thickening involving the periphery of multiple lobes, most marked in the lower lung zones, parahilar/paramediastinal and/or anterior upper lobes with or without adjacent ground-glass opacities) was the most frequently observed (60%). Crazy-paving (figure 2B), peripheral consolidation (figure 2C), peribronchovascular consolidation (figure 2D) and predominantly ground-glass opacities (figure 3E) were seen in 21%, 22%, 16% and 12%, respectively. Among those with contrast-enhanced CTs, 11 of 30 (37%) displayed hyperenhancing lymph nodes (figure 2F), a peculiar finding, previously reported in

unusual conditions.^{20,21} Findings like pattern A have been observed with connective tissue disease-associated interstitial LD or interstitial pneumonia with autoimmune features.²² However, unlike these disorders, radiological signs of fibrosis (honeycombing, traction bronchiectasis) were uncommon in our cohort. Overall, the observed CT findings are unexpected in sJIA; the more typical finding of pleural effusion^{1,7,18} was rare at LD diagnosis (online supplementary table S4).

Histopathology and related genetics

Biopsy or autopsy tissues of 36 of 61 patients were available for centralised analysis (GD). Multicompartment disease (some combination of alveolar, airway, pleural, vascular alterations) was observed in all cases. Using their primary pattern of injury, three subgroups were defined: spectrum of PAP/endogenous lipoid pneumonia (ELP), vasculopathy and other (online supplementary table S4). The pathology typically associated with pattern A on CT is non-specific interstitial pneumonia (NSIP).^{22,23} Surprisingly, in 21 patients with CT pattern A who had histology, only 1 had NSIP. Instead, the predominant pathology (64% of cases reviewed) was PAP/ELP (figure 2G), which was patchy and often accompanied by associated vascular changes (figure 2G, right). PAP/ELP is very rare in rheumatic disease,²⁴ and the CT pattern typically associated with PAP is crazy-paving (pattern B).²⁵

To identify other histological features associated with PAP/ELP-like pathology in our cases, we generated a heat map (online supplementary figure S5A). Not surprisingly, type II alveolar cell hyperplasia was highly associated with PAP/ELP.^{26,27} The next associated finding was lymphoplasmacytic inflammation (71% of PAP/ELP cases). Third, 55% had mild to moderate pulmonary arterial wall thickening. Hypertensive vascular changes are not typically associated with inherited PAP/ELP, suggesting a secondary disease process.^{26–28} Electron microscopy (EM) (available in nine PAP/ELP cases) demonstrated well-formed lamellar bodies within type II alveolar epithelial cells. Variable



Figure 1 Distinctive clinical features in systemic juvenile idiopathic arthritis (sJIA) with lung disease (LD) and survival outcome. (A) Acute erythematous digital clubbing; (B, C) bulbous deformity with erythematous clubbing of fingers (B) and toes (C); (D) typical salmon-coloured, macular sJIA rash (evanescent); and (E, F) atypical rashes that occur before LD detection: (E) oedematous, urticarial, non-evanescent rash (knee) and (F) serpiginous, eczematous, non-evanescent rash with hyperpigmented borders. (G) Mean ± SE blood ferritin values of propensity-matched (online supplementary figure S3) sJIA controls (blue) and LD cases (red) across time points relative to LD diagnosis. n.s., $p > 0.1$, * $p < 0.05$, ** $p < 0.01$, *** $p < 0.001$, by Wilcoxon rank-sum test.

accumulation of macrophages containing lamellar debris, lipid and cholesterol clefts was observed (figure 2H). The EM findings are more characteristic of macrophage overloading or dysfunction than of genetic disorders in surfactant metabolism.^{29 30} When we examined 13 PAP/ELP cases (6 with EM analysis) for genes causing hereditary PAP (*SFTPA1*, *SFTPB*, *SFTPC*, *ABCA3*, *NKX2-1*, *CSF2RA*, *CSFR2B*, *MARS*),^{26 28 31–35} 6 were heterozygous for protein-changing mutations, but none was de novo in trio analyses (online supplementary table S5A). One (*SFTPC* p.R167Q) causes PAP with low penetrance³¹; the others are not known to cause PAP in heterozygotes. While these rare variants (maximum allele frequency <5%) might contribute to LD in these children, they are not likely the full explanation.^{32 36 37}

Vascular abnormalities were the predominant finding in 4 of 36 biopsies (online supplementary figure S5B–D, table S4). Consistent with chest CT findings, interstitial fibrosis was generally mild, with advanced fibrosis/remodelling in only 4 of 36 samples, including 2 autopsies (online supplementary figure S5D).

Candidate risk factors for parenchymal LD

Other genetic factors

No evidence for a shared monogenic explanation for LD was found in WES of the 20 cases analysed (not shown). We also assessed the frequency of HLH/MAS-related gene variants (*PRF1*, *LYST*, *STX11*, *STXBP2*, *UNC13D*, *NRLC4*). Rare

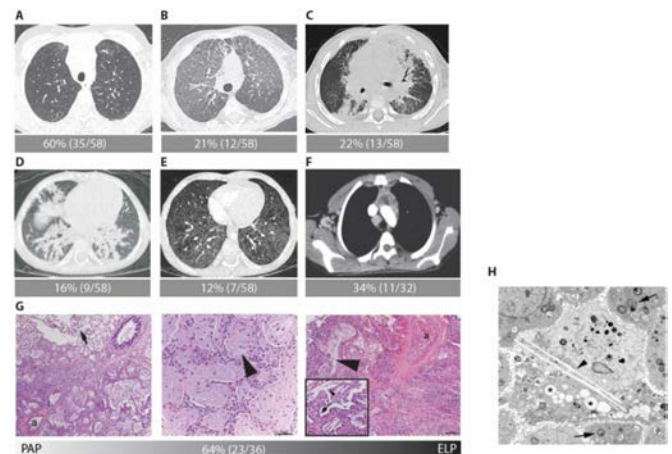


Figure 2 Distinctive radiological and pathological features. Panels A–E: representative axial chest CT images: (A) multilobar, predominantly peripheral septal thickening, most marked in the lower lung, parahilar and/or anterior upper lobes with or without adjacent ground-glass opacities; (B) crazy-paving; (C) peripheral consolidations; (D) peribronchovascular consolidations; (E) predominantly ground-glass opacities; and (F) hyperenhancing lymph nodes on contrast-enhanced CT. Panels G–H: histopathological findings (H&E staining) along the pulmonary alveolar proteinosis/endogenous lipid pneumonia (PAP/ELP) spectrum. Alveolar filling with eosinophilic proteinaceous material (G, left), admixed with a variable degree of ELP, indicated by cholesterol clefts (arrowheads) and foamy (lipid-containing) macrophages (G, middle and right), as described.^{82 83} Regions of PAP/ELP accompanied by type II alveolar epithelial cell hyperplasia (G, right insert, arrow), mild to moderate interstitial infiltration by inflammatory cells and lobular remodelling (airspace widening with increased interstitial smooth muscle). Typically, PAP/ELP findings were patchy, with involved areas juxtaposed to the normal lung (G, left, arrow). Pulmonary arterial wall thickening; a, artery (G, right). In A–G, the number of cases with pattern/number of assessable cases are indicated. (H) Electron micrograph showing normal lamellar bodies within type II cells (arrows) and macrophage (centre), containing lamellar debris, lipid (*) and cholesterol clefts (arrowhead). Original magnification $\times 7000$. Four PAP/ELP cases (one each: *ABCA3* and *CSF2RB* variants), stained for surfactant proteins (SP-B, proSP-C, SP-D, *ABCA3*, TTF-1), demonstrated robust immunoreactivity (not shown).

protein-altering variants, all heterozygous and none de novo, were found (online supplementary table S5B). Concordance between these variants and MAS (at sJIA onset or ever during disease course to data close) was not observed. The frequency of such variants (55%) is higher than reported for sJIA with MAS (36%)³⁸ and could contribute to propensity for inflammation.

Early-onset sJIA

Compared with control subjects with sJIA in the CR, the LD cohort's median age at sJIA onset was substantially younger (table 1; 2.3 years (1.1–5.0) vs 5.2 years (2.8–9.8), $p = 1 \times 10^{-7}$; online supplementary figure S6A). The CR cohort showed the full age of onset range of published sJIA cohorts, whereas the LD cohort was similar to a subgroup with younger onset age in sJIA cohorts^{39 40} (online supplementary figure S6B). Within LD cases, early onset of sJIA/sJIA-like disease was tightly correlated with PAP/ELP-like pathology (Wilcoxon test, $p = 2.3 \times 10^{-4}$; if cut-off for age at sJIA onset <5 years, OR=15, Fisher's $p = 0.001$, compared with older children in the cohort). Of cases, 91% (21

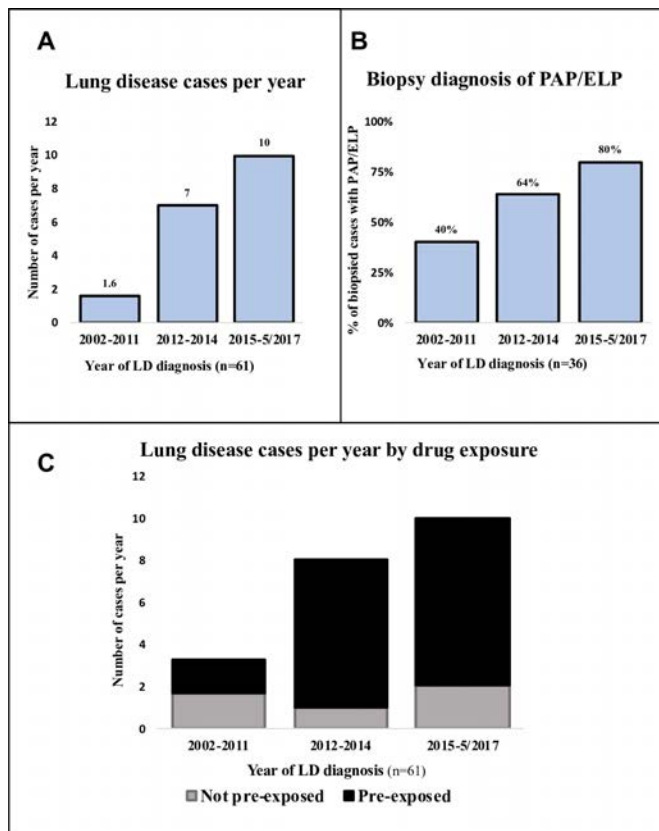


Figure 3 Annual number of reported cases of LD and PAP/ELP pathology. (A) Annual number of LD cases in this series (total n=61). (B) Percentage of biopsied LD cases (n=36) with PAP/ELP pathology, grouped by year of LD diagnosis. (C) Annual incidence of LD, indicating proportions exposed (black) or not (grey) to anti-IL-1/IL-6 inhibitors. ABCA-3, ATP binding cassette subfamily A member 3; IL, interleukin; LD, lung disease; PAP/ELP, pulmonary alveolar proteinosis/endogenous lipid pneumonia; proSP-C, prosurfactant D; SP-B, surfactant protein B; SP-D, surfactant protein D; TTF-1, thyroid transcription factor 1.

of 23) with PAP/ELP had sJIA onset at <5 years (online supplementary figure S6C).

Trisomy 21

In the LD cohort, T21 prevalence (table 1) was strikingly higher (10%) than in sJIA registry cohorts (0.2%; 1 of 471 in the CR and 2 of 914 in PharmaChild, these being similar to the frequency (0.14%) in live births).⁴¹ There were suggestions of more aggressive LD in these children, all of whom developed LD on anti-IL-1/IL-6. Four of six children with T21 were hypoxic (OR=7.8, Fisher's $p=0.08$, compared with the proportion of non-T21 with hypoxia). Two of five with T21 showed advanced interstitial fibrosis/remodelling (OR=8.4, Fisher's $p=0.09$), and two of four children with advanced fibrosis had T21. Five of six (83%) had viral or fungal lung infection at LD diagnosis, compared with 16 of 55 (29%) of non-T21 (OR=12, Fisher's $p=0.02$).

Pre-exposure to cytokine inhibitors

Compared with previously described patients with sJIA,¹⁸ the LD cohort demonstrated rare clinical, radiological and pathological findings. During the time period of the series, the annual number of cases in the LD cohort increased dramatically, although some bias of ascertainment is possible due

to increased awareness of this disease (figure 3A). PAP/ELP pathology increased among biopsied cases (figure 3B). The proportion of cases exposed to IL-1/IL-6 inhibitors increased in the cohort (figure 3C) and in all reported LD cases in sJIA (online supplementary figure S7A). These three trends coincided with increased use of IL-1/IL-6 inhibitors for sJIA.⁴² This prompted us to ask whether, compared with the CR sJIA cohort, the LD cohort was enriched for cases with exposure to IL-1/IL-6 inhibitors prior to LD. We matched the LD cases and CR controls for a number of potential confounders (online supplementary figure S7B). We found no difference in overall exposure to IL-1/IL-6 inhibitors; the exposure level in the CR controls was already high (online supplementary figure 7C; 46 of 53, 87%). Interestingly, among specific drug exposures, we found there was a moderate increase in anakinra exposure (OR=2.2 (0.94–5.5), $p=0.07$). We next asked whether exposure to these inhibitors was related to the prevalence of unusual features. The frequencies of acute clubbing, digital erythema, unexplained abdominal pain, peripheral eosinophilia, CT pattern A or D, hyperenhancing lymph nodes and PAP/ELP pathology, but not PH, were substantially higher ($p<0.1$; false discovery rate <20%) in pre-exposed versus non-pre-exposed subjects (figure 4A–B). These associations were not specific to one inhibitor. The median time from IL-1/IL-6 inhibitor to LD diagnosis was 1.2 years (IQR 0.7–2.0 years, n=46).

Severe or refractory sJIA

A possible bias in the associations with pre-exposure is increased severity of sJIA and related treatment, that is, channel bias. We assessed five clinical features associated with sJIA severity, as there is no validated sJIA severity index. For increased severity, we assessed MAS at sJIA onset, need for calcineurin inhibitors and persistent arthritis; for reduced severity, we assessed 'ever off' steroids and positive treatment response. The small sample of non-exposed subjects prevented us from performing a full analysis within our cohort. We compared the pre-exposed LD subgroup with published cohorts (figure 4C–F; online supplementary table S6). In Russo and Katsicas,⁴³ the proportion of children with early-onset sJIA (<1.5 years) with MAS at sJIA onset was 10× higher than the proportion of children with later sJIA onset (>1.5 years) (32% vs 3%). This difference was interpreted to indicate more severe inflammation in early-onset sJIA. Among pre-exposed subjects with early-onset sJIA LD, the proportion with MAS at onset (27%) was comparable with early-onset subjects in Russo and Katsicas.⁴³ For pre-exposed children with later-onset sJIA LD, a significantly higher proportion had MAS at onset versus the comparable group in Russo and Katsicas⁴³ (26% vs 3%; OR=12.75, $p=0.0004$) and versus another sJIA cohort, Behrens *et al*⁴⁴ (OR=4.83, $p=0.003$). These observations raised the possibility that LD was associated with MAS at onset, resulting in increased inhibitor use. However, there was no association in the LD cohort between MAS at onset and any of the unusual features of LD (figure 4G).

The pre-exposed LD cohort was generally similar to published cohorts for frequency of treatment-responsive disease (lack of calcineurin inhibitor, a period of systemic quiescence or substantially reduced steroid treatment; Figure 4C–F). One exception was that a lower proportion of the LD subgroup treated with inhibitors for ≥ 6 months were ever off steroids, perhaps reflecting more severe disease; nonetheless, this proportion was >50% (figure 4F). In addition, at data close, 58% of the pre-exposed (18 of 31) reported inactive sJIA (on medication) despite continuing LD in 94% (17 of 18). These observations

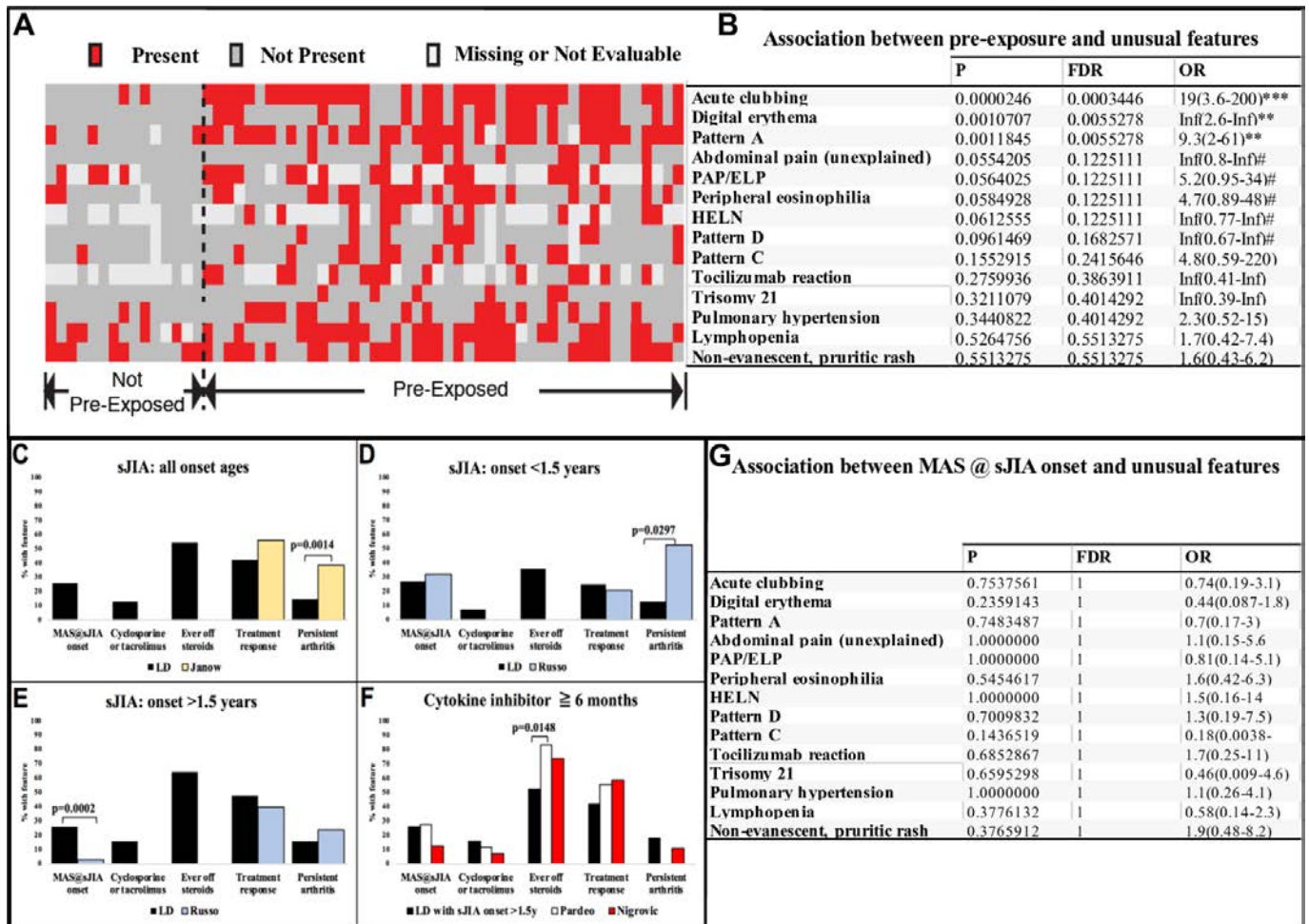


Figure 4 Association between unusual features and pre-exposure to anti-IL-1/IL-6 or MAS at sJIA onset. (A) Heat map indicating occurrence of unusual clinical and radiological features (rows) by subjects (columns), grouped by pre-exposure status. (B) Statistical analysis for panel A, indicating p values, FDR and OR with 95% CI. Inf, infinite, # $p < 0.1$, * $p < 0.05$, ** $p < 0.01$, *** $p < 0.001$. (C–F) Comparison of severity-related features in pre-exposed LD cases versus published sJIA cohorts. (C) Pre-exposed LD cases compared with Janow *et al.*⁴² (D) Pre-exposed LD cases with sJIA onset <1.5 years, compared with comparable age group in Russo and Katsicas⁴³; cut-off at <1.5 years was chosen by Russo and Katsicas, based on developmental difference before versus after 18 months. (E) Pre-exposed LD cases with sJIA onset >1.5 years, compared with comparable age group in Russo and Katsicas.⁴³ (F) Pre-exposed LD cases treated with IL-1/IL-6 inhibitors for ≥ 6 months compared with comparable groups in Pardeo *et al.*⁸⁴ and Nigrovic *et al.*⁸⁰ No bar indicates unavailable data. For details on definitions and published cohorts, see online supplementary table S6. (G) Statistical analysis of associations between MAS at sJIA onset and unusual clinical features of LD in sJIA, indicating p values, FDR and OR with 95% CI. FDR, false discovery rate; HELN, hyperenhancing lymph nodes; IL, interleukin; LD, lung disease; MAS, macrophage activation syndrome; PAP/ELP, pulmonary alveolar proteinosis/endogenous lipid pneumonia; sJIA, systemic juvenile idiopathic arthritis.

argue that refractory sJIA is not required for LD development or persistence.

Survival

The period of follow-up after LD diagnosis was variable (median 1.7 years; IQR 0.75–3 years). Survival was drastically lower in the LD cohort (mortality: 159/1000 person-years; figure 5) than in a UK cohort of patients with sJIA who required biologic agents (mortality: 3.9/1000 person-years).⁴⁵ The predominant cause of death in our cohort was reported as diffuse LD (12 of 22 deaths), with MAS in 5 of 12 (online supplementary table S7). Among 75 categorical variables (online supplementary table S2–S5), male sex, hypoxia at initial LD evaluation, predominantly neutrophilic bronchoalveolar lavage (BAL) ($\geq 40\%$ neutrophils, over 10 times the normal),^{46,47} but not PH, appeared to associate with shortened survival (online supplementary figure S8A–D). These associations were not significant after adjusting for multiple tests. However, BAL neutrophilia ($\geq 50\%$) has been linked to

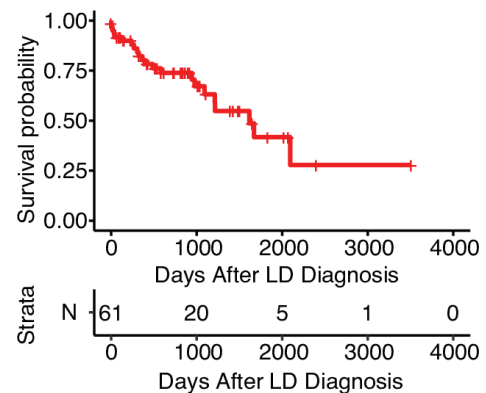


Figure 5 Survival outcome in systemic juvenile idiopathic arthritis cohort with lung disease (LD). The number of survivors at a given time point after LD diagnosis is shown (strata).

fatality,^{48 49} and 100% in our series (12 of 12) with this feature were deceased by data close.

DISCUSSION

LD in sJIA was characterised by young age at sJIA onset and unusual clinical features, including acute erythematous clubbing, atypical rash and anaphylaxis to tocilizumab; severe tocilizumab reaction in sJIA with pulmonary disease was also noted in the data from the PharmaChild registry.⁵⁰ The most prevalent finding on chest CT was peripheral septal thickening ± ground-glass opacities. Crazy-paving, consolidation and hyperenhancing lymph nodes were also observed. On tissue diagnosis, this group showed primarily PAP/ELP-like pathology. Compared with PAP/ELP in other settings, the LD pathology was distinctive for its patchiness and associated vascular changes.

The proportion of LD cases with PAP/ELP-like tissue diagnosis has increased since 2010, coinciding with increasing use of IL-1/IL-6 inhibitors.⁴⁰ Pre-exposure to these inhibitors was characteristic of the predominant phenotypic subtype in our series. It is possible that this association is confounded by concomitant reduction in steroids with inhibitor use or by treatment of severe inflammation; our data do not conclusively rule out these possibilities. However, severe disease has been observed since the initial description of sJIA in 1897,⁵¹ whereas the LD with associated features described here appears to be new and increasing in frequency. Among biopsied cases, PAP/ELP was found in 80% with pre-exposure (includes one with mostly pleural sample and limited PAP foci) vs 36% not pre-exposed (OR=7 (95% CI 1.45 to 33.7), Fisher's $p=0.015$; online supplementary figure S5E) and was independent of PAP/ELP association with young age (online supplementary figure S9). Thus, IL-1/IL-6 inhibitor exposure may promote development of PAP/ELP-like disease and may qualitatively influence LD-associated features in a subset of patients with sJIA, among the substantially larger group of patients who derive striking benefit from these inhibitors.

Autopsy RNA sequencing data from the Genotype-Tissue Expression project show the lung is a major physiological producer of IL-1 and IL-6 in adults (online supplementary figure S10),⁵² and cytokine profiling suggests that circulating IL-1RA levels (reflecting the IL-1 activity) in young (<4 years) healthy children are 2× higher than in older healthy children.⁵³ In addition, NFκB, a key transcription factor downstream of IL-1, stimulates angiogenesis and alveolarisation in the postnatal, developing lung.⁵⁴ These observations raise the possibility of a physiological role of IL-1/IL-6 in the lung, particularly in early childhood. The striking enhancement of LD risk by early age of sJIA onset suggests developmental vulnerabilities that may interact with the inhibitors.

A specific relationship between reduced IL-1 and PAP development is described in mice. IL-1 $\alpha^{-/-}$ mice (but not IL-1 $\beta^{-/-}$ mice) challenged with inhaled silicone, an inflammasome (NLRP3) activator,⁵⁵ develop PAP-like LD.⁵⁶ In the lung, IL-1 regulates granulocyte-macrophage colony-stimulating factor (GM-CSF) levels^{57 58} and macrophage function^{56 57}; disruption of either can lead to surfactant accumulation and PAP.^{59 60} These findings imply a link between reduced IL-1 and PAP, but also suggest that additional triggers may be required for disease development, in line with the rarity of severe parenchymal LD among the overall population of patients with sJIA treated with IL-1/IL-6 inhibitors. The association of PAP and paediatric haematological malignancies, especially myeloid leukaemia, can be ascribed in some cases to dysregulation of the GM-CSF/GM-CSF receptor axis and consequent macrophage dysfunction.⁶¹

We found an outsized risk of LD in children with T21 and sJIA. T21 carries increased susceptibility to adverse drug reactions⁶² and to viral pneumonia.⁶³ Another contributing factor may be underlying type 1 interferonopathy, recently described in T21.⁶⁴ An association of T21 and PAP in the context of haematological malignancy also has been reported.⁶⁵

Drug hypersensitivity reactions can occur in children treated with biologic drugs for rheumatic disease.⁶⁶ A subset of LD cases met the criteria for DReSS (online supplementary tables S1 and S8), a delayed form of severe drug-related hypersensitivity with organ involvement that can include lung.^{17 67 68} DReSS findings included dramatic eosinophilia, often despite concurrent steroids, together with extensive, persistent rash, frequently involving the face, which is uncommon in sJIA.¹⁸ Altered drug metabolism in childhood may increase risk of hypersensitivity reactions.⁶⁹ Another consideration is drug-induced interstitial lung disease (DiILD), previously reported in children with rheumatic disease on biologics.⁷⁰ DiILD has overlapping chest CT findings with LD in sJIA.⁷¹ No pathological findings are pathognomonic of DiILD,^{71 72} but PAP has been described.²⁴ Drug cessation is indicated when DReSS or DiILD is recognised.⁶⁸

Infection may exacerbate LD, trigger its detection or be causally linked. Pathogens identified at initial lung evaluation (online supplementary table S3) included rhinovirus (a cause of severe lower respiratory infection in young children⁷³), herpes viruses and pneumocystis, all of which require IL-1 for optimal host defence.^{55 74 75} Pneumocystis pneumonia (PCP) is a recognised cause of PAP²⁵ and is associated with high mortality in immunocompromised individuals.⁷⁶ PCP risk is also elevated in DReSS.⁷⁷ At least four of our cases had PCP; these were diagnosed by PCR of BAL, the preferred test in non-HIV immunosuppressed patients.⁷⁶ It seems prudent to consider prophylaxis for patients with sJIA with lymphopaenia or steroid use (consistent with recommendations⁷⁸) or T21.

LD in sJIA has been associated with MAS.^{13 79} In 23 out of 61 cases in our series, LD detection occurred with concurrent MAS. Out of these 23, 19 had their first MAS episode at or after LD diagnosis, suggesting that LD may trigger systemic inflammation. Consistent with this possibility, 4 of 11 cases with MAS co-occurred with initial detection of LD during three treatment trials of the inhibitors (n=331 subjects in total).⁴⁻⁶

PH with a range of severity was observed with or without pre-exposure to inhibitors and with or without PAP/ELP pathology. Out of 20 subjects, 2 lacked substantial parenchymal LD at PH detection. Together, these observations argue that PH in this LD cohort has heterogeneous biology.

Persistent arthritis (figure 4F) was less frequent in the pre-exposed LD cohort than in the sJIA cohort in the CARRA legacy registry (2010–2013),⁴² and of comparable frequency to children treated with IL-1 inhibition as first-line sJIA therapy. Inhibitor therapy may attenuate arthritis when given early or the LD cohort may be enriched for children with systemic inflammation-predominant disease.^{18 80}

Over 50 additional LD cases in sJIA have been reported to us since closing this series. The Food and Drug Administration (FDA) adverse event website (FDA Adverse Event Reporting System) shows 39 adults (rheumatoid arthritis (23), AOSD (11), other (5)) developing alveolar disease or PH on IL-1/IL-6 inhibitors and 4 DReSS cases (second quarter, 2019). An apparent discrepancy between adverse event reports and the frequency of sJIA-LD reported here may reflect its underdiagnosis or under-reporting.⁸¹

The association between cytokine inhibition and sJIA-LD and related mechanistic hypotheses demand further investigation. We

acknowledge the limitations of retrospective data, use of historical/published data for controls, possible biases as mentioned and false discovery issues associated with multiple hypothesis testing in a large data set. With these limitations, one cannot assign causality to cytokine inhibition in LD in sJIA. Likewise, it is premature to make treatment recommendations solely on the basis of our findings. Therapeutic decision making for patients with sJIA-associated LD is challenging, and currently individualised management is appropriate. However, in children with risk factors, close attention to subtle pulmonary symptoms is advised, and approaches for early detection of altered pulmonary function, guided by a pulmonary specialist, should be considered. In light of high fatality, efforts to determine LD prevalence, uncover molecular mechanism(s), and devise treatment and prevention approaches are urgently needed.

Author affiliations

- ¹Pediatrics, Stanford University, Stanford, California, USA
- ²Institute for Immunity, Transplantation and Infection, Center for Biomedical Informatics Research, Medicine, Stanford University, Stanford, California, USA
- ³Pathology, Seattle Children's Hospital, Seattle, Washington, USA
- ⁴University of Washington School of Medicine, Seattle, Washington, USA
- ⁵Radiology, Baylor College of Medicine, Houston, Texas, USA
- ⁶Genetics, Stanford University, Stanford, California, USA
- ⁷Pediatrics, Children's Hospital of Pittsburgh of University of Pittsburgh Medical Center, Pittsburgh, Pennsylvania, USA
- ⁸Pediatrics, University of Cincinnati College of Medicine, Cincinnati, Ohio, USA
- ⁹Cincinnati Children's Hospital Medical Center, Cincinnati, Ohio, USA
- ¹⁰Children's Hospital Colorado, Aurora, Colorado, USA
- ¹¹University of Colorado School of Medicine, Aurora, Colorado, USA
- ¹²Radiology, Stanford University, Stanford, California, USA
- ¹³Public Health Services, Biostatistics, University of Miami School of Medicine, Miami, Florida, USA
- ¹⁴Helen DeVos Children's Hospital, Grand Rapids, Michigan, USA
- ¹⁵Michigan State University, East Lansing, Michigan, USA
- ¹⁶Pediatrics, Washington University in Saint Louis, Saint Louis, Missouri, USA
- ¹⁷Pediatrics, Children's Hospital of Philadelphia, Philadelphia, Pennsylvania, USA
- ¹⁸University of Pennsylvania, Philadelphia, Pennsylvania, USA
- ¹⁹Medicine, Metro Health Hospital, Wyoming, Michigan, USA
- ²⁰University of Michigan, Ann Arbor, Michigan, USA
- ²¹Boston Children's Hospital, Boston, Massachusetts, USA
- ²²Harvard Medical School, Boston, Massachusetts, USA
- ²³Pediatrics, Children's Hospital of Los Angeles, Los Angeles, California, USA
- ²⁴University of Southern California, Los Angeles, California, USA
- ²⁵Children's of Alabama, Birmingham, Alabama, USA
- ²⁶University of Alabama at Birmingham, Birmingham, Alabama, USA
- ²⁷Pediatrics, Columbia University Medical Center, New York, New York, USA
- ²⁸Rheumatology, Ospedale Pediatrico Bambino Gesù, Roma, Italy
- ²⁹Pediatrics, Yale University School of Medicine, New Haven, Connecticut, USA
- ³⁰Arthritis Associates of South Florida, Delray Beach, Florida, USA
- ³¹Pediatrics, Vanderbilt University School of Medicine, Nashville, Tennessee, USA
- ³²Joseph M Sanzari Children's Hospital, Hackensack, New Jersey, USA
- ³³Hackensack University Medical Center, Hackensack, New Jersey, USA
- ³⁴Pediatrics, Prince of Wales Hospital, New Territories, Hong Kong
- ³⁵Faculty of Medicine, Chinese University of Hong Kong, New Territories, Hong Kong
- ³⁶Children's Mercy Hospitals and Clinics, Kansas City, Missouri, USA
- ³⁷School of Medicine, University of Missouri Kansas City, Kansas City, Missouri, USA
- ³⁸Pediatrics, University of Utah Health Sciences Center, Salt Lake City, Utah, USA
- ³⁹Children's Hospital of Georgia, Augusta, Georgia, USA
- ⁴⁰Augusta University, Augusta, Georgia, USA
- ⁴¹Pediatrics, Al Mafraq Hospital, Abu Dhabi, United Arab Emirates
- ⁴²Randall Children's Hospital at Legacy Emanuel, Portland, Oregon, USA
- ⁴³Pediatrics, Northwestern University Feinberg School of Medicine, Chicago, Illinois, USA
- ⁴⁴Children's Hospital at Montefiore, Bronx, New York, USA
- ⁴⁵Yeshiva University Albert Einstein College of Medicine, Bronx, New York, USA
- ⁴⁶Johns Hopkins All Children's Hospital, Saint Petersburg, Florida, USA
- ⁴⁷Pediatrics, Kaiser Permanente Roseville Medical Center, Roseville, California, USA
- ⁴⁸Pediatrics, Hospital for Special Surgery, New York, New York, USA
- ⁴⁹Weill Cornell Medical College, New York, New York, USA
- ⁵⁰Pediatrics, Hacettepe University Faculty of Medicine, Ankara, Turkey
- ⁵¹Cook Children's Medical Center, Fort Worth, Texas, USA
- ⁵²Akron Children's Hospital, Akron, Ohio, USA
- ⁵³Northeast Ohio Medical University, Rootstown, Ohio, USA

- ⁵⁴Pediatrics, Emory University School of Medicine, Atlanta, Georgia, USA
- ⁵⁵Children's Healthcare of Atlanta, Atlanta, Georgia, USA
- ⁵⁶Rady Children's Hospital, San Diego, California, USA
- ⁵⁷Pediatrics, University of California San Diego, La Jolla, California, USA
- ⁵⁸Pediatrics, University of Nebraska Medical Center College of Medicine, Omaha, Nebraska, USA
- ⁵⁹Pediatrics, University of Minnesota Medical School Twin Cities, Minneapolis, Minnesota, USA
- ⁶⁰University of Minnesota Masonic Children's Hospital, Minneapolis, Minnesota, USA
- ⁶¹Children's Hospital of Eastern Ontario, Ottawa, Ontario, Canada
- ⁶²Hospital for Sick Children, Toronto, Ontario, Canada
- ⁶³Pediatrics, University of Toronto, Toronto, Ontario, Canada
- ⁶⁴Emma Children's Hospital AMC, Amsterdam, The Netherlands
- ⁶⁵University of Amsterdam, Amsterdam, The Netherlands
- ⁶⁶Pediatrics, Seattle Children's Hospital, Seattle, Washington, USA
- ⁶⁷Pediatrics, University of Wisconsin Madison School of Medicine and Public Health, Madison, Wisconsin, USA
- ⁶⁸Pathology, Boston Children's Hospital, Boston, Massachusetts, USA
- ⁶⁹Medicine, Institute for Stem Cell Biology and Regenerative Medicine, Stanford University, Stanford, California, USA
- ⁷⁰Biomedical Data Science, Stanford University, Stanford, California, USA
- ⁷¹Institute for Immunity, Transplantation and Infection, Microbiology and Immunology, Stanford University, Stanford, California, USA

Acknowledgements The CARRA registry has been supported by the NIH's National Institute of Arthritis and Musculoskeletal and Skin Diseases (NIAMS) and the Arthritis Foundation. We thank all participants and hospital sites that recruited patients for the CARRA registry. The authors thank Drs Joseph A Kovacs, Jay K Kolls and Sergio Vargas for their expert input on pneumocystis pneumonia, Dr James Verbsky for contributing unidentified genetic data, and Dr Xuan Qin for PCP staining of a subset of biopsies. The authors also thank Dr Yuki Kimura for critical reading of the manuscript, Dr Claudia Macaubas for statistical assistance and Ms Melinda Hing for assistance with the manuscript.

Collaborators CARRA registry site principal investigators and research coordinators: K Abulaban, R Agbayani, S Akoghanian, E Anderson, M Andrew, B Badwal, L Barillas-Arias, K Baszis, M Becker, H Bell-Brunson, H Benham, S Bensele, T Beukelman, J Birmingham, M Boncek, H Brunner, A Bryson, H Bukulmez, L Cerracchio, E Chalom, J Chang, N Chowdhury, K Chundru, T Davis, J Dean, F Dedeoglu, V Dempsey, M Dionizovik-Dimanovski, L Dolinsky, J Drew, B Feldman, P Ferguson, B Ferreira, C Fleming, L Franco, I Goh, D Goldsmith, B Gottlieb, T Graham, T Griffin, M Hance, D Helfrich, K Hickey, M Hollander, J Hsu, A Huber, A Hudson, C Hung, A Huttenlocher, L Imundo, C Inman, J Jaquith, R Jerath, J Jones, S Jones, L Jung, P Kahn, D Kingsbury, K Klein, M Klein-Gitelman, S Kramer, A Kufen, S Lapidus, D Latham, S Linehan, B Malla, M Malloy, A Martyniuk, T Mason, K McConnell, D McCurdy, K McKibben, C McMullen-Jackson, K Moore, L Moorthy, E Muscal, W Norris, J Olson, K O'Neil, K Onel, K Phillips, L Ponder, S Prahalad, C Rabinovich, S Rauch, S Ringold, M Riordan, S Roberson, A Robinson, E Rojas, M Rosenkranz, B Rosolowski, N Ruth, K Schikler, A Sepulveda, C Smith, H Stapp, K Stewart, R Syed, A Tangarone, M Teshar, A Thatayatikom, R Vehe, E von Scheven, D Wahezi, C Wang, C Wassink, M Watson, A Watts, J Weiss, P Weiss, A Wolverton, J Woo, A Yalcindag, Q Yu, A Zeft, L Zemel, A Zhu and J Zwering.

Contributors VES, GC, GHD, RPG, ANL, JoB, KJ, JX, RB, LB, YL, IT, TD, GB, MMD, PK, EDM: collection, analysis, discussion and interpretation of data. VES, GC: wrote the manuscript. EDM, PK: checked and revised the manuscript. SC, GS, RD, KA, KB, EMB, JaB, AC, MC, RQC, AD, FDB, TBG, AAG, IF, MF, SIG, LRY, MLS, AH, KH, MH, LAH, MI, CJ, RJ, KK, DJK, MK-G, KL, SL, CL, JL, DRL, DM, JM, KO, SO, MP, KP, SP, SR, AR, MR, NR, JR, RS, DS-M, SS, JAS, HES, CT, SOV, RKV, JY: provided data, and checked and approved the manuscript.

Funding This work was supported by the sJIA Foundation (EDM), the Lucile Packard Foundation for Children's Health (EDM), CARRA-Arthritis Foundation grant (EDM, VES), Life Sciences Research Foundation (GC), Bio-X Stanford Interdisciplinary Graduate Fellowship (JoB), Stanford Graduate Fellowship and the Computational Evolutionary Human Genetics Fellowship (KJ), Bill & Melinda Gates Foundation (PK), and NIH 1U19AI109662 (PK), U19AI057229 (PK) and RO1 AI125197 (PK).

Competing interests VES reports personal fees from Novartis. GD reports personal fees from Novartis. SC reports personal fees from Novartis and grants from AB2 Bio. GS reports personal fees from Novartis. KB reports personal fees from Novartis. RQC is co-PI of an investigator-initiated clinical trial funded by SOBI. RD reports personal fees from Boehringer Ingelheim, other from NowVitals, personal fees and other from Triple Endoscopy, other from Earables, and NowVitals with patents and lung-related device development. AAG reports grants and personal fees from Novartis and grants from NovImmune. SL reports personal fees from Novartis. RS reports personal fees from Novartis, NovImmune and SOBI. SS reports personal fees from Novartis. MLS reports personal fees from Novartis. LRY reports other from Up-To-Date and other from Boehringer Ingelheim, outside the submitted work. EDM reports grants from Novartis.

Patient and public involvement statement Patients were not involved in the research process of this study. Results will be shared via CARRA patient communication mechanisms.

Patient consent for publication Not required.

Ethics approval Ethics approval was obtained through the Stanford University School of Medicine institutional review board. Contributing case reporters obtained approval per local institutional review board requirements. Institutional review board permission was obtained at each institution according to local requirements.

Provenance and peer review Not commissioned; externally peer reviewed.

Data availability statement Data are available upon reasonable request.

ORCID iD

Elizabeth D Mellins <http://orcid.org/0000-0003-2577-139X>

REFERENCES

- Gurion R, Lehman TJA, Moorthy LN. Systemic arthritis in children: a review of clinical presentation and treatment. *Int J Inflam* 2012;2012:1–16.
- Gerfaud-Valentin M, Cottin V, Jamilloux Y, et al. Parenchymal lung involvement in adult-onset still disease: a STROBE-compliant case series and literature review. *Medicine* 2016;95:e4258.
- Minoia F, Davi S, Horne A, et al. Clinical features, treatment, and outcome of macrophage activation syndrome complicating systemic juvenile idiopathic arthritis: a multinational, multicenter study of 362 patients. *Arthritis Rheumatol* 2014;66:3160–9.
- Ruperto N, Brunner HI, Quartier P, et al. Two randomized trials of canakinumab in systemic juvenile idiopathic arthritis. *N Engl J Med* 2012;367:2396–406.
- De Benedetti F, Brunner HI, Ruperto N, et al. Randomized trial of tocilizumab in systemic juvenile idiopathic arthritis. *N Engl J Med* 2012;367:2385–95.
- Ter Haar NM, Dijkhuizen EHP, Swart JF, et al. Treatment to target using recombinant Interleukin-1 receptor antagonist as First-Line monotherapy in New-Onset systemic juvenile idiopathic arthritis: results from a Five-Year Follow-Up study. *Arthritis Rheumatol* 2019;71:1163–73.
- García-Peña P, Boixadera H, Barber I, et al. Thoracic findings of systemic diseases at high-resolution CT in children. *RadioGraphics* 2011;31:465–82.
- Athreya BH, Doughty RA, Bookspan M, et al. Pulmonary manifestations of juvenile rheumatoid arthritis. A report of eight cases and review. *Clin Chest Med* 1980;1:361–74.
- Padeh S, Laxer RM, Silver MM, et al. Primary pulmonary hypertension in a patient with systemic-onset juvenile arthritis. *Arthritis & Rheumatism* 1991;34:1575–9.
- Sato K, Takahashi H, Amano H, et al. Diffuse progressive pulmonary interstitial and intra-alveolar cholesterol granulomas in childhood. *Eur Respir J* 1996;9:2419–22.
- Schultz R, Mattila J, Gappa M, et al. Development of progressive pulmonary interstitial and intra-alveolar cholesterol granulomas (PICG) associated with therapy-resistant chronic systemic juvenile arthritis (CJA). *Pediatr Pulmonol* 2001;32:397–402.
- Leber A, Carette S, Chapman KR, et al. A 21-year-old man with systemic-onset juvenile rheumatoid arthritis, cough and progressive dyspnea. *Can Respir J* 2010;17:e42–4.
- Kimura Y, Weiss JE, Haroldson KL, et al. Pulmonary hypertension and other potentially fatal pulmonary complications in systemic juvenile idiopathic arthritis. *Arthritis Care Res* 2013;65:745–52.
- DeWitt EM, Kimura Y, Beukelman T, et al. Consensus treatment plans for new-onset systemic juvenile idiopathic arthritis. *Arthritis Care Res* 2012;64:1001–10.
- Beukelman T, Kimura Y, Ilowite NT, et al. The new Childhood Arthritis and Rheumatology Research Alliance (CARRA) registry: design, rationale, and characteristics of patients enrolled in the first 12 months. *Pediatric Rheumatology* 2017;15.
- Swart J, Giancane G, Horneff G, et al. Pharmacovigilance in juvenile idiopathic arthritis patients treated with biologic or synthetic drugs: combined data of more than 15,000 patients from Pharmachild and national registries. *Arthritis Res Ther* 2018;20.
- Kardaun SH, Mockenhaupt M, Roujeau J-C. Comments on: DRESS syndrome. *J Am Acad Dermatol* 2014;71:1000–1000.e2.
- De Benedetti F, Schneider R. Systemic Juvenile Idiopathic Arthritis. In: Petty R, Lindsley C, Laxer R, et al, eds. *Textbook of pediatric rheumatology*. 7th edn. Philadelphia, PA: Elsevier, 2016: 206–16.
- van Gent R, van Tilburg CM, Nibbelke EE, et al. Refined characterization and reference values of the pediatric T- and B-cell compartments. *Clin Immunol* 2009;133:95–107.
- Bonekamp D, Hruban RH, Fishman EK. The great mimickers: Castleman disease. *Semin Ultrasound CT MR* 2014;35:263–71.
- Carucci LR, Halvorsen RA. Abdominal and pelvic CT in the HIV-positive population. *Abdom Imaging* 2004;29:631–42.
- Fischer A, Antoniou KM, Brown KK, et al. An official European Respiratory Society/American Thoracic Society research statement: interstitial pneumonia with autoimmune features. *Eur Respir J* 2015;46:976–87.
- Dell S, Cernelc-Kohan M, Hagood JS. Diffuse and interstitial lung disease and childhood rheumatologic disorders. *Curr Opin Rheumatol* 2012;24:530–40.
- Wardwell NR, Miller R, Ware LB. Pulmonary alveolar proteinosis associated with a disease-modifying antirheumatoid arthritis drug. *Respirology* 2006;11:663–5.
- Seymour JF, Presneill JJ. Pulmonary alveolar proteinosis: progress in the first 44 years. *Am J Respir Crit Care Med* 2002;166:215–35.
- Doan ML, Guilleman RP, Dishop MK, et al. Clinical, radiological and pathological features of ABCA3 mutations in children. *Thorax* 2008;63:366–73.
- Deutsch GH, Young LR, Detering RR, et al. Diffuse lung disease in young children: application of a novel classification scheme. *Am J Respir Crit Care Med* 2007;176:1120–8.
- Abou Taam R, Jaubert F, Emond S, et al. Familial interstitial disease with I73T mutation: a mid- and long-term study. *Pediatr Pulmonol* 2009;44:167–75.
- Golde DW, et al. Defective lung macrophages in pulmonary alveolar proteinosis. *Ann Intern Med* 1976;85:304–9.
- Sakagami T, Uchida K, Suzuki T, et al. Human GM-CSF autoantibodies and reproduction of pulmonary alveolar proteinosis. *N Engl J Med* 2009;361:2679–81.
- Wert SE, Whitsett JA, Noguee LM. Genetic disorders of surfactant dysfunction. *Pediatr Dev Pathol* 2009;12:253–74.
- Suzuki T, Maranda B, Sakagami T, et al. Hereditary pulmonary alveolar proteinosis caused by recessive CSF2RB mutations. *Eur Respir J* 2011;37:201–4.
- Suzuki T, Sakagami T, Rubin BK, et al. Familial pulmonary alveolar proteinosis caused by mutations in CSF2RA. *J Exp Med* 2008;205:2703–10.
- Martinez-Moczygemba M, Doan ML, Elidemir O, et al. Pulmonary alveolar proteinosis caused by deletion of the GM-CSFR α gene in the X chromosome pseudoautosomal region 1. *J Exp Med* 2008;205:2711–6.
- Hadchouel A, Wieland T, Griesse M, et al. Biallelic mutations of methionyl-tRNA synthetase cause a specific type of pulmonary alveolar proteinosis prevalent on Réunion island. *Am J Hum Genet* 2015;96:826–31.
- Turcu S, Ashton E, Jenkins L, et al. Genetic testing in children with surfactant dysfunction. *Arch Dis Child* 2013;98:490–5.
- Wambach JA, Wegner DJ, DePass K, et al. Single ABCA3 mutations increase risk for neonatal respiratory distress syndrome. *Pediatrics* 2012;130:e1575–82.
- Kaufman KM, Linghu B, Szustakowski JD, et al. Whole-exome sequencing reveals overlap between macrophage activation syndrome in systemic juvenile idiopathic arthritis and familial hemophagocytic lymphohistiocytosis. *Arthritis Rheumatol* 2014;66:3486–95.
- Ogilvie EM, Fife MS, Thompson SD, et al. The ?174G allele of the interleukin-6 gene confers susceptibility to systemic arthritis in children: A multicenter study using simplex and multiplex juvenile idiopathic arthritis families. *Arthritis Rheum* 2003;48:3202–6.
- Klotsche J, Raab A, Niewerth M, et al. Outcome and trends in treatment of systemic juvenile idiopathic arthritis in the German national pediatric rheumatologic database, 2000–2013. *Arthritis Rheumatol* 2016;68:3023–34.
- Alexander M, Petri H, Ding Y, et al. Morbidity and medication in a large population of individuals with Down syndrome compared to the general population. *Dev Med Child Neurol* 2016;58:246–54.
- Janow G, Schanberg LE, Setoguchi S, et al. The systemic juvenile idiopathic arthritis cohort of the childhood arthritis and rheumatology research alliance registry: 2010–2013. *J Rheumatol* 2016;43:1755–62.
- Russo RAG, Katsicas MM. Patients with very early-onset systemic juvenile idiopathic arthritis exhibit more inflammatory features and a worse outcome. *J Rheumatol* 2013;40:329–34.
- Behrens EM, Beukelman T, Gallo L, et al. Evaluation of the presentation of systemic onset juvenile rheumatoid arthritis: data from the Pennsylvania systemic onset juvenile arthritis registry (PASOJAR). *J Rheumatol* 2008;35:343–8.
- Davies R, Southwood T, Kearsley-Fleet L, et al. Mortality rates are increased in patients with systemic juvenile idiopathic arthritis. *Arch Dis Child* 2017;102:206–7.
- Meyer KC, Raghu G, Baughman RP, et al. An official American Thoracic Society clinical practice guideline: the clinical utility of bronchoalveolar lavage cellular analysis in interstitial lung disease. *Am J Respir Crit Care Med* 2012;185:1004–14.
- Midulla F, Villani A, Merolla R, et al. Bronchoalveolar lavage studies in children without parenchymal lung disease: cellular constituents and protein levels. *Pediatr Pulmonol* 1995;20:112–8.
- Radhakrishnan D, Yamashita C, Gillio-Meina C, et al. Translational research in pediatrics III: bronchoalveolar lavage. *Pediatrics* 2014;134:135–54.
- Meyer KC, Raghu G. Bronchoalveolar lavage for the evaluation of interstitial lung disease: is it clinically useful? *Eur Respir J* 2011;38:761–9.
- DeGroot J, Vastert S, Giancane G, et al. Interstitial lung disease in systemic juvenile idiopathic arthritis in the PharmaChild registry. *Pediatric Rheumatology Online Journal* 2018;16:17.
- Stills GF. On a form of chronic joint disease in children. Medical Chirurgical Trans (Proceedings of the Royal Medical and Chirurgical Society), 1897:47–60.
- Ardlie KG, Deluca DS, Segre AV, et al. The Genotype-Tissue Expression (GTEx) pilot analysis: multitissue gene regulation in humans. *Science* 2015;348:648–60.
- Sack U, Burkhardt U, Borte M, et al. Age-dependent levels of select immunological mediators in sera of healthy children. *Clin Diagn Lab Immunol* 1998;5:28–32.
- Iosef C, Alastalo T-P, Hou Y, et al. Inhibiting NF- κ B in the developing lung disrupts angiogenesis and alveolarization. *Am J Physiol Lung Cell Mol Physiol* 2012;302:L1023–36.

- 55 Shrivastava G, León-Juárez M, García-Cordero J, *et al.* Inflammasomes and its importance in viral infections. *Immunol Res* 2016;64:1101–17.
- 56 Huaux F, Lo Re S, Giordano G, *et al.* IL-1 α induces CD11b^{low} alveolar macrophage proliferation and maturation during granuloma formation. *J Pathol* 2015;235:698–709.
- 57 Periasamy S, Harton JA. Interleukin 1 α (IL-1 α) promotes pathogenic immature myeloid cells and IL-1 β favors protective mature myeloid cells during acute lung infection. *J Infect Dis* 2018;217:1481–90.
- 58 Willart MAM, Deswarte K, Pouliot P, *et al.* Interleukin-1 α controls allergic sensitization to inhaled house dust mite via the epithelial release of GM-CSF and IL-33. *J Exp Med* 2012;209:1505–17.
- 59 Uchida K, Beck DC, Yamamoto T, *et al.* Gm-Csf autoantibodies and neutrophil dysfunction in pulmonary alveolar proteinosis. *N Engl J Med* 2007;356:567–79.
- 60 Huaux F, De Gussem V, Lebrun A, *et al.* New interplay between interstitial and alveolar macrophages explains pulmonary alveolar proteinosis (PAP) induced by indium tin oxide particles. *Arch Toxicol* 2018;92:1349–61.
- 61 Dirksen U, Hattenhorst U, Schneider P, *et al.* Defective expression of granulocyte-macrophage colony-stimulating factor/interleukin-3/interleukin-5 receptor common beta chain in children with acute myeloid leukemia associated with respiratory failure. *Blood* 1998;92:1097–103.
- 62 Hefti E, Blanco JG. Pharmacotherapeutic considerations for individuals with Down syndrome. *Pharmacotherapy* 2017;37:214–20.
- 63 Ram G, Chinen J. Infections and immunodeficiency in Down syndrome. *Clin Exp Immunol* 2011;164:9–16.
- 64 Sullivan KD, Evans D, Pandey A, *et al.* Trisomy 21 causes changes in the circulating proteome indicative of chronic autoinflammation. *Sci Rep* 2017;7:14818.
- 65 Inaba H, Jenkins JJ, McCarville MB, *et al.* Pulmonary alveolar proteinosis in pediatric leukemia. *Pediatr Blood Cancer* 2008;51:66–70.
- 66 Soyer O, Demir S, Bilginer Y, *et al.* Severe hypersensitivity reactions to biological drugs in children with rheumatic diseases. *Pediatr Allergy Immunol* 2019;11.
- 67 Kardaun SH, Sekula P, Valeyrie-Allanore L, *et al.* Drug reaction with eosinophilia and systemic symptoms (dress): an original multisystem adverse drug reaction. results from the prospective RegiSCAR study. *Br J Dermatol* 2013;169:1071–80.
- 68 Martínez-Cabriales SA, Rodríguez-Bolaños F, Shear NH. Drug reaction with eosinophilia and systemic symptoms (dress): how far have we come? *Am J Clin Dermatol* 2019;20:236.
- 69 Kuyucu S, Caubet J-C. Hypersensitivity reactions to antiepileptic drugs in children: epidemiologic, pathogenetic, clinical, and diagnostic aspects. *J Allergy Clin Immunol* 2018;6:1879–91.
- 70 Nisar MK, Östör AJK. Pulmonary complications of biological therapies in children and adults with rheumatic diseases. *Paediatr Respir Rev* 2013;14:236–41.
- 71 Skeoch S, Weatherley N, Swift A, *et al.* Drug-Induced interstitial lung disease: a systematic review. *J Clin Med* 2018;7.
- 72 Flieder DB, Travis WD. Pathologic characteristics of drug-induced lung disease. *Clin Chest Med* 2004;25:37–45.
- 73 Lauinger IL, Bible JM, Halligan EP, *et al.* Patient characteristics and severity of human rhinovirus infections in children. *J Clin Virol* 2013;58:216–20.
- 74 Piper SC, Ferguson J, Kay L, *et al.* The role of interleukin-1 and interleukin-18 in pro-inflammatory and anti-viral responses to rhinovirus in primary bronchial epithelial cells. *PLoS One* 2013;8:e63365.
- 75 Chen Wet *et al.* Interleukin 1: an important mediator of host resistance against *Pneumocystis carinii*. *J Exp Med* 1992;176:713–8.
- 76 Robert-Gangneux F, Belaz S, Revest M, *et al.* Diagnosis of *Pneumocystis jirovecii* pneumonia in immunocompromised patients by real-time PCR: a 4-year prospective study. *J Clin Microbiol* 2014;52:3370–6.
- 77 Kano Y, Ishida T, Hirahara K, *et al.* Visceral involvements and long-term sequelae in drug-induced hypersensitivity syndrome. *Med Clin North Am* 2010;94:743–59.
- 78 Park JW, Curtis JR, Moon J, *et al.* Prophylactic effect of trimethoprim-sulfamethoxazole for pneumocystis pneumonia in patients with rheumatic diseases exposed to prolonged high-dose glucocorticoids. *Ann Rheum Dis* 2018;77:644–9.
- 79 Schulert GS, Yasin S, Carey B, *et al.* Systemic juvenile idiopathic Arthritis-Lung disease: characterization and risk factors. *Arthritis Rheumatol* 2019. doi:10.1002/art.41073. [Epub ahead of print: 5 Aug 2019].
- 80 Nigrovic PA, Mannion M, Prince FHM, *et al.* Anakinra as first-line disease-modifying therapy in systemic juvenile idiopathic arthritis: report of forty-six patients from an international multicenter series. *Arthritis Rheum* 2011;63:545–55.
- 81 Ransohoff JD, Nikfarjam A, Jones E, *et al.* Detecting chemotherapeutic skin adverse reactions in social health networks using deep learning. *JAMA Oncol* 2018;4:581–3.
- 82 Antoon JW, Hernandez ML, Roehrs PA, *et al.* Endogenous lipid pneumonia preceding diagnosis of pulmonary alveolar proteinosis. *Clin Respir J* 2016;10:246–9.
- 83 Fisher M, Roggli V, Merten D, *et al.* Coexisting endogenous lipid pneumonia, cholesterol granulomas, and pulmonary alveolar proteinosis in a pediatric population: a clinical, radiographic, and pathologic correlation. *Pediatr Pathol* 1992;12:365–83.
- 84 Pardeo M, Pires Marafon D, Insalaco A, *et al.* Anakinra in systemic juvenile idiopathic arthritis: a single-center experience. *J Rheumatol* 2015;42:1523–7.

Evidence to support or guide glucocorticoid tapering in rheumatoid arthritis is lacking

Low-dose glucocorticoids (GCs) improve symptoms and physical function and reduce joint damage in rheumatoid arthritis (RA).¹ Over a third of patients with RA are managed with long-term oral GC, defined as daily use for ≥ 3 months.² Current RA management guidelines recommend tapering GCs to the lowest effective dose as quickly as possible^{3,4} to minimise risk of GC-associated side effects, such as infections, cardiovascular events and bone fractures. However, there is little evidence to guide clinicians attempting to taper GCs,^{5,6} leading to widely variable practice patterns. This is of particular importance for patients with established RA who are maintained on long-term GCs. Such patients have higher cumulative GC exposure and increased rates of cardiovascular disease, osteoporosis and insulin resistance relative to early patients with RA,⁷⁻⁹ yet may face disease flare, adrenal insufficiency or other withdrawal symptoms when GC tapering is attempted.¹⁰⁻¹²

We searched clinicaltrials.gov for all registered studies evaluating oral GC tapering in adult patients with RA since September 2008. We found 2300 studies of adult patients with RA, 151 of

which included GCs, and we reviewed these studies. Of these, 80 were excluded as irrelevant due to observational design (n=42), non-oral GC administration (n=34) or other reasons (n=4). An additional 60 studies did not evaluate GC tapering. The remaining 11 studies are presented in table 1¹³⁻¹⁷ along with five additional studies captured by a previously published systematic review on this subject covering the years 1972–2011.^{5,18-21}

Of the 11 studies identified from clinicaltrials.gov, 7 incorporated GC tapers as induction treatment or bridge therapy for early RA (table 1). An additional two studies did not specify starting GC dose or taper duration. One study (NCT02573012) compared RA disease activity among patients randomised to continue versus stop versus taper off long-term oral GCs, but was limited to patients maintained on tocilizumab. The last (NCT02997605) was the only study to compare the efficacy of two different GC tapering regimens in allowing patients with established RA to discontinue long-term oral GCs. Of the five studies identified from the previous systematic review, three incorporated GC tapers as induction treatment for early RA. The remaining two studies compared RA disease activity or radiographic progression among patients randomised to continue vs taper off long-term GCs. None of these studies directly compared the efficacy of different GC tapering regimens. Of the 16 studies reviewed, only one (NCT02997605)

Table 1 Characteristics of included studies

Identifier	Acronym	Subjects	RA population	Duration (weeks)	Primary outcome	GC used	Initial GC dose* (mg/day)	Taper length (weeks)	Goal GC dose* (mg/day)	Additional taper instructions
NCT02466581 NCT01491815	NORD-STAR	812	Early	24	CDAI remission	Prednisone	20	9	5	Stop after 9 months
NCT02930343		150	Early	12	EULAR good response	Prednisolone	7.5	6	0	
NCT02997605	STAR	122	LT-GC	52	GC discontinuation	Prednisone Hydrocortisone	NS NS	52 36	0 0	Reduce 1 mg/month 20 mg/day for 3 months, 10 mg/day for 3 months
NCT03649061 ¹³	CareRA	442	Early	104	Area under DAS-28 curve	Prednisone	30	30	0	
NCT01219933 ¹⁴	ACT-ALONE	68	Current GC	20	DAS-28 LDA	Methylprednisolone	1–25	NS	NS	
NCT02644499		186	Early	12	EULAR good response	Prednisolone	15	6	2.5	
NCT02000336	CORRA	386	Early	52	Radiographic progression	Prednisolone	10 60	12 28	5 7.5 to 5	
NCT01172639 ¹⁵	COBRA	400	Early	104	DAS-28 remission	Prednisone	60 30	7 32	6.25 0	Taper to stop by week 32 Taper to stop by week 32
NCT00480272	CURE	251	Early	52	DAS-28 remission	Prednisone	50	7	6.25	Stop at week 24
NCT02293590	RICE	43	Established	24	ACR50 response	Prednisone	20	NS	0	Taper every 5 days
NCT02573012 ^{16,17}	SEMIRA	261	Established LT-GC	24	DAS-28 change from baseline	Prednisone	5	24	0	
Tengstrand <i>et al</i> ¹⁸		58	Established LT-GC	104	DAS-28 mean	NS	NS	52	0	
Goekoop-Ruiterman <i>et al</i> ¹⁹	BEST	508	Early	52	Dutch HAQ mean, Radiographic progression	Prednisolone	60	7	7.5	
Choy <i>et al</i> ²⁰	CARDERA	467	Early	104	New erosions	Prednisolone	60	28	7.5	Taper to stop by week 34
Pincus <i>et al</i> ²¹		31	LT-GC	NS	Withdrawal for 'lack of efficacy'	Prednisone	5	20	0	
Hickling <i>et al</i> ²²		128	Early	156	Radiographic progression	Prednisone	7.5	4	0	7.5 mg/day for 2 years, then taper

Evidence to support or guide GC tapering in rheumatoid arthritis is lacking.

*In prednisone equivalents.

CAAI, clinical disease activity index; DAS-28, disease activity score, 28-joint; EULAR, European League Against Rheumatism; GC, glucocorticoid; LDA, low disease activity; LT-GC, long-term GC; NS, not specified.

evaluated GC withdrawal symptoms and did so as a secondary outcome. Another study allowed for slower GC taper if 'withdrawal symptoms' occurred but did not specify how such symptoms were to be defined, or how the taper should be adjusted in response.

In sum, although long-term GC use is common in RA and GC tapering is explicitly supported by current RA management guidelines, there are few data to guide clinicians attempting to taper long-term GCs in RA, particularly among patients with established RA. Further work, including placebo-controlled trials of GC tapering, is needed to develop data-driven protocols for GC tapering that also account for GC withdrawal symptoms.

Beth I Wallace ^{1,2}, **David M Wallace**³, **Akbar K Waljee**^{1,4}, **Daniel J Clauw**^{2,5}

¹VA Center for Clinical Management Research, VA Ann Arbor Healthcare System, Ann Arbor, Michigan, USA

²Department of Internal Medicine, Division of Rheumatology, University of Michigan Health System, Ann Arbor, Michigan, USA

³Department of Internal Medicine, Division of General Medicine, University of Michigan Health System, Ann Arbor, Michigan, USA

⁴Department of Internal Medicine, Division of Gastroenterology, University of Michigan Health System, Ann Arbor, Michigan, USA

⁵Department of Anesthesiology, University of Michigan Health System, Ann Arbor, Michigan, USA

Correspondence to Dr Beth I Wallace, Department of Internal Medicine, Division of Rheumatology, University of Michigan Health System, Ann Arbor, MI 48109, USA; brennerb@umich.edu

Handling editor Josef S Smolen

Contributors BIW: study conception and design, interpretation of data, drafting of the manuscript and final approval of the manuscript. DMW: data acquisition, critical revision of the manuscript and final approval of the manuscript. AKW: study conception, critical revision of the manuscript and final approval of the manuscript. DJC: study conception, critical revision of the manuscript and final approval of the manuscript.

Funding Dr Wallace was supported during the time of this research by a VA Advanced Fellowship in Health Services Research and Development.

Competing interests Dr Clauw reports consulting relationships with Aptinix, Daiichi Sankyo, Intec Pharma, Eli Lilly, Pfizer, Samumed, Theravance, Tonix, Zynerba; has served as expert witness for Nix Patterson LLP, Williams & Connolly LLP; receives research support from Aptinix, Pfizer.

Patient consent for publication Not required.

Provenance and peer review Not commissioned; externally peer reviewed.

© Author(s) (or their employer(s)) 2019. No commercial re-use. See rights and permissions. Published by BMJ.



To cite Wallace BI, Wallace DM, Waljee AK, et al. *Ann Rheum Dis* 2019;**78**:1733–1734.

Received 10 July 2019

Revised 18 July 2019

Accepted 18 July 2019

Published Online First 31 July 2019

Ann Rheum Dis 2019;**78**:1733–1734. doi:10.1136/annrheumdis-2019-216009

ORCID iD

Beth I Wallace <http://orcid.org/0000-0003-1802-1427>

REFERENCES

- 1 Kirwan JR, Bijlsma JWJ, Boers M, et al. Effects of glucocorticoids on radiological progression in rheumatoid arthritis. *Cochrane Database Syst Rev* 2007;350.
- 2 Wallace B, Lin P, Kamdar N, et al. Patterns of Glucocorticoid Use and Provider-Level Variation in a Commercially Insured Incident Rheumatoid Arthritis Population [abstract]. *Arthritis & rheumatology* 2018;70(Suppl. 10).
- 3 Singh JA, Saag KG, Bridges SL, et al. 2015 American College of rheumatology guideline for the treatment of rheumatoid arthritis. *Arthritis Rheumatol* 2016;68:1–26.

- 4 Smolen JS, Landewé R, Bijlsma J, et al. EULAR recommendations for the management of rheumatoid arthritis with synthetic and biological disease-modifying antirheumatic drugs: 2016 update. *Ann Rheum Dis* 2017;76:960–77.
- 5 Volkman ER, Rezaei S, Tarp S, et al. We still don't know how to taper glucocorticoids in rheumatoid arthritis, and we can do better. *J Rheumatol* 2013;40:1646–9.
- 6 Gorter SL, Bijlsma JW, Cutolo M, et al. Current evidence for the management of rheumatoid arthritis with glucocorticoids: a systematic literature review Informing the EULAR recommendations for the management of rheumatoid arthritis. *Ann Rheum Dis* 2010;69:1010–4.
- 7 Peters MJL, Symmons DPM, McCarey D, et al. EULAR evidence-based recommendations for cardiovascular risk management in patients with rheumatoid arthritis and other forms of inflammatory arthritis. *Ann Rheum Dis* 2010;69:325–31.
- 8 Caplan L, Wolfe F, Russell AS, et al. Corticosteroid use in rheumatoid arthritis: prevalence, predictors, correlates, and outcomes. *J Rheumatol* 2007;34:696–705.
- 9 Einarsson JT, Willim M, Ernestam S, et al. Prevalence of sustained remission in rheumatoid arthritis: impact of criteria sets and disease duration, a nationwide study in Sweden. *Rheumatology* 2019;58:227–36.
- 10 Joseph RM, Hunter AL, Ray DW, et al. Systemic glucocorticoid therapy and adrenal insufficiency in adults: a systematic review. *Semin Arthritis Rheum* 2016;46:133–41.
- 11 Rodger RS, Watson MJ, Sellars L, et al. Hypothalamic-Pituitary-Adrenocortical suppression and recovery in renal transplant patients returning to maintenance dialysis. *Q J Med* 1986;61:1039–46.
- 12 Margolin L, Cope DK, Bakst-Sisser R, et al. The steroid withdrawal syndrome: a review of the implications, etiology, and treatments. *J Pain Symptom Manage* 2007;33:224–8.
- 13 Verschueren P, De Cock D, Corluy L, et al. Methotrexate in combination with other DMARDs is not superior to methotrexate alone for remission induction with moderate-to-high-dose glucocorticoid bridging in early rheumatoid arthritis after 16 weeks of treatment: the CareRA trial. *Ann Rheum Dis* 2015;74:27–34.
- 14 Ribbens C, Vanhoof J, Maertens M, et al. FRI0304 Glucocorticoid Dose Reduction in Patients with Low Disease Activity Using Tocilizumab: the Act-Alone Study. *Ann Rheum Dis* 2014;73(Suppl 2):495.2–495.
- 15 Boers M, Verhoeven AC, Markuse HM, et al. Randomised comparison of combined step-down prednisolone, methotrexate and sulphasalazine with sulphasalazine alone in early rheumatoid arthritis. *The Lancet* 1997;350:309–18.
- 16 Burmester GR, Buttgerit F, Bernasconi C, et al. A Randomized Controlled 24-Week Trial Evaluating the Safety and Efficacy of Blinded Tapering Versus Continuation of Long-Term Prednisone (5 mg/day) in Patients with Rheumatoid Arthritis Who Achieved Low Disease Activity or Remission on Tocilizumab [abstract]. *Arthritis & rheumatology* 2018;70(suppl 10).
- 17 Buttgerit F, Nebesky M, Burmester GR, et al. Glucocorticoid tapering in monthly 1mg decrements does not result in clinically manifest adrenal insufficiency in patients with rheumatoid arthritis. *learnings from the phase 3/4 SEMIRA study* 2019;78.
- 18 Tengstrand B, Larsson E, Klareskog L, et al. Randomized withdrawal of long-term prednisolone treatment in rheumatoid arthritis: effects on inflammation and bone mineral density. *Scand J Rheumatol* 2007;36:351–8.
- 19 Goekoop-Ruiterman YPM, de Vries-Bouwstra JK, Allaart CF, et al. Clinical and radiographic outcomes of four different treatment strategies in patients with early rheumatoid arthritis (the best study): a randomized, controlled trial. *Arthritis Rheum* 2005;52:3381–90.
- 20 Choy EHS, Smith CM, Farewell V, et al. Factorial randomised controlled trial of glucocorticoids and combination disease modifying drugs in early rheumatoid arthritis. *Ann Rheum Dis* 2008;67:656–63.
- 21 Pincus T, Swearingen CJ, Luta G, et al. Efficacy of prednisone 1-4 mg/day in patients with rheumatoid arthritis: a randomised, double-blind, placebo controlled withdrawal clinical trial. *Ann Rheum Dis* 2009;68:1715–20.
- 22 Hickling P, Jacoby RK, Kirwan JR. Joint destruction after glucocorticoids are withdrawn in early rheumatoid arthritis. arthritis and rheumatism Council low dose glucocorticoid Study Group. *Rheumatology* 1998;37:930–6.

Association of human papillomavirus infection with risk for rheumatoid arthritis: a population-based cohort study

Rheumatoid arthritis (RA) is an autoimmune disease caused by genetic and environmental factors. Infection is proposed to contribute to the pathogenesis.¹ Several viral and bacterial infections, including parvovirus B19, Chikungunya, hepatitis C, Epstein-Barr virus and *Porphyromonas gingivalis*, have been raised to be associated with RA.¹ The mechanism of how infections affect RA remains undetermined, generally considered to be via molecular mimicry and cross-reactions

Table 1 Demographic characteristics of human papillomavirus (HPV) and non-HPV

	Before propensity score matched				Standardised differences	After propensity score matched				Standardised differences
	HPV (N=40 349)		Non-HPV (N=322 792)			HPV (N=40 349)		Non-HPV (N=161 396)		
	n	%	n	%		n	%	n	%	
Age					0					0.002
20–40	21 093	52.3	168 744	52.3		21 093	52.3	84 413	52.3	
40–55	10 975	27.2	87 800	27.2		10 975	27.2	44 008	27.3	
≥55	8 281	20.5	66 248	20.5		8 281	20.5	32 975	20.4	
Mean±SD	41.7±16.2		41.7±16.2		0	41.7±16.2		41.6±16.2		0.003
Gender					0					–0.003
Female	21 015	52.1	168 120	52.1		21 015	52.1	84 280	52.2	
Male	19 334	47.9	154 672	47.9		19 334	47.9	77 116	47.8	
Hypertension	4680	11.6	31 124	9.6	0.064	4680	11.6	18 779	11.6	–0.001
Hyperlipidemia	1960	4.9	11 095	3.4	0.071	1960	4.9	7594	4.7	0.007
Chronic liver disease	1297	3.2	7031	2.2	0.064	1297	3.2	5143	3.2	0.002
Diabetes	1767	4.4	14 826	4.6	–0.01	1767	4.4	6889	4.3	0.005

between self-antigens and viral proteins.¹ Furthermore, recent study postulates that RA may be the result of immunosenescence, meaning premature ageing of the immune system via various mechanisms including telomere shortening.² A recent review article illustrates that the expression of human telomerase reverse transcriptase was influenced by human papillomavirus (HPV) E6/E7.³ Therefore, immunosenescence caused by telomere shortening may be another hypothetical mechanism in RA development followed by HPV infection.

HPV infections have been found to be associated with autoimmune diseases including systemic lupus erythematosus and RA.^{4,5} Immunosuppressed conditions in patients with autoimmune disease are prone to HPV infection.⁶ On the contrary, previous study shows that HPV infection is also a trigger factor for systemic lupus erythematosus in susceptible individuals based on the plausible mechanism of molecular homology.⁵ However, there is currently a lack of evidence to show whether the HPV infection is one of the risk factors for RA. The aim of this population-based cohort study is to examine the association and the causal relationship between HPV infection and risk of developing RA.

This nationwide cohort study was conducted using Taiwan's National Health Insurance Research Database from 1999 to 2013. The cumulative incidence rate of RA was calculated in person-years

and plotted by Kaplan-Meier curves. Log-rank test was used to examine the differences between the cumulative incidence curves. The Cox proportional-hazards regression model was used to estimate the HR and 95% CI to compare the risk of RA between the HPV infection and control cohorts. A total of 40 349 individuals were enrolled in the HPV group, as well as 161 396 controls without HPV infection identified by propensity score matching to reduce the heterogeneity and selection bias, and the sensitivity analysis was also performed (see online supplementary text). The baseline characteristics are revealed in table 1 and showed similar distributions due to the well-balanced matching. The average age was 41.7±16.2 and the gender ratio was 52.1% (female) to 47.9% (male) in patients with HPV infection. There was no significant difference in these comorbidities between the two groups.

The incidence density of RA was higher in the HPV-infected group compared with the non-HPV controls (1.1 vs 0.8 per 1000 person-years; crude HR, 1.41; 95% CI 1.24 to 1.6). After adjusting for age, gender, hypertension, hyperlipidemia, chronic liver disease and diabetes, the adjusted HR of developing RA among the HPV-infected group was 1.40 (95% CI 1.24 to 1.59). The cumulative incidence rates of RA in the HPV and non-HPV groups are shown in figure 1. The Kaplan-Meier analysis revealed that the HPV-infected individuals had a significantly higher RA incidence than the non-HPV controls (log-rank test: $p<0.001$). In the subgroup analysis after stratification for age and gender, the results indicated a significantly increased risk of RA in adults 20–40 years old and 40–55 years old from the HPV group (adjusted HR, 1.76; 95% CI 1.38 to 2.23; adjusted HR, 1.34; 95% CI 1.09 to 1.65, respectively) and female (adjusted HR, 1.45; 95% CI 1.25 to 1.68) with HPV infection (see online supplementary table S3).

In conclusion, this is the first study to examine the relationship between HPV infection and RA under a time-sequential research design, and inferred that HPV infection may be a precipitating factor of RA based on the results implying that HPV infection may be associated with a higher risk of RA development.

Yen-Tze Liu^{1,2,3}, Hsi-Kai Tsou,^{4,5} Jeng-Yuan Chiou,⁶ Yu-Hsun Wang,⁷ Ming-Chih Chou,^{1,8} James Cheng-Chung Wei^{1,9,10}

¹Institute of Medicine, Chung Shan Medical University, Taichung, Taiwan

²Department of Family Medicine, Changhua Christian Hospital, Changhua, Taiwan

³Department of Holistic Wellness, Mingdao University, Changhua, Taiwan

⁴Functional Neurosurgery Division, Neurological Institute, Taichung Veterans General Hospital, Taichung, Taiwan

⁵Department of Rehabilitation, Jen-Teh Junior College of Medicine, Nursing and Management, Miaoli, Taiwan

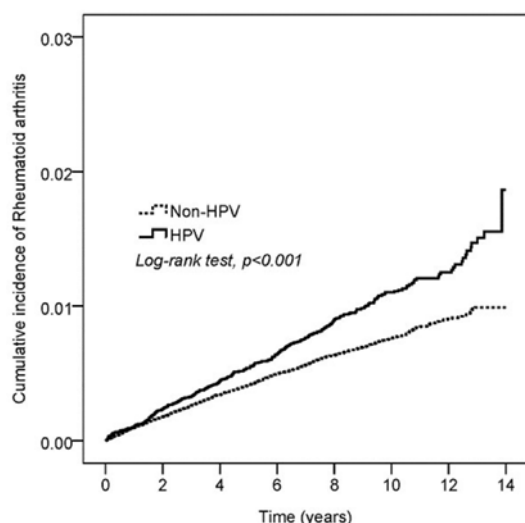


Figure 1 Kaplan-Meier curves of cumulative incidence for rheumatoid arthritis in human papillomavirus (HPV) and non-HPV group.

⁶School of Health Policy and Management, Chung Shan Medical University, Taichung, Taiwan

⁷Department of Medical Research, Chung Shan Medical University Hospital, Taichung, Taiwan

⁸Division of Thoracic Surgery, Department of Surgery, Chung Shan Medical University Hospital, Taichung, Taiwan

⁹Department of Internal Medicine, Chung Shan Medical University Hospital, Taichung, Taiwan

¹⁰Graduate Institute of Integrated Medicine, China Medical University, Taichung, Taiwan

Correspondence to Dr James Cheng-Chung Wei, Institute of Medicine, Chung Shan Medical University, Taichung 402, Taiwan; jccwei@gmail.com

Handling editor Josef S Smolen

Acknowledgements The authors would like to thank all colleagues who contributed to this study.

Contributors Corresponding author JCCW had full access to all the data in the study and takes responsibility for the integrity of the data and the accuracy of the data analysis. Study concept and design: JCCW. Acquisition, analysis or interpretation of data: JCCW and Y-HW. Drafting of the manuscript: Y-TL and M-CC. Critical revision of the manuscript for important intellectual content: JCCW, H-KT, J-YC and Y-HW.

Funding The authors have not declared a specific grant for this research from any funding agency in the public, commercial or not-for-profit sectors.

Competing interests None declared.

Patient consent for publication Not required.

Provenance and peer review Not commissioned; externally peer reviewed.

© Author(s) (or their employer(s)) 2019. No commercial re-use. See rights and permissions. Published by BMJ.

► Additional material is published online only. To view please visit the journal online (<http://dx.doi.org/10.1136/annrheumdis-2019-215931>).



To cite Liu Y-T, Tsou H-K, Chiou J-Y, et al. *Ann Rheum Dis* 2019;**78**:1734–1736.

Received 22 June 2019

Revised 6 August 2019

Accepted 6 August 2019

Published Online First 14 August 2019

Ann Rheum Dis 2019;**78**:1734–1736. doi:10.1136/annrheumdis-2019-215931

ORCID iD

Yen-Tze Liu <http://orcid.org/0000-0002-5922-2295>

REFERENCES

- Smolen JS, Aletaha D, McInnes IB. Rheumatoid arthritis. *Lancet* 2016;388:2023–38.
- Chalan P, van den Berg A, Kroesen B-J, et al. Rheumatoid arthritis, Immunosenescence and the hallmarks of aging. *Curr Aging Sci* 2015;8:131–46.
- Katzenellenbogen R. Telomerase induction in HPV infection and oncogenesis. *Viruses* 2017;9:E180.
- Shi J, Sun X, Zhao Y, et al. Prevalence and significance of antibodies to citrullinated human papilloma virus-47 E2345-362 in rheumatoid arthritis. *J Autoimmun* 2008;31:131–5.
- Shi L-H, Huang J-Y, Liu Y-Z, et al. Risk of systemic lupus erythematosus in patients with human papillomavirus infection: a population-based retrospective cohort study. *Lupus* 2018;27:2279–83.
- Kim SC, Feldman S, Moscicki A-B. Risk of human papillomavirus infection in women with rheumatic disease: cervical cancer screening and prevention. *Rheumatology* 2018;57(Suppl 5):v26–33.

Real-world effectiveness of apremilast in multirefractory mucosal involvement of Behçet's disease

Relapsing oral and genital ulcers (OGUs) represent the stigmata of Behçet's disease (BD) and may be very painful, affecting both quality of life and relationships. A wide number of topical and immunosuppressive drugs can be used to treat ulcers,¹ but failures are commonly reported. The efficacy of the phosphodiesterase-4 inhibitor apremilast has been proven in OGUs of BD in two randomised clinical trials (RCTs),^{2,3} whereas only two case reports are available until now.^{4,5} We aimed at evaluating the real-world effectiveness of apremilast in BD patients with OGUs refractory to conventional and/or biological treatments.

We retrospectively evaluated patients classified as BD, according to International Criteria for BD⁶ and International Study Group⁷ criteria, who underwent apremilast (30 mg two times per day) for multirefractory OGUs from November 2017 to January 2019. The number of OGUs was assessed at baseline and either at 3 and 6 months. Pain from ulcers and BD activity were evaluated via 100 mm visual analogue scale (VAS) and BD current activity form (BDCAF). We also recorded the number of OGU flares both in the 4 weeks prior to apremilast start and

Table 1 Clinical and demographic characteristics of 13 patients with Behçet's disease included in our study

Demographic features		Clinical characteristics at diagnosis, n (%)	
Female, n (%)	9 (69.2)	Ocular involvement	4 (30.8)
Age in years, mean (SD)	44.1 (11.2)	Oral ulcers	13 (100)
HLA-B51 positivity, n (%)	6 (54.5)	Genital ulcers	9 (69.2)
Disease duration at APR baseline, months, mean (SD)	154.2 (167.8)	Other mucocutaneous involvement	7 (53.8)
Previous biological agents, n (%)		Musculoskeletal involvement	10 (76.9)
Tumor necrosis factor- α inhibitors	10 (76.9)	Central nervous system involvement	1 (7.7)
Anakinra	4 (30.8)	Vascular involvement	2 (15.4)
Ustekinumab	2 (15.4)	Gastrointestinal involvement	6 (46.1)
Previous immunosuppressants, n (%)		Combination treatment at baseline, n (%)	
Colchicine	10 (76.9)	Colchicine	4 (30.8)
Cyclosporine A	4 (30.8)	Intravenous immunoglobulins	1 (7.7)
Methotrexate	3 (23.1)	Anakinra	1 (7.7)
Azathioprine	9 (69.2)	Low dose steroids (\leq 10 mg prednisone /day)	10 (76.6)
Others (cyclophosphamide, thalidomide, interferon, sulfasalazine)	7 (53.9)	High dose steroids ($>$ 10 mg prednisone /day)	2 (15.4)
Flares of mucosal involvement in the 4 weeks prior to APR			
Oral ulcer flares, mean (SD)	2.2 (3.1)	Genital ulcer flares, mean (SD)	0.5 (0.7)
APR, apremilast.			

Table 2 Mucosal involvement, VAS pain and BDCAF assessed at baseline and throughout the observation period

	Baseline 13 patients	3 months 12 patients	P value	6 months 8 patients	P value
Number of active oral ulcers, mean (SD)	1.1 (0.6)	0.4 (0.5)	0.02	0.4 (0.5)	0.03
Number of active genital ulcers, mean (SD)	0.5 (0.5)	0.1 (0.3)	0.02	0 (0)	0.07
BDCAF, mean (SD)	4.5 (2.9)	3.2 (3.4)	0.01	2.37 (3.7)	0.01
VAS pain, mean (SD)	67.5 (16.6)	29 (32.1)	0.002	20 (19.1)	0.005

Reported p values are referred to the difference from baseline.
BDCAF, BD current activity form; VAS, visual analogue scale.

throughout the observation period (table 1 and online supplementary table 2). The occurrence of adverse events was also reported. Paired t-test or Wilcoxon matched-pair signed rank test were used for statistical analysis. The off-label use of apremilast was approved by the Hospital Ethics Committee in compliance with the Declaration of Helsinki. All patients provided a written informed consent.

Thirteen patients (females 9/13) with disease duration (mean±SD) of 154±167 months were analysed (table 1) (online supplementary file 1). At 3 months (data from 12/13 patients) active OGUs were significantly less (p=0.02 for both) than baseline (table 2). Three patients stopped the treatment due to diarrhoea. At 6 months, active oral ulcers and oral relapses were still lower than baseline (p=0.03 for both), whereas only a positive trend (p=0.07) for genital ulcers was seen (data from 8/13 patients) (table 2). Ulcer VAS pain was 67±16 at baseline, and a prompt amelioration was observed at 3 months (29±32, p=0.002), and confirmed at 6 months (20±19, p=0.005) (table 2). Likewise, BDCAF dropped from 4.5±2.9 of baseline to 3.2±3.4 at 3 months (p=0.01), and was persistently low up to 6 months (2.3±3.7, p=0.01) (table 2). Serious adverse events were not observed.

Our findings are consistent with a recent RCT on 111 BD patients,² which showed the efficacy of apremilast in reducing both number and pain of oral ulcers.² Preliminary results from another study confirm the significant decrease of total number of oral ulcers and resolution of genital ulcers over 12 weeks in the apremilast group.³ Similarly, in our study the mean number of oral relapses during therapy was significantly lower than that in the 4 weeks prior to apremilast. Interestingly, an appreciable reduction of VAS pain and BDCAF was already seen at 3 months and persisted up to 6 months. Of note, the overall beneficial effect of apremilast also on joint symptoms should be highlighted, as emerged by the BDCAF evaluations. Apremilast was safe and no serious adverse events were observed during the time span of our study. The main limitations of our study were the small sample size and the short-term follow-up. In addition, patients had been referred to our tertiary care centres since they were difficult-to-treat or refractory to therapy, configuring a possible selection bias. Nevertheless, we provide evidence that apremilast may induce a meaningful and early benefit in BD patients with multirefractory OGUs also in real-life settings.

Giuseppe Lopalco¹,²,³,⁴ Vincenzo Venerito,¹ Pietro Leccese,² Giacomo Emmi,³ Luca Cantarini,⁴ Nancy Lascaro,² Gerardo Di Scala,⁵ Claudia Fabiani,⁶ Donato Rigante,⁷ Florenzo Iannone¹

¹Department of Emergency and Organ Transplantation, Rheumatology Unit, University of Bari, Bari, Italy

²Rheumatology Institute of Lucania (IRel), Rheumatology Department of Lucania, San Carlo Hospital of Potenza and Madonna delle Grazie Hospital of Matera, Potenza, Italy

³Department of Experimental and Clinical Medicine, University of Firenze, Florence, Italy

⁴Research Centre of Systemic Autoinflammatory Diseases, Behçet's Disease Clinic and Rheumatology-Ophthalmology Collaborative Uveitis Centre, Department of Medical Sciences, Surgery and Neurosciences, University of Siena, Siena, Italy

⁵Department of Experimental and Clinical Medicine, University of Firenze, Firenze, Italy

⁶Ophthalmology Unit, Department of Medicine, Surgery and Neuroscience, University of Siena, Siena, Italy

⁷Institute of Pediatrics, Fondazione Policlinico Universitario "A. Gemelli" IRCCS, Rome, Italy

Correspondence to Dr Giuseppe Lopalco, Department of Emergency and Organ Transplantation, Rheumatology Unit, University of Bari, Bari 70124, Italy; glopalco@hotmail.it

Handling editor Josef S Smolen

Acknowledgements We would like to thank prof Giovanni Lapadula for his valuable insights.

Collaborators Marco Fornaro, Maria Grazia Giannotta, Elena Silvestri.

Contributors All authors approved the final version of the letter after being involved in drafting and revising the article for important intellectual content. As the corresponding author, GL had full access to the data and takes responsibility for the accuracy of the performed analysis and the integrity of data. GL, VV and FI were involved in the design of the study. Execution, analysis and writing of the manuscript were performed by GL and VV.

Funding The authors have not declared a specific grant for this research from any funding agency in the public, commercial or not-for-profit sectors.

Competing interests None declared.

Ethics approval This study was performed according to the Declaration of Helsinki and obtained the approval by the Ethics Committee in the University of Bari, Italy.

Provenance and peer review Not commissioned; externally peer reviewed.

© Author(s) (or their employer(s)) 2019. No commercial re-use. See rights and permissions. Published by BMJ.

► Additional material is published online only. To view please visit the journal online (<http://dx.doi.org/10.1136/annrheumdis-2019-215437>).

GL and VV contributed equally.



To cite Lopalco G, Venerito V, Leccese P, et al. *Ann Rheum Dis* 2019;**78**:1736–1737.

Received 27 March 2019

Revised 25 July 2019

Accepted 6 August 2019

Published Online First 10 August 2019

Ann Rheum Dis 2019;**78**:1736–1737. doi:10.1136/annrheumdis-2019-215437

ORCID iDs

Giuseppe Lopalco <http://orcid.org/0000-0003-4524-9566>

Giacomo Emmi <http://orcid.org/0000-0001-9575-8321>

Florenzo Iannone <http://orcid.org/0000-0003-0474-5344>

REFERENCES

- Hatemi G, Christensen R, Bang D, et al. 2018 update of the EULAR recommendations for the management of Behçet's syndrome. *Ann Rheum Dis* 2018;**77**:808–18.
- Hatemi G, Melikoglu M, Tunc R, et al. Apremilast for Behçet's syndrome—a phase 2, placebo-controlled study. *N Engl J Med* 2015;**372**:1510–8.
- Hatemi G, Mahr A, Takeno D, et al. Apremilast for Behçet's syndrome: a phase iii randomised, placebo-controlled, double-blind study (RELIEF). *Ann Rheum Dis* 2018;**77**:A9.
- Moya P, Castellví I, Magallares B, et al. Healing of mucocutaneous lesions with apremilast in Behçet disease. *J Clin Rheumatol* 2019. doi:10.1097/RHU.0000000000001005. [Epub ahead of print: 20 Mar 2019].
- Saini A, Ferguson C, Salkey K. Use of Apremilast for Aphthous Ulcers in a Patient With Behçet's Syndrome. *J Drugs Dermatol* 2018;**17**:1328–9.
- International Team for the Revision of the International Criteria for Behçet's Disease (ITR-ICBD). The International criteria for Behçet's disease (ICBD): a collaborative study of 27 countries on the sensitivity and specificity of the new criteria. *J Eur Acad Dermatol Venereol* 2014;**28**:338–47.
- O'Neill TW, Rigby AS, Silman AJ, et al. Validation of the International Study Group criteria for Behçet's disease. *Br J Rheumatol* 1994;**33**:115–7.

'Slope sign': a feature of large vessel vasculitis?

Ultrasound (US) scanning in the diagnosis of large vessel giant cell arteritis (LV-GCA) is becoming more prevalent, with the advantage of being non-invasive and free of ionising radiation.¹ The recent European League against Rheumatism (EULAR) recommendations suggest that US should be the first-line investigation for cases of suspected GCA where adequate equipment and expertise is available.^{2,3} US is also having a more prominent role in disease monitoring. Biologics such as Tocilizumab have now been approved to treat relapsing and refractory LV-GCA; however, it has been noted that while Tocilizumab may suppress serum inflammatory markers (ie, C reactive protein and erythrocyte sedimentation rate (ESR)) it may underestimate on-going vessel wall disease activity.⁴ Consequently, the use of US in disease monitoring has become increasingly important, as traditional biomarkers are not reliable in this instance.

The use of US in cranial GCA is now well established, with the finding of a non-'compressible halo sign' in the temporal arteries to be of important diagnostic value.² In the axillary arteries of patients with suspected LV-GCA, this sign is less helpful due to tissue depth and therefore measuring the intima-medial thickness (IMT) is the preferred method of assessment. The cut-off value for IMT at the axillary arteries is 1.0 mm, with values greater than this suggestive of LV-GCA.⁵ It is recognised that there are other causes of arterial wall thickening, such as atherosclerosis. Atherosclerotic changes on US are usually more localised and discrete; however, it can sometimes be challenging to differentiate between vasculitic and atherosclerotic changes in axillary arteries.⁶

We describe the 'slope sign' as a specific US feature in of the axillary arteries in patients with LV-GCA (figure 1). Unlike atherosclerosis, thickening seen in vasculitis is smooth, homogenous and continuous up to a transitional point where IMT gradually slopes downwards back to a normal level (below 1.0 mm). We postulated that evaluation of this slope may help differentiate vasculitis from atherosclerosis (see online supplementary images) and other causes of arterial wall thickening, and may also be helpful to monitor disease progression (see online supplementary table 1). We recently conducted a review

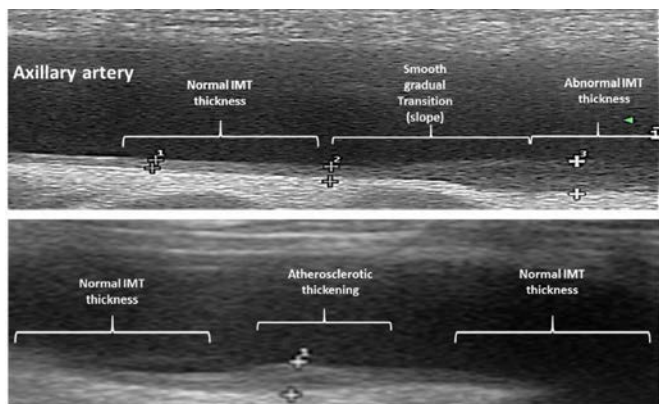


Figure 1 Ultrasound scan images of the axillary artery demonstrating the 'slope sign' of smooth transition from increased to normal intima-medial thickness (IMT) in large vessel giant cell arteritis (upper panel) contrasted with the discrete localised thickening seen in atherosclerosis (lower panel).

of our images at Southend University Hospital, UK (examined from 01.09.2018 to 18.01.2019) and observed the presence of a 'slope sign' in the axillary artery US scan of 24 out of 28 new patients with confirmed LV-GCA. The remaining four patients did not have the transition zone visualised and therefore could not be assessed.

We have observed that this transitional point is often situated near the circumflex artery. Further research is required to determine whether either the position of the slope in relation to the circumflex or the angle of the slope have further value in diagnosis and monitoring.

We suggest the 'slope sign' to be a helpful finding in the US of the axillary arteries in patients with acute and chronic LV-GCA. We propose the 'slope sign' should be included in protocols for axillary artery US scanning in suspected LV-GCA. It may also have utility monitoring disease activity in confirmed LV-GCA.

Bhaskar Dasgupta ¹, **Kate Smith** ^{1,2}, **Abdullah Abu Syeed Khan** ¹, **Fiona Coath**,¹ **Richard J Wakefield**³

¹Rheumatology, Southend University Hospital NHS Foundation Trust, Westcliff-on-Sea, UK

²Rheumatology, Chapel Allerton Hospital, Leeds Biomedical Research Centre, Leeds, UK

³Rheumatology, University of Leeds, Leeds Institute of Rheumatic and Musculoskeletal Medicine, Leeds, UK

Correspondence to Dr Bhaskar Dasgupta, Rheumatology, Southend Hospital NHS Trust, Westcliff-on-Sea SSO ORY, UK; bhaskar.dasgupta@southend.nhs.uk

Handling editor Josef S Smolen

Contributors BD performed the scans; BD, AASK and KS selected the scans, BD, AASK, KS, FC and RJW contributed to data analysis and writing the manuscript.

Competing interests None declared.

Patient consent for publication Not required.

Provenance and peer review Not commissioned; externally peer reviewed.

© Author(s) (or their employer(s)) 2019. No commercial re-use. See rights and permissions. Published by BMJ.

► Additional material is published online only. To view please visit the journal online (<http://dx.doi.org/10.1136/annrheumdis-2019-216213>).



To cite Dasgupta B, Smith K, Khan AAS, *et al.* *Ann Rheum Dis* 2019;**78**:1738.

Received 23 August 2019

Revised 4 September 2019

Accepted 4 September 2019

Published Online First 13 September 2019

Ann Rheum Dis 2019;**78**:1738. doi:10.1136/annrheumdis-2019-216213

ORCID iDs

Bhaskar Dasgupta <http://orcid.org/0000-0002-5523-6534>

Kate Smith <http://orcid.org/0000-0002-1685-2051>

Abdullah Abu Syeed Khan <http://orcid.org/0000-0003-4380-9064>

REFERENCES

- Czihal M, Lottspeich C, Hoffmann U. Ultrasound imaging in the diagnosis of large vessel vasculitis. *Vasa* 2017;**46**:241–53.
- Dejaco C, Ramiro S, Duftner C, *et al.* EULAR recommendations for the use of imaging in large vessel vasculitis in clinical practice. *Ann Rheum Dis* 2018;**77**:636–43.
- Schmidt WA. Ultrasound in the diagnosis and management of giant cell arteritis. *Rheumatology* 2018;**57**(suppl_2):ii22–31.
- Coath F, Gilbert K, Griffiths B, *et al.* Giant cell arteritis: new concepts, treatments and the unmet need that remains. *Rheumatology* 2019;**58**:key326.
- Schäfer VS, Juche A, Ramiro S, *et al.* Ultrasound cut-off values for intima-media thickness of temporal, facial and axillary arteries in giant cell arteritis. *Rheumatology* 2017;**56**:1479–83.
- Schmidt WA. Role of ultrasound in the understanding and management of vasculitis. *Ther Adv Musculoskelet Dis* 2014;**6**:39–47.

Metering the METEOR in methotrexate failure: is propensity score a falling star?

The debate on the preferred treatment of rheumatoid arthritis (RA) after methotrexate (MTX) failure has always been fascinating. Sytske Anne Bergstra and associates have analysed data from patients in the METEOR cohort who had failed MTX monotherapy.¹ It was absorbing to see how they used multiple propensity score (PS) to control for bias in non-randomised data collected from an international registry ('METEOR'). They have pragmatically outlined how the PS was analysed.

The analysis has demonstrated clear superiority of biological disease-modifying anti-rheumatoid drugs (b-DMARDs) over conventional synthetic DMARDs (cs-DMARDs) in both unadjusted and PS-adjusted results at 6 months and at 1 year. There is already plenty of evidence that addition of a bDMARD to MTX (on failure of monotherapy) is better in the short term than addition of a cs-DMARD. A network meta-analysis of 33 trials has shown the superiority of b-DMARDs at 6 months in achieving higher disease control, that is, in the American College of Rheumatology 70% response criteria (ACR70).² Similarly, a meta-analysis of eight such trials demonstrated similar benefits with bDMARDs at 6 months, but the differences disappeared at 24 months.³ The European League Against Rheumatism (EULAR) already recommends adding a bDMARD (over adding a csDMARD) in MTX failure if 'unfavourable factors' are present.⁴ At the present date, the evidence for benefits of this approach is only for the short term, and not beyond 2 years.

The contrast in this analysis is that Bergstra *et al* have used rheumatoid arthritis disease activity score (DAS) as the primary outcome measure. Clinical trials usually use the ACR20 criteria. Even in the RACAT trial that had shown non-inferiority of triple drug therapy versus addition of etanercept in MTX failure, DAS28 reduction was more in the etanercept group at 6 months. Nevertheless, ACR20 and ACR50 were similar at 6 months (and at 2 years). Differences in DAS28 and ACR70 vanished by the end of 2 years.⁵ Again, difference in DAS (includes 44 swollen joint count and 78 tender joint count) may be numerically different than difference in DAS28.

I would have liked to know what proportion of patients in the three groups of the study met ACR20 at the two time points. And, hopefully, the authors will publish the results of the follow-up of the METEOR MTX monotherapy failure cohort at 24 months as well.

It is interesting that the multiple PS adjustments did not change the differences in DAS by much. Improvement in DAS was almost double in the bDMARD group compared with the others. The bDMARD group had higher number of swollen joints and thus seemed likely to show greater difference on adjustment by the PS. But this was not so.

PS basically combines the effect of all known confounders into one covariate. It is good for studies with rare events and multiple confounders.⁶ As the authors have mentioned, the PS cannot control bias due to factors not included in the analyses. One such factor can be the placebo effect of biologicals on patients. Again use of the Ritchie articular index (RAI) and the DAS (that includes the RAI) allows for variability in the subjective evaluation. This might unconsciously augment a bias in the evaluator who is aware that the patient is on biologicals. Another potential confounder was the MTX dose. Patients in the

csDMARD +steroids group were getting almost half the MTX dose compared with the other two groups. If this difference was maintained throughout the observation period, that itself would lead to differences in the DAS. Also, I did not find information on steroid use in the bDMARD group.

This paper has reiterated the short-term superiority of bDMARDs over csDMARD after MTX failure. In a comparison of cost-effectiveness and quality of life, results depended on the methods used.⁷ We are yet to know what is best for the patient in the long term.

The highlight of the paper seems to be use of the PS. But PS-adjusted analysis did not differ much from the unadjusted analysis. Maybe because it has good validity. Maybe its use is superfluous until we understand all the confounders in RA. Either way, it is for the reader to decide if PS is a guiding star or a falling star!

Sakir Ahmed

Correspondence to Dr Sakir Ahmed, Clinical Immunology and Rheumatology, Kalinga Institute of Medical Sciences, Bhubaneswar, Odisha 751024, India; sakir005@gmail.com

Handling editor Josef S Smolen

Contributors The sole author has completely drafted and finalised the manuscript.

Competing interests None declared

Patient consent Not required.

Provenance and peer review Not commissioned; internally peer reviewed.

© Author(s) (or their employer(s)) 2019. No commercial re-use. See rights and permissions. Published by BMJ.



To cite Ahmed S. *Ann Rheum Dis* 2019;**78**:e131.

Received 19 October 2018

Accepted 26 October 2018

Published Online First 8 November 2018



► <http://dx.doi.org/10.1136/annrheumdis-2018-214652>

Ann Rheum Dis 2019;**78**:e131. doi:10.1136/annrheumdis-2018-214612

REFERENCES

- Bergstra SA, Winchow LL, Murphy E, *et al*. How to treat patients with rheumatoid arthritis when methotrexate has failed? the use of a multiple propensity score to adjust for confounding by indication in observational studies. *Ann Rheum Dis* 2019;**78**:25–30.
- Fleischmann R, Tongbram V, van Vollenhoven R, *et al*. Systematic review and network meta-analysis of the efficacy and safety of tumour necrosis factor inhibitor-methotrexate combination therapy versus triple therapy in rheumatoid arthritis. *RMD Open* 2017;**3**:e000371.
- Graudal N, Hubeck-Graudal T, Faurschou M, *et al*. Combination Therapy With and Without Tumor Necrosis Factor Inhibitors in Rheumatoid Arthritis: A Meta-Analysis of Randomized Trials. *Arthritis Care Res* 2015;**67**:1487–95.
- Smolen JS, Landewé R, Bijlsma J, *et al*. EULAR recommendations for the management of rheumatoid arthritis with synthetic and biological disease-modifying antirheumatic drugs: 2016 update. *Ann Rheum Dis* 2017;**76**:960–77.
- O'Dell JR, Mikuls TR, Taylor TH, *et al*. Therapies for active rheumatoid arthritis after methotrexate failure. *N Engl J Med* 2013;**369**:307–18.
- Joffe MM, Rosenbaum PR. Invited commentary: propensity scores. *Am J Epidemiol* 1999;**150**:327–33.
- Kvamme MK, Lie E, Uhlig T, *et al*. Cost-effectiveness of TNF inhibitors vs synthetic disease-modifying antirheumatic drugs in patients with rheumatoid arthritis: a Markov model study based on two longitudinal observational studies. *Rheumatology* 2015;**54**:1226–35.

Response to: 'Metering the METEOR in methotrexate failure: is propensity score a falling star?' by Ahmed *et al*

We thank Dr Ahmed for his response to our article and for his interest in the methodology we used.¹ The aim of our study was twofold: to compare, in daily practice, treatment options after failure of initial methotrexate (MTX) in rheumatoid arthritis (RA) patients, but also to introduce the multiple propensity score (PS) in rheumatology.

As Dr Ahmed mentioned, previous research has been performed into treatment options after MTX failure, including the mentioned network meta-analysis based on clinical trials.² These trials mostly included a selected population and reported response to one or at most two treatment options, either including a biologic disease modifying anti-rheumatic drug (bDMARD) or conventional synthetic (cs) DMARD triple therapy. But in daily practice, there are many scenarios in which rheumatologists consider multiple treatment options aimed to specifically benefit their individual patient, rather than following predefined study protocols. In our large, international daily practice database, we were able to compare three treatment strategies simultaneously, including a combination of csDMARD(s) with glucocorticoids. This is a therapy that has never been compared with triple therapy in clinical trials, but as shown by our data it was the therapy that was most frequently prescribed after MTX failure in daily practice.³

Next, Dr Ahmed asked for the proportion of patients that fulfil the American College of Rheumatology response criteria, which we cannot provide as it is not used in daily practice to monitor individuals' response to treatment and therefore not included in the Measurement of Efficacy of Treatment in the Era of Outcome in Rheumatology (METEOR) database. In addition, Dr Ahmed¹ is interested in the 24-month results of our data. Although undoubtedly long-term outcomes are of interest in a potentially chronic disease as RA, we were specifically interested in the short-term effectiveness of the treatment strategy after MTX failure. With longer follow-up, many patients who do not respond to treatment will have switched to a next treatment step according to a treat-to-target approach. When analysing longer term results, we would not be able to discern the effects of the second treatment strategy, but rather evaluate the treat-to-target concept. Previous studies have shown that long-term outcomes can be greatly improved if a consequent treat-to-target approach aimed at remission or at least low disease activity is maintained.⁴⁻⁶ These long-term benefits make it possible to return to the acute symptoms of having active RA and the intention to suppress disease activity as quickly as possible, hence our focus on short-term outcomes of treatment choices.

Only data regarding treatment effectiveness will not allow us to draw definitive conclusions on the best treatment step after initial MTX failure in daily practice. For this decision, also other factors such as adverse events and cost-effectiveness should be considered. We do not agree that the dose of methotrexate (within a certain range) has a significant impact on short-term outcomes, as in our previous studies in the same database such an association was not found, neither for MTX in combination therapies nor for MTX monotherapy.^{7,8}

Next to the clinical research question, multiple PS played an important role in our study. From the onset of this study, we have been careful to consider bias. We have acknowledged that there was a large risk of confounding by indication and that the

multiple PS would be an appropriate method to handle this bias. Indeed, several of the included baseline variables were unbalanced at baseline. However, it is impossible to determine the eventual influence of the multiple PS on the effect estimates beforehand, and the relatively small differences between crude and adjusted analyses should not be a reason to not include the multiple PS afterwards. We have shown both crude and adjusted analyses, such that the reader can judge both.

Using the multiple PS enabled us to compare three treatment groups simultaneously, which was not done in previous studies, but more in line with relevant scenarios in daily practice. A multiple PS reflects to some extent the prescriber's perspective on a patient's disease severity and prognosis.⁹ As in all methods used to adjust for bias in observational research, unknown or unmeasured factors that influence treatment decisions (cultural, socioeconomic, emotional, other) cannot be included in multiple PS.⁹ We agree that we should always remain critical when interpreting its results. Nevertheless, a well-applied multiple PS can help us shine light on outcomes of daily practice observational studies, specifically in the situation in which multiple treatment options are available.

Sytske Anne Bergstra,¹ Cornelia F Allaart,¹ Robert B M Landewé^{2,3}

¹Department of Rheumatology, Leiden University Medical Center, Leiden, The Netherlands

²Amsterdam Rheumatology & Immunology Center, Amsterdam, The Netherlands

³Department of Rheumatology, Zuyderland Medical Center, Heerlen, The Netherlands

Correspondence to Sytske Anne Bergstra, Department of Rheumatology, Leiden University Medical Center, Leiden 2333 ZA, The Netherlands; s.a.bergstra@lumc.nl

Handling editor Josef S Smolen

Funding The authors have not declared a specific grant for this research from any funding agency in the public, commercial or not-for-profit sectors.

Competing interests None declared.

Patient consent Not required.

Provenance and peer review Commissioned; internally peer reviewed.

© Author(s) (or their employer(s)) 2019. No commercial re-use. See rights and permissions. Published by BMJ.



To cite Bergstra SA, Allaart CF, Landewé RBM. *Ann Rheum Dis* 2019;**78**:e132.

Received 2 November 2018

Accepted 4 November 2018

Published Online First 14 November 2018



► <http://dx.doi.org/10.1136/annrheumdis-2018-214612>

Ann Rheum Dis 2019;**78**:e132. doi:10.1136/annrheumdis-2018-214652

REFERENCES

- Ahmed S, Bergstra SA, Winchow LL. Metering the Meteor in methotrexate failure: is propensity score a falling star? *Ann Rheum Dis* 2019;**78**:e131.
- Fleischmann R, Tongbram V, van Vollenhoven R, *et al*. Systematic review and network meta-analysis of the efficacy and safety of tumour necrosis factor inhibitor-methotrexate combination therapy versus triple therapy in rheumatoid arthritis. *RMD Open* 2017;**3**:e000371. doi:10.1136/rmdopen-2016-000371
- Bergstra SA, Winchow LL, Murphy E, *et al*. How to treat patients with rheumatoid arthritis when methotrexate has failed? the use of a multiple propensity score to adjust for confounding by indication in observational studies. *Ann Rheum Dis* 2019;**78**:25–30.
- Markuse IM, Akdemir G, Dirven L, *et al*. Long-term outcomes of patients with recent-onset rheumatoid arthritis after 10 years of tight controlled treatment: a randomized trial. *Ann Intern Med* 2016;**164**:523–31.
- Rantalaaho V, Korpela M, Laasonen L, *et al*. Early combination disease-modifying antirheumatic drug therapy and tight disease control improve long-term radiologic

- outcome in patients with early rheumatoid arthritis: the 11-year results of the Finnish Rheumatoid Arthritis Combination Therapy trial. *Arthritis Res Ther* 2010;12:R122.
- 6 Boers M, Verhoeven AC, Markusse HM, *et al*. Randomised comparison of combined step-down prednisolone, methotrexate and sulphasalazine with sulphasalazine alone in early rheumatoid arthritis. *Lancet* 1997;350:309–18.
 - 7 Bergstra SA, Allaart CF, Stijnen T, *et al*. Meta-regression of a dose-response relationship of methotrexate in mono- and combination therapy in disease-modifying antirheumatic drug-naïve early rheumatoid arthritis patients. *Arthritis Care Res* 2017;69:1473–83.
 - 8 Bergstra SA, Allaart CF, van den Berg R, *et al*. Similar short-term clinical response to high-dose versus low-dose methotrexate in monotherapy and combination therapy in patients with rheumatoid arthritis. *Arthritis Res Ther* 2017;19:258.
 - 9 Spreeuwenberg MD, Bartak A, Croon MA, *et al*. The multiple propensity score as control for bias in the comparison of more than two treatment arms: an introduction from a case study in mental health. *Med Care* 2010;48:166–74.

Tocilizumab in patients with adult-onset Still's disease refractory to glucocorticoid treatment

I was pleased to read the article by Kaneko and colleagues¹ on the efficacy and safety of tocilizumab in patients with adult-onset Still's disease, because the current information on its biologic efficacy has been mainly obtained from small retrospective case series and not from prospective randomised trials. The authors have presented a randomised controlled trial in which they suggest that tocilizumab is effective in adult-onset Still's disease refractory to glucocorticoid treatment. Information on biologic therapy for the management of adult-onset Still's disease is scarce. In this regard, there is a noteworthy issue. At present, the treatment of patients with adult-onset Still's disease remains empirical.² Corticosteroids are the cornerstones of the initial treatment, and conventional disease-modifying antirheumatic drugs (DMARDs), such as methotrexate, hydroxychloroquine, leflunomide, ciclosporin, tacrolimus and azathioprine, are generally used alone or in combination. DMARDs are effective means of inducing remission, lowering the risk of relapse and minimising glucocorticoid therapy and toxicity in adult-onset Still's disease.³ Thus, DMARDs are therapeutic options in addition to the standard-of-care treatment with glucocorticoids for this disease.⁴ Biologic agents are generally used as the second-line treatment because of their high cost and potential toxicity.⁵ Biologics may be considered in case of failure of DMARDs to control the disease. Although adult-onset Still's disease is a rare systemic inflammatory disorder, biologic therapy represents a major breakthrough in the management of patients with adult-onset Still's disease refractory to DMARDs. For example, anakinra induced more beneficial responses than DMARDs did in patients with refractory adult-onset Still's disease in a randomised study.⁶ However, there is no strong evidence regarding the comparative efficacy of tocilizumab and DMARDs in the management of adult-onset Still's disease. Currently, no randomised trial has shown that tocilizumab is superior to DMARDs in treating adult-onset Still's disease refractory to glucocorticoid treatment. Thus, treatment for adult-onset Still's disease continues to be a challenge. Further randomised studies

are warranted to determine the benefits of tocilizumab in terms of its glucocorticoid-sparing effect, remission and reduction in relapse, compared with DMARD therapy.

Young Ho Lee

Correspondence to Professor Young Ho Lee, Division of Rheumatology, Korea University Medical Center, Seoul 02841, South Korea; lyhcggh@korea.ac.kr

Competing interests None declared.

Patient consent Not required.

Provenance and peer review Not commissioned; internally peer reviewed.

© Author(s) (or their employer(s)) 2019. No commercial re-use. See rights and permissions. Published by BMJ.



To cite Lee YH. *Ann Rheum Dis* 2019;**78**:e133.

Received 23 October 2018

Accepted 26 October 2018

Published Online First 2 November 2018



► <http://dx.doi.org/10.1136/annrheumdis-2018-214653>

Ann Rheum Dis 2019;**78**:e133. doi:10.1136/annrheumdis-2018-214635

REFERENCES

- 1 Kaneko Y, Kameda H, Ikeda K, *et al*. Tocilizumab in patients with adult-onset still's disease refractory to glucocorticoid treatment: a randomised, double-blind, placebo-controlled phase III trial. *Ann Rheum Dis* 2017;**77**:1720–9.
- 2 Castañeda S, Blanco R, González-Gay MA. Adult-onset Still's disease: advances in the treatment. *Best Pract Res Clin Rheumatol* 2016;**30**:222–38.
- 3 Yoo DH. Treatment of adult-onset still's disease: up to date. *Expert Rev Clin Immunol* 2017;**13**:849–66.
- 4 Kalyoncu U, Solmaz D, Emmungil H, *et al*. Response rate of initial conventional treatments, disease course, and related factors of patients with adult-onset Still's disease: data from a large multicenter cohort. *J Autoimmun* 2016;**69**:59–63.
- 5 Pasadhika S, Rosenbaum JT. Update on the use of systemic biologic agents in the treatment of noninfectious uveitis. *Biologics* 2014;**8**:67.
- 6 Nordström D, Knight A, Luukkainen R, *et al*. Beneficial effect of interleukin 1 inhibition with anakinra in adult-onset Still's disease. An open, randomized, multicenter study. *J Rheumatol* 2012;**39**:2008–11.

Response to: 'Tocilizumab in patients with adult-onset Still's disease refractory to glucocorticoid treatment' by Lee

We would like to thank Dr Lee¹ for his interest in our paper² and for his comments providing futuristic insights into the management of adult-onset Still's disease. As he highlights, conventional disease-modifying antirheumatic drugs (DMARDs) are important options for this disease.^{3–5} Although the safety of biological agents including tocilizumab have been shown in patients with rheumatoid arthritis, they are more expensive than conventional DMARDs, and the long-term safety of their use in patients with adult-onset Still's disease is still unknown. Some of patients in our trial had a history of not responding to DMARDs such as methotrexate or ciclosporine, but we did not collect precise information about patients' previous treatment other than glucocorticoids use.

Our trial was a first step, aimed at proving the efficacy of anti-interleukin-6 treatment by a high-levelled evidence rather than case reports. As Dr Lee mentioned, further randomised studies are warranted to determine the optimal management of adult-onset Still's disease, although the rarity and occasional fatal severity of adult-onset Still's disease would hinder determining appropriate endpoints and recruiting active patients who are refractory to glucocorticoids but can tolerate control treatment including placebo or conventional DMARDs. The next step will need worldwide cooperation to establish the optimal management of adult-onset Still's in clinical studies with a proper design and sample size.

Yuko Kaneko,¹ Hideto Kameda,^{1,2} Kei Ikeda,³ Tomonori Ishii,⁴ Kosaku Murakami,⁵ Hyota Takamatsu,⁶ Yoshiya Tanaka,⁷ Takayuki Abe,⁸ Tsutomu Takeuchi¹

¹Division of Rheumatology, Department of Internal Medicine, Keio University School of Medicine, Tokyo, Japan

²Division of Rheumatology, Department of Internal Medicine, Toho University Ohashi Medical Center, Tokyo, Japan

³Department of Allergy and Clinical Immunology, Chiba University Hospital, Chiba, Japan

⁴Department of Hematology and Rheumatology, Tohoku University Graduate School of Medicine, Sendai, Japan

⁵Department of Rheumatology and Clinical Immunology, Kyoto University, Kyoto, Japan

⁶Department of Respiratory Medicine and Clinical Immunology, Graduate School of Medicine, Osaka University, Osaka, Japan

⁷The First Department of Internal Medicine, School of Medicine, University of Occupational and Environmental Health, Kitakyushu, Japan

⁸Department of Preventive Medicine and Public Health, Biostatistics at Clinical and Translational Research Center, Keio University School of Medicine, Tokyo, Japan

Correspondence to Dr Yuko Kaneko, Division of Rheumatology, Department of Internal Medicine, Keio University School of Medicine, Tokyo 160-8582, Japan; ykaneko@z6.keio.jp

Handling editor Josef S Smolen

Contributors This is a response to e-letter.

Funding The authors have not declared a specific grant for this research from any funding agency in the public, commercial or not-for-profit sectors.

Competing interests None declared.

Patient consent Obtained.

Provenance and peer review Commissioned; internally peer reviewed.

© Author(s) (or their employer(s)) 2019. No commercial re-use. See rights and permissions. Published by BMJ.



To cite Kaneko Y, Kameda H, Ikeda K, *et al.* *Ann Rheum Dis* 2019;**78**:e134.

Received 29 October 2018

Accepted 1 November 2018

Published Online First 10 November 2018



► <http://dx.doi.org/10.1136/annrheumdis-2018-214635>

Ann Rheum Dis 2019;**78**:e134. doi:10.1136/annrheumdis-2018-214653

REFERENCES

- Lee YH. Tocilizumab in patients with adult-onset Still's disease refractory to glucocorticoid treatment. *Ann Rheum Dis* 2019;**78**:e133.
- Kaneko Y, Kameda H, Ikeda K, *et al.* Tocilizumab in patients with adult-onset still's disease refractory to glucocorticoid treatment: a randomised, double-blind, placebo-controlled phase III trial. *Ann Rheum Dis* 2018;**77**:1720–9.
- Castañeda S, Blanco R, González-Gay MA. Adult-onset Still's disease: advances in the treatment. *Best Pract Res Clin Rheumatol* 2016;**30**:222–38.
- Yoo DH. Treatment of adult-onset still's disease: up to date. *Expert Rev Clin Immunol* 2017;**13**:849–66.
- Kalyoncu U, Solmaz D, Emmungil H, *et al.* Response rate of initial conventional treatments, disease course, and related factors of patients with adult-onset Still's disease: data from a large multicenter cohort. *J Autoimmun* 2016;**69**:59–63.

Inflammation in SLE-PAH: good news or not?

We read with great interest the recent study of Sun *et al* on the two distinct clinical phenotypes of systemic lupus erythematosus (SLE)-associated pulmonary arterial hypertension (PAH).¹ Based on the baseline characteristics of SLE-PAH, two clusters of patients were identified as vasculitic subtype, which had systemic manifestations and high SLE disease activity, and vasculopathic subtype, which tended to have low disease activity but pure PAH. It showed that the survival of patients with vasculitic subtype was worse than those with vasculopathic subtype. The time interval between the diagnosis of SLE and PAH (<2 years) and Systemic Lupus Erythematosus Disease Activity Index (SLEDAI >9) were identified as two independent predictors of vasculitic subtype. A weighted score ≥ 2 combining these two factors (time interval <2 years and ≥ 2 years were 1 and 0 point, SLEDAI >9, 5–9 and <5 were 2, 1, 0 point) was further developed as prediction model of vasculitic subtype.

Peking Union Medical College Hospital established a prospective cohort of patients with SLE-PAH in China since 2009. A total of 145 patients with SLE-PAH were enrolled. All patients were evaluated by right heart catheterisation to confirm the diagnosis of PAH. The mean pulmonary arterial pressure was 46.4 ± 10.9 mm Hg, the pulmonary vascular resistance was 10.0 ± 4.2 WU and cardiac index was 2.8 ± 0.8 L/min \times m². Other groups of pulmonary hypertension were excluded by chest high-resolution CT scan, pulmonary function test and ventilation/perfusion (V/Q) scan.

According to the weight score combining the time interval between the diagnosis of SLE and PAH and SLEDAI, patients were divided into vasculitic subtype (weight score ≥ 2 , 34 cases) and vasculopathic subtype (weight score <2, 111 cases). Kaplan-Meier analysis showed that the survival of vasculitic subtype tended to be better than vasculopathic subtype with the 3-year survival rates of 92.4% versus 85.5% ($p=0.52$, HR 0.70, 95% CI 0.24 to 2.05; [figure 1A](#)). The conclusion was not changed after adjusting treatment variation (data not shown). Besides mortality, we set a secondary end point as treatment goal achievement (TGA). Treatment goal was defined as achieved when all of the following four aspects were reached, including (1) clinical symptoms: no signs of right heart failure, syncope or progression; (2) WHO functional class (FC) I or II, or six-minute walking distance (6MWD) >380–440 m; (3) serology: brain natriuretic peptide (BNP) <50 ng/L or N terminal-pro brain natriuretic peptide (NT-proBNP) <300 ng/L; and (4) cardiac imaging: normal right atrial area according to echocardiography. Notably, it showed that the vasculitic subtype tended to reach

TGA earlier than vasculopathic subtype with the 3-year TGA rates of 71.2% versus 60.7% ($p=0.31$, HR 1.34, 95% CI 0.76 to 2.31; [figure 1B](#)).

According to the literature, the non-inflammatory subtype and the inflammatory subtype of SLE-PAH was previously being inferred.² Our study also showed that baseline inflammation such as serositis was an independent predictor of TGA, which associated with long-term survival (unpublished data). Patients with serositis at baseline tended to benefit from intensive immunosuppressive therapy and have a better clinical outcome (unpublished data), which indicates that inflammation may play a significant role in the prognosis and treatment response in SLE-PAH. It is indeed necessary to distinguish patients with SLE-PAH into the two phenotypes—vasculitic or vasculopathic subtypes. However, the prognosis of vasculitic subtype may not be worse than vasculopathic subtype and needs to be further studied. Several studies showed improvement from immunosuppressant therapy.^{3,4} It has been reported that patients with a simultaneous diagnosis of PAH and CTD (the diagnosis of PAH and CTD within 6 months) and treated with immunosuppressant therapy were prone to be short-term responders and had the best survival.⁵ Our data showed that the patients with vasculitic subtype tend to get TGA easier and had a higher 3-year survival rate (even without clinical significance), suggesting that the vasculitic subtype has a stronger inflammatory background and may have a better treatment response in immunosuppressant therapy. Notably, the timing of treatment can also affect the prognosis that patients may benefit from early immunosuppressant treatment. Further study is on call to answer these questions.

Junyan Qian,¹ Mengtao Li,¹ Jiuliang Zhao,¹ Qian Wang,¹ Zhuang Tian,² Xiaofeng Zeng¹

¹Department of Rheumatology, Key Laboratory of Rheumatology and Clinical Immunology, Ministry of Education, Peking Union Medical College Hospital, Peking Union Medical College and Chinese Academy of Medical Science, Beijing, China

²Department of Cardiology, Peking Union Medical College Hospital, Peking Union Medical College and Chinese Academy of Medical Science, Beijing, China

Correspondence to Dr Mengtao Li and Dr Xiaofeng Zeng, Department of Rheumatology, Peking Union Medical College Hospital, Beijing, China; mengtao.li@cstar.org.cn, xiaofeng.zeng@cstar.org.cn

Contributors Conception and design: JQ, ML, XZ. Analysis and interpretation: JQ, QW, JZ, ZT. Drafting the manuscript for important intellectual content: JQ, ML, XZ.

Funding The study was supported by the Chinese National Key Technology R&D Program, Ministry of Science and Technology (2017YFC0907601, 2017YFC0907602, 2017YFC0907603), and the Chinese National High Technology Research and Development Program, Ministry of Science and Technology (2012AA02A513).

Competing interests None declared.

Patient consent Obtained.

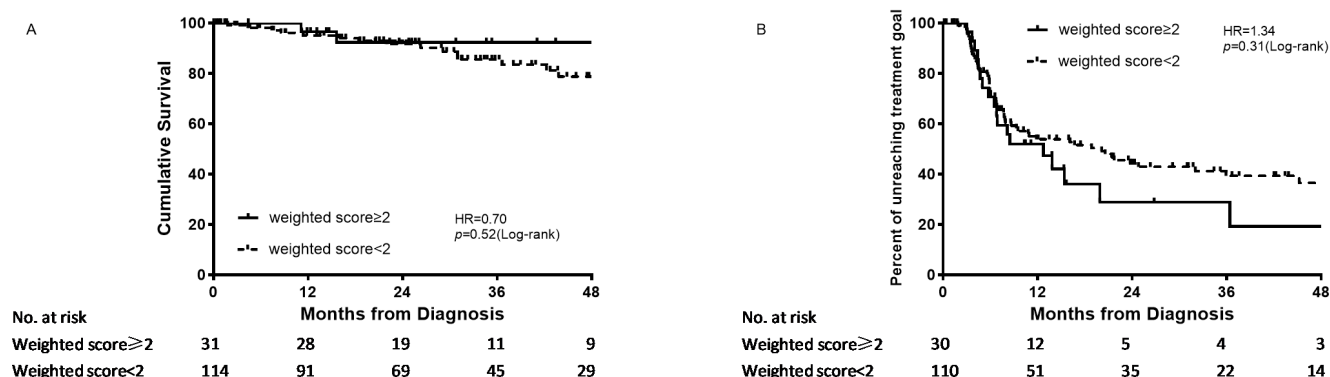


Figure 1 (A) Survival curves of patients with SLE-PAH in two different weighted score groups. (B) TGA curves of patients with SLE-PAH in two different weighted score groups.

Provenance and peer review Not commissioned; internally peer reviewed.

© Author(s) (or their employer(s)) 2019. No commercial re-use. See rights and permissions. Published by BMJ.



To cite Qian J, Li M, Zhao J, *et al.* *Ann Rheum Dis* 2019;**78**:e135.

Received 17 October 2018

Accepted 26 October 2018

Published Online First 14 November 2018



► <http://dx.doi.org/10.1136/annrheumdis-2018-214647>

Ann Rheum Dis 2019;**78**:e135. doi:10.1136/annrheumdis-2018-214605

REFERENCES

- 1 Sun F, Lei Y, Wu W, *et al.* Two distinct clinical phenotypes of pulmonary arterial hypertension secondary to systemic lupus erythematosus. *Ann Rheum Dis* 2019;**78**:148–50.
- 2 Chow SL, Chandran V, Fazlzad R, *et al.* Prognostic factors for survival in systemic lupus erythematosus associated pulmonary hypertension. *Lupus* 2012;**21**:353–64.
- 3 Jais X, Launay D, Yaici A, *et al.* Immunosuppressive therapy in lupus- and mixed connective tissue disease-associated pulmonary arterial hypertension: a retrospective analysis of twenty-three cases. *Arthritis Rheum* 2008;**58**:521–31.
- 4 Huang C, Zhang S, Tian Z, *et al.* Could pulmonary arterial hypertension be an active index of systemic lupus erythematosus? A successful case of SLE-PAH cured by methylprednisolone pulse therapy. *Lupus* 2014;**23**:1533–6.
- 5 Yasuoka H, Shirai Y, Tamura Y, *et al.* Predictors of favorable responses to immunosuppressive treatment in pulmonary arterial hypertension associated with connective tissue disease. *Circ J* 2018;**82**:546–54.

Response to: 'Inflammation in SLE-PAH: good news or not?' by Junyan Qian *et al*

Thank you very much for your interest in our article 'Two distinct clinical phenotypes of pulmonary arterial hypertension secondary to systemic lupus erythematosus', and we are glad to answer the question 'Inflammation in SLE-PAH: good news or not?' as below.

First, referral bias may exist and contribute to the different outcome. As an example, the Peking Union Medical College Hospital (PUMCH) cohort has more patients with pulmonary arterial hypertension secondary to systemic lupus erythematosus (SLE-PAH) with vasculopathic subtype.¹ Among these patients, the 3-year survival is precisely in line with our two cohorts,^{1,2} suggesting those SLE with 'pure' PAH are more homogeneous. Further analysing the more heterogeneous vasculitic subtype, the baseline manifestations and SLE disease activity index (SLEDAI) of our data vary. We totally agree that such patients with more systemic inflammatory components would be a better responder to immunosuppressive therapies, and some patients may even experience a reversible PAH course.³⁻⁵ Nevertheless, when talking about all-cause mortality, it makes sense that a patient who had a pronounced lupus nephritis (LN) or neuropsychiatric systemic lupus nephritis (NPSLE) or haematological manifestations on top of PAH will have a higher probability of poorer outcome.⁶ Another scenario is that when such patients underwent aggressive immunosuppressive therapy and complicated with infection, they tend to be more vulnerable to haemodynamically unstable. In other words, for those more heterogeneous vasculitic SLE-PAH subtype, baseline parameters and other confounders such as comorbidities, complications and treatment protocols should be scrutinised before a definitive conclusion can be made. It seems indisputable that clinical trials should be carried out on such patients in order to justify the appropriate combination of immunosuppressive therapy and PAH-targeted treatment, and improve the overall outcome.

Fangfang Sun,¹ Yunxia Lei,² Xiao Zhang,² Shuang Ye¹

¹Department of Rheumatology, School of Medicine, Ren Ji Hospital South Campus, Shanghai Jiaotong University, Shanghai, China

²Department of Rheumatology, Guangdong General Hospital, Guangzhou, China

Correspondence to Professor Shuang Ye, Department of Rheumatology, School of Medicine, Ren Ji Hospital South Campus, Shanghai Jiao Tong University, Shanghai 200001, China; ye_shuang2000@163.com

Handling editor Josef S Smolen

Contributors All authors participated in drafting and revising the response, and all authors approved the final version for publication. XZ and SY had full access to all the data in the study and take responsibility for the integrity and accuracy of the data.

Funding The authors have not declared a specific grant for this research from any funding agency in the public, commercial or not-for-profit sectors.

Competing interests None declared.

Patient consent Not required.

Provenance and peer review Commissioned; internally peer reviewed.

© Author(s) (or their employer(s)) 2019. No commercial re-use. See rights and permissions. Published by BMJ.



To cite Sun F, Lei Y, Zhang X, *et al*. *Ann Rheum Dis* 2019;**78**:e136.

Received 1 November 2018

Accepted 1 November 2018

Published Online First 14 November 2018



► <http://dx.doi.org/10.1136/annrheumdis-2018-214605>

Ann Rheum Dis 2019;**78**:e136. doi:10.1136/annrheumdis-2018-214647

REFERENCES

- 1 Qian J, Li M, Zhao J. Inflammation in SLE-PAH: good news or not? *Ann Rheum Dis* 2019;**78**:e135.
- 2 Sun F, Lei Y, Wu W, *et al*. Two distinct clinical phenotypes of pulmonary arterial hypertension secondary to systemic lupus erythematosus. *Ann Rheum Dis* 2019;**78**:148–50.
- 3 Yasuoka H, Shirai Y, Tamura Y, *et al*. Predictors of favorable responses to immunosuppressive treatment in pulmonary arterial hypertension associated with connective tissue disease. *Circ J* 2018;**82**:546–54.
- 4 Watanabe R, Fujii H, Shirai T, *et al*. Successful use of intensive immunosuppressive therapy for treating simultaneously occurring cerebral lesions and pulmonary arterial hypertension in a patient with systemic lupus erythematosus. *Intern Med* 2014;**53**:627–31.
- 5 Huang C, Zhang S, Tian Z, *et al*. Could pulmonary arterial hypertension be an active index of systemic lupus erythematosus? A successful case of SLE-PAH cured by methylprednisolone pulse therapy. *Lupus* 2014;**23**:1533–6.
- 6 Wu XY, Yang M, Xie YS, *et al*. Causes of death in hospitalized patients with systemic lupus erythematosus: a 10-year multicenter nationwide Chinese cohort. *Clin Rheumatol* 2018.

Chronic hydroxychloroquine/chloroquine exposure for connective tissue diseases and risk of Alzheimer's disease

I have read with interest the article by Fardet *et al*¹ regarding chronic hydroxychloroquine/chloroquine exposure for connective tissue diseases and risk of Alzheimer's disease. This population-based cohort study reported that people who had been chronically exposed to hydroxychloroquine/chloroquine were not at a higher risk of Alzheimer's disease than the control individuals. However, the manuscript has some issues. The results reported by Fardet *et al* differ from those of another retrospective case-control study² which demonstrated that patients with rheumatoid arthritis who used conventional synthetic disease-modifying antirheumatic drugs (csDMARDs) including hydroxychloroquine showed a significant association with dementia. First, the risk of confounding may be significant in observational studies, and statistical adjustment for confounders in observational studies may not entirely resolve these problems. Second, the results from observational studies might be spurious due to some types of bias, such as reporting and recall biases. Considering the lack of evidence from randomised controlled trials (RCTs), the conclusions by Fardet *et al*¹ that hydroxychloroquine/chloroquine do not confer protection against the development of Alzheimer's disease and those by Chou *et al*² that csDMARD use increases the risk of Alzheimer's disease may be overstated or risky.³ The antimalarial drugs, hydroxychloroquine and chloroquine, have well-documented, anti-inflammatory activity and effectively suppress microglial neurotoxicity induced by β -amyloid protein.⁴ Currently, no RCTs have examined the role of hydroxychloroquine/chloroquine in preventing Alzheimer's disease. Whether hydroxychloroquine/chloroquine increases or decreases the development of Alzheimer's disease cannot yet be confidently stated. With respect to the divergent results from observational studies, well-designed RCTs are required to adequately address the complex problem about the relationship between hydroxychloroquine/chloroquine use and Alzheimer's disease risk.

Young Ho Lee

Correspondence to Professor Young Ho Lee, Department of Rheumatology, Korea University College of Medicine, Seoul 02841, Korea; lyhcg@korea.ac.kr

Handling editor Josef S Smolen

Competing interests None declared.

Patient consent Not required.

Provenance and peer review Not commissioned; internally peer reviewed.

© Author(s) (or their employer(s)) 2018. No commercial re-use. See rights and permissions. Published by BMJ.



To cite Lee YH. *Ann Rheum Dis* 2019;**78**:e137.

Received 27 September 2018

Accepted 29 September 2018

Published Online First 18 October 2018



► <http://dx.doi.org/10.1136/annrheumdis-2018-214515>

Ann Rheum Dis 2019;**78**:e137. doi:10.1136/annrheumdis-2018-214494

REFERENCES

- 1 Fardet L, Nazareth I, Petersen I. Chronic hydroxychloroquine/chloroquine exposure for connective tissue diseases and risk of Alzheimer's disease: a population-based cohort study. *Ann Rheum Dis* 2019;**78**:279–82.
- 2 Chou MH, Wang JY, Lin CL, *et al*. DMARD use is associated with a higher risk of dementia in patients with rheumatoid arthritis: a propensity score-matched case-control study. *Toxicol Appl Pharmacol* 2017;**334**:217–22.
- 3 Rossouw JE, Anderson GL, Prentice RL, *et al*. Risks and benefits of estrogen plus progestin in healthy postmenopausal women: principal results from the women's health initiative randomized controlled trial. *JAMA* 2002;**288**:321–33.
- 4 Giulian D. Microglia and the immune pathology of Alzheimer disease. *Am J Hum Genet* 1999;**65**:13–18.
- 5 Fardet L, Petersen I, Nazareth I. Response to: 'Chronic hydroxychloroquine/chloroquine exposure for connective tissue diseases and risk of Alzheimer's disease' by Lee. *Ann Rheum Dis* 2019;**78**:e138.

Response to: 'Chronic hydroxychloroquine/chloroquine exposure for connective tissue diseases and risk of Alzheimer's disease' by Lee

We agree with Lee¹ that observational studies are limited by unmeasured and unknown confounding which can be best handled by a sufficiently powered randomised controlled trial. As mentioned in the discussion of our paper, we also acknowledge that Chou *et al* in their research on the Taiwanese National Health Insurance Research Database found that conventional synthetic disease-modifying antirheumatic-drugs (csDMARD) increases the risk of Alzheimer's disease rather than providing protection.² It is interesting that both studies failed to epidemiologically capture any positive anti-inflammatory effects or suppression of microglial neurotoxicity induced by β -amyloid protein hypothesised to be triggered by these drugs. Further, as described in our paper,³ the effect of hydroxychloroquine on progression of dementia in early Alzheimer's disease has already been investigated in an 18-month randomised, placebo-controlled trial that included 168 patients with early Alzheimer's disease which showed no effect of the treatment against placebo.⁴ There are no randomised controlled trials to date that evaluate effects of these drugs on primary prevention of Alzheimer's disease. This is because such trials would have to run for several years and would need to recruit very large numbers of people in order to provide a meaningful result. In the absence of such evidence large observational studies offer the best next level of evidence on which we as clinicians can judge the effectiveness and/or safety of drugs.

Laurence Fardet,^{1,2,3} Irene Petersen,¹ Irwin Nazareth¹

¹Department of Primary Care and Population Health, University College London, London, UK

²Department of Dermatology, AP-HP, Henri Mondor hospital, Créteil, France

³EA7379, Université Paris Est Créteil, Créteil, France

Correspondence to Professor Laurence Fardet, Department of Primary Care and Population Health, University College London, London, UK; laurence.fardet@aphp.fr

Handling editor Josef S Smolen

Funding The authors have not declared a specific grant for this research from any funding agency in the public, commercial or not-for-profit sectors.

Competing interests None declared.

Provenance and peer review Commissioned; internally peer reviewed.

© Author(s) (or their employer(s)) 2019. No commercial re-use. See rights and permissions. Published by BMJ.



To cite Fardet L, Petersen I, Nazareth I. *Ann Rheum Dis* 2019;**78**:e138.

Received 3 October 2018

Accepted 4 October 2018

Published Online First 18 October 2018



► <http://dx.doi.org/10.1136/annrheumdis-2018-214494>

Ann Rheum Dis 2019;**78**:e138. doi:10.1136/annrheumdis-2018-214515

REFERENCES

- 1 Lee YH. Chronic hydroxychloroquine/chloroquine exposure for connective tissue diseases and risk of Alzheimer's disease. *Ann Rheum Dis* 2019;**78**:e137.
- 2 Chou MH, Wang JY, Lin CL, *et al*. DMARD use is associated with a higher risk of dementia in patients with rheumatoid arthritis: A propensity score-matched case-control study. *Toxicol Appl Pharmacol* 2017;**334**:217–22.
- 3 Fardet L, Nazareth I, Petersen I. Chronic hydroxychloroquine/chloroquine exposure for connective tissue diseases and risk of Alzheimer's disease: a population-based cohort study. *Ann Rheum Dis* 2019;**78**:279–82.
- 4 Van Gool WA, Weinstein HC, Scheltens P, *et al*. Effect of hydroxychloroquine on progression of dementia in early Alzheimer's disease: an 18-month randomised, double-blind, placebo-controlled study. *Lancet* 2001;**358**:455–60.

'MAINRITSAN2-the future', with some doubts!

We read with great interest the article on 'comparison of individually tailored versus fixed-schedule rituximab regimen to maintain ANCA-associated vasculitis remission: results of a multicentre, randomised controlled, phase III trial (MAINRITSAN2)' by Charles and Terrier.¹ They have tried to address a crucial aspect of rituximab dose titration during remission maintenance of anti-neutrophil cytoplasmic antibody (ANCA)-associated vasculitis (AAV). The key message is that, although AAV relapse rates did not differ significantly among the two groups, the patients in the individually tailored group received fewer rituximab infusions. This outcome has a significant bearing on cost and drug-related side effects. However, certain aspects of this study require further clarification.

First, 'the trial was designed to detect a 20% absolute between-arm difference of relapse, with a 5% alpha risk and 80% power in a two-sided test, with 35% relapses in control group'. It is not clear why the arbitrary figure of 35% relapse rate in the control group was considered when the MAINRITSAN² study had shown a rate of major and minor relapse of 5% and 11%, respectively. The same was evident in the present study where the relapse rate in the control group was only 9.9%. It would be interesting to know the post-hoc power analysis of the present study given the difference between the presumed and observed relapse rates (35% vs 9.9%).

Second, both the total number of relapses and major relapses were higher in the tailored-infusion group compared with the fixed-schedule group. Though these were not statistically significant in the present study, these might become significant on long-term follow-up of a larger cohort. It is interesting to know that half of the patients with total relapses were always negative for CD19+B cells. There might be two reasons for this. First may be the disturbance of b-cell activating factor (BAFF) homeostasis,³ and analysis of BAFF levels in both these groups can provide that answer if it has been carried out or the samples have been preserved. Second, it may be due to the persistence of tissue B cells, despite depletion of the circulatory CD19+ B cell.⁴ If a biopsy was done in any of the patients with relapse then the presence of tissue B cells can be looked at in the biopsy specimens.

Third, it would be good to have the comparison of a composite outcome measure like Q-TWiST [Q-TWiST = (u TOX x TOX)+TWiST + (uProg x PROG)] in both these groups. This has been reported previously in 'CORTicosteroid and cyclophosphamide-based induction therapy for SNV patients AGED ≥65 years (CORTAGE)' trial by the same group,⁵ and this can give a better idea regarding the time in which the patient experienced ≥1 (TOX) serious adverse event (SAE), the time without disease activity and SAE (TWiST) and time with disease activity (PROG).

Fourth, the definition of major and minor relapses is not clear from the supplementary tables. In table S1,¹ the patient at serial no 9 with mononeuritis was considered to have a major relapse, whereas in table S2,¹ the patient at serial number 3 with mononeuritis was considered to have a minor relapse.

Finally, while doing the cost-benefit analysis of lower rituximab pulses in the tailored arm, the costs of frequent ANCA and CD19+ B levels need to be factored in.

Arghya Chattopadhyay, Nupoor Acharya, Debashish Mishra, Vikas Sharma, GRSRNSK Naidu, Aman Sharma

Department of Internal Medicine, Clinical Immunology and Rheumatology services, PGIMER, Chandigarh, India

Correspondence to Dr Aman Sharma, Department of Internal Medicine, Clinical Immunology and Rheumatology services, PGIMER, Chandigarh 160012, India; amansharma74@yahoo.com

Handling editor Josef S Smolen

Contributors All authors (AC, NA, DM, VS, GRSRNSK and AS) were involved in the preparation of the manuscript and reviewed the final version.

Competing interests None declared.

Patient consent Not required.

Provenance and peer review Not commissioned; internally peer reviewed.

© Author(s) (or their employer(s)) 2019. No commercial re-use. See rights and permissions. Published by BMJ.



To cite Chattopadhyay A, Acharya N, Mishra D, *et al.* *Ann Rheum Dis* 2019;**78**:e139.

Received 26 September 2018

Accepted 29 September 2018

Published Online First 12 October 2018



► <http://dx.doi.org/10.1136/annrheumdis-2018-214516>

Ann Rheum Dis 2019;**78**:e139. doi:10.1136/annrheumdis-2018-214486

REFERENCES

- Charles P, Terrier B. Comparison of individually tailored versus fixed schedule rituximab regimen to maintain ANCA associated vasculitis remission: results of a multicentre, randomised controlled, phase III trial (MAINRITSAN2). *Ann Rheum Dis* 2018;**77**:1144–50.
- Guillevin L, Pagnoux C, Karras A, *et al.* Rituximab versus azathioprine for maintenance in ANCA-associated vasculitis. *N Engl J Med* 2014;**371**:1771–80.
- Ehrenstein MR, Wing C. The BAFFing effects of rituximab in lupus: danger ahead? *Nat Rev Rheumatol* 2016;**12**:367–72.
- Ferraro AJ, Smith SW, Neil D, *et al.* Relapsed Wegener's granulomatosis after rituximab therapy--b cells are present in new pathological lesions despite persistent 'depletion' of peripheral blood. *Nephrol Dial Transplant* 2008;**23**:3030–2.
- Pagnoux C, Quéméneur T, Ninet J, *et al.* Treatment of systemic necrotizing vasculitides in patients aged sixty-five years or older: results of a multicenter, open-label, randomized controlled trial of corticosteroid and cyclophosphamide-based induction therapy. *Arthritis Rheumatol* 2015;**67**:1117–27.

Response to: "MAINRITSAN2-the future", with some doubts!' by Chattopadhyay *et al*

We would like to thank Chattopadhyay *et al*¹ for their comments regarding our paper.²

The MAINTenance of Remission Using RITuximab in Systemic ANCA-associated Vasculitis (MAINRITSAN2) trial was designed in 2011. At that time, the MAINRITSAN trial results were not yet available, which explains why a conservative hypothesis was used to calculate the sample size. Given the low relapse rate (9.9%) observed with rituximab maintenance therapy for antineutrophil cytoplasm antibody (ANCA)-associated vasculitides (AAVs), our study was underpowered to detect an absolute relapse rate difference of 7%. However, a post-hoc power calculation is not necessary to reach this conclusion.³ The individually tailored group had more relapses (and major relapses), and these differences might have been statistically significant had the sample size been larger and/or follow-up longer.

To overcome this situation, we compared absolute differences of 7% for relapse rates and 3.7% for major relapse rates with the numbers of infusions needed to prevent those relapses. That is to say, the tailored-infusion or fixed-schedule group, respectively, received 248 or 381 infusions, meaning that 133 infusions were needed to prevent 3 major relapses (ie, ~45 infusions to prevent a major relapse at month 28), which would certainly make a difference for the patients. A lighter therapeutic regimen is always better, as has clearly been supported historically for patients with vasculitis. Indeed, the dramatically improved prognoses for AAVs observed over the 30 last years are mainly attributable to the lower cumulative immunosuppressant and glucocorticoid doses administered. Based on our findings, we concluded that it seems possible to reduce patients' rituximab exposure, thereby avoiding overtreatment and meeting one of our goals.

For the MAINRITSAN and MAINRITSAN2 trials, use of a composite outcome (eg, Q-TWIST) was not planned, so the required data are not available, but we do not think these analyses would have made our message clearer. As previously written, relapses were more frequent in the tailored arm, and at 28 months serious adverse events had occurred in 26 (32.1%) tailored-arm vs 31 (38.3%) systematic infusion-arm patients.

In online supplementary table S1, patient 9 had a minor relapse with purpura and, despite escalating the glucocorticoid dose, he developed mononeuritis multiplex with severe right peroneal nerve motor deficit; he was then considered to have had a major relapse by the Adjudication Committee. Patient 3 (online supplementary table S2) experienced only sensory symptoms without motor deficiency, and the mononeuritis multiplex

was confirmed by electromyogram and neuromuscular biopsy. We acknowledge that the definition of the severity of these AAV peripheral nerve involvements is difficult, but only the former patient's motor deficit warranted being classified as a major relapse. Considering patient 9 (online supplementary table S1) to be misclassified, as suggested by Chattopadhyay *et al*,¹ would have slightly disadvantaged the individually tailored group.

Finally, when we undertake the medical-economic analysis, all direct and indirect costs will have to be accounted for, that is, hospitalisations (with all related costs), rituximab infusions, laboratory tests and so on.

Pierre Charles,^{1,2} Loic Guillevin¹

¹Department of Internal Medicine, Referral Center for Rare Systemic and Autoimmune Diseases: Vasculitis and Scleroderma, Cochin Hospital, Paris Descartes University, Paris, France

²Department of Internal Medicine, Institut Mutualiste Montsouris, Paris, France

Correspondence to Professor Loic Guillevin, Department of Internal Medicine, Referral Center for Rare Systemic and Autoimmune Diseases: Vasculitis and Scleroderma, Cochin Hospital, Paris Descartes University, Paris 75014, France; loic.guillevin@aphp.fr

Handling editor Josef S Smolen

Funding The authors have not declared a specific grant for this research from any funding agency in the public, commercial or not-for-profit sectors.

Competing interests None declared.

Patient consent Not required.

Provenance and peer review Commissioned; internally peer reviewed.

© Author(s) (or their employer(s)) 2019. No commercial re-use. See rights and permissions. Published by BMJ.



To cite Charles P, Guillevin L. *Ann Rheum Dis* 2019;**78**:e140.

Received 12 October 2018

Accepted 13 October 2018

Published Online First 26 October 2018



► <http://dx.doi.org/10.1136/annrheumdis-2018-214486>

Ann Rheum Dis 2019;**78**:e140. doi:10.1136/annrheumdis-2018-214516

REFERENCES

- Chattopadhyay A, Acharya N, Mishra D, *et al*. 'MAINRITSAN2-the future', with some doubts! *Ann Rheum Dis* 2019;**78**:e139.
- Charles P, Terrier B, Perrodeau E. Comparison of individually tailored vs fixed-schedule rituximab regimen to maintain ANCA-associated-vasculitis remission: results of a multicenter, randomized-controlled, phase 3 trial (MAINRITSAN2). *Ann Rheum Dis* 2018;**77**:1144–50.
- Schulz KF, Grimes DA. Sample size calculations in randomised trials: mandatory and mystical. *Lancet* 2005;**365**:1348–53.

Knee osteoarthritis and bisphosphonates: Could BCP crystals be the missing link?

I read with interest your article regarding the potential of bisphosphonates for osteoarthritis (OA).¹ Since OA affects the entire joint, it is unsurprising that there has been great difficulty developing an effective targeted treatment. The lifetime risk of symptomatic knee OA has been estimated to be as high as 44.7%,² and therefore, we are in urgent need of finding a disease-modifying OA drug.³

Basic calcium phosphate (BCP) crystals have been found in 100% of OA knee and hip cartilages removed at joint replacement and therefore might represent a potential therapeutic target in OA.⁴ BCP crystals include various calcium phosphates, including partially carbonate-substituted hydroxyapatite, octacalcium phosphate, tricalcium phosphate and magnesium whitlockite.⁵ BCP crystals have multiple biologic effects in vitro. They have the ability to stimulate prostaglandins, cytokines and matrix metalloproteinase synthesis in various cells including macrophages, synovial fibroblasts and chondrocytes.⁶ BCP crystals also contribute to inflammation in OA via the innate immune system.

Bisphosphonates are well-known analogues of endogenous pyrophosphate. They have a strong affinity for bone mineral and therefore tightly bind to hydroxyapatite crystals.⁷ This may be the reason behind the potential therapeutic effect of bisphosphonates in knee OA. With OA being the most prevalent rheumatic disease, affecting millions of patients worldwide, it is essential we urgently find a treatment for this much neglected disease. There is ample evidence that BCP crystals are a pathogenic mediator of OA and bisphosphonates as a potential OA treatment should be explored further.

Claire-Louise M Murphy,¹ Geraldine McCarthy²

¹Department of Rheumatology, Homerton University Hospital NHS Foundation Trust, London, UK

²Department of Rheumatology, Mater Misericordiae University Hospital, Dublin, Ireland

Correspondence to Dr Claire-Louise M Murphy, Department of Rheumatology, Homerton University Hospital NHS Foundation Trust, London E9 6SR, UK; claire-louise.murphy@nhs.net

Competing interests None declared.

Patient consent Not required.

Provenance and peer review Not commissioned; internally peer reviewed.

© Author(s) (or their employer(s)) 2019. No commercial re-use. See rights and permissions. Published by BMJ.



To cite Murphy C-LM, McCarthy G. *Ann Rheum Dis* 2019;**78**:e141.

Received 10 September 2018

Revised 23 September 2018

Accepted 24 September 2018

Published Online First 9 October 2018



► <http://dx.doi.org/10.1136/annrheumdis-2018-214493>

Ann Rheum Dis 2019;**78**:e141. doi:10.1136/annrheumdis-2018-214421

REFERENCES

- 1 Lems WF. Bisphosphonates: a therapeutic option for knee osteoarthritis? *Ann Rheum Dis* 2018;**77**:1247–8.
- 2 Murphy CL, McCarthy GM. Why basic calcium phosphate crystals should be targeted in the treatment of osteoarthritis. *EMJ Rheumatology* 2014;**1**:96–102.
- 3 Murphy L, Schwartz TA, Helmick CG, et al. Lifetime risk of symptomatic knee osteoarthritis. *Arthritis Rheum* 2008;**59**:1207–13.
- 4 Rosenthal AK. Crystals, inflammation, and osteoarthritis. *Curr Opin Rheumatol* 2011;**23**:170–3.
- 5 McCarthy GM, Cheung HS. Point: Hydroxyapatite crystal deposition is intimately involved in the pathogenesis and progression of human osteoarthritis. *Curr Rheumatol Rep* 2009;**11**:141–7.
- 6 McCarthy GM, Dunne A. Calcium crystal deposition diseases - beyond gout. *Nat Rev Rheumatol* 2018;**14**:592–602.
- 7 Manolagas SC. Birth and death of bone cells: basic regulatory mechanisms and implications for the pathogenesis and treatment of osteoporosis. *Endocr Rev* 2000;**21**:115–37.

Response to: 'Knee osteoarthritis and bisphosphonates: Could BCP crystals be the missing link?' by Murphy *et al*

I read with great interest the letter from Murphy and McCarthy¹: 'knee osteoarthritis and bisphosphonates: could BCP crystals be the missing link?'.¹

I recently gave comments on two case-control studies,² in which the need for a total knee prosthesis was around 25% lower in bisphosphonate (BP) users than in controls.^{3,4} What could be the explanation? It could be related to epidemiology: BP-users have a healthier lifestyle than non-users, by doing more exercise therapy, preventing overweight and so on. The other option is a biological effect, for example, an effect of BPs on the underlying subchondral bone in patients with osteoarthritis (OA).⁵

Murphy and McCarthy bring in that BPs have a strong affinity for basic crystal phosphates (BCPs) and that this might inhibit inflammatory reactions in the synovial fluid.¹ They argued that BCPs have been found in the cartilage of 100% of patients with OA at the time of joint replacement and that BCPs might contribute to inflammation in OA.

Although this is certainly a valuable suggestion, the incidence of clinically manifest knee-osteoarthritis based on BCP-crystals is low in patients with OA. Since knee-OA is a whole joint disease, cartilage, bone, synovial inflammation and muscular weakness all play a role,⁶ it is very likely that other factors are among the mean determinants of inflammation and pain in patients with knee-OA. So, BCP-crystals are probably not 'the' missing link, but might be a 'missing link'.

Nevertheless, since the pathogenesis of OA is not fully elucidated and therapeutic options are scarce, further research in the direction of BCPs and BPs in patients with knee-OA is very welcome.

Willem Lems

Correspondence to Willem Lems, Department of Rheumatology, VU University Medical Center, Amsterdam 1007MB, The Netherlands; wf.lems@vumc.nl

Handling editor Josef S Smolen

Funding The authors have not declared a specific grant for this research from any funding agency in the public, commercial or not-for-profit sectors.

Competing interests None declared.

Patient consent Not required.

Provenance and peer review Commissioned; internally peer reviewed.

© Author(s) (or their employer(s)) 2019. No commercial re-use. See rights and permissions. Published by BMJ.



To cite Lems W. *Ann Rheum Dis* 2019;**78**:e142.

Received 12 October 2018

Accepted 13 October 2018

Published Online First 2 November 2018



► <http://dx.doi.org/10.1136/annrheumdis-2018-214421>

Ann Rheum Dis 2019;**78**:e142. doi:10.1136/annrheumdis-2018-214493

REFERENCES

- Murphy CM, McCarthy G. Knee osteoarthritis and bisphosphonates: could BCP crystals be the missing link? *Ann Rheum Dis* 2019;**78**:e141.
- Lems WF. Bisphosphonates: a therapeutic option for knee osteoarthritis? *Ann Rheum Dis* 2018;**77**:1247–8.
- Neogi T, Li S, Peloquin C, *et al*. Effect of bisphosphonates on knee replacement surgery. *Ann Rheum Dis* 2018;**77**:92–7.
- Fu SH, Wang CY, Yang RS, *et al*. Bisphosphonate use and the risk of undergoing total knee arthroplasty in osteoporotic patients with osteoarthritis: a nationwide cohort study in taiwan. *J Bone Joint Surg Am* 2017;**99**:838–46.
- Roman-Blas JA, Castañeda S, Largo R, *et al*. An OA phenotype may obtain major benefit from bone-acting agents. *Semin Arthritis Rheum* 2014;**43**:421–8.
- Bijlsma JW, Berenbaum F, Lafeber FP. Osteoarthritis: an update with relevance for clinical practice. *Lancet* 2011;**377**:2115–26.

Correction: *Mitochondrial DNA haplogroups influence the risk of incident knee osteoarthritis in OAI and CHECK cohorts. A meta-analysis and functional study*

Fernández-Moreno M, Soto-Hermida A, Vázquez-Mosquera M, *et al.* Mitochondrial DNA haplogroups influence the risk of incident knee osteoarthritis in OAI and CHECK cohorts. A meta-analysis and functional study. *Ann of Rheum Dis* 2017;76:1114–22. doi: 10.1136/annrheumdis-2016-210131

The second corresponding author was not listed.

The corresponding details are:

Francisco J Blanco MD PhD
Rheumatology Service
Clinical Research Unit
INIBIC-Complejo Hospitalario Universitario A Coruña
15006-A Coruña, Spain
flblagar@sergas.es

Open access This is an open access article distributed in accordance with the Creative Commons Attribution Non Commercial (CC BY-NC 4.0) license, which permits others to distribute, remix, adapt, build upon this work non-commercially, and license their derivative works on different terms, provided the original work is properly cited, appropriate credit is given, any changes made indicated, and the use is non-commercial. See: <http://creativecommons.org/licenses/by-nc/4.0/>.

© Author(s) (or their employer(s)) 2019. Re-use permitted under CC BY-NC. No commercial re-use. See rights and permissions. Published by BMJ.

Ann Rheum Dis 2019;78:e143. doi:10.1136/annrheumdis-2016-210131corr1



Correction: *Multi-dimensional analysis identified rheumatoid arthritis-driving pathway in human T cell. A meta-analysis and functional study*

Takeshita M, Suzuki K, Kondo Y, *et al.* Multi-dimensional analysis identified rheumatoid arthritis-driving pathway in human T cell. A meta-analysis and functional study. *Ann of Rheum Dis* 2019;78:1346-56. doi:10.1136/annrheumdis-2018-214885.

The abbreviation for Temra in the legends of figures 1 and 2 should be CD45RA-positive effector memory T cell.

Open access This is an open access article distributed in accordance with the Creative Commons Attribution Non Commercial (CC BY-NC 4.0) license, which permits others to distribute, remix, adapt, build upon this work non-commercially, and license their derivative works on different terms, provided the original work is properly cited, appropriate credit is given, any changes made indicated, and the use is non-commercial. See: <http://creativecommons.org/licenses/by-nc/4.0/>.

© Author(s) (or their employer(s)) 2019. Re-use permitted under CC BY-NC. No commercial re-use. See rights and permissions. Published by BMJ.

Ann Rheum Dis 2019;78:e144. doi:10.1136/annrheumdis-2018-214885corr1

